Joachim Ihme

Rail Vehicle Technology

Springer

Rail Vehicle Technology

Joachim Ihme

Rail Vehicle Technology

Springer

Joachim Ihme
Ostfalia HaW
Wolfenbüttel, Germany

ISBN 978-3-658-36968-2 ISBN 978-3-658-36969-9 (eBook)
https://doi.org/10.1007/978-3-658-36969-9

This book is a translation of the original German edition „Schienenfahrzeugtechnik “ by Ihme, Joachim, published by Springer Fachmedien Wiesbaden GmbH in 2019. The translation was done with the help of artificial intelligence (machine translation by the service DeepL.com). A subsequent human revision was done primarily in terms of content, so that the book will read stylistically differently from a conventional translation. Springer Nature works continuously to further the development of tools for the production of books and on the related technologies to support the authors.

© The Editor(s) (if applicable) and The Author(s), under exclusive license to Springer Fachmedien Wiesbaden GmbH, part of Springer Nature 2022
This work is subject to copyright. All rights are solely and exclusively licensed by the Publisher, whether the whole or part of the material is concerned, specifically the rights of translation, reprinting, reuse of illustrations, recitation, broadcasting, reproduction on microfilms or in any other physical way, and transmission or information storage and retrieval, electronic adaptation, computer software, or by similar or dissimilar methodology now known or hereafter developed.
The use of general descriptive names, registered names, trademarks, service marks, etc. in this publication does not imply, even in the absence of a specific statement, that such names are exempt from the relevant protective laws and regulations and therefore free for general use.
The publisher, the authors and the editors are safe to assume that the advice and information in this book are believed to be true and accurate at the date of publication. Neither the publisher nor the authors or the editors give a warranty, expressed or implied, with respect to the material contained herein or for any errors or omissions that may have been made. The publisher remains neutral with regard to jurisdictional claims in published maps and institutional affiliations.

This Springer imprint is published by the registered company Springer Fachmedien Wiesbaden GmbH part of Springer Nature.
The registered company address is: Abraham-Lincoln-Str. 46, 65189 Wiesbaden, Germany

Preface

This book originated from lectures on rail vehicle technology that I have held since 1990 at the Ostfalia University of Applied Sciences in Wolfenbüttel and Wolfsburg for students of mechanical engineering, automotive engineering and electrical engineering.

Unfortunately, over the last 30 years, the teaching of rail vehicle technology and railway engineering has been cut back at technical universities and universities of applied sciences, although Germany still has important locations for the rail vehicle and supply industry. In addition, the interest in railways and rail vehicles among first-year students is rather low, since model railways have essentially become a collector's item for older gentlemen and railways have withdrawn from many regions.

This is why the German rail vehicle industry and rail operators are finding fewer and fewer engineers specially trained for them. According to reports, there is therefore a need to provide new employees with the necessary basic knowledge and special skills in the company. This book aims to make an introductory contribution to this in the field of rail vehicle technology. Apart from being used as a lecture material, it is also suitable for self-study. However, not all aspects of rail vehicle technology and rail transport can be dealt with and deepened here.

At the request of the readership, a new chapter on "Engineering in rail vehicle construction" has been included in the second edition.

The target group for this book are students at colleges and universities after the basic studies of mechanical or vehicle engineering. Also the interested layman, e.g. the railway enthusiast, can expand his knowledge in this book. However, he will largely miss steam locomotives and landscape photographs of railway trains.

I would like to thank all the companies and institutions that supported me with information and picture material, especially the companies Alstom, Bombardier, Siemens, Voith and Vossloh. I would also like to thank Springer Vieweg Verlag and Dipl.-Ing. Thomas Zipsner for the pleasant cooperation. Last but not least, I would like to thank my dear wife, who had to forego many joint activities with me during the preparation of the manuscript.

All unmarked illustrations and photos are by the author. I am grateful for suggestions from readers and for information on errors.

Braunschweig
in October 2021

Wolfenbüttel, Niedersachsen, Germany Joachim Ihme

Contents

1 Introduction 1

2 Running Resistances of Rail Vehicles 31
- 2.1 Running Resistance 32
- 2.2 Air Resistance 33
- 2.3 Additional Resistance 35
- 2.4 Line Resistance 38
- 2.5 Acceleration Resistance 39
- 2.6 Air Resistance According to the Hanover Formula 40
- 2.7 Total Resistance and Wheel Power 42
- 2.8 Examples and Tasks for Chap. 2 44

3 Driving Machines, Power Transmission 51
- 3.1 Steam Engine 54
- 3.2 Electric Motor 58
  - 3.2.1 DC Motor 61
  - 3.2.2 Single-Phase AC Motor 63
  - 3.2.3 Three-Phase Motor 69
  - 3.2.4 Mechanical Part of the Electric Drives 74
- 3.3 Internal Combustion Engine 80
  - 3.3.1 Mechanical Power Transmission 83
  - 3.3.2 Hydrodynamic Power Transmission 85
  - 3.3.3 Electrical Power Transmission 91
- 3.4 Gas Turbine 96
- 3.5 Hybrid Vehicles 99

4 Brakes for Railway Vehicles 107
- 4.1 Frictional Brakes 109
  - 4.1.1 Through Brakes 116
  - 4.1.2 Mechanical Brake Components 124
  - 4.1.3 Electric (Regenerative) Brake 127
  - 4.1.4 Hydrodynamic Brake 129

4.2 Brakes Independent of Wheel-Rail Adhesion 129
4.3 Calculation of Braking Distances 134
4.4 Brake Weight 140

5 Wheelset Guidance, Suspension and Damping 143
5.1 Vibration Perception of the Human Being 144
5.2 Vehicle Vibrations Due to Track Unevenness 145
5.3 Theoretical Principles of Vibration Simulation 148
5.3.1 Simulation in the Frequency Domain 151
5.3.2 Simulation in the Time Domain 157
5.4 Interaction Between Vehicle and Track 160
5.5 Dynamic Behaviour of the Wheelset 164
5.6 Running Gears of Rail Vehicles 184
5.6.1 Bogies for Railway Vehicles 185
5.6.2 Running Gear of Tramcars 196
5.7 Curve Entry and Exit 203
5.8 Air Suspension 206

6 Supporting Structures and Superstructures of Railway Vehicles 215
6.1 Strength Requirements for Rail Vehicle Bodies 216
6.1.1 Static Load Assumptions 216
6.1.2 Dynamic Load Assumptions 219
6.1.3 Static Tests 220
6.1.4 Crashworthy Design 220
6.2 Historical Development and Current Status of Railway Passenger Carriages 226
6.3 Metro, Light Rail and Tram Vehicles 247
6.4 Locomotives 253
6.5 Freight Wagons 258
6.6 Bogies and Running Gear 264

7 Engineering in Rail Vehicle Construction 271
7.1 Product Creation Process in Rail Vehicle Construction 273
7.2 Computer-Aided Product Creation 282

References 297

Index 301

Formula Symbols, Indices and Abbreviations Used

Formula Symbols Used

A [m^2, cm^2, mm^2]	Area
A_1 [m^2]	Transverse clamping surface
A_2 [m^2]	Train surface
B [N, kN]	Braking force
C [diverse]	Integration constant
D [–]	Damping factor according to Lehr
E [kWh]	Energy
F [N, kN]	Force general
F_B [N, kN]	Braking force
F_{GR} [N, kN]	Weight force on wheel/wheels
F_{MG} [N, kN]	Braking force of the magnetic rail brake
F_{WR} [N, kN]	Rolling resistance force of a wheel
G [N, kN]	Weight force
I [A]	Current
I [mm^4]	Second moment of an area
J [kgm^2]	Mass moment of inertia
Im [–]	Imaginary part of a complex number
K_W [–]	Ratio of average drag coefficients
L [m]	Length, train length
L [m]	Uneven wavelength
M [Nm]	Moment, torque
M_{Kipp} [Nm]	Stall torque (for three-phase motor)
M_{RL} [Nm]	Bearing frictional torque
N [N, kN]	Normal force
P [kW]	Power
P_{1h} [kW]	Hourly output (for electric locomotives)
P_{Start} [kW]	Starting power (for electric locomotives)
P_{Cont} [kW]	Continuous power (for electric locomotives)

P_V [kW]	Power loss
R [m]	Radius of the track curve
Re [–]	Reynolds number
Re [–]	Real part of a complex number
S [N, kN]	Lateral force
T [N, kN]	Tangential force
T [s]	Time(point)
U [V, kV]	(Electr.) Voltage
U [N, kN]	Circumferential force
U_{gl} [V, kV]	DC voltage average
V [m^3]	Volume
W_{Drive} [N, kN]	Driving resistance force
W [cm^3, mm^3]	Resistance torque
W_a [N, kN]	Air resistance nose and tail
W_{Acc} [N, kN]	Acceleration resistance
W_b [N, kN]	Air resistance train surface (air friction)
W_{Cur} [N, kN]	Curve resistance
W_{Run} [N, kN]	Running resistance
W_{Air} [N, kN]	Air resistance
W_R [N, kN]	Rolling resistance
W_{Imp} [N, kN]	Impact resistance
W_{Lin} [N, kN]	Line resistance
Z [N, kN]	Traction force
Z_{max} [N, kN]	Maximum traction force
a [m, mm]	Distance, wheelset distance
a [m/s^2]	Braking deceleration
b [m/s^2]	Acceleration
c	Coefficient (general)
c [N/m]	Spring constant
c' [N/m]	Gravitational stiffness (gravitational spring stiffness)
c_d [–]	Coefficient for impact resistance
c_W [–]	Drag coefficient
c'_W [–]	Drag coefficient for inclined air flow
$c_{W,L}$ [–]	Drag coefficient locomotive
$c_{W,W}$ [–]	Drag coefficient wagon
e [m, mm]	Distance, eccentricity
f [Hz]	Frequency
f_R [–]	Rolling resistance coefficient
g [m/s^2]	Acceleration due to gravity
h [m, mm]	Height; unevenness (amplitude)
i [–]	Imaginary Unit, $i = \sqrt{-1}$

k [Ns/m]	Damper constant
k [–]	Slip coefficient
l [m, mm]	Distance, length
m [kg, t]	Mass
m' [kg/m]	Specific mass (for rails)
n [–]	Number, number of wagons of a train
n [min^{-1}]	Rotational speed
n [–]	Polytropic exponent
p [bar]	Pressure
q [$\mathrm{N/m}^2$]	Dynamic pressure
r [m, mm]	Radius
r_0 [mm]	Rolling circle radius of the wheelset with central alignment in the track
s [‰]	Gradient (slope)
s [m, mm]	Distance
s_B [rad/m]	Drilling slip
s_B [–]	Brake slip
s_T [–]	Traction slip (drive slip); Tangential slip
s_U [–]	Circumferential slip
s_B [m]	Braking distance
s_R [mm]	Rolling circle distance of the wheels of a wheelset
t [s]	Time
t_A [s]	Response time
t_B [s]	Braking duration (duration until standstill)
t_S [s]	Threshold duration
u [mm]	Superelevation (in the track curve)
v [m/s, km/h]	Driving speed
v_0 [m/s, km/h]	(Vehicle) reference/initial speed
v_res [km/h]	Resultant flow speed
x, y, z	Coordinates of the (fixed) coordinate system
Φ_h [m^3/rad]	Spectral density of a track unevenness
Ω [rad/m]	Travel circle frequency
α [°]	Angle, pitch angle
γ [rad]	Taper angle
γ_e [rad]	Effective taper of the wheelset
δ [rad/s]	Decay constant
δ [$\mathrm{rad/s}^2$]	Angular acceleration
ε [rad]	Yaw angle
η [–]	Efficiency
κ [–]	Exponent for adiabatic compression
λ [–]	Torque mass (surcharge) factor

μ [–]	Coefficient of friction
μ_g [–]	Sliding coefficient
μ_h [–]	Adhesion coefficient
μ_K [–]	Coefficient of friction brake pad (brake lining) – wheel
μ_L [–]	Bearing coefficient of friction
ν [rad/s]	Eigen(circuit) frequency
ξ, η, ς	Coordinates of the wheel-set coordinate system
ρ [kg/m^3]	Airtight
τ [°, rad]	Angle of attack
φ [rad]	Phase angle
ψ [rad]	Roll angle
ω [rad/s]	Excitation (circuit) frequency
ω [rad/s]	Angular velocity
ω_B [rad/s]	Drilling angle velocity

Indexes

0	Initial value, reference value
I	Input
II	Output
c	Spring
d	Damper
eff	RMS value
F	Air spring
Gen	Generator
H	at the back
K	Code converter
l	left
L	Catenary
M	Motor
max	maximum, maximum~
R	Wheel
r	right
rel	relatively
res	resulting
Ü	Transmission
V	front

Abbreviations

ABB	ASEA-Brown-Boveri, Swedish-Swiss electrical company
Adtranz	Subsidiary of Daimler-Benz AG, merged from AEG and ABB, acquired by Bombardier in 2001
AEG	(German) General Railway Act
AEG	Allgemeine Elektrizitätsgesellschaft, merged into Adtranz
Alstom	Alstom Transport Germany GmbH
Bombardier	Bombardier Transportation (division of the Canadian group Bombardier Inc.)
BOStrab	(German) Construction and operating regulations for tramways
CAF	Construcciones y Auxiliar de Ferrocarriles S. A.; Spanish rail vehicle manufacturer
CRRC	China Railway Rolling Stock Corporation, Beijing, PRC
DB	Deutsche Bahn AG (from 1994); Deutsche Bundesbahn (until 1993)
DIN	German Institute for Standardization
DR	Deutsche Reichsbahn (State railway of the GDR, until 1993)
Duewag	Duewag AG (Düsseldorf-Uerdinger Waggonfabrik), today part of Siemens Mobility
EBO	(German) Railway Construction and Operation Regulations
EN	European Standard (Europa Norm)
FEM	Finite Element Method
HeiterBlick	HeiterBlick GmbH, Leipzig; tramcar manufacturer
ICE	Intercity-Express (German high-speed train)
ISO	International Standard Organization
LHB	Linke-Hofmann-Busch GmbH, Salzgitter (now Alstom Transport Germany)
MAN	Maschinenfabrik Augsburg-Nürnberg AG (now part of the VW Group)
Siemens	Siemens AG, Mobility Division
SNCF	Societé Nationale des Chemins de Fer français (French National Railway Company)
SO	Top of rail
Solaris	Solaris Bus & Coach S.A., based in Posnan (PL); in 2018 the bus division was taken over by CAF and the tram division by Stadler Rail
Stadler	Stadler Rail AG, Headquarters: Bussnang (CH); Swiss rail vehicle manufacturer
Tatra	CKD Tatra Vagonka, Prague, Czech manufacturer of trams, among other things (Siemens Mobility site since 2001)
TGV	Train à Grande Vitesse (French high-speed train)
TEE	Trans-Europ-Express (high-speed train system between Western European countries 1957 to 1987)
TSI	Technical specification for interoperability

Üstra	Üstra Hannoversche Verkehrsbetriebe AG (Tram and Bus operator in Hanover)
UIC	Union International des Chemins de Fer (International Union of Railways)
VDB	Verband der Bahnindustrie in Deutschland e. V. (Association of the Railway Industry in Germany)
VDV	Verband Deutscher Verkehrsbetriebe e. V. (Association of German Transport Operators)

Introduction

1

The theoretical principles of rail vehicle technology are the same worldwide. They are explained in this book using examples from Germany and Europe. It should be noted that laws, regulations and standards outside Germany and the European Union differ from those presented in this book.

The railway has not had a good reputation in Germany since the Second World War. As the state-owned "Deutsche Bundesbahn" (German Federal Railways), it was regarded as an "official railway": backward, inflexible, expensive and customer-unfriendly. Road transport was considered to be a modern, flexible and much cheaper alternative, which among other things led to the fact that the route network in the old federal states shrank from 30,500 to 27,000 km and the length of passenger transport from 29,000 to 21,000 km between 1950 and 1990.[1] It was not until 1977 that the last steam locomotives were taken out of service on the DB – many years later than on other Western European railways. At the Deutsche Reichsbahn (DR) in the GDR, numerous lines were dismantled as reparations after the Second World War and many main lines lost their second track. Also due to the lack of modernization of the network and the rolling stock (e.g. the DR did not retire the last steam locomotives until 1988), the image of the railway in the GDR was not the best,[2] although it provided high passenger and freight transport services. After the merger of the Deutsche Bundesbahn and the Deutsche Reichsbahn in 1994 to form the Deutsche Bahn AG,[3] the image of the railway in Germany has unfortunately hardly improved: delays, train cancellations due to snow, sleet and storms, non-functioning air-conditioning systems,

[1] See: Bundestag (German Federal Parliament) Printed Matter 13/2569 (2013).

[2] In the GDR there was a saying about the six natural enemies of the Reichsbahn: spring, summer, autumn, winter, day and night.

[3] Deutsche Bahn AG: German Railways plc.; the shares are still 100% held by the state.

© The Author(s), under exclusive license to Springer Fachmedien Wiesbaden GmbH, part of Springer Nature 2022

J. Ihme, *Rail Vehicle Technology*,
https://doi.org/10.1007/978-3-658-36969-9_1

signal boxes and traction unit failures are topics in the media almost daily. In the meantime, the route network in the new federal states has also been thinned out considerably.

The situation was not much different in the second area of rail transport, the tramways in Germany: Between 1945 and today, the number of cities in Germany with tram operations nearly halved, and even in the remaining cities, the networks have mostly shrunk. For a long time, buses were considered to be cheaper and more flexible, and when there was sufficient demand for transport, people preferred to replace the tram with an underground railway that did not interfere with individual traffic. This development has now been partially halted: many cities are expanding their networks and Saarbrücken and Oberhausen have reintroduced trams. On the other hand, some operations are still threatened with closure. The construction and operation of underground railways has proved so costly in many places[4] that underground cities such as Berlin, Munich and Nuremberg are extending tram routes again, even though they were originally intended to be abolished. The tram is currently experiencing a renaissance in the USA, France and Great Britain – countries where only a few tram companies existed 40 years ago. New tram networks have also been created in China and in emerging countries such as Morocco, Tunisia and Turkey.

However, the poor image of rail transport in Germany is not a problem of rail transport per se, but rather caused by the operator and the political framework conditions. For example, the stock market flotation of Deutsche Bahn from 1994 onwards and the associated cost-cutting policy of the company are certainly a reason for the problems described above. In Germany, the strong automobile lobby also has considerable influence on political guidelines in the transport sector. For example, "electromobility" was subsidised to the tune of €1.4 billion until 2016, although the funding was limited to electric road vehicles, energy storage technology and charging point infrastructure on roads. It was not intended to promote existing electromobility on the railways, e.g. the construction of new tram lines. In 2018, a subsidy programme is still running, where the acquisition costs of pure electric road vehicles are subsidised with €2000 each and plug-in hybrid cars with €1500. The programme is designed for up to 300,000 vehicles.

As a counter-example to the situation of the railways in Germany, the railways in Switzerland and Japan may serve, for example, whose image is far better. The performance of railway systems can be seen in Australia, Russia, China and the USA: In these territorial countries, the share of railways in freight transport[5] is around 40%, while in Germany it is around 20%. In Germany, around 60% of freight is transported by truck. In local transport,

[4]The construction costs of tram or metro are of course dependent on numerous parameters. As a rough guide, one can calculate €10 million per km of tram line and €100 million per km of metro line (in each case including energy supply and signalling). The operation of metro lines is also much more expensive than the operation of tram lines due to the operation of the stations (lighting, cleaning, escalators, lifts, etc.) and tunnel maintenance.

[5]Freight transport performance is measured in tkm (tonne-kilometres), the product of the weight of cargo transported and the transport distance.

trucks can certainly hardly be replaced by rail, but in long-distance transport, rail transport could make a considerable contribution to relieving road congestion if there were the political will to expand the railway infrastructure. The major rail hubs in particular are bottlenecks here, but so are the routes from inland to the North Sea ports.

There are still major discrepancies in the financing of infrastructure within the transport sector in Germany. For example, railways and road transport have to pay the full mineral oil tax rate on diesel oil, while inland waterways and aviation (including private aviation with small aircraft) are exempt. Long-distance buses do not have to pay motorway tolls in Germany, while each train is subject to a route usage charge per km of journey and a station charge for each stop at a station. In freight transport, trucks pay a toll only for the use of motorways and federal roads, while rail freight pays a toll for each kilometre travelled. Diesel oil used in rail operations and electrical energy are also subject to the eco-tax.

Nevertheless, rail transport is the most resource-efficient means of transport. Thanks to low driving resistances, energy consumption is lower than in road or air transport. An electric rail vehicle on an overhead line or conductor rail can be operated 100% from regenerative energy sources, without a battery with poor efficiency (approx. 70%, increasing the energy input). The land consumption of a railway line is much lower than that of a waterway or a motorway [43]. Railways are also still the safest means of transport.

So what actually is a railway?

On 17th March 1880, the German Imperial Court (Reichsgericht) defined the term "railway" as follows:

> An undertaking aimed at the repeated movement of persons or objects over not entirely insignificant distances on a metal basis, which is intended by its consistency, construction and smoothness to enable the transport of large masses of weight or the achievement of a relatively significant speed of transport movement, and by this characteristic in conjunction with the natural forces also used to produce the transport movement (such as steam, electricity, animal, human muscular activity, in the case of an inclined plane of the railway also already the own weight of the transport vessels and their load, etc.) is capable of producing a relatively violent effect in the operation of the company on the same (depending on the circumstances only in a useful way, or also destroying human life and injuring human health).[6]

A railway system is characterized by the following subsystems [43]:

- Administrative subsystem (management),
- Operational subsystem (operation, production),

[6]This definition by the Reichsgericht does not provide a useful technical definition of the term "railway", but establishes the principle of strict liability for a railway undertaking: the operation of a railway is dangerous, and in the event of damage, the railway undertaking is generally liable. It would have to prove that it was not the railway undertaking itself that caused the damage, but the injured party. Strict liability also applies to the operation of motor vehicles, which is why motor vehicle liability insurance must be taken out.

- Technical subsystem (technology),
- Commercial system (purchasing and sales).

Here we will mainly deal with the technical subsystem, which consists of the following components:

- Rail Vehicle Engineering,
- Track Technology,
- Track Guidance Technology,
- Energy (Supply) Technology,
- Communications and Signaling (Computer Science).

Our topic will mainly be vehicle technology, which in the case of railways cannot be separated from track technology and track guidance technology, just as energy supply also plays a role for rail vehicle technology. In this respect, rail vehicle technology is subject to stronger restrictions and boundary conditions than motor vehicle technology, because compatibility with existing equipment and vehicles must also be ensured.

Railways are mechanically guided means of transport that use the wheel-rail system. They are also referred to as rail transport systems. Rail vehicles either have their own traction drive (locomotive, railcar) or are pulled or pushed by a locomotive, see Fig. 1.1. Special cases of mechanically guided systems are suspension railways (e.g. Wuppertal "Schwebebahn", a single rail suspension railway) as well as systems with vehicles without their own drive, e.g. cable railways where the drive is provided by a stationary motor. An example is shown in Fig. 1.6: The Oberweißbacher Bergbahn is a funicular railway in which rail-guided carriages are pulled by a fixed drive on a rope in order to overcome a large gradient. For one uphill car a second downhill car serves as a counterweight. In the middle of the line, the uphill and downhill carriages are guided past each other via a switch.

Railways also include tramways, underground railways and rack railways (Fig. 1.4). In contrast to railways, which have their own track system, trams usually run on a track system embedded flush in the road (Fig. 1.2). Whereas the operation of railways is controlled by train protection devices (e.g. signals), trams run on sight, i.e. they have to adapt to the peculiarities of road traffic, e.g. by braking performance accordingly. Like railways, metros are operated by means of train protection systems. A mixture of metro and tramway are the light railways, which can run in the street, on their own track or in tunnels (e.g. in Dortmund, Düsseldorf, Duisburg, Essen, Frankfurt/Main, Hanover (see Fig. 1.3), Cologne, Stuttgart) (Fig. 1.4).

Metros belong to the railways. While in Hamburg and Berlin (Fig. 1.5) they are independent systems, in Munich, Stuttgart, Frankfurt and in the Ruhr area they are integrated into the railway network both in terms of track and rolling stock and run partly or completely (e.g. Hanover) on normal railway lines.

Fig. 1.1 Railway. (**a**) Double-decker push-pull train, (**b**) Through freight train

Fig. 1.2 Classic tramway in the street space (Halberstadt)

According to the standard DIN 25003,[7] rail vehicles belong to the track-guided vehicles. They are mainly divided into railway vehicles and tramway vehicles, Fig. 1.7.

[7] DIN e. V. (Ed.): Systematics of rail vehicles. DIN 25003, Beuth Verlag, Berlin (2001).

Fig. 1.3 Light rail on its own track with elevated platforms (Hanover); *in the background*: tunnel ramp and tunnel

Fig. 1.4 Rack railway (Drachenfelsbahn)

The term "rail vehicles" stands for rail-bound vehicles that run on wheels fitted with wheel flanges on rails arranged in pairs and parallel and that transport both goods and passengers. The connection between the wheelset of the rail vehicle and the rail is the essential interface in the

Fig. 1.5 Metro (S-Bahn) Berlin (note: conductor rail, centre buffer coupling)

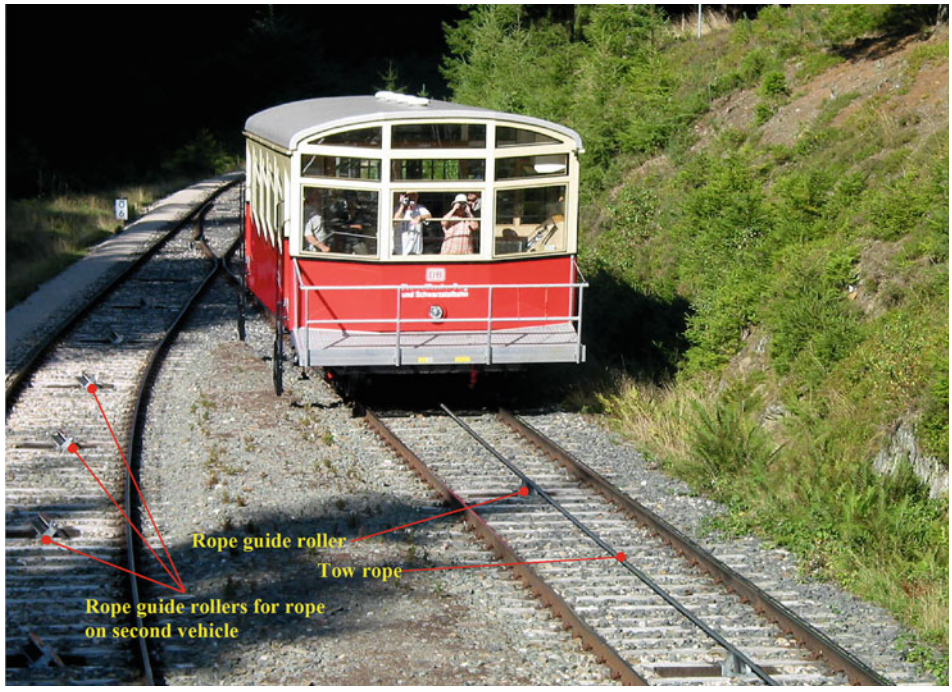

Fig. 1.6 Funicular railway (Oberweißbacher Bergbahn) in the switch in the middle of the line; uphill travelling carriage

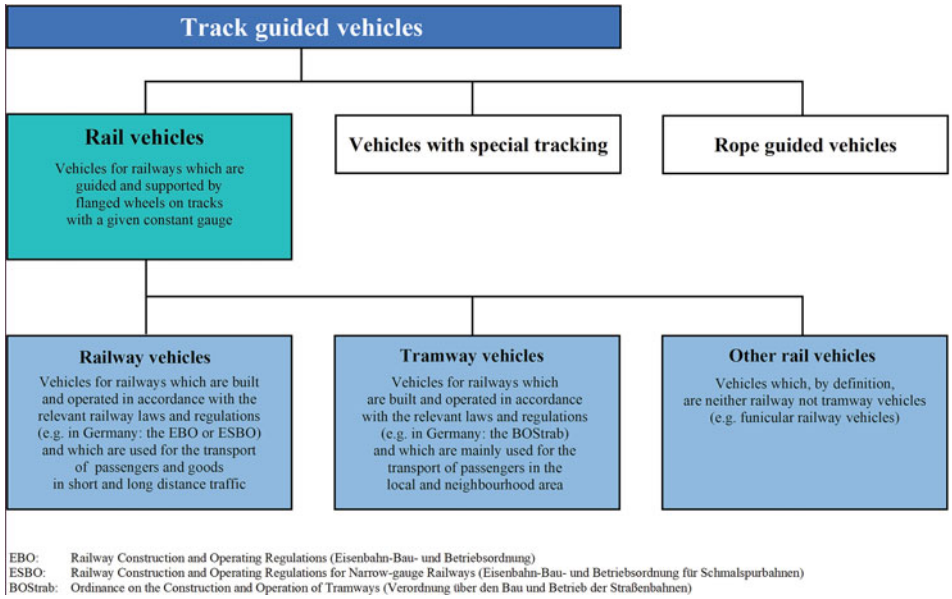

Fig. 1.7 Classification of rail vehicles within track guided vehicles. [34]

> railway system. The wheelset guides the vehicle, supports the weight of the vehicle and transmits the tractive and braking forces required to move the vehicle [34, p. 1].
>
> Rail vehicles are track-bound vehicles that are guided and supported by wheels fitted with wheel flanges on tracks of a specific gauge [DIN 25003].

Figure 1.8 shows the German legal bases of the railway systems, which differ substantially for tramways and railways. The General Railway Act (AEG) covers not only regional and long-distance trains but also regional railways of other operators (often also referred to as "non-federally owned railways" or not quite correctly as "private railways"). The latter include, for example, the Harz narrow gauge railroads (HSB), which are owned by the federal states and municipalities located in the transport area.

The construction of the railway lines and the construction of the vehicles as well as the operation of these railway systems of public transport are regulated[8] in the EBO (Railway construction and operating regulations) and in the ESBO (Railway construction and operating regulations for narrow-gauge railways). For non-public railways (e.g. for the internal traffic of industrial companies), the BOA (Ordinance on the Construction and Operation of Connecting Railways) and the EBOA (Railway Construction and Operating

[8] Larger narrow-gauge railway networks in Germany are operated, for example, by the Rhein-Neckar Transport services (RNV) and the Harz narrow gauge railroads (HSB). There are also a number of other narrow-gauge railway lines, e.g. in Saxony, on the island of Rügen and on the North Sea islands.

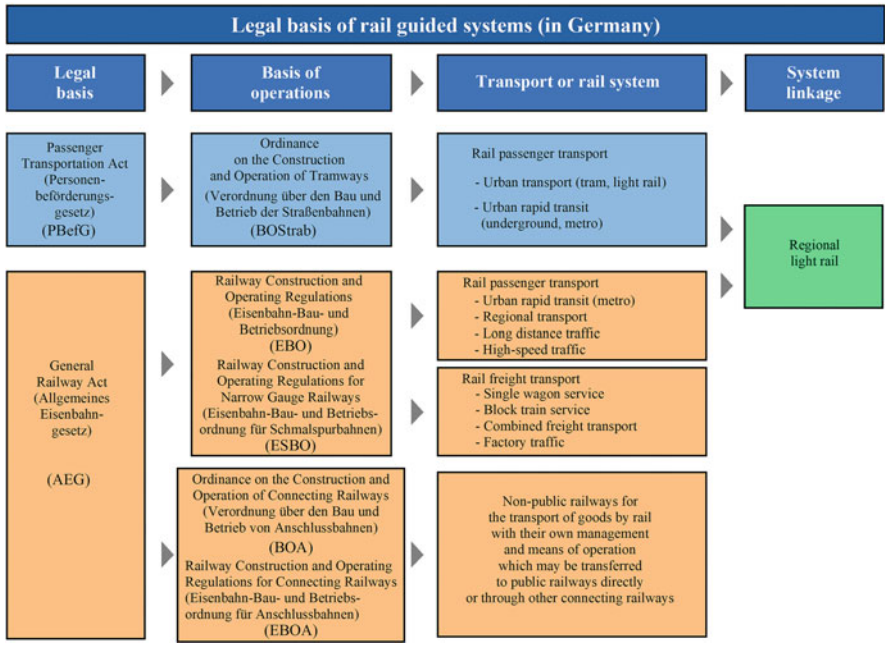

Fig. 1.8 Legal basis of the rail guided systems. [34]

Regulations for Connecting Railways) apply. Examples of connecting railways are, for example, the works railway of BASF in Ludwigshafen or that of Volkswagen AG in Wolfsburg.

Tramways are subject to the PBefG (Passenger Transport Act); the regulations for their construction and operation are the BOStrab (Tramway Construction and Operation Regulations) [34]. Due to the historical development of tramway operations, the regulations of the BOStrab are not as narrowly defined as those of the EBO, as tramway operations usually represent closed systems and e.g. vehicles of different operations do not necessarily have to be compatible. This is reflected, for example, in different track gauges, carriage widths,[9] platform heights, minimum track radii, supply voltages, brake designs, coupling systems, etc.

The classification of railway vehicles is shown in Fig. 1.9; some examples of passenger and freight railway vehicles are shown in Fig. 1.10.

The classification of the tram vehicles can be seen in Fig. 1.11. Figure 1.12 shows different tramcar types. Due to the historical development and the different capacity requirements, there is an almost unmanageable variety of types of tram vehicles in the 59 tramway

[9]For example, older tram cars in Würzburg only have a width of 2100 mm, while in Schwerin vehicles with a width of 2650 mm are in use. The decisive factor for this is, among other things, the distance between track centres on double tracks.

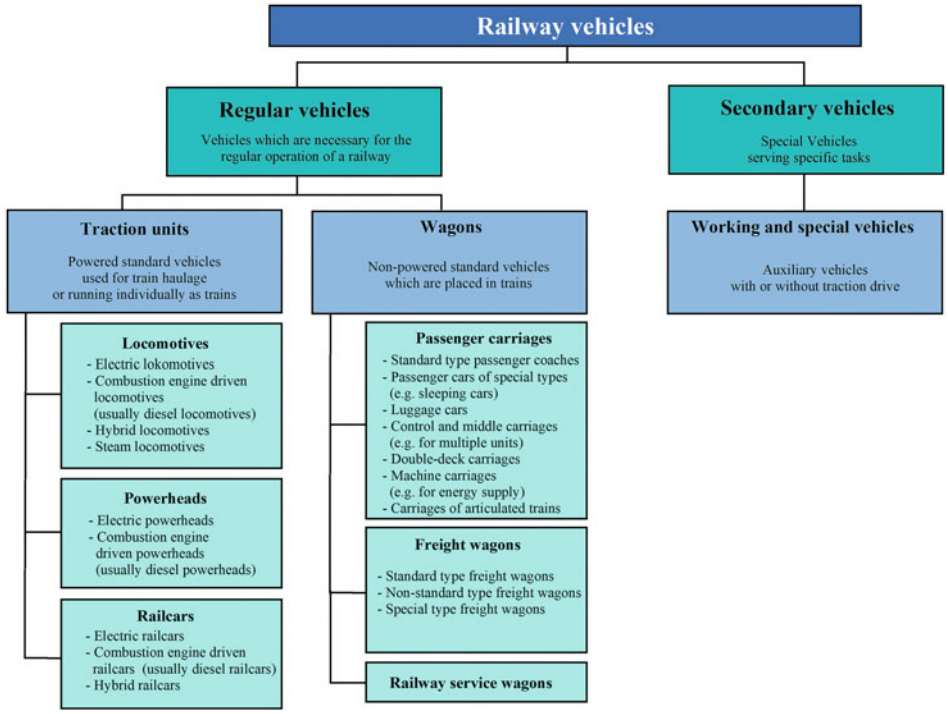

Fig. 1.9 Classification of railway vehicles in the area of validity of the EBO. (According to [34])

companies in Germany. In France, most of the tramway systems were built only in the last 40 years, so that a standardization of the vehicles could take place there.

Figure 1.13 shows the wheelset arrangements of traction units.[10] The designation method is also called "axle formula". Other designations are common in other countries.[11] Driving axles are marked with capital letters, running axles with numbers. A small zero indicates a single-axle drive. For example, C means a mechanical coupling of three drive axles via driving rods or cardan shafts. Co stands for three individually driven axles (e.g. with electric motors) in one frame. An apostrophe after letter-number combinations indicates that the axles are mounted in a separate frame (usually a bogie) under the main frame of the traction unit. The axle arrangement 1A1 was possessed, for example, by the first locomotives of the Nuremberg-Fürth railway line opened in 1835, "Adler" and "Greif"

[10] In rail vehicle technology, rail vehicles are usually represented with the direction of travel to the right. In order to adapt the axle formulae (notation from left to right) to the symbolic representation, the direction of travel to the left was selected here as a deviation.

[11] For example, in Switzerland an electric locomotive with six driven axles for a maximum speed of more than 100 km/h is called Ae 6/6 (A: maximum speed, e: electric, 6/6: six driven by six axles); Dm 2/2: shunting locomotive (D) with combustion engine (m), two driven by two axles (2/2).

Fig. 1.10 Railway vehicles and trains

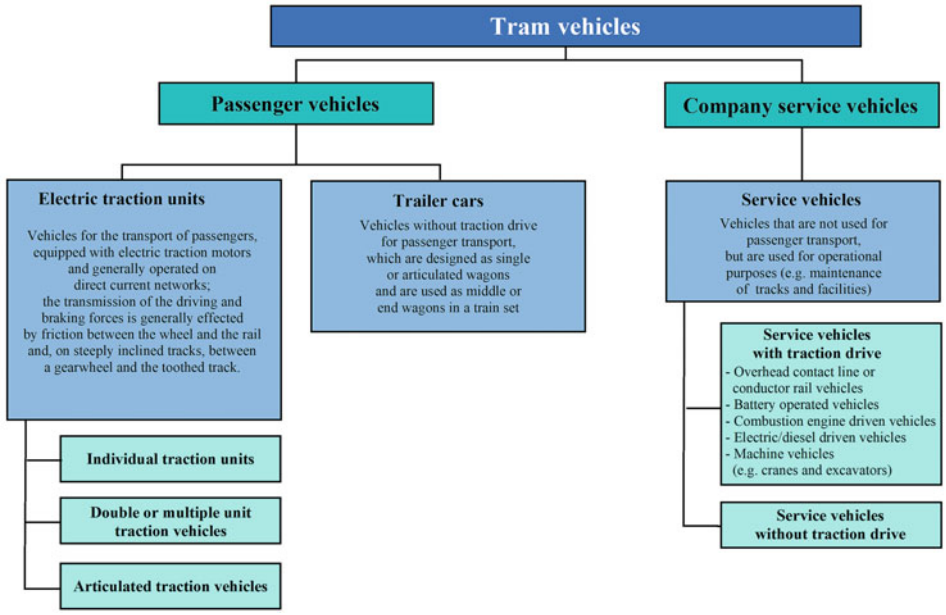

Fig. 1.11 Classification of tram vehicles. [34]

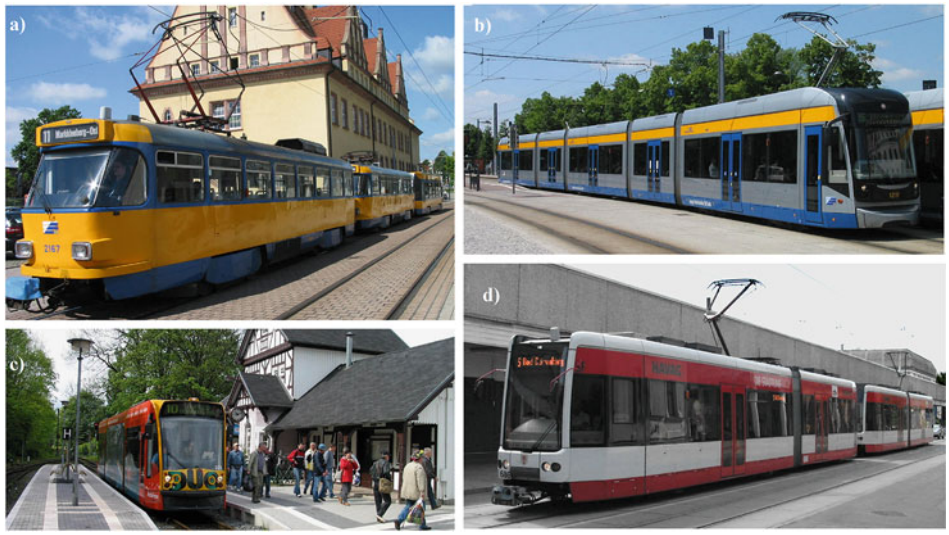

Fig. 1.12 Types of tramcar. (**a**) Single tramcar in double traction with trailer (Leipzig), (**b**) 12-axle articulated tramcar (Leipzig), (**c**) Hybrid articulated tramcar with diesel unit (Nordhausen), (**d**) 6-axle articulated tramcar in double traction (Halle/Saale)

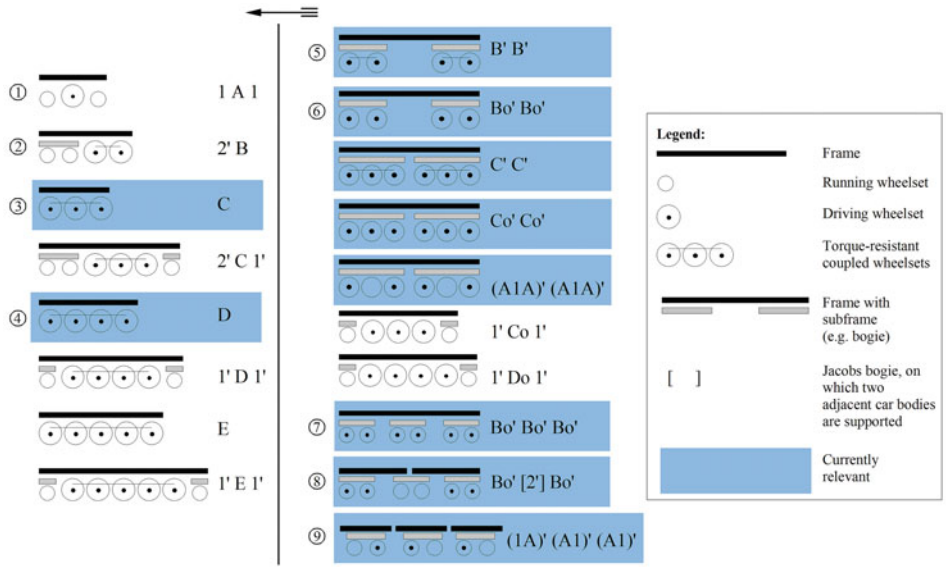

Fig. 1.13 Designation of wheelset arrangements of traction units in Germany. (See: DIN e. V. (Ed.): Schienenfahrzeuge – Kennzeichnung der Radsatzfolge. DIN 30052, Beuth Verlag, Berlin (2006))

①. The locomotive "General" from the Buster Keaton film "The General" had the axle arrangement ②: 2′B. Diesel shunting locomotives still use the axle arrangement C (e.g. DB series 360–365, ③) and D (DB series 245 ex DR V 60, ④) today. Many diesel locomotives have the B′B′ ⑤ wheelset arrangement, with two wheelsets arranged in each bogie and connected by cardan shafts. On four-axle electric locomotives, the axle formula is usually Bo′Bo′ ⑥ when the wheelsets each have a motor and are mounted in pairs in bogies. The Ae 6/6 electric locomotive of the Swiss Federal Railways has three two-axle bogies, each with two individually driven axles, under a continuous main frame in the series version, i.e. the wheelset sequence Bo′Bo′Bo′ ⑦.

Classical (two-part) articulated tramcars often have the B′[2′]B′ wheelset sequence (longitudinal motor in the driven bogies driving two axles each), or, as shown in Fig. 1.13 ⑧ Bo′[2′]Bo′, when each driving wheelset has a separate motor. A Jacobs bogie (see Chap. 5) is usually arranged under the joint. The wheelset sequence (1A)′ (A1)′(A1)′ ⑨ is used, for example, on three-car tramcars of the MAN/AEG type used in Braunschweig, Jena, and Zwickau, among other places. In this designation method, the brackets indicate that a driven and a non-driven wheelset are installed in a common frame. This frame is arranged under each car section similar to a bogie, but with only a smaller turning angle.

The common characteristic of all rail vehicles is the track guidance by wheelset and track. In contrast to motor vehicles, the choice of track on railways is not made by the driver, but is controlled by the signal box. Course keeping is not the task of the vehicle

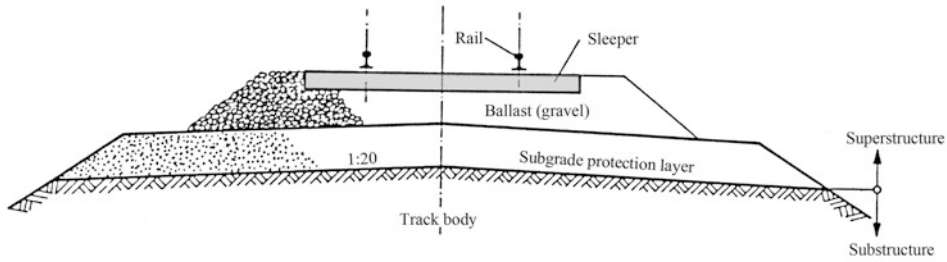

Fig. 1.14 Ballasted track with transverse sleepers. (After [43])

driver (called "train driver" on the railway), but is taken over by the track guidance by wheelset and track.

Figure 1.14 first shows a section through the (classic) railway superstructure with ballast bedding. The railway body is referred to as the substructure. The formation protection layer is the lower part of the superstructure and serves to drain it. On top of this is the ballast. It ensures the elasticity of the superstructure, i.e. the ballast has spring and damping properties. The ballast accommodates the (cross-)sleepers on which the rails are fastened by means of the so-called small iron (shims, screws or spring clips). Together, sleepers and rails form the track grid. Rails, sleepers and ballast ensure high lateral stability of the track and distribute the wheel loads over a larger area in the direction of the track body.

In curves, vertical ties are often placed in the track bed at the sleeper ends to increase lateral stability. Since the rails in Germany today are usually welded end-to-end, the superstructure must absorb longitudinal compressive forces due to the thermal expansion of the rails at higher outside temperatures without the track grid buckling. At low temperatures, this results in corresponding tensile stresses.

The cross sleeper superstructure shown here has become the standard design worldwide. The sleepers are mostly made of wood or concrete; steel sleepers are used less frequently. Due to the necessary impregnation of the wooden sleepers, which is hazardous to health and the environment, they are replaced by concrete sleepers. Since many different sleeper dimensions are required for turnouts, wooden sleepers were still used here. In the meantime, plastic sleepers are used for switches, but also on the track. Track-laying machines are used to align the track and compact the ballast under the sleepers. On DB's new lines, the so-called "slab track" is also used. Here, the concrete sleepers are cast into a continuous concrete slab. Compared to ballasted track, the maintenance effort is lower, but the production costs are higher.

Figure 1.15a shows the ballast superstructure with concrete sleepers as used on DB main lines. Figure 1.15b shows the so-called Y-steel sleeper in ballast superstructure (Brocken line of the Harzer Schmalspurbahnen). The Y-sleeper consists of double-T profiles and is intended to increase the lateral displacement resistance of the track due to its Y shape. It was developed by Salzgitter AG and is also used on standard gauge lines.

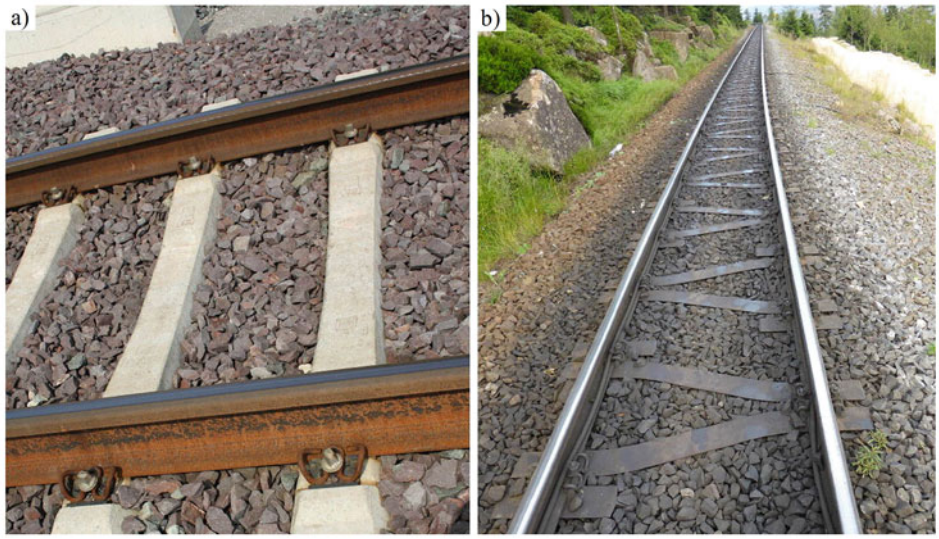

Fig. 1.15 Ballasted track with concrete sleepers (**a**) and Y-steel sleepers (**b**)

Figure 1.16 shows a wheelset. The two wheels are firmly connected to the wheelset shaft; i.e. wheels and wheelset shaft rotate at the same speed. In the wheelset design shown, the wheel consists of the wheel disc and the wheel tyre. As the latter is subject to wear on the tread and wheel flange (terms explained in Fig. 1.17), the wheel tyre profile is machined and reprofiled after a certain mileage. If a limit is reached in the wheel tyre thickness, the wheel must be re-tyred. The wheel disc and wheel tyre are connected by an interference fit and secured by a snap ring (see Fig. 1.16). The wheel tyres are fitted by heating them in a gas ring burner and sliding them onto the cold wheel disc. After cooling, the wheel tyre sits firmly on the wheel disc. In addition, the connection is then secured by the rolled-in snap ring.

Since centrifugal force causes the wheel tyre to expand at high speeds in high-speed traffic, there is a risk that the pressure between the wheel tyre and wheel disc will be lost, causing the wheel tyre to loosen. For this reason, vehicles for high-speed traffic use solid wheels in which the wheel disc and wheel tyre are made in one piece. If the wheel profile is worn, the entire wheel must be replaced. To remove the wheels, a hydraulic hose can be connected to the front of the steering knuckle. By means of an existing bore in the wheelset shaft up to the hub, the wheel bore can be expanded hydraulically and the wheel can be pulled off mechanically.

If trams run on rails in the road surface, structure-borne noise can be transmitted into buildings. To reduce structure-borne noise, wheels for tram vehicles are often designed as rubber-sprung wheels, Fig. 1.18. This reduces the natural frequency of the wheel tyre; the material damping of the rubber reduces vibration amplitudes. However, the rolling

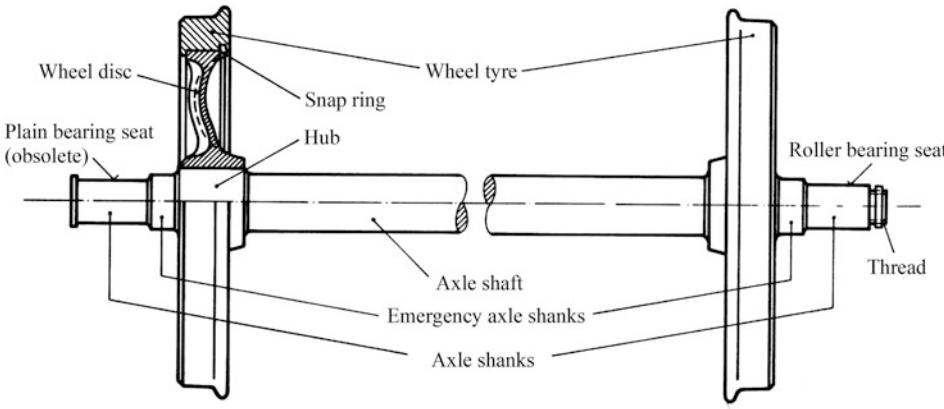

Fig. 1.16 Railway wheelset. (According to [43])

resistance of the wheel increases. Figure 1.18 shows on the right a tram bogie with inner bearings of the wheelsets (TATRA design).

The characteristic feature of railways is the interaction between wheelset and track. Therefore, the dimensions of the wheels and wheelsets must be matched to the dimensions of the track. The distance between the two rails of a track is called track gauge, see also Fig. 1.19.

> In Germany, the track gauge is the clear distance between the rail heads, measured perpendicular to the track axis 14 mm below the top of the rail [§5 EBO].

Tracks of different gauges are[12] in use worldwide, Fig. 1.20. This is mainly for historical reasons. The standard gauge is considered to be 1435 mm, which goes back to the English measurement of 4′ 8 1/2″. Smaller gauges are called narrow gauge, larger ones broad gauge. The most important gauges worldwide are 1670 mm (about 5% of the world railway network), 1600 mm (1%), 1520 mm (11%), 1435 mm (65%), 1067 mm (7%), 1000 mm (7%) and 750/760 mm (1%). The choice of gauge was partly made for strategic military reasons (e.g. Spain: broad gauge, France: standard gauge), but also to save on investment costs (narrow gauge).

The track gauge, i.e. the distance between the rail heads, is specified as 1435 mm. On the wheelset, the distance between the flanges is measured 10 mm below the line joining the flanges. This distance must be at least 1410 mm and must not exceed 1426 mm. The tolerance allows a certain amount of wear on the wheel flanges until re-profiling of the wheel tyres is necessary. There is therefore a difference of 9–25 mm between the track gauge and the wheelset flange distance, depending on wheel tyre wear, and more in the case

[12] Metzeltin, G.H.: Die Spurweiten der Eisenbahnen. Deutsche Gesellschaft für Eisenbahngeschichte e. V., Karlsruhe (1974).

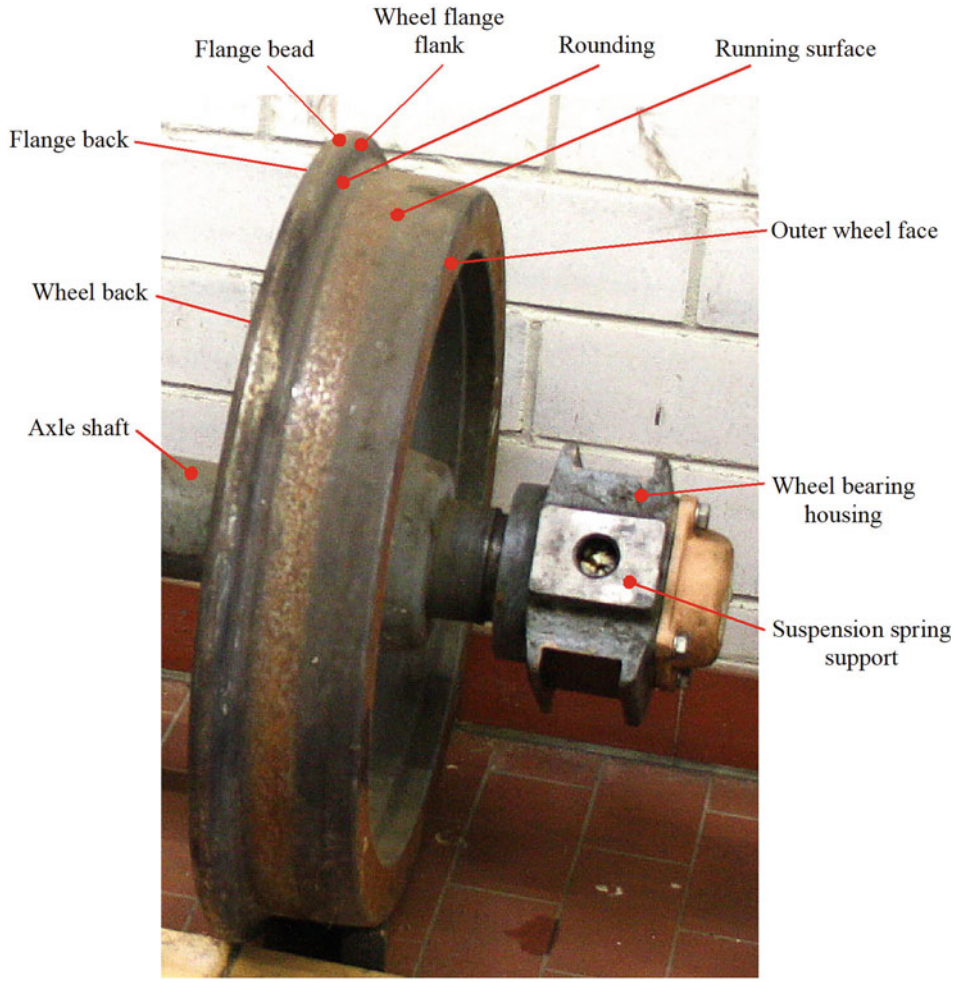

Fig. 1.17 Markings on the wheelset and wheel tyre profile

of rail wear. This is the so-called track play, which the wheelset can use in its transverse movement in the track.

The choice of gauge for a railway line was often random. As long as no connection to foreign railways was planned, an individual gauge was not a problem. An example of disadvantages in choosing an unusual gauge is the tramway in Braunschweig with 1100 mm. This gauge is now unique in the world. The tramway was financed by an English company; possibly this was a reason for the choice of gauge (3′ 7″ engl. = 1105 mm). Or was 3′ 1/2″ Pruss. = 1098.5 mm the basis? All vehicle procurements by the Braunschweig tramway involve a great deal of engineering effort due to this gauge, as standard running gear cannot be used. Also, the transition of tram cars as “Regio-Tram”

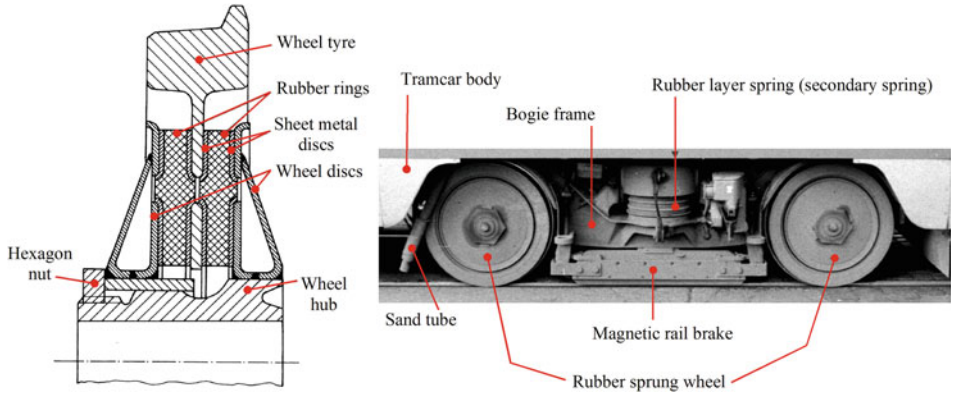

Fig. 1.18 Rubber sprung tram wheel (according to [53]) and installation in bogie

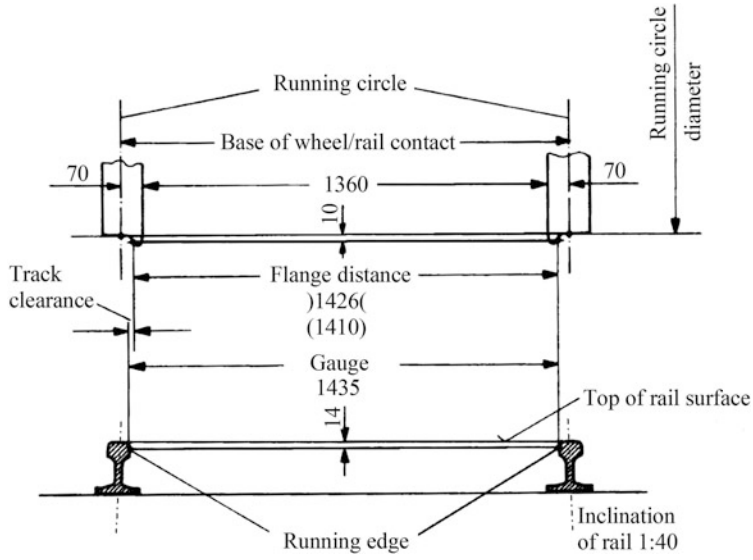

Fig. 1.19 Dimensions of track and wheelset for standard gauge. (According to [43])

into the standard gauge network of the DB as in Chemnitz, Karlsruhe, Kassel and Saarbrücken is not possible in Braunschweig.

Since at switches (Fig. 1.21) and crossings a back flank guidance of the wheelset by so-called check rails in the area of the frogs is necessary, the value 1360 mm applies as dimension for the distance of the wheel backs. In Fig. 1.21, the back flank guidance can be seen in the right part of the picture by the wear marks on the check rail at the front of the picture.

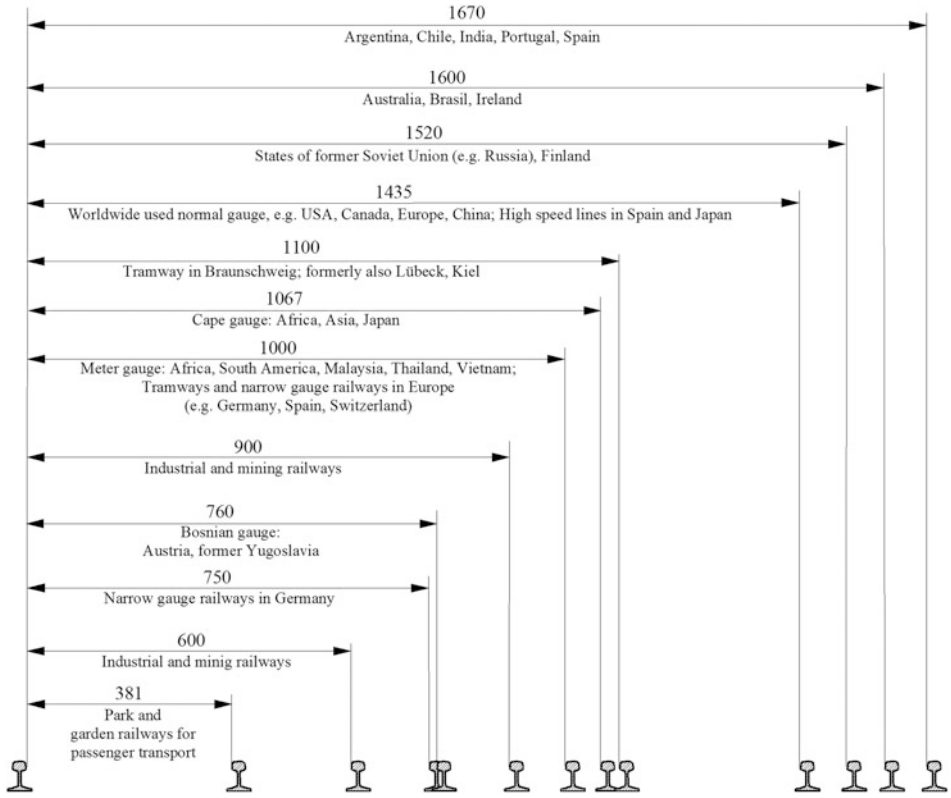

Fig. 1.20 Important track gauges of railways

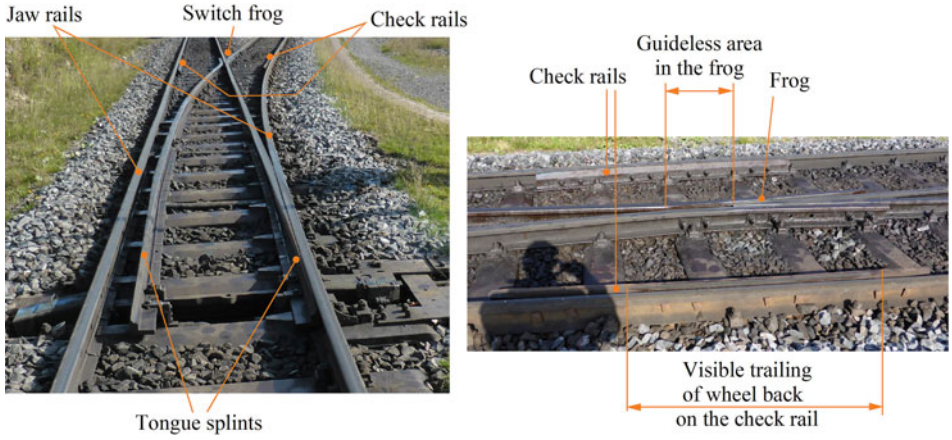

Fig. 1.21 Components of a switch (right turnout)

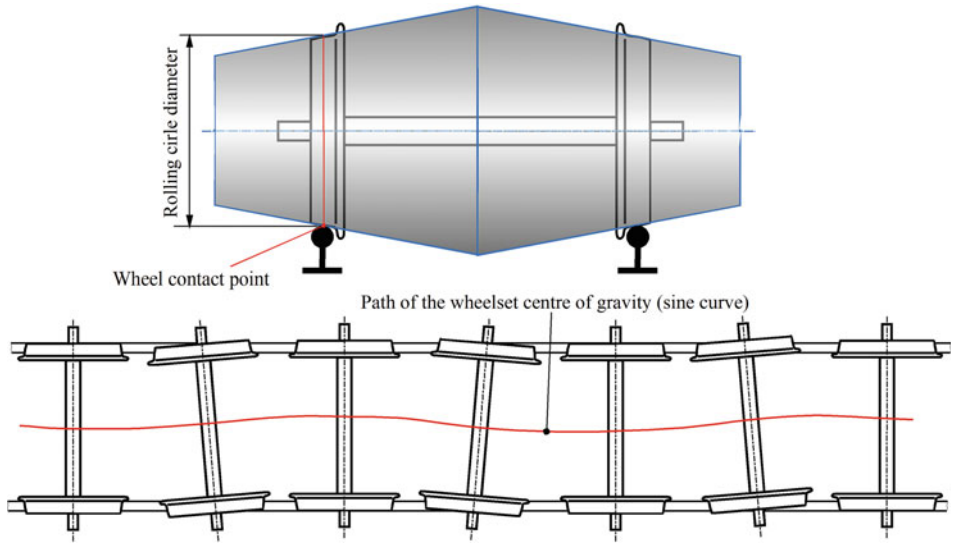

Fig. 1.22 Wheelset as a double cone; formation of the sine or rolling motion

To ensure that the wheelset is centred in the track and does not constantly touch the rail flank with a wheel flange, wheel profiles are tapered (this is dealt with in more detail in Chap. 5), Fig. 1.22. This is also intended to enable steering of the wheelset in the track curve, as the outer wheel on the curve rolls on a larger diameter than the inner wheel on the curve. Both wheels have the same angular velocity due to the torsionally rigid connection with the wheelset shaft.

The wheelset therefore behaves like a rolling double cone when it is deflected from the track centre within the scope of the track clearance: It then rolls on one side on a larger rolling circle diameter, thus deflecting back to the track centre, rolls on the opposite side on a larger rolling circle diameter, deflecting back to the center, etc. The resulting form of motion of an untethered[13] wheelset is called sine run, wave run, or wobble run. The term "Klingel run" after JOHANNES KLINGEL,[14] who provided a mathematical derivation of the path curve in 1883, is also used. We will deal with this inherent motion of the wheelset in detail in Chap. 5.

The rails are also part of the track technology. In the case of transverse sleeper superstructures, they are subjected to bending (and shear) by the wheelset loads, to surface pressure in the wheel contact surfaces[15] and to tension or compression by thermal

[13] I.e. not coupled to a vehicle via springs and dampers.

[14] Johannes Klingel (1819–1888), senior civil engineer at the Baden State Railway.

[15] The wheel contact area of a rail vehicle wheel is about the size of a 2-cent EURO coin with a wheel load of up to 12.5 t in Europe. This surface is used to transmit braking and tracking forces and, in the case of traction units, also drive forces.

expansion. The rail profiles used by DB are shown in Fig. 1.23.

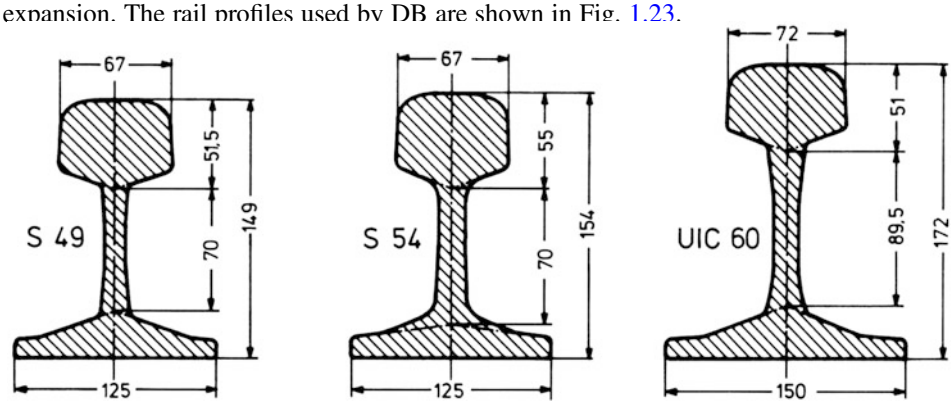

Fig. 1.23 Rail profiles used by DB. (According to [43])

The designation of the rails is derived from the specific mass (S 54: rail with approx. 54 kg/m). On branch lines and in sidings, the S 49 rail is still fitted; main lines and station tracks are fitted with S 54 rails, which are compatible with S 49 rails without changing the rail plates on the sleepers due to their foot and rail head width. On heavily loaded lines with high wheel loads and high speeds, the UIC[16] 60 profile is used. It requires different rail fastenings than S 49 and S 54 due to the larger foot width. In order to limit the deflection of the rails under the wheel loads, the second degree moment of area I_x about the horizontal axis is large. In contrast, the second degree moment of area I_y about the vertical axis is significantly lower. As a result, the rails can be laid well in the curve radius of the track. Rails are produced in lengths of 120 m, for example, and transported to the installation site loaded on several flat freight cars. In the process, they adapt to the curvature of the track without the freight cars derailing.

The possible cross-sectional shape and size of vehicles is determined, among other things, by the clearance gauge, the so-called standard clearance (in Germany according to §9 EBO) Fig. 1.24. This space is kept clear of parts of buildings, signals and overhead line masts around the centre of the track. The standard clearance is not to be confused with the vehicle boundary profile.

> The standard clearance is the envelope of the space to be kept clear which is necessary for the passage of rail vehicles and railway operational purposes. It is composed of the boundary line of fixed installations and the additional safety spaces required. The fixed installations must be located outside this line [37].

For the vehicle boundary profile, for example, the vehicle length (curve overhang) as well as transverse and roll spring travel, among other things, must be taken into account. For

[16] UIC: Union International des Chemins de Fer – International Union of Railways, headquarters: Paris.

	S 49	S 54	UIC 60
Cross section A	6297 mm^2	6948 mm^2	7686 mm^2
Spec. mass m'	49.43 kg/m	54.54 kg/m	60.34 kg/m
Moment of area I_x	1819 cm^4	2073 cm^4	3055 cm^4
Moment of area I_y	320 cm^4	262 cm^4	336 cm^4
Section modulus W_x	240 cm^3	262 cm^3	336 cm^3
Section modulus W_y	51 cm^3	57 cm^3	68 cm^3

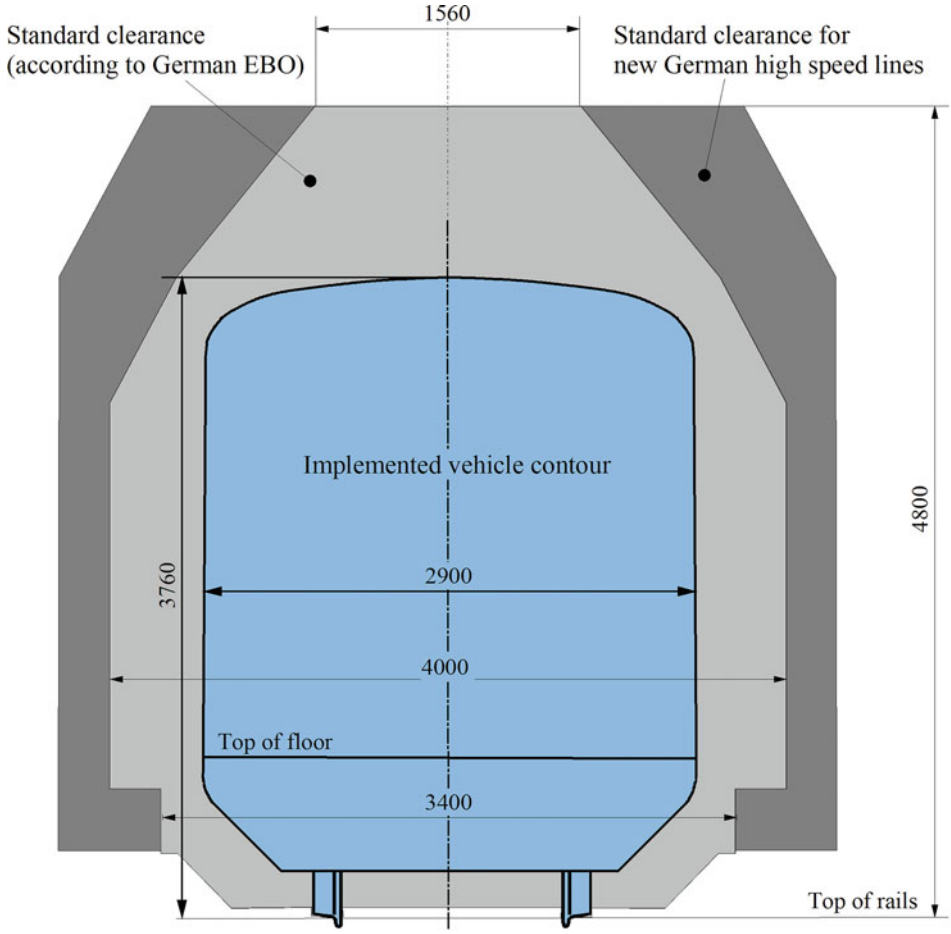

Fig. 1.24 Standard clearance according to § 9 EBO (simplified) and vehicle cross-section

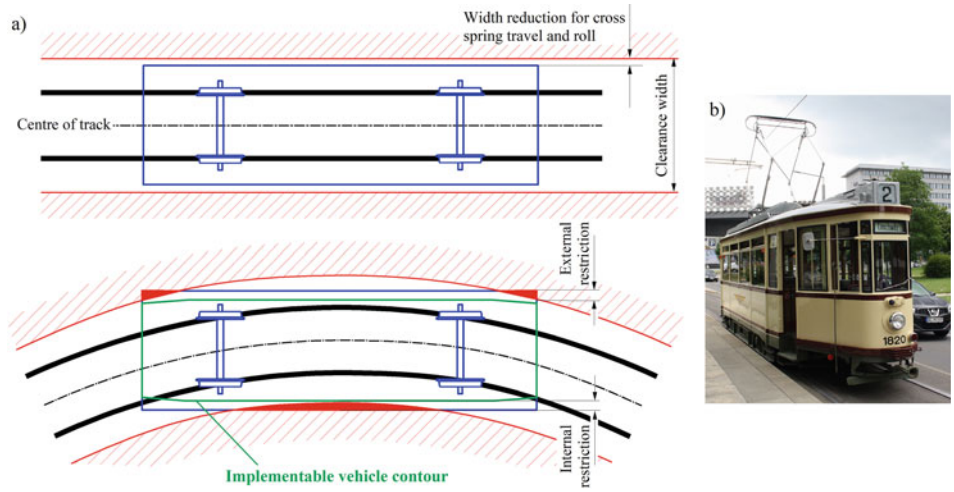

Fig. 1.25 (**a**) Restriction of vehicle width in track curves, (**b**) Older two-axle tram railcar with severe external restriction

vehicles with tilting technology, for example, the vehicle width decreases considerably due to the possible roll angle towards the roof. The vehicle outline profile is determined for each vehicle type by a restriction calculation[17] (see Fig. 1.25). It is always smaller than the loading gauge. Nevertheless, mainline vehicles are usually wider than road vehicles, for which 2550 mm is permissible according to StVZO.[18]

In older two-axle tramcars, a short wheelbase was usually chosen, often around 3000 mm, because of the curve running properties. With an overall vehicle length of 10,000 mm, this results in large front and rear transitions, so that the ends of the car bodies had to be very strongly retracted, Fig. 1.25b.

On DB's new lines, a larger (wider) profile was implemented compared to the standard clearance gauge, e.g. in order to limit the pressure surges occurring during train encounters and tunnel entrances and exits. Due to the height of the overhead contact lines on the rest of the network, the height of the profile has not been changed so that electric traction units can be used freely on the old and new line network.

In other countries, other standard clearance profiles are implemented: Great Britain has a significantly smaller clearance, so that normal continental European vehicles cannot run in Great Britain. Special multiple-unit trains are used for traffic, e.g. Paris-London through the Channel Tunnel. The Channel Tunnel itself has a larger clearance profile for the transport of lorries on railway wagons. However, the rail vehicles used for this purpose can only run between Dover and Calais. In Switzerland, due to the numerous tunnels, the standard

[17] The restriction calculation is carried out according to UIC guideline 505.

[18] StVZO: Road Traffic Licensing Regulations in Germany.

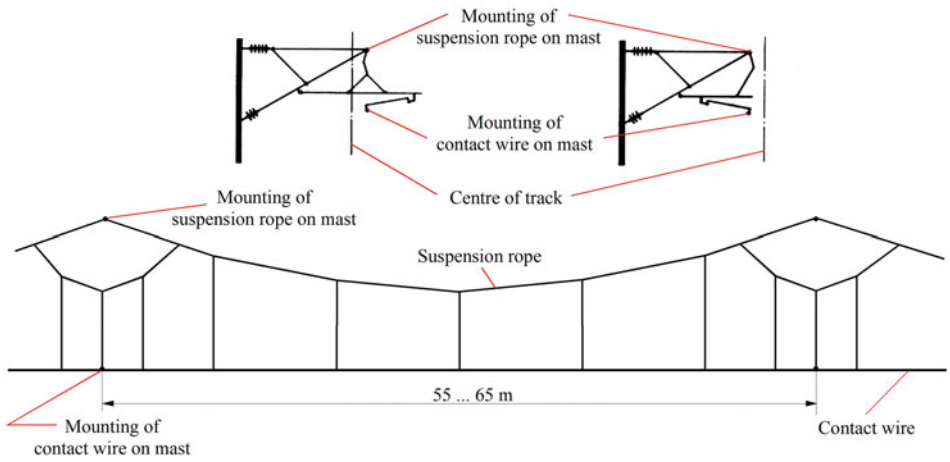

Fig. 1.26 Constructive design of a DB overhead contact line for 250 km/h speed: (**a**) masts with long and short cantilever, (**b**) side view. (According to [43])

clearance is narrower at the top, which means narrower pantographs.[19] In the USA, the standard clearance is generally much wider and higher, so that three-storey car transport wagons can be used, for example. On some lines, containers can be transported double-decker.

For the power supply of electric traction units, overhead contact lines[20] are mainly used on mainline railways. Figure 1.26 shows the design of a DB overhead contact line for 250 km/h. The contact wire and supporting rope are laid in a zigzag pattern, with a catenary mast with a long cantilever following a mast with a short cantilever. This ensures even wear of the collector contact strips. The collector strips as a wearing part are made of electric carbon.

The suspension rope and contact wire are tensioned via weights on catenary masts so that the pantograph maintains a permanently secure contact with the catenary. The contact wire should not sag like a clothesline. After all, currents of about 500 A must flow over the contact between the contact wire and the carbon contact strip for a locomotive with approx. 7500 kW power and 15,000 V voltage. Despite the lower power, the currents are similarly high on trams due to the lower catenary voltages (between 500 and 750 V). Current collectors for the power car of the ICE-1 (DB series 401) as well as for the ICE-T (a tilting train) are shown in Fig. 1.27.

The pantograph of the ICE-T is mounted on a frame so that it can be moved sideways, since the pantograph has to be adjusted due to the track curve-dependent tilting device of the vehicle bodies in order not to lose contact with the overhead line.

[19] DB traction units for transport to Switzerland are therefore equipped with additional narrower pantographs.

[20] In the UK, some lines in southern England, e.g. the Dover-London line, are electrified with contact rail.

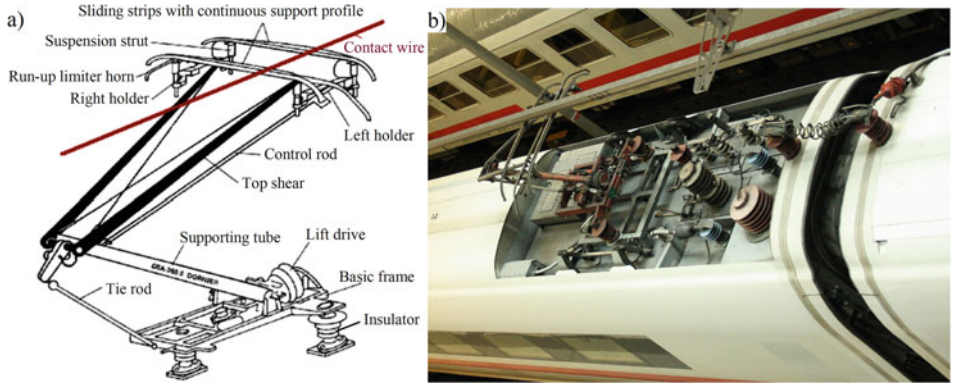

Fig. 1.27 (**a**) Current collector of the ICE-1 [10], (**b**) Current collector of the ICE-T (*right*)

For trams, which usually only reach maximum speeds of 70 km/h, single overhead contact lines without a suspension rope are often used. The catenary is also laid in a zigzag pattern.

In order to keep the tunnel cross-section small on metros and underground railways with long tunnel sections, conductor rails are installed instead of overhead lines, Fig. 1.28. On the "small profile sections" of the Berlin underground,[21] the conductor rail is swept from above (Fig. 1.28, left). On the Berlin "large profile lines", on the Berlin metro and on the Hamburg underground, the pantograph brushes the conductor rail from below (better protection against touch by persons!). On the Hamburg metro, the current collector is guided to the side of the conductor rail. Due to the larger cross-section of the conductor rail compared to an overhead contact line, the voltage drop is lower and fewer feed points or substations are required for the power supply. On the other hand, the design of the conductor rails at points and crossings is complicated, Fig. 1.29, top left.

At the end of this introductory chapter, the importance of the railways in Germany will be briefly presented. Figure 1.30 shows the share of rail in passenger transport ("modal split"), Fig. 1.31 in freight transport.

The total passenger transport performance in 2012 (passengers transported multiplied by travel distance) was 1068 billion passenger-kilometres (pkm). The share of the railway was 88.4 billion pkm.

Freight transport performance in 2013 amounted to around 645 billion tkm (freight weight transported multiplied by transport distance); the railways thus accounted for around 109 billion tkm. Road transport dominates in both passenger and freight transport. Apart from the transport costs, this is also due to the network access of rail and road and the length of the available route network (rail: 37,900 km, of which DB AG: 33,500 km; roads

[21] The older underground lines in Berlin (lines U1 to U4) have a smaller loading gauge than the later built lines U5 to U9; the vehicles are not compatible. In Berlin, Hamburg and Munich metro and underground are separated networks.

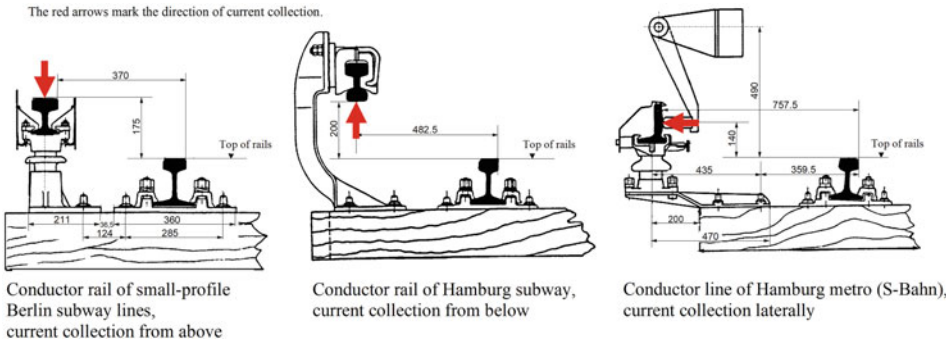

Fig. 1.28 Conductor rail systems. (According to [19])

interurban: 230,000 km, of which motorways: 12,880 km). Due to political decisions, many localities have lost their passenger stations and stops. In addition, due to line closures, many freight customers no longer have a siding.

Important markets and manufacturers worldwide for passenger rail vehicles are shown in Fig. 1.32. The largest market for passenger rail vehicles is in China.[22] The largest manufacturers are also located there. The two most important Chinese rail vehicle manufacturers, CNR and CSR, merged in June 2015 to form CRRC (China Railway Rolling Stock Corporation). As a result, the gap with the rest of the companies in the global market has become huge. The Chinese state-owned company is targeting rolling stock markets in North and South America, Africa, Asia and Australia. There are still a number of hurdles to market entry in Europe, including the complex approval procedures for rolling stock.[23]

Five of the ten (nine) largest manufacturers in Fig. 1.32 (Alstom, Bombardier, Siemens, Stadler, CRRC) operate plants in Germany. Alstom took over the Bombardier railway activities in 2020. In 2017, the rail industry in Germany employed about 50,200 people.

[22] The Chinese railway network alone has grown from approx. 40,000 km to over 70,000 km in the last 30 years. In addition, there has been a considerable expansion of subway networks and the construction of new tram systems.

[23] Hinrichs, L.: China Corp. Unlimited. Privatbahn Magazin (2015) H. 5, pp. 16–19.

Small-profile Berlin subway lines: current collection from above

Berlin metro (S-Bahn) and Berlin large-profile subway lines: current collection from below

Hamburg metro (S-Bahn): current collection laterally

Fig. 1.29 Conductor rail systems and current collectors

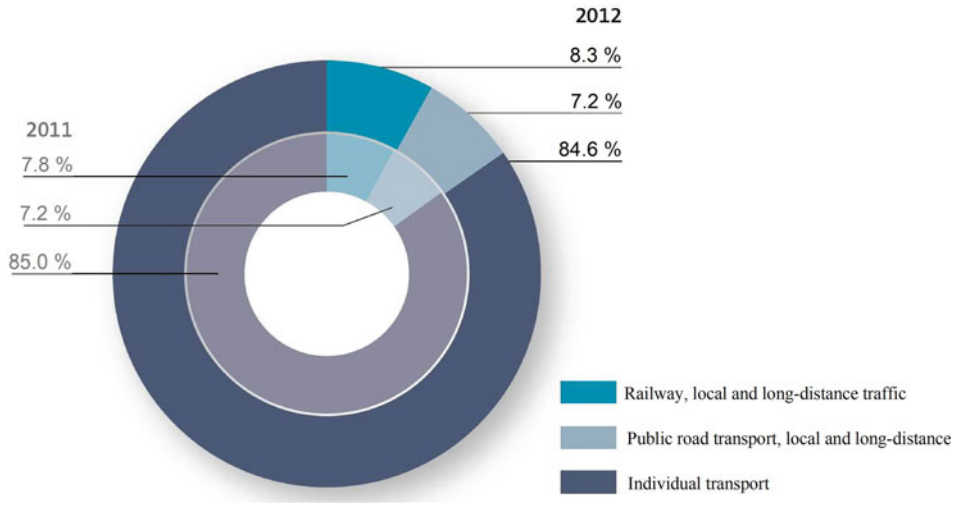

Fig. 1.30 Modal split in passenger transport in the Federal Republic of Germany. [62]

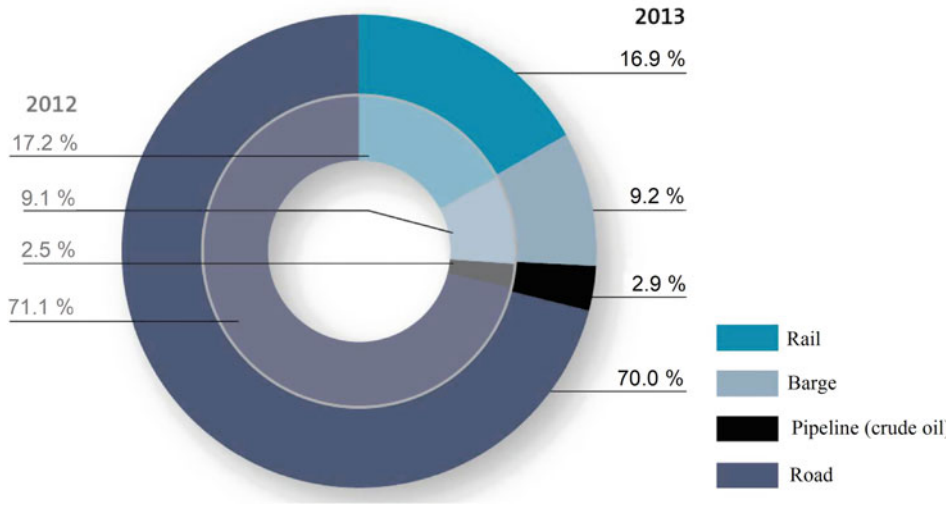

Fig. 1.31 Modal split in freight transport in the Federal Republic of Germany. [62]

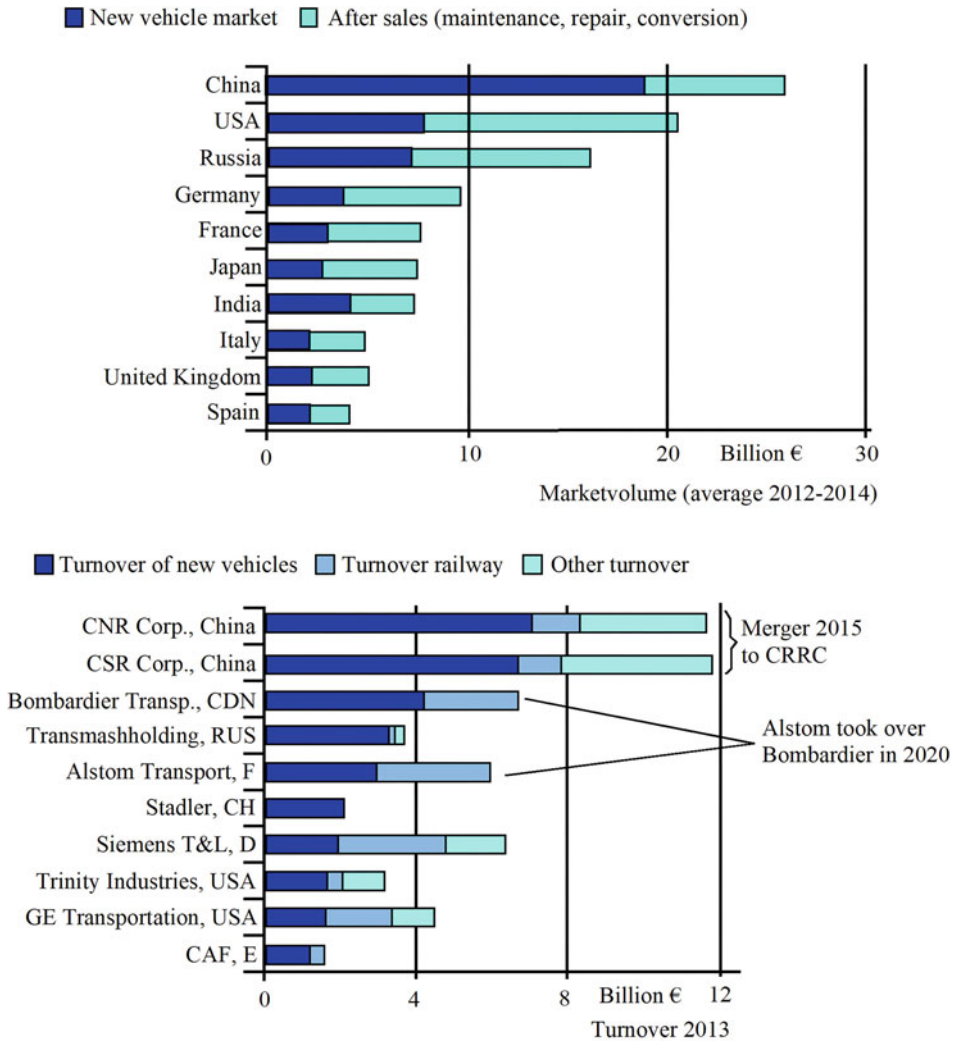

Fig. 1.32 Market volume for passenger rail vehicles (local and long-distance) and manufacturers. (Leenen, M.; Wolf, A.: Urban transport will determine growth over the next 5 years. Privatbahn Magazin (2014) H. 5, p. 95/96)

Running Resistances of Rail Vehicles

2

Like all land vehicles, rail vehicles also have running resistances. These are forces that oppose the movement of the vehicle and must be overcome by driving forces (tractive forces) if movement is to take place. The road vehicle and the rail vehicle have largely the same resistance components. Only the impact resistance does not exist in road vehicles. However, the magnitude of the resistance forces is different. Figure 2.1 shows the total resistance of rail vehicles in its systematic composition.

The total resistance therefore consists of the running resistance at a certain speed ($v = \text{const}$) and the acceleration resistance. In the case of running resistance, a distinction is made between the running resistance of the vehicle and the line resistance. The latter results from the gradient resistance as well as the curvature resistance when driving on track curves. The running resistance consists of the air resistance and the additional resistance. In the case of rail vehicles, the additional resistance is the combined resistance of bearing friction and rolling resistance. In addition, there is the impact resistance resulting from the oscillatory movement of a rail vehicle transverse to the direction of travel. Whereas in the case of road vehicles the drag of the nose and tail and the air friction on the roof, sides and underside are combined in the drag coefficient, in the case of rail vehicles the drag is separated into that of the nose and the tail and that of the train surface. This makes sense because rail vehicles operate less as individual vehicles than as a train. The nose and tail drag occurs at the first and last vehicle of a train set, while the vehicles in between essentially only contribute to the surface friction.

For the movement of a (rail) vehicle applies:

© The Author(s), under exclusive license to Springer Fachmedien Wiesbaden GmbH, part of Springer Nature 2022

J. Ihme, *Rail Vehicle Technology*,
https://doi.org/10.1007/978-3-658-36969-9_2

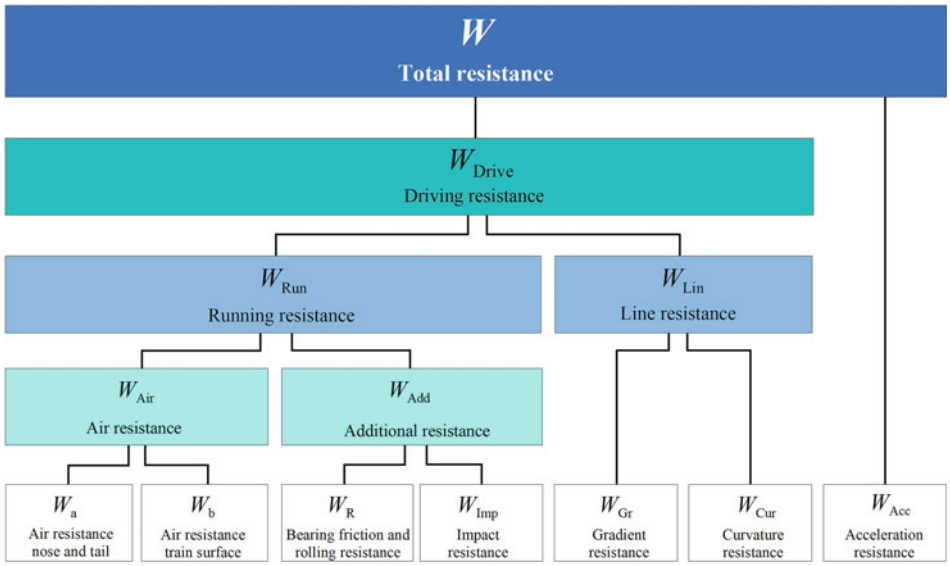

Fig. 2.1 Composition of the total resistance of rail vehicles. (According to [43])

$$Z = \sum W, \qquad \text{Tractive force} = \text{sum of the resistive forces.} \tag{2.1}$$

The further explanations of the total resistance are based on the study of a high-speed railway in Germany [49]. The calculation of the total resistance is carried out according to the so-called "synthetic formula". Here, the total resistance is composed of individual components as shown in Fig. 2.1. According to the formulas presented in this chapter, the power to be installed for a given driving program can be determined for the design of rail vehicles, for example. In practice, it is common to verify the running resistance experimentally for specific vehicles or vehicle units, e.g. from run-out tests.

2.1 Running Resistance

We first look at the running resistance of the vehicle. In general, the running resistance is made up of three components. The first is constant, the second is linearly dependent on the driving speed and the third increases with the square of the driving speed:

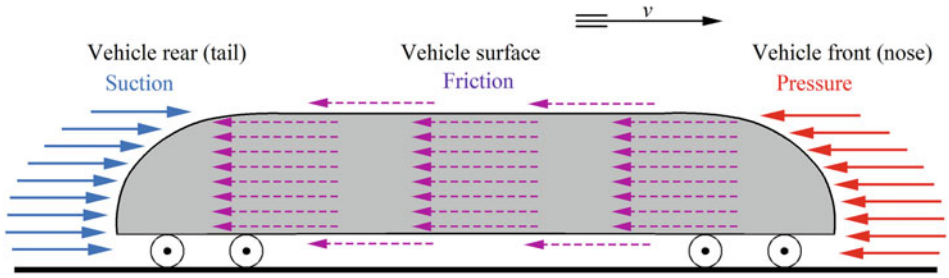

Fig. 2.2 Air resistance from pressure, friction and suction forces

$$W_{\text{Run}} = c' + c'' \cdot v + c''' \cdot v^2 \quad [\text{N}] \tag{2.2}$$

with:

W_{Run}:	Running resistance,
v:	Driving speed in [km/h],
c', c'', c''':	Constant coefficients.

2.2 Air Resistance

The air resistance W_{air} results from the air resistances of nose and tail as well as the train surface according to Fig. 2.1. In front of the nose surface of a train there is an overpressure, at the tail there is a suction. In between, the air resistance is determined by the air friction on the train surface (sideways, above and below), see Fig. 2.2.

The air resistance W_{a} of nose and tail is calculated as follows:

$$W_{\text{a}} = (c_1 + c_2) \cdot A_1 \cdot q \quad [\text{N}], \tag{2.3}$$

c_1:	Coefficient for air resistance nose [–],
c_2:	Coefficient for air resistance tail [–],
A_1:	Vehicle cross-sectional area including pantograph [m^2], see Fig. 2.3,
q:	Dynamic pressure [N/m^2].

For the dynamic pressure you get:

$$q = \frac{\rho}{2} v^2. \tag{2.4}$$

In railway engineering, the speed v is usually used in km/h. In addition, a headwind surcharge of $v_W = 15$ km/h is taken into account. This results in for the dynamic pressure:

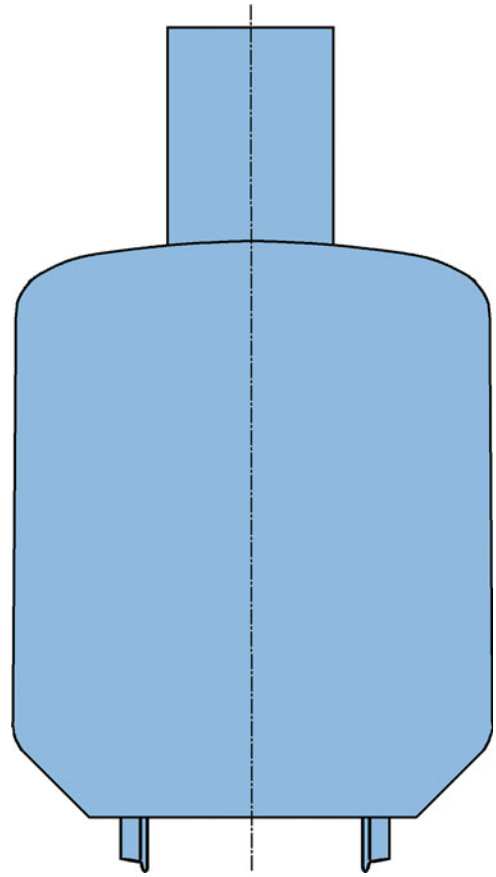

Fig. 2.3 Cross-sectional area A_1 (transverse clamping area) of a rail vehicle with pantograph

$$q = \frac{\rho \cdot (v + 15)^2}{2 \cdot 3.6^2} = 0.048(v + 15)^2 \tag{2.5}$$

with

ρ: Air density; $\rho \approx 1.25$ [Ns^2/m^4],
v: Driving speed in [km/h].

The coefficients c_1 and c_2 depend on the shape of the vehicles (corresponding to the c_W value for motor vehicles).

Air resistance also includes air friction at the train surface (W_b in Fig. 2.1):

$$W_b = (c_3 + c_4 + c_5 + c_6 + c_7) \cdot A_2 \cdot q, \tag{2.6}$$

A_2: Train surface [m^2],
q: Dynamic pressure according to Eq. 2.5,

c_3: Coefficient for air resistance of the train surface as a cylindrical body, see Eq. 2.7,
$c_4 = 0.0004$ Coefficient for angular train cross section,
$c_5 = 0.0002$ Coefficient for technical roughness of the train surface,
$c_6 = 0.0020$ Coefficient for ground effect between train and track,
$c_7 = 0.0005$ Coefficient for separating joints between the train members as well as for running gear and protruding parts.

The coefficient c_3 is calculated according to the PRANDTL-SCHLICHTING[1] resistance law for cylindrical bodies:

$$c_3 = \frac{0.455}{(\log Re)^{2.58}}, \tag{2.7}$$

Re: REYNOLDS number; $Re = 1.9 \cdot 10^4 \cdot L \cdot v_m$ [–],
L: Train length [m],
v_m: Average driving speed [km/h]; $v_m \approx v_{max}/2$.

For the total air resistance you get:

$$W_{Air} = W_a + W_b. \tag{2.8}$$

2.3 Additional Resistance

The additional resistance (Fig. 2.1) consists of the bearing friction and rolling resistance as well as the impact resistance. The bearing friction and rolling resistance is proportional to the weight of the vehicle [46]:

$$W_R = f_R \cdot m \cdot g. \tag{2.9}$$

The rolling resistance results because the wheel contact force F_{GR} acts in front of the wheel centre due to the contact surface formation in the wheel contact area around the lever arm of the rolling friction e, Fig. 2.4.

Thus the rolling resistance force F_{WR} is calculated from the moment equilibrium:

[1] Ludwig Prandtl (1875–1953), German physicist and fluid engineer. Hermann Schlichting (1907–1982), German fluid mechanic, professor at the TU Braunschweig.

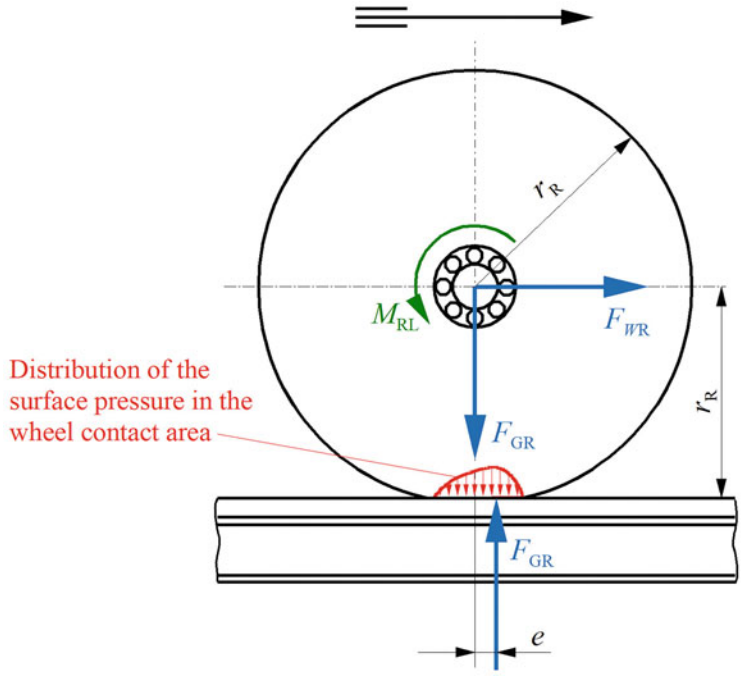

Fig. 2.4 Derivation of the rolling resistance

$$F_{WR} \cdot r_R = F_{GR} \cdot e. \tag{2.10}$$

In addition, the bearing frictional torque in the wheel or axle bearing is also included:

$$F_{WR} \cdot r_R = F_{GR} \cdot e + M_{RL}. \tag{2.11}$$

The bearing frictional torque results from the product of the bearing load F_{GR} and the bearing frictional coefficient μ_L:

$$M_{RL} = F_{GR} \cdot \mu_L. \tag{2.12}$$

Finally, you get for the rolling resistance force:

$$F_{WR} = \frac{F_{GR} \cdot e + M_{RL}}{r_R} = \frac{F_{GR} \cdot e + F_{GR} \cdot \mu_L}{r_R} = \frac{e + \mu_L}{r_R} F_{GR} = f_R \cdot F_{GR}.$$

Usually the rolling resistance coefficient is assumed to be the same for all wheels, so that one can write simplified (see above):

$$W_R = f_R \cdot m \cdot g.$$

The rolling resistance coefficient f_R for the steel wheel/steel rail pairing is about one power of ten smaller than for the road vehicle with the tyre/road surface pairing:

$$f_R = 0.001 \ldots 0.0015 \ldots 0.002 \text{ (Rail vehicle)},$$
$$f_R = 0.015 \ldots 0.03 \text{ (Road vehicle on asphalt or concrete roadway)},$$
$$f_R = 0.3 \text{ (Road vehicle on loose sand)}.$$

This is also due to the size of the contact surface and thus the size of the lever arm e in Fig. 2.4: While it is about the size of a 2€-cent coin in the steel wheel-steel rail pairing, it is about the size of a postcard in the tyre-road surface pairing.

In railway engineering, one usually calculates with the vehicle or train weight in t (in tonnes, although this is the unit of mass) and with the travel speed in km/h. This results in somewhat different formulas and coefficients than known from motor vehicle engineering. For the bearing friction and rolling resistance one then obtains:

$$W_R = f_R \cdot m \tag{2.13}$$

with

f_R: Rolling resistance coefficient; $f_R = 15$ [N/t],
m: Train mass in [t].

The rolling resistance is therefore assumed to be independent of the speed and proportional to the vehicle or train weight. The impact resistance is linearly dependent on the speed. It was determined experimentally from driving tests and combines all speed-dependent components of the running resistance. Physically, the impact resistance can be explained as follows: Rail vehicles are guided transversely by the track. For this reason, they also have transverse suspension and perform oscillations transverse to the axis of movement. The vibration energy comes from the forward movement of the vehicle.

$$W_{Imp} = c_d \cdot m \cdot v \tag{2.14}$$

with

m: Train mass in [t],
v: Driving speed in [km/h].

For the coefficient c_d there is the empirical value:

$$c_d \approx 0.025 \left[\frac{N}{t \cdot \frac{km}{h}} \right].$$

From Eqs. 2.8, 2.13 and 2.14 it finally follows for the running resistance:

$$W_{Run} = W_R + W_{Imp} + W_{Air}, \tag{2.15a}$$

$$W_{Run} = 15 \cdot m + 0.025 \cdot m \cdot v + [(c_1 + c_2) \cdot A_1 + (c_3 + 0.00031) \cdot A_2] \cdot 0.048 \cdot (v + 15)^2 \ \text{[N]}. \tag{2.15b}$$

2.4 Line Resistance

Next, we will now deal with the line resistance. According to Fig. 2.1, it is composed of the gradient resistance (Fig. 2.5) and the curvature resistance:

$$W_{Lin} = W_{Gr} + W_{Cur}. \tag{2.16}$$

Gradients for railway lines are limited by the EBO and are significantly lower than for roads: According to § 7 EBO, $s = 12.5‰$ applies to main lines, $s = 40‰$ to branch lines (s: gradient; 40‰ corresponds to 4%, i.e. there is a 4 m difference in height for every 100 m of length). For tramways, gradients of around 100‰ occur (e.g. in Würzburg).

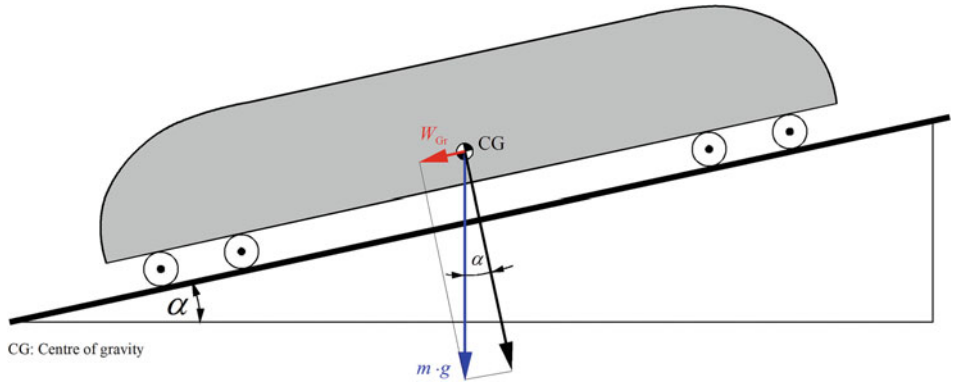

Fig. 2.5 Gradient resistance

$$W_{\mathrm{Gr}} = m \cdot g \cdot \sin\alpha \approx m \cdot g \cdot \tan\alpha \approx m \cdot g \cdot s \quad [\mathrm{N}] \tag{2.17}$$

with

m: Mass in [t],
s: Gradient (slope) in [‰].

The resistance to curvature for railway vehicles on standard gauge tracks is determined according to RÖCKL's[2] formulae found experimentally:

$$W_{\mathrm{Cur}} = m \cdot g \cdot \frac{650}{R - 55} \quad [\mathrm{N}] \quad \text{for R} < 300\ \text{m}, \tag{2.18a}$$

$$W_{\mathrm{Cur}} = m \cdot g \cdot \frac{500}{R - 30} \quad [\mathrm{N}] \quad \text{for R} \geq 300\text{m}, \tag{2.18b}$$

m: Mass in [t],
R: Radius of curve in [m].

For tram vehicles, which have to[3] pass through much smaller curve radii than railway vehicles, according to [66] on grooved rails:

$$W_{\mathrm{Cur}} = m \cdot g \cdot \frac{0.158 \cdot a + 0.033 \cdot s_{\mathrm{R}}}{R}, \tag{2.19}$$

a: Wheelset spacing in the vehicle or bogie in [m],
s_{R}: Wheelset pitch in [m]; equal to track gauge plus 0.05 m.

Thus, all components of the driving resistance are known when driving at constant speed.

2.5 Acceleration Resistance

When the driving speed is increased – in the acceleration state – the translational and rotational masses must be accelerated. For the acceleration resistance of the rotatory masses, the transmission ratio between the wheelset (circumferential speed ≈ driving speed) and the respective mass under consideration plays a role in addition to the rotating mass, the mass moment of inertia. The higher the transmission ratio to the mass to be accelerated and the greater the mass moment of inertia, the greater the acceleration torque. For simplification, one relates the rotatory masses to the translatory masses by the so-called

[2] Alois von Röckl (1822–1885), Lawyer, medic and engineer; Bavarian railway director.
[3] Some trams have curve radii down to 12 to 15 m.

torque mass surcharge factor λ [19, 43, 66]. Then one obtains for the acceleration resistance:

$$W_{\mathrm{Acc}} = 10^3 \cdot m \cdot b \cdot \lambda \quad [\mathrm{N}], \tag{2.20}$$

m: Mass of the train or vehicle in [t],
b: Acceleration in [m/s^2],
λ: Torque mass surcharge factor:

$\lambda \approx 1.15 \ldots 1.30$ for electric locomotives,
$\lambda \approx 1.20 \ldots 1.30$ for diesel locomotives,
$\lambda \approx 1.04$ for ICE-3,
$\lambda \approx 1.03 \ldots 1.10$ for carriages and freight wagons,
$\lambda \approx 1.06 \ldots 1.08$ for long locomotive-hauled trains,
$\lambda \approx 1.09 \ldots 1.11$ for short locomotive-hauled trains,
$\lambda \approx 1.15$ for empty freight trains,
$\lambda \approx 1.06$ for loaded freight trains.

The higher the proportion of rotational masses (traction units!) and the higher the rotational speed of rotational masses, the greater the torque mass surcharge factor. For vehicles with variable gear ratios between the engine and the drive wheels (diesel drive vehicles), the torque surcharge factor is higher for large gear ratios ("low gear") than for small gear ratios ("high gear"). A loaded vehicle has a lower torque mass surcarge factor than the same vehicle when unloaded, because the rotational masses are related to the translational mass. This finally allows us to specify the total resistance *W:*

$$W = W_{\mathrm{Run}} + W_{\mathrm{Lin}} + W_{\mathrm{Acc}}. \tag{2.21}$$

2.6 Air Resistance According to the Hanover Formula

In addition to the "Synthetic Formula" just discussed, the "Hanover Formula"[4] is also used to calculate air resistance. It is initially based on the equation also used for road vehicles [46]:

$$W_{\mathrm{Air}} = \frac{\rho}{2} \cdot c_{\mathrm{W}} \cdot A \cdot v^2, \tag{2.22}$$

c_{W}: Drag coefficient for angle of attack $\tau = 0$.

[4] Voß, G.; Gackenholz, L.; Wiebels, R.: A new formula (Hanover formula) to determine the air resistance of track-bound vehicles. Glasers Annalen-ZEV 96 (1972) H. 6, pp. 166–171.
The formula was developed by experiments at the Technical University of Hanover.

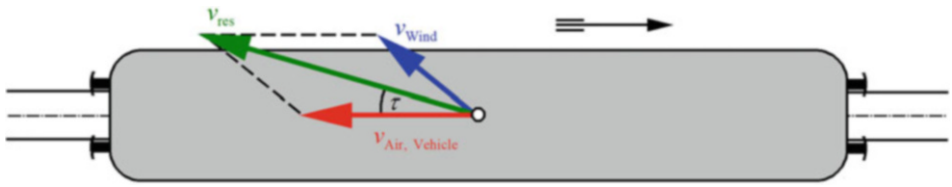

Fig. 2.6 Vehicle inflow in crosswind. $v_{\text{Air, Vehicle}}$ inflow velocity due to vehicle motion, v_{Wind} wind velocity, v_{res} resulting inflow velocity, τ inflow angle

As already shown, there are three components of air resistance in trains (see Fig. 2.2):

- Potential flow (pressure resistance at the front of the train),
- Boundary layer flow (air friction at the middle part of the train),
- Trailing flow (suction resistance at the end of the train).

Since trains can be put together in different ways, it is difficult to determine the total drag coefficient. On top of this, the angle of attack also plays a role. The angle of attack τ is the angle between the direction of travel and the vector of the resulting inflow velocity v_{res}, Fig. 2.6.

The drag coefficient c_{W} is divided among the vehicles of a train set, i.e. the locomotive, first wagon, middle wagons and last wagon. In addition, the drag coefficients are related to a standard area of $A_{\text{norm}} = 10\ \text{m}^2$. Deviations in the cross-sectional area of vehicles are thus taken into account via the c_{W} values. This gives the aerodynamic drag of a vehicle combination:

$$W_{\text{Air}} = \begin{bmatrix} c_{\text{W,L}} + c'_{\text{W,L}} + c_{\text{W,W1}} + c'_{\text{W,W1}} + (n-2) \cdot c_{\text{W,Wm}} \\ +(n-2) \cdot c'_{\text{W,Wm}} + c_{\text{W,Wn}} + c'_{\text{W,Wn}} \end{bmatrix} \cdot \frac{\rho}{2} \cdot A_{\text{standard}} \cdot v_{\text{res}}^2 \qquad (2.23)$$

with

A_{standard}:	Standardised reference cross-sectional area of a vehicle; $A_{\text{standard}} = 10\ \text{m}^2$,
$c_{\text{W,L}}$:	Drag coefficient of the locomotive,
$c_{\text{W,W1}}$:	Drag coefficient of the first wagon following the locomotive,
$c_{\text{W,Wm}}$:	Drag coefficient of a wagon in the middle,
$c_{\text{W,Wn}}$:	Drag coefficient of the last wagon,
c'_{W}:	Addition to the c_{W} value due to oblique flow ($\tau \neq 0$),
ρ:	Air density; $\rho \approx 1.25\ [\text{Ns}^2/\text{m}^4]$,
v_{res}:	Resulting inflow velocity,
n:	Number of wagons in the train set.

Relating the average values of to c'_W the average values of c_W,

$$K_W = \frac{\overline{c'_W}}{\overline{c_W}},$$

finally results for the air resistance of a vehicle convoy:

$$W_{Air} = [c_{W,L} + c_{W,W1} + (n-2) \cdot c_{W,Wm} + c_{W,Wn}] \cdot (1 + K_W) \cdot \frac{\rho}{2} \cdot A_{standard} \cdot v_{res}^2. \quad (2.24)$$

Examples of c_W values:

Electric 6-axled express locomotive class 103	$c_{W,L} = 0.26$
Intercity car as first car	$c_{W,W1} = 0.13$
Intercity car as second to (n – 1) car:	$c_{W,Wm} = 0.10$
Intercity car as the last car:	$c_{W,Wn} = 0.23$
Three car diesel powered multiple unit:	$c_W = 0.75$
Diesel locomotive with a center cab:	$c_{W,L} = 0{,}45$
Electric 6-axled freight locomotive class 151:	$c_{W,L} = 0.48$
Box freight car as the first wagon:	$c_{W,W1} = 0.30$
Box freight car as second to (n – 1) wagon:	$c_{W,W1} = 0.10$
Box freight car as the last wagon:	$c_{W,Wn} = 0.30$

2.7 Total Resistance and Wheel Power

The total resistance is calculated according to Fig. 2.1:

$$W = W_R + W_{Imp} + W_{Air} + W_{Gr} + W_{Cur} + W_{Acc} \quad (2.25)$$

Only in a few cases do all resistance components occur simultaneously. In order for a vehicle or vehicle combination to move, a tractive force must be applied:

$$Z = W \quad (2.26)$$

Neglecting the slip at the driving wheels, the wheel power can be determined from this:

$$P_R \approx Z \cdot v \quad (2.27)$$

To calculate the engine power, the efficiency η_{PT} of the power transmission must be taken into account:

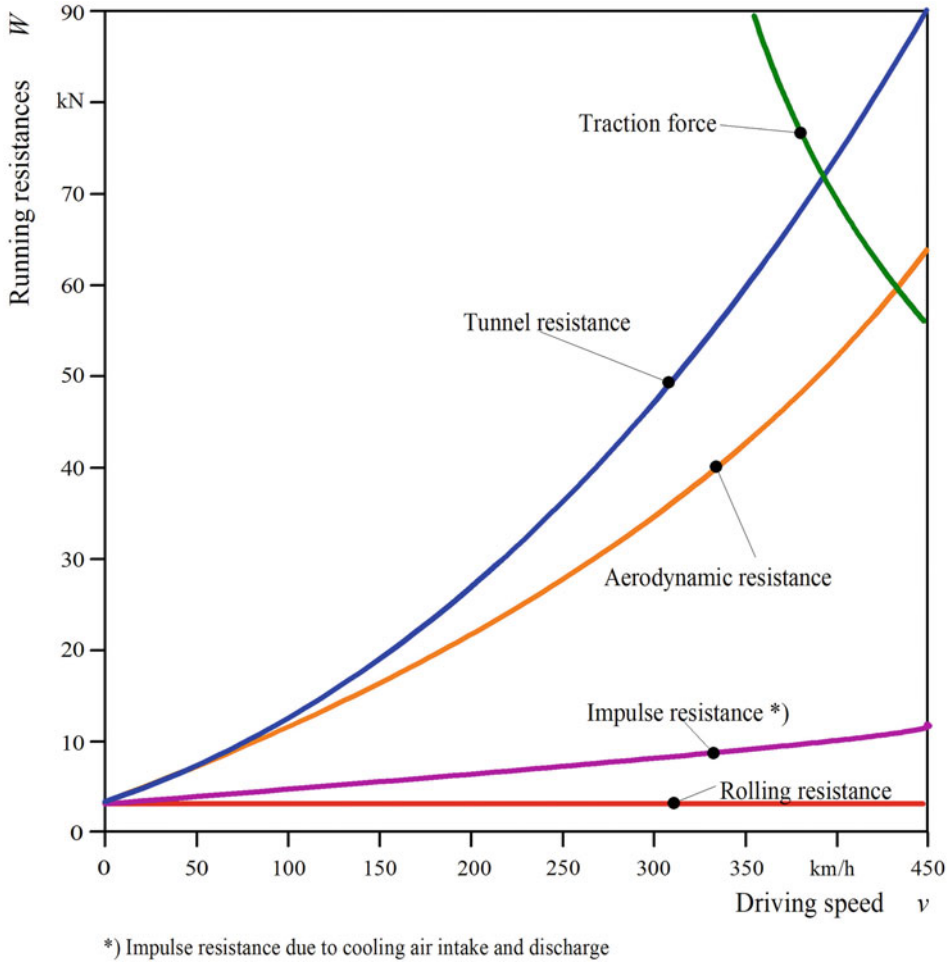

Fig. 2.7 Distribution of the driving resistances of the four-part ICE test vehicle. (Peters, J. L.: Determination of the aerodynamic resistance of the ICE/V in tunnel and on free track by run-out tests. ETR 39(1990) H. 9, pp. 559–564)

$$P_{\text{engine}} = \eta_{\text{PT}} \cdot P_{\text{R}} \tag{2.28}$$

Figure 2.7 shows the measured driving resistances for the four-car ICE test train. The air resistance (called "aerodynamic resistance" in Fig. 2.7) already outweighs the other resistance components at unaccelerated travel on the level from approx. 40 km/h onwards. Tunnel resistance is an additional factor when driving through tunnels. Despite the large tunnel cross-sections on the new DB lines, a vehicle in a tunnel acts like a piston in a cylinder and pushes a column of air in front of it.

The impulse resistance results from the cooling air intake and discharge, which takes place through ventilation grilles located on the side of the power car and thus perpendicular to the longitudinal inflow. The cooling of the traction motors, the transformers and the converters of the power cars is provided by electrically driven fans. No calculation formulas are available for the impulse resistance.

To get an idea of the necessary cooling power, one can read from Fig. 2.7 the driving resistance (orange line) at the intersection with the tractive force (green line) on the vertical axis of the diagram: approx. 58 kN. This intersection point belongs to the highest attainable driving speed (see Chap. 3 for this) of approx. $v_{max} \approx 430$ km/h ≈ 120 m/s. The power at v_{max} is therefore about $P \approx W \cdot v_{max} \approx 58{,}000\ \text{N} \cdot 120\ \text{m/s} = 6960$ kW, i.e. about 7 MW power at the driving wheels. If the efficiency of the traction motors is assumed to be $\eta \approx 0.94$, about 417 kW of power loss from the motors must be dissipated to the environment as heat. In addition, there is a similarly large power loss of the transformers and converters. Therefore, considerable cooling air flows are led to the outside via the ventilation grilles.

2.8 Examples and Tasks for Chap. 2

Example 2.1
In the past, so-called light railways were often used in sand pits and quarries, i.e. transport took place with trolleys (Fig. 2.8) on rails. In most cases, the trolleys were moved by muscle power. A loaded trolley has a mass of approx. 1200 kg.

Fig. 2.8 Trolleys for bulk materials

Fig. 2.9 Two-car diesel railcar LINT 54 (class 622)

Since the speed is low, only the bearing friction and rolling resistance occurs, which can be determined according to Eq. 2.9 with $f_R = 0.0015$: $W_R \approx 18$ N. This force for in-plane motion can be easily applied by a person pushing. Using carts on road surfaces, the force would be about 240 N for $f_{R,road} \approx 0.02$, which is what a person exerts when pushing. On loose sand, $f_{R,road} \approx 0.3$ and the rolling resistance is $W_R \approx 3600$ N. This is too much for a single person to handle.

Example 2.2
The diesel commuter railcar LINT 54 (Fig. 2.9) from ALSTOM has the following data:

Mass occupied with 75% stocks[5]:	$m = 125$ t
Drag coefficient:	$c_W = 0.33$

The driving resistances are determined as a function of the speed and the line gradient ($s_{max} = 40‰$).

We use Eq. 2.15a and calculate the aerodynamic drag according to Eq. 2.22, since the c_W value is available from tests for the two-piece vehicle.

Then, according to Eq. 2.17, for $s = 1, 2, 3, 4, 10$, and 40‰, we determine the gradient resistance (e.g.: $W_{Gr}(s = 10‰) = 12.5$ kN; $W_{St}(s = 40‰) = 50.0$ kN). The result is shown in Fig. 2.10. In order not to have to represent the vertical axis of Fig. 2.10 too large, only $s = 10‰$ was considered as the largest slope.

[5] In the case of rail vehicles, the vehicle mass is specified as 75% full storage containers – in the case of a diesel railcar, e.g. the supplies of diesel fuel and sand as well as water for the sanitary facilities .

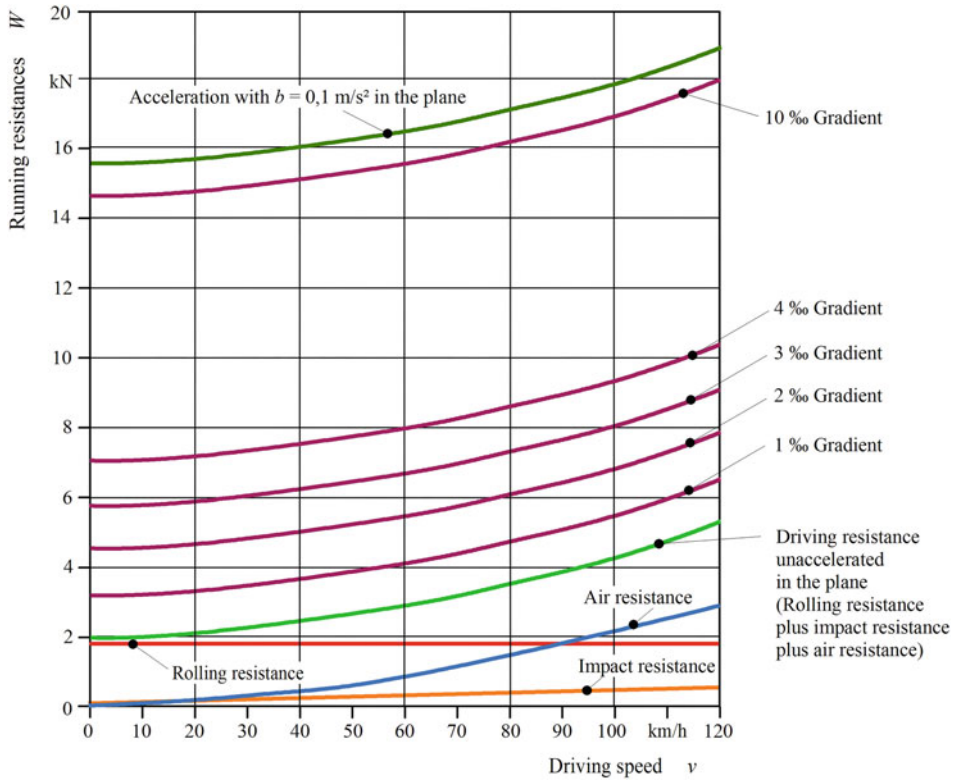

Fig. 2.10 Driving resistance lines for the two-car diesel multiple unit LINT 54

It can be seen that the acceleration capacity in particular determines the total resistance. For a required acceleration of e.g. $b = 1.75$ m/s^2 (estimated: $\lambda \approx 1.1$), the acceleration resistance for the vehicle under consideration is $W_{\mathrm{Acc}} = 240$ kN. This could just be achieved for the LINT 54 with six driven axles (axle load approx. 16 t) with dry rails ($\mu \approx 0.3$) as starting acceleration (see Chap. 3). The vehicle requires a wheel power of about 583 kW ($P_{\mathrm{R}} = W \cdot v$) on a gradient $s = 10‰$ at maximum speed $v_{\max} = 120$ km/h. However, the installed drive power is three times 335 kW (three drive units) to achieve high accelerations.

Task 2.1

(a) The running resistance of a freight train consisting of a class 151 electric locomotive and 60 two-axle sliding wall wagons is to be calculated. The train is supposed to run at a constant speed of 80 km/h. There is no wind.
(b) Determine the necessary power and energy consumption for a distance of 80 km.
(c) What energy would be required to transport the same payload by road truck?

Given: Mass of locomotive: 120 t; total mass per wagon: 40 t, of which payload 25 t
Mass of road truck: 40 t, of which payload 25 t; rolling resistance coefficient $f_R = 0.01$; $c_W \cdot A = 9\ m^2$

Result
The running resistance on level ground for the freight train (with air resistance according to the Hanover formula $W_{Air} \approx 21.24$ kN) is: $W_{Run,plane} \approx 102$ kN. The wheel power for this is $P_R \approx 2270$ kW, the energy consumption for 1 h travel at constant speed: $E_{Train} \approx 2270$ kWh.

To transport the same net load by truck, 60 trucks with trailers are required. Per truck with trailer the driving resistance $W_{Truck} \approx 6.8$ kN, the power $P_{Truck} \approx 151$ kW and the energy consumption $E_{Truck} \approx 151$ kWh. 60 trucks therefore require $E_{sum} \approx 9060$ kWh.

The ratio of energy consumption is therefore $E_{Truck}/E_{Train} \approx 4$. In order to transport 1500 t of load at the same speed, the energy consumption on the road is about four times higher than on the rail in this example.

Task 2.2
Determine the air resistance of the train from Task 2.1 for $v = 80$ km/h according to

(a) Hanover formula
(b) Synthetic formula

Given: Locomotive class 151: length over buffers 19,490 mm; length of body 18,200 mm,
Width 3129 mm, height 3570 mm
Wagon: length 14,020 mm; box length 12,780 mm; width 2676 mm, height 2290 mm

Result
According to the Hanover formula, the air resistance of the train is $W_{Air} \approx 21.24$ kN (see 2.1). According to the synthetic formula: $W_a \approx 2.4$ kN; $W_b \approx 11.55$ kN (with $A_2 \approx 7860\ m^2$; $Re = 6.54 \cdot 10^8$; $c_3 \approx 0.00166$), thus $W_{Air} \approx 13.95$ kN.

The Hanover formula provides a value that is approx. 50% larger than the synthetic formula. The reason is probably that the Hanover formula for freight trains takes into account the corresponding drag coefficients found experimentally, while the synthetic formula for high-speed trains with smoother vehicle surfaces was derived from flow theory. In this case, the Hanover formula probably provides the more realistic value.

Task 2.3

(a) What wheel power is required by a train set corresponding to ICE-1 at $v = 200$ km/h and a gradient of $s_{max} = 2‰$?
(b) What is the required wheel power at $v_{max} = 270$ km/h on level ground?

In both cases, the impact resistance must be taken into account!

Data: Train mass: $m = 792$ t
Rolling resistance coefficient: $f_R = 15$ N/t
Cross-sectional area: $A = 10$ m^2
Drag coefficient: $c_W = 0.95$
Air density: $\rho = 1.25$ kg/m^3 $= 1.25$ Ns^2/m^4

Result

(a) The wheel power is calculated according to Eq. 2.27. The tractive force required for this is calculated from the running resistance according to Eq. 2.15a plus the gradient resistance according to Eq. 2.17. The running resistance is made up of rolling, impact and air resistance.
Rolling resistance according to Eq. 2.13: $W_R = 11{,}880$ N
Impact resistance according to Eq. 2.14: $W_{Imp} = 3960$ N
Air resistance according to Eq. 2.22: $W_{Air} = 21.178$ N (consider headwind with 15 km/h!)
From this running resistance: $W_{Run} = 36.318$ N
Gradient resistance: $W_{Gr} = 158{,}400$ N
Required tensile force: $Z = W_{Run} + W_{Gr} = 194.718$ N ≈ 195 kN
Wheel power $P_R \approx 10.9$ MW (This power corresponds approximately to the installed power of an ICE-1.)
(b) At $v = 270$ km/h, impact and air resistance become greater compared to (a): $W_{Imp} = 5346$ N, $W_{Air} = 37{,}212$ N $\rightarrow Z \approx 55$ kN $\rightarrow$ wheel power $P_R \approx 4.1$ MW

Task 2.4
For an electric road vehicle with the given data are to be calculated:

(a) the wheel power at the intended maximum speed of $v_{max} = 120$ km/h $= 33.33$ m/s
(b) the wheel power for driving on a car park ramp with $s = 0.15$ (15%) and $v = 3$ m/s (10.8 km/h)
(c) Is the wheel power calculated in (b) provided by the electric motor?

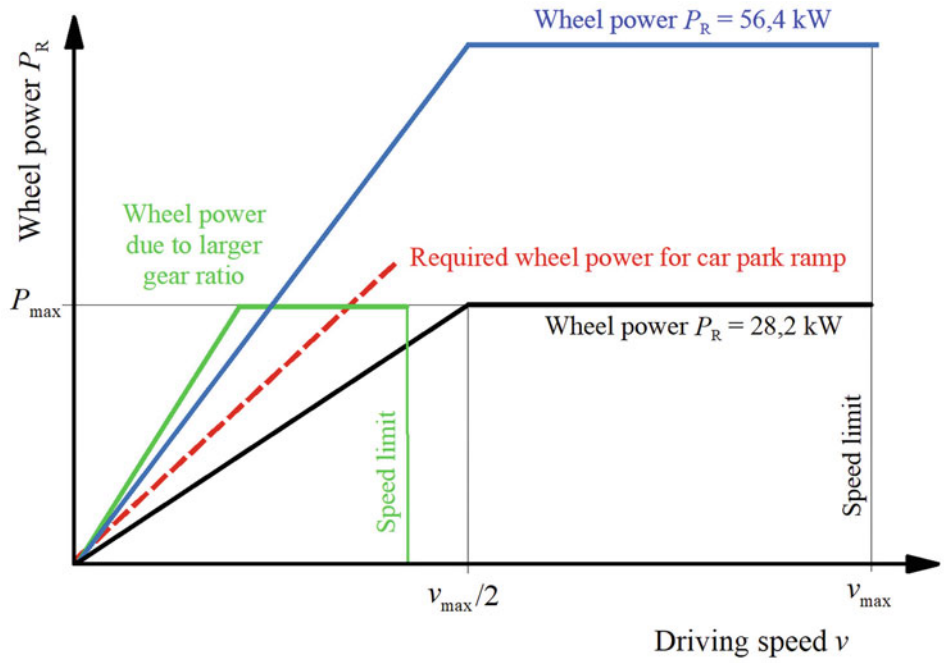

Fig. 2.11 For Task 2.4: Variation of the motor power characteristic for an electric road vehicle

Data: Weight force: $G = 18{,}000$ N
Rolling resistance coefficient: $f_R = 0.02$
Drag coefficient: $c_W = 0.35$
Cross sectional area: $A = 2\ \text{m}^2$
Air density: $\rho = 1.25\ \text{Ns}^2/\text{m}^4$

Result

(a) Wheel power according to Eq. 2.27; therefore tractive force from rolling (Eq. 2.13) and air resistance (Eq. 2.22):

$$P_R = \left(0.02 \cdot 18{,}000\,\text{N} + 1.25/2\,\text{Ns}^2/\text{m}^4 \cdot 2\,\text{m}^2 \cdot 0.35 \cdot 33.33^2\,\text{m}^2/\text{s}^2\right) \cdot 33.33\,\text{m/s}$$
$$= (360\,\text{N} + 486\,\text{N}) \cdot 33.33\,\text{m/s} \approx 28.197\,\text{W} \approx \underline{28.2\,\text{kW}} \quad (\text{at } v_{max} = 120\,\text{km/h})$$

This is not an arithmetical error – many commercially available electric road vehicles nevertheless have outputs of 250 to 400 kW!

(b) Rolling resistance (Eq. 2.13) and gradient resistance (Eq. 2.17) occur (air resistance neglected due to low speed):

$$W = f_R \cdot G + s \cdot G$$
$$W = 0.02 \cdot 18,000\,\text{N} + 0.15 \cdot 18,000\,\text{N} = 360\,\text{N} + 2700\,\text{N}$$
$$= 3060\,\text{N}$$

Wheel performance $P_R = 3060\,\text{N} \cdot 3\,\text{m/s} = 9180\,\text{W} \approx \underline{9.2\,\text{kW}}$

(c) The basic power curve of an electric motor is shown in Fig. 2.11. The full motor power is only available from approx. $v_{max}/2$ (see also Fig. 3.23). At low speeds (revolutions per minute) the power is lower. The power of the electric motor increases approximately linearly in the lower speed range:

$$P \approx \frac{2P_{max}}{v_{max}} v \qquad \left(v \leq \frac{v_{max}}{2}\right)$$

With $P_{max} = 28.2$ kW and $v_{max} = 33.33$ m/s applies:

$$P = 1.692\,\text{kW} \cdot \text{s/m} \cdot v = 1.692\,\text{kW} \cdot \text{s/m} \cdot 3\,\text{m/s} \approx \underline{5\,\text{kW}}$$

At 3 m/s, only $P \approx 5$ kW is available. This is not sufficient for driving up the parking garage ramp. Either a motor with a higher output has to be installed or a manual gearbox with a corresponding transmission ratio must be used for driving slowly up such gradients. These possibilities are illustrated in Fig. 2.11: The dashed red line represents the power requirement for driving up the car park ramp. Black is the approximated course of the wheel power when using an electric motor with 28.2 kW. Since the power requirement is higher than the available power, the ramp cannot be driven on. By installing a larger gear ratio ("first gear"), green line, more power is available at low driving speeds, i.e. the ramp can be driven (slowly). However, the achievable top speed on the level becomes lower due to the engine speed limit. Alternatively, the installed motor power could be doubled (blue line). This would make it possible to drive on the parking garage ramp without a second gear ratio. The fact that rail vehicles with electric drive manage without a manual gearbox is due to the low gradients of railway lines compared to roads.

Driving Machines, Power Transmission

3

After we have dealt with the driving resistances in Chap. 2, we now have to clarify which prime movers are capable of providing tractive forces at the wheel so that motion of the vehicle is possible.

Figure 3.1 shows the driving resistance lines over the driving speed (green: unaccelerated driving on the level; violet: driving on a gradient or driving with constant acceleration). Limit lines of the vehicle drive are drawn into this diagram in red: Because the drive torques at the wheels of land vehicles are usually transmitted via the frictional connection between the wheel and the track (exception: cogwheel tracks), the wheel loads on the drive wheels and the coefficient of adhesion determine the frictional connection limit (drawn horizontally at the top of Fig. 3.1):

$$Z_{\max} = \mu \cdot F_{\mathrm{R}} \tag{3.1}$$

with:

$Z_{\max}$:	max. tractive force,
μ:	Coefficient of adhesion between wheel and rail,
F_{R}:	Wheel loads on the drive wheels.

Because vehicles are limited in width, length and height as well as in weight, the installable traction power is also not arbitrary.[1] Since the tractive forces are plotted in Fig. 3.1, $Z = P/v$

[1] For diesel locomotives in Europe, for example, the limit is around 4000 kW engine power due to the possible vehicle contour and the permissible wheelset loads.

© The Author(s), under exclusive license to Springer Fachmedien Wiesbaden GmbH, part of Springer Nature 2022

J. Ihme, *Rail Vehicle Technology*,
https://doi.org/10.1007/978-3-658-36969-9_3

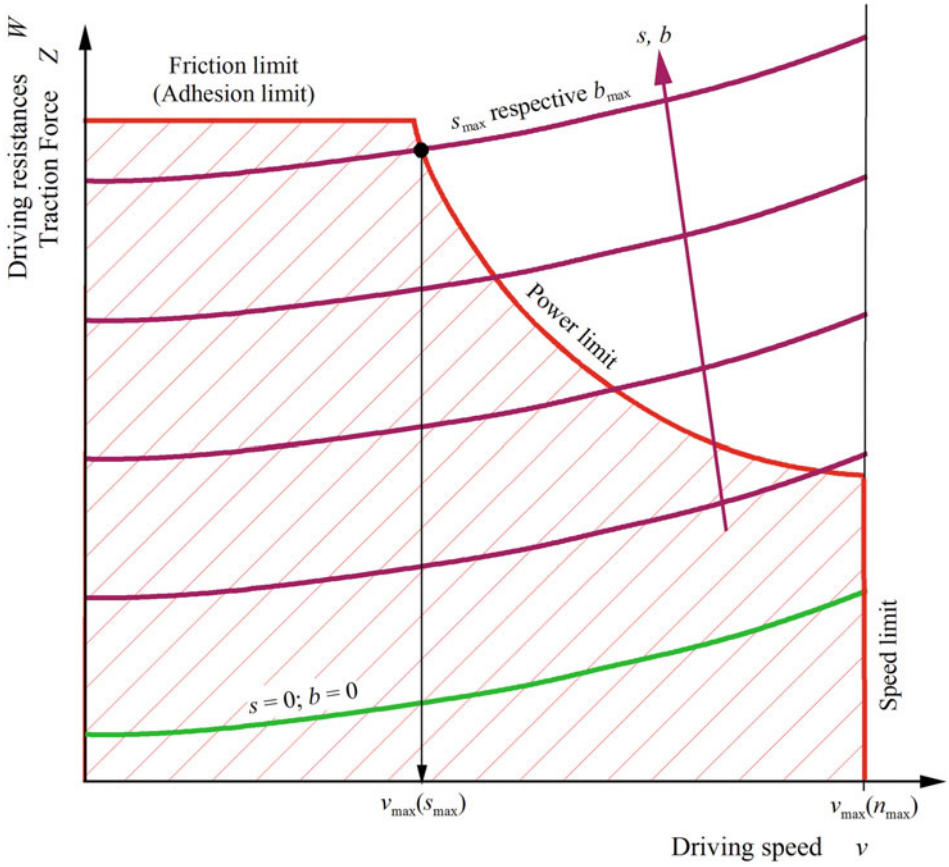

Fig. 3.1 Demand map of a land vehicle

(tractive force equals power divided by driving speed). If one assumes that the prime mover can deliver its maximum power over a larger range of travel speeds, the further limit is the hyperbola drawn on the right ("power limit"). Finally, each drive unit reaches a certain maximum rotational speed. This results in the vertical red line on the far right.

All driving conditions within the red shaded area can thus be achieved. However, this also means that, for example, the maximum gradient (upper violet parabola) cannot be driven on with v_{max} at maximum rotational speed $n_{max,}$ since the following applies to the point of intersection with the red hyperbola: $W(S_{max}) = Z_{max}(v)$. The "desired" characteristic diagram of the prime mover of a land vehicle shaded in red in Fig. 3.1 is also referred to as the "ideal delivery characteristic diagram" [46].

The adhesion limit is examined in more detail in Fig. 3.2. The curves of the adhesion coefficient between the wheel and the rail as a function of the driving speed entered there originate from tests. The values in the shaded area are usually used for calculations; the formulae are given in Fig. 3.2.

As can be seen from Fig. 3.1, the adhesion limit determines the tractive force of rail vehicles only in the lower speed range; at higher speeds, the installed power is the limit and

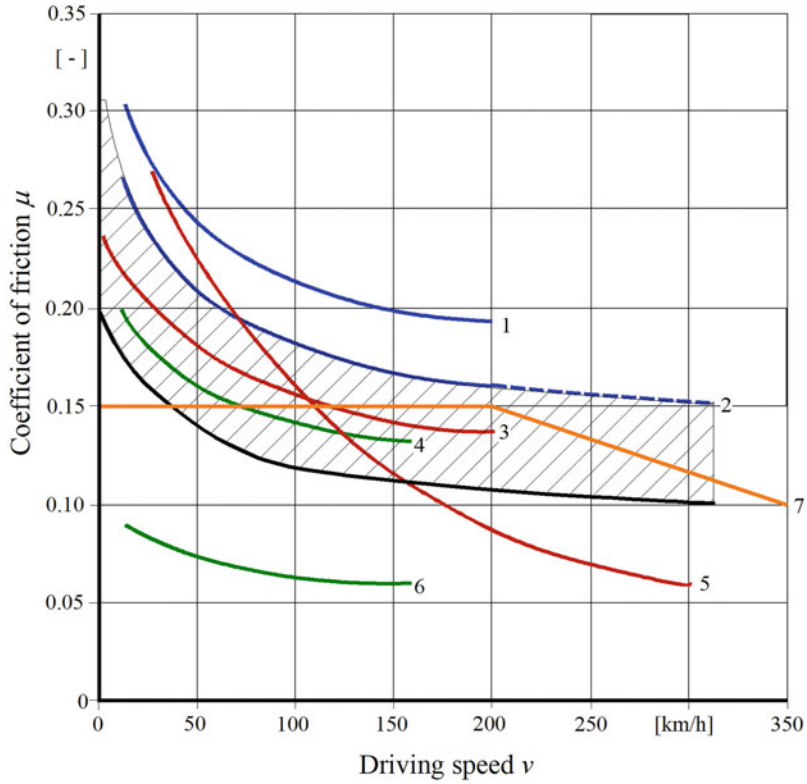

1 Curtius-Kniffler for dry, sanded rails: $\mu = 0.161 \cdot \frac{7.5}{v+44}$

2 Curtius-Kniffler for wet, sanded rails: $\mu = 0.24 \cdot \frac{8+0.1 \cdot v}{8+0.2 \cdot v}$

3 SNCF*) for anti-skid protection device without sanding: $\mu = 0.13 \cdot \frac{7.5}{v+44}$

4 DB for wet, clean

5 Minimum measured values of SNCF

6 DB für smeary, leaf fall (lowest measured values)

7 Exploitable for high-speed trains, after [57]

usable for calculations

*) SNCF: Societé Nationale des Chemins de Fer Francais
(French State Railways)
DB: Deutsche Bahn AG (German Railways)

Fig. 3.2 Static friction curves for wheel/rail system. (According to Lehmann [43] and Schindler [57]; Curtius, E. W.; Kniffler, A.: Neue Erkenntnisse über die Haftung zwischen Rad und Schiene. Elektrische Bahnen 21 (1950) H. 9, pp. 201–210)

the adhesion coefficient is no longer utilised. In order to increase tractive forces when starting (and braking forces when braking), "sanding" is common. Traction units are equipped with sanding devices for this purpose. Fine-grained, dry sand is spread on the rails via pipes directly in front of the driving wheels and increases the static friction coefficient.

Figure 3.3 shows the ideal delivery identification in tractive force and in power representation. According to Fig. 3.2, the adhesion limit is no longer a straight line, but decreases with increasing driving speed. The representation has been supplemented by the ideal braking characteristics: To protect the friction brakes in the vehicle, braking via the drive system is desirable. Most prime movers generate a braking torque and thus a braking power in overrun mode.

According to Fig. 3.4, the following results for the powers:

$$\text{Power at the drive wheels} : P_{\mathrm{R}} = \eta_{\mathrm{K}} \cdot P_{\mathrm{M}}, \tag{3.2}$$

$$\text{Power dissipation} : P_{\mathrm{v}} = (1 - \eta_{\mathrm{K}}) \cdot P_{\mathrm{M}} \tag{3.3}$$

with

P_{M}:	Engine Performance,
η_{K}:	Efficiency of the characteristics converter.

We will now investigate which prime movers have a map corresponding to the ideal delivery map. Since this is not the case for all known prime movers, the task also consists of adapting the map of the prime mover to the ideal delivery map via a so-called characteristic converter [46], Fig. 3.4.

3.1 Steam Engine

From the operation of the first railway lines in the nineteenth century until well into the twentieth century, the steam engine was a common drive for rail vehicles.[2] Figure 3.5 shows the delivery map of a three-cylinder steam locomotive of the DB class 011[3] (the locomotive is shown in Fig. 3.6).

[2] Steam operation on the German Federal Railways ended in 1977; in China and South Africa, steam locomotives were still used until the turn of the millennium. Within the EU, steam locomotives are now only found on tourist and museum railways.

[3] The class 011 was a coal-fired three-cylinder express steam locomotive with $v_{\max} = 140$ km/h and a power of about 1500 kW. The class 012 locomotive installed as a locomotive monument at Braunschweig Central Station is its oil-fired variant.

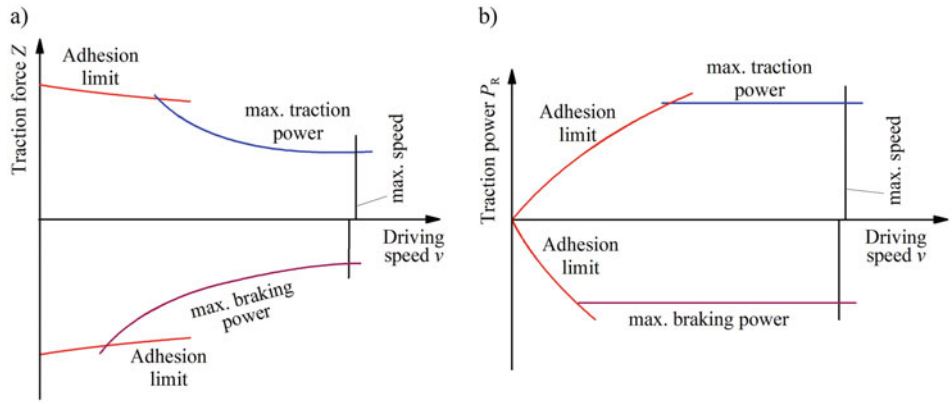

Fig. 3.3 Ideal delivery identification. (**a**) Tractive force or braking force versus driving speed, (**b**) Wheel power versus driving speed. (According to [46])

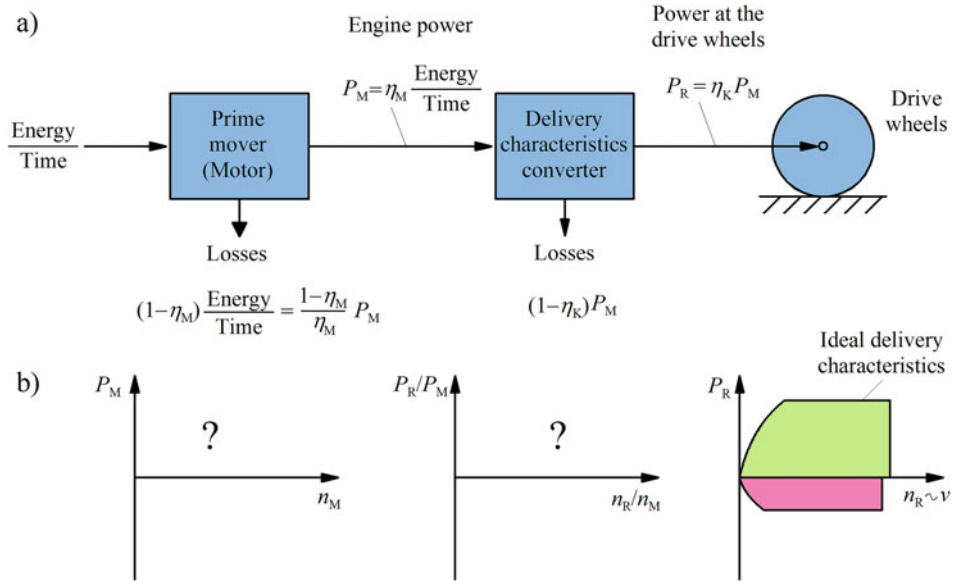

Fig. 3.4 (**a**) Block diagram of the drive system, (**b**) Search for motor and transformer maps to obtain the ideal delivery map. (According to [46])

In the left diagram, the torque $M/M(P_{max})$ related to the torque at maximum power is plotted instead of the tractive force; however, tractive force and torque are proportional. On the horizontal axis, the speed is plotted in relation to the speed at maximum power. It can be seen that both diagrams are close to the ideal delivery identification, since the steam engine is a prime mover of (almost) constant power (as long as the steam boiler delivers enough steam). That is why steam locomotives do not need a characteristic converter, i.e. no

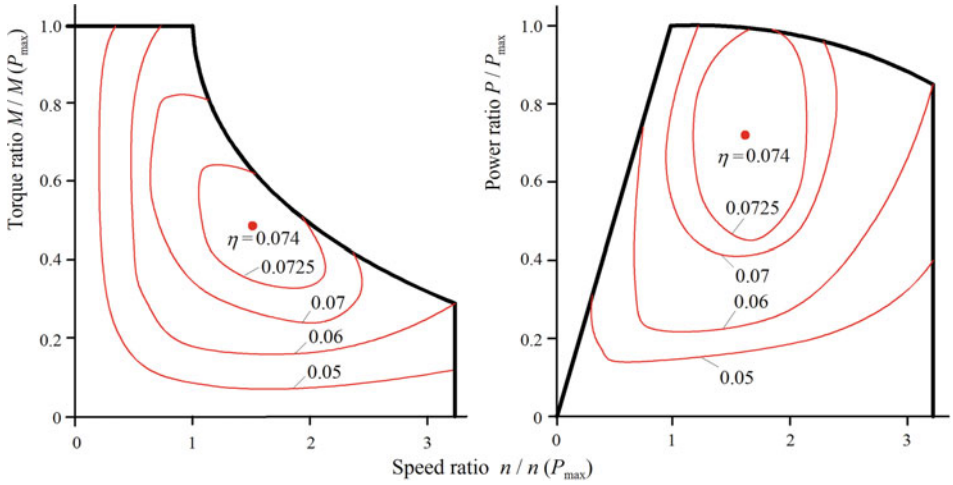

Fig. 3.5 Characteristic diagrams of the DB class 011 three-cylinder express steam locomotive. (According to documents of the German Federal Railway Central Office in Minden)

Fig. 3.6 Three-cylinder express steam locomotive class 011 (August 1972)

gearbox. The fact that they are no longer used is due to their lack of economy: They require high maintenance, need two-man crews (driver and stoker) and have a limited driving

range, as they have to replenish fuel and especially water.[4] On top of this, as can be seen from the red lines in Fig. 3.5, they have a poor efficiency, which is 7.4% at the best point here. The red lines of constant efficiency drawn in Fig. 3.4 are called "shell curves" because of their shape. They can be found in a similar form in all drive machines.

Figure 3.5 also shows that the efficiency in the partial power range is very poor (<5%). When shunting, locomotives are predominantly operated in the partial power range. This is why shunting steam locomotives were phased out a long time ago. In addition, the boiler heat losses mean that energy is also consumed when the locomotive is at a standstill. Finally, the power that can be installed in steam locomotives is limited to about 1800 kW for Western European vehicle dimensions. This is no longer sufficient for heavy trains and high speeds today.

In the ideal delivery characteristic diagram according to Fig. 3.2, a brake characteristic diagram is also required. Steam locomotives, e.g. for mountain routes, were equipped with the so-called RIGGENBACH[5] counter-pressure brake for this purpose. This allowed the steam engine to work as a compressor in braking mode: Air was sucked in, compressed and expelled via a throttle. This made the brake map shown in red in Fig. 3.7 possible, although it only partially corresponds to the ideal map, since, for example, the braking torque decreases with decreasing speed and is also zero for speed $n = 0$. Thus, the back-pressure brake cannot be used to brake to a standstill, but an additional friction brake is required. However, on downhill gradients, the RIGGENBACH counter-pressure brake can be used as a continuous brake for steady-state braking.[6] This considerably reduces the wear of the friction brake. To cool the steam cylinders, which heat up due to air compression, feed water from the tender supply can be injected into them. The RIGGENBACH counter-pressure brake is still used today on steam-powered rack railways.

The map of the steam engine corresponds to a large extent to the ideal map. However, the steam locomotive does not need a gearbox simply because there are only slight gradients on railway lines and the required acceleration values are low with regard to standing passengers and dining car passengers. A steam vehicle in road traffic, on the other hand, would need a multi-gear transmission in order, on the one hand, to be able to negotiate ramps with a greater gradient (e.g. in a multi-storey car park), to enable high accelerations and, on the other hand, to reach motorway speeds.

[4] The tenders of steam locomotives are often mistakenly called "coal cars" by laymen. The tender of the locomotive shown in Fig. 3.6, for example, holds 10 t of coal and 38 m^3 (38 t) of water, so it is not so much a coal car as a water car. Water must be replenished several times during a long trip, depending on the locomotive's exertion. The coal supply is usually only replenished at the terminal station.

[5] Nikolaus Riggenbach (1817–1899), Swiss engineer and inventor of the rack railway.

[6] Steady-state braking: braking to maintain a constant speed on a downhill gradient.

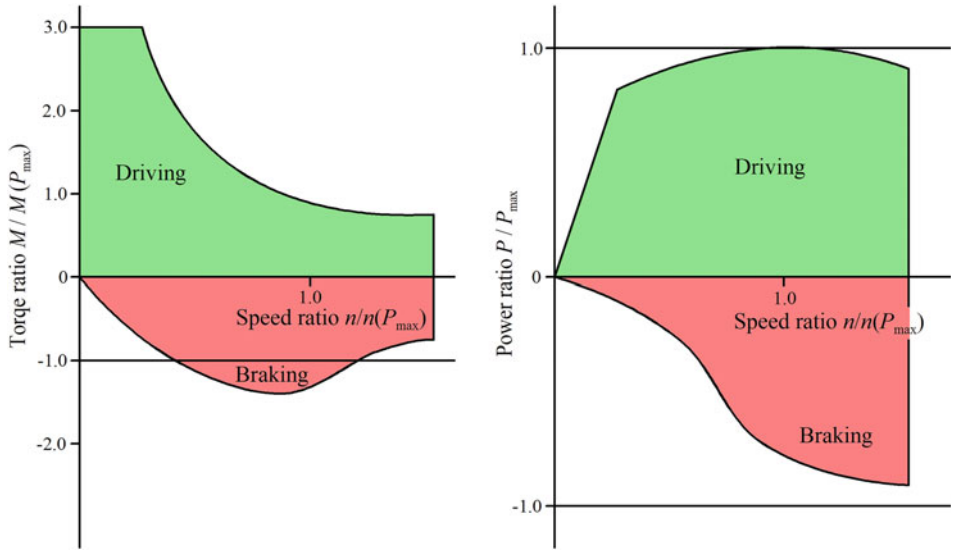

Fig. 3.7 Characteristic diagram of the three-cylinder freight steam locomotive with RIGGENBACH counter-pressure brake DB class 044 (according to documents of the German Federal Railway Central Office Minden)

3.2 Electric Motor

The electric motor as a rail drive cannot be considered without the energy supply system, since in electric rail vehicles the energy source is not carried along as a battery, but the power supply is provided via overhead line or conductor rail. The German Federal Railways had battery railcars in service until the eighties of the twentiethth century, but they were finally taken out of service because of the high battery maintenance costs. A renewed procurement of traction vehicles powered purely by accumulators is not to be expected in the foreseeable future. More likely is the procurement of electric rail vehicles operated by both overhead line or generator and accumulator. In the case of battery-electric vehicles, also in road traffic, the losses in the charger and battery of approx. 30% must be taken into account. If the vehicle is fed by overhead line or conductor rail, these losses do not apply.

In 1866, WERNER VON SIEMENS[7] discovered the electrodynamic principle, which made the construction of the electric motor possible. As early as 1879, SIEMENS showed the first electric locomotive at the Berlin Trade Exhibition (Fig. 3.8). The power was supplied via a central rail, the return line via the two running rails. In 1881, the first electric tramway was

[7] Werner (von) Siemens (1816–1892), German engineering officer, inventor, and entrepreneur.

Fig. 3.8 First electric locomotive at the Berlin Trade Exhibition in 1879. (Photo: Siemens Archive)

opened in Berlin; in 1882, Siemens & Halske supplied the first electric mine locomotive, whose power supply was already via catenary.

The first electric mainline railway operated in the USA in 1895 with direct current 650 V. Since direct current cannot be transformed, mainline railways require either numerous substations to feed in power or a large catenary cross-section to limit the voltage drop due to the electrical resistor of the catenary. According to OHM's law, the voltage drop $U_A = R \cdot I$. Since the transmitted power $P_{el} = U \cdot I$ depends on the current I for a given mains voltage, the line resistor R determines the voltage drop.

For this reason, tests have also been carried out in Germany more than 120 years ago with alternating current and three-phase current. Here, a high voltage is possible in the catenary, which keeps the voltage drop low at the same power due to lower currents. On the traction units, a transformer reduces the voltage to a value that is favourable for the traction motors. The three-phase supply, however, requires a multi-pole catenary, Fig. 3.9. The high-speed railcar shown here already reached a maximum speed of 210 km/h in 1903 [13].

Finally, alternating current electrification with 15 kV voltage and a frequency of 16 2/3 Hz (today 16.7 Hz) became established in Germany. Single-phase alternating current can be transformed on the traction unit and only requires a single-pole contact line. The frequency of 16 2/3 Hz is a compromise between the usual mains frequency of 50 Hz and direct current. The reason for this is the "brush fire" on the commutator of the motor that occurs with alternating current, which causes high wear. With low frequency it

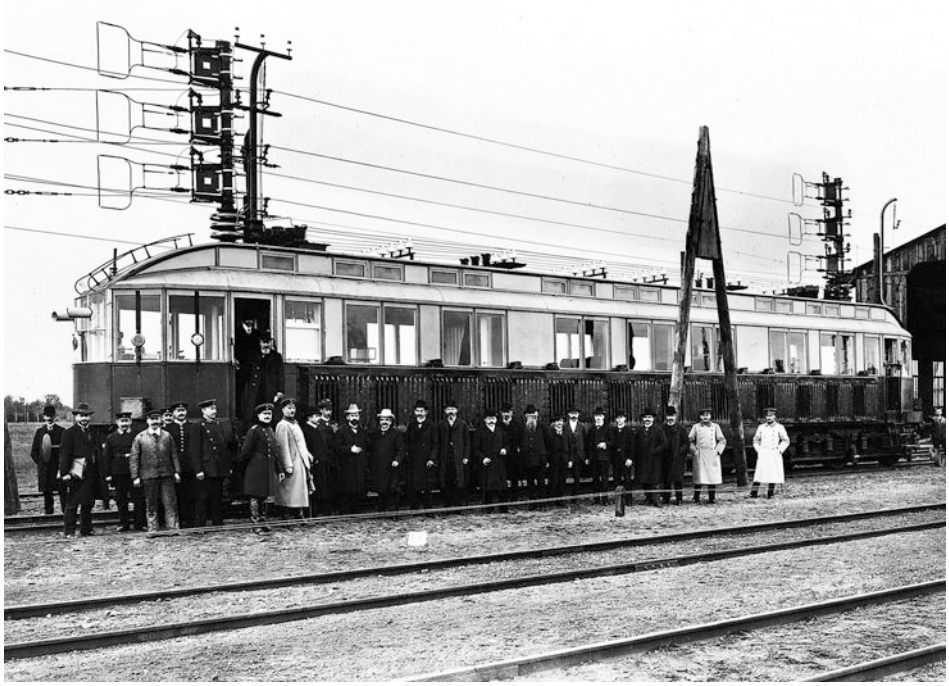

Fig. 3.9 Electric high-speed railcar for three-phase current 1903. (Photo: Siemens Archive)

can be limited. On the other hand, with decreasing frequency the transformer becomes heavier, since the iron weight is approximately inversely proportional to the frequency. The frequency of traction current at 16 2/3 Hz is one third of the frequency of 50 Hz. This means that a generator with three pole pitches for traction current can be operated in the power station at the same turbine speed as for mains current. Today, frequency conversion by means of semiconductor circuits is no longer a technical problem, but the foundations of today's traction current supply were already laid at the beginning of the twentieth century.

Due to the necessary insulation in the motors, the motor voltage was usually 1500 V maximum. With direct current supply, the catenary voltage is limited to this value if the motors are fed directly; if two motors are connected in series, 3000 V are also possible. Today, the overhead line voltage for trams is between 500 and 750 V DC; underground trains and some metro lines are sometimes operated with 800, 1200 or 1500 V DC.

Figure 3.10 shows a map of Europe with the power systems used on the mainline railways. In Norway, Sweden, Germany, Austria and Switzerland the single-phase AC system with 15 kV voltage is used, the frequency being 16.7 Hz in Germany, Austria and Switzerland and 16 2/3 Hz in Sweden and Norway. In southern France and the Netherlands 1500 V direct current is used, in Spain, Italy, Belgium and in many countries of Eastern Europe 3000 V, in southern England 800 V. Electrification started relatively early in these countries. Countries that did not electrify their railway lines until after World War II were

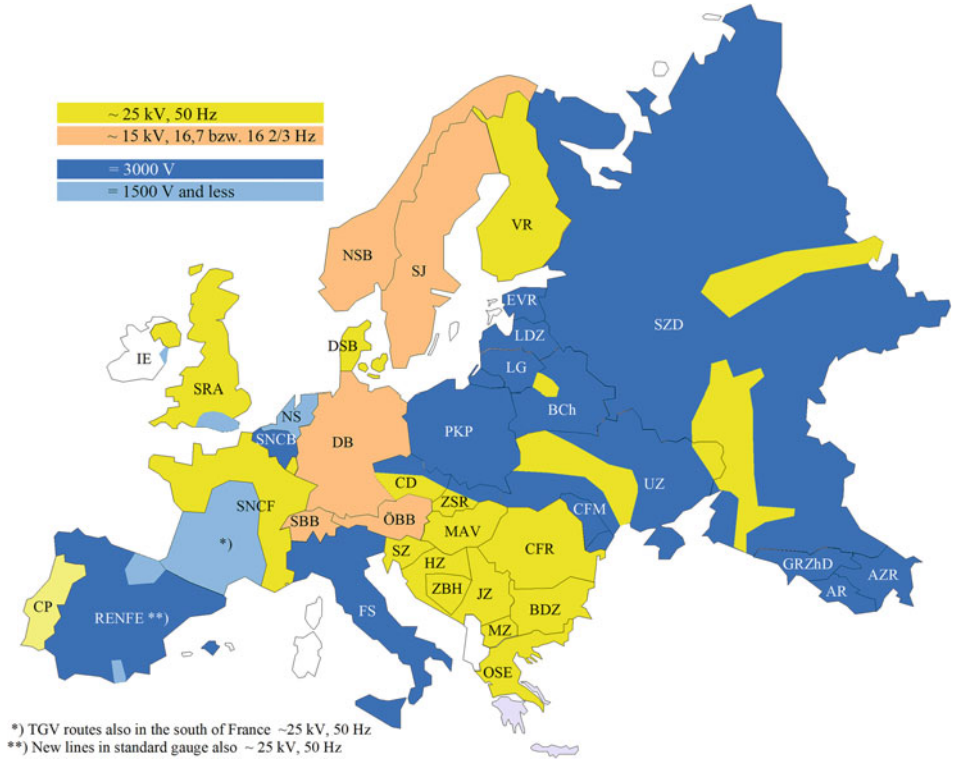

Fig. 3.10 Electric power systems of mainline railways in Europe

able to use single-phase alternating current at 25 kV and 50 Hz due to further developments[8] and thus avoid having their own supply network. In the USA, some lines are also operated with single-phase alternating current 25 Hz.

3.2.1 DC Motor

Whereas 30 years ago almost every transition from one power system to another required a change of traction unit, today universal locomotives are conceivable and in some cases even implemented due to semiconductor technology and the three-phase motor, see Sect.

[8] In Germany the Rübelandbahn in the Harz Mountains (Blankenburg – Elbingerode) is also electrified with 25 kV, 50 Hz. Considerable freight traffic is handled on this mountain railway; for rationalisation purposes, the line was electrified by the Deutsche Reichsbahn from 1965. Since it is an island operation without connection to the rest of the electrified railway network, the deviating power system was chosen to avoid a long traction current feed line.

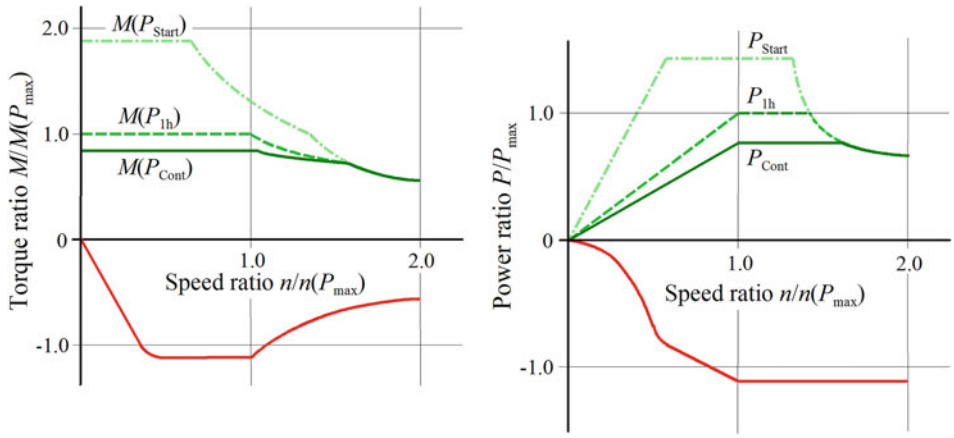

Fig. 3.11 Torque and power characteristics of a DC motor with resistor brake for trams. (According to Siemens company documents)

3.2.3 First, however, we want to consider the classic DC traction motor. Figure 3.11 shows the characteristic curves for a tram motor.

Three characteristic curves are distinguished in the drive map for this motor:

- The starting power (P_{Start}) and the associated starting torque,
- The hourly power (P_{1h}) and the hourly torque and
- The continuous power (P_{Cont}) with the continuous torque.

For railway motors, a distinction is often made between these three powers, which can be delivered over different periods of time. Since every electric machine has an electrical resistor, it heats up during power consumption or power output. The temperature rise in the motor must be limited so that the insulation of the windings is not damaged or the connections at the commutator become unsoldered. Tram motors are usually self-ventilated motors, i.e. the cooling air is supplied via a fan wheel mounted on the motor shaft (comparable to the cooling of an electric hand drill). This means that the cooling capacity is dependent on the motor speed. Electric motors for mainline vehicles are usually externally cooled, i.e. they are supplied with cooling air by fans that are driven independently of the traction motor. Liquid cooling is also available for highly loaded motors.

Thus, if the self-ventilated motor according to Fig. 3.11 has to deliver a high torque at low speed during start-up, it heats up strongly and then needs time to cool down. Therefore, the starting power can only be applied for a short time, usually 5 or 10 min depending on the application. Over an hour, the engine would be able to deliver the hourly power slightly above the continuous power, e.g. for driving on longer inclines. Unlimited time the continuous power and the corresponding torque are available. All in all, it can be seen that the characteristic curves of the electric motor also largely correspond to the ideal

characteristic curve. Electric traction units therefore only require a fixed transmission ratio between the motor and the wheelset; no further characteristic converters are required.

The braking characteristic curve does not fully correspond to the ideal characteristic curve, since the braking torque approaches zero as the speed decreases. During braking, the motor is operated as a generator and converts the kinetic energy of the vehicle and the train. The electrical energy generated is converted into heat in resistors. Tramcars have braking resistors on the roof for this purpose. In winter, it is possible to switch to heating resistors inside the car. If the appropriate conditions exist on the grid side, the braking energy can also be fed back into the grid.

The control of DC motors when fed from a DC overhead contact line or conductor rail is done either via series resistors or a DC chopper, Fig. 3.12. In older DC vehicles, resistors are connected upstream of the motor with the aid of the master controller so that the motor is only operated with a voltage lower than the supply voltage U_L via the voltagedrop at the series resistors. At the series resistors, however, a part of the supplied power is converted into heat. The DC chopper is a type of "DC transformer" [20]. It blocks or releases the current passage in short intervals, thus acting like a fast switch. Figure 3.13 shows the voltage curve with different clocking of the DC chopper.

3.2.2 Single-Phase AC Motor

Next, we will now look at the single-phase AC motor. Locomotives and railcars with AC motors are still in use at German Railways (DB, Deutsche Bahn); the last class procured was the class 111 from 1979 on. After that, the three-phase asynchronous motor generally prevailed as the drive in rail vehicles in Germany because the frequency converter was ready for series production. In France, for example, the synchronous motor also plays a role as a rail drive.

Figure 3.14 shows the performance map of the German class 194 electric freight locomotive. Although only a few examples of this locomotive series are still in service, the published map is one of the few to contain the already mentioned shell curves of equal efficiency. The locomotive with Co′Co′ axle arrangement has six AC traction motors. The efficiency of the locomotive from the contact wire ranges from 77.7% at the 'best point' to 70% at part load – the electric drive is thus significantly better than the steam engine, with only a small drop in efficiency at part load. Although AC motors of the power class considered (hourly output per motor 550 kW) achieve efficiencies of around 85%, the overall efficiency is lower because the motors are preceded by the transformer and auxiliary units also require energy, e.g. the traction motor fans and the compressor for the air brake.

If one takes into account the efficiency of a thermal power plant that generates the electrical energy and the efficiency of the energy transmission up to the locomotive, the highest efficiency is just under 30%. There is hardly any difference between this and the diesel traction unit; only in the partial load range the electric locomotive is better. However, it must be taken into account that 1 kWh of traction current causes lower costs than 1 kWh

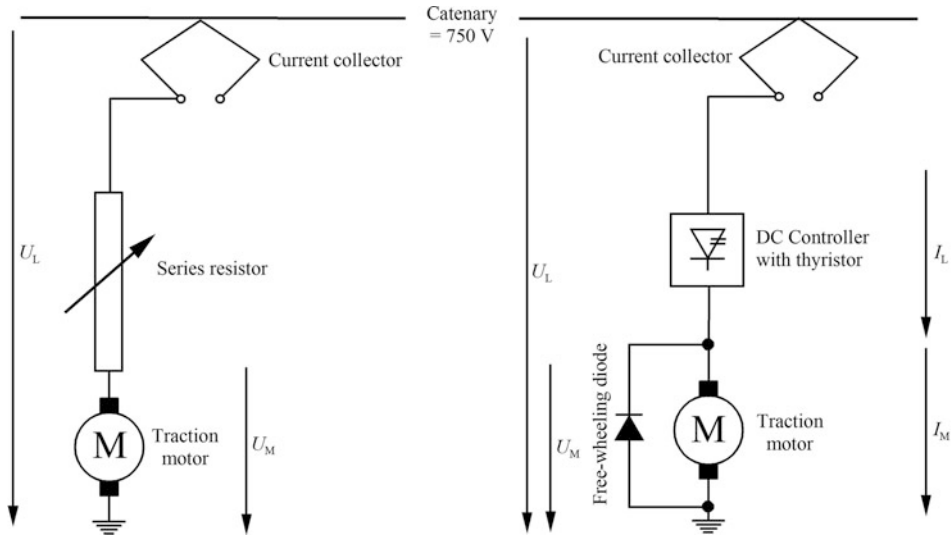

Fig. 3.12 Control of DC motors on DC mains. (According to [20])

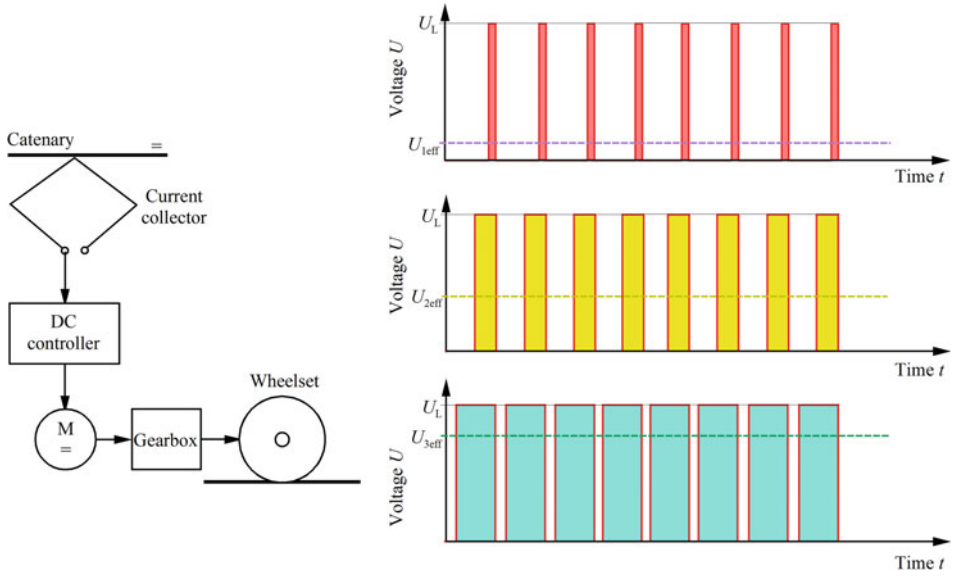

Fig. 3.13 Course of the voltage in the DC controller (pulse width control). (According to [20])

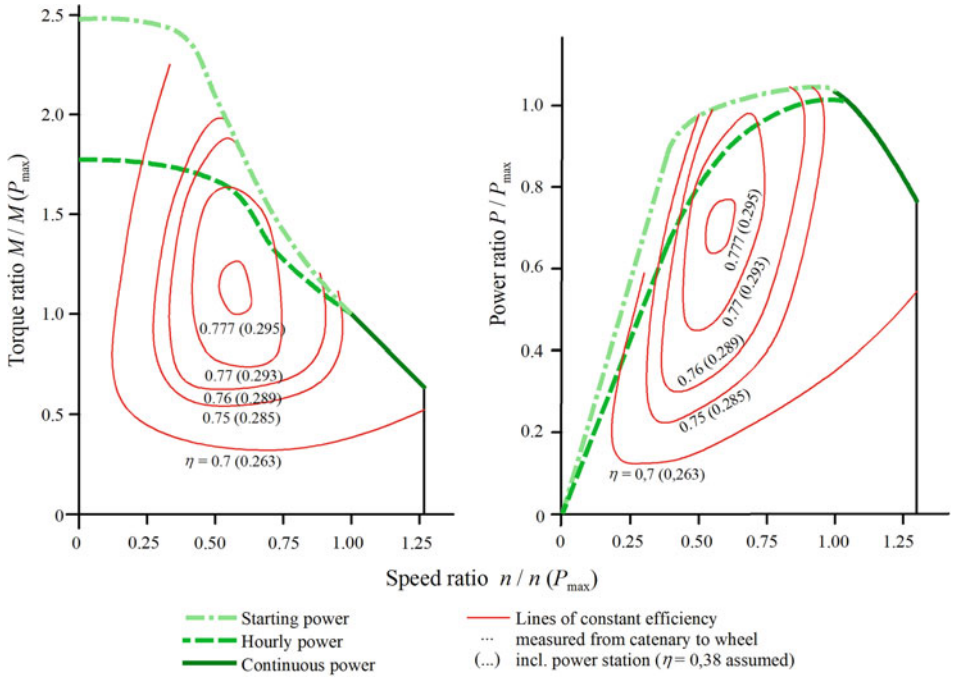

Fig. 3.14 Characteristic diagram of the DB class 194 six-axled electric freight locomotive. (o. Verf.: Das Kennlinienfeld der elektrischen Lokomotive. Eisenbahntechn. Rundschau 3 (1954) H. 11)

of energy from diesel oil.[9] DB generates traction current not only in thermal power plants, but also in hydroelectric and wind power plants; a complete supply with green electricity would be possible with the appropriate investments.

The control of vehicles with AC motors is done either by transformers with several taps or by power converters. Figure 3.15 shows the amplitude control of a single-phase AC locomotive. The overhead line voltage of 15 kV is transformed on the locomotive to a motor voltage of 1000–1500 V maximum. Low-voltage control was used for locomotives of lower power (e.g. DB class 141). Here, the transformer has taps on the secondary side of the winding so that the motors can be operated with different voltages. Due to the low voltage, high currents have to be transmitted by the switching mechanism here, which is only possible with overall lower power ratings. The high voltage control switches the primary side of the transformer. This means that higher voltages have to be switched, but only smaller currents, even for larger installed powers. Figure 3.16a shows the voltage curve at the motor with low voltage and high voltage control. Both are amplitude control.

[9]For diesel oil, railway companies in Germany have to pay mineral oil tax and eco-tax like road vehicles. At DB, the price of diesel is only cheaper than at the road filling station because of bulk purchasing. One litre of diesel oil has an energy content of approx. 11 kWh.

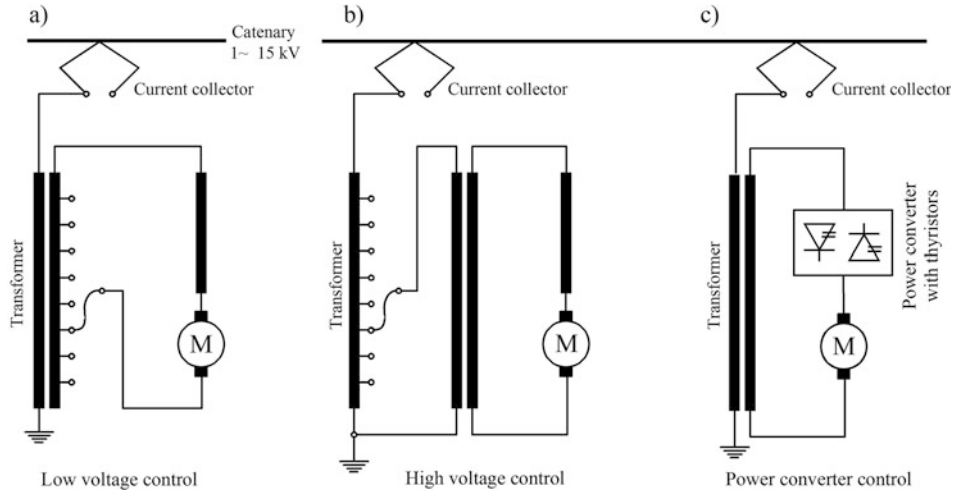

Fig. 3.15 Control of single-phase AC vehicles

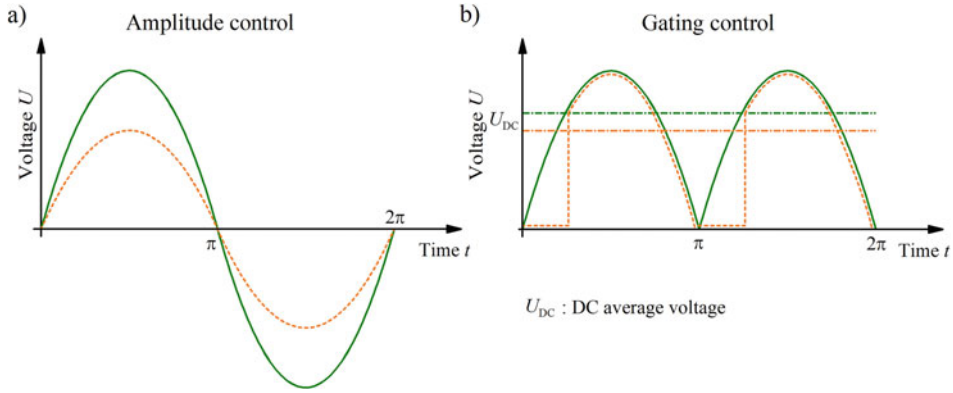

Fig. 3.16 Motor voltage curve with amplitude control (**a**) and gating control (**b**). (According to [43])

The converter control with thyristors (gating control; Fig. 3.15c) only requires a transformer with a fixed winding ratio. The alternating current is rectified in the converter. This results in a wavy direct current, Fig. 3.16b. The time at which the converter switches within a half-wave determines the DC average motor voltage. The converter for AC vehicles was developed to series maturity in Sweden; the Swedish state railway still uses converter locomotives.

Figure 3.17 shows the tractive effort-speed characteristic diagram of the six-axle Co′Co′ class 151 freight locomotive of the DB. This locomotive is equipped with a resistor brake, i.e. it can brake without wear by switching the traction motors as generators and converting

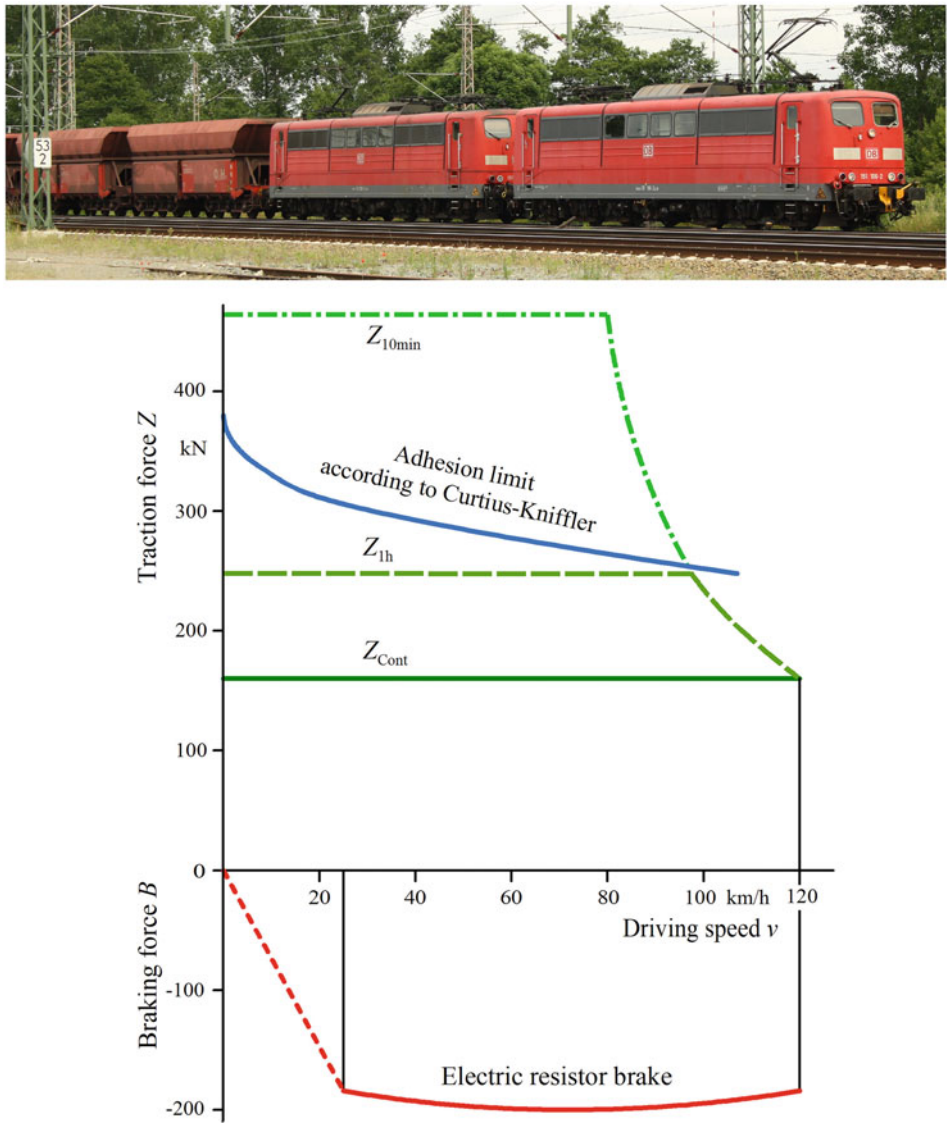

Fig. 3.17 (**a**) DB class 151 electric freight locomotive in double traction, (**b**) Map of a class 151 locomotive. (Map according to documents of German Federal Railway Central Office Munich)

the generated energy into heat in resistors. The resistor brake is used in operation between 120 and 25 km/h.

When starting at the adhesion limit, the locomotive can apply a tractive effort of about 400 kN in the 10-min power range. Between the Hansaport in Hamburg and the Salzgitter-Beddingen station (transfer to the Salzgitter steelworks), the DB currently runs the heaviest

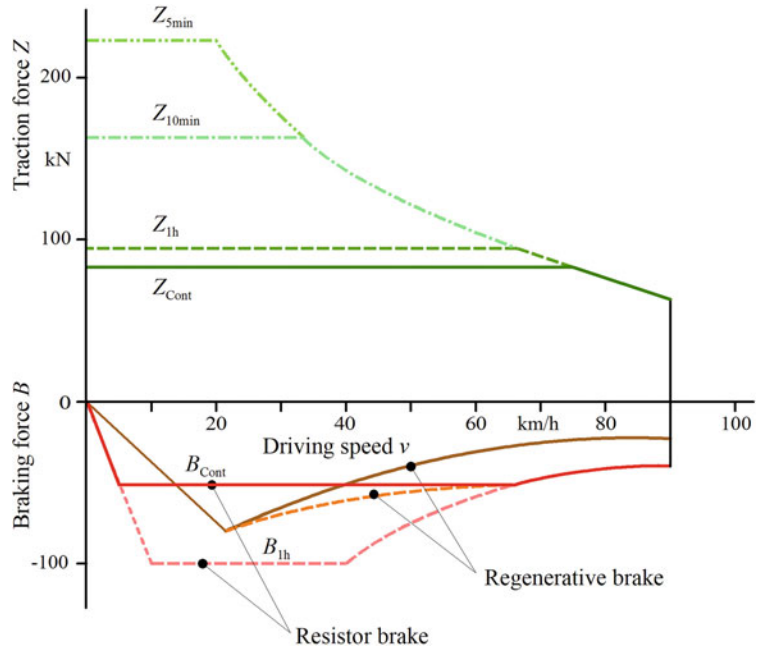

Fig. 3.18 Characteristic diagram of the DB electric multiple unit class ET 45.01. (According to documents of German Federal Railway Central Office Munich)

trains. With a gross weight of 6000 t, 4300 t of iron ore pellets are transported. The trains are hauled by two class 151 electric locomotives. Due to the high tractive forces, the wagons and locomotives are equipped with center buffer couplers.

Instead of converting the energy generated by the traction motors during braking into heat in resistors, it makes sense to feed the energy back into the grid. With AC motors, this is complex, as the supply frequency and the mains frequency have to match. Only with vehicles with three-phase motors and frequency converters is this possible as standard. DB has investigated both resistor braking and regenerative braking on an older electric railcar, Fig. 3.18. The regenerative braking has not been adopted in other vehicles with single-phase AC motors.

An impression of the size of an AC traction motor is given in Fig. 3.19. The motor shown from a DB class 141 electric locomotive is, at 578 kW, the smallest traction motor in a post-war new locomotive. The largest single-phase AC motors at the DB had about 1300 kW continuous power (class 103).

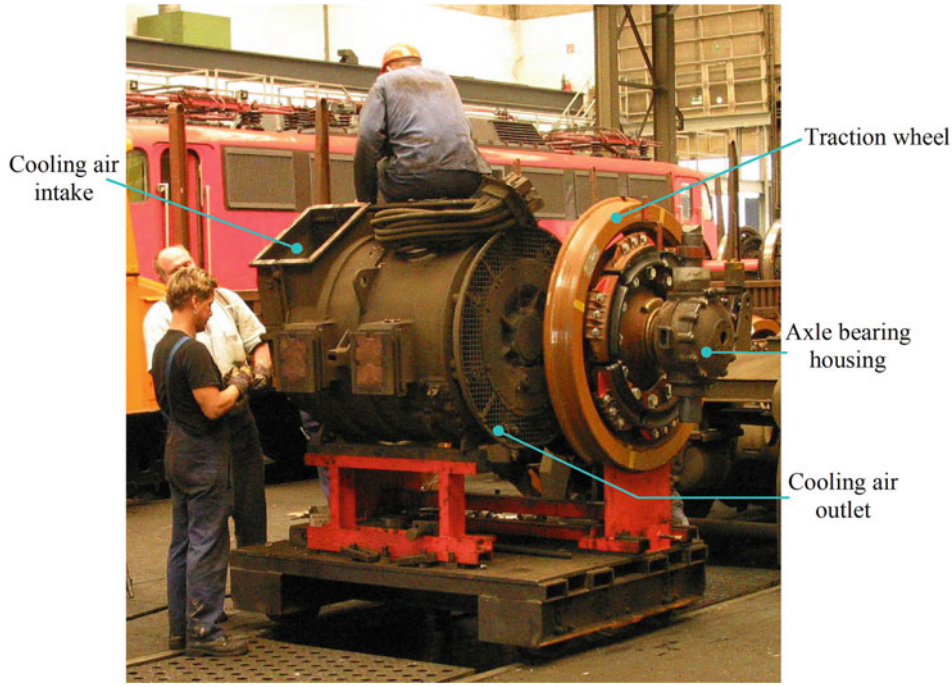

Fig. 3.19 Single-phase AC motor of a DB class 141 electric locomotive; continuous motor power 578 kW

3.2.3 Three-Phase Motor

Neither DC motors nor single-phase AC motors are ideal traction motors, as they are relatively long and require a lot of maintenance due to the commutator (see Fig. 3.20). In contrast, the three-phase asynchronous motor has the advantage of not requiring a commutator. Thus, the only wearing parts are the roller bearings of the armature. The three-phase motor has compact dimensions (length and diameter) and therefore a lower mass, Fig. 3.21 and Table 3.1. Due to the smaller diameter, higher rotational speeds are possible (mechanical tensions from centrifugal forces!). However, for operation on a single-phase alternating current or direct current network, it requires a converter which supplies it with three-phase current of variable frequency. Static converters for railway operation have only been available since the further development of semiconductor technology in the mid-seventies of the last century.[10]

[10]Previously, rotating converters were used: On an alternating current network, an alternating current motor drove a direct current generator, which supplied the traction motors with direct current. By means of a phase converter and frequency converter group, frequency-controlled three-phase motors

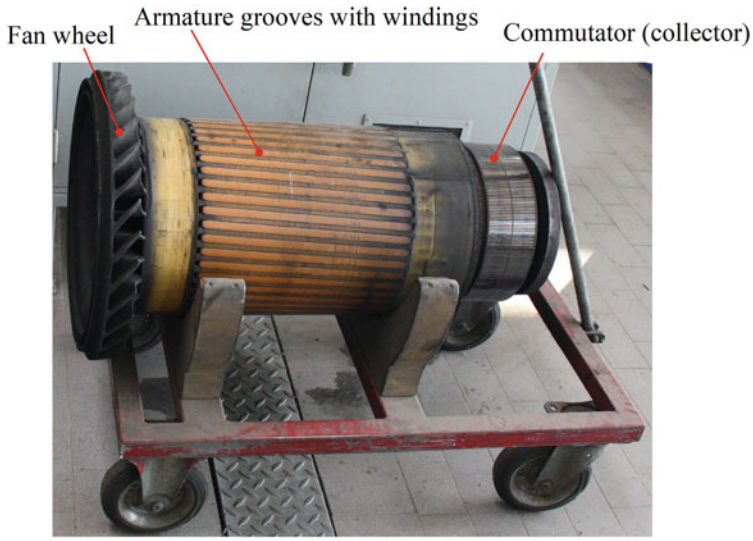

Fig. 3.20 Armature (rotor) of a self-ventilated tram DC motor 600 V, 120 kW

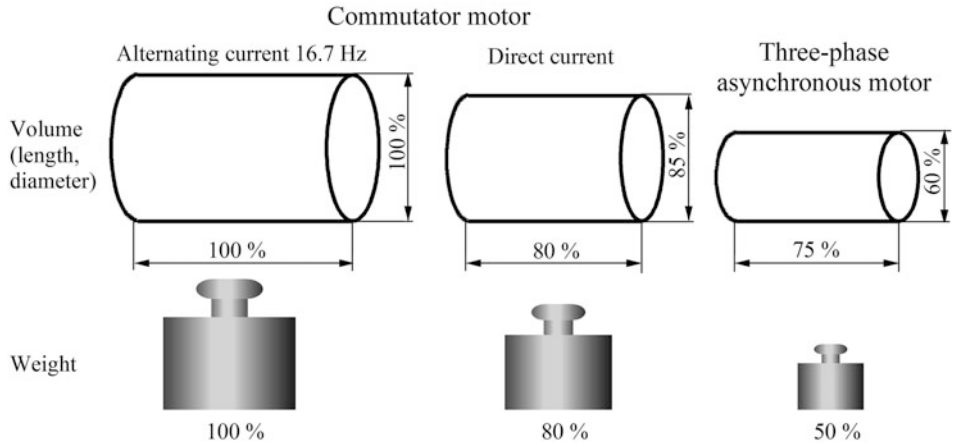

Fig. 3.21 Comparison of single-phase alternating current motor, direct current motor and three-phase asynchronous motor. (According to Siemens documents)

The main advantage of three-phase drive technology is that the same components can be used to build vehicles for both direct current and alternating current feed. The technology is also suitable for power transmission in diesel traction units. Figure 3.22 shows schematic

could also be supplied. This technology, which was tested in northern France about 60 years ago, did not catch on [20, p. 96/97].

Table 3.1 Data on different traction motors for mainline locomotives. (According to: Baur, K. G.: Die Geschichte der Drehstromlokomotiven. Eisenbahnkurier Verlag, Freiburg (2005))

First year of manufacture	1956	1975	1979	1999
Locomotive class	DB 110, 140	DB 181.2	DB 120	DB 182 (Taurus)
Motor design	1 ~ Series wound	Mixed flow	Three-phase	Three-phase
Max. Voltage	585 V	1050 V	2200 V	2027 V
Continuous current	2250 A	830 A	360 A/phase	690 A
Continuous output	0.95 MW	0.8 MW	1.4 MW	1.64 MW
Max. Speed	1525 min^{-1}	2210 min^{-1}	3600 min^{-1}	3900 min^{-1}
Diameter	1164 mm	950 mm	930 mm	810 mm
Mass	3.9 t	3.1 t	2.4 t	2.8 t

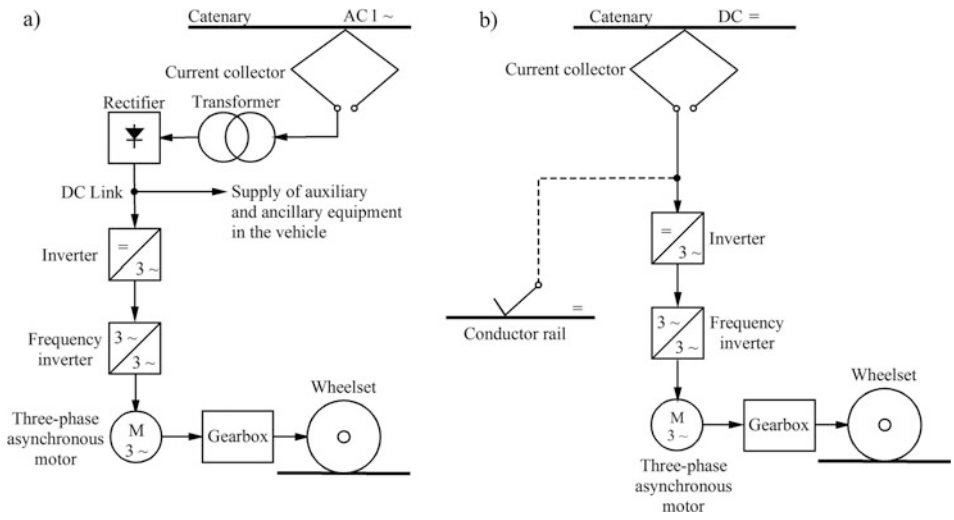

Fig. 3.22 Schematic diagrams for rail vehicles with three-phase asynchronous motors. (**a**) on the single-phase AC mains, (**b**) on the DC mains

diagrams of electric traction units with asynchronous motors. In the case of AC supply, there is a DC link in the vehicle to which the frequency inverter is connected. For this purpose, the alternating current is first transformed to motor voltage (max. approx. 2000 V) and then rectified. In diesel drive vehicles, a synchronous generator is usually driven by the diesel engine, which supplies the DC link via the rectifier.

In the case of rail vehicles on the DC mains, the frequency inverter is supplied directly with DC current. This technology has the advantage that multi-system vehicles can also be implemented relatively easily. For example, in the case of alternating current 50 or 16.7 Hz, the power is fed before the transformer, and in the case of direct current 1500 or 3000 V, the power is fed directly into the DC link. This means that the system boundaries shown in

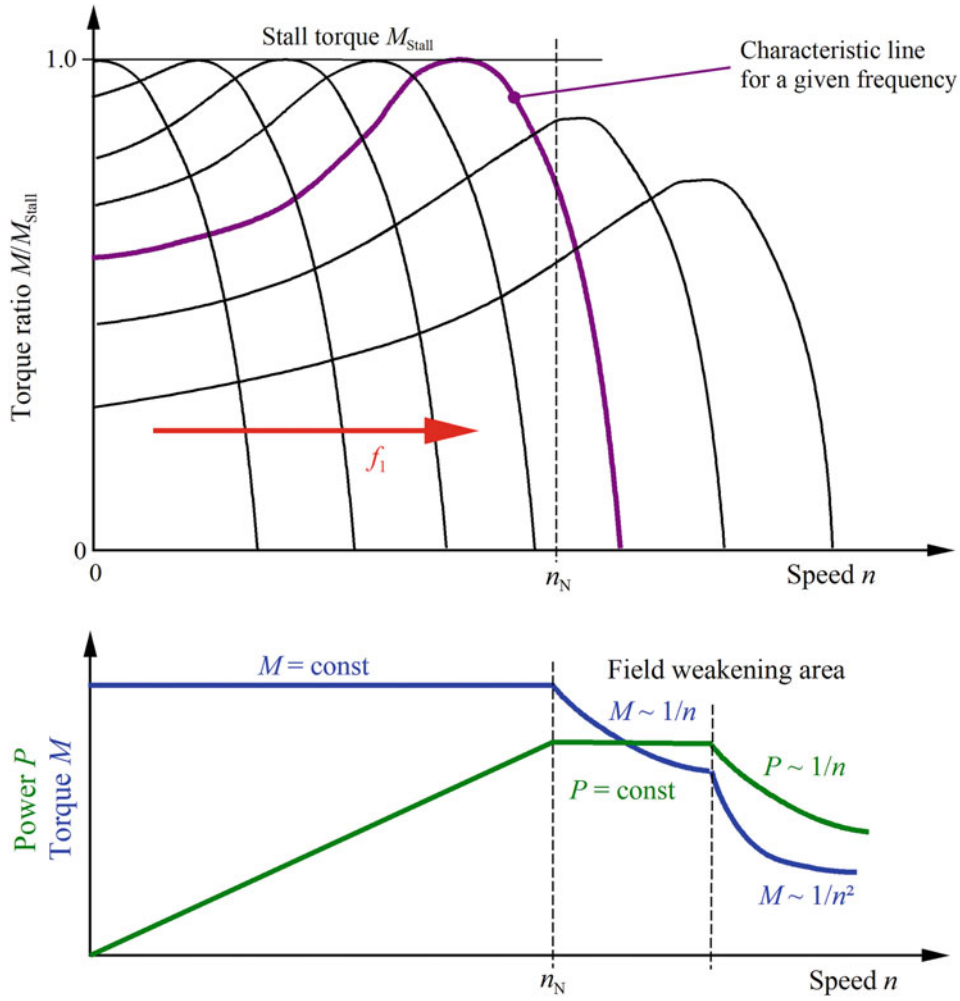

Fig. 3.23 Characteristic curves of the frequency-controlled asynchronous machine. [2]

Fig. 3.10 no longer play a role due to the different power systems in Europe, i.e. there is no longer any need to change locomotives at national borders.[11]

In Fig. 3.23, the torque-speed characteristic at a given supply frequency is shown in purple in the upper figure. If three-phase current of variable frequency is supplied to the motor, the torque output can be kept constant up to the speed n_N. Above this, the field of the

[11] Unfortunately, it is not only the electricity systems that differ in Europe. The different track safety systems are also a particular obstacle when travelling across national borders. For this reason, it is not possible to travel across all national borders in Europe today without changing locomotives.

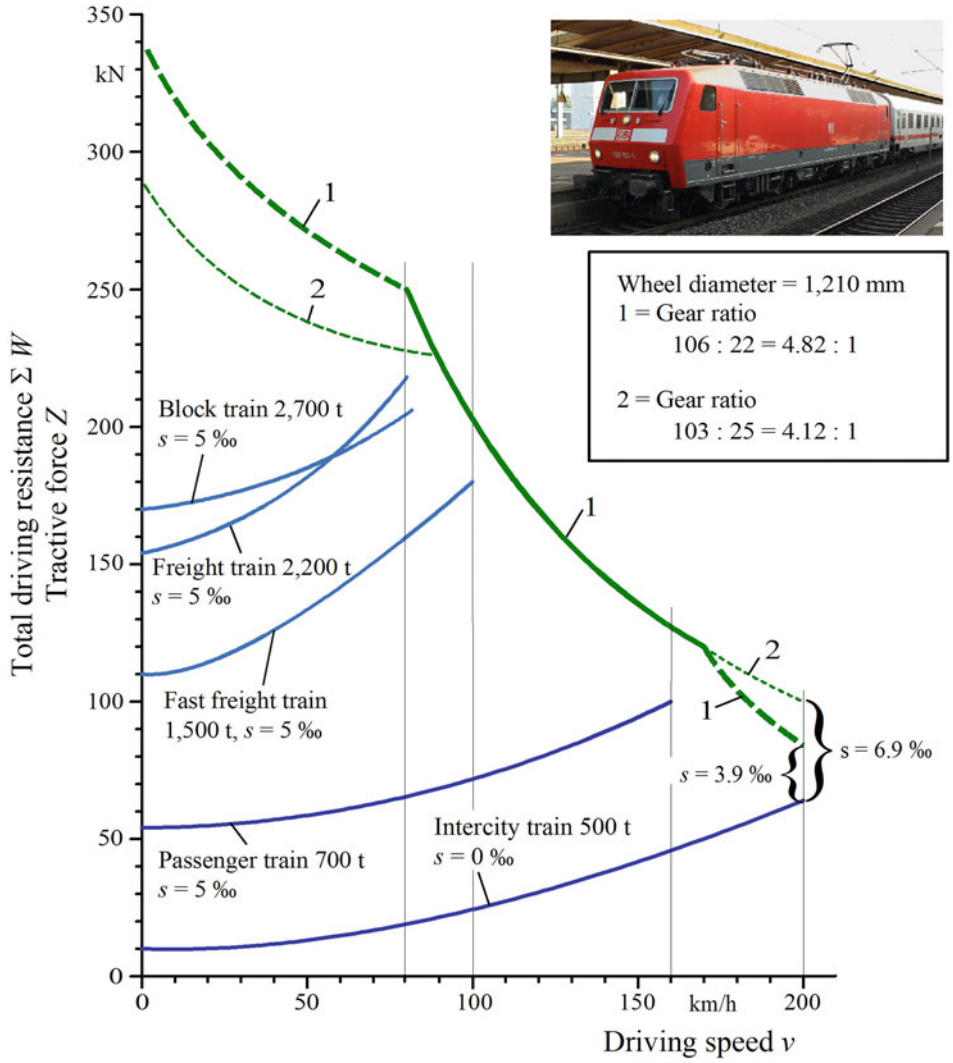

Fig. 3.24 Tractive effort-speed diagram of the Bo′Bo′ class 120.1 electric locomotive with three-phase drive technology. (Characteristic diagram according to: Rappenglück, W.: Die Serienlokomotive Baureihe 120.1. Eisenbahn Ingenieur Kalender '90, Tetzlaff-Verlag, Darmstadt (1989), pp. 247–266)

motor must be weakened, e.g. by series resistors. Thereby the asynchronous machine is a machine of constant power. At even higher speeds, the power decreases with the speed.

Figure 3.24 shows the tractive force/speed diagram of DB class 120.1, which was the first series-produced electric locomotive with three-phase drive technology. In addition to the lines of tractive effort, the lines of driving resistance for various types of trains are also shown. The class 120 was planned as a universal locomotive. Locomotives were procured

with two different gear ratios between the motor and the wheel (not switchable!). However, the idea of only one type of locomotive for all types of trains could not be realized. The operational advantage of a universal locomotive would be that it could be used for fast passenger trains during the day and for heavy freight trains at night. This would result in a high capacity utilization and a lower need for locomotives.

Figure 3.24 no longer distinguishes between short-time power, hourly power and continuous power. In DB's long-distance network, new and upgraded lines mean that trains are now driven more frequently at high or maximum speed, so that the motors have to run at maximum power for about 2/3 of the journey time. 40 years ago, only 20% of the time was covered at maximum power [43]. A distinction between continuous power and short-time power is therefore no longer meaningful.

Figure 3.25 shows the characteristic diagram of an electric locomotive from the Bombardier TRAXX[12] family. The class 145 is used for passenger and freight transport. On the basis of TRAXX components, Bombardier builds electric locomotives for various power systems (also as multi-system locomotives) and diesel-electric locomotives. The locomotives are represented in Europe and the USA. For the class 145 only the continuous power characteristic is given. The locomotive has a regenerative brake, i.e., kinetic energy is converted into electrical energy during braking and fed back into the catenary system.

3.2.4 Mechanical Part of the Electric Drives

It has already been mentioned that in the case of electric rail vehicle drives only a fixed transmission ratio is required between the motor and the driving wheelset. The oscillation excitation due to horizontal and vertical track unevenness (see Chap. 5) causes the wheelset mass to oscillate. This results in forces on the track. In order to limit these forces, the wheelset mass must be as small as possible. An unsprung motor connected to the wheelset should therefore have a mass as low as possible or the running speed must not be too high. For this reason, a constructive attempt is made to decouple the electric traction motor from the wheelset mass. Figure 3.26 presents the most important design principles of the mechanical part of electric drives.

The traverse-bearing drive is the oldest and simplest type of motor connection to the wheelset. Half of the mass of the traction motor is supported directly on the wheelset shaft via roller bearings. On the opposite side, the motor is usually spring-mounted in the bogie frame (or in the vehicle frame on vehicles without bogies). On a mainline locomotive, the unsprung mass is thus 4.5–5 t per wheelset. The travers-bearing drive was used on tramcars and on locomotives and railcars with low to medium maximum speeds. Due to the lower mass of three-phase motors, the traverse-bearing drive is used again today, e.g. in the

[12] According to Bombardier's definition, TRAXX stands for "*Locomotives Platform for Transnational Railway Applications with Extreme Flexibility*".

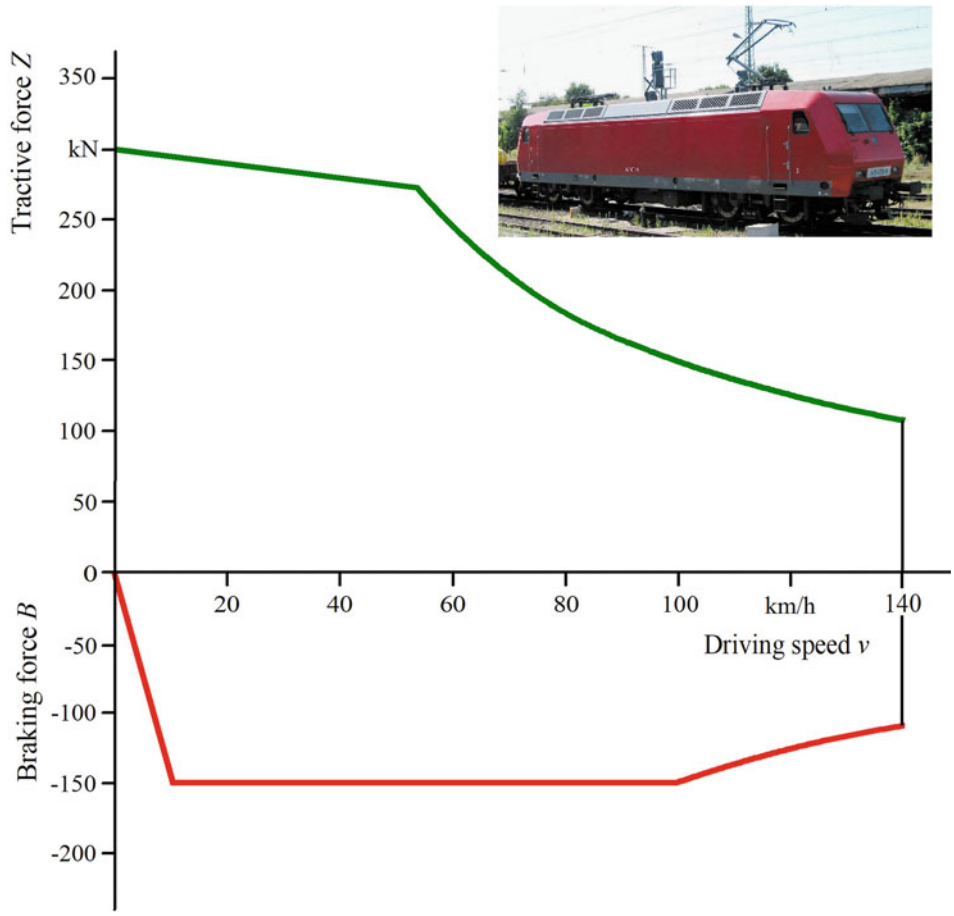

Fig. 3.25 Tractive force and braking force characteristics of the Bo′Bo′ electric locomotive class 145 of DB. (Characteristic diagram according to Bombardier documents)

TRAXX family of locomotives for locomotives with maximum speeds of up to 140 km/h. Figure 3.27 shows the design of the class 145 trolley drive.

A further development of the axlebox drive is the hollow shaft axlebox drive (Fig. 3.26 centre), which is used on DB locomotives as a rubber ring spring drive. Here the motor is mounted on the wheelset side on a hollow shaft through which the wheelset shaft passes. The hollow shaft has star-shaped outriggers on the outside on both sides, with which it is connected to the driving wheels via rubber elements (Fig. 3.28). The rubber elements allow vertical and axial spring travel; the motor is therefore fully cushioned relative to the wheelset. Vibrations are damped by the material damping of the rubber. In addition, rotation angles between the hollow shaft and the driving wheels are possible. This means that the motor can already perform small angles of rotation during heavy starting processes,

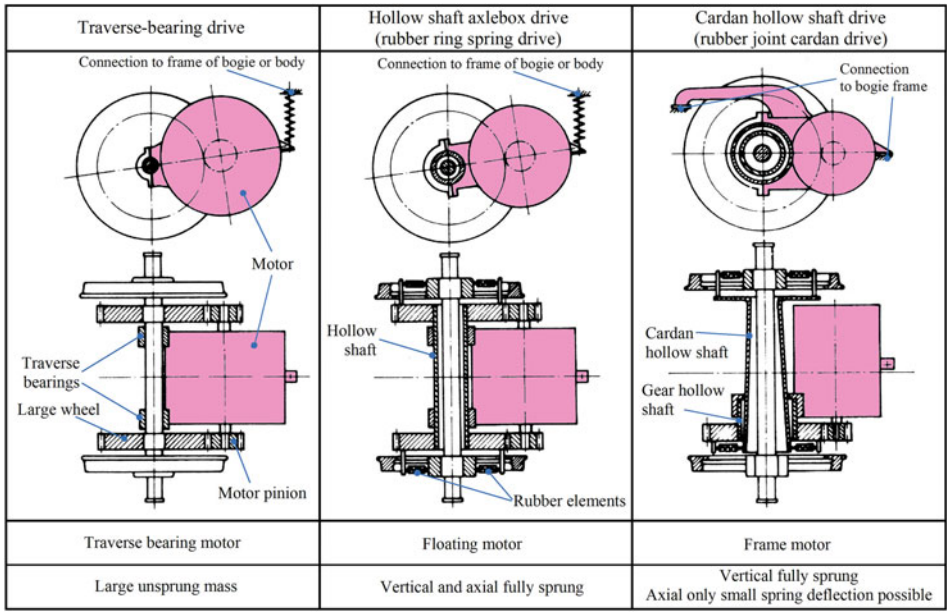

Fig. 3.26 Design principles of the mechanical part of electric drives. [43]

even if the driving wheels are still at rest. This prevents excessive loading of individual motor windings with high motor currents.

A similar design solution for coupling the motor to the wheelsets is the two-axle longitudinal drive for trams, metro and underground trains, Fig. 3.29. The longitudinal DC motor drives a hollow shaft via two angular gears, which are connected to the wheelset shaft by means of a so-called wedge pack coupling via rubber elements. The motor is thus spring-mounted in relation to the wheelsets. Figure 3.29 also shows the rubber-sprung design of the wheel (see Chap. 1).

In traction units with high maximum speeds (>200 km/h), the traction motors are usually mounted in the bogie frame. Due to the suspension between wheelsets and bogie frame (primary suspension; see Chap. 5) there are relative movements between bogie frame and wheelset which have to be compensated by the connection between motor and wheelset. The cardan hollow shaft drive was developed for this purpose. A cardan shaft, which is designed as a hollow shaft for space reasons, is arranged between the output shaft of the gearbox, which is designed as a hollow shaft, and the wheelset shaft. It includes the wheelset shaft and is connected to a driving wheel on one side via articulated levers, and to the hollow gearbox shaft of the motor output on the other side via articulated levers, Fig. 3.30. The hollow cardan shaft lies inside the hollow gearbox shaft, see also Fig. 3.26. The ICE-1 drive heads have solid steel brake discs; the brake linings are made of sintered metal. The gears between the motor shaft and the gear shaft are arrow toothed: helical

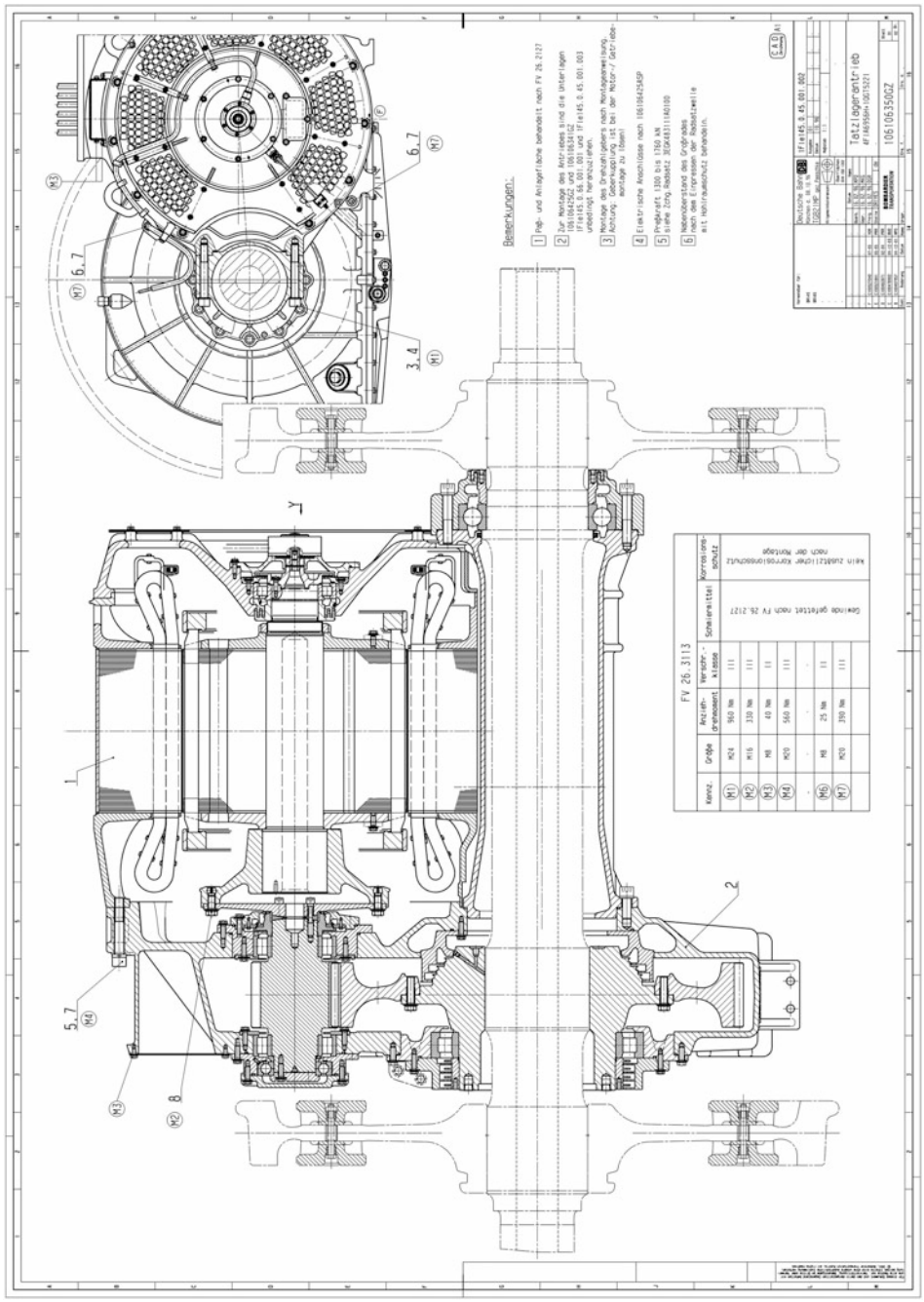

Fig. 3.27 Traverse-bearing drive of the TRAXX class 145 locomotive. (Drawing: Bombardier)

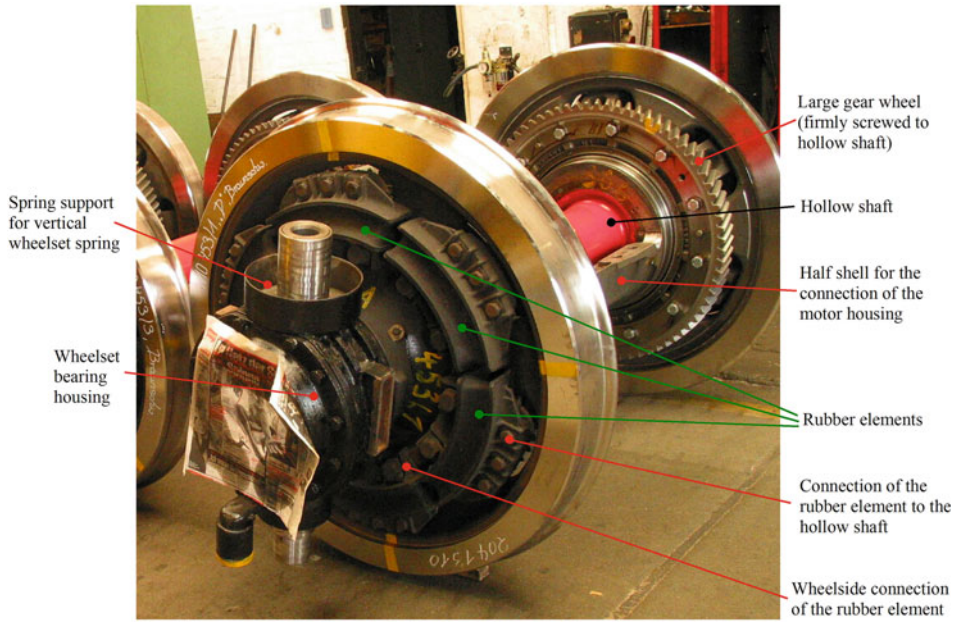

Fig. 3.28 Rubber spring drive (hollow shaft axlebox drive) of the DB class 110 electric locomotive

gearing results in narrower wheels than straight gearing. However, helical gearing results in an axial force. Due to the opposite direction of the teeth in the case of arrow toothed gearing, the axial forces cancel each other out.

Figure 3.31 shows the drive arrangement of the TGV.[13] The TGV has two power cars with the axle arrangement Bo′Bo′, between which the intermediate cars are arranged on Jacobs bogies (see Chap. 5). The traction motors are mounted in the bogie frame. The relative travels between the wheelset and the motor are balanced by a cardan shaft with two universal joints and a tripod length extension. A two-stage reduction gear is arranged between the motor and the cardan shaft. As a result, the rotational speed of the cardan shaft is lower than that of the engine. The cardan shaft transmits a torque of 3000 Nm. It drives into the final drive, which contains another reduction stage and increases the torque. Only the mass of the final drive and half the mass of the propshaft rest unsprung on the wheelset. The tripod length extension ensures low axial extension forces (approx. 500 N) of the cardan shaft.

[13] TGV: Train à Grande Vitesse – high-speed train of the French national railway.

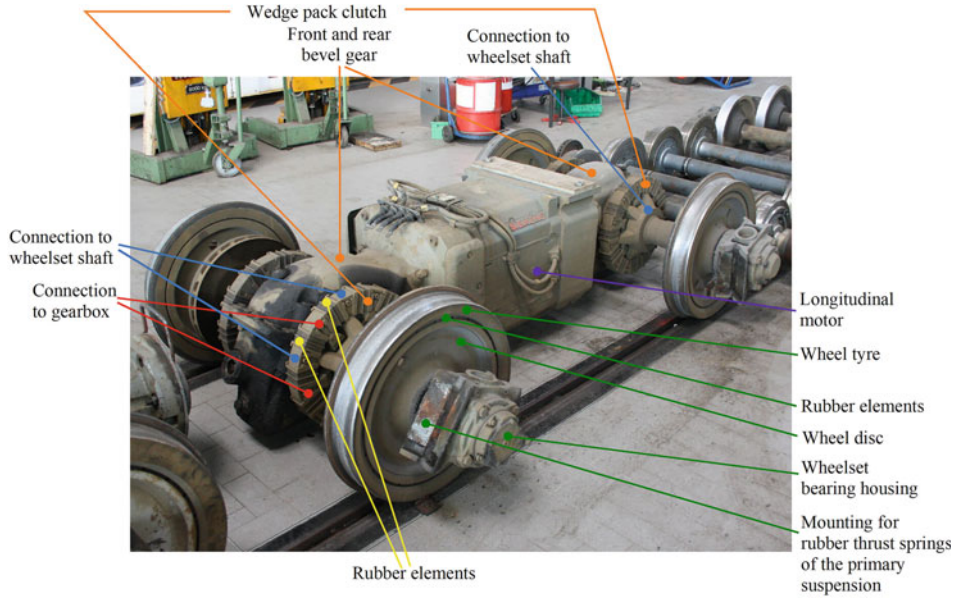

Fig. 3.29 Two-axle longitudinal drive for trams with wedge pack clutch; self-ventilated DC motor 120 kW

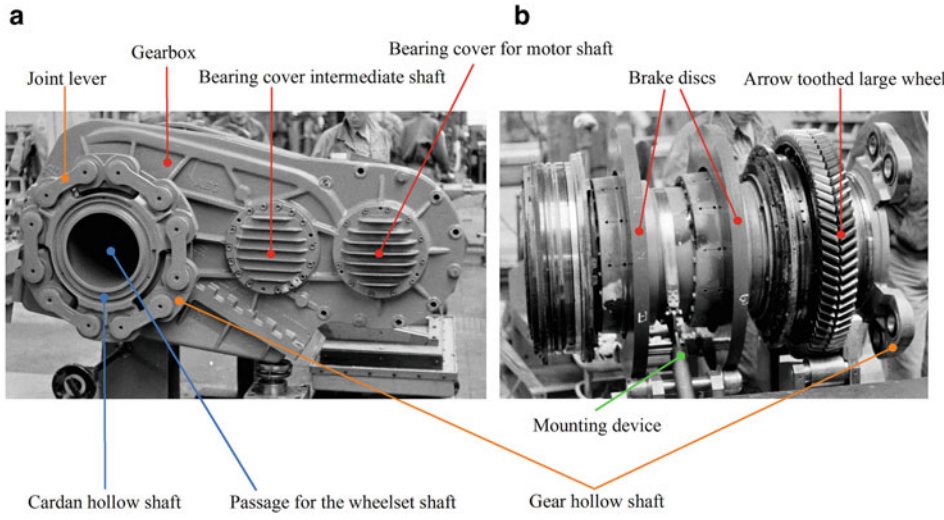

Fig. 3.30 Cardan hollow shaft drive of the ICE-1. (**a**) Side view of the removed gearbox, (**b**) View of the outer hollow shaft of the gearbox output drive

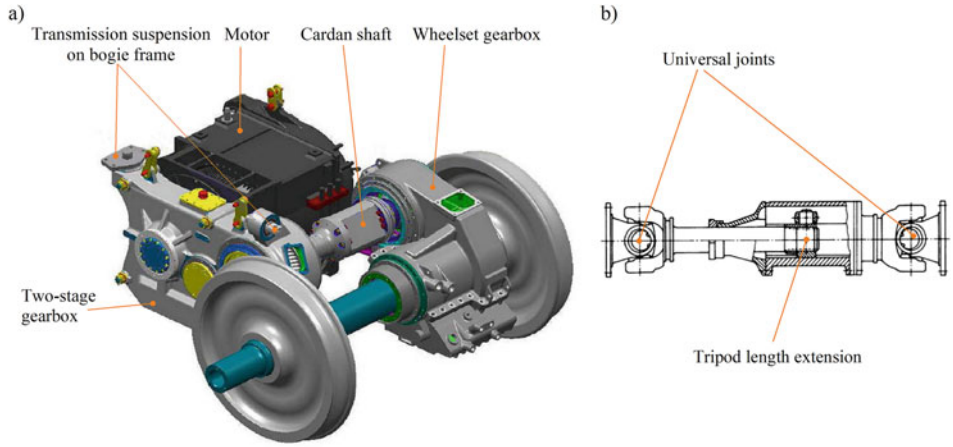

Fig. 3.31 Cardan drive of the TGV. (**a**) Motor, gearbox and wheelset arrangement (according to Alstom drawing), (**b**) Cardan shaft with tripod length extension. (From: von Seherr-Thoss, H.-Chr.; Schmelz, F.; Aucktor, E.: Gelenke und Gelenkwellen. Calculation, design, applications. Vieweg Verlag, Wiesbaden (2002), p. 325)

3.3 Internal Combustion Engine

The spark-ignition internal combustion engine was invented by Nikolaus Otto[14] in 1867. Named the Otto engine after its inventor, the internal combustion engine was initially intended as a stationary drive using town gas as fuel. Gottlieb Daimler[15] built the first four-stroke gasoline engine for liquid fuel, thus making vehicle propulsion by means of the internal combustion engine possible. The petrol engine was not able to establish itself as a drive for rail vehicles, although there were numerous railcars and (small) locomotives with petrol engines in the 1920s and 1930s. One example is shown in Fig. 3.32: The rail bus developed by the Waggonfabrik Wismar in 1932 had two Ford four-cylinder petrol engines from the automotive industry, which were housed in front structures on the body of the car. Each engine drove the respective front wheel set via a four-speed manual gearbox. The clutch was operated by the driver using a foot pedal. Since the transmissions were also from the automobile industry and had only one reverse gear, there was one motor for each of the two directions of travel. Engines with 40 or 50 hp (29 or 37 kW) were installed. The manufacturer of the railcar, Waggonfabrik Wismar, advertised that any Ford workshop could supply the appropriate spare parts and that the engines were only in operation for half

[14] Nikolaus Otto (1832–1891), German inventor and entrepreneur, co-founder of Gasmotorenfabrik Deutz, now Deutz AG.

[15] Gottlieb Wilhelm Daimler (1834–1900), German engineer and entrepreneur, founded Daimler-Motoren-Gesellschaft, now Daimler AG.

Fig. 3.32 "Hanover" type railcar of the Waggonfabrik Wismar (Wismar wagon factory) with a Ford petrol front-mounted engine at each end of the vehicle

of the vehicle's travel distance. With these railcars, the expensive steam operation could be replaced on branch lines and narrow gauge railroads. After all, 78 vehicles of this type could be sold; the last ones were in service until the end of the 1960s. Several are still available on museum railways.[16]

In 1892 Rudolf Diesel[17] built the first compression-ignition internal combustion engine at MAN in Augsburg. As early as 1913, the first diesel locomotive based on plans by Diesel and Klose[18] was delivered by Borsig-Lokomotivwerke in Berlin and Gebr. Sulzer AG in Winterthur, Fig. 3.33. In this locomotive, direct drive was chosen, i.e. the crankshaft of the main diesel engine was connected to the driving wheels of the locomotive via driving rods. Since the diesel engine cannot start from a standstill (no torque at zero speed; see Fig. 3.34), it was started with compressed air generated by a compressor driven by the auxiliary diesel engine. At about 8–10 km/h speed, the main diesel engine was ignited by fuel injection. The locomotive did not prove itself. Due to the expansion of the compressed air during the starting process in the working cylinders, they cooled down so much that the ignition of the engine did not work safely. Other locomotives with direct drive did not prove themselves either [18].

The problem of the internal combustion engine drive of rail vehicles consists in its characteristic diagram: It does not deliver any torque at zero rotational speed and its running is only quiet and smooth above a certain speed, the idling speed. Figure 3.34 shows the characteristic diagrams of a diesel engine.

[16] Bohlmann, D. Th.: Die Wismarer Schienenomnibusse der Bauart Hannover. Zeunert-Verlag, Gifhorn (1976).

[17] Rudolf Diesel (1858–1913), German engineer.

[18] Adolf Klose (1844–1923), chief engineer of the Royal Württemberg State Railways.

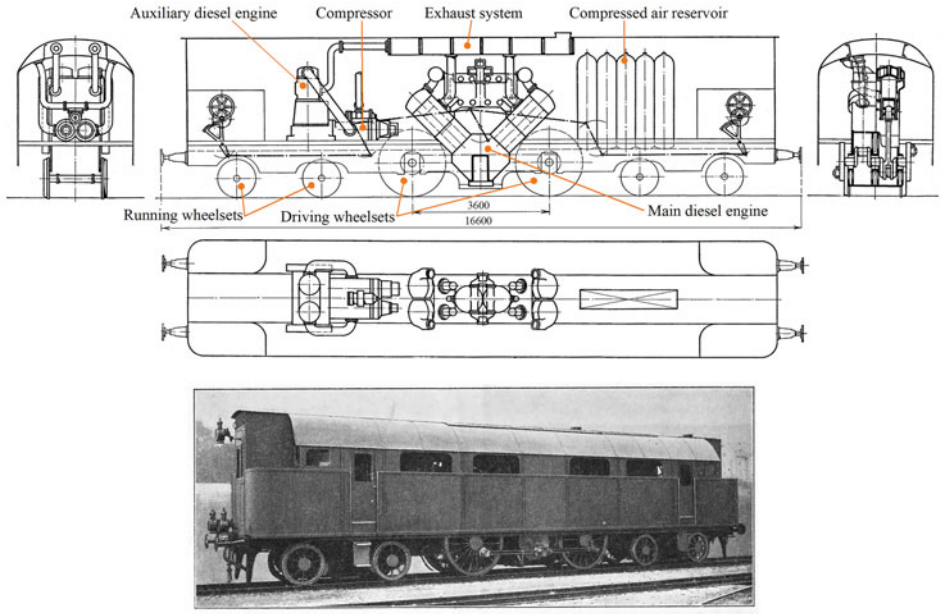

Fig. 3.33 First large diesel locomotive in the world (with direct drive) by Diesel and Klose. (After: Sternenberg, F.: Die erste Thermolokomotive. Z-VDI (1913) pp. 1325–1330])

You can see the so-called speed gap, which must be bridged in vehicles by a speed converter (clutch). The remaining characteristic diagram of the diesel engine also bears little resemblance to the "ideal delivery characteristic diagram" discussed at the beginning. For this reason, the diesel engine in vehicle operation must also be equipped with a torque converter in addition to the speed converter in order to adapt its characteristic map to the demand characteristic map. A particular problem in railway operation is posed by gear switching operations, which interrupt the tractive force of the traction unit and can lead to longitudinal jolts in train formations. The aim in the development of power transmission systems, especially for internal combustion engine locomotives, was therefore the uninterrupted transmission of torque. However, as already shown in the example of the Wismar railcar, the use of manual transmissions is possible for light railcars.

The diesel engine (as well as the petrol engine) delivers a braking torque (Fig. 3.34), the so-called drag torque, during coasting operation. It results from the internal friction torques of the engine (piston sealing, bearing friction, friction at the valve control, etc.). When the fuel supply is interrupted, internal combustion engines therefore deliver a braking torque. In the case of diesel engines, the braking torque can be further increased by the engine brake. Here, the engine draws in air, compresses it and pushes it out via a throttle valve (see dashed braking characteristics in Fig. 3.34). The engine brake is used on diesel railcars, but not on locomotives.

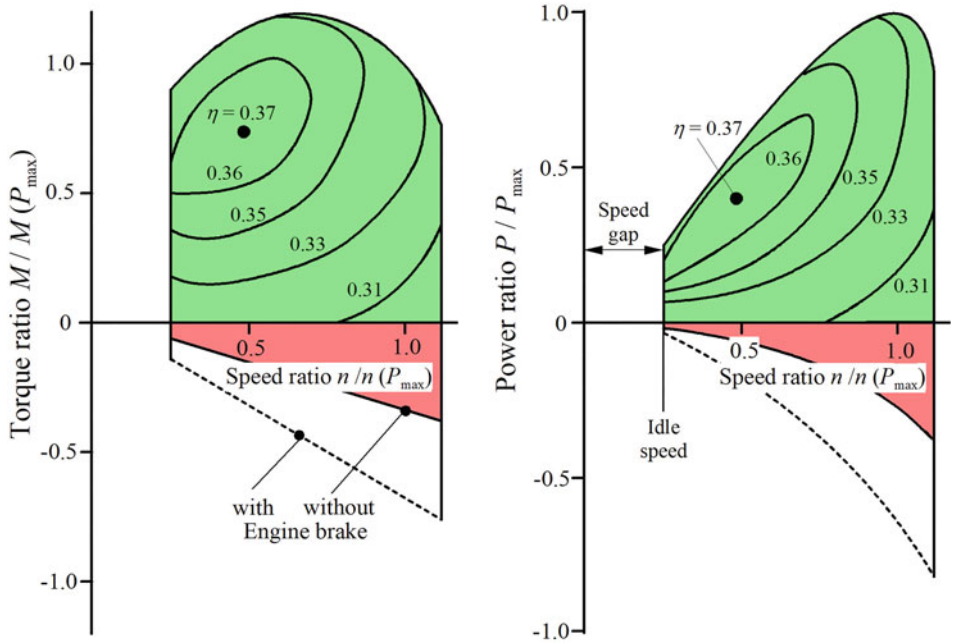

Fig. 3.34 Characteristic diagrams of a diesel engine. (According to [46])

3.3.1 Mechanical Power Transmission

In vehicles with engine outputs of up to about 400 kW per engine unit, i.e. especially in light railcars, mechanical power transmission by means of a stepped gearbox is common. Figure 3.35 shows the engine characteristic converted in the stepped gearbox; the engine characteristic in the four gears is shown as green fields. It can be seen that an adaptation to the demand characteristic has taken place. The speed gap at start-up is bridged by a clutch. In this process, part of the engine power is converted into heat until the two halves of the clutch are in synchronism. When changing from one gear to the other, the connection between engine and transmission is interrupted by the clutch. The higher the tractive forces have to be at low speeds or the higher the top speed is to be, the more gear ratios a stepped transmission must have.[19]

Since, as already mentioned, the interruptions in tractive force occurring when changing gears are undesirable in a train set, so-called powershift transmissions are used in rail vehicles, Fig. 3.36. In the six-speed transmission shown, there are four electromagnetically actuated multi-plate clutches with which individual gear pairs can be switched into the torque flow. In first gear, for example, the torque flow goes from the input shaft via clutch

[19] This is why, for example, heavy trucks have up to 12 gear steps because of the high tractive forces and cars with a high top speed have, for example, six gear steps.

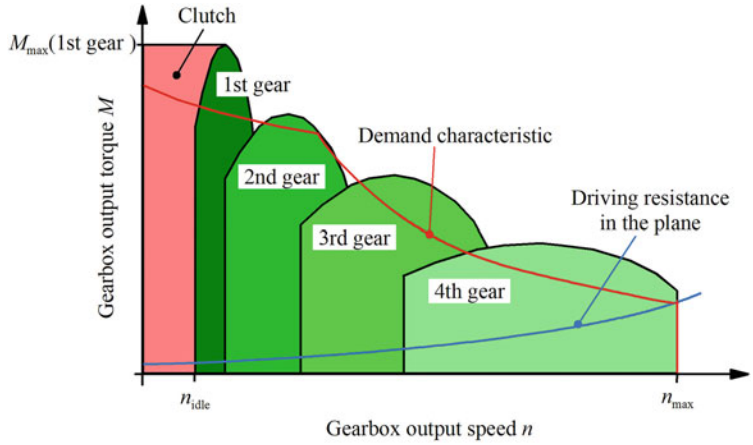

Fig. 3.35 Vehicle map with diesel engine, clutch and four-speed gearbox

a and gear pair **I** to the intermediate shaft and from there via clutch **s** and gear pair **IV** to the output shaft. When shifting into second gear, clutch **a** is disengaged, while at the same time clutch **b** is engaged and the torque flow now occurs via gear pair **II** to the intermediate shaft and via **IV** to the output shaft. By simultaneously disengaging and engaging the magnetic clutches, interruptions in tractive force are avoided.

In the event of a power failure, an emergency gear can be engaged on the gearbox via the claw clutches **k1** and **k2** with the aid of a spanner. In this way, the track can be cleared at reduced speed. This strategy attempts to avoid longer track closures due to vehicle malfunctions.

The transmission shown in Fig. 3.36 was installed in the DB rail buses. The class 798 had two power units of 110 kW each and could haul a trailer and a cab control car at $v_{max} = 90$ km/h. Except for a few examples, the vehicles are no longer in service.

Modern railcars also have mechanical transmissions, but these are often constructed from planetary gear sets. This allows powershift transmissions with many transmission stages to be implemented in a compact design.

Gear drives have relatively high efficiencies. Losses occur due to bearing friction, friction between the meshing teeth and churning losses, as bearings and gears run in an oil bath. Nevertheless, the efficiencies are 92–96%. Another advantage is the rigid connection between input and output, which makes it possible to use the motor brake, which is not the case with hydraulic gearboxes and electric power transmission.

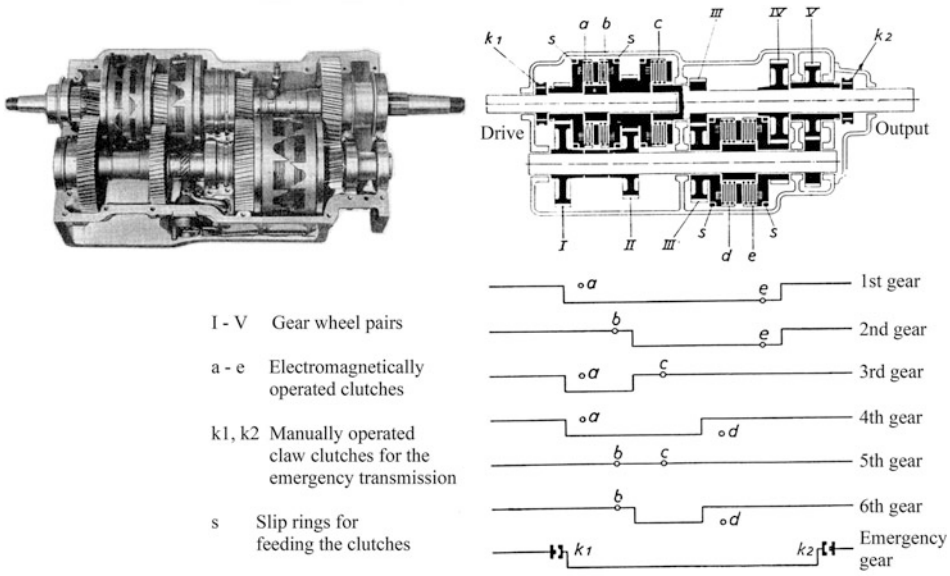

Fig. 3.36 Six-speed powershift transmission for DB class 795/798 rail buses (input power 110 kW). (According to documents of Zahnradfabrik Friedrichshafen)

3.3.2 Hydrodynamic Power Transmission

Purely mechanical power transmission is no longer possible for larger engine outputs. For power transmission in motor ships, FÖTTINGER[20] had already invented the hydrodynamic clutch and the hydrodynamic converter before the First World War. The hydrodynamic clutch is the combination of a (centrifugal-)pump and a turbine in one housing as a speed converter. If the turbine wheel is firmly installed in the housing, this results in a hydrodynamic brake (retarder). With the hydrodynamic converter, a guide wheel is added on which torques can be supported, so that a torque converter is created, see Fig. 3.37.

The characteristic curves of the hydrodynamic clutch and the hydrodynamic converter (also called hydraulic clutch and hydraulic converter or Föttinger clutch and Föttinger converter) are shown in Fig. 3.38. Important are the curves of the output torques, the efficiencies and the power loss.

With the hydraulic clutch (Fig. 3.38a) with constant input speed (pump speed), the efficiency increases linearly with increasing output speed (turbine speed) up to 100%. However, without slip, i.e. without a speed difference between pump and turbine, no torque transmission is possible. Therefore, hydraulic clutches are designed in such a way that at the nominal output torque the slip $s = 1 - (n_{II}/n_I)$ is approx. 3%. This results in the

[20] Hermann Föttinger (1877–1945), German engineer, inventor and university lecturer.

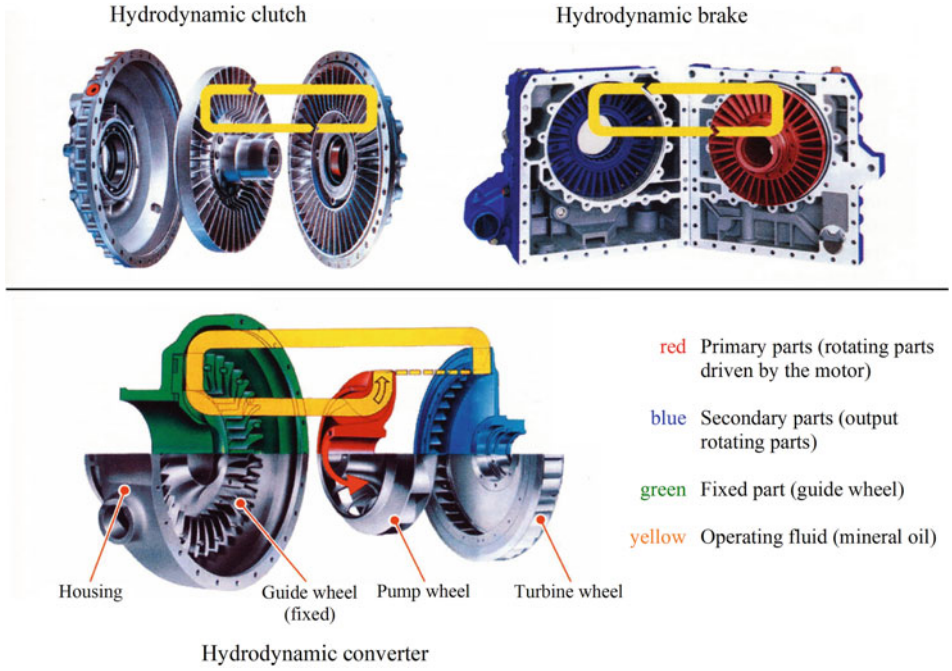

Fig. 3.37 Hydrodynamic clutch, hydrodynamic brake, hydrodynamic converter. (According to drawing of Voith)

efficiency $\eta = 1 - s$ at 97% [18]. The power loss of the clutch, which must be dissipated as heat, is shown as a red area in the characteristic diagram in Fig. 3.38a.

The situation is different for the hydraulic converter (Fig. 3.38b): First of all, the output torque can be greater than the input torque at low output speeds and constant input speed. However, the efficiency curve has the form of a downward opening parabola, i.e. the efficiency reaches its maximum in the range of medium output speeds. As the output speeds continue to increase, the efficiency drops towards zero. With the hydraulic converter, therefore, only the range of medium output speeds should be utilised, and for start-up also the range from zero output speed to the medium speed range.

In practice, a hydrodynamic transmission therefore consists of a combination of several converters and possibly a clutch, Fig. 3.39. One converter serves as a starting converter with a large transmission ratio. One or two further converters are used as march converters, whereby the second march converter can also be replaced by a hydraulic clutch. In this way, a favourable efficiency curve is achieved. Switching between the converters is done by draining one and filling the other with hydraulic oil.

The design of a two-converter gearbox is shown in Fig. 3.40. The converters are preceded by a so-called high drive, with which the input speed is translated into high speed compared to the engine speed, since the converter diameter can be kept smaller at high pump speed. The auxiliary machine drive (15) is required for the brake air compressor,

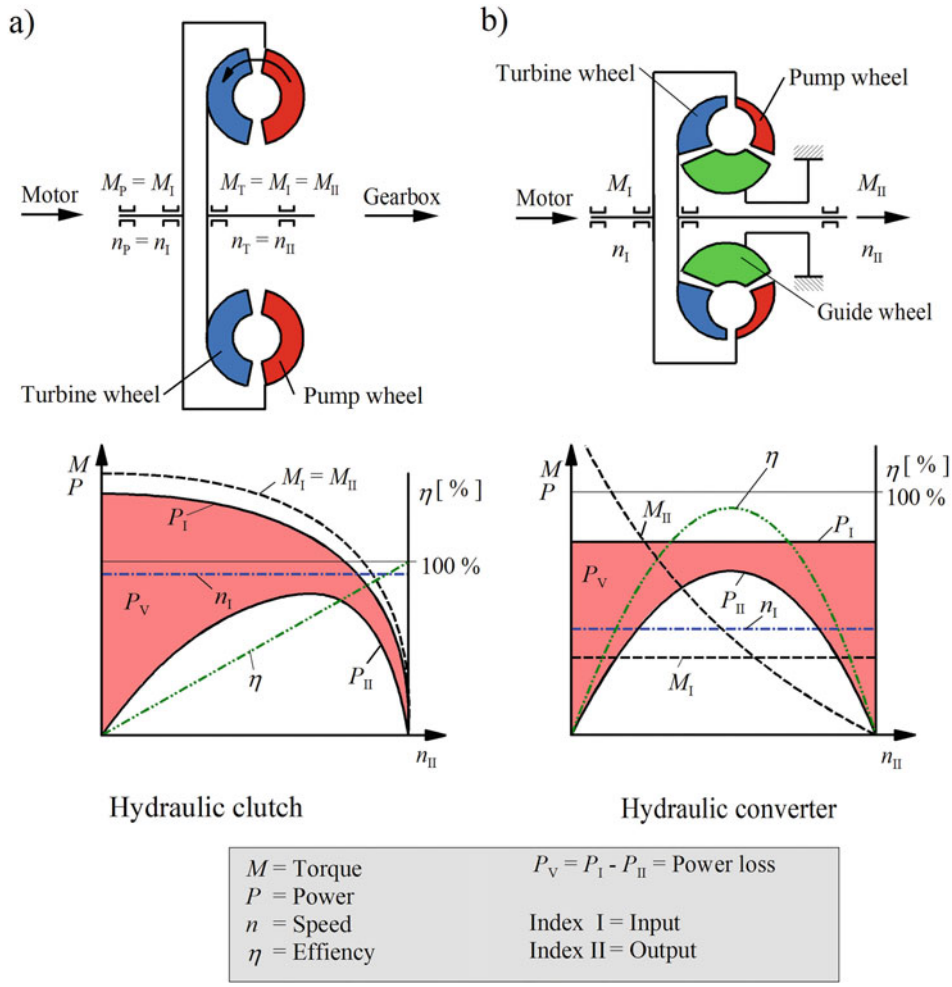

Fig. 3.38 Characteristics of the hydraulic clutch (**a**) and the hydraulic converter (**b**). (According to [43, 46])

radiator fan and alternator. The sliding shaft shown in green in Fig. 3.40 and the reversing wheels (5, 7) are used to reverse the direction of travel. They can only be switched when the vehicle is stationary.

Figure 3.41 shows the overall arrangement of all units of a heavy shunting diesel locomotive. A central driver's cab is useful for shunting service so that the driver does not have to change the driver's cab when changing the direction of travel. Narrow, low engine front ends ensure that the driver has a good view of the buffers. At first glance, it is astonishing how little space the diesel engine and converter gearbox take up in the locomotive body. From the converter gearbox, the torque is transmitted via cardan shafts

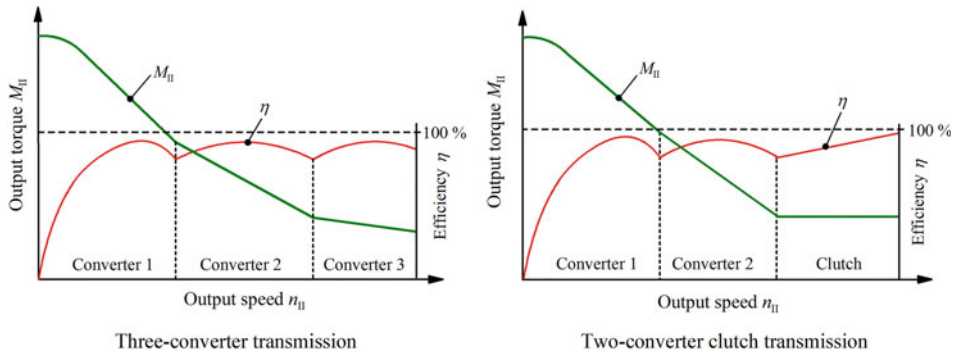

Fig. 3.39 Torque and efficiency curve for torque converter transmissions. (According to [43])

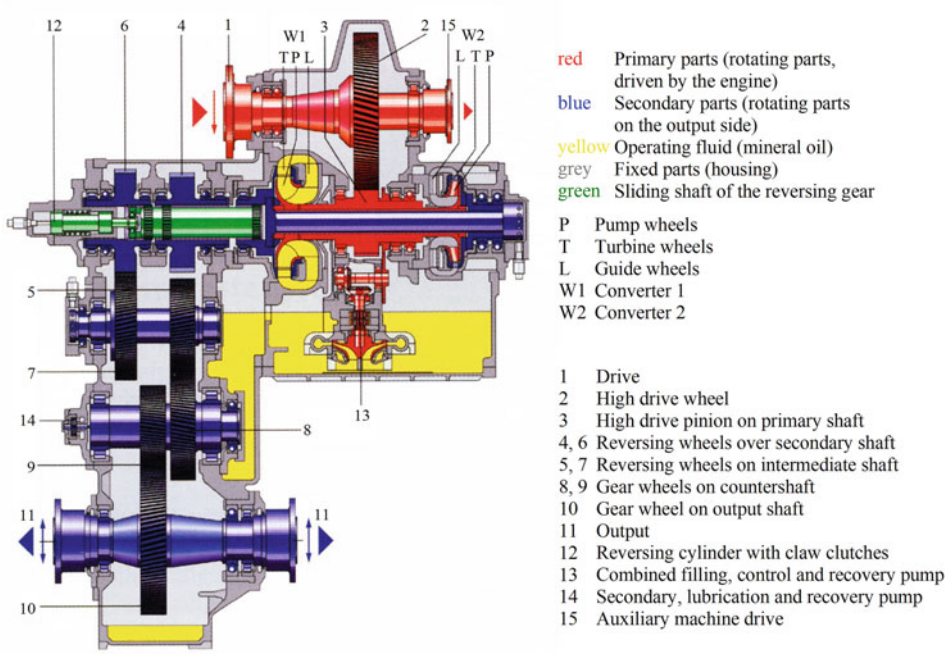

Fig. 3.40 Two-converter transmission L620r from Voith. (According to Voith drawing)

to the final drives of the inner wheelsets of the two bogies. These two final drives each have a through drive via which cardan shafts lead to the final drives of the outer wheelsets. All wheelsets are thus connected in a rotationally fixed manner, so that the axle formula for this locomotive is B′B′.

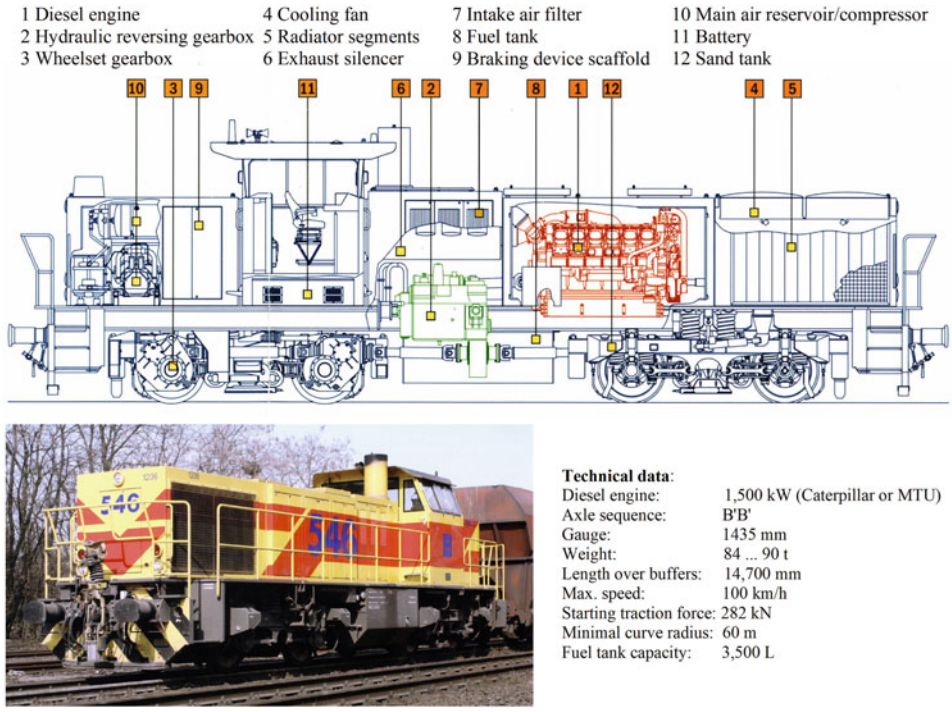

Fig. 3.41 Diesel-hydraulic locomotive G 1206 from Vossloh Locomotives for mainline service and heavy shunting service. (According to Vossloh documents)

The converter transmission here is a turbo reversing transmission, i.e. there are converters for each direction of travel. This makes it possible to switch from forward to reverse during manoeuvring without stopping for a long time and without mechanical switching. Only the corresponding converters are emptied or filled.

We have seen that the hydrodynamic converter can be used very well as a continuously variable transmission, but with the disadvantage of poor efficiency outside of medium output speeds. During start-up, the disadvantage is not so serious, since even a mechanical clutch gives off a large part of the supplied motor energy as heat during the engagement process.

A way out of the problem of poor efficiency in the higher speed range is offered by the differential converter transmission (DIWABUS transmission from Voith). This transmission is used in city buses and railcars (e.g. in the Regio-Shuttle of Stadler Rail). Its principle is based on power split by means of a differential gear, which in the case of the DIWABUS transmission is designed as a planetary gear so that the input shaft is coaxial with the output shaft, Fig. 3.42.

The motor drives the drive shaft, on the left in Fig. 3.42. The transfer case brake is released. At the moment of starting, the output shaft (light blue in Fig. 3.42) is stationary

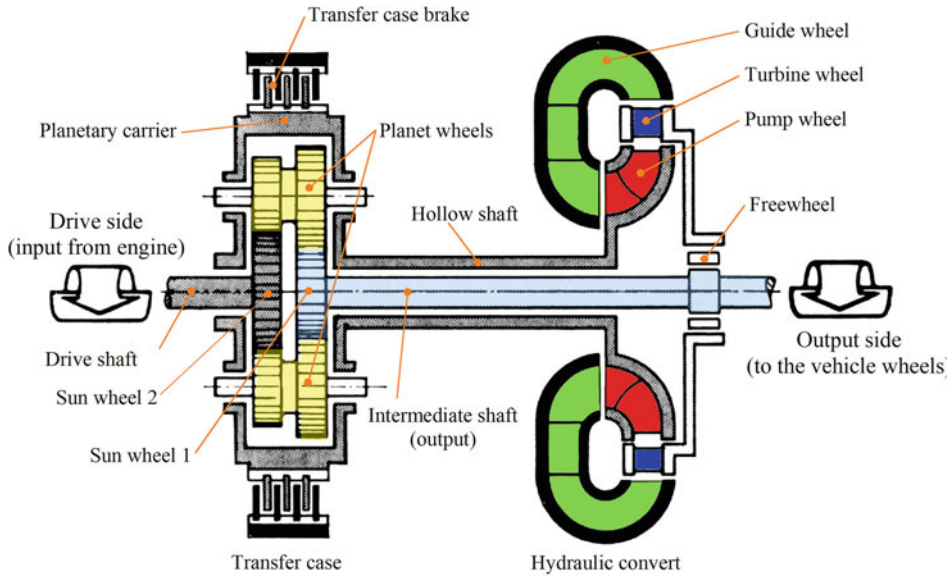

Fig. 3.42 Differential converter gearbox with power split. (According to [61])

because the vehicle's drive wheels are not turning. Along with the output shaft, the sun wheel **1** is also stationary. All the power is now transmitted to the pump wheel of the converter via the planet carrier and the hollow shaft which is connected in a rotationally fixed manner. The turbine starts to rotate and drives the output shaft via the locked freewheel. This also causes the vehicle's drive wheels to rotate. At this point, the large gear ratio of the converter is utilized for starting. As the speed of the output shaft and sun wheel **1** increases, an increasing proportion of the engine power is transmitted to the vehicle wheels via the mechanical branch; the power proportion of the converter decreases.

When the converter has exceeded the maximum of the efficiency curve, the transfer case brake (multi-disk brake) is engaged and thus the planet carrier and the pump wheel are firmly braked. All engine power is now mechanically transmitted to the vehicle wheels with good efficiency. Due to the freewheel, the output shaft can rotate freely when the turbine wheel is stationary. Due to the now rigid mechanical coupling between the engine and the drive wheels, the engine brake can also be used as a wear-free continuous brake, which is useful, for example, in city bus applications, but also for light railcars.

Hydrostatic power transmission by means of a hydraulic pump and hydraulic motor, which is widely used for agricultural and construction machinery, is hardly ever used for traction units in the rail vehicle sector. For this reason, it will not be discussed further here.

3.3.3 Electrical Power Transmission

Electric power transmission was already used for railcars more than one hundred years ago – initially, sufficiently powerful diesel engines were not available for locomotives. Until World War II, diesel locomotives with electric power transmission were developed, especially in the USA. In the 1950s, diesel traction largely replaced steam locomotives in the USA. This development was promoted there by the low cost of diesel oil as well as by a larger loading gauge of the railways and higher permissible axle loads. This meant that heavy and large, slow-running diesel engines from marine technology could be installed in the locomotives. The higher weight of electrical power transmission at the time also did not play a role as great as in Europe. The development in the former Soviet Union was similar to that in the USA. In Germany, electric power transmission for diesel railcars and diesel locomotives did not become established in larger numbers until the development of three-phase drive technology in the 1980s. Until then, diesel hydraulics dominated in Germany. The considerations were the more compact design and the lower weight.

In diesel-electric power transmission, the diesel engine drives a generator that supplies electrical energy for the electric traction motors. The oldest system is the direct current generator, which feeds direct current motors. Here, the DC catenary is replaced, so to speak, by the diesel engine and DC generator. The interaction of diesel engine and DC generator is explained in Fig. 3.43.

The generator current is plotted horizontally, the generator voltage vertically. The connection between current and voltage is represented by the thinly drawn current-voltage curves as characteristic curves of the generator. The power consumption of the generator is obtained from the product of current and voltage: $P_{\mathrm{Gen}} = U_{\mathrm{Gen}} \cdot I_{\mathrm{Gen}}$, which can be seen as the blue characteristic curve. In the middle range, the generator power (dashed blue curve) is higher than the engine power (green straight line) when the engine is running at constant (maximum) power. In this range, the engine speed would decrease and the engine would eventually stall. Therefore, in the range $P_{\mathrm{Gen}} > P_{\mathrm{Mot}}$, the generator power must be reduced by field weakening – connecting resistors in front of the field winding. If, on the other hand, the generator power were to be designed smaller so that $P_{\mathrm{Gen}} = P_{\mathrm{Mot}}$ only at one operating point, the power of the diesel engine could not be utilized in wide ranges; it could only be operated in the partial load range. The red curve in Fig. 3.43 shows the efficiency curve; it lies between 70 and 80%.

The principle structure of a diesel locomotive or diesel railcar with three-phase power transmission is shown in Fig. 3.44. Compared with the principle of the electric locomotive, the power supply system is replaced by a diesel engine and an asynchronous generator. The possible modular structure of traction unit families should be pointed out here once again.

As there is no mechanical connection between the traction wheel and the diesel engine in the case of electric power transmission, the engine brake cannot be used. However, as indicated in Fig. 3.44 by the dashed red arrows, wear-free braking is possible by running the electric traction motors as generators and converting the energy generated into heat in

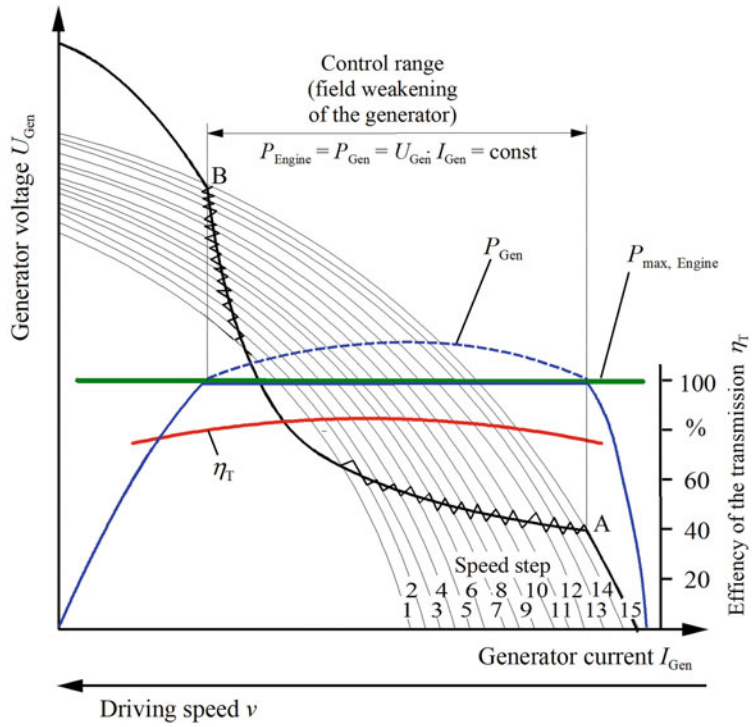

Fig. 3.43 Diesel-electric power transmission with direct current generator and direct current motors; current-voltage curves and efficiency of the transmission. (According to: Gössl, N.: Dieselhydraulik und Dieselelektrik. Eisenbahntechnische Rundschau 4 (1953) H. 10)

braking resistors. In this case, the braking resistor replaces the mains supply for regeneration that is present in an electric three-phase locomotive.

With three-phase power transmission, the efficiency can be increased considerably compared to the values shown in Fig. 3.43. In particular, a better adaptation of the power transmission to the engine characteristic curve is possible than with diesel hydraulics, Fig. 3.45.

Figure 3.45 shows the performance maps of three diesel engines including the curves of equal consumption ("shell curves"). The MTU[21] engines are medium-speed engines; the MaK engine[22] is a low-speed engine. The power consumption curve of the hydraulic transmission is shown in blue with a dashed line. This is the characteristic pump curve, a

[21] MTU: Motoren -und Turbinenunion GmbH, Friedrichshafen; today part of Rolls Royce Power Systems.

[22] MaK: Maschinenfabrik Kiel, today Vossloh Lokomotivtechnik. The construction of diesel engines has since been transferred to Caterpillar.

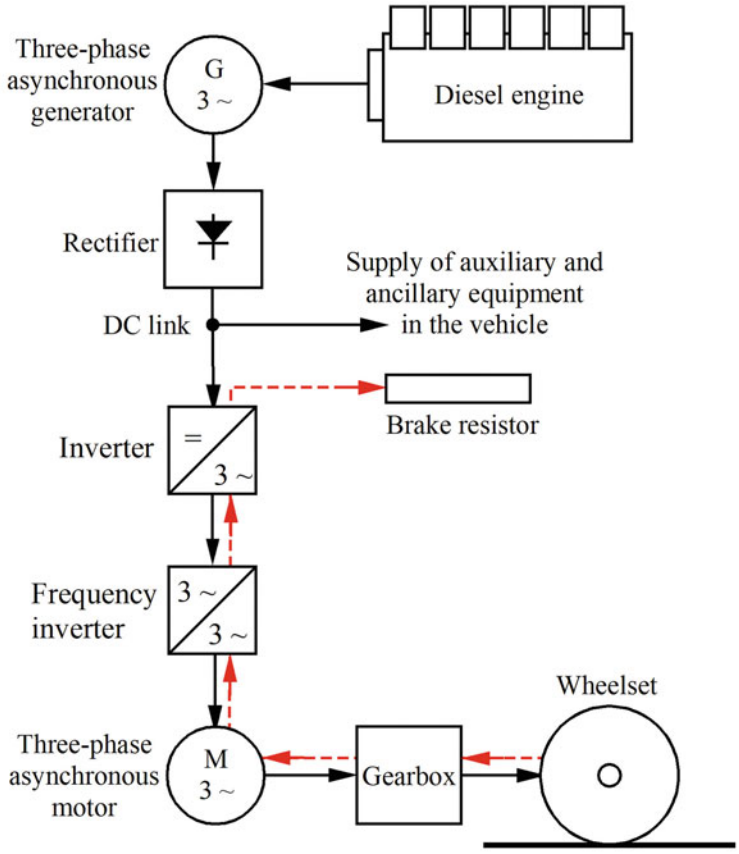

Fig. 3.44 Principle of three-phase power transmission for diesel locomotives

parabola. All points below parabola are possible operating points. The point of lowest consumption in each motor characteristic curve is outside the pump characteristic curve, i.e. the motor cannot be operated with hydraulic transmission at the optimum consumption point. With three-phase transmission, the power consumption curve (drawn in green in Fig. 3.45) can be better matched to the motor curve; the points of minimum consumption are reached in all characteristic diagrams. The table in Fig. 3.45 shows that at 75% power output (frequent in shunting operation!) the motors can run at lower speed with electrical power transmission. This has a favourable effect on the service life of the motors, since the mass forces and not the gas forces are decisive for the mechanical stress. In addition, according to Fig. 3.45, the consumption values are lower with diesel-electric drive.

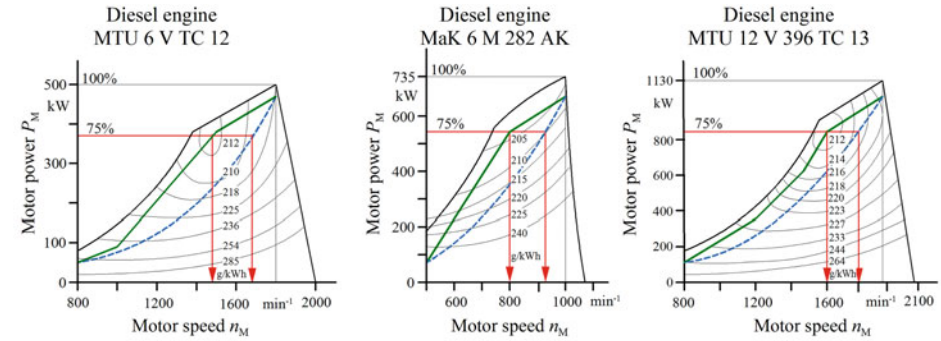

Diesel electric	1480 min⁻¹, 210 g/kWh	800 min⁻¹, 204 g/kWh	1610 min⁻¹, 212 g/kWh
Diesel hydraulic	1670 min⁻¹, 212 g/kWh	930 min⁻¹, 209 g/kWh	1780 min⁻¹, 214 g/kWh

Fig. 3.45 Comparison of three-phase transmission/hydraulic transmission in diesel locomotives: speeds and consumption values of the diesel engines for 75% power. (According to: Teich, W.: Essential system differences between three-phase drive technology and hydraulic transmission. Elektrische Bahnen 81 (1983) H. 4, pp. 124–132)

The question arises as to why traction units with hydraulic transmissions are still being built at all. The reason is the higher investment costs for diesel-electric vehicles.[23] In addition to the specialist personnel for the mechanical components of the vehicles, smaller railway companies often do not have the corresponding specialist personnel for electrical components, in particular for the power electronics.

Figure 3.46 shows the overall construction of a diesel-electric shunting and mainline locomotive. Compared to Fig. 3.41, hardly any serious differences are noticeable, although both locomotives come from different manufacturers. The locomotive shown in Fig. 3.46 has the 12-cylinder MTU engine with the map in Fig. 3.45 on the right. Due to the single axle drive it has the Bo′Bo′ axle arrangement.

It has already been mentioned that traction units are not operated at maximum power all the time. The part-load efficiency of the diesel engine is significantly worse than the efficiency at peak power. This leads to the idea of equipping vehicles with several engine systems and switching individual systems on or off depending on the power requirement. In the case of railcars, the total power is often divided among several engine systems. In this case, however, space considerations are more of a factor, since the systems have to be arranged underfloor, for example, in order to be able to use (almost) the entire length of the vehicle as a passenger compartment. In the case of diesel locomotives, it was initially not possible in the 1950s to achieve high performance using only one engine system. The first heavy diesel locomotive of the DB, the class V 200 (later class 220 or 221), had two engine

[23] An empirical formula states that 1 kg of mechanical components costs about the same as 1 kg of pork, while 1 kg of electrical components costs about the same as 1 kg of veal. On 06/06/2014, 1 kg of veal cutlet cost about €27–€30, while 1 kg of pork cutlet cost €8–€10 (in Germany).

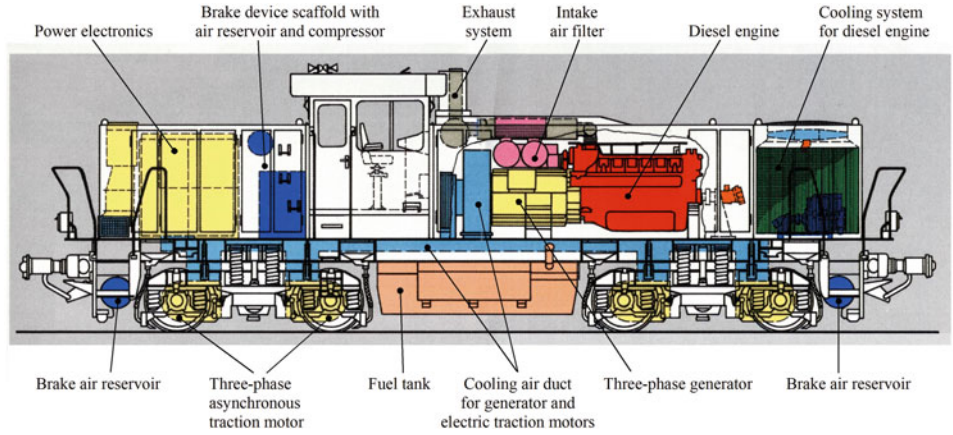

Fig. 3.46 Diesel-electric locomotive for heavy shunting and mainline service. (According to Krauss-Maffei documents)

systems with a combined output of about 1600 and 2000 kW. The advantage of this is that in the event of a failure of one unit, it is still possible to clear the track with reduced power (and thus speed); the disadvantage are the higher maintenance and repair costs of two units compared to one. Later heavy diesel locomotives of the DB, e.g. the classes 216 and 218, therefore had only one machine unit. In the meantime, however, considerations of fuel economy play an important role in diesel locomotives due to rising fuel costs.

Bombardier has therefore developed a diesel locomotive with four engines[24] (DB class 245; factory designation TRAXX P160 DE ME; ME = Multi Engine), whereby each diesel engine drives its own synchronous generator. However, the locomotive has a common DC link, Fig. 3.47. The locomotive is driven by four electric traction motors, two of which are fed from the DC link via a frequency converter. This makes it possible to run the locomotive with only one diesel engine in operation.

The four Caterpillar diesel engines, each with an output of 563 kW, are switched on and off depending on the power requirement. The number of operating hours and the cooling water temperature are taken into account by the engine coordination when selecting the engine to be switched on or off. Since these are large-series diesel engines, the overall procurement costs and maintenance costs should be comparable with single-engine locomotives, whose engines, however, are small(est) series products. Spare parts supply is easier and cheaper with large-series engines. Due to the heavy weight of the four engine

[24] Bikle, U.; Pöpper, C.; et al.: Die Diesellokomotive TRAXX DE Multi-Engine. Eisenbahntechn Rundschau 61 (2012) H. 9, pp. 58–64.

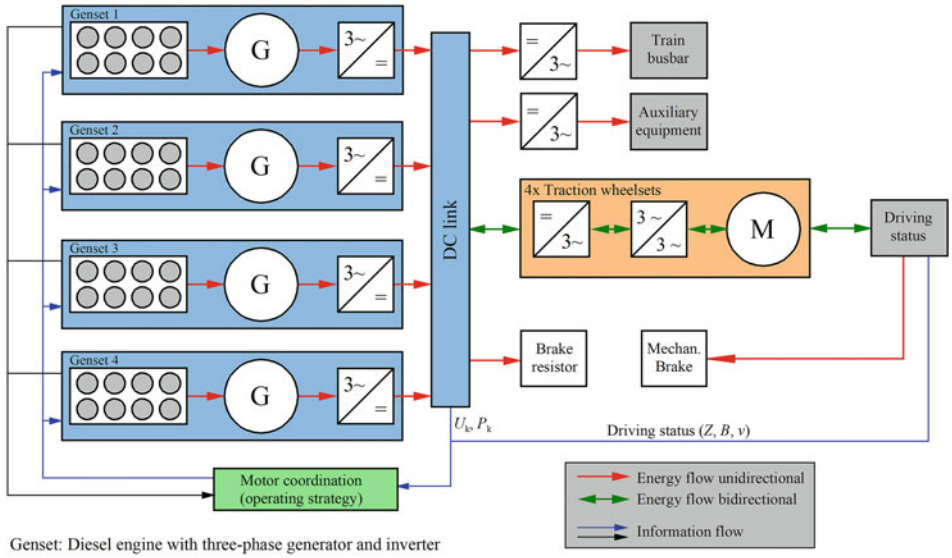

Fig. 3.47 Drive diagram of the DB class 245 multi-engine diesel locomotive. (According to Bombardier documents)

units, the class 245 (Fig. 3.48) has a fuel tank capacity of only 2700 L, whereas 4000–6000 L are common in comparable locomotives.[25] The total weight of the locomotive is 83 t.

3.4 Gas Turbine

In France, the former Soviet Union, and the USA, pure gas turbine drives were tested and used in rail vehicle technology. The DB also had some diesel TEE railcars[26] converted to gas turbine drive. Only the two-shaft gas turbine can be used as a vehicle drive, the characteristic curves of which are shown in Fig. 3.49.

The characteristic diagrams of the two-shaft gas turbine come relatively close to the ideal delivery characteristic diagram, so that the gas turbine is suitable as a vehicle drive. Its main advantage is its compact design. This allows high power to be accommodated in the vehicle. However, as can be seen from the constant efficiency curves in Fig. 3.49, the part-load efficiencies and the maximum efficiency are considerably worse than for the diesel engine. Therefore, the gas turbine is only economical to use in railway operations when

[25] Depending on the driving program and the route, the consumption of a diesel locomotive with an output of approx. 2000 kW is between 300 and 400 L/100 km.

[26] TEE: Trans Europ Express – trains for international travel in Europe with a high level of comfort; this type of train is no longer offered.

Fig. 3.48 DB class 245 multi-engine diesel locomotive

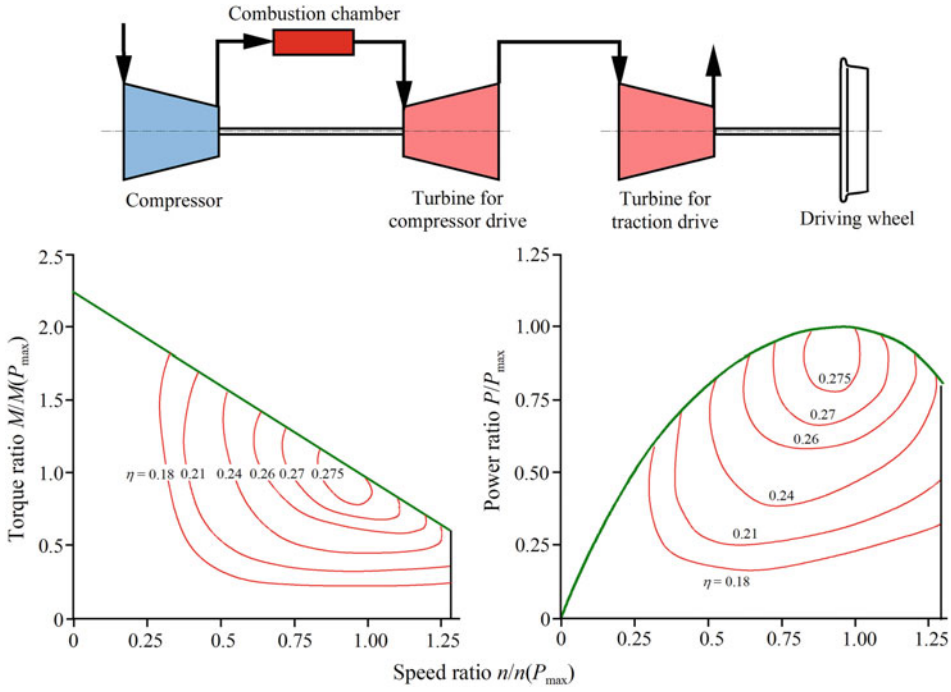

Fig. 3.49 Schematic and characteristics of the two-shaft gas turbine. (According to [46])

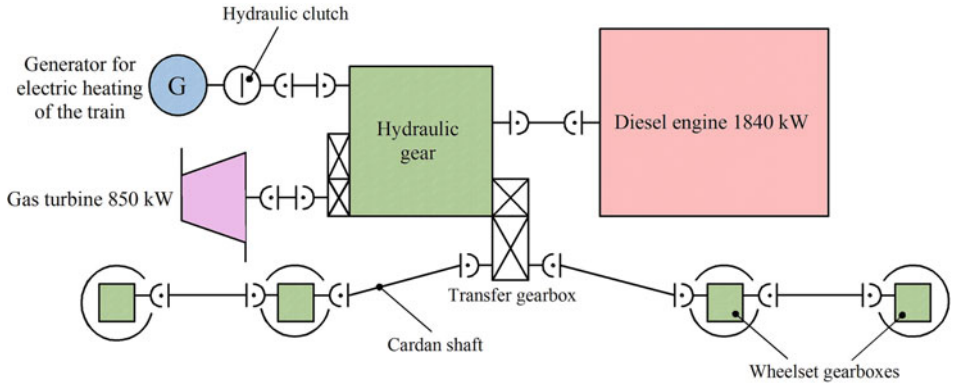

Fig. 3.50 Drive scheme of the former DB series 210 with additional gas turbine. (According to [43])

fuel costs are low. However, because the power that can be installed in diesel locomotives is limited, as already mentioned, gas turbines were used as boosters in diesel locomotives at DB.

The problem with diesel operation of locomotive-hauled passenger trains is the heating. In the steam locomotive era, passenger trains were steam-heated. The first electric locomotives and diesel locomotives therefore also had steam boilers to supply the heating equipment of the passenger coaches with heating steam. With increasing electrification, passenger coaches received electric (resistor-)heaters in addition to steam heating, which were supplied with power from the electric locomotive via the so-called train busbar.[27] Since the retirement of the steam locomotives and the older diesel locomotives, passenger trains are heated exclusively electrically.

The necessary power of about 35–50 kW per passenger coach must be provided by the diesel locomotive in diesel traction. For this purpose, the diesel locomotives used in front of passenger trains are equipped with generators that feed up to 480 kVA of power into the train busbar. For intercity trains with eight to twelve cars including dining cars, this power is utilized and reduces the traction power. For this reason, some diesel locomotives of the 218 family were fitted with gas turbines (class 210), which were used as an additional prime mover in parallel with the diesel engine, Fig. 3.50. The gas turbine was to take over the basic load of heating and traction power in order to run in the usable efficiency range at full load, while the diesel engine with its better part-load efficiency was to cover the remaining power requirement. For freight trains, the high total output from the diesel engine and the gas turbine could be used for traction.

[27] The train busbar is a connecting line of all vehicles of a train set for the supply of heating, air conditioning, lighting and other consumers. The power is supplied from the locomotive.

The gas turbines from the helicopter sector did not prove themselves in railroad service in either the class 210 or the TEE multiple units. The fuel consumption and maintenance costs were allegedly too high.

The problem of diesel-powered Intercity trains with high heating power requirements has been largely solved in Germany by almost complete electrification of the long-distance routes: Only on the Hamburg-Westerland and Munich-Lindau routes do diesel-powered Intercity trains still run, which are currently hauled by two class 218 locomotives. The power of both locomotives is sufficient for traction and heating.

3.5 Hybrid Vehicles

> A hybrid vehicle is a vehicle with at least two different energy converters and two different energy storage systems (in the vehicle) for the purpose of vehicle propulsion.[28]

The aim of most road vehicles with hybrid drive is to use braking energy for vehicle propulsion.[29] For vehicles with internal combustion engine drive, a separate energy converter and storage system is necessary for this purpose, since no liquid fuel can be recovered during the braking process. This also applies to rail vehicles with internal combustion engines, while electric rail vehicles can feed braking energy back into the grid as electrical energy, as already described.

The use of hybrid drive systems is therefore interesting for rail vehicles that are equipped with combustion engine drives. Electric accumulators and pressure accumulators can be used to store energy. In the case of diesel-electric power transmission as shown in Fig. 3.44, for example, the braking resistor could be replaced by an accumulator with charger in order to store braking energy and make it usable for the drive.

Another possibility would be the use of hydraulic pumps and pressure accumulators. The pressurized liquid quantity delivered during braking via the hydraulic pump, e.g. into a piston or bladder accumulator, could be used for starting by means of a hydraulic motor.

A hybrid technology from Alstom for shunting diesel locomotives that is currently being tested is shown in Fig. 3.51. Here, relatively large traction batteries (energy content 2×100 kWh) are used. Since the maximum power is rarely required in shunting operation, in the Alstom hybrid locomotive H3 (see Fig. 3.52) the base load is covered by the diesel engine(s). The engine can run at the operating point of lowest consumption. If its power is not fully required for traction, intermediate charging of the batteries can take place. Peak demand in traction power is covered by the traction batteries. In enclosed factory buildings, the diesel engine can be switched off and shunting can be carried out with zero emissions

[28] Definition for hybrid vehicles by the UN in 2003.

[29] In the case of so-called "plug-in" hybrid vehicles, the batteries can also be charged at charging stations or at household sockets. The aim here is to enable longer distances to be covered without exhaust emissions by means of inexpensive electric power.

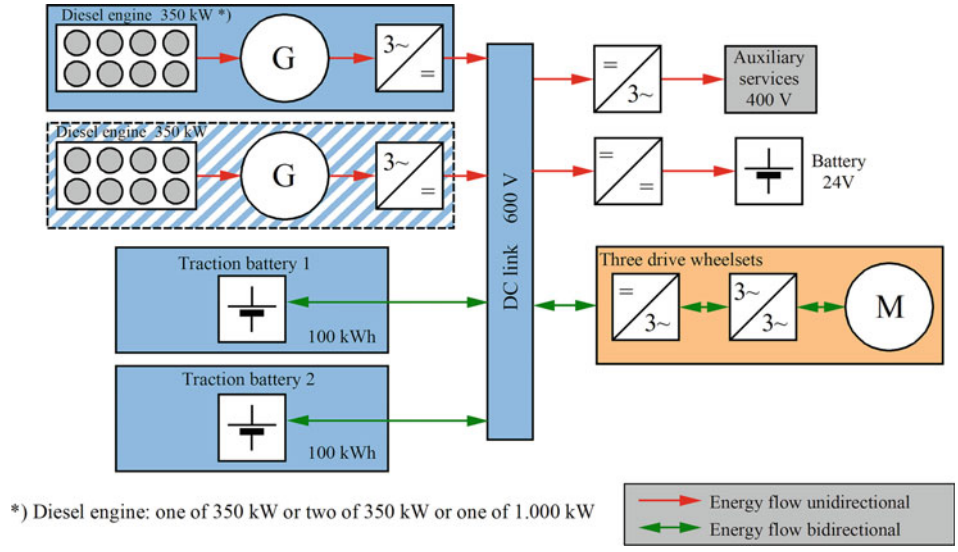

Fig. 3.51 Schematic of the drive of the Alstom hybrid locomotive H3. (According to Alstom documents)

Fig. 3.52 Alstom hybrid locomotive H3. (Photo: Alstom)

Fig. 3.53 Hybrid locomotive TRAXX "Last Mile". (Photo: Bombardier)

using only electric traction from the batteries. Alstom has measured a fuel saving of 11 L per operating hour in trial operation.

Another application of hybrid technology results from the operation of sidings and short branch line sections without electrification in freight train operation: With electric traction, a separate diesel shunting locomotive must be kept available for the delivery of freight wagons and wagon groups in non-electrified track sections. By installing a diesel generator system on an electric locomotive (Bombardier TRAXX "Last Mile", class 187, see Fig. 3.53), shunting and delivery runs can be carried out directly by the electric locomotive of the freight train, even in track sections without overhead lines. The diesel engine power of the mentioned locomotive is 180 kW, the maximum speed in diesel operation is 50 km/h.[30] Alternatively, it would also be possible to use a battery or capacitors ("Super Caps") as energy storage for short-term operation without overhead contact line.

In Germany, about half of the railway network is[31] electrified (in Switzerland, almost 100%). For electric traction on non-electrified railway lines, energy conversion in the vehicle with the aid of fuel cells is a possibility. Fuel cells are based on the principle of

[30] Bombardier (ed.): Die nächste Generation TRAXX – Weiterentwicklung einer erfolgreichen Lokomotivplattform. Vortragsunterlagen zur Schienenfahrzeugtagung Graz, Sept. 2011; Internet: http://www.schienenfahrzeugtagung.at/download/PDF2011/5-Altmann.pdf/

[31] However, about 90% of the transport service is provided on the electrified network.

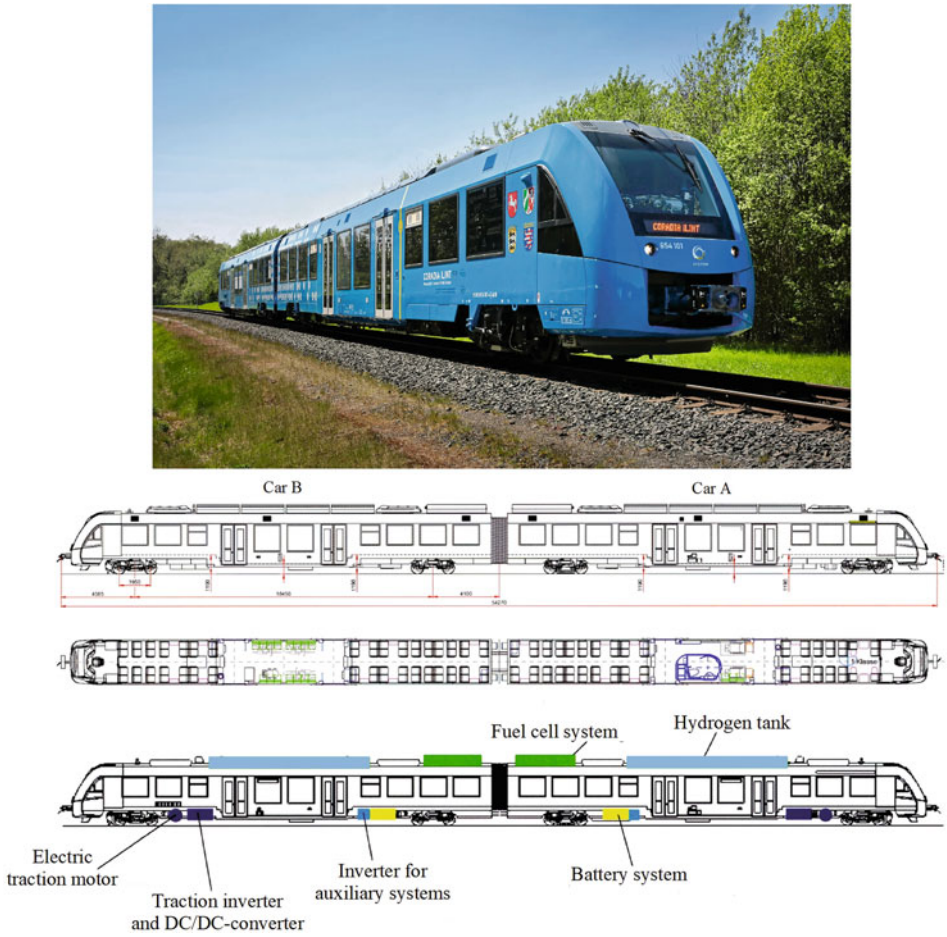

Fig. 3.54 Alstom Coradia iLINT fuel cell multiple unit. (Photo and drawings: Alstom)

"cold combustion" and generate electrical energy from hydrogen and (atmospheric) oxygen. This concept was implemented by Alstom with the "Coradia iLINT" multiple unit train presented in 2016, Fig. 3.54.[32]

This vehicle is based on the two-part diesel powered LINT 54. Instead of the "power pack" of diesel engine and transmission, a three-phase motor with 320 kW continuous power is installed in each vehicle part, each of which is connected to the final drive via a cardan shaft. As with the diesel-powered LINT, the axle arrangement is B′2′ + 2′B′. The two sections of the vehicle have an identical drive system. The vehicle is designed for a maximum speed of 140 km/h.

[32] See also: Hondius, H.: Der Brennstoffzellen-Hybrid-Zug Alstom Coradia iLint. Der Stadtverkehr 61 (2016) H. 11, pp. 6–8.

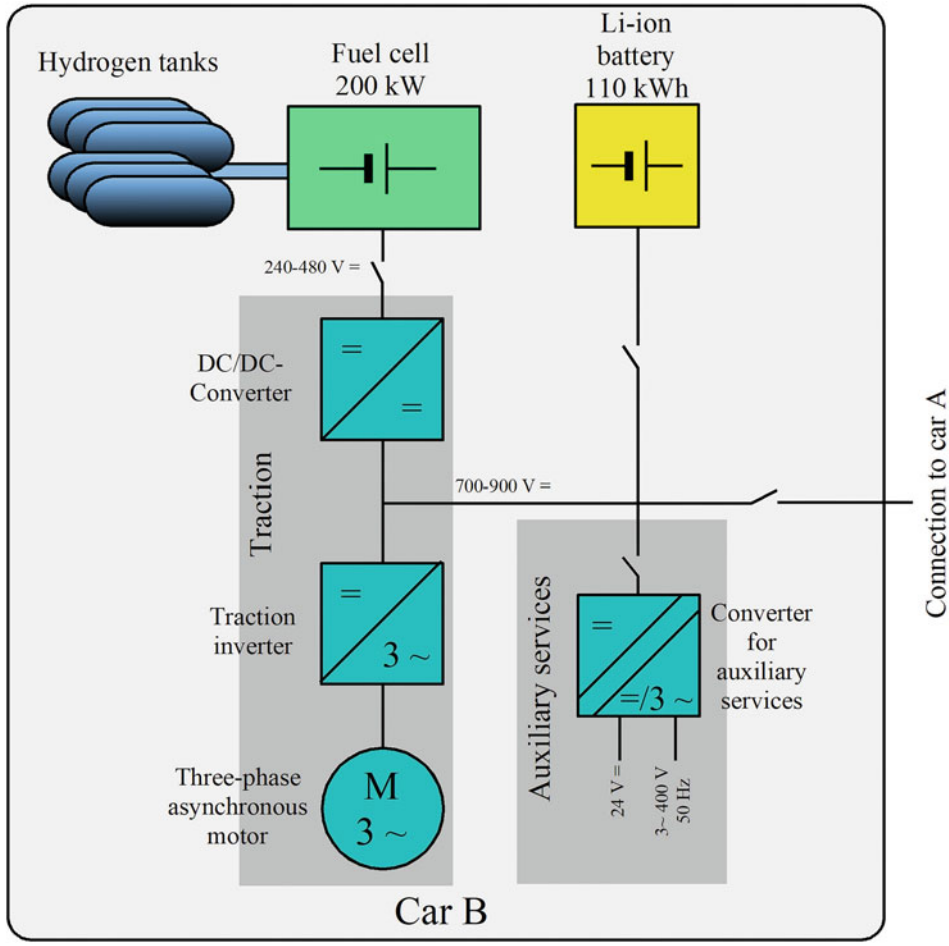

Fig. 3.55 Schematic of the power supply of the iLINT. (According to [53])

Electrical energy is supplied by a fuel cell system with an output of 200 kW installed on the roof of each vehicle. The hydrogen supply of 90 kg is carried in each case in 24 pressure tanks in gaseous form under 350 bar also on the roof. The range of the train is about 800–1000 km. The principle of the energy supply of the train is shown in Fig. 3.55.

Since the efficiency of the fuel cell decreases with increasing load current, a lithium-ion accumulator with a capacity of 110 kWh and a continuous output of about 200 kW is provided. It is used to store braking energy during recuperative braking with the traction motor. It also absorbs excess energy generated in the fuel cell system. In addition to providing traction energy, it can in particular cover power peaks, e.g. during starting and acceleration. The fuel cell system can thus be operated in a favourable efficiency range with

largely constant power. The efficiency of a fuel cell system consisting of individual cells in cell stacks is 60% [47].

The air conditioning in the passenger compartments is provided by one air conditioning unit each with a cooling capacity of 25 kW and a heating capacity of 30 kW. In addition, an electric heating system with a maximum output of 30 kW is installed in each vehicle section. This is supplied by the auxiliary converter (Fig. 3.55). Lighting, fan, control system, brake air compressor etc. are also connected to the auxiliary converter.

Hydrogen can be produced electrolytically from water, which would be possible in the future e.g. via electrical energy from wind, sun and hydropower without CO_2. The existing problem of storing electrical energy from wind and hydropower at night could thus be at least partially solved. At present, however, about 90% of hydrogen in Germany is produced from natural gas (methane, CH_4), with CO_2 being captured. The overall efficiency from electrolysis to the output of the fuel cell is given as about 25%.[33] The electrolytic production of hydrogen via electrical energy from thermal power plants (approx. 40% efficiency) results in a total efficiency at the output of the fuel cell of approx. 10%. From the point of view of energy efficiency and ecology, this method is therefore also out of the question. The use of fuel cells only makes technical sense if regeneratively generated electrical energy is used for hydrogen production. The economic viability can only be assessed after longer periods of operation of larger vehicle fleets. The efficiency of an energy supply via overhead line is comparatively better: from the power station via substations and overhead line to the vehicle's current collector it is about 90% (including thermal power station it is about 35%).

The iLINT's operations planned to date envisage using hydrogen produced as a by-product in the chemical industry (e.g. from chlor-alkali electrolysis). Thus, the first passenger deployment of two iLINT multiple units on the network of the "Eisenbahnen und Verkehrsbetriebe Elbe-Weser GmbH" (evb) in northern Lower Saxony is planned from the end of 2018. The hydrogen will be supplied by a chemical plant in Stade. A hydrogen filling station will be built in Bremervörde for the trains, which will be supplied by truck.[34] The Landesnahverkehrsgesellschaft Niedersachsen (LNVG; State Transport Company of Lower Saxony) intends to order another 14 iLINT multiple units. At the beginning of 2018, Alstom had received letters of intent for a total of 60 trains.

The narrow-gauge Zillertalbahn in Tyrol/Austria is also to be operated with fuel cell vehicles in the future.[35] The hydrogen for this is to be produced electrolytically, preferably at night, using energy from nearby hydroelectric power stations. The additional costs for a multiple unit with fuel cell hybrid drive are estimated at 20% compared to an AC multiple

[33] Herzog, K.: Kraftfahrzeugantriebe. Vorlesungsskript, Techn. Hochschule Mittelhessen, Gießen (n.d.), on the Internet at: https://www.thm.de/me/images/user/herzog-91/Kfz-antriebe/Kfz_Antriebe_5_Elektromotoren_und_Hybridantriebe.pdf; last accessed on 21.08.2018.

[34] NN.: LNVG Lower Saxony – the hydrogen pioneers. Privatbahn Magazin (2018) H. 1, p. 90/91.

[35] Schreiner, H.: With hydrogen through the Zillertal. Eisenbahn-Revue International (2018) H. 4, pp. 182–185.

unit with catenary. The costs for the alternatively required overhead line including the substations[36] for the 32 km long Zillertal Railway were calculated at €22 million.

The advantages of hybrid fuel cell vehicles in general are:

- Electric drive, thus less noise than with diesel drive
- Energy saving through recuperation (estimated 20–40%)
- Climate-neutral transport if hydrogen is produced from renewable sources
- Avoidance of the investment of an overhead contact line and the traction current supply (substations)

However, there are also disadvantages:

- Limited service life of the fuel cell system (approx. 10,000–20,000 operating hours [47]; a multiple unit has approx. 3000 operating hours per year)
- Limited battery life (approx. 10 years, with frequent deep discharging the life can be reduced to three years [47])
- Higher vehicle procurement costs (according to [47] approx. 65% more than electric multiple units, according to Zillertalbahn approx. 20%)
- Tank and supply infrastructure for hydrogen required
- Special safety measures required in depot and vehicle workshop

In addition to the diesel-battery hybrid drive for shunting locomotives mentioned at the beginning of this section, the same principle is also possible for railcars.[37] Another hybrid technology for rail vehicles is the catenary/battery power supply.[38, 39] Siemens and Bombardier are testing this technology for railcars. If the overhead line is available at 15 kV/16.7 Hz, the vehicles are powered from it. The battery is also charged via the current collector from the overhead line. With a charged battery, approx. 35–40 km (peak up to 80 km) can be covered on non-electrified lines.

According to studies by the Technical University of Dresden, the electrification of a railway line makes economic sense as soon as there is at least an hourly frequency (i.e. at least one train per hour and direction) [47]. At present, there is a partial surplus of electrical

[36] Substation: It is used to feed energy into the catenary. In order to limit the voltage drop due to the ohmic resistor of the overhead line, a railway line is divided into several feeder sections. Each feeder section requires a substation that takes the energy from the national grid or a railway's own grid, transforms it into the overhead line voltage and, in the case of DC railways, also rectifies it.

[37] Lehmann, I.; Nedic, D.; Oszfok, B.: Quiet, clean, fast: MTU hybrid drive for the Bodenseegürtelbahn. Eisenbahntechn. Rundschau 67 (2018) H. 9, pp. 111–114.

[38] Stephan, A.; Wittemann, N. T.; Müller, A.: Alternative drive concepts: Which hybrid for which line? Eisenbahningenieur 69 (2018) H. 9, pp. 60–66.

[39] Von Mach, S.; Buschbeck, J.; et al: The development and market introduction of the TALENT 3 battery multiple unit. Eisenbahntechn. Rundschau 67 (2018) H. 9, pp. 115–119.

energy available. Due to the proposed shutdown of coal and nuclear power plants in Germany, the politically desired use of electric vehicles in road traffic and digitalisation (computers also require electrical energy), the aspect of energy efficiency will become more important in the future. In rail transport, trolley vehicles will then have a clear advantage.

Brakes for Railway Vehicles

4

Rail vehicle brakes, like brakes in motor vehicles, have the following tasks:

- Decrease speed,
- Securing stationary vehicles,
- Keeping the speed constant on downhill stretches,
- Stopping vehicles within the designated limits.

Figure 4.1 shows the classification of brakes on rail vehicles. Brakes with contact are divided into free-acting and wheel-rail friction brakes. The mechanical brakes are divided as friction brakes into block brakes, disc brakes and – more rarely – drum brakes. The block brake is still the most widespread rail vehicle brake because it is used almost exclusively on freight wagons. Due to the development towards higher speeds and the resulting higher braking performance, the trend is towards disc brakes, which are largely standard on passenger coaches. Freight wagons with maximum permissible speeds above 120 km/h also have disc brakes.

In addition to the brakes listed in Fig. 4.1, steam locomotives had the counter-pressure brake already mentioned and vehicles with mechanical transmission had the engine brake also used in (diesel-)commercial vehicles.

The first brakes on rail vehicles were hand brakes, designed as single-block levers or weight brakes, later also spindle brakes. These brakes required the wagons to be constantly accompanied by so-called "brakemen" – railwaymen who applied or released the brakes in accordance with the locomotive driver's whistle signals. In 1872, the first continuous self-acting brake came into use in the form of a rope brake from Heberlein.[1] From about 1870

[1] Jacob Heberlein (1825–1881), German engineer, chief engineer of the Royal Bavarian State Railway.

© The Author(s), under exclusive license to Springer Fachmedien Wiesbaden GmbH, part of Springer Nature 2022

J. Ihme, *Rail Vehicle Technology*,
https://doi.org/10.1007/978-3-658-36969-9_4

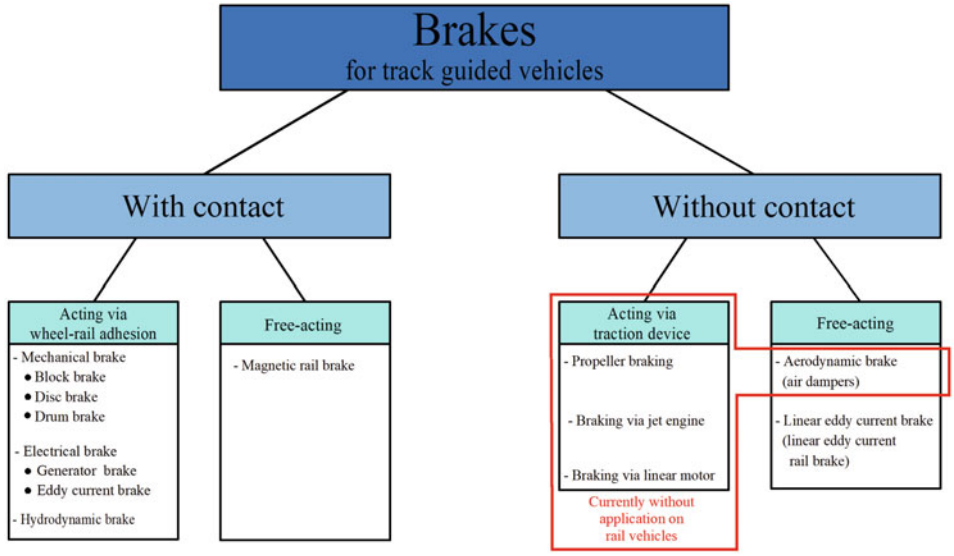

Fig. 4.1 Brakes for track guided vehicles. (According to [43])

onwards, the first experiments were carried out with continuous air brakes by WESTINGHOUSE[2] and vacuum brakes by HARDY.[3] A "continuous brake" can be released from the traction unit or from a brake car for the entire train. Further improvements were made in 1902 with the "KNORR fast brake" invented by KNORR.[4]

Since a suitable brake that could stop long and loosely coupled (freight-)trains safely and quietly had not yet been developed, only passenger trains ran with air brakes until the First World War. From 1931 onwards, the first multi-release air brakes were used for freight and passenger trains. A significant improvement in air brakes began in 1953 with the KNORR brake with uniform action (KE brake). From this time onwards, the KE brake was approved by the International Union of Railways (UIC) for use in international rail traffic. Today, this brake is the most widely used railway brake. Figure 4.2 shows the systematics of frictional brakes for rail vehicles.

Braking also means energy conversion in rail vehicles. In the process, kinetic energy is converted into thermal energy or electrical energy, whereby the latter can be fed back into the catenary network or converted into thermal energy in braking resistors. In the stopping braking process of freight trains, power of 300 kW per wheelset is converted, and in the case of high-speed trains, power of 1.2 MW per wheelset. This shows that the braking power of rail vehicles clearly exceeds their drive power.

[2] George Westinghouse (1846–1914), American engineer, inventor, and entrepreneur.

[3] John George Hardy (1851–1914), English engineer with the Austrian Southern Railway Company.

[4] Georg Knorr (1859–1911), German engineer and entrepreneur.

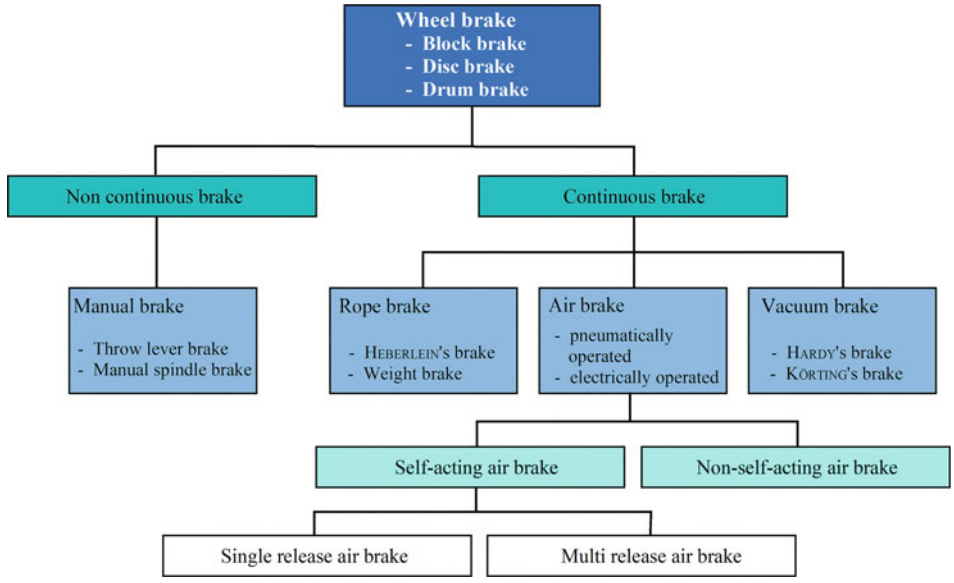

Fig. 4.2 Frictional brakes for rail vehicles

4.1 Frictional Brakes

The performance, traction and braking capacity of rail vehicles is determined both by the design and construction of the vehicle and by physically determined limits (adhesion). Influencing parameters for the adhesion coefficients are (Fig. 4.3):

- Weather conditions,
- Impurities,
- Material pairing,
- Use of auxiliary materials to improve the coefficients of adhesion, for example sand.

In Germany, the switch from grey cast iron brake blocks to plastic brake blocks is currently taking place as part of noise reduction measures in rail transport. Plastic brake blocks have the following advantages over grey cast iron brake blocks:

- The rolling noise of the wheels is lower because plastic brake pads do not roughen the wheel treads.
- The brake dust has no electrically conductive properties (important for electric railway operation, as electric traction vehicles also suck in dust via the fans).
- The coefficient of friction of plastic brake blocks is less dependent on the friction speed than is the case with grey cast iron brake blocks (see Fig. 4.3b). As a result, the “braking

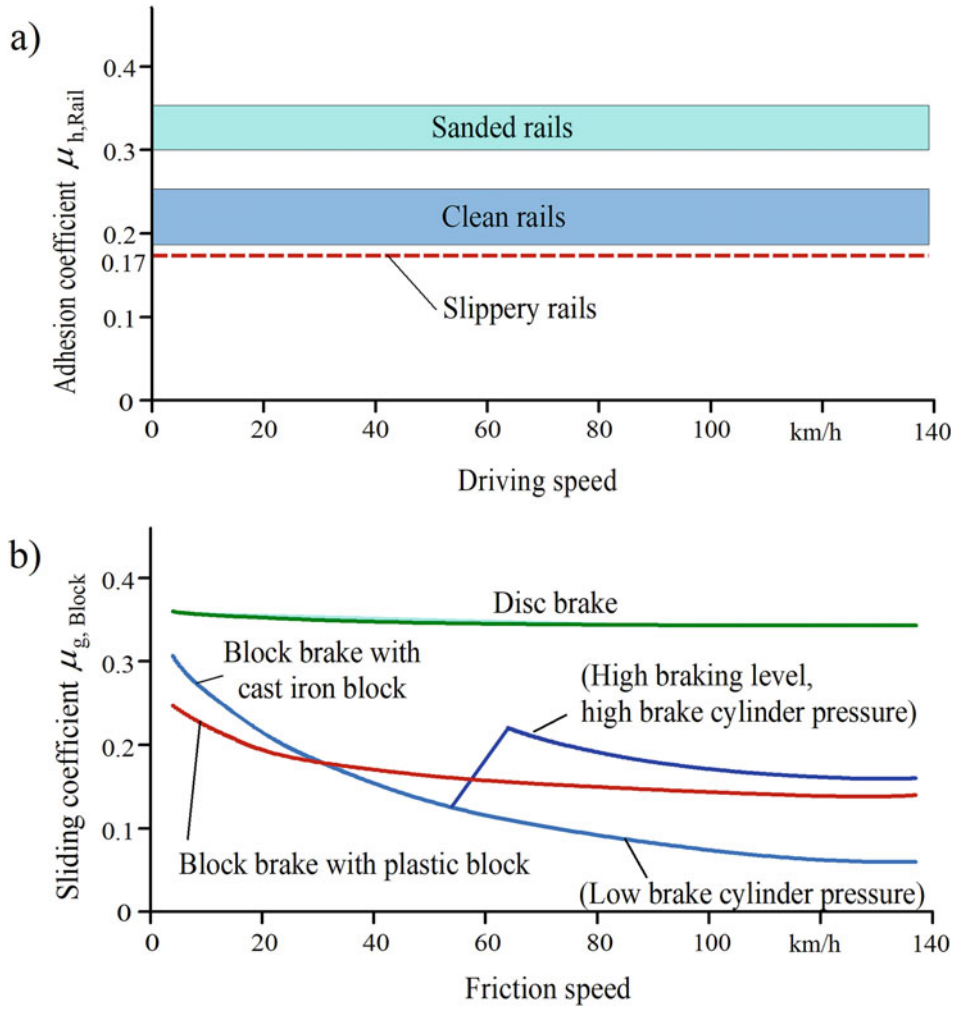

Fig. 4.3 Coefficients of adhesion between wheel and rail (**a**) and between brake disc and lining or wheel and brake pad (**b**). (According to training documents of DB AG)

jerk" is less pronounced with plastic brake blocks (the lower the friction speed, the higher the coefficient of friction: the braking effect increases with decreasing driving speed. This effect is lowest with disc brakes).

On the braked wheel, a distinction is made between two adhesion coefficients:

- μ_S = wheel/rail adhesion coefficient,
- μ_K = Coefficient of adhesion wheel/brake pad or brake disc/brake lining.

Consequences of worsened adhesion conditions for braking are:

- Blocking of the wheel sets, associated with damage to the wheel tyres (flat spots),
- Braking distance extension.

For the improvement of the adhesion ratios are used:

- Sand spreading equipment,
- Cleaning Blocks,
- Plasma torch for cleaning the rails,
- Slip-controlled brakes (see anti-lock braking systems on motor vehicles),
- Magnetic rail brakes (MG brakes).

Any transmission of tangential forces on the rolling wheel is basically associated with slip. The slip is defined as follows:

$$\text{Drive slip (traction slip)}: \qquad s_{\mathrm{T}} = 1 - \frac{v_0}{r \cdot \omega}, \tag{4.1a}$$

$$\text{Brake slip}: \qquad s_{\mathrm{B}} = 1 - \frac{r \cdot \omega}{v_0} \tag{4.1b}$$

with

r:	Rolling radius of the wheel,
ω:	Wheel Angle Speed,
v_0:	Vehicle Speed.

The traction slip is $s_{\mathrm{T}} = 1$ when starting with spinning wheels ($v_0 = 0$); the brake slip is $s_{\mathrm{B}} = 1$when the wheels are locked ($\omega = 0$). When the wheel is rolling momentum-free (= slip-free), $v_0 = r \cdot \omega$ and thus $s_{\mathrm{T}} = 0$ and $s_{\mathrm{B}} = 0$, respectively.

The dependence of the coefficient of adhesion on slip is shown in Fig. 4.4.

From Fig. 4.4 it can be seen that the maximum adhesion for dry rails is at a slip $s \approx 0.01$. For the tyre/road surface pairing, the maximum adhesion is at $s \approx 0.1$. In principle, the range shown in Fig. 4.4 for $s > 0.01$ is not stable, i.e. if the slip increases, the coefficient of adhesion jumps from adhesion to the lower coefficient of sliding and the wheel locks during braking or spins ("skids") during propulsion. Since these processes are more sensitive in the wheel/rail system than in a motor vehicle, a mechanical anti-lock system was installed in rail vehicles as early as the 1930s.

Next, we consider the forces on a braked rail vehicle, see Fig. 4.5. At the center of gravity of the braked (decelerated) vehicle attack:

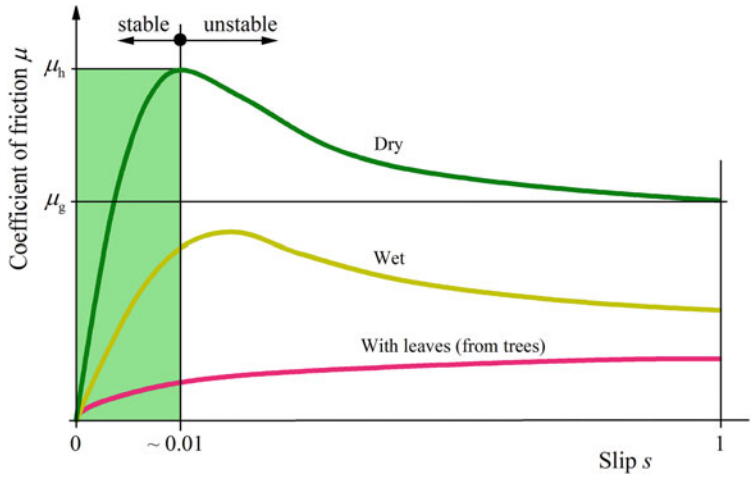

Fig. 4.4 Dependence of the adhesion coefficients on slip for wheel/rail pairing

- Weight force $m \cdot g$,
- Inertial force $m \cdot a$.

On the wheelsets attack:

- Bearing forces $F_{A1/2}$, $F_{B1/2}$,
- Wheel contact forces $F_{C1/2}$.

In the presence of slip:

- Force $\mu_{S1/2} \cdot F_{C1/2}$,
- Moments from wheel inertia $M = J_R \cdot \delta_{1/2}$ with $\delta =$ angular acceleration and $J_R =$ moment of inertia of the wheel.

The braking force of the magnetic rail brake F_{MG} is supported by the distance e on the car body.

The equilibrium conditions at the wheel sets result in (changing signs due to the consideration of the two wheel sets):

$$\sum F_{ix} = 0 \rightarrow F_{A1/2} = \mu_{S1/2} \cdot F_{C1/2} \pm F_K, \tag{4.2}$$

$$\sum F_{iy} = 0 \rightarrow F_{B1/2} = F_{C1/2} \pm \mu_K \cdot F_K, \tag{4.3}$$

$$\sum M_{\mathrm{i}} = 0 \rightarrow J_{\mathrm{R}} \cdot \delta_{1/2} = -\mu_{\mathrm{K}} \cdot F_{\mathrm{K}} \cdot r \pm \mu_{\mathrm{S1/2}} \cdot F_{\mathrm{C1/2}} \cdot r. \tag{4.4}$$

From Eq. 4.4 it can be seen that the condition

$$\mu_{\mathrm{K}} \cdot F_{\mathrm{K}} < \mu_{\mathrm{Si}} \cdot F_{\mathrm{Ci}}$$

must be fulfilled if δ_{i} is to assume negative values (= deceleration). The consequence of non-fulfilment is the sliding of the wheelsets.The balance of forces on the vehicle requires:

$$m \cdot a = -\mu_{\mathrm{S1}} \cdot F_{\mathrm{C1}} - \mu_{\mathrm{S2}} \cdot F_{\mathrm{C2}} - F_{\mathrm{MG}}. \tag{4.5}$$

The deceleration *-a* is caused by the adhesion coefficients $\mu_{\mathrm{S1/2}}$ utilized at the wheels, which cause some slip between the wheel and the rail (see Fig. 4.4), and not directly by the braking forces $\mu_{\mathrm{K}} \cdot F_{\mathrm{K}}$.

From the moment equilibria around the contact points of wheelsets 1 and 2 follows:

$$F_{\mathrm{C1/2}} = \frac{1}{2} m \cdot g \mp \frac{1}{2} m \cdot a \cdot \frac{h}{l} \pm \frac{1}{2} F_{\mathrm{MG}} \cdot \frac{e}{l}. \tag{4.6}$$

With the help of Fig. 4.5 it can be seen that a deceleration *-a* results in a relief of the rear wheelset and a load on the front wheelset. Due to the small distance *e,* the reverse reaction as a result of the MG brake is negligible.

For low slip, the approximation $a \approx r \cdot \delta_{\mathrm{i}}$ holds.

Using this approximation and adding Eqs. 4.4. and 4.5 (divided by *r*) one obtains:

$$m\left(1 + \frac{\sum J_{\mathrm{i}}}{m \cdot r^2}\right) a = -\sum \mu_{\mathrm{K}} \cdot F_{\mathrm{K}} - F_{\mathrm{MG}}, \tag{4.7}$$

Mass fraction = Brake force fraction.

From this it is clear that the braking forces must also contribute to the deceleration of the rotating masses, which is formally taken into account by the introduction of the so-called rotating mass factor λ (see Chap. 2). For example, for passenger coaches $\lambda \approx 1.03$ and for locomotives $\lambda \approx 1.10$.

The kinetic energy of the train is converted into heat in the components involved in the friction process during braking and released into the environment. In order to absorb the heat generated for a short time during stop braking, the components must have a high heat capacity so that no excessive temperatures occur. Nevertheless, during stop braking of high-speed trains, temperatures of up to about 500 °C occur at the brake linings. For inertia braking (e.g. on downhill gradients), high heat transfer coefficients are required at the components, which are achieved in the case of brake discs, for example, by a ribbed, internally ventilated design (see also Figs. 4.16 and 4.17).

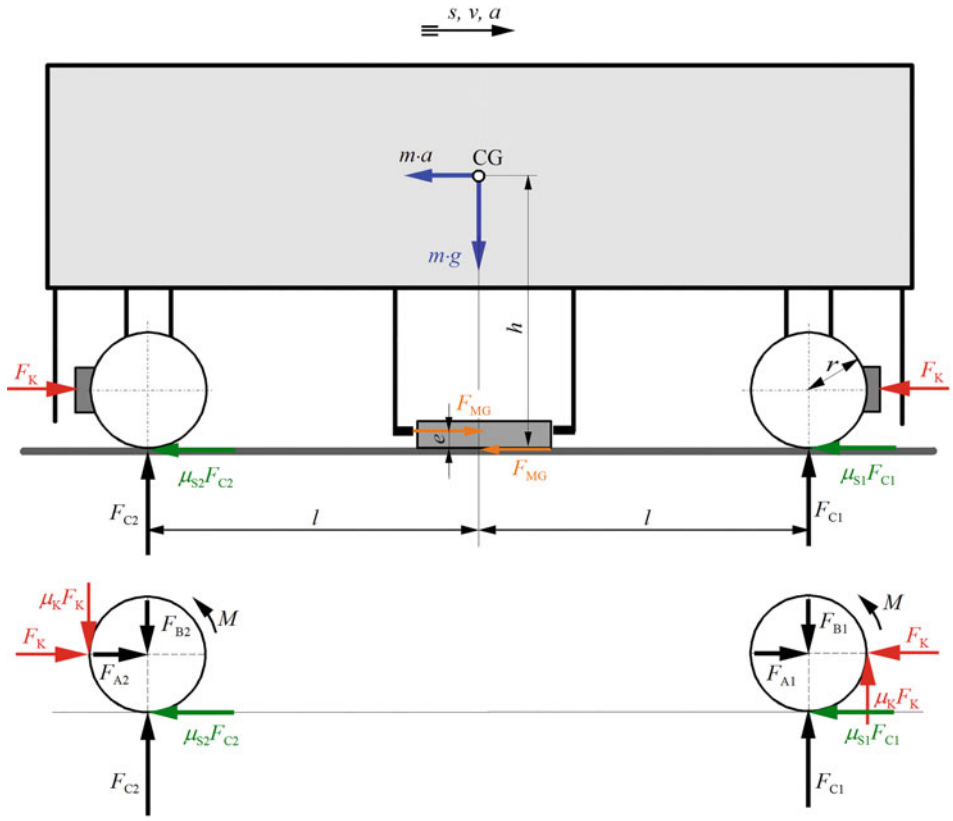

Fig. 4.5 Forces on braked two-axle rail vehicle. (According to [56])

We return to Fig. 4.2 and now briefly consider the various embodiments of friction brakes.

Hand brakes are purely mechanical brakes. Today they are mainly used as parking brakes to secure parked vehicles against unintentional movement (see Fig. 4.6). Parking brakes only act on a number of the wheelsets and must therefore not be used for the braking force calculation of rail vehicles.

Throw lever brakes (formerly used on steam locomotives) act on the brake linkage by shifting a weight using its weight force. This weight force is transferred to the brake blocks by means of the brake linkage.

In locomotives and railcars, a so-called spring brake is usually used instead of the hand brake, Fig. 4.7. It is mounted on the air brake cylinders. The brakes are applied by venting the spring brake line. Vehicles parked without pressure are thus braked by the spring brake. When compressed air is applied, the brake is released again. A mechanical release device, e.g. by means of a spindle and spanner, enables the brake to be released without compressed air in the event of a fault. In contrast to mainline vehicles, modern metro and light

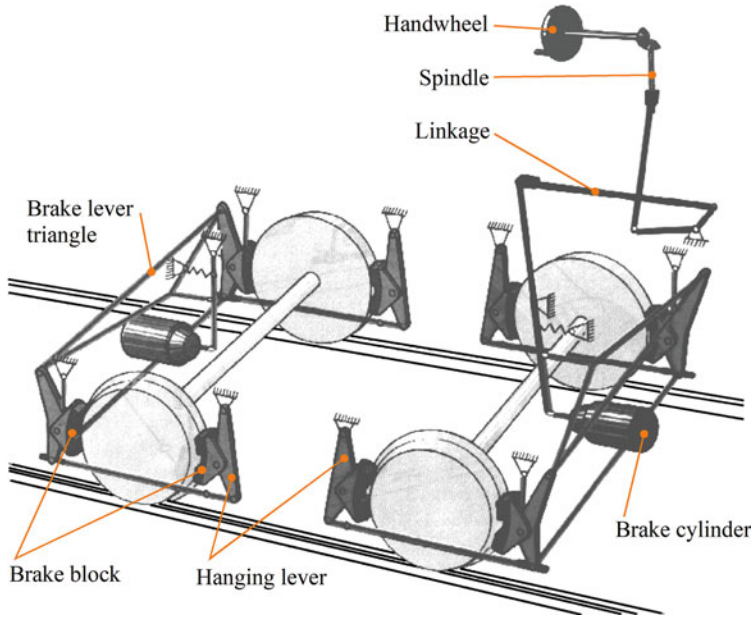

Fig. 4.6 Hand brake as block brake. (According to [56])

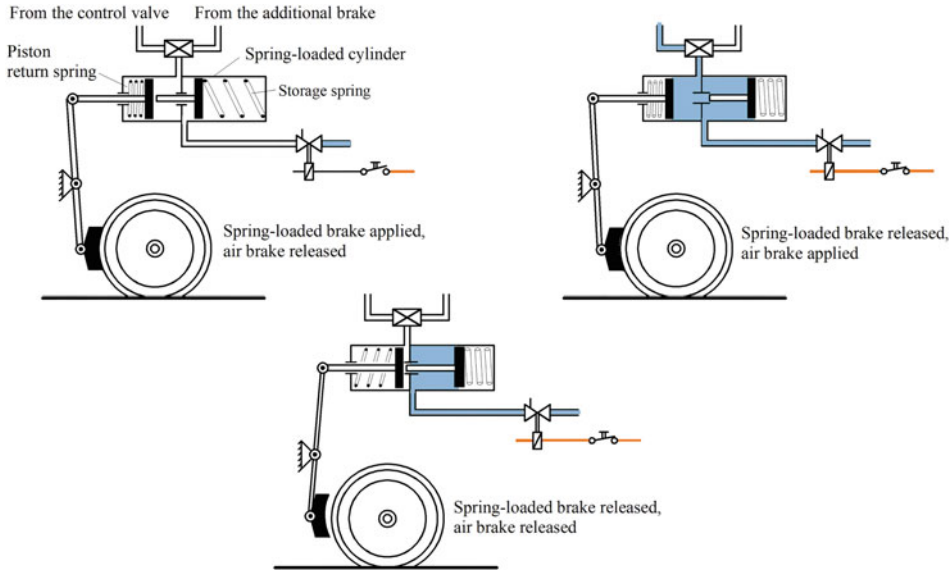

Fig. 4.7 Mode of operation of a spring brake. (According to: Workbook Fundamentals of Locomotive Technology, DB AG, 129/7 84)

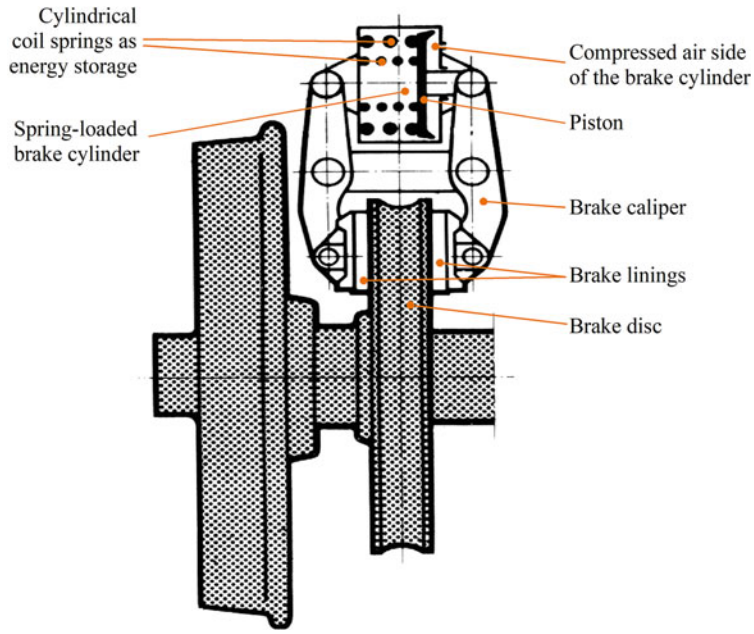

Fig. 4.8 Spring-loaded brake as compact unit. (According to drawing: Bosch-Rexroth)

rail vehicles are equipped with controllable compressed air spring brake systems. These brake systems are controlled electro-pneumatically and in parallel to the purely electric brake. The spring-loaded brake serves here as a service brake in the lower speed range and as a parking brake. A spring brake unit as a compact assembly for disc brakes is shown in Fig. 4.8.

4.1.1 Through Brakes

Through brakes can be operated from one point in the train, usually from the leading traction unit, and act on all vehicles in the train. In Central Europe, the compressed air brake has become established. The vacuum brake[5] was in use in Great Britain until the 1970s; it is still used in India and South Africa, as well as on some narrow-gauge railways and museum railways.

[5]The vacuum brake requires larger brake cylinders than the air brake, since in practice a vacuum of approx. 0.7 bar can be achieved compared to the ambient pressure. Larger piston diameters are therefore required for defined piston forces. The vacuum brake has the advantage that it cannot freeze due to condensation. Trains with a length of more than approx. 500 m cannot be braked safely, as the vacuum in the brake pipe decreases with the length due to unavoidable leaks and pipe resistance.

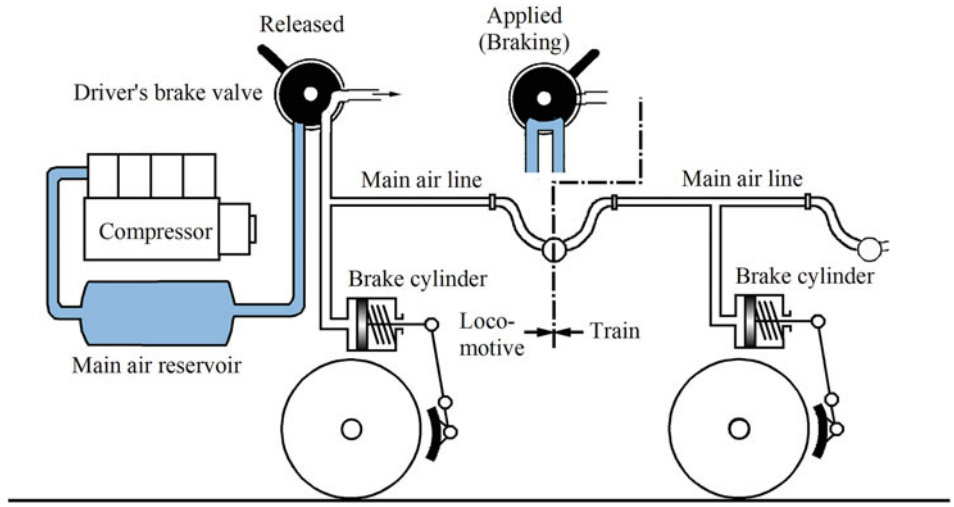

Fig. 4.9 Direct-acting air brake (non-automatic). (According to [51])

The rope brakes such as the Heberlein brake and the (Görlitz) weight brake require rope hoists, usually over the roofs of the cars to the locomotive or to the brake car. This means considerable effort when assembling and separating trains. Rope brakes are therefore only used on museum railways.

Mode of Operation of the Air Brakes

In all **air brakes, the braking** force is generated by pressing the brake pads/brake linings against the wheels using compressed air. Compressed air is fed into the cylinders and acts on the brake pads or brake linings via pistons and linkages. The braking force can be regulated by varying the dosage of the air pressure.

In the case of the **direct-acting brake** (Fig. 4.9), compressed air from the main air reservoir is present at the brake valve. The compressed air flows into the brake cylinders as long as the brake valve is set to the brake position. The compressed air supply is interrupted in the closing position of the brake valve. If the release position is selected, the brake cylinder is vented to the atmosphere. A gradual increase or decrease of the braking force is possible with this brake. This brake is not self-acting, as a continuous brake line would be open in the event of a train separation, and the compressed air required for braking would therefore flow into the atmosphere. For this reason, this system is not suitable as a train brake. A brake is described as "self-acting" if automatic braking takes place in the event of train separation or leaking or breaking lines.

With the **indirectly acting air brake** (Fig. 4.10), each vehicle has a control valve and an auxiliary air holder. The compressed air required for braking is reduced to control pressure (5 bar) in the driver's brake valve during the filling and release process and stored in the

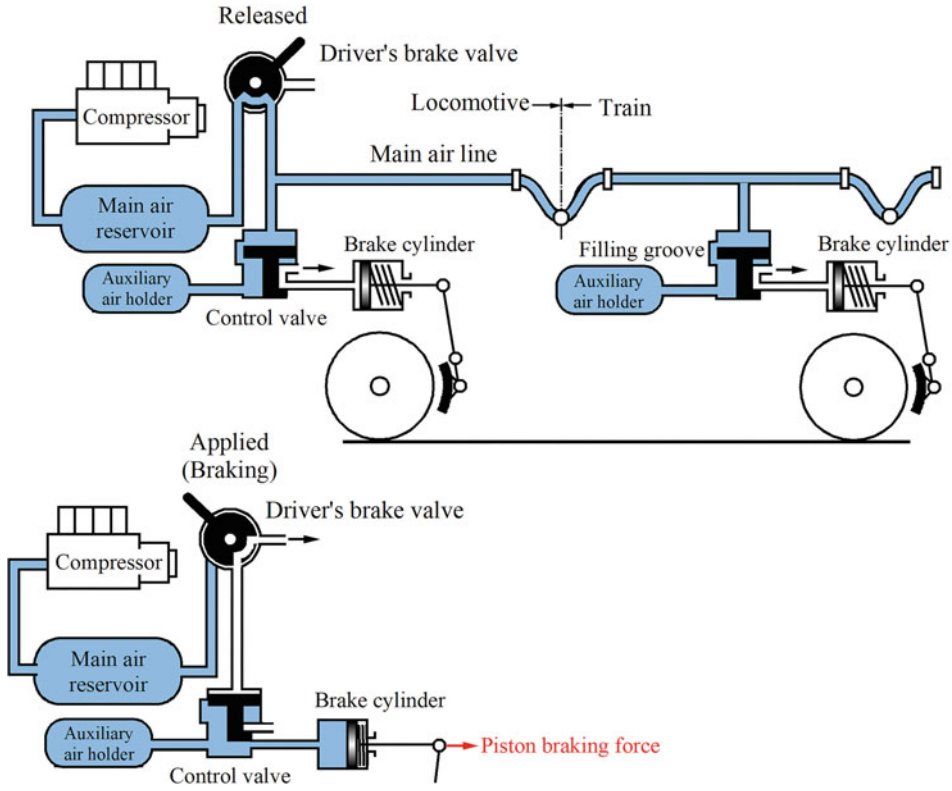

Fig. 4.10 Indirectly acting air brake (self-acting). (According to [51])

auxiliary air holders via the continuous brake line (main air line) and the control valves. When the main air line pressure is reduced, the control valves switch to the brake position and the compressed air stored in the auxiliary air holders flows into the brake cylinders.

Since this process also occurs with any other type of pressure reduction in the main air line (e.g. when the air line is torn off during train separations), it is also referred to as a "self-acting" compressed air brake. It is suitable as a train brake. The simplified form of the automatic air brake shown in Fig. 4.10 can be exhausted, as no compressed air is added to the auxiliary air holders during braking. Repeated braking at short intervals reduces the auxiliary air holder pressure and thus the available braking force.

The **control valve** is the essential component for the automatic air brake. The control valve regulates the ventilation of the brake cylinders as well as the filling of the auxiliary air holder or supply air reservoir by means of the induced pressure change in the main air line. Basically, control valves are divided into single-release and multi-release types.

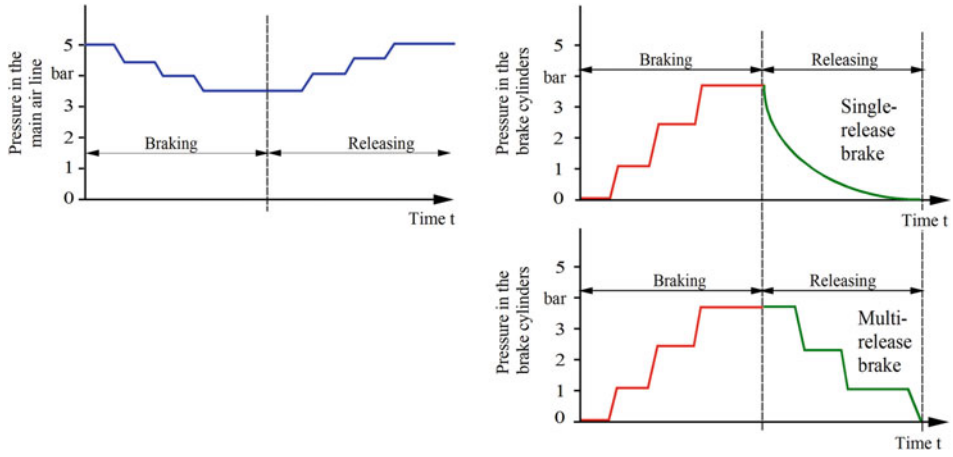

Fig. 4.11 Pressure curves for single-release and multi-release brakes. (According to [42])

Single-Release Control Valves

At a slight increase in pressure, the control valves are fully released. The release process is no longer interrupted automatically. The auxiliary air holder is only filled up again from the start of the release process. Once the constant control pressure has been reached in the main air line, the brake is fully operational again (for pressure curves, see Fig. 4.11). As single-release brakes no longer meet the requirements standard of modern rail vehicles, these brakes and their mode of operation will not be discussed further.

Multi-Release Control Valves

With a small pressure increase, the control valves release the brake cylinders only according to the newly set main air line pressure. This means that the brake can be released in stages, see Fig. 4.11. The brake is not fully released until the control pressure is reached. The multi-release effect is achieved in all modern brake designs by applying the three-pressure principle.

The operation of a **multi-release control valve** is shown in Fig. 4.12: Three pressures act on the piston set: the main air line pressure p_L, the control pressure p_A and the brake cylinder pressure p_C. The slider connected to the piston either allows the brake cylinders to be released or, in the braking position, connects the supply air holder to the brake cylinders. The supply air holder and the control chamber are filled from the main air line via non-return valves.

Release Position

In the release position, the pressures p_A, p_L and p_R are equal; the piston set is in its lower end position under the influence of the spring acting on the upper control piston.

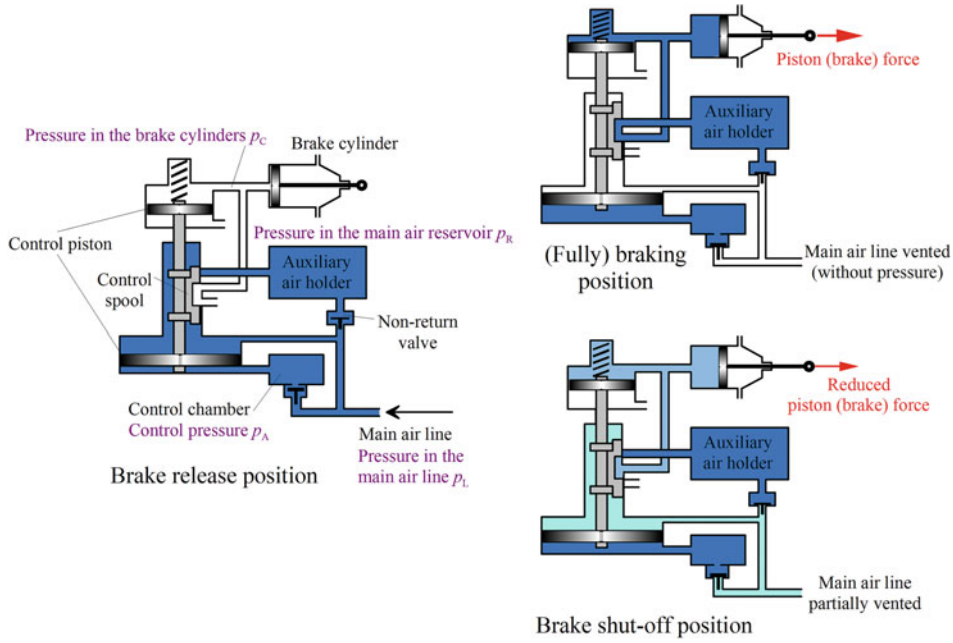

Fig. 4.12 Multi-release control valve. (According to [51])

Braking Position

If the pressure in the main air line is reduced, the check valve to the control chamber closes and the piston set moves upwards under the influence of the now higher pressure p_A. Air flows from the supply air holder to the brake cylinder via the slide valve. This also closes the non-return valve to the supply air holder. The brake cylinder pressure also acts on the upper control piston of the piston set. When the resulting force becomes greater than the force resulting from the pressure difference between p_L and p_A at the lower piston, the piston set is pushed back down slightly into the brake shut-off position. The connection to the brake cylinder is thus interrupted. With further air outlet, the process is repeated until full brake pressure is reached at an outlet of 1.3–1.6 bar.

Release

During release, due to the increase in pressure in the main air line, the upward force acting on the large control piston becomes less than the downward force acting on the smaller piston. The piston therefore moves downwards to the release position, in which the brake cylinder is vented until the upward force again prevails and brings the piston set into the final position. In this way, during both braking and release, each line pressure corresponds to a clearly defined brake cylinder pressure, which is precisely controlled by movements of the piston set between the braking and end positions on the one hand and between the release and end positions on the other. The brake is not fully released until there is no

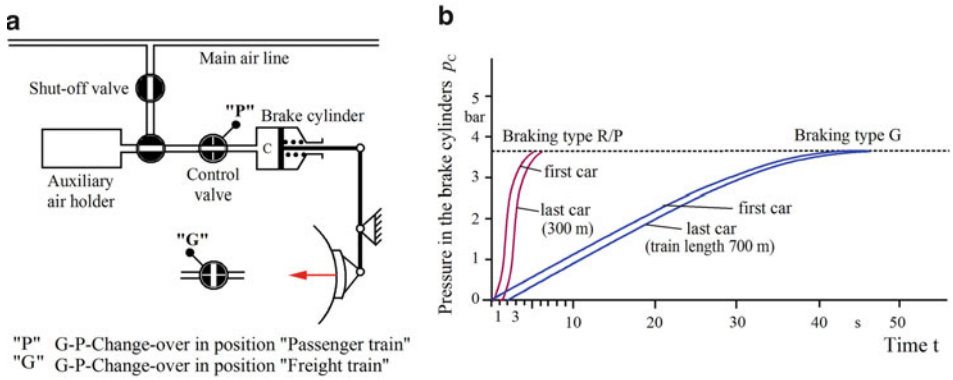

Fig. 4.13 (**a**) Brake type change R/P – G, (**b**) Pressure curves. (According to [42, 51])

longer any pressure difference acting on the large piston, i.e. the line pressure p_L is equal to the control chamber pressure p_A. When the control pressure is reached again, the air reservoir is also filled again, so that a brake of this type is inexhaustible.

Brake Types

Under the influence of sudden and unevenly acting forces, jolts and strains occur in a train consisting of coupled individual vehicles, which could significantly reduce the comfort of the passengers. At higher values, vehicles and loads can be damaged and train separations can be caused. For this reason, braking forces should be applied to all vehicles simultaneously if possible. Due to the speed of propagation of the pressure wave in the main air line (less than the speed of sound of 343 m/s) and the length of the train, the brakes of vehicles running at the front react much earlier than the brakes at the rear of the train. To reduce the problem, shock-absorbing buffers, brake type changes and, in modern vehicles, electro-pneumatic brake control systems are used.

When changing the brake type, the brake cylinder filling time is determined by two different cross sections (brake type R/P (Rapid/Passenger train) = large cross section, brake type G (Goods train) = small cross section), Fig. 4.13. For passenger or fast freight trains up to a certain train weight, brake type R/P is used for faster brake response. Heavy and slower freight trains are braked in braking mode G. For certain vehicles (e.g. locomotives) the braking mode R/P can be subdivided into even more finely dosed braking positions.

Electropneumatic Brake Control (Ep-Brake)

Since the low propagation speed of the pressure reduction or pressure increase as described above has some disadvantages, one tries to circumvent this problem by the electropneumatic brake control. The ep-brake is used on all high-speed trains and works as follows: A device on the driver's brake valve energizes the brake and release solenoids

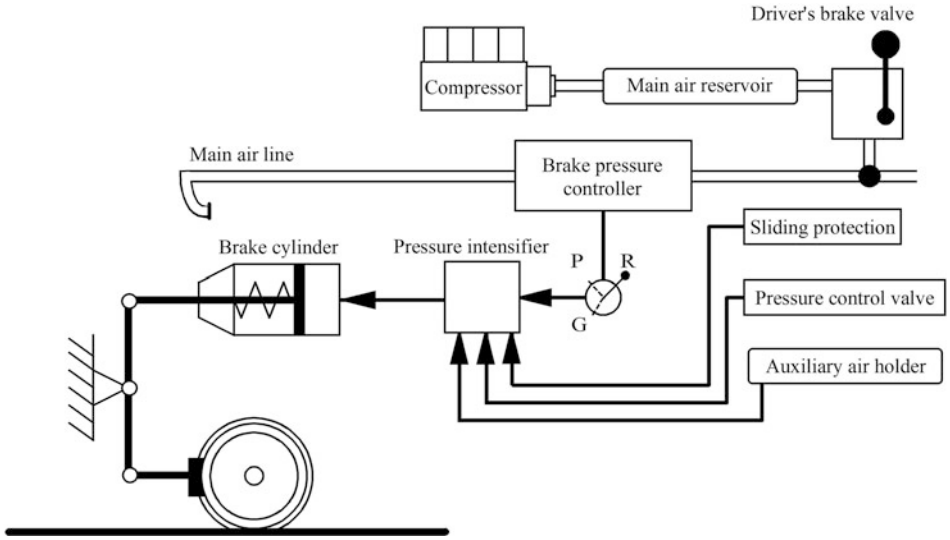

Fig. 4.14 Simplified compressed air diagram of a KE brake

attached to the control valves via a cable connection to the cars (the so-called UIC cable). This means that all control valves respond immediately when the driver's brake valve is actuated. During the release process, the release solenoids immediately release air from the auxiliary air holders into the main air line. An additional 10 bar air line (main air reservoir line) is coupled through from the locomotive to the last vehicle. This line supplements the air consumption of the auxiliary air holders.

Other Components of the Compressed Air System

The **driver's brake valve** (for this and other components see Fig. 4.14) is operated exclusively by the driver of the leading traction unit and must meet the following criteria in its function: The main air line must be filled and a constant pressure must be maintained in it (control pressure of the main air line corresponds to 5 bar), even in the event of minor air losses due to leaks. In the event of emergency braking, the main air line must be emptied over a large cross-section.

In the case of service braking (e.g. for speed regulation), the driver's brake valve shall allow a gradual pressure reduction of the main air line, adapted in time to the sensitivity of the control valves. It shall be possible to shut off a filling of the main air line, e.g. if a locomotive is to be carried as a wagon in the train.

The **brake pressure regulator** (Fig. 4.14) controls the maximum achievable brake cylinder pressure in block brakes with cast iron brake blocks depending on the brake position and the speed by means of a pressure intensifier. High braking is initiated at increasing speed from approx. 70 km/h and low braking at decreasing speed from approx.

50 km/h. High braking means high maximum brake cylinder pressure (on wagons max. 3.8 bar) and low braking means lower maximum brake cylinder pressure (on wagons max. 1.7 bar).

The **load change** regulates the brake cylinder pressure according to the load of a vehicle in such a way that a higher brake cylinder pressure can be achieved with a larger load and the maximum brake cylinder pressure is reduced with a smaller load in order to prevent overbraking and thus sliding of the vehicle's wheelsets. This control can be set manually before the start of the journey on the individual vehicles at the so-called load change[6] or automatically by means of a weighing valve in the vehicle.

A possible sliding of the braked wheelsets is to be prevented in the beginning by the wheel **slide protection.** For this purpose, the brake cylinder pressure is reduced at the beginning of the sliding process or at a measured differential speed between the wheelsets. There are mechanical and electronic wheel slide protection devices. For modern vehicles, only electronic wheel slide protection devices are used, which operate on the basis of differential speeds between the measured wheelsets and a pre-programmed "substitute speed" (see "Antilock Braking Systems" on road vehicles). Since the brake cylinder pressure that is set depends on various parameters such as speed, brake position, main air line pressure reduction introduced and wheel slide protection, the **pressure intensifier** exists to provide the final required pressure for the brake cylinders from all these parameters. The pressure intensifier works as follows:

Braking
- By means of driver's brake valve: pressure reduction in the main air line,
- Control valve switches to "Braking",
- Depending on the wheel slide protection, brake pressure regulator, brake position and the amount of pressure reduction, the pressure intensifier allows the "brake air" to flow from the auxiliary air holders into the brake cylinders.

Release
- Increase the pressure in the main air line to max. 5 bar by means of the driver's brake valve,
- Control valve switches to "Release",
- Depending on the brake position and pressure increase, the pressure intensifier releases the brake cylinders.

[6] A two-stage load braking can be set manually at the load change ("empty" or "loaded"). The changeover is made by changing the linkage ratio, by connecting another brake cylinder or by gradually changing the maximum brake cylinder pressure [37]; see also Sect. 4.4 and Fig. 4.27.

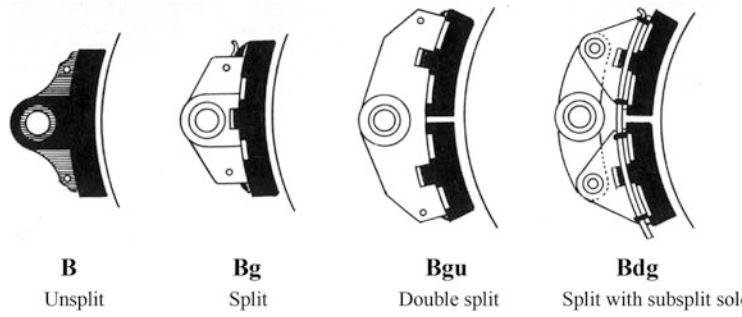

Fig. 4.15 Brake block shapes. (According to [51])

4.1.2 Mechanical Brake Components

The force generated by the brake cylinders is amplified by the **brake linkage** (see Fig. 4.6) and transmitted as evenly as possible to the brake shoes. Automatic brake slack adjusters can be interposed to compensate for brake block wear. The brake linkage consists of numerous levers, shafts and joints, which is why the efficiency is not particularly high (80–90%). **Block brake units** are used on almost all vehicles exclusively in split design, consisting of a bracket and one or two brake block soles, Fig. 4.15. Several small blocks promote more even pressure distribution and more favourable heat generation. In the case of split brake blocks, only the soles are replaced when worn.

Brake block materials are grey cast iron (EN-GJL) or special plastics. Plastic blocks have a higher coefficient of friction than grey cast iron blocks, which is also largely independent of speed. For this reason, grey cast iron blocks are not used in vehicles with high deceleration. Another disadvantage in electric train operation is the (magnetic and electrically conductive) abrasion of the grey cast iron blocks, which may be sucked in by the fans of the electric locomotives. Due to the noise caused by brakes with cast iron blocks (brake squeal, higher rolling noise due to roughening of the wheel treads, hitting of the loose brake blocks against the wheel disc when the brake is released), the cast iron blocks are increasingly being replaced by the (more expensive) plastic blocks.

Disc brakes (Figs. 4.16 and 4.17) have become widely accepted in passenger coaches, suburban, metro and light rail vehicles (and also in freight transport at speeds above 120 km/h) for the following reasons:

- Higher performance than block brakes,
- Lower maintenance costs,
- Better ride comfort (no squeaking, no holding jerk),
- Lower dependence of the coefficient of friction on pressure and speed, consequently no high braking stage necessary,
- More compact design with shorter response times.

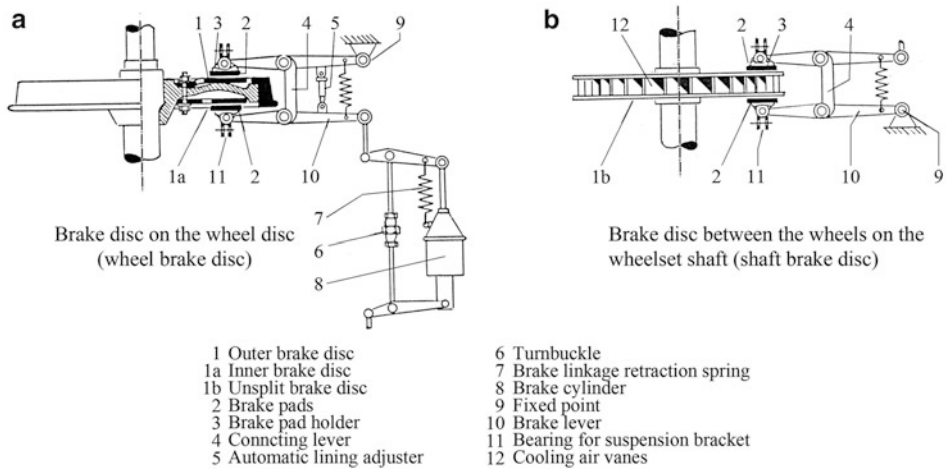

Fig. 4.16 Disc brakes with wheel brake disc (**a**) and shaft brake disc (**b**). (According to [51])

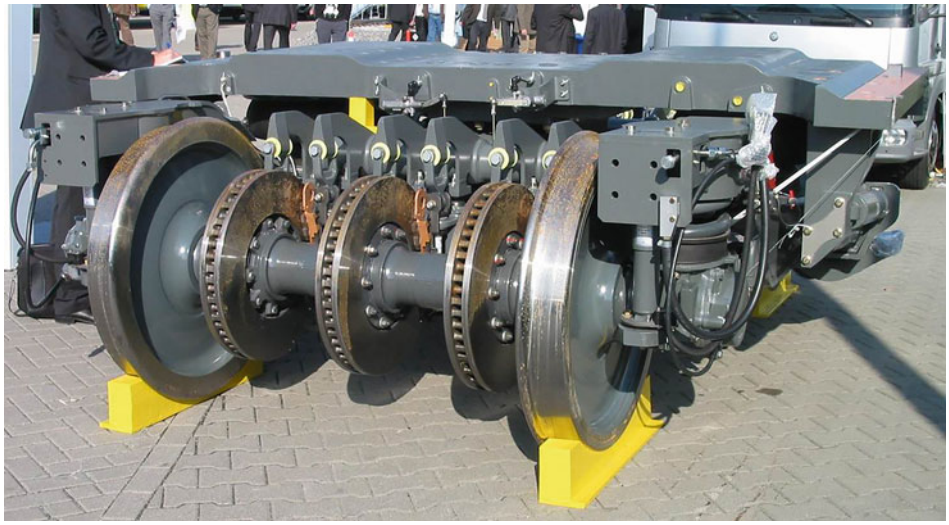

Fig. 4.17 Three brake discs on a wheelset shaft of the Siemens Velaro RUS (high-speed train for Russia)

The disc brakes are controlled by the same air brake system as the block brakes with plastic blocks (no high braking level). The brake discs can either be attached to the wheel body (e.g. on railcars with axle drives or electric motors) or individually to the wheelset shaft. For better heat dissipation, brake discs are usually internally ventilated with cooling air vanes. Cast iron with nodular graphite (EN-GJS) is used as the brake disc material; steel is also used for the ICE drive heads, although the brake linings are made of sintered metal in

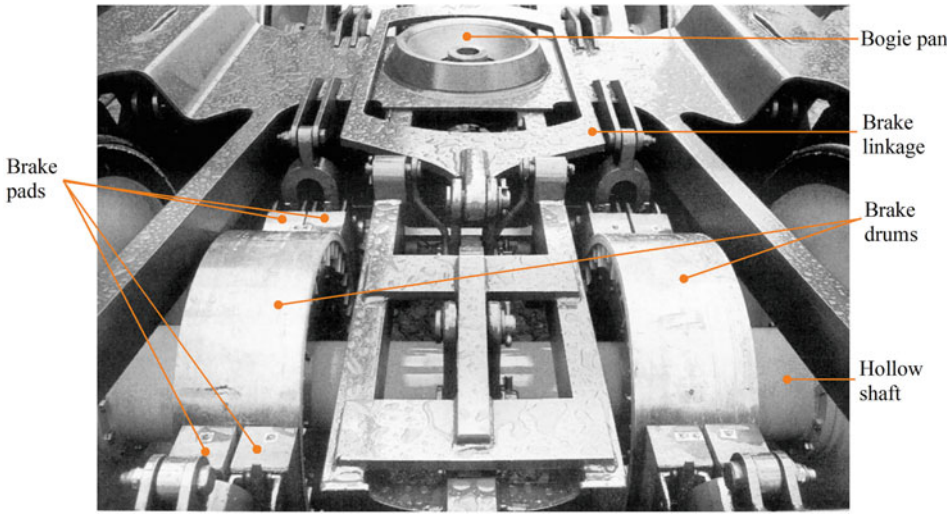

Fig. 4.18 External drum brake in a freight wagon bogie. (Eisenbahn Revue International (1994)H. 1/2, p. 38)

this case. The brake pads are pressed against the brake discs by the brake cylinders via a linkage. Automatic pad adjusters can be interposed to compensate for pad wear. Becorite sintered materials are used for the brake linings in high-speed traffic.

High stresses due to increased speed and high wheelset loads led to wheel damage in vehicles with block brakes, and unfortunately accidents also occurred due to wheel breakage. BSI traffic technology,[7] together with other companies, has developed an external drum brake (Fig. 4.18) and tested it on the test bench and in road trials. This brake combines the advantages of disc brakes

- Low noise,
- Constant friction value,
- No wheel heating,
- Long service life of brake drum and lining,

with those of block brakes

- Cost-effective solution,
- Easy conversion of existing block brake systems.

[7] BSI: Bergische Stahlindustrie – today Faiveley Transport SA.

The drum brake uses the same air brake system as the conventional air brakes. Its components are essentially:

- Brake body: consisting of a drum and a hollow shaft flanged to the wheel, optimum ribbing for good heat dissipation, material grey cast iron or grey cast iron with nodular graphite.
- Brake pads: similar shape to the brake pads with service life up to 20,000 km and made of plastic.

4.1.3 Electric (Regenerative) Brake

The regenerative brake plays an essential role in most diesel-electric or electric traction units, and in particular in suburban, underground, urban and tramway vehicles (see also Sect. 3.2). The constantly increasing traction power of traction units also results in increased demands on the braking systems. In addition to the mechanical braking systems that are always available, electric traction units offer the possibility of electrodynamic braking: the traction motors are operated as generators during braking. The regenerative brake is characterised by the following properties compared to the mechanical brake:

- Wear-free and low-maintenance operation,
- Fine adjustment of the braking force,
- More favourable braking characteristics through the choice of appropriate braking and control circuits,
- Possibility of energy recovery into the mains with appropriate switching,
- Protection of the wheel tyres.

Only the driven wheelsets are braked with the regenerative brake, not all wheelsets of a train. A clever combination of electric and mechanical brakes achieves an almost constant braking force in conventional vehicles and can thus compensate for the decreasing braking force of the electric brake as the speed decreases.

In Fig. 4.19 the types of brake circuits are distinguished. This overview shows the variety of regenerative brakes and circuit types that exist.

Figure 4.20 shows a simplified example of the brake circuit of a catenary voltage-dependent, externally excited DC resistor brake. On the basis of this representation, the mode of operation can be explained as follows:

- The traction motors (M1 to M4) are switched as generators to braking resistors.

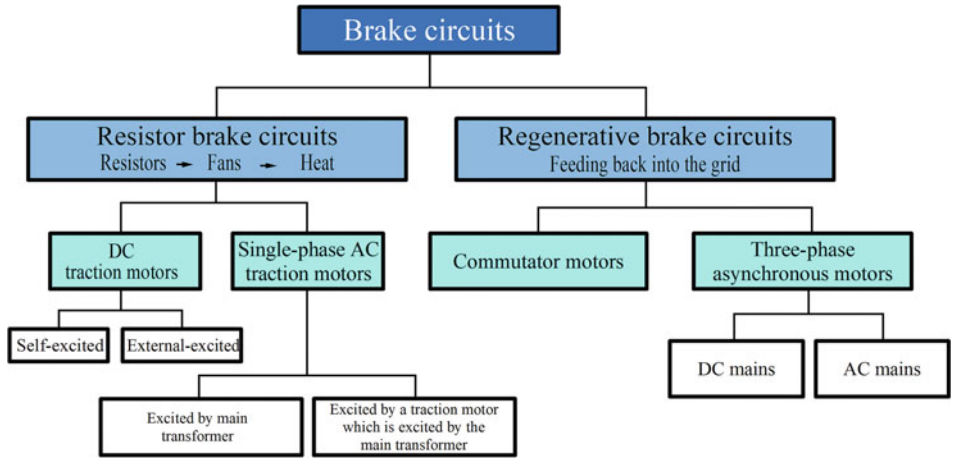

Fig. 4.19 Overview: Brake circuits for electric traction units. [4]

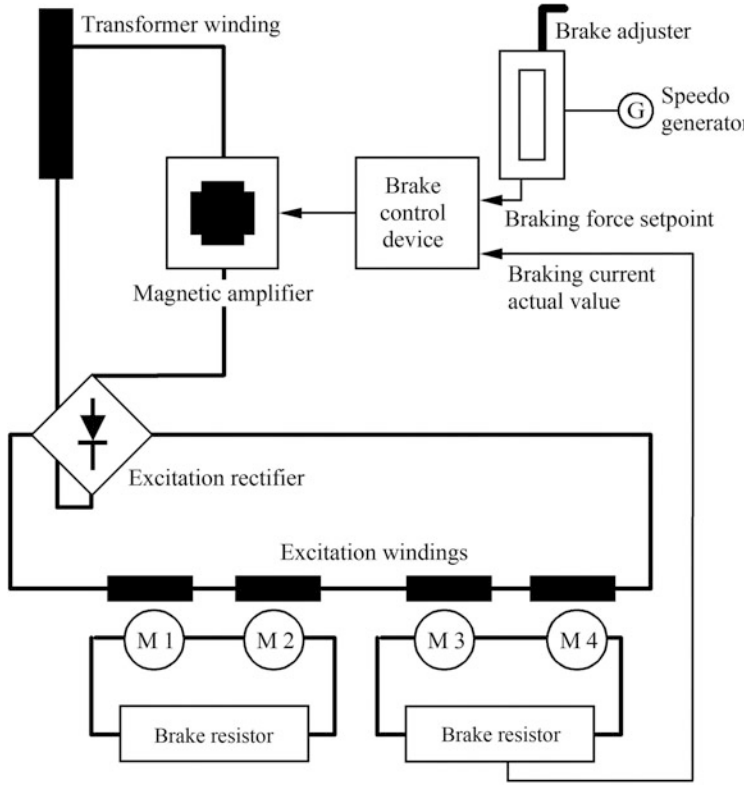

Fig. 4.20 Externally excited DC resistance brake. (According to: DB AG Workbook for the Initial and Further Training of Locomotive Drivers No. 129/7 23)

- The excitation of the generators takes place via the excitation windings supplied with direct current.
- The brake control device controls the magnetic amplifier depending on the actual braking current value, the speed and the applied braking stage (brake actuator).
- The magnetic amplifier controls the braking exciter current on the AC side of the braking excitation rectifier and thus the braking force acting in the traction motors.

The decreasing braking force with decreasing driving speed (see characteristic curves of the electric motors in Chap. 3) is compensated for in rail vehicles with this braking circuit by combining it with other braking systems.

The application of newer drive concepts allows energy to be fed back into the grid over the entire speed range by means of a regenerative braking circuit. However, the energy fed back must be absorbed by other vehicles. Only in very few cases is it possible to feed energy back into the public grid. The energy that cannot be absorbed by the catenary system is converted into heat in braking resistors. At DB AG today, approx. 10% of the electrical energy absorbed for traction is fed back by regenerative braking.

4.1.4 Hydrodynamic Brake

Two types of hydrodynamic brakes are used on rail vehicles: The hydraulic retarder works like a "water vortex brake". The pump wheel is connected to the drive wheelsets. The turbine wheel is part of the housing, i.e. it cannot rotate. The pump wheel thus works against the fixed turbine wheel. During the braking process, kinetic energy is converted into heat energy of the retarder oil. This heat must be dissipated to the environment via an oil cooler (heat exchanger).

The turbo reversing transmission has a hydraulic starting converter for each direction of travel of the traction unit. Braking is effected by applying pressure to the starting converter for the opposite direction of travel. Hydraulic brakes operate without wear. These brakes are used on diesel-hydraulic locomotives and railcars.

4.2 Brakes Independent of Wheel-Rail Adhesion

In the comments on the wheel-rail adhesion coefficient, reference was made to unfavourable environmental conditions which could result in a drastic increase in the braking distance, e.g. dampness and wet leaves on the rails. Under such conditions, brakes that apply their braking force independently of the wheel-rail adhesion are absolutely necessary for safety reasons.

The magnetic rail brake (MG brake, Fig. 4.21) is widely used on passenger coaches for the reasons mentioned above. For speeds above 140 km/h, magnetic rail brakes are prescribed by various railway administrations. The background to this is the existing signal

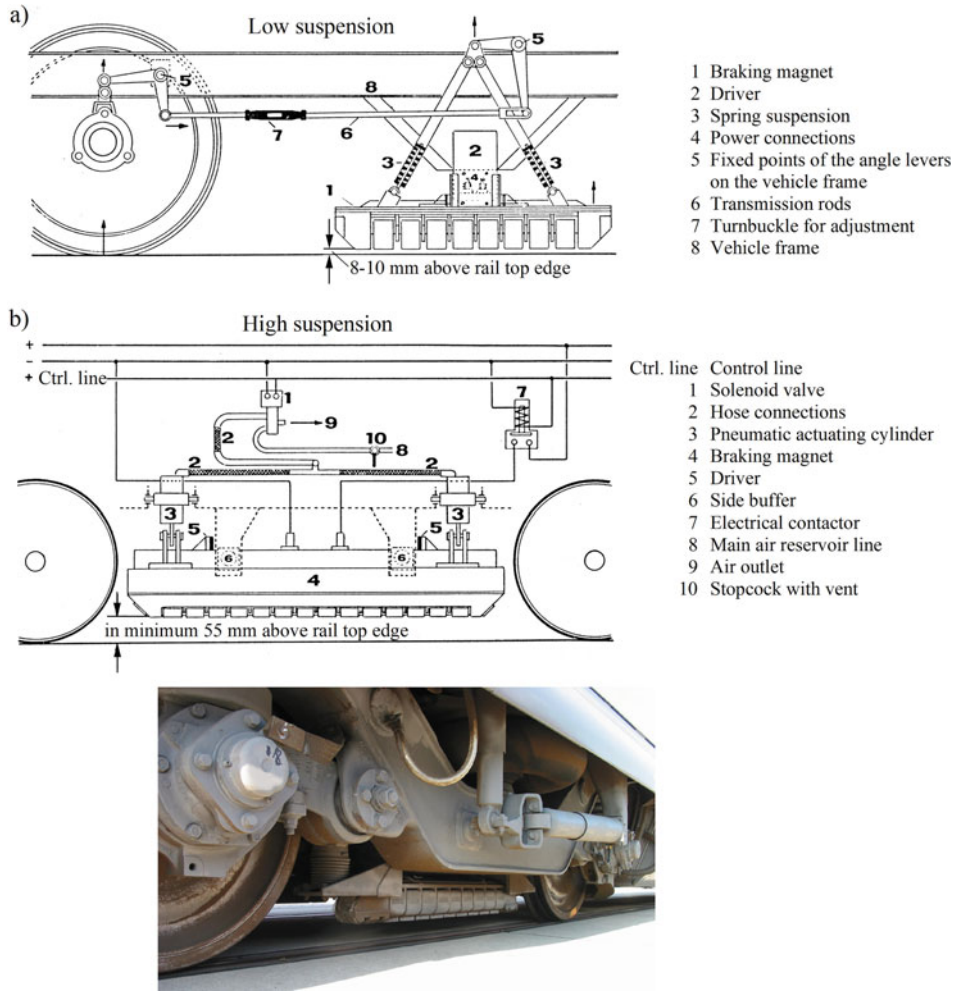

Fig. 4.21 Magnetic rail brake (according to [51]), *below* magnetic rail brake in high suspension on ÖBB-Railjet (ÖBB: Austrian Federal Railways)

distances, for which the braking distance at high speeds would be too long without magnetic rail brakes. The use of the MG brake has been tested for speeds above 250 km/h and implemented as an emergency brake or rapid brake. Further applications of the MG brakes can be found in urban, underground, tramway and mine railways as well as in railcars for regional traffic.

The MG brake is a friction brake in which brake pads are pressed electromagnetically onto the rail heads. The braking effect results from friction between the pole shoes and the rail, but also from eddy current effects between the brake magnet and the rail head. The MG brake is subject to wear, i.e. the pole shoes must be replaced from time to time. MG brakes

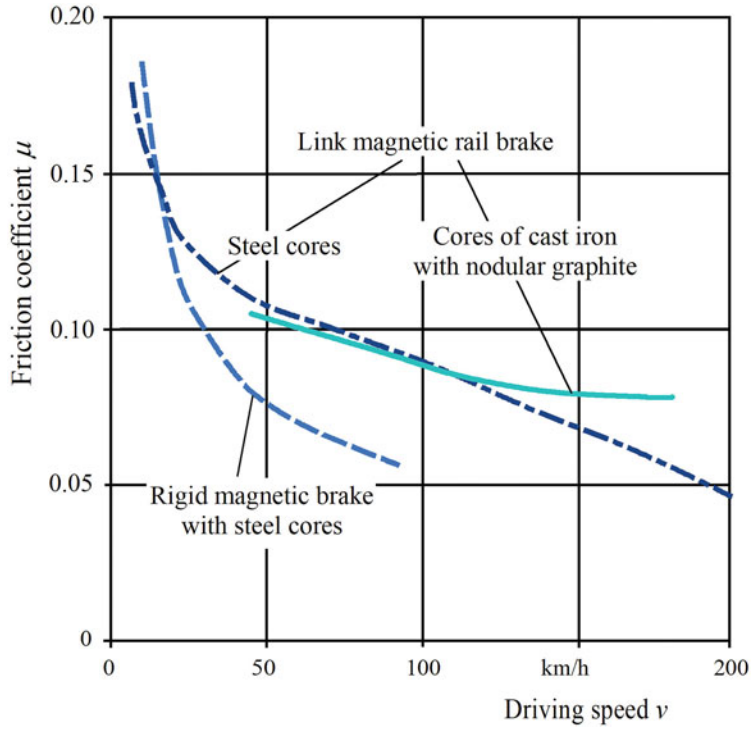

Fig. 4.22 Friction value of MG brake of different designs as a function of speed. (According to [56])

are also designed in the form of link magnets for better adaptation to unevenness in the rail run.

With regard to the suspension, a distinction is made (Fig. 4.21):

- the low suspension: for trams and light railways with low speeds up to 100 km/h, magnet distance to the rail top edge of approx. 6–12 mm, Fig. 4.21a.
- the high suspension: for vehicles in high-speed traffic with speeds above 100 km/h, magnetic distance to the rail top edge of 60–130 mm, Fig. 4.21b.

Since the braking force of the MG brake increases sharply below 50 km/h (see friction coefficient curve in Fig. 4.22) and the MG brake cannot be controlled, the MG brakes are switched off in this range for railway vehicles. The further deceleration of the vehicles until standstill is done by a combination with other brakes. In combination with the block brake, decelerations of 1.5 m/s^2 are achieved; higher values are unacceptable for passengers not wearing seat belts or standing passengers.

The linear eddy current brake is used in rail transport as a braking system that is actually independent of the coefficient of adhesion. It is controllable and wear-free and can apply

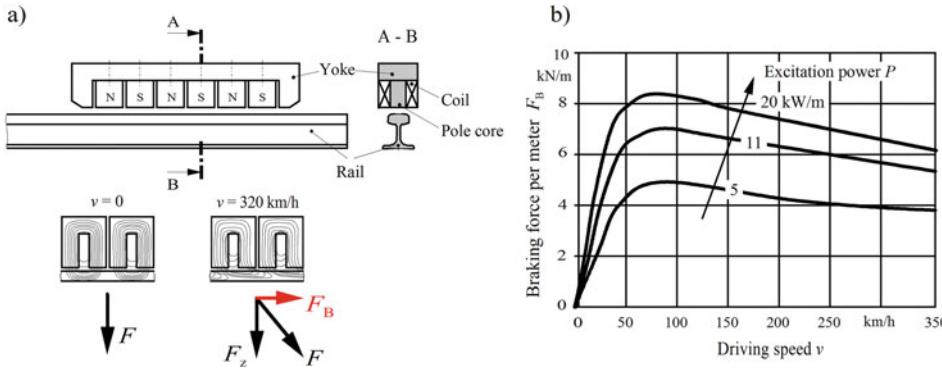

Fig. 4.23 Structure (**a**) and characteristic values (**b**) of the linear eddy current brake. (According to [37])

higher braking forces than the MG brake, particularly in the upper speed range, with the appropriate power design. Due to its controllability, it can also be used with partial braking forces for service braking and is particularly suitable for high-speed traffic.

The installation of the eddy current brake in the bogie is similar to that of the MG brake. However, in contrast to the MG brake, the eddy current brake does not touch the rail during the braking process, but hangs about 7 mm above it and therefore brakes without wear. For a constant distance, the brakes must be supported by a longitudinal beam on the wheel bearings. The eddy current brake consists of a solid magnet yoke and several pole cores screwed to it, which are surrounded by copper coils. The coils of these brakes are alternately switched from north to south pole in the direction of the rail, Fig. 4.23a. To build up the strong magnetic fields, a high excitation power is required, which is usually available from regenerative brakes at a sufficient level.

At standstill, the magnetic field is symmetrical and generates a vertical attractive force F, Fig. 4.23a. If the brake is moved relative to the rail, a transient magnetic field is generated in the rail. This generates voltages which result in eddy currents, distort the magnetic field in the opposite direction to the direction of travel and form a horizontal force component $F_{B.}$

The characteristic of the linear eddy current brake (Fig. 4.23b) shows, as already mentioned, a braking force at standstill which is zero. It reaches its braking force maximum at constant excitation in the range of approx. 75 km/h. The strong heating of the rails and the magnetic influence on signalling devices on the track can be mentioned as disadvantages in the operation of the linear eddy current brake. The linear eddy current brake was successfully tested for the first time in DB AG's ICE-V high-speed train. It is used as standard in the ICE-3.

Figure 4.24 shows the interaction of different braking systems on the ICE-1, with the braking forces and braking decelerations plotted against the running speed. According to the source given for Fig. 4.24, the power heads of the ICE-1 can apply a significant

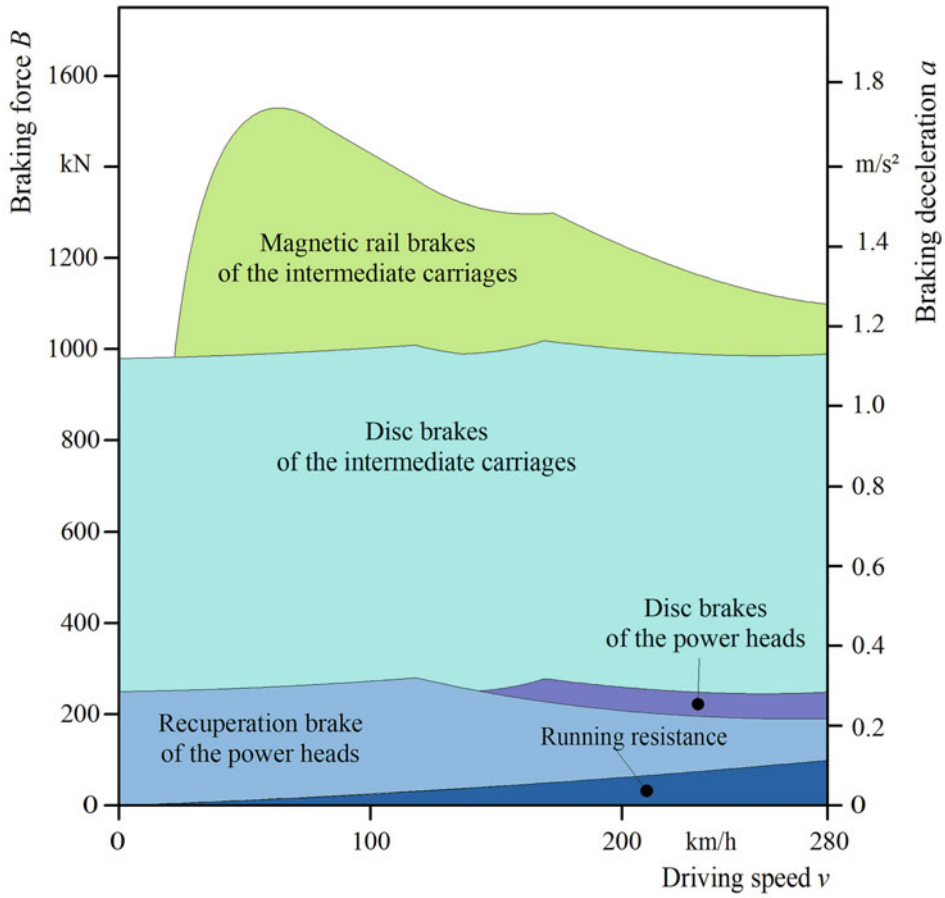

Fig. 4.24 Braking force distribution of the ICE 1 on different braking systems. (Braun, A.: Experiences with friction brakes of the InterCity Express. ZEV + DET Glas. Annalen 117(1993)H. 11, S. 352–357)

regenerative braking force (approx. 250 kN at $v = 0$) even at low speeds. This is to be doubted, since usually the braking force during regenerative braking is zero at $v = 0$.

The magnetic rail brake is switched off at low speeds. The series ICE-1 and 2 do not have an eddy current brake.

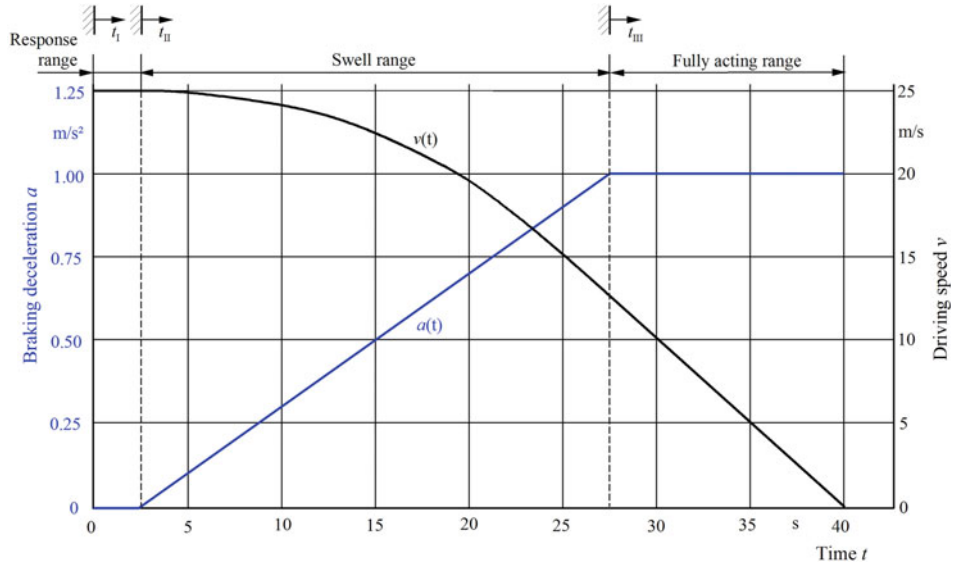

Fig. 4.25 Course of braking deceleration and speed during deceleration braking of a freight train to a standstill. (According to [24])

4.3 Calculation of Braking Distances

The calculation of braking distances is described in DIN EN 14531-1.[8] A simplified procedure for the approximate determination is to be shown here. In order to calculate the braking distance of a rail vehicle or a train, it is first necessary to understand the course of the braking deceleration during a braking process, Fig. 4.25. This figure schematically shows the braking course – braking deceleration (blue line) and speed (black line) – over time for a freight train. Some simplifications have been made here:

- The braking effect of the running resistances is neglected.
- The braking process takes place on level ground (no uphill or downhill gradient).
- After a response time of $t_A = 2.5$ s, the braking effect starts, assuming a linear increase of the braking deceleration.
- The maximum braking deceleration of $a = -1$ m/s^2 = const is reached after a threshold duration of $t_S = 25$ s.

[8] DIN e. V.: Railway applications – Methods for the calculation of stopping and deceleration braking distances and parking braking. Part 1: General algorithms for individual vehicles and vehicle groups taking into account average values. pr DIN EN 14531–1 (draft), Beuth-Verlag, Berlin (2012).

With these simplifications, the blue line in Fig. 4.25 results for the time course of the braking deceleration.

As known from Fig. 4.13, the build-up of brake pressure in freight trains is slow. Here, 25 s were assumed until the full brake pressure is available ($t = 27.5$ s) and thus the maximum deceleration of the train occurs. This maximum deceleration then acts constantly until the train comes to a standstill. The initial speed in this example is $v_0 = 90$ km/h $\triangleq$ 25 m/s. The duration until the train comes to a standstill t_B results from three components:

- Response time t_A,
- Threshold duration t_S,
- Full effective time t_V,

$$t_B = t_A + t_S + t_V. \tag{4.8}$$

Analogously, one obtains for the braking distance:

$$s_B = s_A + s_S + s_V. \tag{4.9}$$

The acceleration a is the derivative of the velocity v with respect to the time t:

$$a = \frac{dv}{dt} \rightarrow dv = a \cdot dt \rightarrow v(t) = \int a \cdot dt. \tag{4.10}$$

The velocity v is the derivative of the path s with respect to the time t:

$$v = \frac{ds}{dt} \rightarrow ds = v \cdot dt \rightarrow s(t) = \int v \cdot dt. \tag{4.11}$$

Since the blue function shown in Fig. 4.25 is discontinuous, it is advisable to consider it range-wise. In the response range, the speed of the train is equal to the initial speed $v_0 = 25$ m/s. The distance covered in this range up to $t_I = t_A$ is therefore

$$s_A = 25 \text{ m/s} \cdot 2.5 \text{ s} = 62.5 \text{ m}.$$

In the threshold range, the braking deceleration increases linearly from zero to $a_{max} = 1.0$ m/s^2; its course thus corresponds to the straight-line equation

$$a(t_{II}) = \frac{a_{max}}{t_S} \cdot t_{II}. \tag{4.12}$$

Eq. 4.10 can now be used to calculate the velocity profile in this range:

$$v(t_{\mathrm{II}}) = \frac{a_{\max}}{t_{\mathrm{S}}} \int t_{\mathrm{II}} \cdot \mathrm{d}t = \frac{a_{\max}}{2t_{\mathrm{S}}} \cdot t_{\mathrm{II}}^2 + C_1. \tag{4.13}$$

In the threshold range it applies that at $t_{\mathrm{II}} = 0$ the train is still moving with the initial velocity v_0. C_1 can be determined from this:

$$C_1 = v_0 \rightarrow v(t_{\mathrm{II}}) = \frac{a_{\max}}{2t_{\mathrm{S}}} \cdot t_{\mathrm{II}}^2 + v_0. \tag{4.14}$$

We get the distance traveled within the threshold duration by integrating Eq. 4.13:

$$s(t_{\mathrm{II}}) = \frac{a_{\max}}{6t_{\mathrm{S}}} \cdot t_{\mathrm{II}}^3 + v_0 \cdot t_{\mathrm{II}} + C_2. \tag{4.15}$$

At time $t_{\mathrm{II}} = 0$, the distance traveled in area II is zero, thus:

$$C_2 = 0 \rightarrow s(t_{\mathrm{II}}) = \frac{a_{\max}}{6t_{\mathrm{S}}} \cdot t_{\mathrm{II}}^3 + v_0 \cdot t_{\mathrm{II}}. \tag{4.16}$$

Using Eq. 4.16, we calculate the distance traveled in the threshold region ($a_{\max} = -1$ m/s^2; $t_{\mathrm{S}} = 25$ s; $v_0 = 25$ m/s):

$$s_{\mathrm{S}} = s_{\mathrm{II}}(t_{\mathrm{II}} = 25\ \mathrm{s}) = \frac{-1\ \mathrm{m/s^2}}{6 \cdot 25\ \mathrm{s}} \cdot (25\mathrm{s})^3 + 25\frac{\mathrm{m}}{\mathrm{s}} \cdot 25\ \mathrm{s} = 521\ \mathrm{m}.$$

The speed of the train at the end of the threshold range is given by Eq. 4.14:

$$v(t_{\mathrm{II}} = 25\ \mathrm{s}) = \frac{-1\ \mathrm{m/s^2}}{2} \cdot 25\ \mathrm{s} + 25\frac{\mathrm{m}}{\mathrm{s}} = 12.5\frac{\mathrm{m}}{\mathrm{s}} = v(t_{\mathrm{III}} = 0) = v_{\mathrm{S}}.$$

This is the initial velocity in the full effective range. Equation 4.10 applies here accordingly, since the acceleration is constant:

$$v(t_{\mathrm{III}}) = \int a_{\max} \cdot \mathrm{d}t = a_{\max} \int \mathrm{d}t = a_{\max} \cdot t_{\mathrm{III}} + C_3. \tag{4.17}$$

At time $t_{\mathrm{III}} = 0$, the velocity is $v(t_{\mathrm{III}} = 0) = v_{\mathrm{S}} = 12.5$ m/s. Thus $C_3 = v_{\mathrm{S}}$,

$$v(t_{\mathrm{III}}) = a_{\max} \cdot t_{\mathrm{III}} + v_{\mathrm{S}}. \tag{4.18}$$

Thus, for the distance travelled in the full effective range:

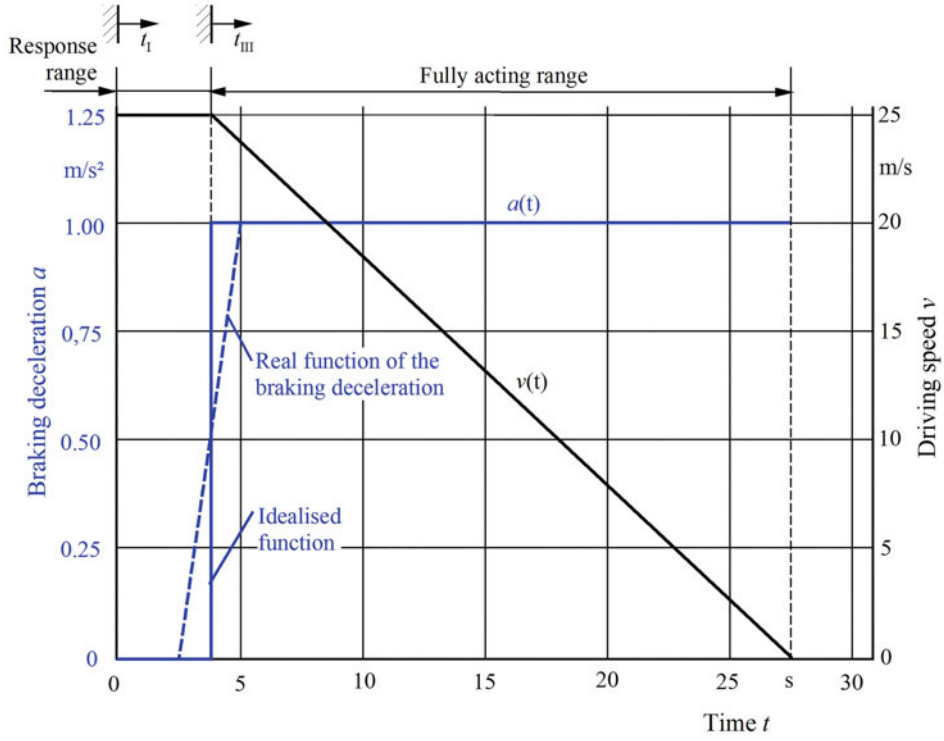

Fig. 4.26 Course of braking deceleration and speed during deceleration braking of a passenger train (local train) to a standstill. (According to [24])

$$s(t_{III}) = \frac{a_{max}}{2} t_{III}^2 + v_S \cdot t_{III} + C_4. \tag{4.19}$$

With $s(t_{III} = 0) = 0$, $C_4 = 0$ and thus

$$s(t_{III}) = \frac{a_{max}}{2} t_{III}^2 + v_S \cdot t_{III}. \tag{4.20}$$

The duration until standstill results from Eq. 4.18:

$$v(t_{III} = t_V) = 0 = a_{max} \cdot t_V + v_S \rightarrow t_V = -\frac{v_S}{a_{max}} = -\frac{12.5 \text{ m/s}}{-1 \text{ m/s}^2} = 12.5 \text{ s}. \tag{4.21}$$

This value inserted in Eq. 4.20 provides for the travel in the full effective range (until the train comes to a standstill):

$$s_V = \frac{-1\ \text{m/s}^2}{2}(12.5\ \text{s})^2 + 12.5\ \text{m/s} \cdot 12.5\ \text{s} = 78.125\ \text{m}.$$

Finally, we obtain for the total braking distance: $s_B = 671.625\ \text{m} \approx 672\ \text{m}$.

For passenger trains – brakes in brake position P – the brake pressure is built up much faster, Fig. 4.26. To calculate the braking distance, the threshold range can be neglected here if the threshold duration (here 2.5 s) is divided equally between the response range and the full-acting range. The step function shown in Fig. 4.26 is then obtained: Up to $t = 3.75$ s the train moves at full speed. Then the full deceleration sets in abruptly. Therefore, only two ranges need to be considered. In the response range, the train covers the following distance at $v_0 = 90$ km/h $\triangleq$ 25 m/s:

$$s_A = 25\ \text{m/s} \cdot 3.75\ \text{s} = 93.75\ \text{m}.$$

Then the full braking effect starts with $a = -1\ \text{m/s}^2$. From Eqs. 4.20 and 4.21 we obtain for the distance to standstill at constant deceleration:

$$s_V = -\frac{v_0^2}{2a_{max}} = -\frac{(25\ \text{m/s})^2}{2(-1\ \text{m/s}^2)} = 312.5\ \text{m}.$$

The total braking distance is therefore $s_B = s_A + s_V = 406.25\ \text{m} \approx 406\ \text{m}$.

Often one finds as a formula to calculate the braking distance at constant braking deceleration:

$$s_{(B)} = \frac{v_0^2}{2a} \tag{4.22}$$

with

$v_0 =$	Output speed and
$a =$	mean braking deceleration (to be used with a positive sign).

The braking distances just calculated are quite acceptable for railway operation, although they are very long compared to road vehicles. However, railways do not run on sight as in road traffic, but on signalling. On main lines, for example, the driver is informed of the position of the main signal by the approach signal 1000 m ahead. If, for example, the signal aspect of the approach signal is “Expect stop at main signal”, target braking is possible up to the main signal showing “Stop”.

$$v_{max} = \sqrt{2s \cdot a} = \sqrt{2 \cdot 1000\ \text{m} \cdot 1\ \text{m/s}^2} \approx 44\frac{\text{m}}{\text{s}} \approx 160\ \text{km/h}.$$

On lines with higher maximum permissible speeds, DB transmits the current permissible speed to the traction unit via an antenna in the track, the so-called "line conductor".

Trams, on the other hand, are driven on sight, especially if the tracks are laid in the roadbed. Assuming that standing passengers, e.g. in trams, should be subjected to a maximum deceleration of $a = 1.0$ m/s^2, then at $v_0 = 50$ km/h ≈ 13.89 m/s and a response time of 1 s a braking distance of

$$s_B = 13.89\ \text{m/s} \cdot 1\text{s} + (13.89\ \text{m/s})^2/(2 \cdot 1.0\ \text{m/s}^2) \approx 110.4\ \text{m}.$$

This is possible for target braking (stopping at stops or in front of signalling equipment showing stop), but not for hazard braking. The BOStrab[9] prescribes an average deceleration of $a = 2.47$ m/s^2 for emergency braking from 50 km/h, which means a braking distance of

$$s_B = 13.89\ \text{m/s} \cdot 1\text{s} + (13.89\ \text{m/s})^2/(2 \cdot 2.47\ \text{m/s}^2) \approx 53.0\ \text{m}$$

Cars can achieve average decelerations of approx. 8 m/s^2 on dry roads, so that their braking distance from 50 km/h at 1 s response time is

$$s_B = 13.89\ \text{m/s} \cdot 1\text{s} + (13.89\ \text{m/s})^2/(2 \cdot 8.0\ \text{m/s}^2) \approx 26.0\ \text{m}$$

In tram vehicles, higher braking decelerations than the 2.47 m/s^2 mentioned can be achieved with the aid of the magnetic rail brake. It should be noted, however, that standing passengers may fall and that seated passengers who are not wearing seat belts may also be injured.

Example 4.1
What is the braking distance of a passenger train from $v = 280$ km/h with a braking deceleration of $a = 1$ m/s^2 and a response time $t_A = 3.75$ s?

Solution: The braking distance results from the response -and full effective distance: $s_B = s_A + s_V$. The speed is 280 km/h $\triangleq$ 77.8 m/s.

$$s_B = v_0 \cdot t_A + \frac{v_0^2}{2a} = 77.8\frac{\text{m}}{\text{s}} \cdot 3.75\text{s} + \frac{\left(77.8\,\frac{\text{m}}{\text{s}}\right)^2}{2 \cdot 1\,\frac{\text{m}}{\text{s}^2}} = 271.5\ \text{m} + 3026.4\ \text{m} = 3297.9\ \text{m}$$

The braking distance from 280 km/h is thus around 3300 m.

[9] See BOStrab, Annex 2 to § 36.

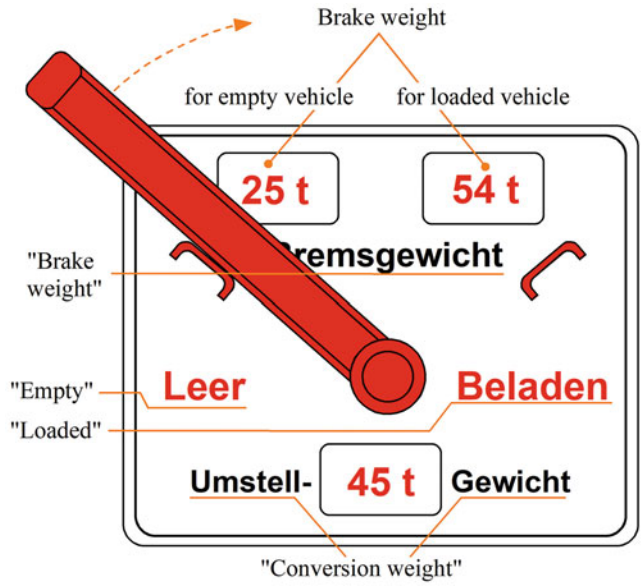

Fig. 4.27 Illustration of the brake weights at the load change of a railway freight wagon

4.4 Brake Weight

In railway operation, the term "brake weight" is used. This term is neither a weight nor a force. The brake weight is used by an operating railway undertaking to determine whether the braking performance of a train set is possible for running on a given railway line at a given speed.

> Brake weight is a term introduced in railway operation that describes the performance capacity of the vehicle brake associated with a braking position. The brake weight of a railway vehicle is usually determined by tests and uniformly specified for a vehicle type [42].

The brake weight of a vehicle can be seen from the markings on the vehicle. In the case of freight wagons, for example, it can be seen from the load change, Fig. 4.27. In the case of freight wagons, the load change is used to manually set the loading condition. For example, this is a four-axle vehicle with a maximum permissible mass of 80 t (20 t per wheelset). At the load change in Fig. 4.27, the red lever is used to change from "Empty" to "Loaded" when the vehicle mass is more than 45 t. The position "Empty" is shown. The vehicle mass is determined after loading, e.g. on a track scale. From the values on the load change plate it can be seen that in the "Empty" position the vehicle has a brake weight of 25 t, and in the "Loaded" position of 54 t.

The "braking hundredths" are calculated from the brake weights of all vehicles in a train and from the sum of all vehicle weights:

$$\text{Braking hundredths } [\%] = \frac{\text{Total brake weight[t]} \times 100}{\text{Total train weight[t]}}.$$

The so-called "book timetables", which are available to the operating staff, show the binding "minimum braking hundredths" for a particular section of line. If a train reaches or exceeds the prescribed minimum braking hundredths, it is ensured that the train can come to a halt from the maximum permissible speed within the available braking distance[10] [42]. The responsible train crew, usually the train leader[11] (the train manager), compares the braking hundredths available for the train with the minimum braking hundredths required for the route to be travelled. If the braking hundredths are not sufficient, special provisions apply, e.g. reduction of the maximum speed. The brake weights can therefore be used by the operating staff to determine, by means of a simple calculation, whether the train's braking capacity is sufficient for a particular route. This is particularly important for trains whose composition changes as a result of wagons being taken on or parked.

[10] The existing braking distance results, for example, from the approach signal spacing on a line.

[11] The train leader is the train chief. He is not to be confused with the locomotive driver.

Wheelset Guidance, Suspension and Damping

5

In contrast to road vehicles, rail vehicles – railways and trams – are track-guided. Adherence to the intended course is therefore not the task of the vehicle driver, but is achieved by the interaction of the track or rails on the one side and wheelsets on the other. Track guidance was already briefly discussed in Chap. 1. This will now be dealt with in more detail. In doing so, we will deal with the running gear of rail vehicles. While freight wagons are in service as two-axled vehicles as well as with bogies, railway vehicles for passenger traffic – passenger coaches and railcars – are almost exclusively used with bogies (an exception is shown at the end of this chapter with the Copenhagen commuter train). Some types of low-floor tram cars are equipped with single-axle – and single-wheel running gear.

As requirements for running gears of rail vehicles can be mentioned:

- Guidance of the vehicle in straight track and in curved track,
- Transmission of forces and moments from the vehicle to the track,
- High vibration comfort for passengers or protection of the load,
- Low forces on the track superstructure,
- Low wheel tyre and rail wear,
- Low noise level,
- Derailment safety, especially at curve entry and exit (see Sect. 5.4),
- Low maintenance.

© The Author(s), under exclusive license to Springer Fachmedien Wiesbaden GmbH, part of Springer Nature 2022

J. Ihme, *Rail Vehicle Technology*,
https://doi.org/10.1007/978-3-658-36969-9_5

5.1 Vibration Perception of the Human Being

In order to assess vibration comfort or to design a vehicle with acceptable vibration comfort for passengers, one must know the vibration perception of humans. People perceive mechanical vibrations differently depending on the vibration direction and frequency. The body posture (sitting, standing, lying) and the introduction of the vibrations to the body (via feet, buttocks, hands, etc.) also play a role. The vibration acceleration that occurs is essentially decisive for the vibration comfort of humans.

Guidance on vibration assessment is given in VDI Guideline 2057.[1] The same evaluation functions for ride comfort in rail vehicles are also shown in DIN EN 12299.[2] Furthermore, the International Union of Railways (UIC) has published leaflet 513.[3] Finally, an assessment of vibration comfort can be found in ISO 2631.[4] The four standards are suitable for assessing the vibration comfort from measured (or from simulations obtained) vibration responses of rail vehicles; indications for the design can only be obtained roughly from the evaluation functions presented there; in some cases even the evaluations differ. The older Wz method of,[5,6] the DB (running quality value) indicates the ranges around 1 Hz and above 10 Hz as favourable in the vibration directions vertical and horizontal-transverse. The range between 4 and 6 Hz is considered unfavourable for both vibration directions.

From the above sources and from [46], the following can be summarized about the vibration sensation of humans:

- Humans are insensitive to vibration in the frequency range between 0 and 0.15 Hz.
- In the range between 0.2 and 0.5 Hz, kinetosis ("seasickness") occurs in humans; humans react less to the vibration acceleration than to the vibration velocity.
- Between 0.5 and 2 Hz, humans perceive vertical vibrations as little disturbing (see the "rocking to sleep" of small children).
- In the range of 2–4 Hz, the vibration acceleration must become smaller with increasing frequency so that it is not perceived as unpleasant.

[1] VDI e. V.(Ed.): Einwirkung mechanischer Schwingungen auf den Menschen – Ganzkörper-Schwingungen. VDI Guideline 2057, Sheet 1, Beuth-Verlag, Berlin (2002).

[2] DIN e. V. (Ed.): Railway applications – Ride comfort – Measurement and evaluation. DIN EN 12299, Beuth-Verlag, Berlin (2009).

[3] UIC (Ed.): Guidelines for the assessment of passenger vibration comfort in railway vehicles. Union Int. des Chemins de Fer, Paris (1994).

[4] ISO (Ed.): Mechanical vibration and shock – Evaluation of human exposure to whole-body vibration. ISO 2631, parts 1–5, Int. Standard Org., Geneva (1997–2010).

[5] Sperling, E.; Betzhold, C.: Contribution to the assessment of ride comfort in rail vehicles. Glasers Annalen ZEV 89(1956)H. 10, pp. 314–317.

[6] DB (Ed.): DB Wz Procedure. Deutsche Bundesbahn, DB Central Office Munich (1973).

- Humans have the highest vibration sensitivity between 4 and 8 Hz, with little dependence on the acceleration amplitude.
- Above 8 Hz, the vibration sensitivity of humans to whole-body vibrations decreases; only the hand-arm system is most sensitive between 8 and 16 Hz.
- ISO 2631 rates the range between 0.5 and 2 Hz highest for horizontal vibrations. Humans would thus be most sensitive in this range. However, the DB Wz procedure considers this range to be uncritical.

The aim in the design of vehicles must therefore be to avoid resonances of the vehicle system in the range between 4 and 8 Hz, since every resonance is associated with large amplitudes. It is therefore attempted to place the rigid body natural frequency of vehicles in the range of 1–2 Hz. As will be seen, this is not possible without compromises due to the necessary static spring deflections (soft springs are needed!) and due to the change in mass when loaded.

5.2 Vehicle Vibrations Due to Track Unevenness

While the rails are "scanned" directly by the wheels in the vertical direction, the coupling between wheel and rail in the horizontal-transverse direction is friction-locked as long as the wheel flange does not touch the rail running edge. Since the latter is associated with wear on the wheel and rail (and usually also with noise), attempts are made to design the running gear of rail vehicles in such a way that contact between the wheel flange and the rail running edge is avoided as far as possible. Due to the large curve radii of mainline railways ($R > 180$ m for branch lines, $R > 300$ m for main lines; see § 6 EBO), this is usually possible, but not for tramways, where the smallest track radii of 12–15 m occur. In the usual design of wheelsets, both wheels are non-rotatably connected to the wheelset shaft, i.e. their rotational speed is the same. Due to the large track radii mentioned above, the system does not require a differential gear as in road vehicles. Nevertheless, there are also so-called loose-wheel running gears,[7] in which the two wheels are not connected by a wheelset shaft, but can rotate independently of each other. This type of construction is common in trams, especially in low-floor cars, since a continuous wheelset shaft requires a higher position of the floor.

Since tracks, like roads, have unevenness (see Fig. 5.1), rail vehicles must be sprung to achieve good vibration comfort and to protect the load. However, tracks have positional errors (unevenness) not only in the vertical direction but also in the horizontal-transverse direction. As a result, rail vehicles are also excited to horizontal vibrations and must

[7] See for example: Abdelfattah, B.; Dellmann, T.: Comparison of the dynamic properties of wheelset and idler pair – A theoretical contribution to an almost forgotten technique. ZEVrail 136(2012)H. 10, pp. 380–390.

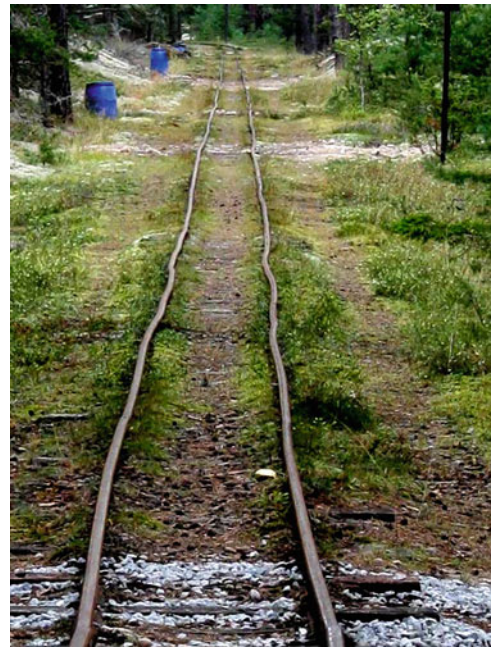

Fig. 5.1 To illustrate track position errors – track of a Swedish forest railway

therefore also have transverse suspension. Both spring systems, vertical and horizontal-transverse, must be equipped with suitable dampers so that introduced vibration amplitudes decay. Rolling vibrations (torsional vibrations about the longitudinal axis of the vehicle) are also excited by different heights of the two rails.

Figure 5.2 shows the vehicle coordinate system used. The possible oscillating movements are designated as follows:

- x-direction: longitudinal oscillations (twitching; not considered further here),[8]
- y-direction: transverse/horizontal vibrations,
- z-direction: vertical vibrations (stamping/diving),
- ψ-direction (around the longitudinal axis): rolling oscillations,
- φ-direction (around the transverse axis): pitching vibrations,
- ε-direction (around the vertical axis): yaw oscillations.

The excitation of a rail vehicle to vibrate is essentially caused by the track unevenness. Engine vibrations and out-of-round wheels, for example, can also cause vehicle vibrations. However, these are not considered here. The unevenness of a track is shown in Fig. 5.3.

In Fig. 5.3, the origin of the space-fixed coordinate system is in the middle of the horizontal connecting line between the two rails. The origin of the wheelset-fixed

[8] Twitch oscillations can be caused by tractive and braking forces in the train set.

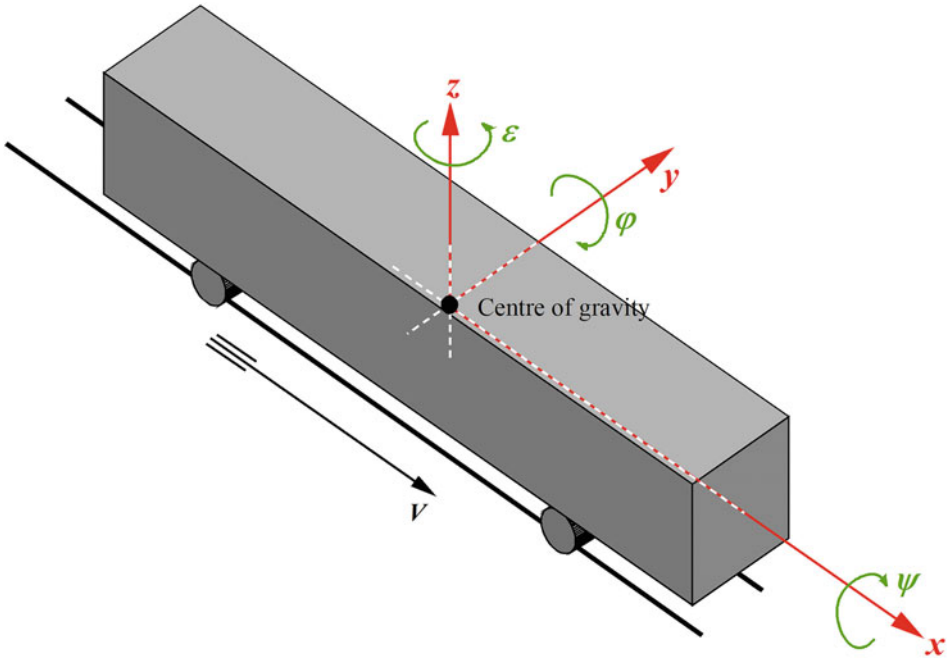

Fig. 5.2 Vehicle coordinate system

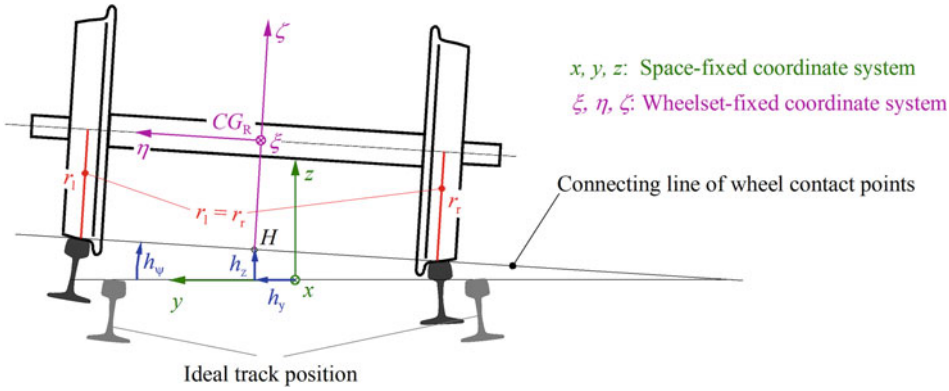

Fig. 5.3 Track unevenness. h_y directional, h_z elevation, h_ψ transverse elevation

coordinate system is located at the wheelset centre of gravity. The wheelset on the track with unevenness is aligned so that it is on the same rolling circle radius at the right and the left wheel. The elevation of the track h_z is then the perpendicular distance between the y-axis and the intersection point H of the negative ζ-axis with the line connecting the wheel contact points. The track position in the horizontal-transverse h_y direction (directional

position) is the horizontal distance of this point H from the z-axis of the space-fixed coordinate system. If the positions of point H are connected in the direction of the x-axis, i.e. along the track, $h_y(x)$ is the so-called rolling line:

> The rolling line is the geometric location of all wheelset points H of a wheelset aligned to equal rolling circle radii at the left and right wheel.[9]

The rolling line simplifies the two-track excitation by right and left rail to a single-track excitation. For the rolling line, measured values are available in the form of unevenness spectra.[10] Another track unevenness is the transverse elevation h_ψ. It is the angle between the y-axis of the space-fixed and the η-axis of the wheelset-fixed coordinate system.

Unevenness of tracks and roads are represented as spectra (power density spectra). Spectra are the result of a Fourier transformation of the measured unevenness. In this way, the unevenness functions are decomposed into individual harmonic components, i.e. converted as the sum of sinusoidal functions of different wavelength, amplitude and phase. The representation is usually over frequency. Figure 5.4 shows spectra of track unevenness provided by DB for the simulation of rail vehicle running (marked in blue in Fig. 5.4). Instead of the frequency, the wavelength (as reciprocal of the frequency) of the unevenness is shown on the horizontal axis. These are the unevenness spectra of very good tracks. For comparison, the green lines in Fig. 5.4 show the results of measurements on a secondary line used only for freight traffic [30]. In all the spectra plotted, it is noticeable that the spectral density of long waves is considerably greater than that of short waves (note the logarithmic representation!). The higher the spectrum, the larger the unevenness. For the elevation, the spectrum of vertical unevenness of a very good road from [46] is plotted in the middle part of the figure for comparison. The spectrum of track elevation slopes more steeply for small wavelengths than the spectrum of vertical road unevenness: Short wavelength unevenness has lower intensity on tracks than on roads. This can be illustrated graphically: rails cannot be bent into short waves with large amplitudes.

5.3 Theoretical Principles of Vibration Simulation

With the help of the spectra of track unevenness, the dynamics of rail vehicles can be simulated. Simulations are used, for example, for the preliminary design of newly developed vehicles. In simulations, vehicle parameters such as spring and damper characteristics, masses, speeds, geometric variables, etc. can be varied with considerably

[9] According to: Wickens, A. H.: New investigations on transverse vibrations on railway vehicles for high speeds. Monthly Journal of the International Railway Congress Association 45(1968)H. 4, pp. 1–25.

[10] See e.g.: Strothmann, W.: Horizontal disturbance function of a track. Archiv für Eisenbahntechnik, Folge 35(1980), p. 7–18.

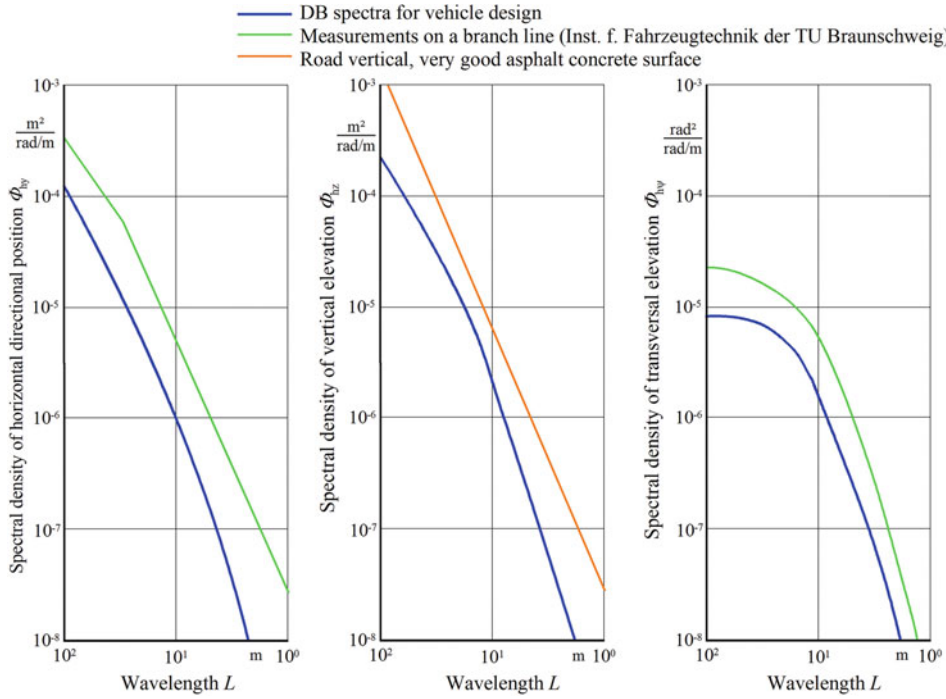

Fig. 5.4 Spectral density of track irregularities (and road irregularities for comparison). (According to [30, 44, 46])

less time and at a fraction of the cost compared to driving tests. Figure 5.5 gives a rough overview of the simulation process and the possibilities for comparison with road tests, e.g. for verification and checking of simulation results.

The basis of a simulation is data of the vehicle and the roadway (green box in Fig. 5.5). The vehicle data must be known, e.g. by measurements or, in the case of new developments, also by estimation. By abstraction, the vehicle becomes a vibration substitute model (blue or red box in Fig. 5.5).

There are basically two possibilities for the simulation of (rail) vehicle vibrations: One is the simulation in the frequency domain. Sinusoidal functions are used as vibration excitation, i.e. a track with unevenness in the form of sinusoidal functions. The vehicle parameters must then be linearized, e.g. spring and damper characteristics, contact functions (see Sect. 5.4), etc. All non-linearities (examples see Fig. 5.10) cannot be taken into account. On the other hand, the computational solution method is very fast and therefore many simulation runs can be made. The vibration responses in the simulation in the frequency domain are called magnification functions. They give the magnitude of motion parameters related to the magnitude of the unevenness amplitude as a function of the excitation frequency. The track unevenness must be available in the form of spectra. A comparison of measurements and calculations is possible via response spectra and rms

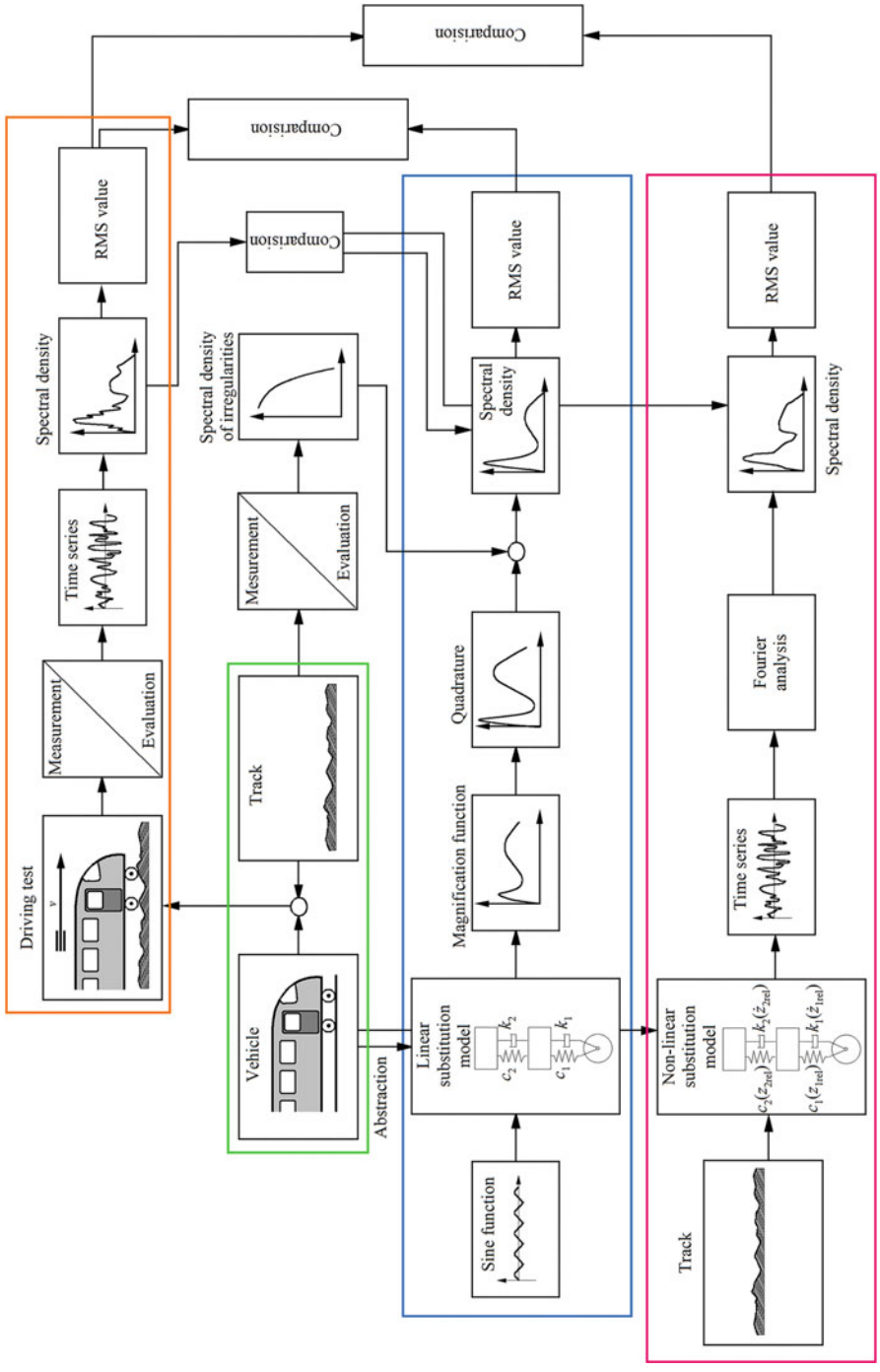

Fig. 5.5 Overview: Simulation of rail vehicle dynamics

values of motion parameters (vibration displacements, velocities, accelerations, forces, moments). The deviations between simulation and experimental results are usually relatively large. Linear substitute models are, however, very useful for sensitivity calculations, for example, if the influence of individual vehicle parameters is to be investigated.

On the other hand, it is possible to simulate in the time domain, i.e. to perform a time step simulation. In this case, all non-linearities of the initial system, the vehicle, can be taken into account. However, the computational effort and thus the time and costs for a simulation run are considerably higher. Track unevenness can be directly incorporated into the simulation as measured variables of a real track. Likewise, it is possible to synthesize[11] an unevenness-distance or time curve from unevenness spectra. The comparison of measurements and calculations is again possible via rms values and spectra of motion quantities. Both in linear and nonlinear simulations, the human vibration perception can be taken into account via evaluation functions.

Today, the equations of motion of the simulation models no longer have to be explicitly set up and solved. Corresponding simulation programs (e.g. ADAMS Rail[12] or SIMPACK[13]) considerably simplify the simulation of dynamic systems. Nevertheless, a basic understanding of the procedure, the running dynamics, the vehicle parameters and the vehicle data is also necessary for this, so that the simulation models can be set up in a targeted manner and simulation results can be interpreted competently. For simulation calculations it is generally true that the number of degrees of freedom of the substitute model, i.e. the number of masses with their movement possibilities, influence the preparation effort and the computational effort. The more degrees of freedom are taken into account, the higher this effort is.

5.3.1 Simulation in the Frequency Domain

Using a simple model, we will explain the procedure for calculating vibrations in the frequency domain. We take the model of a two-axle rail vehicle and combine the masses, the springs and the dampers respectively. This results in a simple one-mass system, Fig. 5.6. The wheelset mass has no degree of freedom of its own; it follows the unevenness of the track without lifting off.

The simplified model can no longer represent the pitching of the vehicle about the transverse axis. We have already created a flat single-track model in the abstraction, i.e. rolling oscillations cannot be simulated with it either. Lifting of the wheelset mass

[11] However, the original unevenness function cannot be generated because the information about the phase angles is lost in the calculation of spectra. In Fourier synthesis, therefore, the phase angles must be calculated using a distribution function.

[12] ADAMS Rail is distributed by MSC Software GmbH. Internet: http://www.mscsoftware.com/de//

[13] SIMPACK is distributed by SIMPACK AG. Internet: http://www.simpack.com//

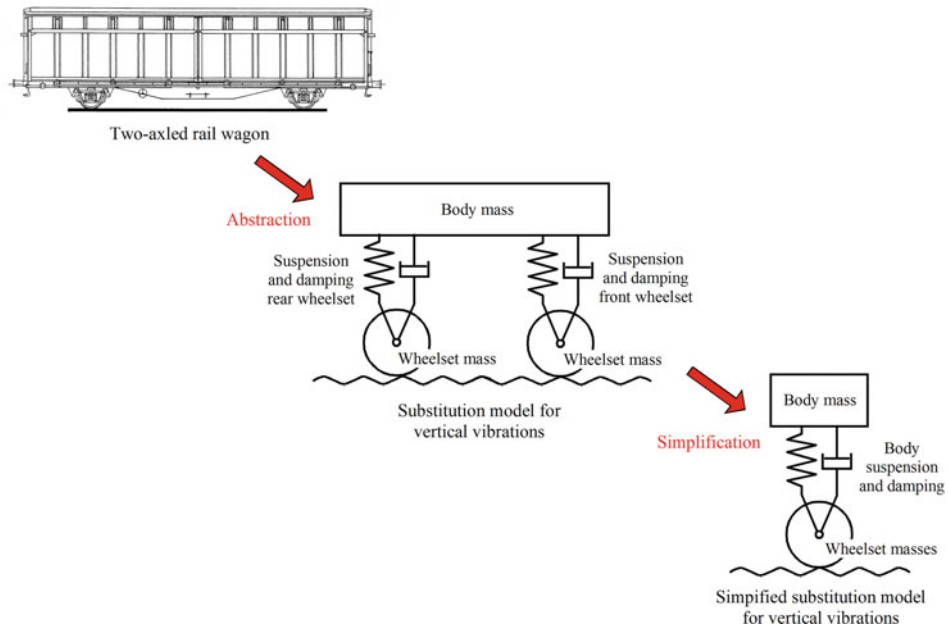

Fig. 5.6 From the real vehicle to the simple vibration replacement model

from the rails is excluded. The spring characteristics must be linearized and the friction damping of the leaf springs must be replaced by a linear hydraulic damper. For this, the establishment of the equations of motion and their solution in the frequency domain are not very complex.

We cut the body mass free and apply the acting forces, Fig. 5.7. The spring force F_c depends on the relative distance between wheelset and body mass, the damper force F_d on the relative speed:

$$\begin{aligned} F_c &= c(z - h_z), \\ F_d &= k\left(\dot{z} - \dot{h}_z\right). \end{aligned} \tag{5.1}$$

According to NEWTON's fundamental law, the following follows for the superstructure mass m:

$$m\ddot{z} = -F_d - F_c \rightarrow m\ddot{z} + k\left(\dot{z} - \dot{h}_z\right) + c(z - h_z) = 0, \tag{5.2}$$

$$m\ddot{z} + k\dot{z} + cz = k\dot{h}_z + ch_z. \tag{5.3}$$

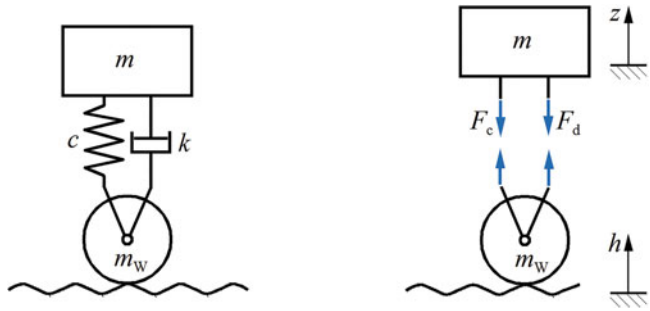

Fig. 5.7 Free cut single mass model

Equation 5.3 represents a second order inhomogeneous differential equation. As solution approach for the particulate solution (for the steady state) harmonic functions come into question:

$$h_z = \widehat{h} \sin(\omega t + \varphi) \tag{5.4}$$

with

$\widehat{h}$:	Excitation amplitude,
ω:	Excitation frequency,
φ:	Phase angle.

It is convenient to use the complex notation for the function in Eq. 5.4:

$$h_z = \widehat{h} e^{i\omega t}. \tag{5.5}$$

This allows the oscillation to be represented as a pointer diagram in the GAUSSIAN number plane. In Eq. 5.5 the unevenness h_z is composed of the real part $\mathrm{Re}\{h_z\} = \widehat{h} \cos(\omega t + \varphi)$ and the imaginary part $\mathrm{Im}\{h_z\} = \widehat{h} \sin(\omega t + \varphi)$.

In the case of linear oscillatory systems and harmonic excitation, the oscillatory response of the system is also harmonic, so that one can write for the forced build-up motion:

$$z = \widehat{z} e^{i\omega t}. \tag{5.6}$$

For the derivatives after time *t,* it follows from Eqs. 5.5 and 5.6 with the derivative rule and $\frac{\mathrm{d}(e^{i\omega t})}{\mathrm{d}t} = i\omega \cdot e^{i\omega t}$ $(i\omega^2) = -\omega^2$ $\left(\text{for } i = \sqrt{-1}\right)$:

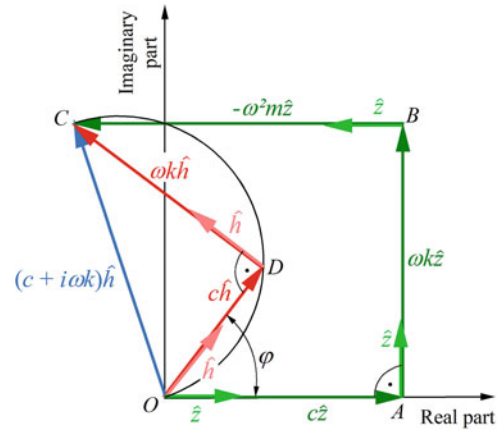

Fig. 5.8 Pointer diagram to Eq. 5.8. (According to [46])

$$\dot{h}_z = i\omega h_z; \quad \dot{z} = i\omega z, \quad \ddot{z} = -\omega^2 z. \tag{5.7}$$

Using the expressions in Eq. 5.7, we obtain from Eq. 5.3:

$$\left(-m\omega^2 + i\omega k + c\right)\widehat{z} = (i\omega k + c)\widehat{h}. \tag{5.8}$$

Figure 5.8 shows the pointer diagram associated with Eq. 5.8: Right and left sides are equal. If the mass m, the damper constant k and the spring constant c are known for a vibration system, the motion of the vehicle body $\widehat{z}$ can be calculated for each frequency ω from the unevenness amplitude $\widehat{h}$ and vice versa. Let us assume $\widehat{z}$ is known. Then, starting from the origin O in Fig. 5.8, we place the pointer $\widehat{z}$ on the real axis and multiply the length of the pointer by c. Thus we find the point A. In A the imaginary part is connected vertically $\omega k\widehat{z}$ with the pointer tip in point B. The left side of Eq. 5.8 has another term as real part: $-\omega^2 m\widehat{z}$. This pointer applied horizontally in B in negative direction gives the point C. The connection from O to C (blue arrow in Fig. 5.8) is the left side of Eq. 5.8, which is the same as the right side. So the blue arrow represents the quantity $(i\omega k + c)\widehat{h}$. Real part and imaginary part are again perpendicular to each other, i.e. we can enter them accordingly in the semicircle (THALES' theorem!) above the blue arrow and thus find the pointer length of $\widehat{h}$. As can be seen from Fig. 5.8, $\widehat{z}$ and $\widehat{h}$ are of different lengths. Both are out of phase by the angle φ. Since the length of several arrows depends on ω and ω^2, respectively, a different pointer diagram results for each frequency ω.

The magnification functions are used to assess the vibration behaviour in the frequency range. They are the ratio of a response variable of the system related to the excitation amplitude. For example, the following applies to the motion of the vehicle body:

$$\frac{\widehat{z}}{\widehat{h}} = \frac{c + i\omega k}{c - \omega^2 m + i\omega k} = \frac{A + iB}{C + iD}. \tag{5.9}$$

The magnitude of the magnification function is calculated according to the rules for complex numbers as follows

$$\left|\frac{\widehat{z}}{\widehat{h}}\right| = \sqrt{\frac{A^2 + B^2}{C^2 + D^2}} = \sqrt{\frac{c^2 + \omega^2 k^2}{\left(-\omega^2 m + c\right)^2 + \omega^2 k^2}}. \tag{5.10}$$

Figure 5.9 shows magnification functions for the body of the single-mass equivalent system shown in Fig. 5.7. The ratio of excitation frequency ω to natural frequency ν is plotted on the horizontal axis. The natural frequency for the single-mass system is given by

$$\nu = \sqrt{\frac{c}{m}}. \tag{5.11}$$

In Fig. 5.9, Lehr's damping factor D was varied:

$$D = \frac{k}{2\sqrt{c \cdot m}}. \tag{5.12}$$

The magnification functions start for $\omega = 0$ at magnification factor 1, i.e. the system follows the unevenness function at low excitation frequencies. The factor 1 states that the system responds with a vibration amplitude of the mass of 1 mm for e.g. 1 mm unevenness amplitude. In the range of natural frequency ($\omega/\nu = 1$) the functions have a maximum. With increasing damping, this maximum becomes smaller. For $\omega/\nu = \sqrt{2}$ all magnification functions have the value 1. Above this frequency ratio, the magnification functions show larger values, the higher the damping ratio D is.

The curve shown in black is valid for $D = 0$. For $\omega = \nu$ it has the value ∞: An oscillating system without damping shows infinitely large amplitudes when excited with its natural frequency – this is of course only valid under the assumption of a linear spring characteristic. In real systems, on the one hand, there is always some inherent damping of the springs and, on the other hand, the spring deflections are limited by, for example, stops. The latter however can not be represented within a linear system. It should be pointed out here that vibration substitute models with rigid bodies can only be used up to below the range of the first bending natural frequency of the car body. This concerns the frequency range of $f = \omega/2\pi$ between 0 to 8 (10) Hz.

The vertical acceleration of the vehicle body mass is important for human vibration perception. We obtain its magnification function via the relation $\ddot{z} = -\omega^2 z$:

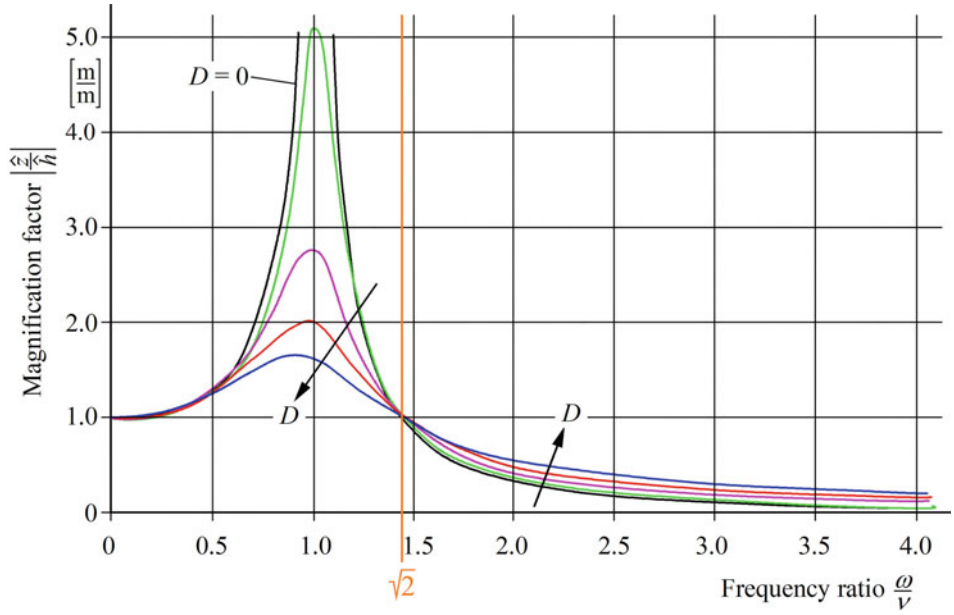

Fig. 5.9 Magnification function of the vehicle body motion of a single mass system as a function of the damping factor D

$$\left|\frac{\hat{\ddot{z}}}{\hat{h}}\right| = \omega^2 \left|\frac{\hat{z}}{\hat{h}}\right| = \omega^2 \sqrt{\frac{c^2 + \omega^2 k^2}{(-\omega^2 m + c)^2 + \omega^2 k^2}}. \tag{5.13}$$

In order to obtain the magnification function of a vibration acceleration, it is therefore only necessary to multiply the magnification function of the associated vibration displacement by ω^2.

As shown, the magnification functions apply to pure sinusoidal excitation. In Sect. 5.2, unevenness spectra of tracks with real, stochastic unevenness were presented. With their mathematical description one can calculate response spectra of a vibration substitute model, which can be used among other things for the comparison of measurements and calculations or for orientation calculations in the design of new vehicles. The spectrum of a system response, here e.g. the body acceleration, with stochastic excitation results as follows:

$$\Phi_{\ddot{z}}(\omega) = \Phi_{\mathrm{hz}}(\omega) \cdot \left(\frac{\hat{\ddot{z}}}{\hat{h}}(\omega)\right)^2. \tag{5.14}$$

Thus, for each frequency of interest ω, the spectral density of the unevenness Φ_{hz} is to be multiplied by the square of the magnification factor of the considered motion quantity

belonging to this frequency. By integration, its rms value (root mean square) z_{eff} can be calculated from the spectrum of a motion quantity[14]:

$$\overline{z}^2 = \int_{\omega_1}^{\omega_2} \Phi_{\text{hz}}(\omega) \cdot \left(\frac{\hat{\ddot{z}}}{\hat{h}}(\omega) \right)^2 \cdot \mathrm{d}\omega \rightarrow z_{\text{eff}} = \sqrt{\overline{z}^2}$$

$$= \sqrt{\int_{\omega_1}^{\omega_2} \Phi_{\text{hz}}(\omega) \cdot \left(\frac{\hat{\ddot{z}}}{\hat{h}}(\omega) \right)^2 \cdot \mathrm{d}\omega}. \tag{5.15}$$

If, as in Fig. 5.4, the unevenness spectra are available as a function of the unevenness wavelength L, they can be converted as follows. The path angular frequency Ω is given by $\Omega = 2\pi/L$ and thus the ("time") angular frequency $\omega = \Omega/v$. For the spectral density one thus obtains:

$$\Phi_{\text{hz}}(\omega) = \frac{1}{v} \cdot \Phi_{\text{hz}}(\Omega) = \frac{1}{v} \cdot \Phi_{\text{hz}}\left(\frac{2\pi}{L} \right). \tag{5.16}$$

On the basis of the rms values – assuming a GAUSSIAN normal distribution – statements can be made about the probability of exceeding certain values of the motion quantities: The rms value itself is not exceeded by 68.3% of the occurring values, the double rms value is not exceeded by 95.4%, and 99.7% of all occurring values are smaller than the triple rms value. For example, if we assume that the rms value of the suspension spring travel was calculated using a simulation with 15 mm, then 2·15 mm = 30 mm of suspension spring travel will not be exceeded with a probability of 95.4%. For 3·15 mm = 45 mm, the probability of not exceeding is already 99.7%. This means that the spring deflection to be provided can be estimated in this example.

5.3.2 Simulation in the Time Domain

If non-linearities of the original system are to be considered, a simulation in the time domain is possible. Such non-linearities can be, for example:

- Progressive spring characteristics (Fig. 5.10a),
- Stops in spring steps (Fig. 5.10a),
- Different characteristics of hydraulic dampers in rebound or compression (Fig. 5.10b),
- Friction damping (Fig. 5.10c),

[14] Theoretically, the RMS value must be integrated from $\omega_1 = 0$ to $\omega_2 = \infty$. However, because of the validity of the substitute models, this does not make sense here.

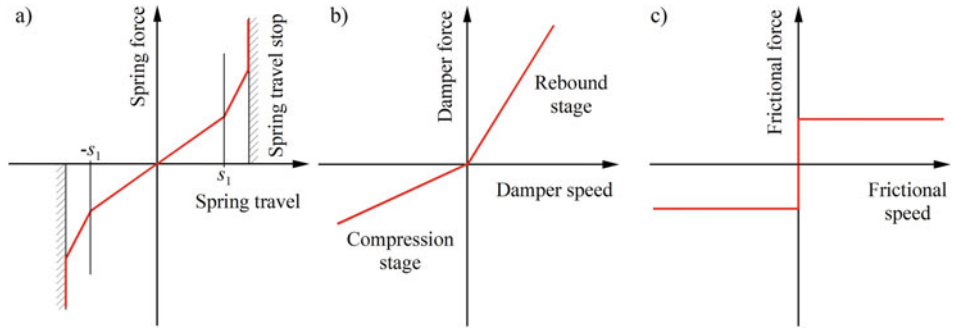

Fig. 5.10 Examples of non-linearities. (**a**) progressive spring with stop, (**b**) damper characteristic curve different in rebound and compression, (**c**) friction damping

- Adhesion-slip functions (see Sect. 5.4),
- Wheel/rail contact functions (see Sect. 5.4).

We start from the equation of motion, again using as an example the one-mass system according to Fig. 5.7 and thus Eq. 5.3:

$$m\ddot{z} + k\dot{z} + cz = k\dot{h} + ch. \tag{5.3}$$

We divide by m

$$\ddot{z} + \frac{k}{m}\dot{z} + \frac{c}{m}z = \frac{k}{m}\dot{h} + \frac{c}{m}h$$

and rearrange the equation according to $\ddot{z}$:

$$\ddot{z} = -\frac{k}{m}\dot{z} - \frac{c}{m}z + \frac{k}{m}\dot{h} + \frac{c}{m}h. \tag{5.17}$$

In this system, the spring and the damper, for example, can have non-linear characteristics. Therefore, only a time step simulation can be considered as a solution method for Eq. 5.17. The state at time $T_1 + \Delta t$ is calculated from the initial position of a state variable (displacement, angle, etc.) at time T_1 by determining the next value of the state variable via the gradient of the state variable (the first derivative with respect to time), Fig. 5.11.

The time step Δt must not be chosen too large. Starting from the value of the state variable at time T_1 (marked in Fig. 5.11 as a point in orange with a tangent in orange), the value of the state variable at time $T_1 + \Delta t$ (green point) is determined. If Δt is chosen too large (time T_2), the "correct" value is no longer determined, but the point marked in red.

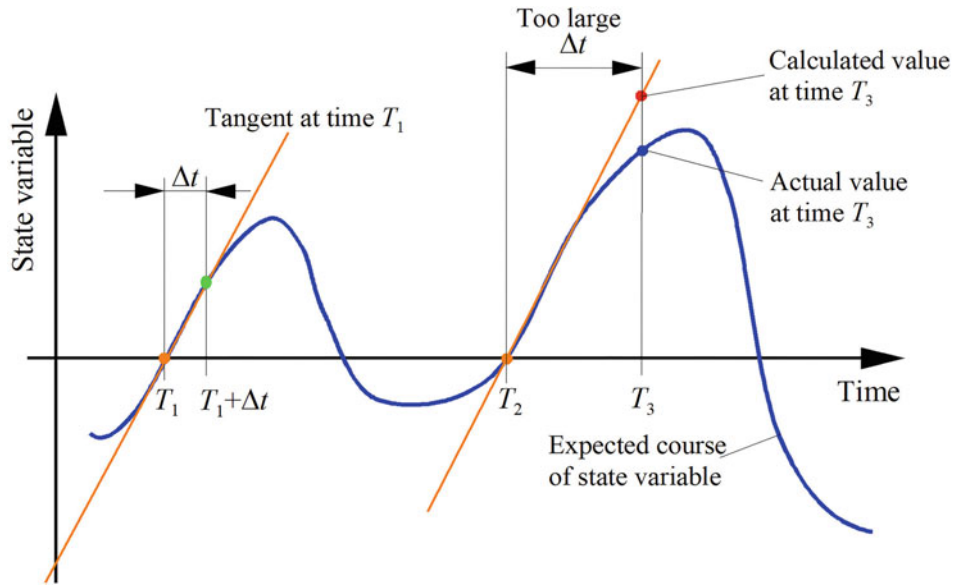

Fig. 5.11 Principle of time step integration

Rule of thumb is that the step size Δt should not be larger than 1/10 of the oscillation period of the highest natural frequency of the system under consideration.[15]

Since only the first derivative can be considered in time step integration, the following substitution is made:

$$\dot{z} = u. \tag{5.18}$$

Thus, Eq. 5.17 reads:

$$\dot{u} = -\frac{k}{m}u - \frac{c}{m}z + \frac{k}{m}\dot{h} + \frac{c}{m}h. \tag{5.19}$$

Equations 5.18 and 5.19 can now be summarized in matrix notation:

$$\begin{bmatrix} \dot{u} \\ \dot{z} \end{bmatrix} = \begin{bmatrix} -k/m & -c/m \\ 1 & 0 \end{bmatrix} \cdot \begin{bmatrix} u \\ z \end{bmatrix} + \begin{bmatrix} k/m \\ 0 \end{bmatrix} \cdot \begin{bmatrix} \dot{h} \\ 0 \end{bmatrix} + \begin{bmatrix} c/m \\ 0 \end{bmatrix} \cdot \begin{bmatrix} h \\ 0 \end{bmatrix}, \tag{5.20}$$

[15] Thus, for a highest natural frequency of 10 Hz (corresponding to an oscillation period of 0.1 s), the step size must not exceed $\Delta t = 0.01$ s.

$$\overline{\dot{u}} = \overline{\overline{A}} \cdot \overline{u} + \overline{N_1} \cdot \overline{\dot{h}} + \overline{N_2} \cdot \overline{h}. \tag{5.21}$$

Overstriked quantities in Eq. 5.21 are vectors, double overstriked ones are matrices.

Equations 5.20 or 5.21 contain besides the state vectors only their first derivatives and can be integrated with a time step method. However, the number of equations has doubled by the substitution according to Eq. 5.18.

Non-linear characteristics are taken into account by determining the corresponding forces and moments from the characteristics of springs and dampers, for example, after each integration step on the basis of the current state variables (deflections, velocities, angles, etc.). The results of a time step simulation are the temporal progressions of the considered state variables. Like the results of driving tests, they can be further processed to spectra and RMS values.

5.4 Interaction Between Vehicle and Track

It was mentioned in Chap. 1 that rail vehicle wheels have roughly spoken a conical profile, see Fig. 1.22. This is to ensure that curves can be negotiated without a flange contact between the outer wheel and the rail. In straight track, self-centering of the wheelset should be ensured so that the wheel flanges do not constantly have contact to the rails.

Figure 5.12 shows a double cone rolling through a track curve. If only the kinematics are considered, i.e. forces and moments on the double cone are neglected, the double cone could travel through the track curve without flanges.

Figure 5.13 shows DB wheel tyre outline profiles. In the past, wheel tyres were designed conical with an inclination of 1:20/1:40 (Fig. 5.13a). With increasing mileage, these conical profiles showed a very similar wear contour (Fig. 5.13b).[16] This eventually led to the development of so-called "wear profiles" which correspond to the profile of a wheel after high mileage and whose contour remains largely constant regardless of mileage. DB uses the DB II profile (UIC-ORE 1002), Fig. 5.13c. The wear profiles minimise the necessary material removal from the wheel tyre during re-profiling. However, the wear profiles have a higher effective taper, which, according to Eq. 5.22, see Sect. 5.5, increases the frequency of sinusoidal running. The use of wear profiles therefore requires a different vibration tuning of the wheelset linkage than a tapered profile.

Wheel tyres of tram vehicles are often still profiled cylindrically, as it is assumed that the track guidance is essentially carried out by the wheel flange and the rail running edge due to

[16] The wheel profile 1: 20/1: 40 has a flank angle at the wheel flange of 60°. This flank angle is said to have been arbitrarily determined by the designers of the first rail vehicles in England at the beginning of the nineteenth century, because the design office had a drawing triangle 90°/60°/30° (lecture by Prof. Dr.-Ing. K. Althammer, TU Braunschweig, winter semester 1972/73). As can be seen in Fig. 5.13b, the worn wheel profile has a larger flank angle. Therefore, the DB II profile has a flank angle of 70° (Fig. 5.13c).

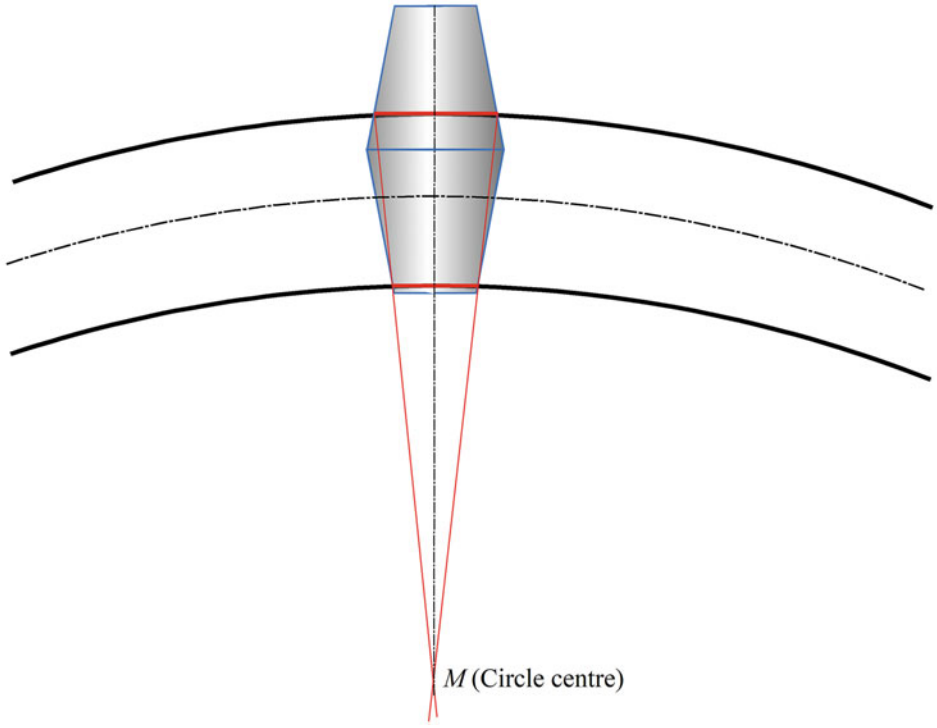

Fig. 5.12 Double cone "wheelset" in the track curve

the tight curve radii and due to the numerous lines with grooved rails. However, cylindrical wheel profiles also result in conical forms of wear. Some tramway companies therefore also assume wear-adapted profiles when re-profiling. Where tram vehicles also run on railway lines, special profiles are used. As a rule, tram wheels are narrower than railway wheels, which would cause problems especially in railway switches and crossings. Figure 5.14 shows on the left the profile of a solid disc railway wheel and on the right the profile of a tram wheel tyre.

Both profiles shown in Fig. 5.14 are from original wheels. On the tram wheel tyre it can be seen that the worn profile has become conical compared to the original cylindrical state. The flat flange crest serves as a running surface when driving through flat frogs, i.e. the wheel lifts off the actual running surface and rolls on the flange crest in the frog area, see Fig. 5.15. Disadvantages here are the vertical shocks and the change in wheel speeds due to the change in wheel diameter.

Incidentally, cylindrical wheel tyres are also not technically useful for trams, as they become conical after longer mileage as shown in Fig. 5.14. The wear shapes of rails also adapt to this, Fig. 5.16.

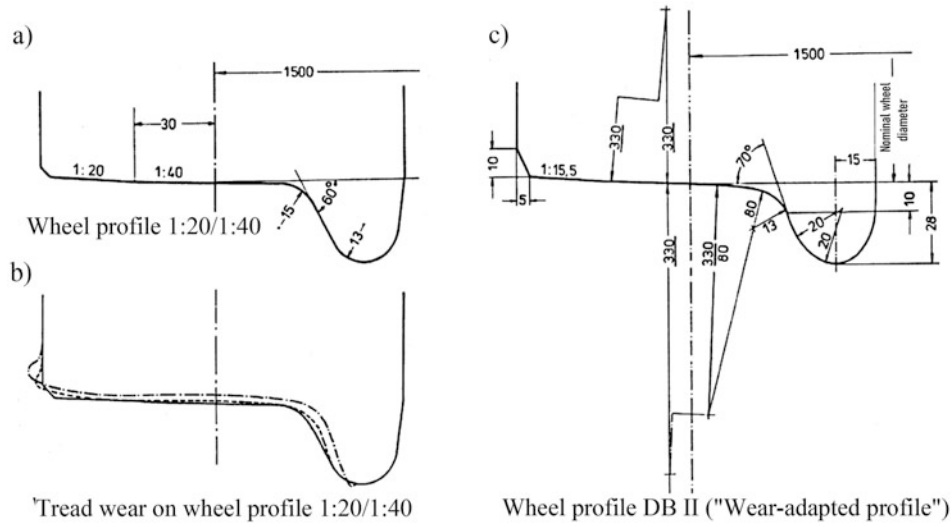

Fig. 5.13 Wheel tyre profiles. (**a**) Wheel tyre profile 1: 20/1: 40, (**b**) Wear progress, (**c**) Wear profile DB II. [40]

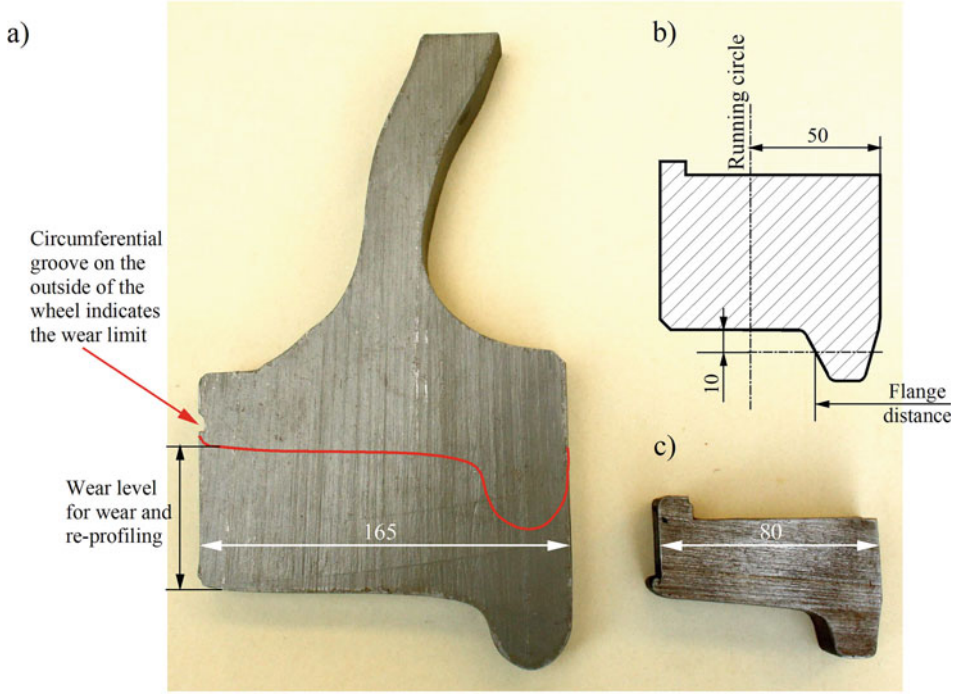

Fig. 5.14 Wheel profiles. (**a**) newly profiled railway solid wheel with corrugated wheel disc, (**b**) dimensions of a tram wheel tyre in new condition, (**c**) tram wheel tyre in worn condition

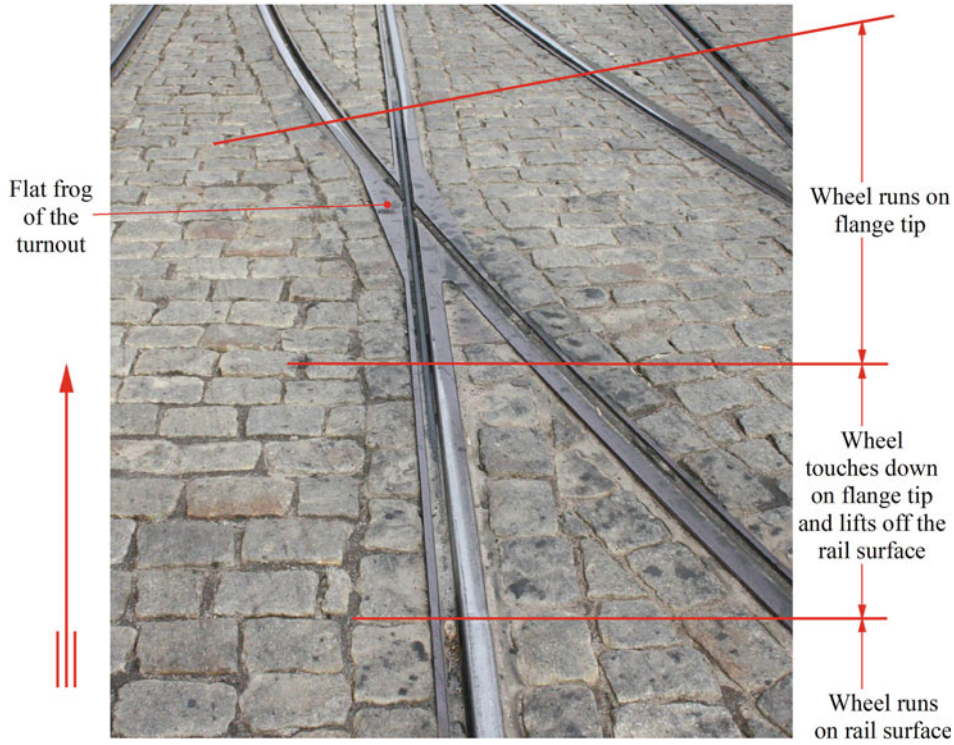

Fig. 5.15 Track guidance in the flat frog of a tramway switch

In Fig. 5.16a, it can be seen that a new rail profile, to whose running surface a horizontal tangent can be applied, adapts to the tapered wear profiles of the wheel tyres over time. In Fig. 5.16b, there is a point contact between the wheel tyre and the rail with a correspondingly high surface pressure, while in Fig. 5.16c the wheel tyre outline and the rail profile have adapted to each other. This results in a line contact with a correspondingly larger contact area and lower surface pressure and thus lower wear.

Why some tramway companies still profile wheel tyres cylindrically when new cannot be fathomed.[17] Track-guided systems, however, are difficult to change in certain parameters because they depend on the interaction between wheelset and track.

When light rail vehicles transition to mainline tracks, as in Chemnitz, Karlsruhe, Kassel, and Saarbrücken, the wheel tread is designed wider than on tram cars but narrower than on rail vehicles. The wheel flange has the same shape as on the mainline vehicle, but is narrower so that both mainline switches and grooved rails can be driven on.

[17] When asked about certain facts in the rail vehicle business, one often hears the response, "We've always done it that way".

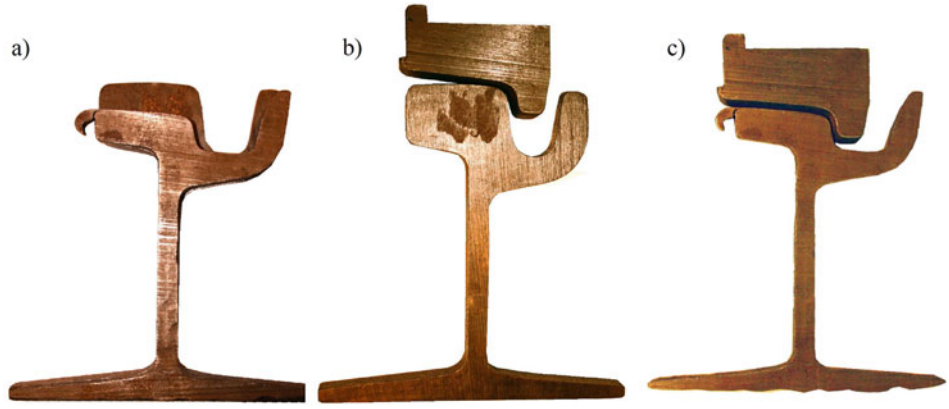

Fig. 5.16 (**a**) Comparison of grooved rail profile new – worn, (**b**) worn wheel tyre on new grooved rail, (**c**) worn wheel tyre on worn rail

5.5 Dynamic Behaviour of the Wheelset

In a straight track, a lateral deflection of the wheelset within the scope of the track clearance causes the wheelset to perform the sinusoidal run already mentioned in Chap. 1. From a purely kinematic point of view, the centre of gravity of the wheelset performs a sinusoidal path. As a result of the wheelset being coupled to a bogie via spring and damper and due to inertia forces, the wheelset does not roll over the rails without slippage, but instead slippage occurs at the wheel contact points. As a result, the movement behaviour of a wheelset is considerably influenced and can become unstable under certain circumstances, i.e. zigzag running occurs with shock-like contact between the wheel flange and the rail running edge. In this case, the system is not sufficiently damped; instead of decaying, the amplitudes of the wheelset run would be fanned and thus increase. Only the wheel flange and rail running edge limit the amplitudes in the horizontal-transverse direction. The energy for the fanning of the oscillation comes from the forward movement of the vehicle.

For the case of slip-free rolling, KLINGEL derived the wavelength of the path curve and the frequency of wheelset running as early as 1883[18]:

[18] Klingel, J.: Über den Lauf der Eisenbahnwagen auf gerader Bahn. Organ für die Fortschritte des Eisenbahnwesens 20(1883)H. 4, pp. 113–123.

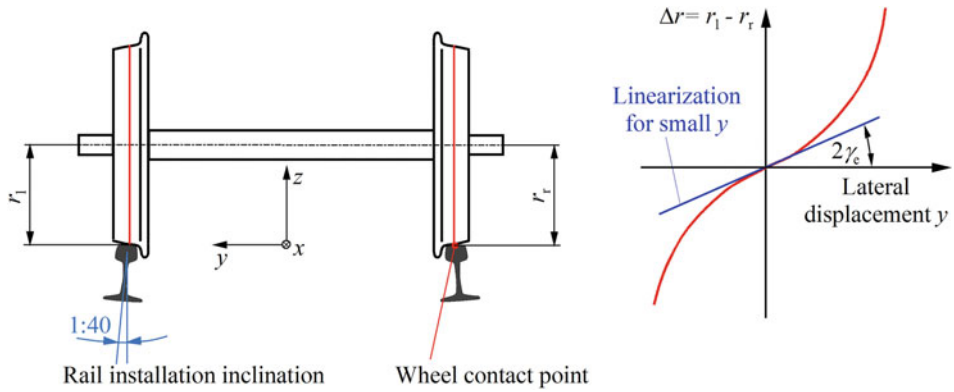

Fig. 5.17 Δr-function (schematic)

$$\begin{aligned} \text{Wavelength} &: L = 2\pi\sqrt{\frac{r_0 \cdot s_R}{2 \cdot \gamma_e}}, \\ \text{Frequency} &: f = \frac{v}{L} = \frac{v}{2\pi}\sqrt{\frac{2 \cdot \gamma_e}{r_0 \cdot s_R}}. \end{aligned} \tag{5.22}$$

In Eq. 5.22 mean:

v:	Driving speed,
γ_e:	Effective taper – Results from the difference of the rolling radii of both wheels when the wheelset is shifted transversely; see below and Fig. 5.17,
r_0:	Wheel radius with central alignment in the track (for standard wheelsets: $r_0 = 500$ mm),
s_R:	Distance between the wheel contact points of a wheelset (for standard gauge: $s_R = 1500$ mm).

Except for the driving speed, all parameters are constant; i.e. the frequency of the sine wave is linearly dependent on the driving speed of the vehicle. This means that depending on the driving speed, resonances with other natural frequencies of the vehicle can occur.

It has already been mentioned that wear profiles lead to a high effective conicity γ_e. This parameter shall now be explained. Consider a wheelset placed on a track in such a way that the rail/wheel contact points on both wheels result in the same rolling circle radius ($r_l = r_r$ in Fig. 5.17). Now the wheelset is moved in transverse direction. This changes the contact points[19] between wheels and rails and thus also the rolling circle radii. If the resulting difference in the rolling circle radii is plotted against the transverse displacement of the wheelset, the so-called Δr-function ($\Delta r = r_l - r_r$) is obtained in Fig. 5.17, right. This

[19] Strictly speaking, there are no contact "points" between the wheel and the rail, but contact surfaces due to the elasticity of the two bodies in contact. Nevertheless, the term "point of contact" or "wheel contact point" is usually used.

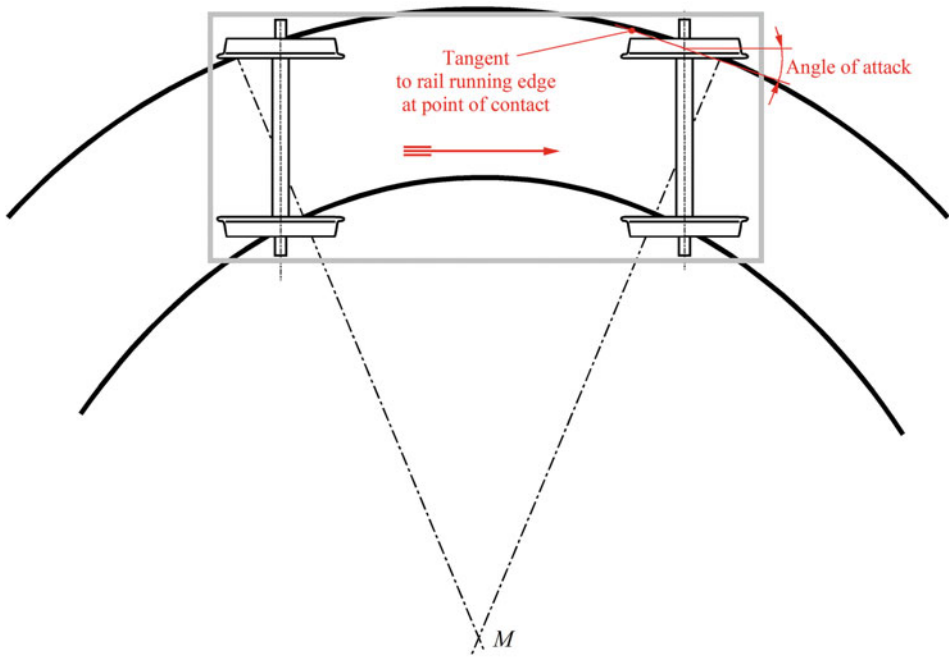

Fig. 5.18 Curved position of a two-axle vehicle with longitudinally rigid wheelset guide

function is non-linear, partly even discontinuous, since the rolling circle radii increase sharply as the wheel flange is approached, while they change only slightly towards the outside of the wheel. The Δr-function depends on the wheel tyre and the rail profile, on the track gauge and on the installation inclination of the rails. For small wheelset transverse paths, the Δr-function can be linearised. The slope of the straight line (Fig. 5.17, right, blue straight line) is defined as $2{\cdot}\gamma_e$. For a wheelset with wear profile DB II and for rails installed with an inclination of 1:40 to the track centre (standard for DB; see Fig. 5.17), $\gamma_e \approx 0.25$ for small wheelset deflections in lateral direction.

This allows the speed-dependent natural frequency of a wheelset to be calculated roughly for the values given in the comment to Eq. 5.1:

$$f = \frac{v}{2\pi} \cdot \sqrt{\frac{2 \cdot \gamma_e}{r_0 \cdot s_R}} \approx 0,13 \cdot v[\mathrm{Hz}] \qquad \text{with } v[\mathrm{m/s}]. \tag{5.23}$$

In practice, however, there are no "untethered" free-rolling wheelsets, but the wheelsets are connected to the bogie or the vehicle undercarriage via springs and dampers or links. Let us first consider a simple two-axle vehicle travelling through a track curve, Fig. 5.18. If the wheelsets are longitudinally rigidly coupled to the vehicle body, large angles of attack of the curve's outer leading wheel will occur in the track curve. This can lead to derailment of

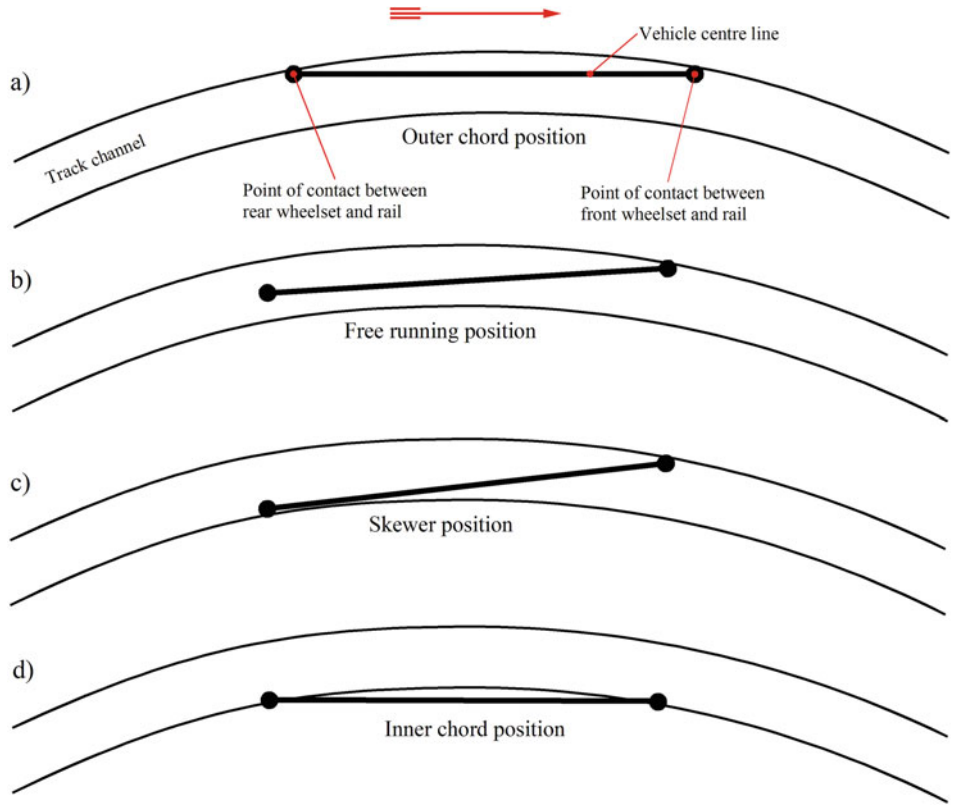

Fig. 5.19 Possible positions of a rail vehicle in the track curve

the vehicle as the wheel flange climbs onto the rail running surface. Even without the risk of derailment, large guiding forces and wear occur.

Irrespective of the wheelset guidance, a distinction is made in the track curve between four possible positions of a rail vehicle, Fig. 5.19. The distance of the outer to the inner rail is shrunk there to the "gauge channel". The two rails have the distance of the track clearance. The vehicle is reduced to its centre line, thus has zero width. Four possible positions of the vehicle occur during curved travel:

- Figure 5.19a shows the outer chord position. Due to the centrifugal forces, the front and rear wheelsets run against the outer rail with the wheel flange of the outside wheel.
- Figure 5.19b shows the freewheeling of the vehicle. The vehicle is guided by the front outer wheel of the curve; the rear wheel set has no wheel flange contact with the rails.
- The skewer position, Fig. 5.19c, occurs, for example, when a vehicle drives slowly through a narrow curve. In this case, the front wheelset runs against the outer rail with

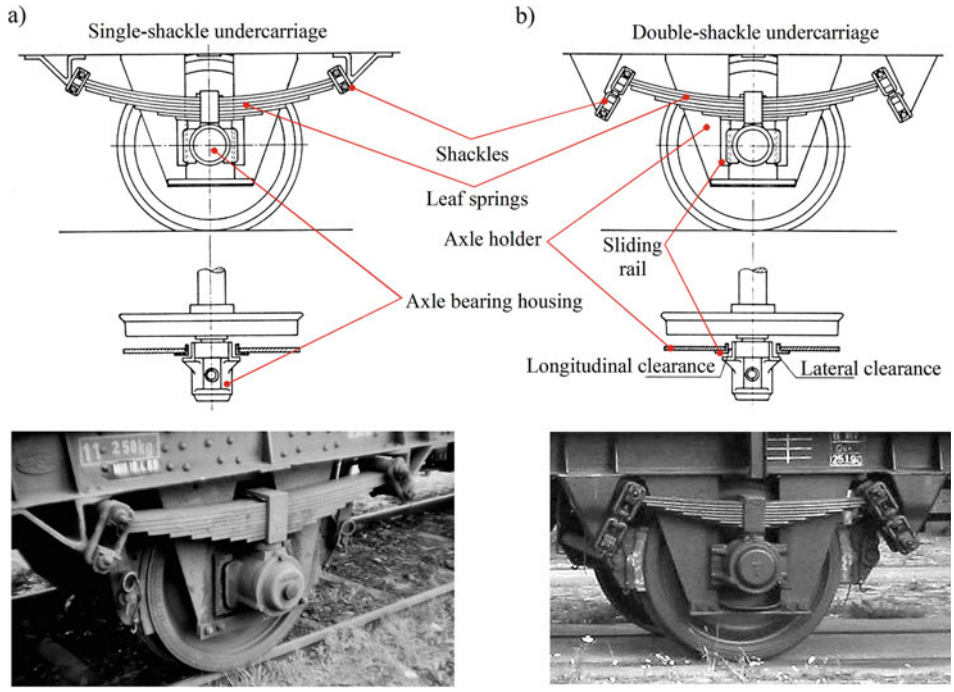

Fig. 5.20 Shackels running gears as longitudinally elastic wheelset guides. (Sketches according to [40])

the wheel on the outside of the curve, while the rear wheelset runs against the inner rail with the wheel on the inside of the curve.

- The inner chord position, Fig. 5.19d, results when a vehicle is pulled slowly through a narrow track curve within a train formation, for example.

A longitudinally rigid wheelset guidance, as in Fig. 5.18, is only conceivable with short wheelbases and with bogies[20]; otherwise safe passage through narrow curves is not possible. Two-axle railway vehicles with large axle distances therefore have longitudinally elastic wheelset guides, Fig. 5.20.

Figure 5.20 shows so-called shackles running gears: (a) an older single-shackle running gear, (b) a double-shackle running gear of a two-axle freight wagon. The shackles act as inclined pendulums, which allow a longitudinal and a transverse movement of the wheelset housing and thus of the wheelset between the sliding rails of the axle holders. Figure 5.21 illustrates the restoring effects due to the inclined position of the shackles during longitudinal and transverse deflections of the wheelset. In the middle position (Fig. 5.21a), the

[20] Older two-axle tramcars, for example, have an axle base of 3000 mm for a body length of 10,000 mm; railway bogies usually have axle bases from 1800 over 2500 to 3000 mm.

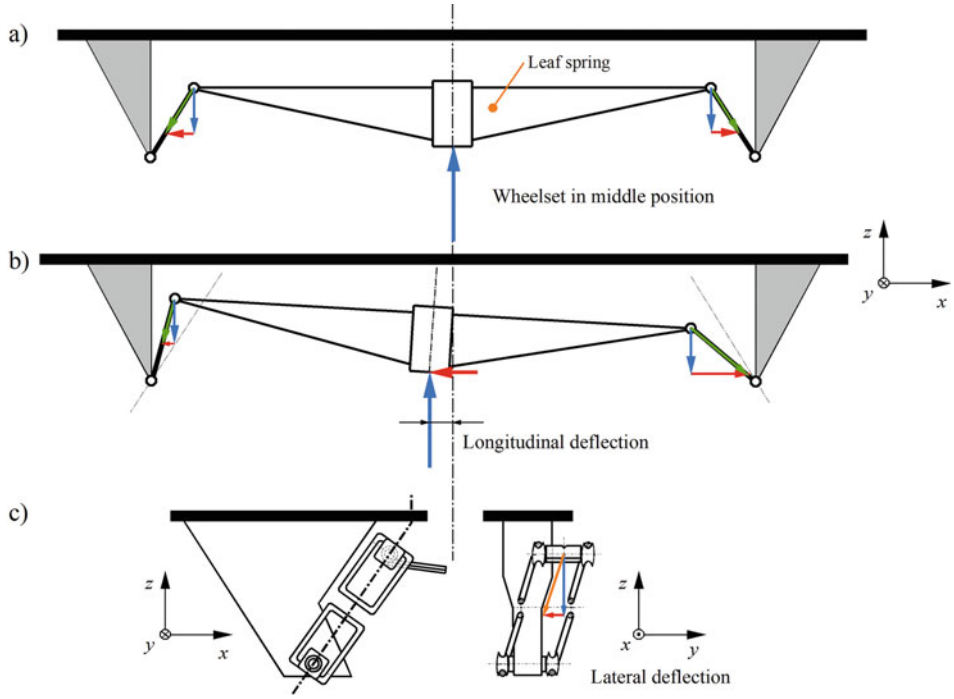

Fig. 5.21 Shackle running gear in middle position (**a**), under longitudinal forces (**b**) and under transverse forces (**c**). (According to [40])

longitudinal forces shown in red cancel each other out. If an external longitudinal force acts on a wheel (Fig. 5.21b) and deflects the wheel bearing in the longitudinal direction, a restoring force results due to the different inclination of the two shackles on a spring.

It has already been mentioned that tracks also have unevenness in the horizontal-transverse direction, so that rail vehicles also require transverse suspension. This is achieved with shackle running gears by the pendulum effect in the transverse direction, Fig. 5.21c. Shackles thus produce a longitudinal and a transverse suspension by their pendulum property. Their spring effect can be determined using the equations for a thread pendulum, Fig. 5.22. For the restoring force on the thread pendulum (Fig. 5.22a), taking into account that the deflection y is small:

$$F_{\mathrm{y}} = m \cdot g \cdot \tan \frac{y}{l} \approx \frac{m \cdot g}{l} y. \tag{5.24}$$

This gives the spring constant c:

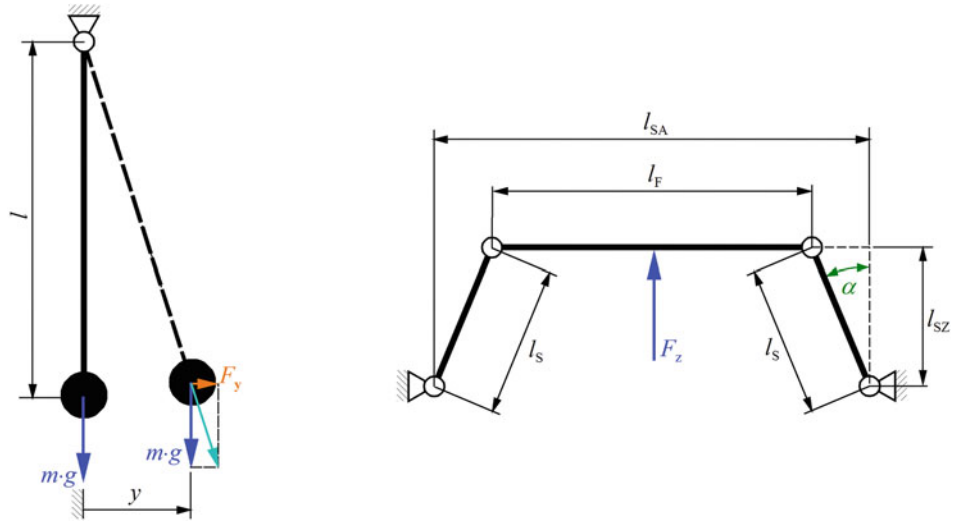

Fig. 5.22 Forces at the thread pendulum (**a**), calculation of the effective pendulum length l_{sz} for the shackle running gear (**b**)

$$F_y = c \cdot y \rightarrow c = \frac{m \cdot g}{l}. \tag{5.25}$$

Finally, the natural frequency ν of a string pendulum can be calculated as

$$\nu = \sqrt{\frac{c}{m}} \rightarrow \nu = \sqrt{\frac{m \cdot g}{m \cdot l}} = \sqrt{\frac{g}{l}} \quad \left(\text{in } \left[\frac{\text{rad}}{\text{s}}\right]\right). \tag{5.26}$$

The natural frequency of a pendulum therefore depends, if we assume that the acceleration due to gravity is constant, only on the length of the pendulum. We will see later that pendulum linkages are often used for transverse suspension in rail vehicles. Their natural frequency is constant according to Eq. 5.26, so that, for example, a vibration comfort independent of the load can be achieved.

In the case of the shackle running gear, longitudinal suspension is also implemented via pendulums, Fig. 5.21a and b. The effective pendulum length l_{sz} required to determine the transverse spring stiffness can be calculated using Fig. 5.22b.

$$\sin \alpha = \frac{l_{SA} - l_F}{2 \cdot l_S}, \tag{5.27}$$

$$\cos\alpha = \frac{l_{SZ}}{l_S} \rightarrow l_{SZ} = l_S \cdot \cos\alpha \tag{5.28}$$

with

l_{SA}:	Spacing of the hook suspension on the spring shackles,
l_F:	Spring length (from spring eye to spring eye),
l_S:	Shackle length.

Due to the longitudinal suspension, the wheelset can "turn in" in the curve, i.e. its central axis can align itself with the centre of the curve. This can be explained as follows: If a wheelset runs on the outside of the curve with the wheel flange in the direction of the rail running edge, the running circle diameter on the outer wheel increases with the wear profiles, while the running circle diameter on the wheel on the inside of the curve decreases. Since both wheels have the same angular velocity, the outer wheel covers a greater distance than the inner wheel and the wheelset steers into a radial position. In the process, restoring forces become effective at the shackle running gear. They are counteracted by forces on the wheel, which are caused by the slip between the wheel and the rail. This results in an equilibrium between the slip forces on the wheel and the forces on the shackle gear. At curve run-out, the wheelset returns to the central position as soon as it rolls on the right and left wheel on the same running circle diameter.

Even with horizontal track unevenness, the points of contact between the wheel and the rail shift so that circumferential and tangential forces are generated at the wheels. These result via the adhesion-slip functions from relative speeds at the wheel contact points. Due to its tethering to the bogie frame or wagon body, the wheelset can no longer roll without slip.

Figure 5.23 shows the forces and moments on a wheelset. The *x*-*y*-*z* coordinate system is fixed in space (inertial system). ξ, η and ζ are the coordinates of the wheelset fixed coordinate system with the origin at the wheelset centre of gravity. F_y is the force on the wheelset resulting from the wheelset restraint on the bogie frame or wagon body; likewise, M_x and M_z are moments resulting from the wheelset restraint (e.g. spring and damper moments; shown in blue in Fig. 5.23).

Lateral and circumferential forces as well as moments occur in the wheel contact surfaces (simplified called contact points). They depend on the magnitude of the normal forces and on the relative movements between wheel and rail. According to Fig. 5.23, the lateral forces result:

$$\begin{aligned} S_l + S_r &= S \\ &= T_l \cos(\gamma_l + \psi_R) + N_l \sin(\gamma_l + \psi_R) + T_r \cos(\gamma_l - \psi_R) \\ &\quad - N_r \sin(\gamma_l - \psi_R) \end{aligned} \tag{5.29}$$

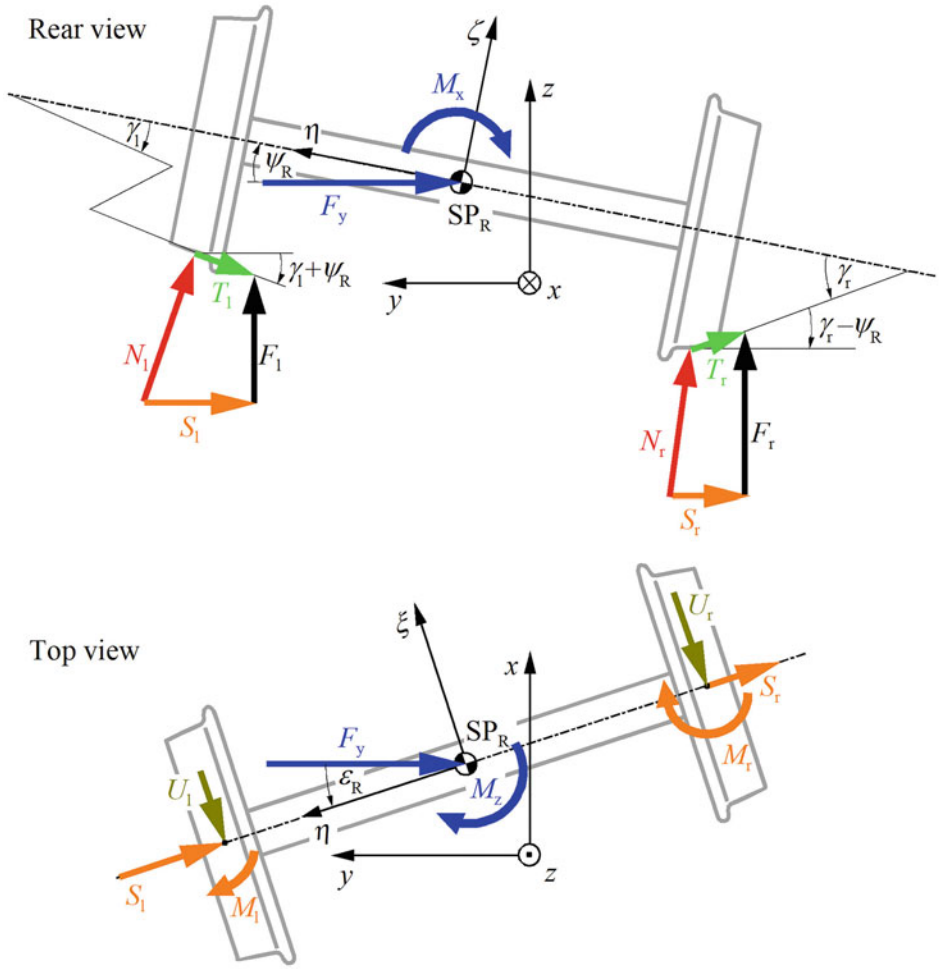

Fig. 5.23 Forces and moments on the wheelset (angles shown enlarged)

with

S_l, S_r:	Lateral forces (in the direction of the η-axis),
T_l, T_r:	Tangential forces (tangential in contact surfaces),
N_l, N_r:	Normal forces (perpendicular to contact surfaces),
γ_l, γ_r:	Effective cone inclinations in the contact surfaces,
ψ_R:	Roll angle of the wheelset (about the ξ-axis), where $\psi_R = (r_l - r_r)/s_R$

Since the occurring angles are small, one can write with $\cos(\gamma + \psi) \approx 1$ and simplified $\sin(\gamma + \psi) \approx \gamma + \psi$:

$$S_\mathrm{l} + S_\mathrm{r} = S = T_\mathrm{l} + T_\mathrm{r} + (N_\mathrm{l} \cdot \gamma_\mathrm{l} - N_\mathrm{r} \cdot \gamma_\mathrm{r}) + (N_\mathrm{l} + N_\mathrm{r})\psi_\mathrm{R}. \tag{5.30}$$

The normal forces can be expressed via the wheel loads:

$$\begin{aligned} F_\mathrm{l} &= N_\mathrm{l} \cos(\gamma_\mathrm{l} + \psi_\mathrm{R}) - T_\mathrm{l} \sin(\gamma_\mathrm{l} + \psi_\mathrm{R}) \approx N_\mathrm{l}, \\ F_\mathrm{r} &= N_\mathrm{r} \cos(\gamma_\mathrm{r} - \psi_\mathrm{R}) - T_\mathrm{r} \sin(\gamma_\mathrm{r} - \psi_\mathrm{R}) \approx N_\mathrm{r}. \end{aligned} \tag{5.31}$$

For simplicity, we can neglect wheel load changes due to vertical and roll vibrations. With this

$$F_\mathrm{l} = F_\mathrm{r} = F, \text{thus equal to the static wheel load.} \tag{5.32}$$

Using Eqs. 5.31 and 5.32, Eq. 5.30 reads:

$$S_\mathrm{l} + S_\mathrm{r} = T_\mathrm{l} + T_\mathrm{r} + F(\gamma_\mathrm{l} - \gamma_\mathrm{r}) + 2F \cdot \psi_\mathrm{R}. \tag{5.33}$$

As mentioned above, the tangential forces (T_l and T_r) and the circumferential forces (U_l and U_r) between wheel and rail arise via relative speeds of the wheelset with respect to the rails. These forces are slip forces. To calculate them, we must therefore deal with the slip at the wheel contact point. Circumferential and transverse slip are the velocities in the longitudinal direction and in $\dot{\xi}$ the transverse direction $\dot{\eta}$ at the wheel contact point, related to the running speed *v:*

$$s_\mathrm{U} = \frac{\dot{\xi}}{v}, s_\mathrm{T} = \frac{\dot{\eta}}{v} \tag{5.34}$$

with

$\dot{\xi}, \dot{\eta}$:	Relative velocities in the wheel contact patch in the wheelset-fixed ξ-η-ζ coordinate system in the ξ-η-plane.

Longitudinal forces arise from longitudinal slip, which is commonly referred to as circumferential slip, and transverse forces arise from transverse slip, which is also referred to as tangential slip.

If a straight path is imposed on a rolling cone as a simplification of a wheel profile, the so-called drilling slip occurs, Fig. 5.24. In the lower part of the figure, the slip-free rolling direction of the cone is shown as a green arrow; however, the direction of movement indicated as a red arrow is imposed on the cone. This results in an angular velocity ω_B, the drilling angular velocity, at the wheel/rail contact point.

The drilling slip can thus be defined as follows:

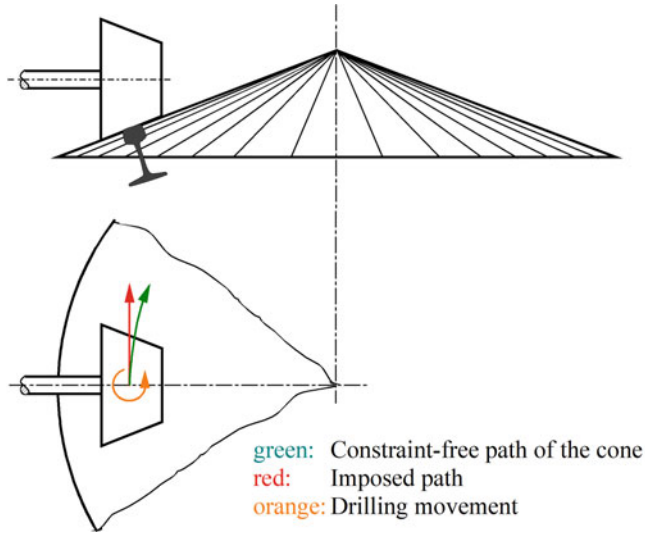

Fig. 5.24 Formation of the drilling slip. (According to [40])

$$s_B = \frac{\omega_B}{v}, \tag{5.35}$$

with ω_B = drilling angular velocity. The drilling slip is not dimensionless with the definition given by Eqs. 5.35, it is not dimensionless like longitudinal and transverse slip. The drilling slip results in a moment in the wheel contact surface.The relationship between tangential, circumferential and drilling slip on the one hand and the resulting adhesion coefficients on the other hand was investigated by KALKER[21] at the TU Delft. Nonlinear functions are obtained, Fig. 5.25. For small slip values, the adhesion-slip functions can be linearized.[22] The slopes of the functions at the origin are then the adhesion coefficients. The forces and moments in circumferential, tangential and drilling direction can be calculated from the adhesion coefficients and the wheel contact force.

First, however, we must determine the velocities at the points of contact; see Fig. 5.26. Different velocities overlap at the wheel contact points:

- Running speed v,
- Wheel peripheral speed $r \cdot \dot{\varphi}$,
- Velocity from yawing motion of wheelset $(s_R/2) \cdot \dot{\varepsilon}_R$,

[21] Kalker, J. J.: On the Rolling Contact Between Two Elastic Bodies in the Presence of Dry Friction. Doctoral thesis TU Delft (1967).

[22] KALKER divides the contact surface into an adhesion and a sliding region and can thus recalculate measured adhesion force functions very well. The linearization means that only an adhesion area exists in the contact surface.

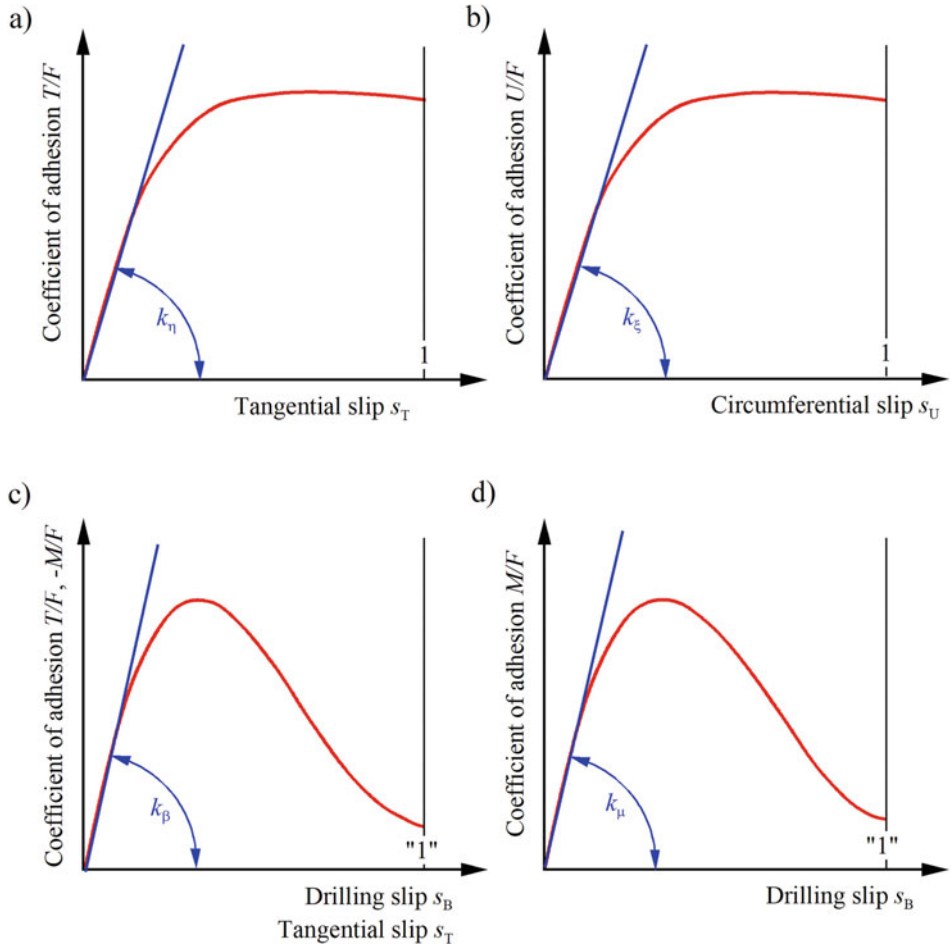

Fig. 5.25 Adhesion-slip functions for tangential, circumferential and drilling slip

- Velocity from transverse wheelset movement $\dot{y}_R$,
- Velocity from track unevenness ($\dot{h}_y$ change in track unevenness as a function of time).

As a description of the track unevenness horizontal-transverse one can use e.g. the rolling line $h_y(x)$ (see Sect. 5.2). The velocity $\dot{h}_y$ is the derivative of the rolling line with respect to time, i.e. the change of the transverse unevenness with time.

The drilling angle velocity results from the following proportions:

- Yaw angle speed $\dot{\varepsilon}_R$ of the wheelset (rotation around the vertical axis),
- Angular velocity component $\gamma \cdot \dot{\varphi}$ in the contact plane.

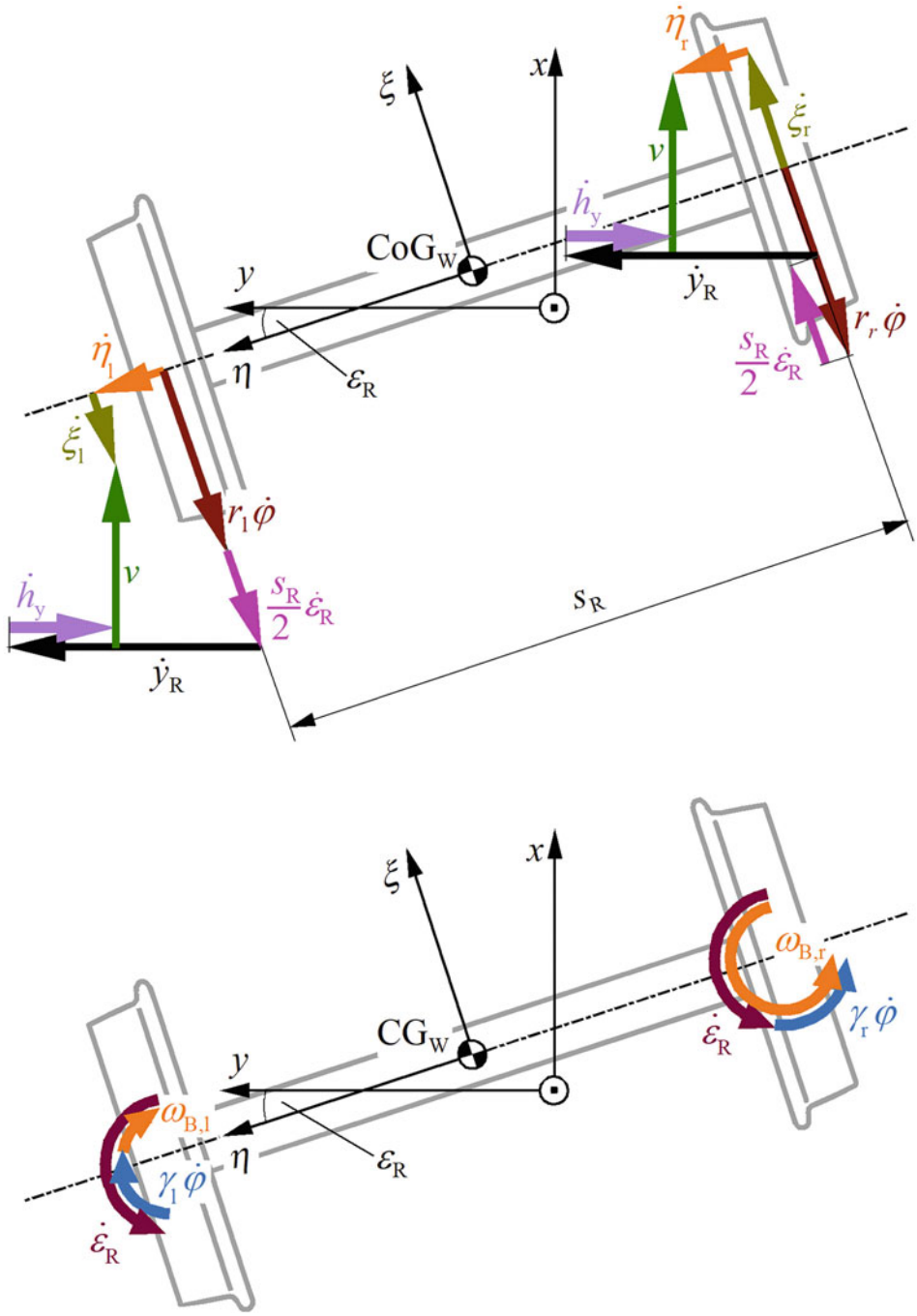

Fig. 5.26 Velocities at the wheelset for calculating the slip values (top view; angle shown enlarged)

For the calculation of the lateral and circumferential forces, the relative velocities in the contact surfaces between wheel and rail in the wheelset coordinate system are required:

$$\begin{aligned}\dot{\eta}_{\mathrm{l/r}} &= \dot{y}_{\mathrm{R}} - \dot{h}_{\mathrm{y}} - v \cdot \varepsilon_{\mathrm{R}},\\ \dot{\xi}_{\mathrm{l/r}} &= r_{\mathrm{l/r}} \cdot \dot{\varphi} \pm \frac{s_{\mathrm{R}}}{2}\dot{\varepsilon}_{R} + v,\\ \omega_{\mathrm{B\,l/r}} &= \dot{\varepsilon}_{\mathrm{R}} \mp \gamma_{\mathrm{l/r}} \cdot \dot{\varphi}.\end{aligned} \tag{5.36}$$

The angular velocity of the wheels is approximately

$$\dot{\varphi} = \frac{v}{r_0} \tag{5.37}$$

with the radius r_0 of the wheels in the centre position (nominal running circle radius).Using the relative velocities from Eq. 5.36, the lateral and circumferential forces as well as the moments for small slip values can be calculated via the adhesion-slip functions:

$$\begin{aligned}S_{\mathrm{l}} + S_{\mathrm{r}} &= S\\ &= \frac{2F \cdot k_{\eta}}{v}\left(\dot{y}_{\mathrm{R}} - \dot{h}_{\mathrm{y}} - v \cdot \varepsilon_{\mathrm{R}}\right) + \frac{2F \cdot k_{\beta}}{v}\dot{\varepsilon}_{\mathrm{R}} + 2P\left(1 - \frac{k_{\beta}}{r_0}\right)\frac{\gamma_{\mathrm{l}} - \gamma_{\mathrm{r}}}{2} + 2F\\ &\quad \cdot \psi_{\mathrm{R}},\end{aligned} \tag{5.38}$$

$$U_{\mathrm{l}} - U_{\mathrm{r}} = U = -\frac{2F \cdot k_{\xi}}{v}\left(\frac{\Delta r}{r_0} + s_{\mathrm{R}} \cdot \dot{\varepsilon}_{\mathrm{R}}\right), \tag{5.39}$$

$$M_{\mathrm{l}} + M_{\mathrm{r}} = M = -\frac{2F \cdot k_{\beta}}{v}\left(\dot{y}_{\mathrm{R}} - \dot{h}_{\mathrm{y}} - v \cdot \varepsilon_{\mathrm{R}}\right) + \frac{2F \cdot k_{\beta}}{v}\left(\dot{\varepsilon}_{\mathrm{R}} - \frac{\gamma_{\mathrm{l}} - \gamma_{\mathrm{r}}}{2r_0}\right) \tag{5.40}$$

with

S:	Lateral force,
U:	Circumferential force,
M:	Moment,
F:	Wheel load.

The forces and moments on the wheelset are shown in Fig. 5.23. F_{y}, M_{x} and M_{z} result from the tethering of the wheelset to the wagon body or bogie frame. In Eqs. 5.38 and 5.40 is the expression $F(\gamma_{\mathrm{l}} - \gamma_{\mathrm{r}})$, the wheel load multiplied by the difference of the contact surface inclinations at the left and right wheels. This difference is called the $\Delta\gamma$-function. It is a nonlinear function for wear profiles depending on the transverse displacement of the wheelset, Fig. 5.27. Its slope for small displacements is $2c'$.

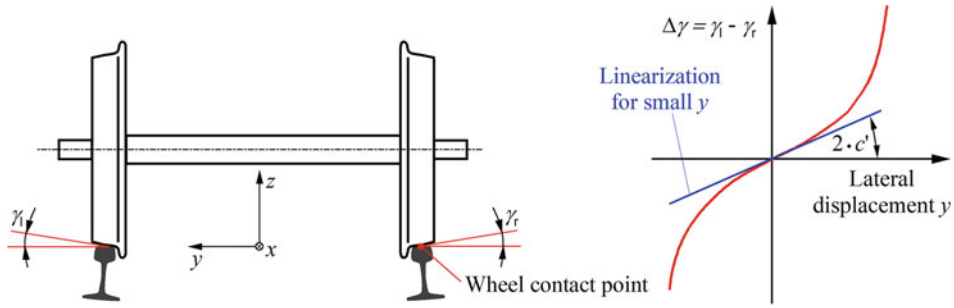

Fig. 5.27 $\Delta\gamma$-function (schematic)

The $\Delta\gamma$-function provides a restoring effect in the case of transverse deflection of the wheelset like a spring loaded by the deflection. The product ($F \cdot c' = c_R$ with F = wheel load) has the dimension of a spring constant and is called "gravitational stiffness". One thus obtains:

$$F(\gamma_l - \gamma_r) = 2Fc'(y_R - h_y) = 2c_R(y_R - h_y). \tag{5.41}$$

We already got to know the Δr-function in Fig. 5.17. Linearized it can be written as

$$\Delta r = r_l - r_r = 2\gamma_e(y_R - h_y). \tag{5.42}$$

With Eqs. 5.41 and 5.42, the relations for the forces and moments in the contact surfaces are finally:

$$S = \frac{2F \cdot k_\eta}{v}(\dot{y}_R - \dot{h}_y) + \frac{2F \cdot k_\beta}{v}\dot{\varepsilon}_R + 2c_R\left(1 - \frac{k_\beta}{r_0}\right)(y_R - h_y) - 2F \cdot k_\eta \cdot \varepsilon_R, \tag{5.43}$$

$$U = \frac{2F \cdot k_\xi \cdot \gamma_e}{r_0}(y_R - h_y) + \frac{2F \cdot k_\xi (s_R/2)}{v}\dot{\varepsilon}_R, \tag{5.44}$$

$$M = -\frac{2F \cdot k_\beta}{v}(\dot{y}_R - \dot{h}_y) + \frac{2F \cdot k_\mu}{v}\dot{\varepsilon}_R - \frac{2c_R \cdot k_\mu}{r_0}(y_R - h_y) + 2F \cdot k_\beta \cdot \varepsilon_R. \tag{5.45}$$

In Eqs. 5.43–5.45 terms occur which depend on the transverse movement of the wheelset in the track ($y_R - h$) and on the wheelset yaw angle ε_R. They can be interpreted as spring forces or spring moments (displacement or angle dependent). Further terms depend on the time derivative of the paths and angles (dotted quantities, velocities). They can be interpreted as damper forces resp. moments. In these expressions, the driving speed v is in the denominator, i.e. the damping effect decreases with increasing driving speed.

With the derived Eqs. 5.43–5.45, the equations of motion of a wheelset bound to a vehicle or bogie mass by spring and damper can be given, e.g. in matrix form:

$$\overline{\overline{M}} \cdot \ddot{\bar{y}} + \overline{\overline{K}} \cdot \dot{\bar{y}} + \overline{\overline{C}} \cdot \bar{y} = \overline{R_1} \cdot \dot{h}_y + \overline{R_2} \cdot h_y \tag{5.46}$$

with

$\overline{\overline{M}}$:	Mass matrix,
$\overline{\overline{K}}$:	Damper matrix,
$\overline{\overline{C}}$:	Spring matrix,
$\bar{y}$:	State vector,
$\dot{\bar{y}}, \ddot{\bar{y}}$:	First or second derivative of the state vector with respect to time,
$\overline{R_1}, \overline{R_2}$:	"Right-side" vectors,
$h_y, \dot{h}_y$:	Unevenness, change of unevenness over time.

The state vector contains as components all movement possibilities (degrees of freedom) of the overall system, e.g. transverse path y_R and yaw angle ε_R of a wheelset or several wheelsets, the bogie frames and the wagon body. The "right-hand side" vector $\overline{R_1}$ contains as components all terms that are multiplied by $\dot{h}_y$ corresponding to $\overline{R_2}$ terms multiplied by h_y.

This system of equations can no longer be solved in closed form. If the described linearizations are carried out, a solution in the frequency domain is possible (calculation of magnification functions or, if the track unevenness, the right side of the equation, is not taken into account, of eigenvalues). If the non-linear contact and adhesion-slip functions are to be used, numerical integration in the time domain is required (see Sect. 5.3.2). The equations and functions presented here are only intended to provide a basic understanding of the theory of wheelset running.

The guidance of a wheelset in a straight track occurs as shown via the slip forces and moments in the wheel contact points. The forces contain components that can be interpreted as spring and damper forces, see above. As the slip values depend on the running speed, unstable wheelset running can occur, i.e. the amplitudes of the rolling motion are no longer sufficiently damped. As a result, the wheelset starts to slide transversely; its amplitudes in the horizontal-transverse direction are only limited by the contact of the wheel flange with the rail running edge. This unstable condition, which sets in at the so-called "critical speed", must be avoided within the planned speed range by appropriate design of the wheelset connection via springs and dampers on the bogie frame or wagon body.

An example of the running of a rail vehicle at different running speeds is shown in Figs. 5.28 and 5.30. Running tests were carried out on a straight section of track with a two-axle open freight wagon of the type Kbs 442 ("stake wagon"). The wheelset lateral force at the rear wheelset and the wheelset lateral displacement in the track were evaluated.

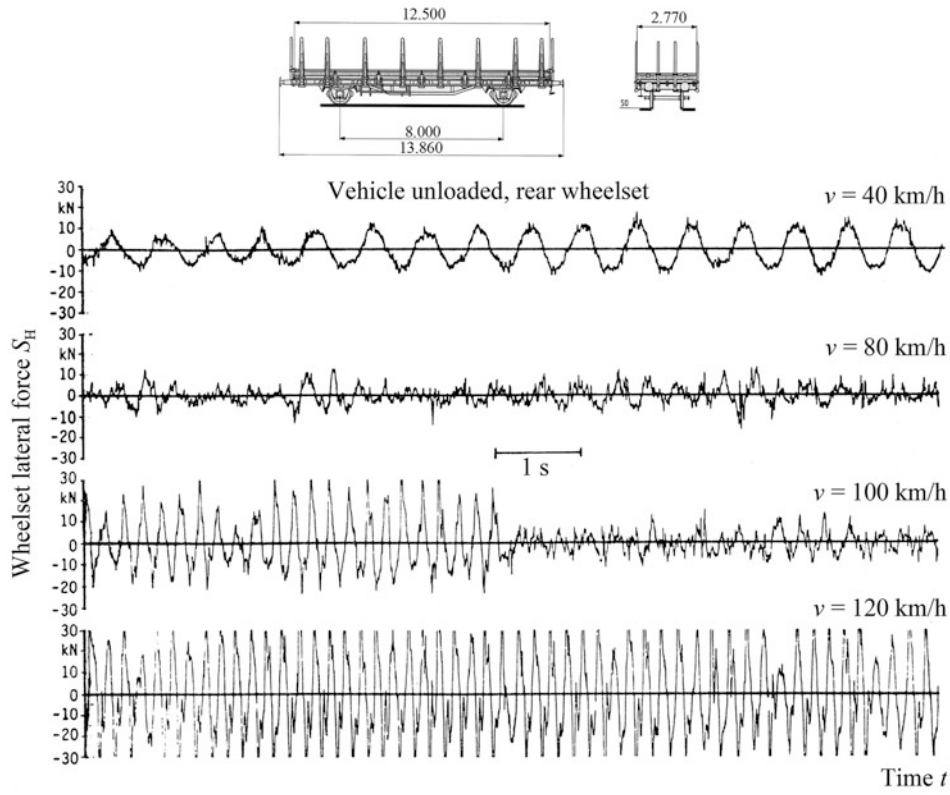

Fig. 5.28 Time functions of the wheelset side force at the rear wheelset of an open freight wagon at different running speeds. [30]

Figure 5.28 shows the time functions of the wheelset side force for $v = 40$, 80, 100 and 120 km/h.

While a dominant frequency can be identified at 40 km/h, the amplitudes of the wheelset side force at 80 km/h are smaller than at 40 km/h, whereby the dominant frequency cannot be identified. At 100 km/h there are initially large amplitudes, which become smaller after a certain distance of travel. At 120 km/h, the wheelset side force peaks at over 30 kN during almost the entire test run.

The course determined by a dominant frequency with its considerable amplitudes for the low driving speed can be explained with the help of Fig. 5.29. The vehicle was equipped with the wheelset profile DB II (wear profile) during the test runs.

The lateral movements of the wheelset and the wagon body are decisive for the lateral forces of the wheelset. The test track was a branch line used only for freight traffic. Due to the existing track unevenness, the vehicle is excited to vibrate with a wide frequency spectrum, i.e. also in its natural frequencies. For small deflections, the shackle running gear

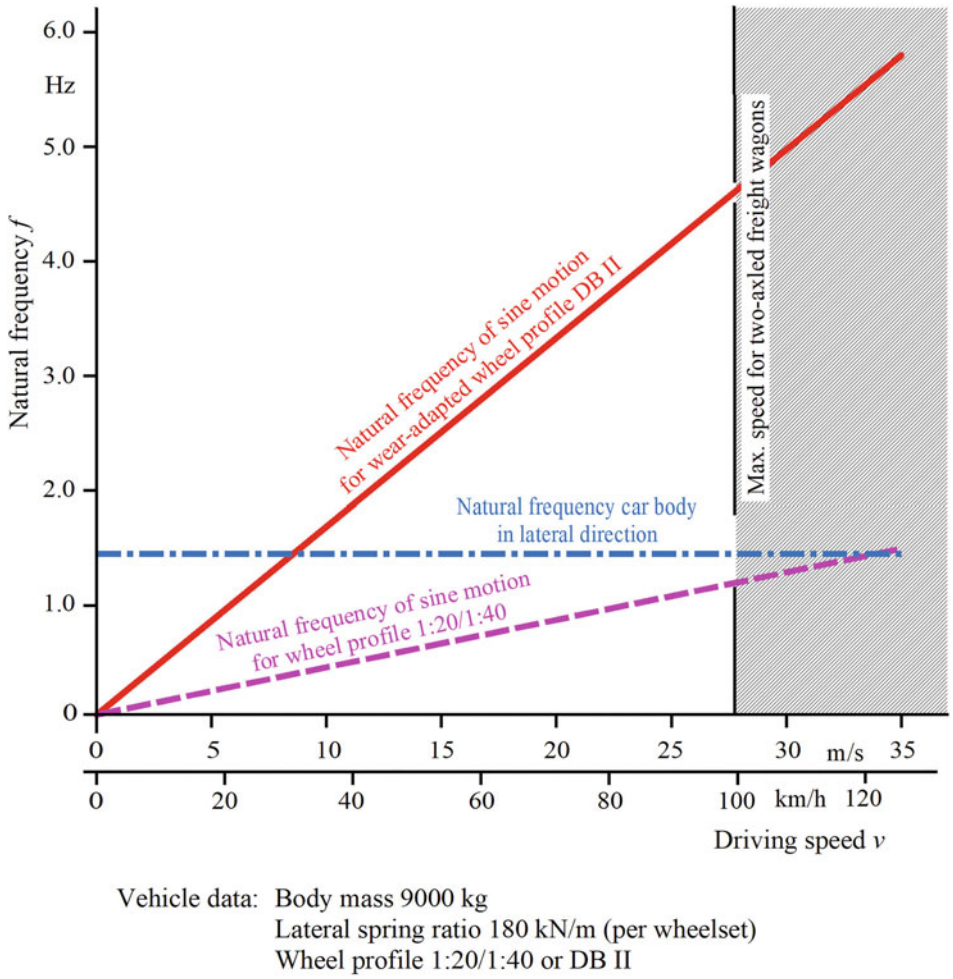

Fig. 5.29 Natural frequencies of the test vehicle from Fig. 5.28

results in a largely linear transverse suspension, which leads to the natural frequency of the car body of about 1.4 Hz shown in light blue.

Due to the wheel profile DB II, there is an effective conicity of $\gamma_e = 0.25$, which results in a speed-dependent frequency of the sinusoidal run according to Eq. 5.22, see red straight line in Fig. 5.29. The red straight line results according to the formula of KLINGEL, i.e. due to purely kinematic considerations and under linearisation of the Δr-function, and is therefore only a rough approximation. It can be seen that at the test speed of 40 km/h there is a resonance of the natural frequency of the sine motion of the wheelsets and the transverse natural frequency of the car body. Resonances always mean large amplitudes. At 80 km/h, the natural frequencies are so far apart due to the increase in the sine motion frequency that

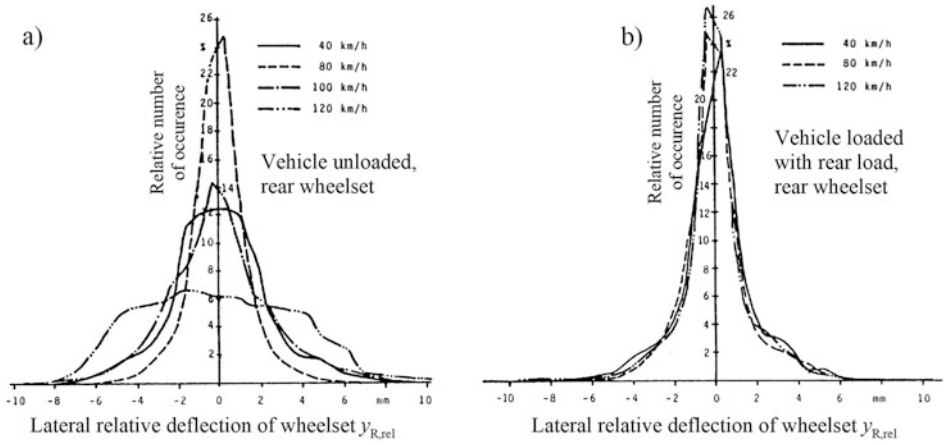

Fig. 5.30 Distribution of wheelset relative deflections during test runs with the vehicle shown in Fig. 5.29; variation of running speed and load. [30]

resonance no longer occurs and only small amplitudes of the wheelset lateral force are measured.

Apparently, the critical speed of the vehicle is just above 100 km/h, because as the time course of the wheelset side force shows, large amplitudes result, which, however, decrease to a lower level after half of the measurement time. This may be due to a change in the contact functions: The track of the test section had been welded together from used track yokes. A change in track gauge or rail profile would lead to different contact functions.

At 120 km/h the critical speed is reached; the wheelset shows a running behaviour that obviously makes full use of the track clearance. Flanges and rail running edges are in contact with each other. This becomes clear when looking at the distribution of the wheelset lateral deflections relative to the rails in Fig. 5.30.

The relative number of occurrence is plotted vertically, the size of the measured wheelset relative deflections horizontally. The narrower and higher a distribution is, the smaller were the amplitudes of wheelset movement in the track. In Fig. 5.30a it can be seen that at 80 km/h the smallest wheelset transverse paths occurred. They were smaller than at 40 km/h. At 120 km/h, one can see almost an equal distribution of the wheelset lateral travels, i.e. the wheelset has fully utilised the track clearance. Figure 5.30b shows for the rear-loaded test vehicle transverse wheel set travels that are largely independent of the driving speed, i.e. a considerably less oscillatory driving behaviour. Due to the large inertial mass of the car body, the wheelset can support itself better.

In Fig. 5.29, the natural frequency of the sine motion for a wheel profile 1:20/1:40 is also drawn in pink-violet due to the lower effective conicity, the natural frequency increases more flatly with the running speed than with the wear profile DB II. Resonance between sinusoidal running and wagon body natural frequency in the transverse direction would only occur here at approx. 120 km/h. The maximum speed of two-axle freight cars is

limited to 100 km/h, however. In this case, one spoke of a "subcritical" running gear, whereas with the DB II wheel profile, a "supercritical" running gear would be present. What was meant by this was that in the case of the former, the critical running speed would not be reached in operation, whereas in the case of the latter, it would be passed at low running speeds and correspondingly lower force levels. However, this view is incorrect. The critical speed depends on the damping in the system; in the case of the experimental vehicle, it is approximately between 100 and 120 km/h. What used to be called "critical speed" is only the speed at which there is resonance between the transverse motion of the body and the sine motion of the wheelset. Unstable wheelset running is not associated with this.

From the equations of motion Eq. 5.46, the critical speed can be calculated. To do this, consider the homogeneous differential equation:

$$\overline{\overline{M}} \cdot \ddot{\overline{y}} + \overline{\overline{K}} \cdot \dot{\overline{y}} + \overline{\overline{C}} \cdot \overline{y} = 0. \tag{5.47}$$

Its solution leads to the so-called "characteristic equation"

$$\det\left(\widehat{p}^2\overline{\overline{M}} + \widehat{p}\overline{\overline{K}} + \overline{\overline{C}}\right) = 0, \tag{5.48}$$

where

$$\widehat{p} = \delta + i\nu.$$

From this, the complex eigenvalues $\widehat{p}$ can be calculated. Their real part is the decay constant δ and the imaginary part is the damped natural frequency ν. Due to the velocity-dependent slip forces, the eigenvalues are also velocity-dependent; the decay constants can have a negative sign (oscillation decays, system stable), be zero (oscillation is undamped) or have a positive sign (fanned oscillation, system unstable).

From δ and ν one can calculate the damping factor *D:*

$$D = \frac{-\delta}{\nu}. \tag{5.49}$$

The critical speed v_{krit} of a wheelset is the speed at which the damping factor of the system reaches zero. From this speed onwards, the amplitude of the wheelset in the horizontal-lateral direction is only limited by the contact of the flanges at the rail running edges. The critical speed must be above the intended operating speed.

Considering a single wheelset tied to an (infinite) mass, Fig. 5.31, the dependence of the critical speed on the transverse- and longitudinal spring stiffness of the wheelset linkage can be represented as an area in space [38].

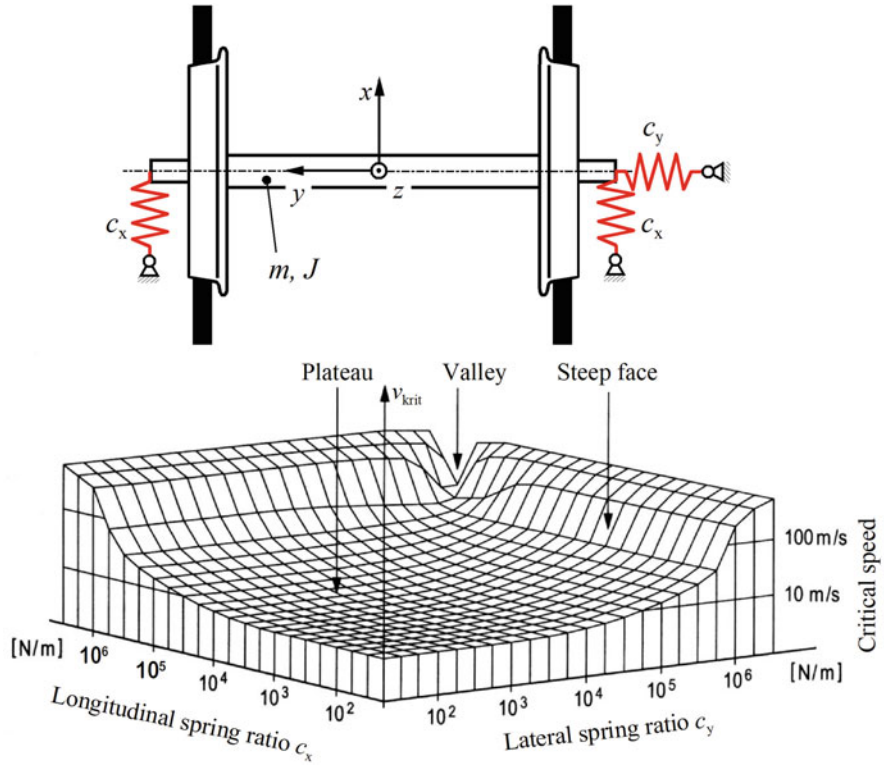

Fig. 5.31 Critical speed of a wheelset tethered to the environment as a function of longitudinal spring constant c_x and transverse spring constant c_y. (According to [38])

It can be seen in Fig. 5.31 that the critical speed increases sharply, especially in the area of the "steep face". This area is reached by increasing the stiffness of one of the two springs c_x or c_y. If both are designed stiffly, one is in the "valley", i.e. at a lower critical speed. Since the transverse suspension c_y cannot be designed with any degree of stiffness due to the requirements for passenger comfort or the vibration load on the vehicle load, the longitudinal suspension c_x is usually designed stiffly in vehicles or running gear for higher speeds. However, with regard to running in curves, there are also limits here depending on the axle spacing.

5.6 Running Gears of Rail Vehicles

Railroad passenger vehicles, many freight cars and locomotives as well as many tram cars are built as bogie vehicles. Due to the short wheelset distances in the bogie frame, good curved running behaviour is achieved even with long vehicles. In addition, the arrangement of a further spring stage is possible. In exceptional cases, there are also railway vehicles

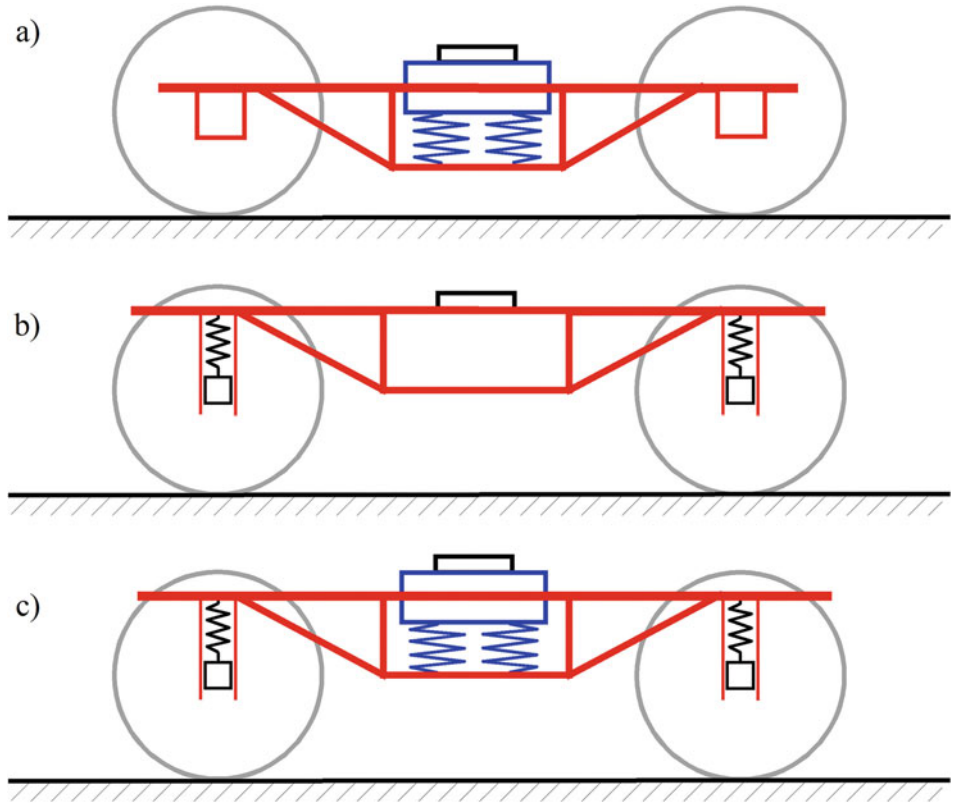

Fig. 5.32 Basic types of bogies. (**a**) Secondary suspension only (traction units, freight wagons), (**b**) Primary suspension only (traction units, freight wagons), (**c**) Primary and secondary suspension. (According to [25])

with single wheelset bogies, e.g. the metro trains built by Alstom for Copenhagen. Single wheelset bogies are also sometimes used for tram vehicles. Bogies for railway vehicles are now discussed first (Sect. 5.6.1). The basic design features are also found in tram vehicles. However, the trend towards low-floor tramcars has led to special solutions there, which are discussed in Sect. 5.6.2.

5.6.1 Bogies for Railway Vehicles

Figure 5.32 shows schematically the basic types of bogies. In Fig. 5.32a the wheelset bearing boxes are firmly connected to the bogie frame (the latter is shown in red in Fig. 5.32). Between the bogie frame and the car body is the cradle (shown in blue), which is supported on the bogie frame by the secondary suspension. This design is used on traction units (e.g. the Tatra tramcars) and some types of freight wagon bogies

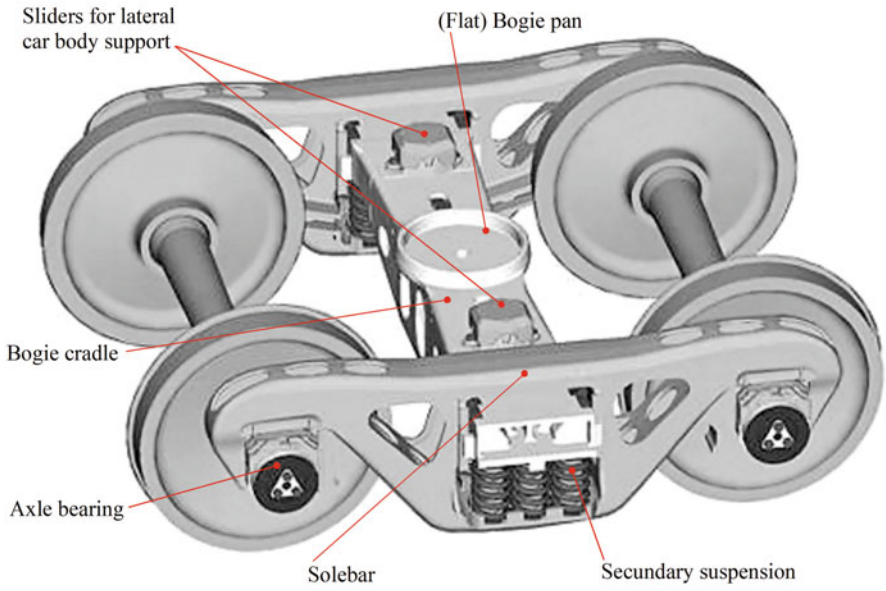

Fig. 5.33 American freight car bogie "Barber" made of cast steel without primary suspension with sprung cradle. (After a computer graphic from: http://www.progressiverailroading.com/; accessed on 06.10.2014)

(especially USA, countries of the former Soviet Union, South America, Australia, Africa), see Fig. 5.33.

In the "Barber" bogie shown in Fig. 5.33 there is no complete bogie frame; the two solebars are connected transversely only by the cradle. The solebars are supported directly on the wheelsets via the axleboxes. As a result, the unsprung masses from wheelsets and solebars are relatively high. The solebars and cradle are made of cast steel, which ensures low procurement costs but not necessarily fatigue strength. This type of bogie is used for axle loads up to 40 t.

Figure 5.32b shows a type of bogie commonly used in Europe for traction units and freight wagons: Here the bogie frame is supported on the wheelsets by a primary suspension; there is no secondary suspension. Figures 5.34 and 5.35 show two examples of this type of bogie. Compared to the "Barber" bogie shown in Fig. 5.33, the bogie frame is also sprung. In the case of the Y 25 freight car bogie (Fig. 5.34), which is standardised in Europe, there are both welded and cast bogie frames. In this type of bogie, the wheelsets are guided longitudinally rigidly, i.e. they cannot adjust themselves radially to the curve. Due to the short wheelbase of 1800 mm, this is not a disadvantage on normal railway lines, but only on sidings with small curve radii. The vertical suspension is provided by coil springs. As steel springs, these have minimal inherent damping, so that additional dampers must be provided. For this purpose, friction dampers are fitted to the axle bearing housings (Fig. 5.34b), to which a normal force dependent on the axle load is applied via shackles.

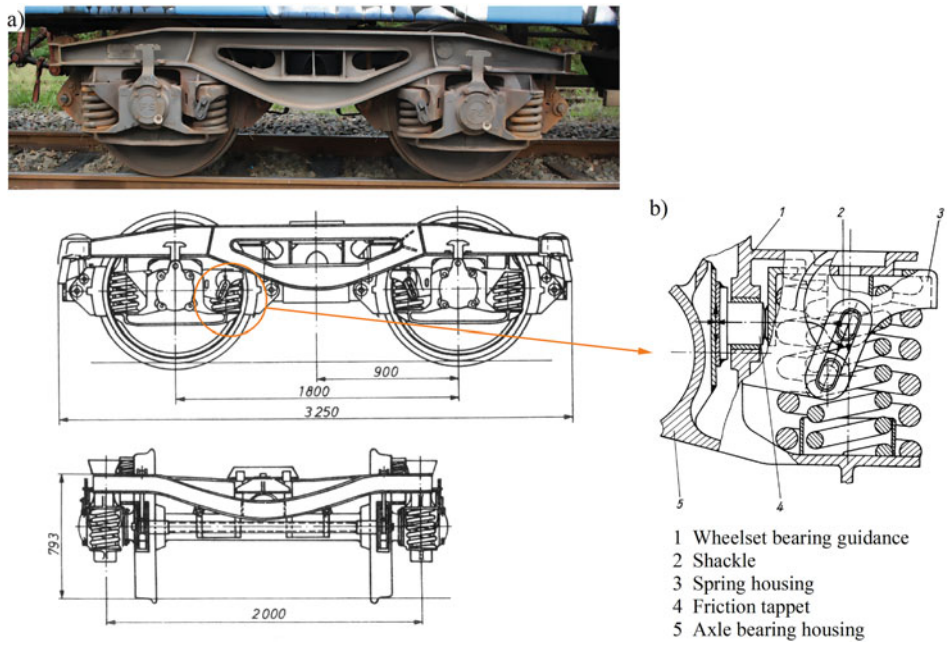

Fig. 5.34 Bogie with primary suspension. (**a**) Freight car bogie type Y 25, (**b**) load-dependent friction damper. (Sketches according to [25])

The LHB 82[23] freight car bogie (Fig. 5.35) also has only a primary suspension, which is implemented via (parabolic) leaf springs suspended in shackles. The wheelsets can therefore adjust themselves curve-radially and the bogie frame is also sprung in the horizontal-transverse direction in analogy to the discussed shackle running gears. The friction in the shackles and between the spring leaves provides damping.

The only unsprung masses on the Y 25 and LHB 82 are the wheelsets. However, the achievable vibration comfort would not be sufficient for passenger vehicles at higher speeds.

Bogies with two suspension levels are predominantly installed in rail vehicles for passenger transport. The secondary suspension is usually realised by a cradle. The necessary transverse suspension is achieved by a pendulum linkage of the cradle, Figs. 5.36 and 5.37.

Two pendulums hinged at the top of the bogie frame support a cradle trough at the lower end, which holds the secondary springs (Fig. 5.36). The cradle rests on these at the top. The body of the wagon is supported on the cradle by the rotary pan. The cradle can therefore spring in and out vertically and also move sideways via the pendulum linkage. Longitudinal movements are prevented by stops.

[23] LHB: Linke-Hofmann-Busch GmbH, Salzgitter; now Alstom Transport Deutschland GmbH.

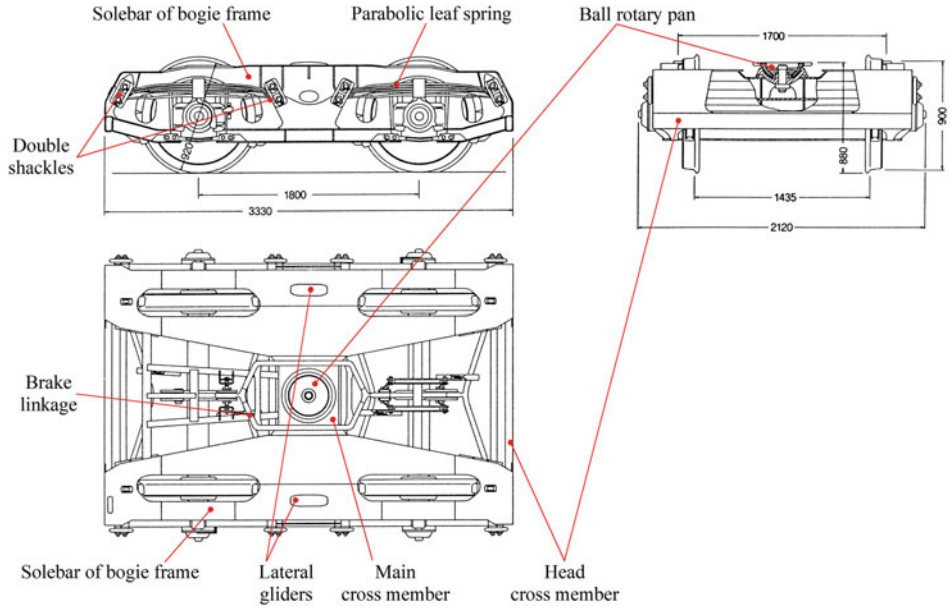

Fig. 5.35 LHB 82 freight car bogie (here with parabolic leaf springs). (According to drawing: LHB)

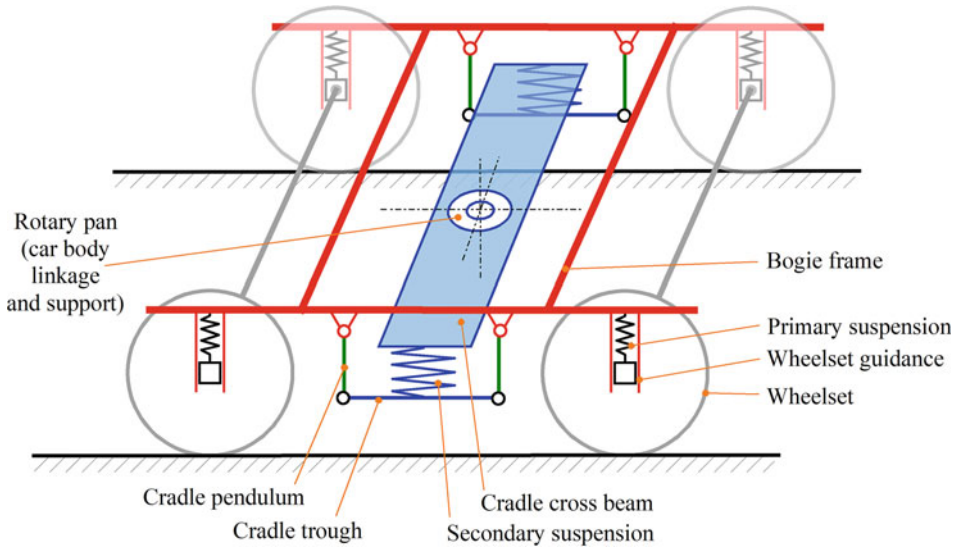

Fig. 5.36 Basic design of a bogie with cradle suspension

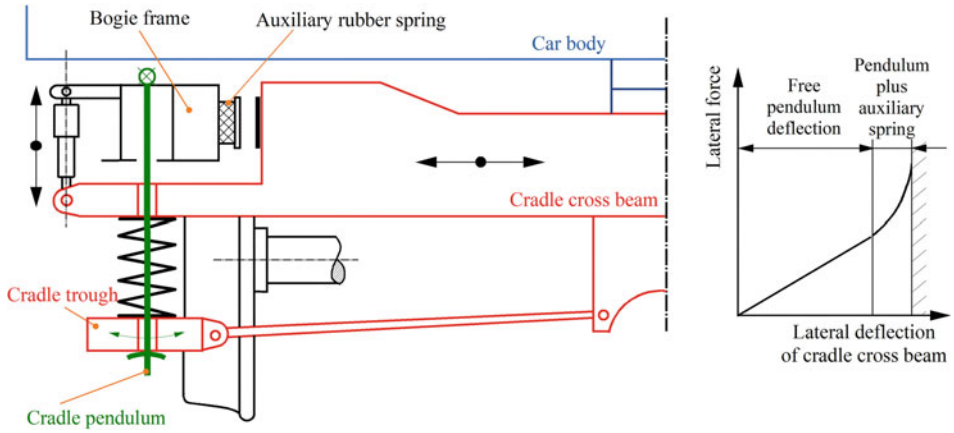

Fig. 5.37 Pendulum support of the bogie cradle (**a**), characteristic curve of the cradle transverse suspension (**b**). (According to [25])

Spring-loaded stops of the cradle on the bogie frame are often provided to limit the transverse spring travel, Fig. 5.37. The use of coil springs requires the use of additional, usually hydraulic, dampers. It should be noted here that leaf springs are often installed without additional dampers. The friction between the spring leaves during compression and extension then provides the damping of the vibrations. However, with only small excitation forces (driving over very good tracks), the friction between the spring leaves is not "broken up" and the leaf spring acts as a single rigid beam. Vibration comfort can thus be poor when the track is good. Passenger vehicles are therefore usually fitted with coil or air springs. Both types of spring require the installation of additional dampers due to their low inherent damping.

Figure 5.38 shows the older but still used bogie type MD 36[24] for passenger coaches in Germany and abroad. It has a cradle transverse suspension via a double pendulum: For small cradle transverse travels in the bogie frame, the pendulum acts with its entire length. The upper part of the pendulum comes to a stop at larger transverse travels, so that only the lower, shorter part of the double pendulum can deflect further in the horizontal-transverse direction. This results in a progressive spring characteristic of the cradle transverse suspension.

In this bogie, the wheelsets are rigidly guided in leaf spring control arms in the longitudinal and transverse directions (c_x and $c_y \rightarrow \infty$). The vertical wheelset suspension and the vertical cradle suspension are provided by coil springs. Hydraulic dampers are

[24] The letters MD stand for "Minden-Deutz". The bogie was developed in cooperation between the Federal Railroad Central Office in Minden and the Westwaggon Company in Cologne-Deutz. The Westwaggon company withdrew from rail vehicle construction at the beginning of the 1970s. The license for the MD bogies was transferred to Bombardier.

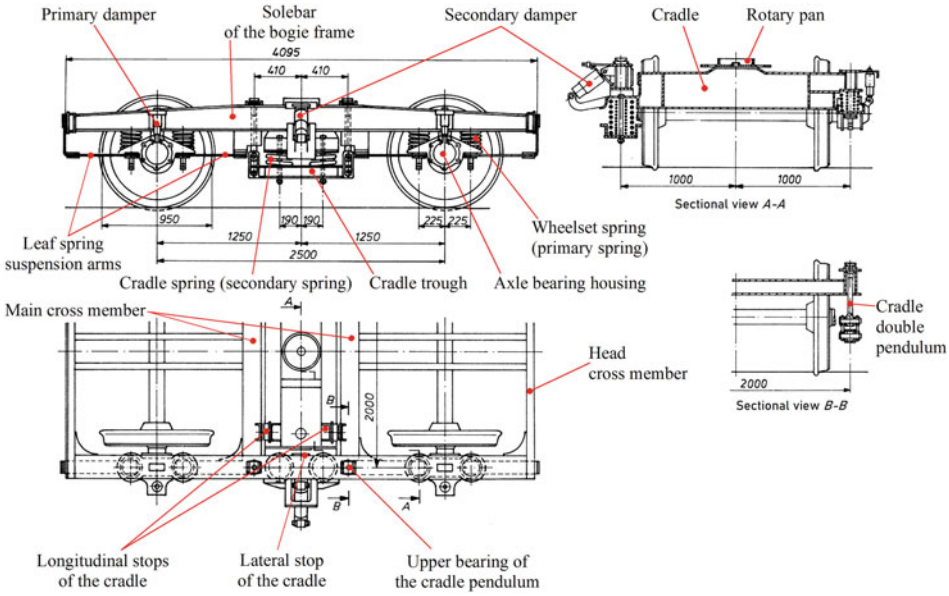

Fig. 5.38 MD 36 passenger bogie. (according to: DB printed matter DV 939d)

connected in parallel to the wheelset springs. The cradle damper is at an angle and takes over the damping of the horizontal and vertical cradle movement. However, this damper arrangement also results in an unfavourable coupling of the vertical and horizontal vibrations. A substructure type of this bogie ("MD 36 light", e.g. in older carriages for regional transport) is equipped with rubber springs on the wheelsets. The hydraulic damper is not necessary because of the material damping of the rubber. The bogie frame including cradle, springs, dampers and brake components has a mass of about 1.5 t. Each wheelset including wheelset bearings and housings also has a mass of 1.5 t, so that a ready-to-run MD 36 bogie has a mass of approx. 4.5 t.

The further development of the bogie MD 36 for higher speeds, the passenger bogie type MD 52, is shown in Fig. 5.39. In order to reduce the mass moment of inertia of the bogie about the vertical axis, the bogie frame has no head cross member. The masses are concentrated near the bogie pan. A small mass moment of inertia around the vertical axis ensures low mass moments and thus lower wheelset side forces.

The wheelsets are guided by double leaf links. Here, too, the wheelset guidance is rigid in the longitudinal and transverse directions (c_x and $c_y \rightarrow \infty$). Instead of stops to limit the longitudinal movement of the cradle, links are used. Separate dampers are provided for the vertical and lateral movements of the cradle. The bogie, designed for 200 km/h, has disc brakes and magnetic rail brakes. It is used under many passenger coaches in Intercity traffic.

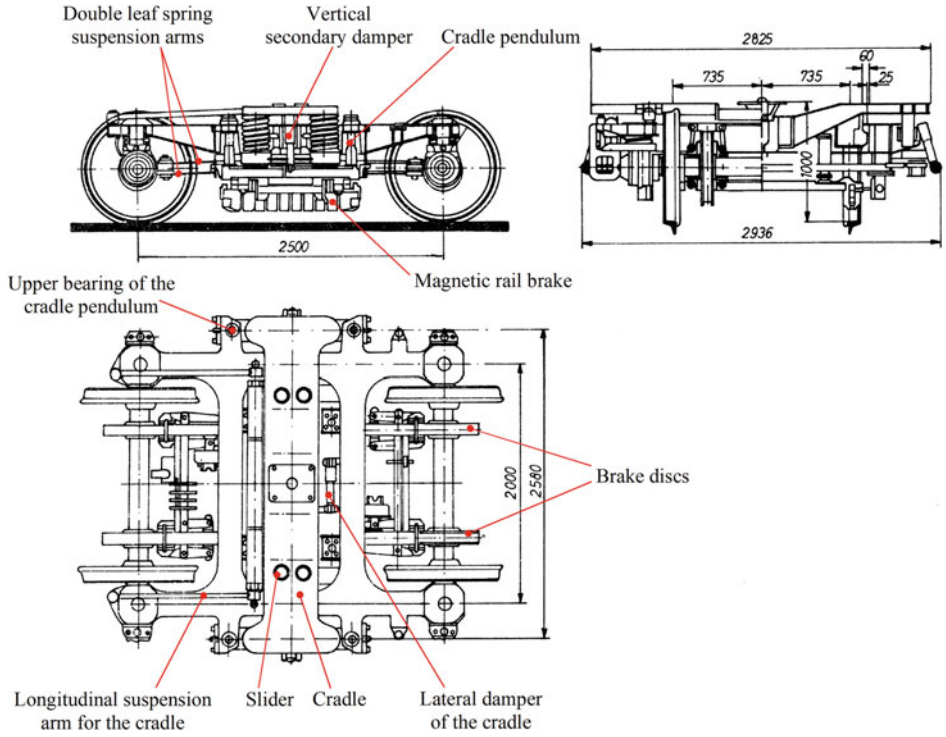

Fig. 5.39 MD 52 passenger bogie. (according to: DB printed matter DV 939d)

For ICE traffic, the MD 52 bogie was further developed into type MD 522 (Fig. 5.40). Noticeable differences to the MD 52 are the guidance of the cradle via links on both sides, the sliding pieces on the cradle that are further out and the four brake discs per wheelset.

In railcars and locomotives, drive elements such as electric motors or axle drives must be accommodated in the bogie. Therefore, there is usually no space for a cradle construction. For this reason, a "flexicoil suspension" is often used as secondary suspension on locomotives. An example is shown in Fig. 5.41. This bogie is from the Siemens "VECTRON" locomotive series.[25] The locomotive body is supported by coil springs on the cradleless bogie.

The turning of the bogie relative to the locomotive body in track curves is achieved by a displacement of the upper relative to the lower contact surface of the coil springs. This "flexicoil effect" of the coil springs results in a restoring moment at the spring base of the four springs, which rotates the bogie back into a straight position when the curve runs out. Longitudinal forces, tractive and braking forces, cannot be transmitted via this spring arrangement, so that lever arrangements are necessary for this.

[25] N.N.: Consistently modular – Siemens Vectron. Privatbahn-Magazin (2014)H. 4, pp. 16–20.

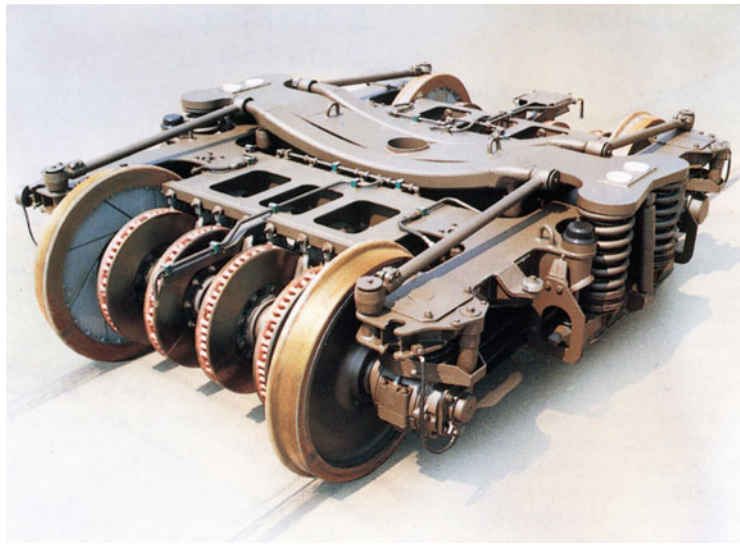

Fig. 5.40 MD 522 bogie for ICE-1 ($v_{max} = 270$ km/h). (Photo: Arge Mittelwagen)

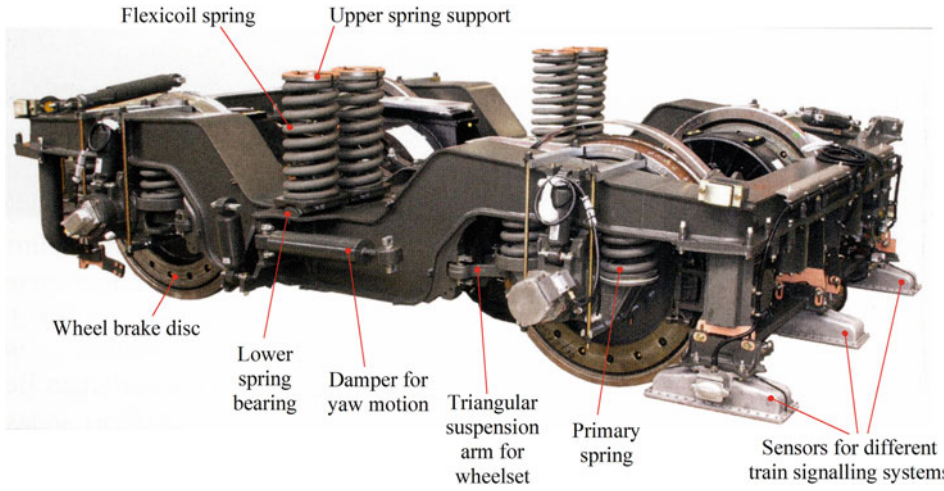

Fig. 5.41 Bogie of the Siemens locomotive series "VECTRON" with Flexicoil suspension. (According to photo: Siemens)

In the bogie design with triangular links shown in Fig. 5.42, the wheelsets are steered in the curve: In the track curve, the outer side of the bogie is loaded more heavily by the centrifugal force. This causes the primary springs to compress. Due to the installation position of the wishbones, the wheelset bearing housings not only move upwards in relation to the joint, but the horizontal distance between the wheelset bearing housings

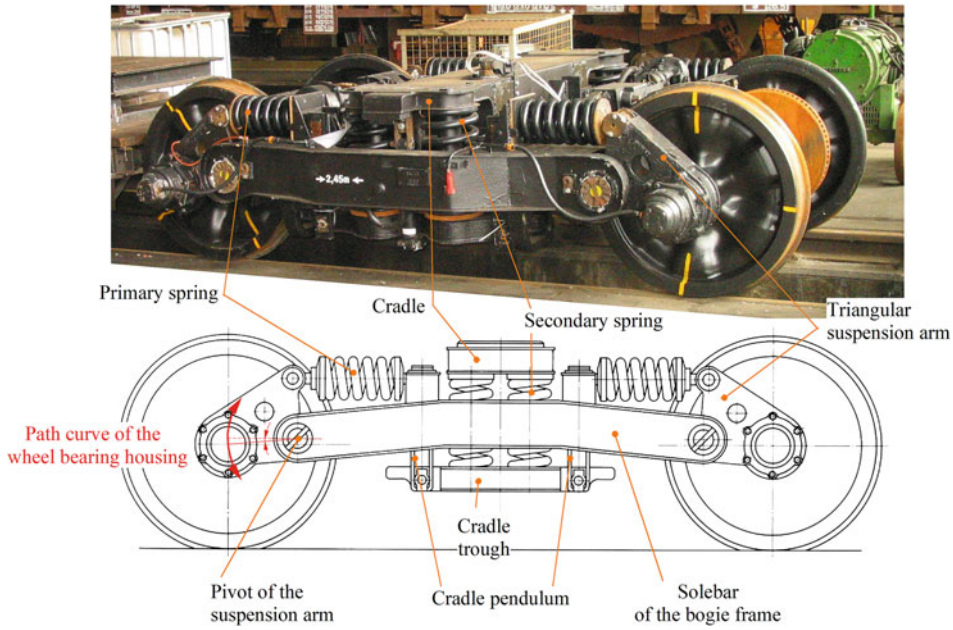

Fig. 5.42 Bogie "Munich-Kassel" with triangular control arms. (Sketch according to [17])

on the outside of the curve increases. On the inner side of the curve, the primary springs deflect, i.e. the wheelset bearing housings move towards each other. The distance between the wheelsets on the inside of the curve is thus shortened and the wheelset centre lines are ideally directed towards the centre of the curve. This makes it possible to drive through a track curve without constraint.

The LD 730 bogie shown in Fig. 5.43 has air springs in the secondary stage. The air springs cannot absorb longitudinal forces (e.g. braking forces), so that the longitudinal forces between the vehicle body and the bogie are transmitted by an articulated rod. It is mounted on the car body in a rubber joint.

On the LD 730 bogie, the primary springs are designed as rubber-metal springs with very hard identification. This is why they are also referred to as frame support bearings. They can be designed with different stiffness in longitudinal, transverse and vertical direction. The comfortable suspension of the car body is achieved by the air suspension with level control (see Sect. 5.8).

The air spring bellows are mounted on a spring carrier that can rotate around the vertical axis relative to the bogie frame. In order to dampen the bogie yaw motion, there is an anti-rotation device as friction damping between the bogie frame and the air spring carrier. The vehicle body is supported on the air springs. The air springs do not spin out with the bogie.

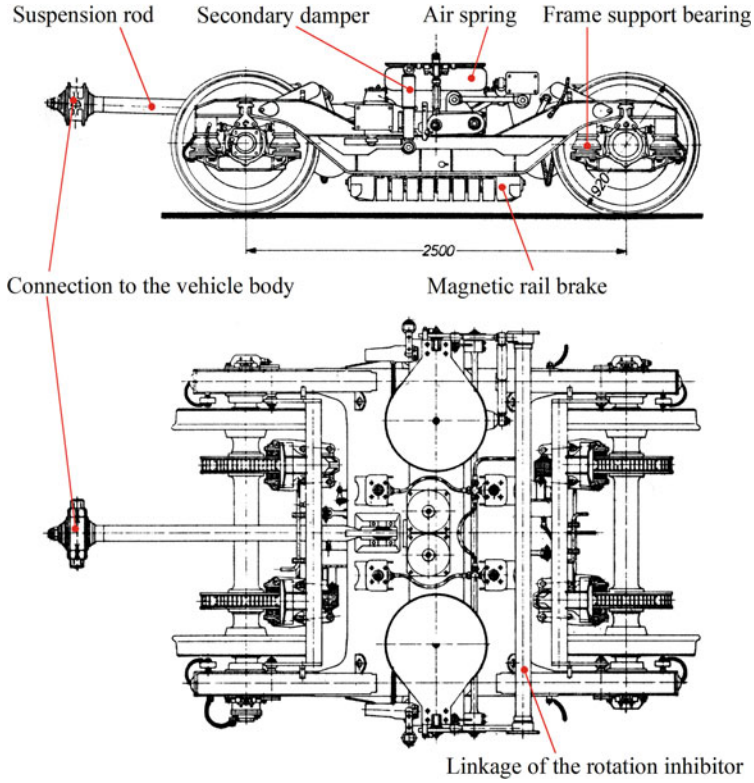

Fig. 5.43 Air-suspended passenger coach bogie LD 730. (According to: Documents of DB AG)

The so-called[26] JAKOBS arrangement of the bogies is used for articulated vehicles. Here, two adjacent vehicle bodies are supported on a common bogie. Figure 5.44 shows the principle and an example. The primary springs of the bogie shown in the photo in Fig. 5.44 are so-called rubber roller springs.

Figure 5.45 shows a bogie of a metro car. This is also a JAKOBS bogie. The section through the rubber roller spring (also called Clouth spring after the manufacturer) shows its structure: A mandrel tapering upwards is attached to the axle bearing housing. A rubber ring is slid over it, the outer contour of which lies in a bell that is bolted to the bogie frame. When the bogie springs in, the mandrel is pushed into the rubber ring. The rubber ring then rolls with its inner contour over the mandrel and with its outer contour inside the bell. As the free space inside the bell decreases with spring deflection due to its shape and that of the mandrel, the rubber ring is compressed. This results in a strongly progressive spring characteristic. The spring characteristic can be influenced by the contour of the mandrel and the bell. With an oval contour, for example, different spring stiffnesses can be achieved

[26] Wilhelm Jakobs, railway engineer (1858–1942).

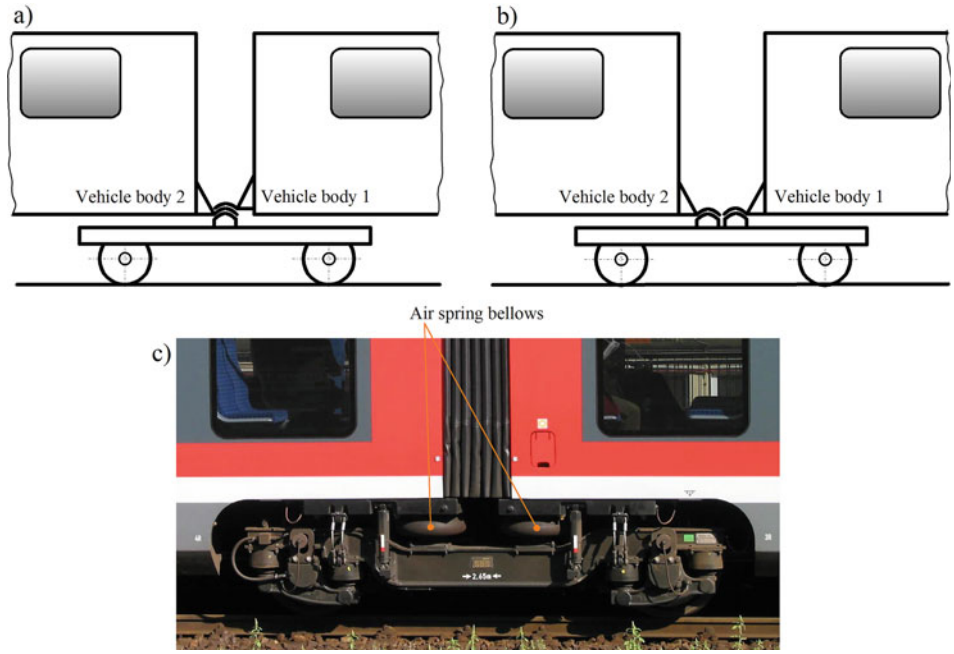

Fig. 5.44 Bogie in JAKOBS arrangement. (**a**) Principle with one common bogie pin, (**b**) two separate bogie pins, (**c**) JAKOBS bogie of the Siemens diesel railcar "DESIRO" with air springs (one pair per car body)

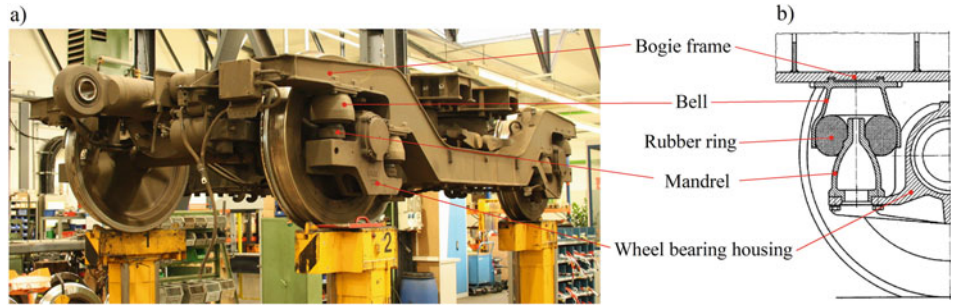

Fig. 5.45 (**a**) Non-driven JACOBS bogie of a subway car with rubber roller springs as primary springs, (**b**) Section through rubber roller spring. (According to drawing: Clouth)

in the vertical, transverse and longitudinal directions. Due to the material damping of the rubber, no additional damper needs to be provided.

While the rubber roller spring allows small longitudinal and transverse spring deflections of the wheelsets in relation to the bogie frame, the lemniscate guide as shown in Fig. 5.46 can be used to achieve (almost) rigid wheelset guidance in the longitudinal

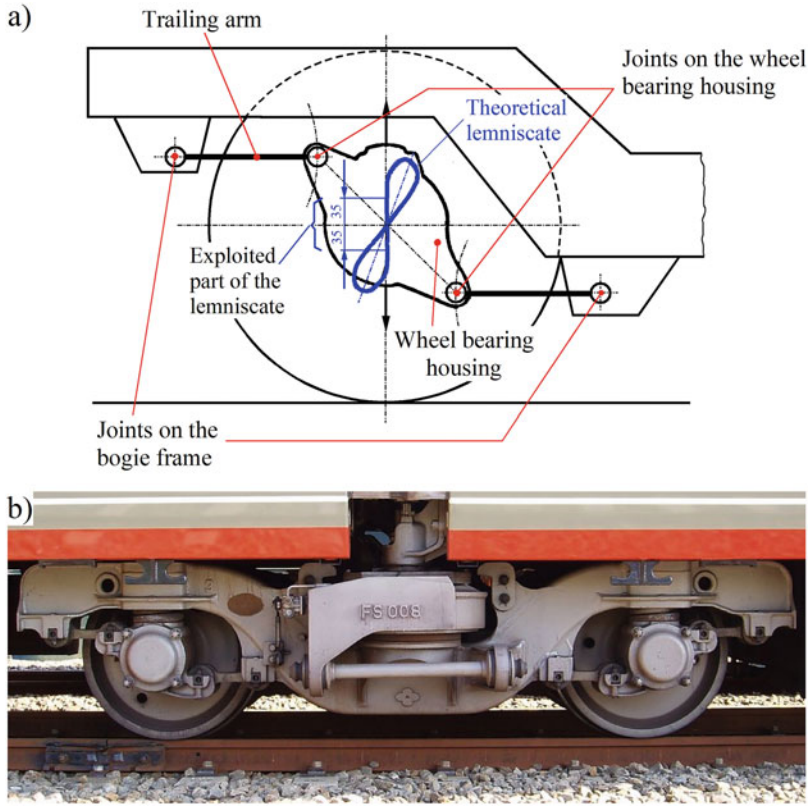

Fig. 5.46 Wheelset linkage by means of lemniscate links. (**a**) Theoretical linkage curve (*blue*). (according to [25]) (**b**) Bogie of a Japanese electric multiple unit with lemniscate guidance of the wheelsets. (Photo: Wikimedia, https://de.wikipedia.org/wiki/Lemniskatenlenker#/media/File:Truck-FS008.jpg/; accessed on 04.02.2016)

direction. Two parallel but offset links are fitted to the top and bottom of the wheel bearing housing. The centre of the wheel bearing housing describes a lemniscate as a coupling curve through this linkage (drawn in blue in Fig. 5.46a, in the form of an 8). The vertical spring travel uses only the approximately straight central part of the lemniscate; the wheel bearing housing therefore moves on a straight vertical path during compression and rebound. Both wheelsets are thus guided in parallel in the plan view.

5.6.2 Running Gear of Tramcars

For tram vehicles running in the street space, the low-floor arrangement is mostly preferred today, Fig. 5.47. Due to the faster passenger change at stops, low-floor vehicles also offer advantages to tram operation: The average speed is increased and thus the attractiveness is

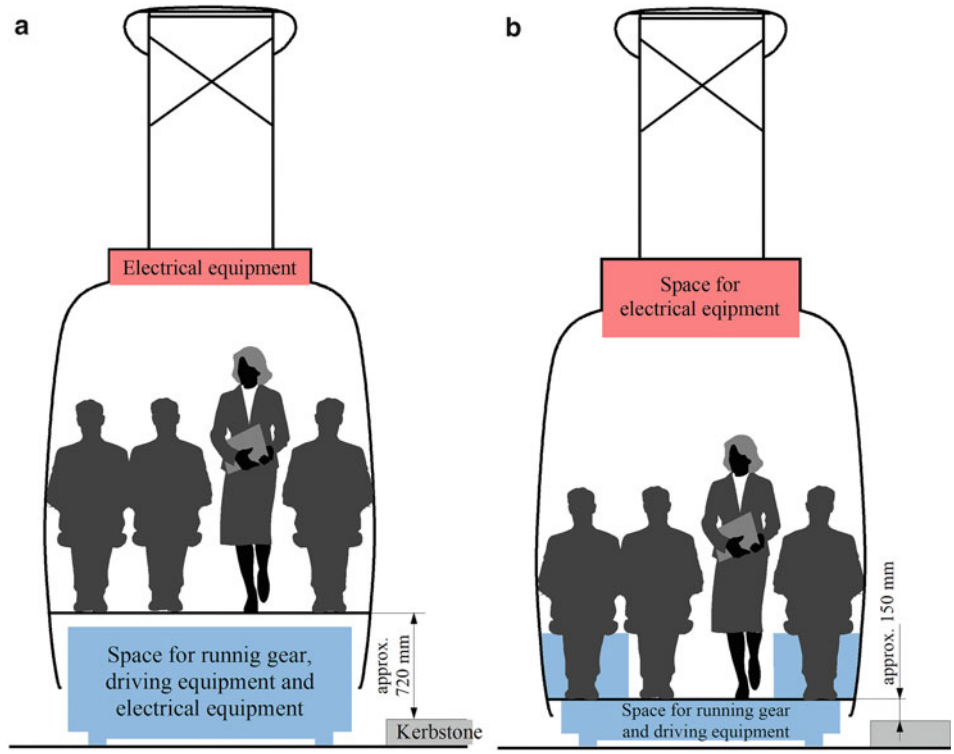

Fig. 5.47 Arrangement of running gear, drive and electrical equipment on tram vehicles in high-floor (**a**) or low-floor type (**b**)

improved. On longer lines, the operation often manages with one vehicle less, as the circulation time is shorter. For passengers with limited mobility (the elderly, wheelchair users, parents with prams), access to the vehicle is made much easier by the low entrance. In most cases, the floor height inside the car is around 300–350 mm. However, this limits the space available for the drive and running gear, Fig. 5.47. Most of the electrical equipment is stored on the roof. Small-wheeled undercarriages can be used to lower the floor compared with a conventional tramcar, but this does not allow a continuous low floor. Steps must therefore be arranged inside the car between the boarding areas and the area above the bogies. In the "classic" tramcar, the floor height is usually more than 900 mm above the top of the rails. For boarding from the kerb, two to three steps are therefore arranged in the entrances.

A tramcar with 70% low floor is shown in Fig. 5.48. The three-car vehicle has two motor bogies, each with two three-phase traction motors. The wheel diameter is 590 mm. In the high-floor area above the motor bogies the floor is 585 mm above rail level. However, platforms are installed below the seats to cover the motor bogies. The powered bogies have metal-rubber springs as primary suspension. The car body is supported on the motor bogies

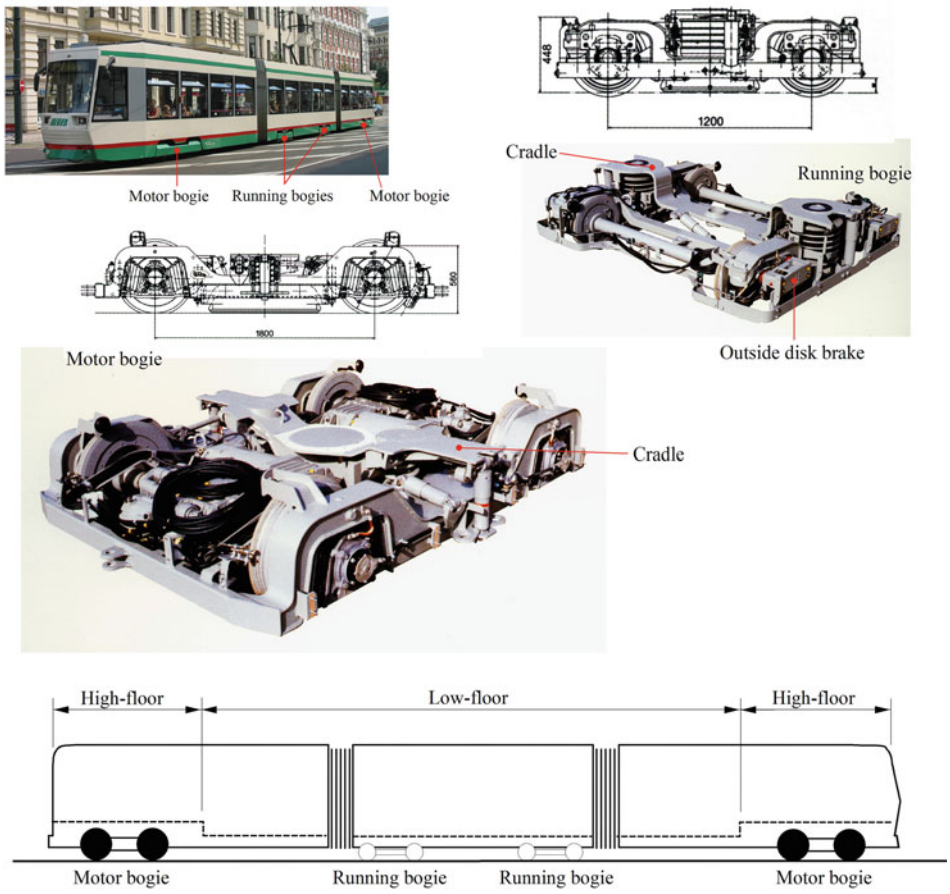

Fig. 5.48 Running gear of a tramcar with 70% low floor (Magdeburg). (According to photos: Alstom)

by a cradle construction. The middle car, on which the front and rear cars are mounted via a joint, has a floor height of only 350 mm. The entrance height is lowered to 300 mm by slight ramps at the doors. The running bogies of the middle section have continuous wheelset shafts with small wheels of only 410 mm diameter. The bogies in the middle section are also covered by platforms under the seats. Similar cars are also running in the cities of Braunschweig (1100 mm gauge), Darmstadt, and Gera (both meter gauge).

The vehicle in Fig. 5.48 runs on standard gauge and has outer frame bogies. On tramcars for standard gauge, inner frame bogies are often used for space reasons (car width), Fig. 5.49a. The primary suspension is provided by rubber thrust springs. The motor bogie has a cradle, which is not shown in Fig. 5.49. The associated vehicle also has a low floor of 70%. The centre carriage, on which the front and rear carriages are semi-mounted by means of an articulation, runs on single-wheel running gears. They have idler

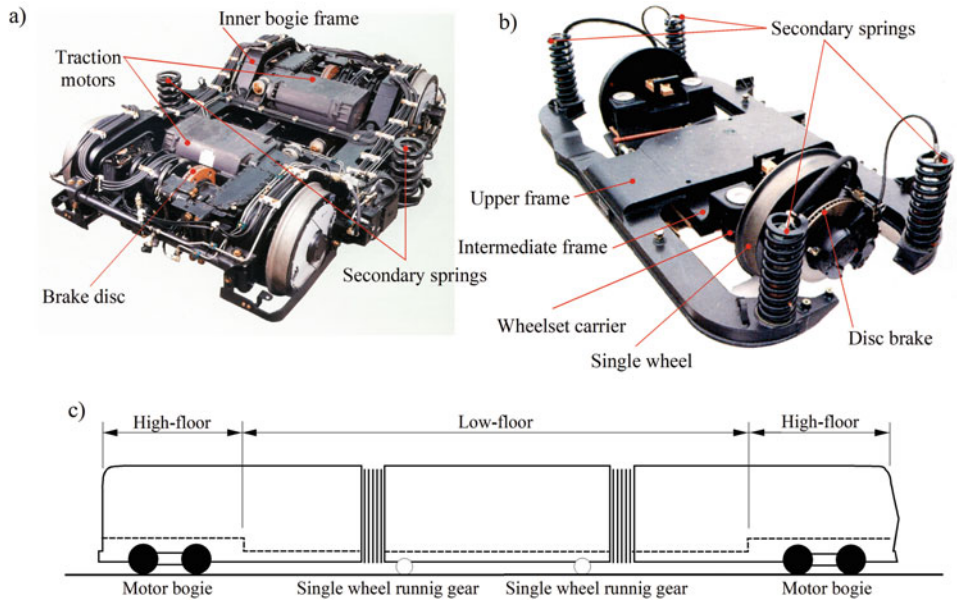

Fig. 5.49 (**a**) Drive bogie and (**b**) running gear of a tramcar with 70% low floor (Bonn) (according to photos: Siemens), (**c**) Overall arrangement

wheels, i.e. the two wheels are not connected by an axle shaft, Fig. 5.49b. Each idler wheel is fitted with a brake disc. The wheels are mounted in the wheelset carrier. The primary suspension is located between the wheelset carrier and the intermediate beam and is responsible for the transverse and longitudinal guidance of the wheelset carrier. The intermediate beam has a ball bearing slewing ring on which the upper frame is supported. The secondary springs on the upper frame provide the connection to the body. Longitudinal control arms between the upper frame and the body guide the running gear. A steering linkage is used to radially adjust the idler gear in curves. In the process, the articulation angle between the middle section and the end sections is transferred to the intermediate frame accordingly.

Tram vehicles with a continuous low-floor can only be reached via loose-wheel running gears. Figure 5.50 shows the drive running gear of the "Variobahn".[27] Each of the four wheels is driven by an asynchronous wheel hub motor. The wheels are connected to the undercarriage by a lever and a joint with a horizontal joint axis and are supported on the undercarriage frame by a helical spring which is not visible in Fig. 5.50a. You can see in Fig. 5.50b the low-lying cross-connections between the left and right sides of the running gear frame. This is not a bogie in the classical sense. Rather, the vehicle consists of short

[27] The Variobahn was developed by the companies ABB and Adtranz. Today it is manufactured by Stadler Rail.

Fig. 5.50 Variobahn (Chemnitz). (**a**) Chassis side view, (**b**) front view, (**c**) wheel hub motor (according to photos: ABB), (**d**) principle of vehicle arrangement, (**e**) vehicle view, (**f**) carriage interior with 100% low-floor floor; covering of the running gear

two-axle car bodies on bogies, between which the middle sections are suspended in joints in the manner of sedan chairs. Since the end carriages are very short, they do not have to be retracted at the ends, but appear very wide (Fig. 5.50e). The higher sides of the chassis with the wheel hub motors are covered inside the car by boxes on which the seats are located (Fig. 5.50f). The vehicle type "Variobahn" is used in Chemnitz, Bochum-Gelsenkirchen, Potsdam and in the Ludwigshafen-Mannheim-Heidelberg area.

Another type of bogie that allows a continuous low floor is shown in Fig. 5.51. A pair of driven and a pair of non-driven loose wheels are arranged in a bogie frame. This type of bogie is also not a bogie in the conventional sense, but allows only a small turning angle in

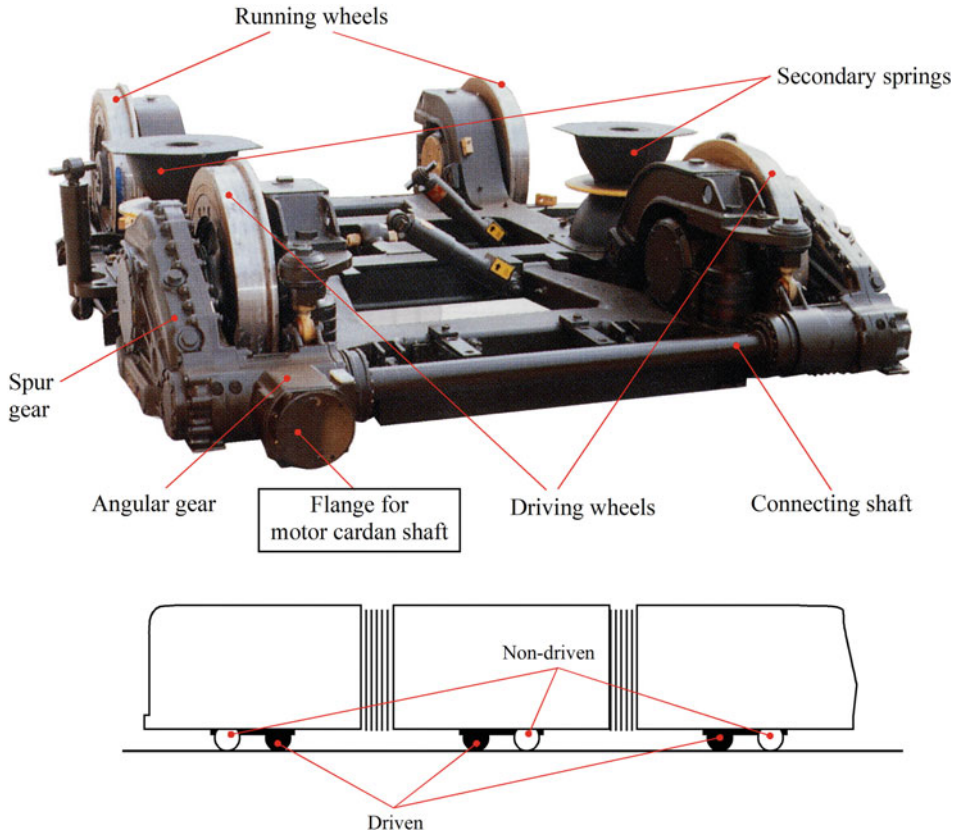

Fig. 5.51 Running gear of the AEG low-floor cars. (According to photo: AEG rail vehicles)

relation to the car body. The traction motor lies longitudinally sideways in the car body and drives the angular gear shown on the left in Fig. 5.51 (highlighted by a rectangle in Fig. 5.51) via a cardan shaft. The right wheel is driven via a connecting shaft lying transversely in front of the drive wheels. A spur gear is arranged externally between the connecting shaft and each of the two driving wheels. The brake disc for the mechanical brake is mounted on the motor shaft. Braking torques, both electrical and mechanical, are therefore transmitted from the motor shaft to the wheels via all the gearboxes. The non-driven wheels are unbraked. Since the rubber secondary springs are not centered between the wheels on one side of the running gear, but are offset toward the driving wheels, the driving wheels have greater wheel loads than the running wheels. In the passenger compartment, the undercarriages and the engine are covered by platforms and boxes under the seats.

Tram vehicles with undercarriages according to Fig. 5.51 are used in Berlin, Braunschweig, Bremen, Jena, Mainz, Munich and Zwickau. The licence for the

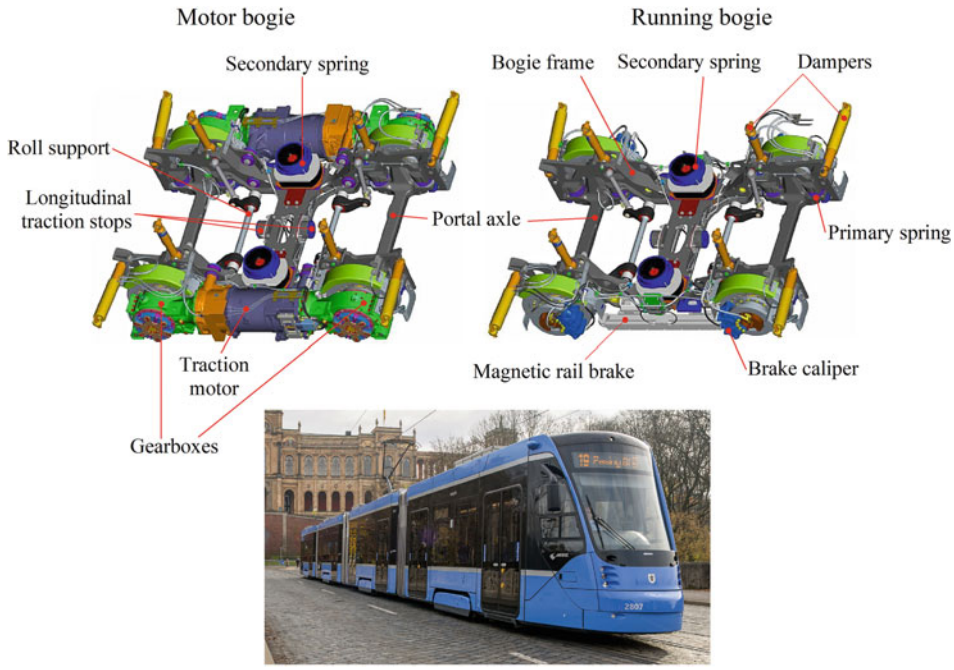

Fig. 5.52 Running gears of the 100% low-floor tramcar "Avenio" (Munich). (According to images: Siemens)

construction of these running gears has been transferred to the Solaris company, so that the vehicles supplied by Solaris for Jena and Braunschweig also have this type of running gear.

As a further example of 100% low-floor vehicles, Fig. 5.52 shows the bogies of the "Avenio" from Siemens. Again, these are not classic bogies. The bogies can only turn out horizontally by 4.5° relative to the car body. The motor bogies and the running bogies are of the same basic construction. On the motor bogie, the motors are arranged on the outside of the bogie frame and drive the two loose wheels on one side of the bogie via angular gears and hollow shafts with elastomer couplings. Traction and braking forces are transmitted to the car body via the traction stops. The roll supports are torsion bar springs similar to the stabilizers on a motor vehicle. They increase the roll stiffness of the secondary suspension and thus reduce the roll angle of the car body under lateral forces (e.g. when cornering). The four-part vehicle for Munich is equipped with three motor bogies and one running bogie.

5.7 Curve Entry and Exit

Special requirements for the design of the running gear or the design of the wagon underframes result from the routing of track curves: At the transition from a straight track section to a curved track with a constant radius, a transition curve is interposed. This has the form of a cubic parabola. This approximates the course of a clothoid for which the curvature increases linearly with the arc length (see [19, pp. 58–62]). The radius of the transition curve connects to the straight line with $R = \infty$ and ends at the track curve with its constant radius. To compensate for the centrifugal forces during curved travel, the outer rail of the track is raised from the beginning of the transition curve by means of a cant ramp. In the track curve (with constant radius), the minimum cant is min u. This is the difference in height between the outer and inner rails (see Fig. 5.53). It is calculated as follows:

$$\min u = \frac{11,8 \cdot v^2}{R} - 100 \quad \left(v \left[\frac{\text{km}}{\text{h}} \right], R[\text{m}], u[\text{mm}] \right)$$

(see [19, p. 52]).The position of a rail vehicle in the banked curve is shown in Fig. 5.53. The component $G{\cdot}\sin\alpha$ of the weight force G is opposite to the component $F{\cdot}\cos\alpha$ of the centrifugal force F. This compensates for some of the centrifugal force on the passengers, thus increasing comfort. As a maximum cant, max $u = 180$ mm is permissible in mixed operation of passenger and freight trains.

As the leading wheel on the outer rail could derail at the end of the curve due to the lowering of the rail as a result of the reduction in the wheel contact force (Fig. 5.54), an appropriately soft suspension must be used to ensure that the wheel unloading remains limited. This can also be achieved by a suitably low torsional stiffness of the bogie frame or by an articulated frame in which the two solebars can be twisted against each other about the horizontal transverse axis. In the case of long two-axle vehicles, the lifting of the leading wheel at the end of the curve is particularly critical, so that here derailment safety must be ensured by means of soft wheelset suspension or torsionally soft wagon underframes.[28]

As the LD 730 bogie shown in Fig. 5.43 has a very hard axle suspension, the bogie frame is designed to be torsionally soft: The main cross member consists of two bending-resistant but torsionally soft open double-T sections. The frame of a similar bogie from the same manufacturer[29] is shown in Fig. 5.55.

[28] See also the standard DIN EN 14363:2016. In the past, the determination of derailment safety was carried out according to ORE-B55-RP08. ORE: Office des Recherches et d'Essaies – Research and Testing Office of the European Railways.

[29] The developer and manufacturer of the LD 730 and the torsionally soft bogie frame was Wegmann & Co, Kassel, which has withdrawn from rail vehicle construction.

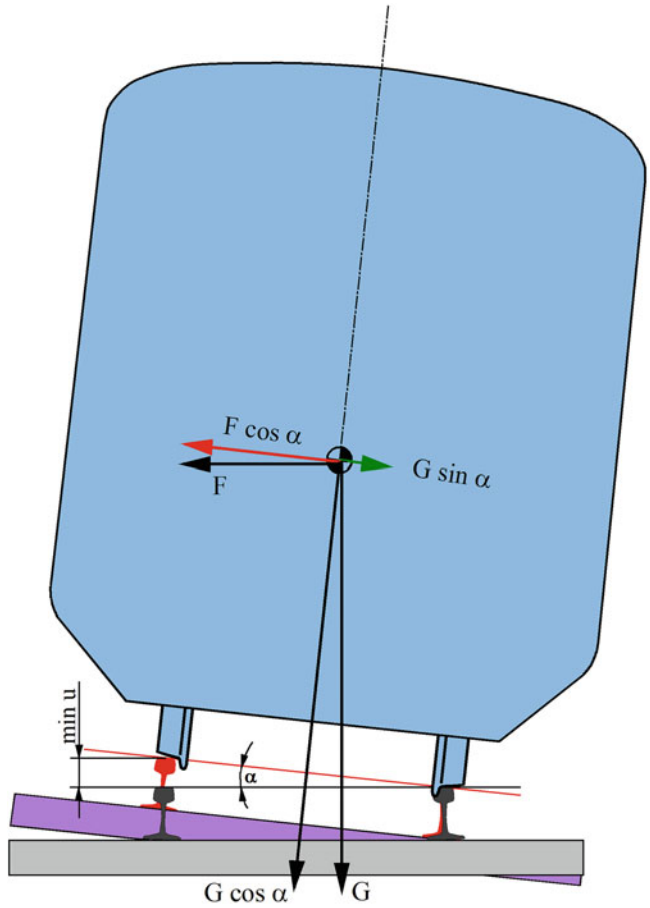

Fig. 5.53 Vehicle in a banked track curve

In the Barber bogie shown in Fig. 5.33, play between the cradle and the solebars is used to allow the two girders to twist against each other about a horizontal transverse axis in the cant ramp. This makes it possible to compensate for the entanglement of the wheel contact plane.

In order to increase the travel speeds of passenger trains in track curves, the centrifugal force on the passengers must be at least partially compensated. Since the track cant is limited on lines in mixed traffic, this can only be achieved by tilting the car body. Some diesel railcar series and one ICE series are therefore equipped with tilting technology at DB. Depending on the curve radius and speed, the car body on the bogies is tilted towards the inside of the curve. In the DMU class 612, Fig. 5.56, this is done by an electric actuator. Since the passengers feel less centrifugal force due to the inclination of the car body, the curved speed can be increased, whereby shorter journey times can be achieved on curved

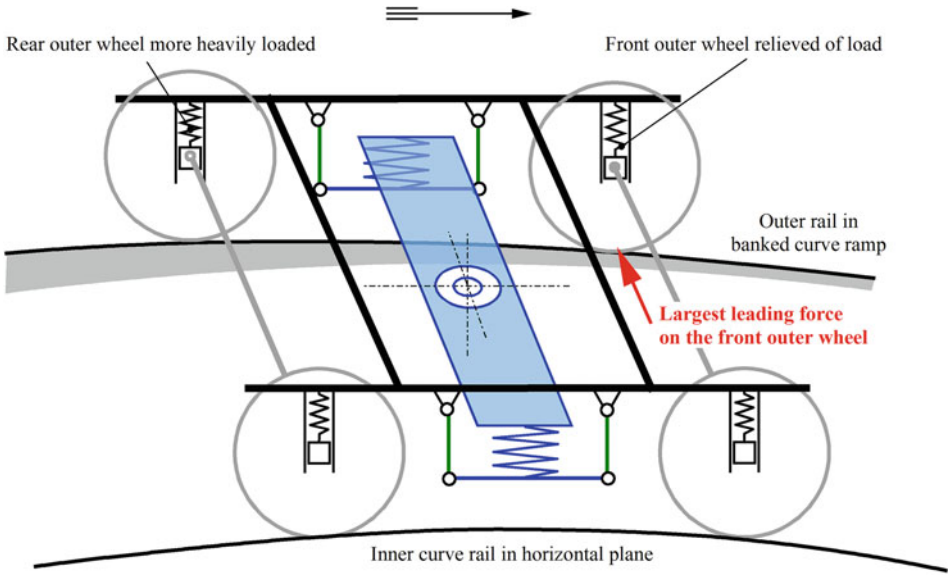

Fig. 5.54 Relief of the front outer wheel of a bogie at the exit of the curve in the cant ramp

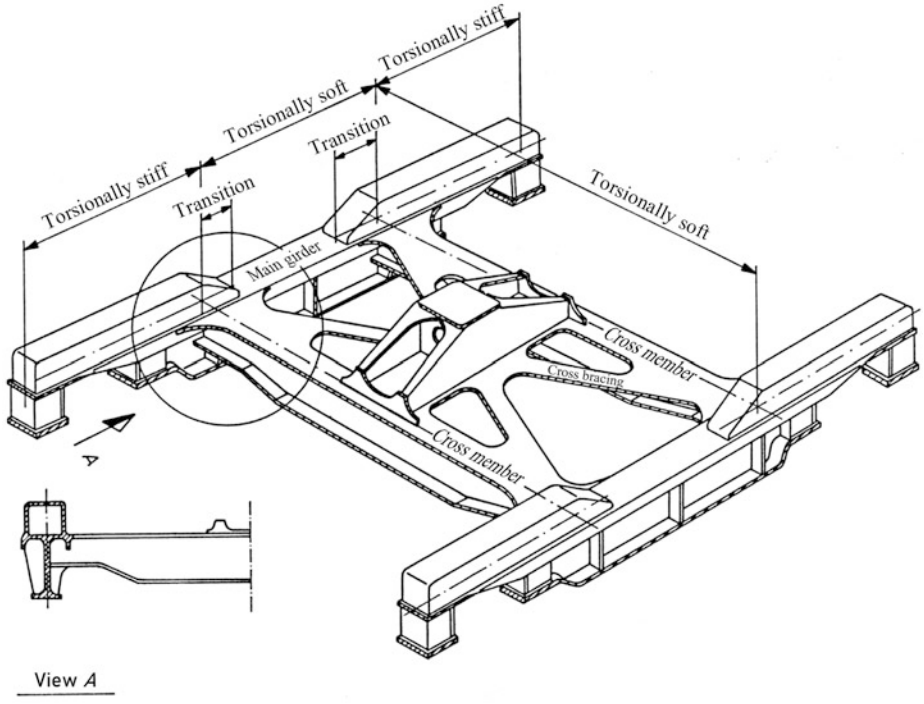

Fig. 5.55 Torsionally soft bogie frame for hard wheelset suspension. (According to drawing: Wegmann)

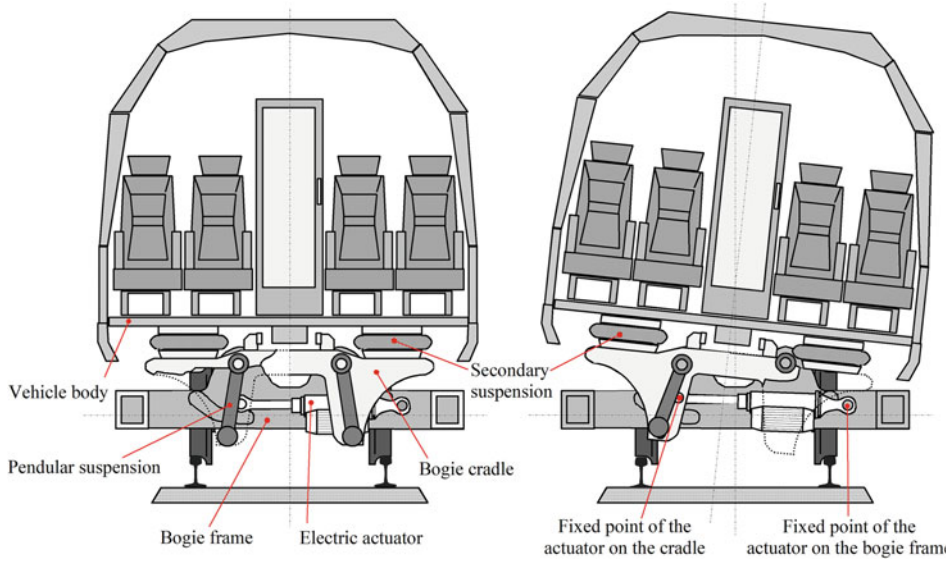

Fig. 5.56 Car body tilting device on DMU class 612 of DB AG

lines. However, the higher curved speeds increase the horizontal forces between wheel and rail due to the higher centrifugal force. The track superstructure must therefore be reinforced accordingly.

5.8 Air Suspension

Similar to commercial vehicles, air suspension has been increasingly used in rail vehicles since around 1960. Air springs are used to achieve a high level of comfort with regard to vibrations and noise, particularly in mainline railcars, but also in passenger coaches (e.g. the ICE-2) and in individual tramcar types. In the case of railcars, air suspension offers a further advantage: since the springs can realize not only the vertical suspension but also movements in the horizontal-transverse direction as well as the turning movement of the bogie relative to the car body, a cradleless bogie design is possible (see Fig. 5.57), which is favourable for accommodating the drive technology (electric motors or axle drives and cardan shafts). In the case of air springs with level control, it is possible to achieve a vehicle entry height that is independent of the load, as well as vibration characteristics that are independent of the load.

The calculation of air springs is relatively complicated and should be left to the manufacturer. In the following, some essential properties of the air spring will be explained. Figure 5.58 schematically shows a loaded air spring at rest (left) and under additional load (right). p_A is the atmospheric pressure (ambient pressure).

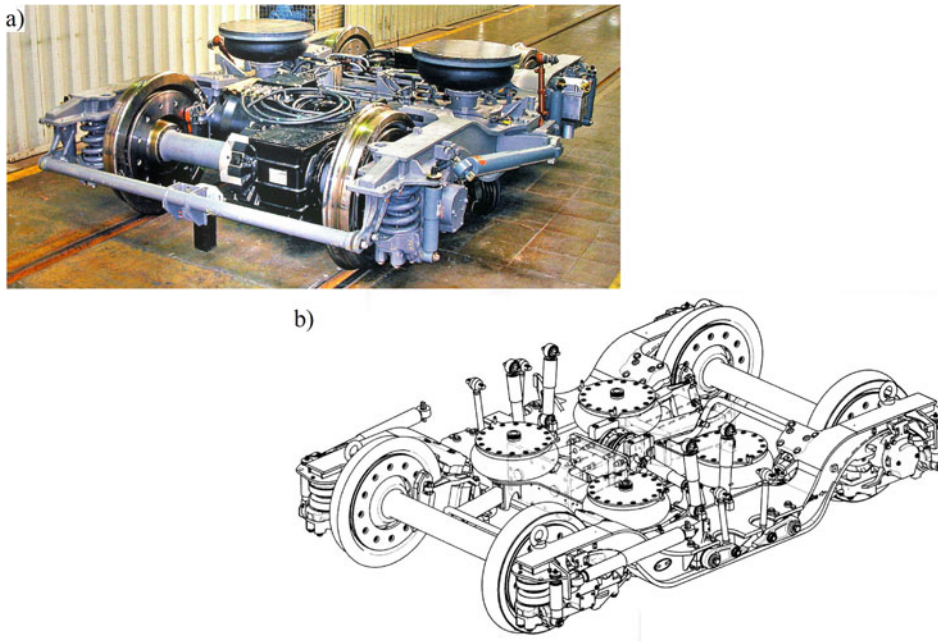

Fig. 5.57 Cradleless air suspension bogies FLEXXcompact of the French diesel multiple unit AGC. (**a**) Powered bogie, (**b**) Jakobs bogie. (According to photos: Bombardier)

We can initially imagine an air spring as an air-filled cylinder whose piston is pushed in under additional load and compresses the air in the cylinder. During the transition from the rest condition to the compressed state, a polytropic compression takes place: The compression is neither adiabatic (= without exchange of heat; this is approximately only true for very fast dynamic processes) nor isothermal (= without increase of temperature). The polytropic law is therefore applied:

$$p \cdot V^n = p_0 \cdot V_0^n$$

with

n	= polytropic exponent.

The numerical value of n is between 1 (isothermal compression) and $\kappa = 1.4$ (adiabatic compression). The air spring has a progressive spring characteristic, Fig. 5.59, because the gas volume becomes smaller with increasing compression and the spring thus becomes harder. Since the progression is very small, the spring characteristic at the operating point can be approximated by the tangent (Fig. 5.59).

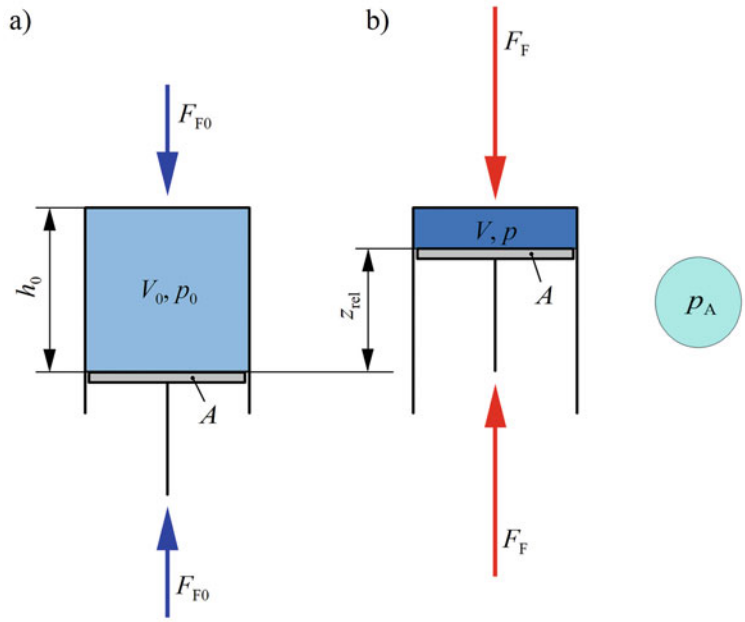

Fig. 5.58 For calculation of the air spring. (**a**) rest condition, (**b**) compressed condition; A = piston area, p_A = atmospheric pressure (ambient pressure)

The spring constant is obtained as the slope of the tangent at the operating point for the spring in the empty state ($z_{rel} = 0$):

$$c = \frac{n \cdot p_0 \cdot A}{h_0} = \frac{n \cdot p_0 \cdot A^2}{V_0} \quad \text{with } h_0 = \frac{V_0}{A}. \tag{5.50}$$

It can be seen that a soft spring, i.e. a small spring constant c, can be achieved by a small surface area (which, however, reduces the load-bearing capacity) and by a large volume of the spring. In practice, one therefore works with additional volume, see Fig. 5.61.

The corresponding natural angular frequency ν for a mass m supported by an air spring is calculated as follows

$$\nu = \sqrt{\frac{c}{m}} = \sqrt{\frac{n \cdot g}{h_0} \cdot \frac{p_0}{p_0 - p_A}}. \tag{5.51}$$

We put in Eq. 5.51 the polytropic exponent $n \approx 1.4$ (fast motions) and for $g = 9.81$ m/s^2. Furthermore, we assume that the pressure p_0 in the spring is much higher than the ambient pressure p_A, i.e. $\frac{p_0}{p_0 - p_A} \approx 1$, and obtain:

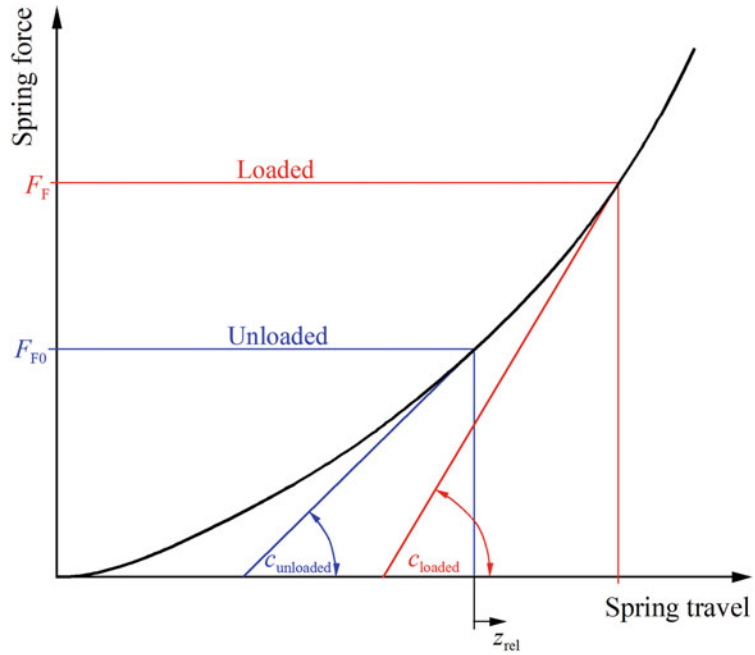

Fig. 5.59 Linearization of the spring characteristic curve of an air spring in the operating points "empty" and "loaded"

$$\nu = \sqrt{\frac{13,734[\mathrm{m}]}{h_0}}. \tag{5.52}$$

Thus, the natural (circular) frequency is only dependent on the height h_0, but independent of the sprung mass:

$$\nu \sqrt{\frac{\tilde{1}}{h_0}}. \tag{5.53}$$

All springs shown in Fig. 5.60 therefore have the same natural frequency but different load capacities. Therefore, air springs with larger diameters are required for heavy vehicles.

Air springs can be raised again to the level of the spring in the empty state by feeding compressed air in the loaded state. When the load is increased, enough air is fed in (see Fig. 5.61) so that the volume V_0 remains constant. This is done by a level control valve which reacts to the distance between the car body and the bogie. If the distance decreases due to higher loading, the valve feeds air into the spring from the reservoir. If the distance increases during unloading, air is released from the spring into the atmosphere. Due to the level control, the boarding height of e.g. passenger trains and railcars is independent of the

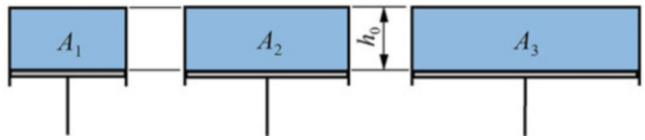

Fig. 5.60 Air springs with the same natural frequency but different load capacity

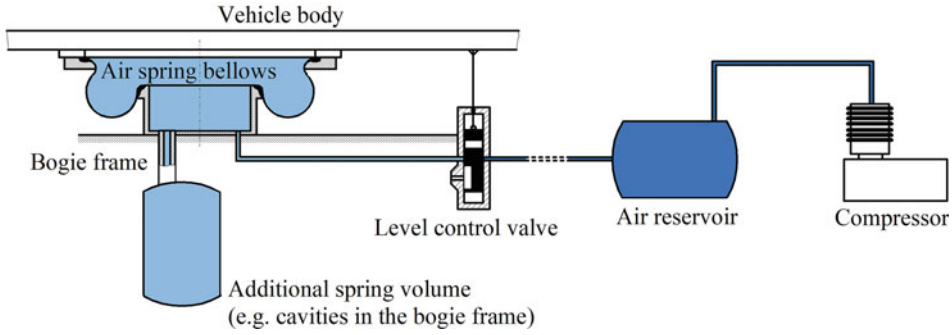

Fig. 5.61 Air spring with level control

occupation status. In addition, the vertical natural frequency of the vehicle and thus the vibration comfort remain constant within narrow limits. This property of an air suspension with level control is not as important in mainline vehicles due to the high dead weight (and thus the low ratio between loaded and empty vehicle, m_{load}/m_{empty}) as in trams or buses (in the latter, $m_{load}/m_{empty} \approx 2.0$).

Figure 5.61 also shows the application of an additional volume. In this way, a large volume of the air spring is achieved without having to expand the installation space for the spring and a soft spring is obtained. In some cases, cavities, e.g. of box girders in the bogie frame, are used as additional volumes. However, the pressure vessel regulations then apply to these structure parts, so that additional, usually commercially available pressure vessels are often installed.

The air spring is not only being used in trams and buses but also increasingly in the railway sector, as

- A good structure-borne sound insulation can be achieved,
- The entry and exit height can be kept constant and
- Simple, cradleless bogie designs are possible.

The disadvantage is the effort for the compressed air supply.

Figure 5.62 shows various forms of air spring bellows for rail vehicles. The half bellows is used in cradleless bogies for mainline vehicles. It can absorb all relative movements between the car body and the bogie. Belted bellows are suitable in tight spaces where a high

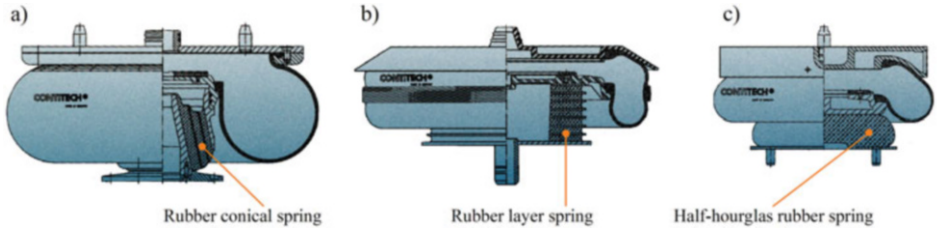

Fig. 5.62 Bellows with air springs. (**a**) Half-bellows with conical spring, (**b**) Belt bellows with laminated spring, (**c**) Guided rolling lobe bellows with Half-Hourglass rubber spring. (According to drawings: Contitech)

load-bearing capacity of the air spring is required, e.g. in mass transit vehicles and subway and commuter trains. Rolling lobe bellows with half hourglass rubber springs allow large spring deflections in the horizontal-transverse direction, but have a low installation height. The rubber springs shown in Fig. 5.62 take over the emergency suspension in case of failure of the air springs.

Examples of the use of air springs in rail vehicle construction are shown in Figs. 5.63 and 5.65. The cradleless motor bogie for the class 474 commuter train shown in Fig. 5.63 has air spring rolling bellows for the secondary suspension. Transverse and vertical movements are hydraulically damped.

Figure 5.64 shows the articulation of the wagon body for the bogie of class 474. The direction of view is in the direction of the longitudinal axis of the vehicle. The longitudinal and transverse forces are transmitted via a pivot between the bogie and the vehicle body. The air springs take over the longitudinal travel when the bogie is turned out about the vertical axis.

Figure 5.65 shows the curve-controlled single wheelset bogies ("KERF") of the commuter train for Copenhagen supplied by Alstom. The bogies are hydraulically controlled in a curve-radial manner depending on relative angles between the vehicle links in order to minimise wheel tyre and rail wear. Since the permissible wheelset loads for bogies on rail vehicles for passenger transport are significantly undercut, but the bogies themselves contribute significantly to the unladen weight of the vehicle, single wheelset bogies were used here. The wheelset load is 22 t with a fully loaded vehicle. The number of wheelsets in a train and the unladen weight could be reduced by the single wheelset bogies.

The bogies are air-suspended in the secondary stage by means of guided rolling bellows (see Fig. 5.62c). They allow the necessary turning and transverse movements. Rubber springs take over the emergency spring function in case of failure of the air springs. The primary suspension is provided by rubber roller springs arranged on both sides of the axle bearing housings.

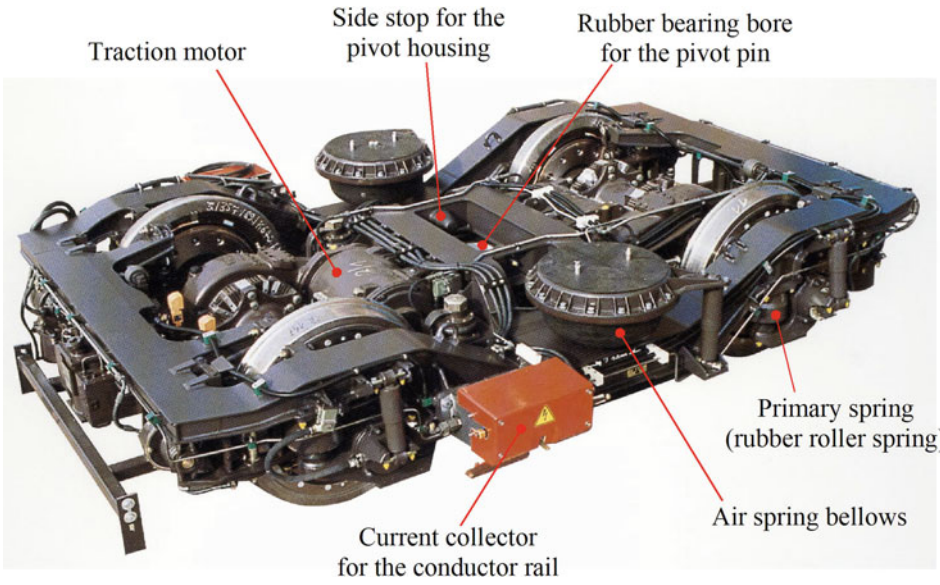

Fig. 5.63 Motor bogie of the electric commuter train railcar class 474 for Hamburg. (According to photo: Alstom)

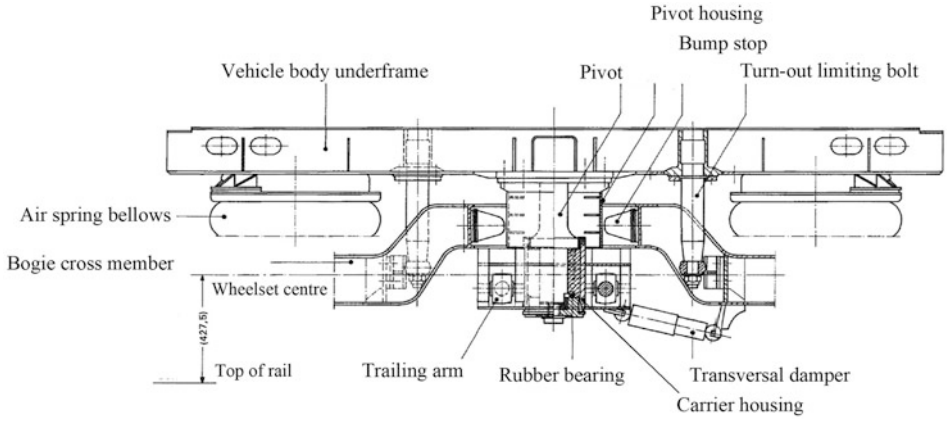

Fig. 5.64 Cross-section of the articulation of the class 474 motor bogie to the wagon body via pivot. (According to drawing: Alstom)

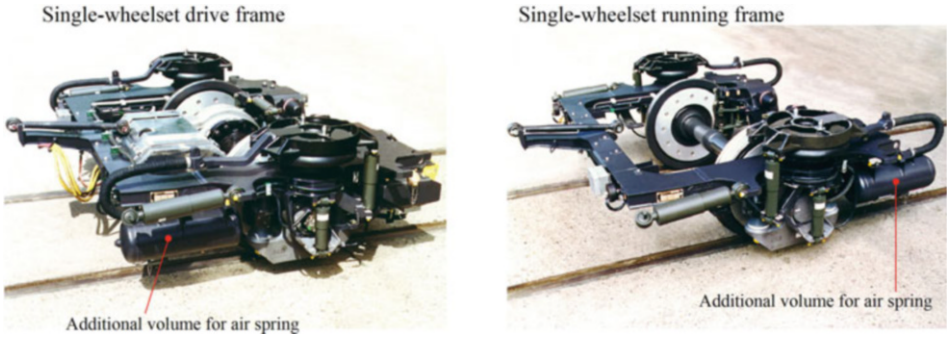

Fig. 5.65 Controlled single wheelset bogies for Copenhagen commuter train. (According to photos: Alstom)

Supporting Structures and Superstructures of Railway Vehicles

6

> Car bodies of railway vehicles must withstand the maximum load according to their operational requirements and achieve the required service life under normal operating conditions with a reasonable probability of survival [DIN EN 12663-1].[1]

Rail vehicles are exposed to high tensile and compressive forces due to driving in a train formation. Even under exceptional loads, e.g. overcrowding of local transport wagons, full operational capability must be maintained. The design service life is assumed to be 30 years; however, the vehicles usually reach a higher age.[2]

The supporting structures of rail vehicles have to meet numerous requirements:

- Absorption and transmission of tensile and compressive forces from railway operations,
- Absorption of loads from payloads – passengers, baggage, operating materials, goods,
- Absorption of aerodynamic loads from train encounters and tunnel entrances,
- Ensuring survival space for passengers in the event of an accident,
- High rigidity; avoidance of impermissible elastic deformations,
- Bending and torsional natural frequency outside the sensitivity range of humans,
- Sufficient structural damping for bending and torsional vibrations,
- Fatigue strength; at least operational strength,

[1] DIN e. V. (Ed.): Railway applications – Strength requirements for rail vehicle bodies.
Part 1: Locomotives and passenger vehicles (and alternative method for freight wagons). DIN EN 12663–1, Beuth Verlag, Berlin (2015).
Part 2: Freight wagons. DIN EN 12663–2, Beuth Verlag, Berlin (2010).

[2] For example, some of the DB class 139 and 140 electric freight locomotives still in use in 2016 are over 50 years old. Many of the passenger coaches currently used in DB Intercity traffic date from the 1950s (although they have been redesigned several times in the passenger compartment).

© The Author(s), under exclusive license to Springer Fachmedien Wiesbaden GmbH, part of Springer Nature 2022

J. Ihme, *Rail Vehicle Technology*,
https://doi.org/10.1007/978-3-658-36969-9_6

- Long service life, not susceptible to corrosion,
- Rational production, favourable costs for procurement and maintenance,
- Environmental compatibility in production, operation and disposal,
- Compliance with TSI[3] (for locomotives and railway passenger rolling stock; European Union Directive 2011/291/EU (2011)).

6.1 Strength Requirements for Rail Vehicle Bodies

The standard DIN EN 12663 defines strength requirements for rail vehicle bodies. Load assumptions for the design of locomotives and wagons can be taken from this. The strength requirements must be verified by calculations and tests. The various load cases can only be presented here in abbreviated form. It is urgently recommended that information is obtained from the applicable regulations, particularly as these have been subject to numerous amendments in the past.

Rail vehicles are divided into the following categories according to DIN EN 12663:

L:	Locomotives,
P-I:	E.g. passenger carriages,
P-II:	E.g. trainsets (DMU, EMU)
P-III:	E.g. Subway, metro vehicles and light railcars,
P-IV:	E.g. light subway vehicles and light rail vehicles,
P-V:	E.g. Tram vehicles,
F-I:	E.g. freight wagons that can be shunted without restriction,
F-II:	E.g. freight wagons that may not be shunted over a hump or by pushing off.

6.1.1 Static Load Assumptions

Figure 6.1 shows static compressive and tensile forces to be absorbed by the car bodies for these categories of vehicles.

Furthermore, vertical loads are defined as static load cases in DIN EN 12663–1. They depend on the vehicle reference masses, which are shown in the draft of DIN EN 15663.[4] This draft standard divides rail vehicles into three categories:

[3] TSI: *T*echnical *S*pecifications for *I*nteroperability, issued by the Commission of the EU. They are intended to ensure that rail vehicles can run as consistently and safely as possible on the railway lines of different countries.

[4] DIN e. V. (Ed.): Bahnanwendungen – Definition der Fahrzeugreferenzmassen. pr DIN EN 15663 (Entwurf), Beuth-Verlag, Berlin (2015).

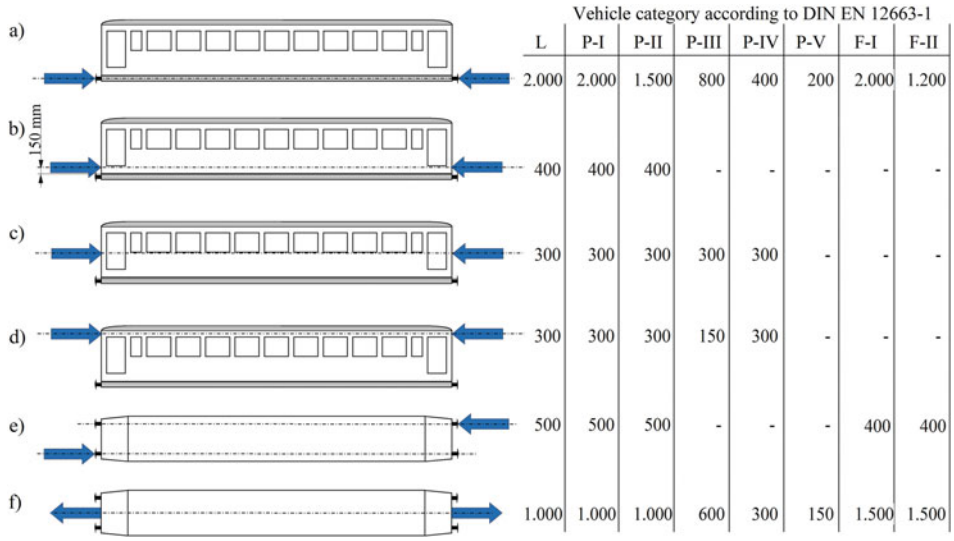

	Vehicle category according to DIN EN 12663-1							
L	P-I	P-II	P-III	P-IV	P-V	F-I	F-II
2.000	2.000	1.500	800	400	200	2.000	1.200
400	400	400	-	-	-	-	-
300	300	300	300	300	-	-	-
300	300	300	150	300	-	-	-
500	500	500	-	-	-	400	400
1.000	1.000	1.000	600	300	150	1.500	1.500

Fig. 6.1 Compressive and tensile forces for car bodies according to DIN EN 12663–1; data in kN

(1) High-speed and long-distance trains,
(2) Passenger rolling stock with the exception of high-speed and long-distance trains,
(3) Freight vehicles.

The normal load for (1) is 100% occupancy of the seats. Each passenger has a mass of 80 kg (incl. luggage). In luggage compartments, 300 kg/m^2 is to be expected. An additional 320 kg per m^2 (four persons per m^2) on standing areas in passenger compartments is considered as an exceptional load.

For category (2), the occupancy of the seats is also 100%. Each passenger has a mass of 70 kg. In addition, 280 kg per m^2 of standing area, 100 kg per m^2 in baggage areas and 300 kg/m^2 in baggage compartments shall be applied. An exceptional load of 500 kg/m^2 (seven persons) is calculated for standing-room areas instead of 280 kg/m^2 (four persons).

For goods vehicles according to cat. (3), the highest permissible load is always used.

The maximum masses from unladen mass (without bogies) and maximum payloads are multiplied by an impact factor of 1.3·g, Fig. 6.2a. According to pr DIN EN 15663, the unladen mass is the mass of the vehicle in the as-delivered condition including the interior fittings and the specified quantities of lubricants and liquid operating fluids, tools and emergency equipment.

For goods vehicles, the unladen mass and the permissible payload, also multiplied by 1.3·g, are taken as the vertical load. For both passenger vehicles and goods vehicles, the so-called lever load case must also be taken into account. This comes into question firstly in the workshop and secondly when a derailed rail vehicle is lifted by means of hydraulic cylinders and pushed back onto the track. The bogies are lifted at the same time (their mass

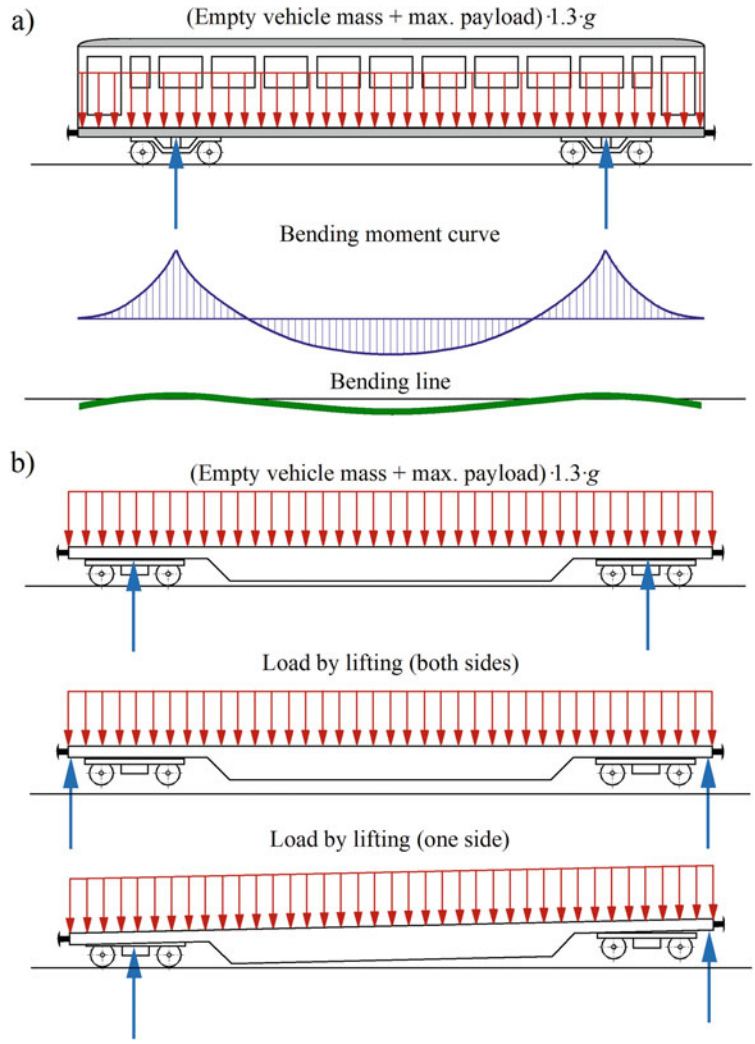

Fig. 6.2 Vertical static loads. (**a**) on passenger vehicles (with bending moment curve and bending line), and (**b**) on goods vehicles

must be taken into account). Passenger vehicles are lifted at defined lifting points when empty. The mass multiplied by an impact factor of $1.1 \cdot g$ must be applied in each case. It shall be possible to lift goods vehicles in the laden condition at defined lifting points. Lifting on one side and lifting on both sides shall be taken into account. The impact factors are assumed to be 1.0 (see also DIN EN 12663–2).

Furthermore, for static considerations, load cases from longitudinal loads (according to Fig. 6.1a, buffer pressure) and weight loads (empty mass + max. Payload without impact factor) must be combined.

For the attachment of equipment, the following loads from acceleration or deceleration shall be considered: x-direction up to $5 \cdot g$, y-direction up to $1 \cdot g$ and z-direction up to $3 \cdot g$.

For freight wagons, DIN EN 12663–2 provides for further load cases, e.g. for

- Crossing flaps on flat wagons,
- Side walls on high-sided wagons,
- Fastening of swap bodies and containers,
- Side doors (sliding doors) of closed wagons,
- Side stakes and end stakes.

The specifications for these load cases should be taken directly from the standard. Furthermore, impact tests (overrun tests) on a freight wagon with fixed brakes and a mass of 80 t are provided for in DIN EN 12663–2 for empty and loaded freight wagons.

6.1.2 Dynamic Load Assumptions

In addition to static load cases, DIN EN 12663–1 also provides for fatigue load cases. These result from cyclic loads that can cause fatigue damage:

- Changes in payload, especially for suburban and metro trains and some freight vehicles,
- Loading and unloading cycles, especially for rail vehicles with large load to empty weight ratios,
- Loads from the track, i.e. from the track unevenness mentioned in Sect. 5.2,
- Aerodynamic loads from train encounters, tunnel travel and crosswinds,[5]
- Driving and braking.

Loads from the track may be obtained from dynamic models (simulations), from measured data on routes to be travelled or similar routes, and from empirical data (accelerations, displacements, etc.). An equivalent dynamic load is given in DIN EN 12663–1 in the form of acceleration levels. For example, accelerations in the x-direction of $\pm$ $0.15 \cdot g$ up to $\pm 0.3 \cdot g$, in the y-direction of $\pm 0.15 \cdot g$ up to $\pm 0.2 \cdot g$ and in the z-direction of $(1.0 \pm 0.15) \cdot g$ up to $(1.0 \pm 0.3) \cdot g$ are given for passenger vehicles of categories P-I to P-V. The acceleration values are to occur 10^7 times.

For passenger vehicles of the categories P-IV and P-V (light subway, light rail and tram vehicles), load cases are specified in VDV[6]-Document 152 [8]. This guideline was revised

[5] See the series of standards DIN EN 14067: DIN e. V.. (Ed.): Railway applications – Aerodynamics. Part 1–6, Beuth Verlag, Berlin (2003–2011).

[6] VDV: Verband Deutscher Verkehrsbetriebe e. V. (Association of German Transport Companies); registered office: Cologne.

in 2016 [66] to extend it to the requirements of low-floor tram cars. For the latter, the limited secondary spring deflections apparently result in higher fatigue loads than specified in DIN EN 12663–1. The standard therefore recommends that the load assumptions for the fatigue loads be verified by means of track tests.

6.1.3 Static Tests

DIN EN 12663–1 stipulates static tests in a test rig for a series-conforming vehicle body for all newly designed vehicle body structures. The mathematical results are to be verified. The stresses are determined by means of strain gauges for the areas of the vehicle body structure that are identified as being subject to high stresses on the basis of the mathematical verifications. The following load cases are to be investigated:

- Compressive loads,
- Tensile loads,
- Vertical loads,
- Lifting loads,
- Unfavourable load combinations of compressive and vertical load.

Strains shall be measured at critical points, e.g. at the solebar, at top chords and at the corners of doors and window openings. Also to be determined is the bending deflection between the support points as well as any possible permanent deflection and any permanent elongation.

Dynamic tests and tests on the track are not generally provided for in DIN EN 12663–1. Fatigue tests should be carried out "*if the calculation includes critical uncertainties or if no data on structural performance exist for this detail*".

Figure 6.3 shows the preparation of a test on a tramcar in a test rig. The horizontal loads are applied by hydraulic cylinders. For the vertical loads from loading, weights are usually placed in the car body. The application of vertical loads by hydraulic cylinders is also possible on certain pressure stands and simplifies the test preparation and execution.

6.1.4 Crashworthy Design

> It is recognised that it is not practically possible to design the vehicle structure in such a way that the occupants are protected in all possible accident situations, nor to consider all possible vehicle combinations. It is therefore necessary to provide a certain level of protection corresponding to the usual collision risks [DIN EN 15227].[7]

[7] DIN e. V. (Ed.): Railway applications – Requirements for the collision safety of rail vehicle bodies. DIN EN 15227, Beuth Verlag, Berlin (2011).

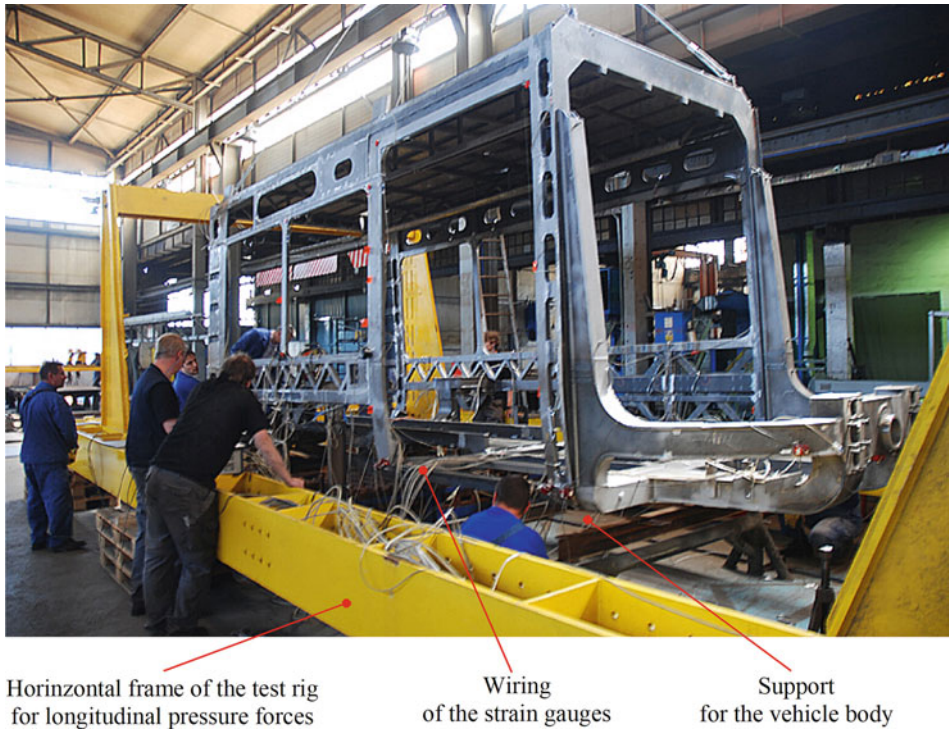

Fig. 6.3 Insertion of a tramcar body into a test rig for static tests. (According to photo: PJ-Messtechnik)

In rail transport, active safety measures are used to avoid collisions. The operational concept of railways basically already allows for a much higher level of safety than in road traffic. The crash-compatible design of rail vehicles therefore protects the vehicle occupants if the active safety measures fail. The consequences of the accident are reduced and sufficient survival space is ensured.

DIN EN 15227 defines collision safety design categories for rail vehicles:

- C-I: Rolling stock intended for operation on trans-European networks (TEN), international, national and regional lines (with level crossings), e.g. locomotives, passenger coaches and railcars,
- C-II: Urban vehicles exclusively for a closed network without interfaces with road transport, e.g. metro vehicles,
- C-III: Light local transport vehicles for urban and/or regional networks with shared track use of mainline railway lines and with interfaces to road transport, e.g. light multiple units and regional light rail vehicles,
- C-IV: Light local transport vehicles exclusively for urban networks with interfaces to road transport, e.g. tram vehicles.

Design collision scenarios are also defined for the above design categories:

(1) Frontal collision of two identical train units; for C-I at 36 km/h, for C-II and C-III at 25 km/h and for C-IV at 15 km/h,
(2) Collision with an 80 t freight wagon, for C-I at 36 km/h and for C-III at 25 km/h (C-II and C-IV are not affected),
(3) Collision at 110 km/h with a 15 t moving deformable obstacle (lorry at level crossing) for C-I and at 25 km/h for C-III (C-II is not concerned); for C-IV collision with 3 t rigid obstacle at 25 km/h.

The standard requires the following measures to protect vehicle occupants in the event of a collision:

- Reduction of the climbing risk (see below),
- Controlled absorption of collision energy,
- Maintaining survival space and structural integrity of areas occupied by people (see Fig. 6.4),
- Limiting delays (for scenarios (1) and (2) to $5 \cdot g$ and for scenario (3) to $7.5 \cdot g$),
- Reduction of the risk of derailment and limitation of the consequences of a collision with obstacles in the track (for this purpose, requirements for track clearers are defined in DIN EN 15227).

A climbing protection (see Fig. 6.6) prevents a vehicle body from sliding over the underframe of another vehicle body in the event of a collision with its longitudinally stiff underframe and thereby deforming or destroying the softer structure and thus the survival space above the solebar. According to DIN EN 15227, the corresponding verifications can be carried out by means of crash simulations (non-linear finite element calculations), since crash tests on real rail vehicles would involve very high costs. Dynamic tests must be carried out on individual components of the vehicle structure, e.g. on the special crash elements, in order to obtain data for the calibration of the calculation models.

The impact energy in the case of collisions is absorbed in railway vehicles according to a three-stage system, Fig. 6.5, where the deformation force is plotted over the deformation path. First, the impact energy is absorbed by elastic deformation via the buffers or via elastic elements in the linkage of the central buffer coupling (i). In the case of railway side buffers, the elastic deformation path is 105–150 mm, depending on the buffer design. Usually the characteristic curve of the buffer springs is kinked linear. These deformations are reversible. Further energy absorption then proceeds irreversibly in crash elements (ii) and (iii). In these areas, the impact energy is absorbed by plastic deformation. The aim here is not to reach the static body test force. After a corresponding impact, the body would remain undeformed; only the crash elements (and the cladding covering them) would have to be replaced.

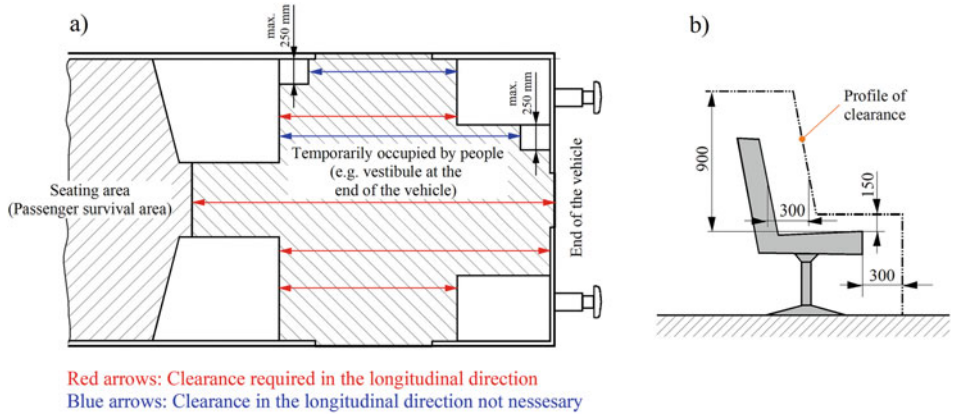

Fig. 6.4 Clearances in accordance with DIN EN 15227, (**a**) at compression zones, e.g. in the vestibule, (**b**) for the driver's seat

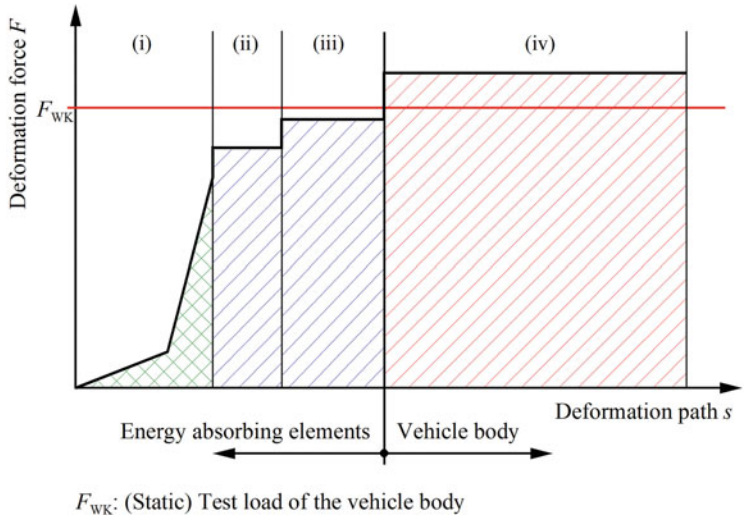

Fig. 6.5 Absorption of impact energy by elastic and plastic deformation. (According to DIN e. V. (Ed.): Longitudinal strength of vehicle bodies of light railcars. DIN 5560, Beuth Verlag, Berlin (2002))

This is illustrated by Fig. 6.6. It shows the crash elements on the vehicle body of an electric locomotive. The deformation path denoted by (i) is purely elastic and is applied by the buffer spring. The deformation path (ii) takes place through plastic deformation of the buffer housing. If the impact energy or the impact force remains limited, only the buffer housing needs to be replaced. If the impact force is even greater, the shock absorber also deforms by the deformation distance (iii). In this case, the buffer and shock absorber would

Fig. 6.6 Deformation elements on an electric locomotive. (According to photo: Uwe Beika, TU Berlin, https://www.schienenfzg.tu-berlin.de/menue/forschung/passive_sicherheit//, accessed on 10.02.2016)

have to be replaced. In any case, the structure of the vehicle body remains undamaged apart from reversible elastic deformations.

Several crash elements covering the collision scenarios according to DIN EN 15227 are installed under the front mask of an electric multiple unit, see Fig. 6.7: Crash elements for the impact on similar vehicles or the freight wagon with fixed brakes (scenarios (2) and (3), see above) are installed at the level of the side buffers of standard vehicles. The crash elements for the impact on the lorry according to scenario (3) are installed somewhat higher. One elastic and one further plastically deforming crash element has the automatic Scharfenberg coupling, which is still missing in Fig. 6.7. In the latter, for example, a tube is used into which a tapered mandrel is inserted in the event of a crash and expands it plastically. In the process, impact energy is converted into deformation energy. The crash elements in the form of a truncated pyramid in Fig. 6.7 absorb impact energy by plastic buckling, which is supported by the shape of the side surfaces of the elements.

The Voith company has developed a lightweight design concept for vehicle heads under the product name “Galea”. Here, crash elements and structural components made of steel have been replaced by corresponding elements made of glass-fiber-reinforced plastic and aluminum honeycomb structures to reduce weight. The mentioned crash standards are fulfilled. The outer head shape can be adapted to the design of the respective vehicle concept.

Fig. 6.7 "Crash head" of the Coradia Continental electric multiple unit. (According to photo: Alstom)

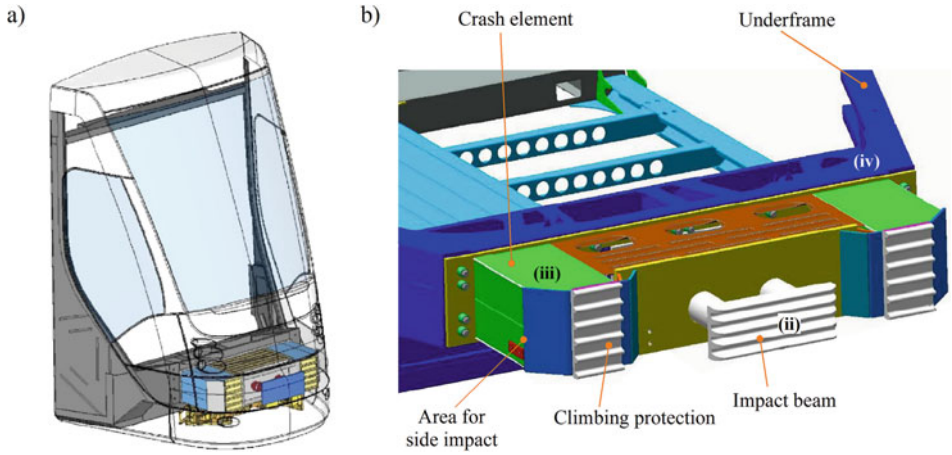

Fig. 6.8 Crash elements in the "Avenio" tramcar. (According to drawings: Siemens)

Figure 6.8 shows the structure of the crash modules for a tram vehicle. Since the vehicle is not intended for driving in a train formation, elastic deformation elements are missing. For impact speeds of up to 5 km/h, only the impact beam is deformed. The head fairing of the vehicle remains largely undamaged. For higher impact speeds up to 15 km/h (vehicle against identical vehicle, see above, collision scenario (1) for C-IV), the second stage of the crash absorber is deformed at a defined force level ((iii) according to Fig. 6.5). This causes

limited damage to the vehicle head, but the vehicle undercarriage remains protected. The area designated in Fig. 6.8 for side impact protection fulfils another requirement of DIN EN 15227, the impact of C-IV vehicles against a 45° obstacle. Figure 6.8 (as well as Fig. 6.7) also shows the climbing protection mentioned above: The horizontal "interlocking" of these elements is intended to prevent climbing by interlocking the collision partners.

6.2 Historical Development and Current Status of Railway Passenger Carriages

An overview of the construction methods of railway passenger vehicles used since the introduction of the railway until today is given in Fig. 6.9. The first railway vehicles at the beginning of the nineteenth century were built by wheelwrights in traditional wooden construction corresponding to the carriages and horse-drawn lorries known at that time. Both passenger and freight vehicle bodies were made of wood. Only fittings and connecting elements such as bolts and screws were made of steel. An example of a passenger carriage is shown in Fig. 6.10.

The underframe and body are made of wood. Even the buffers are made of wood; the leather "buffer pads" are padded with hay. Only the wheelset holders, wheel bearings, springs, wheelsets, and draw gear were made of metal. The car is built as a compartment car consisting of three compartments with six outer doors. This type of passenger coach was

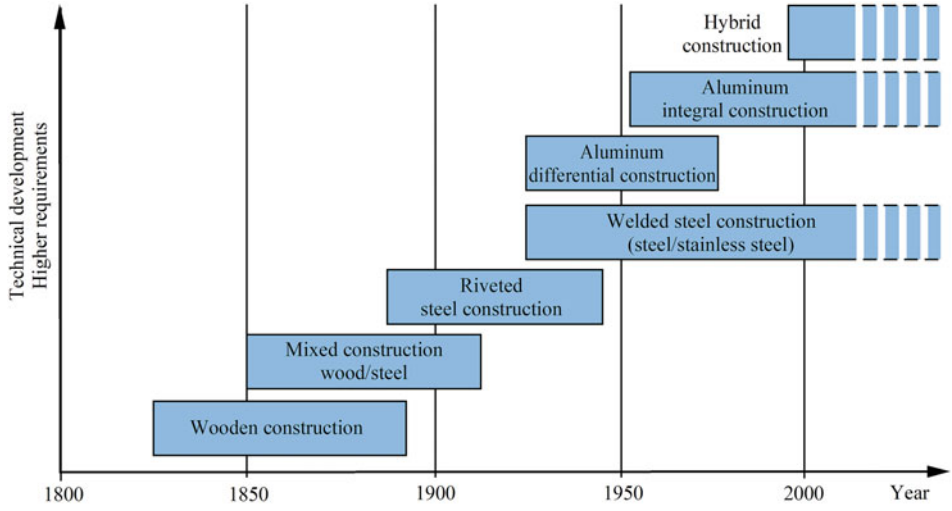

Fig. 6.9 Construction methods of rail vehicles. (After: Gerhard, T.; Meyer, G.; Altenburg, K.: Revolution or Evolution? – Observations on materials and construction methods for rail vehicles. Eisenbahntechn. Rundschau 51(2002)H. 1/2, p. 13–23)

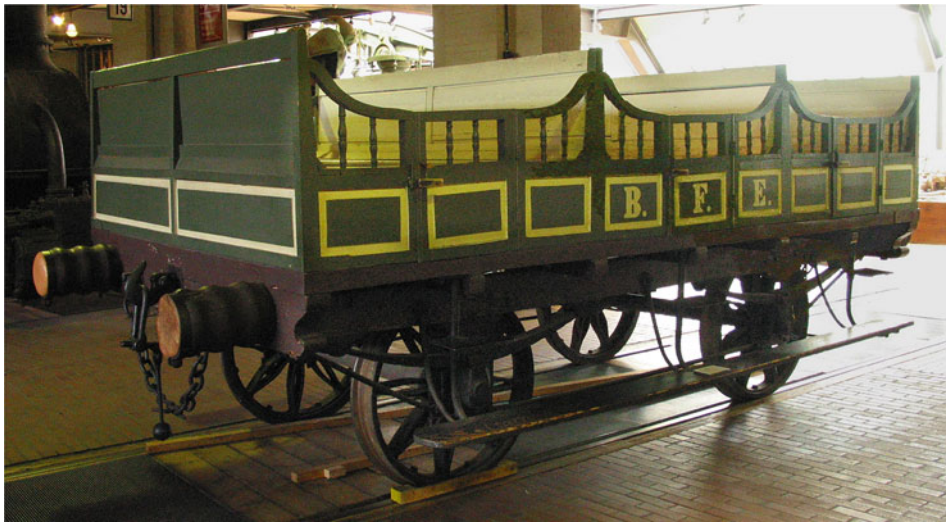

Fig. 6.10 Open wooden passenger carriage for the Breslau-Schweidnitz-Freiburg railway, 1842; original in the Museum of Transport and Technology in Berlin

developed from carriage superstructures placed one behind the other on an underframe. Only the first class coaches had closed superstructures. Second class coaches were roofed, but open above the parapet. The third class car shown has neither a roof nor windows.[8]

In accidents, wooden railway vehicles usually offered passengers no survival space because the superstructures were largely destroyed. Splintering wood led to serious injuries and the vehicles often caught fire. When, in the middle of the nineteenth century, the price of wood also rose due to high demand, the steel underframe with a wooden superstructure continued to prevail in railway carriages, Fig. 6.11. The outer sheeting of the sides and end walls was made of steel. In order to improve the connection between the wooden vehicle body and the underframe and to increase the rigidity of the body, diagonal tension bands made of flat steel were bolted to the outside of the vertical and horizontal squared lumber members of the walls, see Fig. 6.11. Since it was essentially the underframe that had to absorb the longitudinal forces and bending moments, it was reinforced with tension rods (see Fig. 6.11). Here, the bending tensile stresses on the underside of the subframe were reduced by tensile stresses in the rods.

[8] On the history of passenger carriages and freight car construction, see also: Ihme, J.: 150 years of railway passenger car construction in Germany. Eisenbahntechn. Rundschau 34(1985)H. 7/8, S. 589–594, and: Schwerin, G.: The freight wagon in Germany in historical view. Eisenbahntechn. Rundschau 34(1985)H. 7/8, S. 595–602.

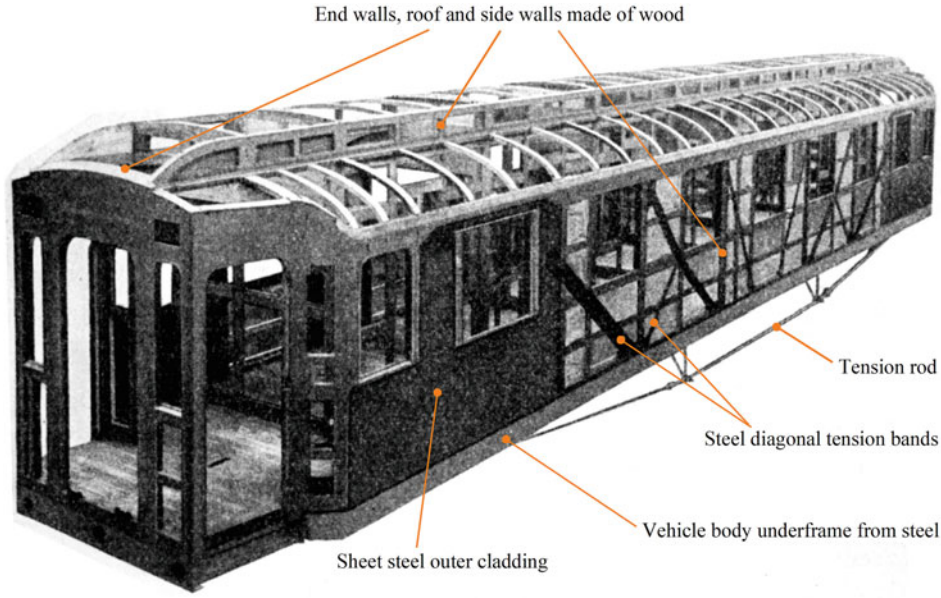

Fig. 6.11 Passenger coach in mixed wood/steel construction. (According to photo: LHB)

In accidents, the car bodies were often separated from the underframes by[9] overriding the buffers. The protection of the passengers was low in this case. Due to the functional separation of the underframe (load-bearing function) and the vehicle body (passenger accommodation), the vehicles had a relatively high mass.

Towards the end of the nineteenth century, the all-steel construction method therefore prevailed. As welding technology was not yet sufficiently developed, the wagon bodies were riveted, Fig. 6.12. Standard hot rolled sections were predominantly used, e.g. U-, T- and L- sections, but also special rail vehicle construction sections, e.g. Z-sections and sections folded from sheet metal. Except for the joining technique (rivets instead of welded joints), the car bodies already show many characteristics of today's steel car bodies. In particular, the first efforts towards lightweight construction can be seen, since in addition to the underframe, the side walls and roof also take on load-bearing functions. However, riveting requires an overlap of the components to be joined, so that the mass is generally higher than with butt welding.

[9] In the case of overriding of buffers, the underframes of the cars are pushed over each other, e.g. in the case of train collisions. Wooden car bodies were usually "shaved off" the underframe and destroyed.

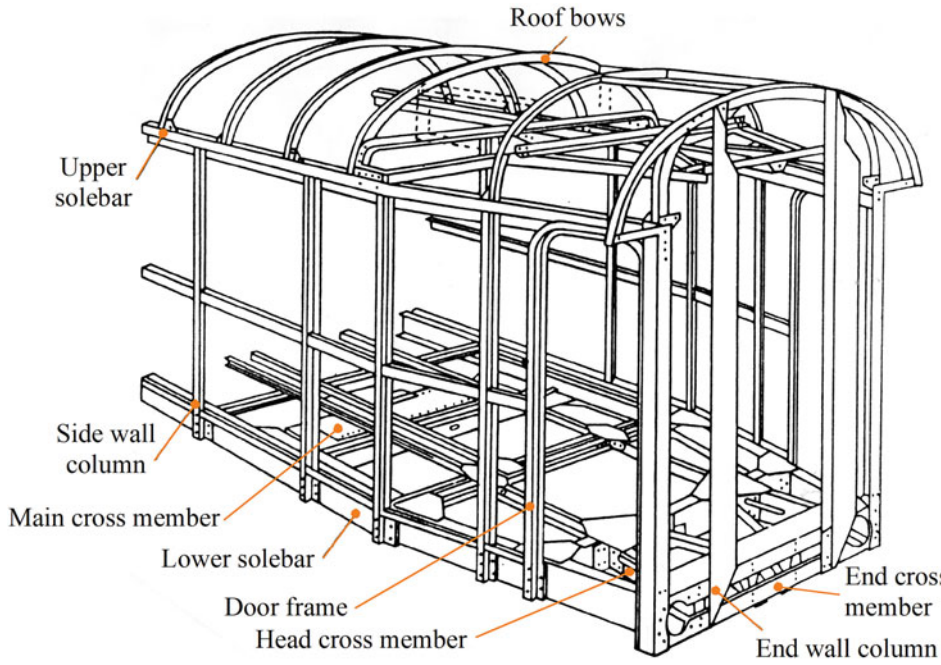

Fig. 6.12 Box frame of a passenger coach in riveted steel construction. (According to: [14])

The lower solebar[10] is usually a U-section. The head piece accommodates the traction and impact equipment (draw hook and buffer). The tensile and impact forces must be transmitted from the end cap to the solebars. For this reason, the headstock has a correspondingly strong design. It usually consists of the head cross member and a further cross member lying parallel behind it, which are connected by diagonal bars and reinforcing plates. The running gear is located on the main cross member, and in the case of bogie vehicles the pivot pin and the lateral slide members (see also Chap. 5). The main cross member is therefore also an assembly made up of several sections, stiffeners and cover plates. The side wall frame is a truss construction made of open sections to which the outer sheet is riveted. Closed (steel) sections (round, oval, rectangular tubes) are still less common as load-bearing components in rail vehicle construction because internal corrosion due to condensation water is difficult to control.[11]

A further development step in the thirties of the twentieth century was the self-supporting car body, which fulfilled the requirements for lowering the vehicle mass. At this time, butt welding had been developed ready for use. Figure 6.13 shows the body of a

[10] In the case of rail vehicles, this is referred to as the "solebar", while the corresponding component in trucks and truck trailers is called the "longitudinal member".

[11] In some cases, closed profiles are also used for today's vehicle bodies. However, measures must then be taken to prevent internal corrosion, e.g. by using stainless steels or cataphoretic dip painting.

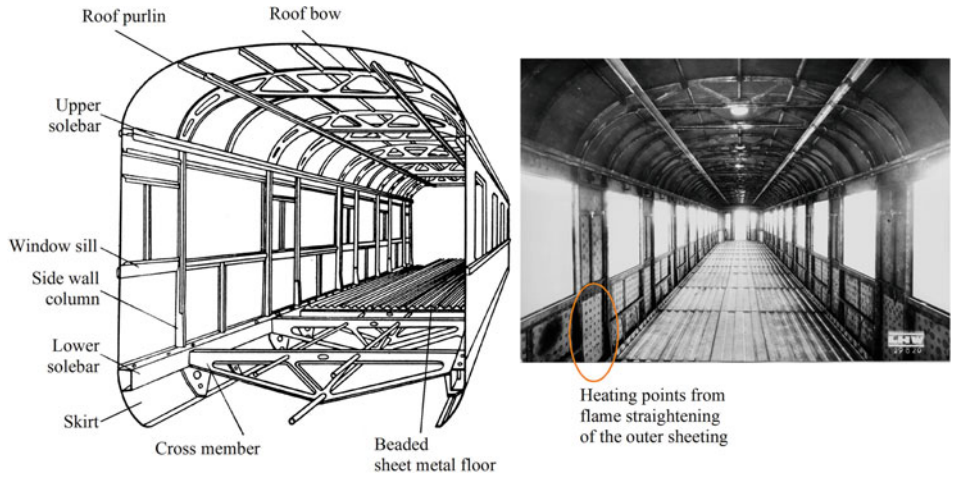

Fig. 6.13 Vehicle body skeleton of a passenger coach in self-supporting construction. (According to [14] and photo: LHB)

four-axle passenger coach from 1942. In addition to a reduction in vehicle mass (associated with a reduction in rolling, gradient and acceleration resistance; see Chap. 2), the coach bodies were fitted with lowered side skirts to reduce air resistance. Rolled sections are no longer used in the body frame, but folded sheet metal sections and lightweight extruded sections. The frame is stiffened by the outer sheet. The side walls and roof also support the frame. The base frame is lighter because it only has to bear lower loads [14].

The dots visible in the photo in Fig. 6.13 on the inside of the outer sheeting originate from flame straightening. The sheeting is welded to the side wall frame on the inside by short (step-)welds. Due to the associated heat input, the sidewall sheets bulge locally and the sidewall surface appears very uneven. With the help of the flame straightening process, a largely even surface of the sidewall can be achieved. In this process, the thermal expansion on one side of the sheet is impeded by means of e.g. clamping magnets, while from the other side the sheet is heated spot wise through a perforated mask by means of an oxy-acetylene flame until it reaches bright red heat. Due to the inherent stresses in the sheet metal, plastic compression of the material occurs in the area of the heat points, resulting in a tightening of the sheet metal after cooling.[12] This process requires a large number of working hours. In most cases, the wall surface must be additionally filled and sanded before painting in order to achieve an even outer skin even under the incidence of light, which is

[12] A detailed description of this process can be found in a bachelor thesis prepared at HAW Hamburg: Weidke, T.: Thermisches Richten im Schienenfahrzeugbau. Bachelor thesis HAW Hamburg (2012); retrieved on 12.01.2015 at: http://edoc.sub.uni-hamburg.de/haw/volltexte/2012/1726/pdf/Thermisches_Richten_im_SFbau.pdf/.

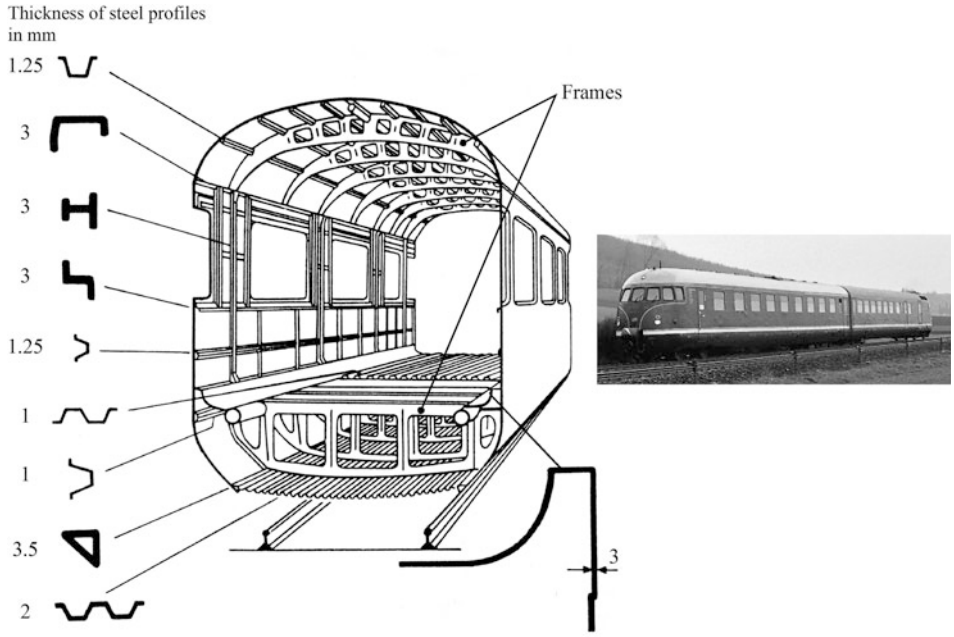

Fig. 6.14 Carbody of the diesel railcars class VT08.5/VT12.5 from 1952. (sketch *left* according to [59])

also associated with high costs. By using spot or laser welding when joining the sidewall structure to the cladding sheets, the buckling behaviour can be reduced.

The competition between motor cars and railroads required a reduction in train hauling costs as early as about 1930, i.e., a move away from labor-intensive steam locomotive operation, especially in light passenger service. High-power internal combustion engines were not yet available, so the solution was to develop lightweight (diesel-)railcars. Findings from the now highly developed lightweight construction of aircraft were transferred to rail vehicle construction. This resulted in lightweight, self-supporting car bodies in frame or tubular construction. Figure 6.14 shows an example of the body of a diesel railcar from 1952 (former DB class VT 08.5/VT 12.5).

The wagon body forms a closed tube with high compressive, bending and torsional stiffness. Typical of this design (see also Fig. 6.13) is the use of beaded plates in the floor and (see Fig. 6.14) also as the lower end of the floor pan. Beaded plates have a much higher bending, buckling and compressive stiffness than a plain plate. In some cases, corrugated sheets are also used for the side walls and roof of car bodies of this design. This makes it possible to avoid the flame straightening mentioned above. The floor pan, which is closed at the bottom, also ensures a lower noise level in the passenger compartment.

However, the self-supporting construction also has disadvantages: The manufacturing effort is high and it is hardly possible to prefabricate large sections (underframe, side walls,

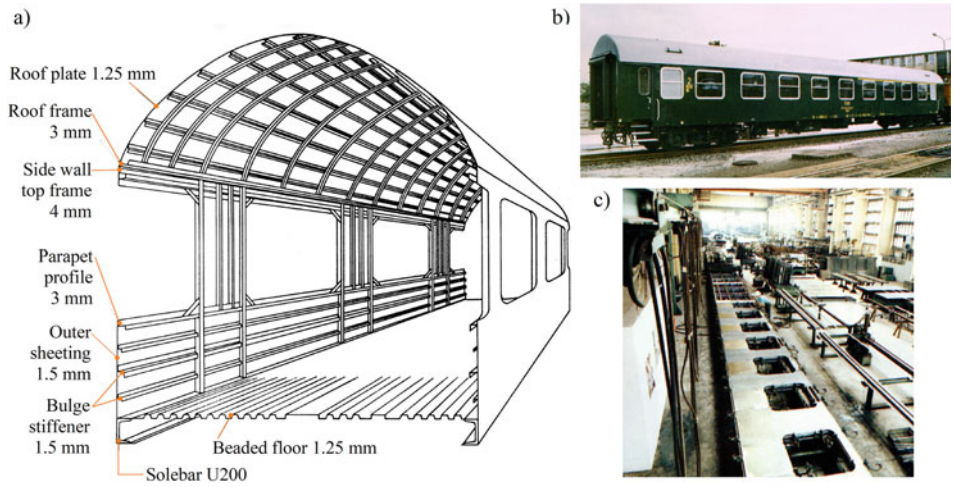

Fig. 6.15 (**a**) Sectional construction of a type Y passenger coach (according to [14]), (**b**) View of the vehicle, (**c**) Production of side walls on a cycle line in large-scale jigs. (Photos: DWA, Bautzen works)

roof). The closed floor pan makes it difficult to install and access underfloor units (e.g. engine/gearbox, heating, air conditioning, tank, waste water tank for toilets, etc.). The tube construction method was therefore not able to gain widespread acceptance, but remained limited to special applications, e.g. in railcar construction. For the reasons mentioned, the diesel railcar shown in Fig. 6.14, for example, had what is known as a machine bogie, i.e. the engine and hydraulic transmission were located in the drive bogie and not underfloor.

Figure 6.15 shows a passenger coach body in a steel construction suitable for production, in the so-called sectional construction method.[13] The large sub-frame, side walls, end walls and roof can be prefabricated and then welded to form the body in appropriate jigs. This allows rational production with partial automation of the welding work. The order throughput time can also be shortened by parallelizing the subassemblies and the vehicle body assembly. The sectional construction method is therefore used particularly in the series production of passenger trains and railcars.

Figure 6.16 shows the body of a two-part diesel-electric commuter railcar for the Altona-Kaltenkirchen-Neumünster (AKN) railway company. Each vehicle section has an underfloor diesel engine with a flange-mounted three-phase generator. The wheelsets of the

[13] Passenger cars were standardized by the International Union of Railways (UIC) at the beginning of the 1960s. The types X and Z are 26,400 mm long over buffers, the type Y 24,500 mm (UIC standard 567). Large series of the type Y cars were built by the GDR's rail vehicle industry for Eastern European railroads and the DR.

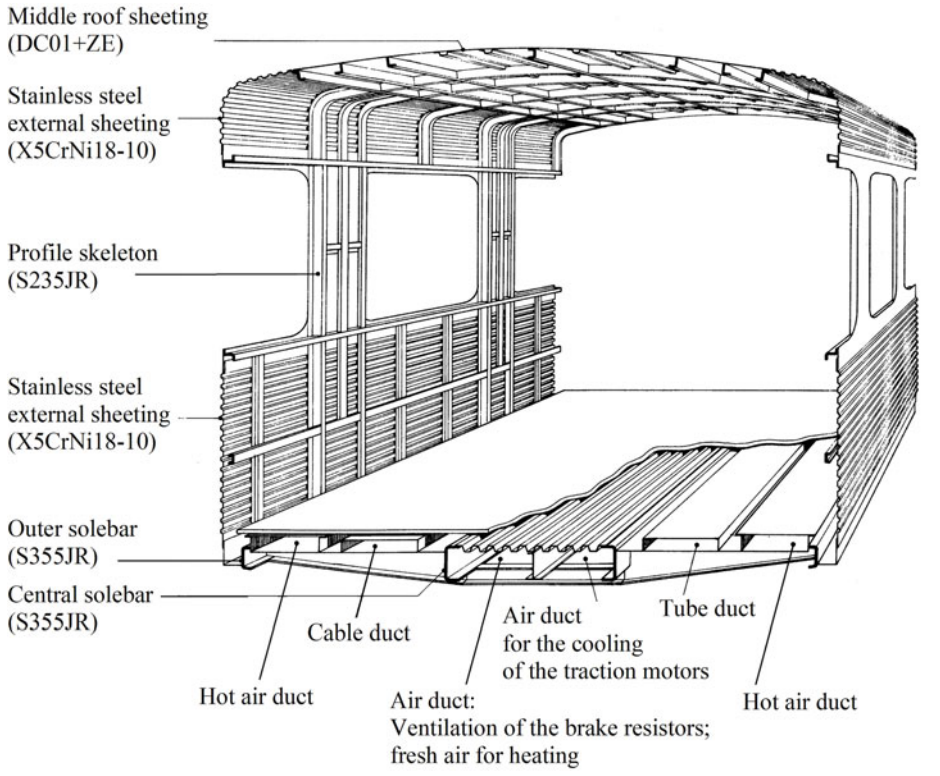

Fig. 6.16 Body of the diesel-electric double railcar VT2E; combined construction of structural steels S235JR and S355JR and stainless steel X5CrNi18-10. (Sketch *above* from: Haug, A.: Waggonbau als Stahlbau. Der Stahlbau 47(1978)H. 6, p. 161–169 and H. 7, p. 205–211)

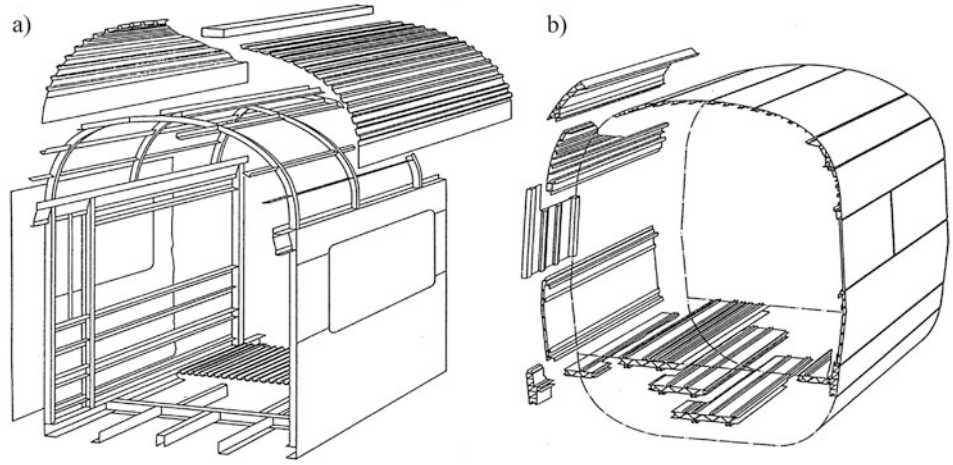

Fig. 6.17 Comparison of the differential design (**a**) with the integral design (**b**). (According to sketches: VAW Aluminium)

two outside bogies are each driven by a self-ventilated DC motor. The central JACOBS bogie is without drive (Bo′[2′]Bo′ wheel arrangement).

In this vehicle, stainless steel sheets were welded onto a body skeleton made of structural steels S235 and S355. In the area of the skirts and the window band, smooth plates were used, while the side walls between the skirts and the window sill are beaded as well as the roof edge trim. The beaded outer sheets are unpainted. Ducts for cables and tubes and air ducts are integrated in the underframe: The vehicles have electric traction motors, which decelerate the vehicle generatively via braking resistors during service braking from v_{max} up to the speed of 20 km/h. From 20 km/h until standstill, the mechanical disc brake kicks in. The air ducts are required for cooling the brake resistors and the traction motors. Warm air ducts are used to heat the passenger compartment. The vehicle has Scharfenberg-type central buffer couplings. This is why the central longitudinal girders have a strong design, because they essentially take on the tractive and compressive forces when driving in a train formation.

The examples shown in Figs. 6.12, 6.13, 6.14, 6.15 and 6.16 are steel constructions in which weight advantages were achieved by means of the moulded lightweight construction described. As early as the 1930s, individual car bodies for railcars were built from light metal. Initially, the steel construction method was imitated, i.e. simple profiles and sheet metal were used ("differential design"). The material aluminum, however, offers the possibility of producing complicated profile shapes by extrusion. This means that functions of the supporting structure can be combined in a few large profiles ("integral design"). Figure 6.17 shows a comparison of the two construction methods.

A transition from differential to integral construction in aluminum is represented by the EMU class 420 from 1969/1970,[14] Fig. 6.18. This car body was constructed from approx. 30 different extruded aluminium profiles. Many of these were still open profiles. Sheet metal was still used as plain and as beaded sheet metal. The joining effort was therefore high. For this three-car multiple unit, the two end cars were made of steel in the first series, and of aluminum construction with the same dimensions in later series. This allows a direct comparison of the body-in-white dimensions:

- Gross vehicle weight of the steel car: 11,000 kg, ratio of gross vehicle weight to unladen mass: 22.2%; vehicle mass/seat: 762 kg,
- Gross vehicle mass of the aluminum car: 6000 kg, ratio of gross vehicle mass to unladen mass: 13.5%; vehicle mass/seat: 683 kg.

In the case of rail vehicles, weight does play a role in rolling, gradient and acceleration resistance. As shown in Chap. 2, the rolling resistance is low overall and the gradient resistance is also not dominant due to the low gradients on main lines. The acceleration resistance, on the other hand, determines the power to be installed and the energy consumption for local and regional vehicles with short stop distances. Due to the simpler interior equipment of these vehicles compared to mainline vehicles, the proportion of unladen mass in the vehicle is also higher. Reductions in the unladen mass therefore have a strong effect on the vehicle mass and thus in particular on acceleration resistance and energy consumption. In addition, the reduction of wheelset loads has an influence on the maintenance costs of the track superstructure. This aspect is also important for mainline vehicles.

Today's integral construction method is based on the use of extruded aluminum (hollow-)profiles, which combine several functions: due to their cross-sectional areas and their second degree moments of area, they are able to absorb forces and moments. At the same time, they form the outer sheeting. By shaping them appropriately, they can be used to accommodate attachments. Figure 6.19 shows the structure of the base plate of an aluminium car body in integral design for a diesel railcar. The bottom plate consists of three different sections (i) to (iii), of which the centre section (i) is used once, sections (ii) and (iii) are used to the right of as shown, and additionally (not shown) in mirror image to the left of (i). The base plate is thus assembled from five extruded sections. Using portal welding machines, the five profiles are longitudinally welded along the length of the car body (approx. 25 m), first on the upper side. Then the bottom plate is turned over by crane and the longitudinal seams of the underside are produced in the supine position. For welding, the profiles can be pushed together by means of the locking lugs shown in Fig. 6.19 and thus virtually tacked. At the same time, these locking lugs serve to secure

[14] "Olympia-Triebzug", electric multiple unit for the Munich S-Bahn network established for the 1972 Olympics.

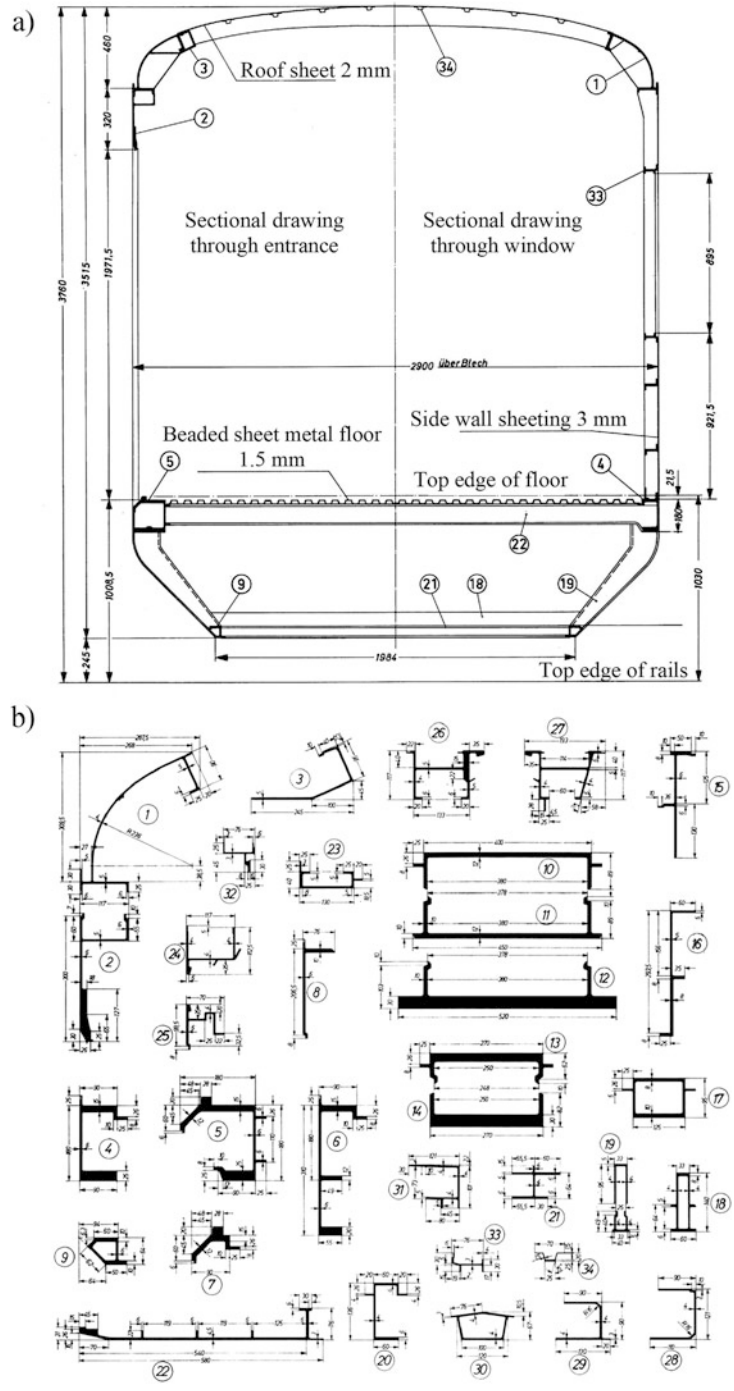

Fig. 6.18 (**a**) Cross-section of the vehicle body of the EMU class 420, (**b**) extruded profiles used; the circled numbers in **a** refer to the profiles in **b.** (According to: Bönisch, M.: Die Leichtbaukonstruktion des dreiteiligen elektrischen S-Bahn-Zuges ET 420/421. Leichtbau der Verkehrsfahrzeuge 16(1972) H. 5, pp. 175–186)

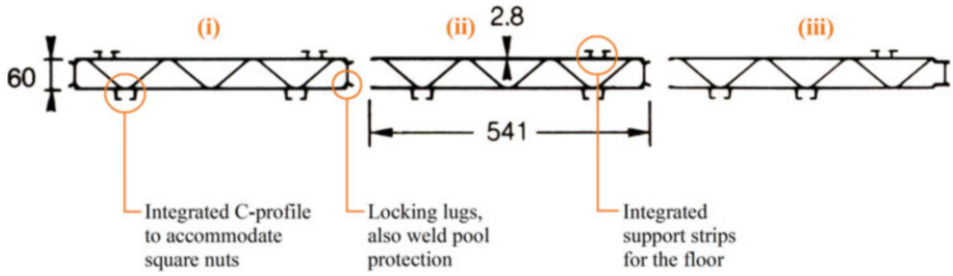

Fig. 6.19 Cross-section through extruded aluminum profiles for the floor plate of a diesel railcar. (According to sketch: VAW Aluminium)

the weld pool on the underside of the weld seams. The hollow chamber profiles have sufficient bending stiffness so that, for example, cross members can be dispensed with except in the area of the head pieces and the bogie connection.

The C-profiles integrated on the underside of the hollow chamber profiles are used to accommodate square nuts via which underfloor units such as the tank, air-conditioning system, electrical equipment, etc. can be attached. For the alignment of these aggregates, the square nuts are longitudinally adjustable in the C-rails. On the top side, the profiles have integrated support strips for the floor construction (thermal insulation, wood ply boards, etc.).

Extruded aluminum profiles can be produced up to approximately 30 m in length. The profile size is defined by a circumscribing circle with a diameter of up to 700 mm (tool diameter of the extrusion press). The integral construction method considerably reduces the labour hours required for welding compared to the differential construction method. The longitudinal seams can be produced largely automatically on portal welding machines as described above. However, some of the cost savings are eaten up by higher semi-finished product costs. Another disadvantage is that extruded profiles can only be produced with a constant cross-section. Cross-section parts that are not required over the entire length can therefore not be omitted or reduced in wall thickness.

Friction stir welding can also be used to join extruded profiles. In this process, the material in the weld joint is plasticized to just below the melting point by the applied friction energy with the aid of a wear-resistant, rotating tool. The longitudinal movement of the tool in the weld joint causes the material to flow together behind the tool. Advantages of the process are the welding without filler material, the lower heating and thus the lower workpiece distortion. A disadvantage is the high feed force required. The process is mainly suitable for seams lying in one plane.[15]

Figure 6.20 shows the structural design of the carriage body of a intermediate carriage from the ICE-1 in integral design. Ten different extruded profiles are sufficient for the

[15] See, for example: Kallee, S. W.; Davenport, J.; Nicholas, E. D.: Railway Rolling Stock Manufacturer Implement Friction Stir Welding. Welding Journal 81(2002)H. 10, pp. 47–50.

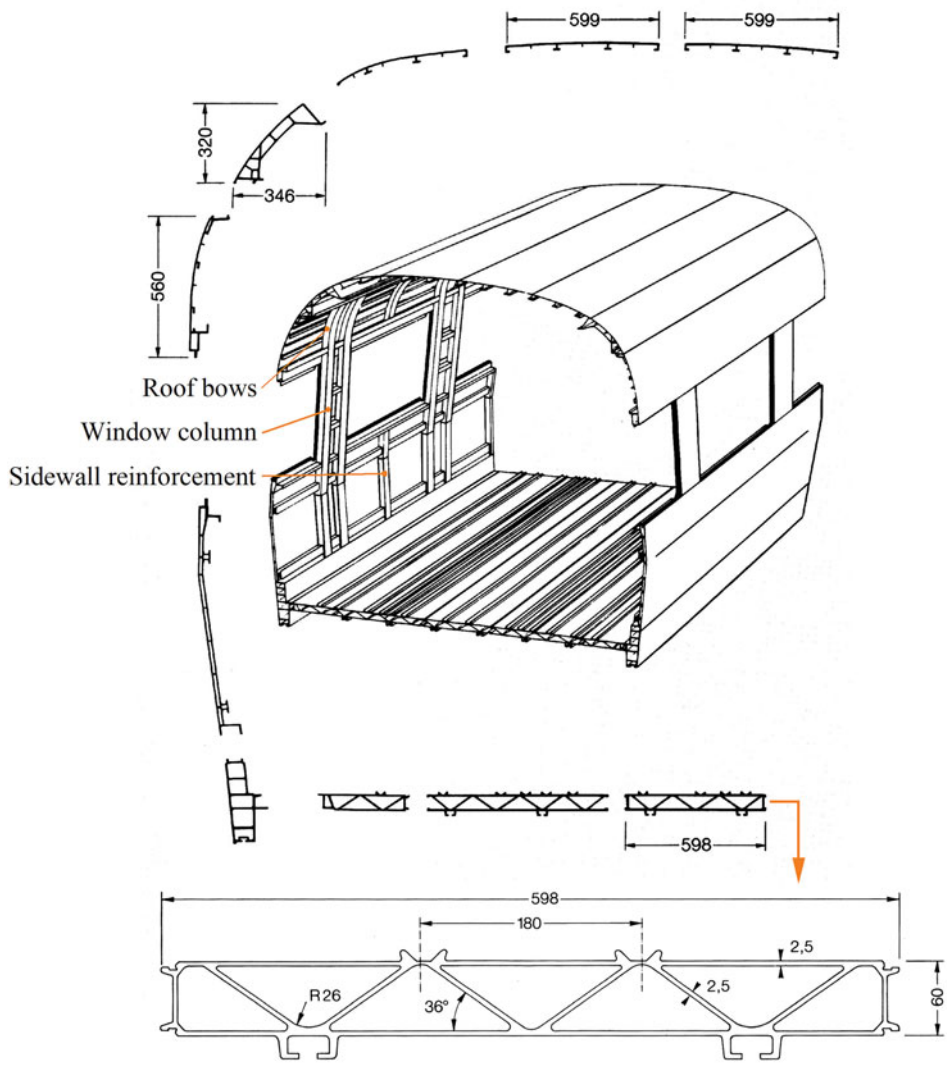

Fig. 6.20 Structural design of an ICE-1 intermediate carriage. (According to drawing: VAW Aluminium)

cross-section of the vehicle body. Except for the floor centre profile, the profiles are used twice (left and right arranged in mirror image). The roof bows, window stems and side wall reinforcements consist of further extruded profiles which are mechanically machined to fit before welding. The roof bows are additionally bent.

While the intermediate cars of the ICE-1 and 2 used both closed and open extruded profiles, the body of the ICE-T (a tilting train) is constructed entirely from closed profiles.

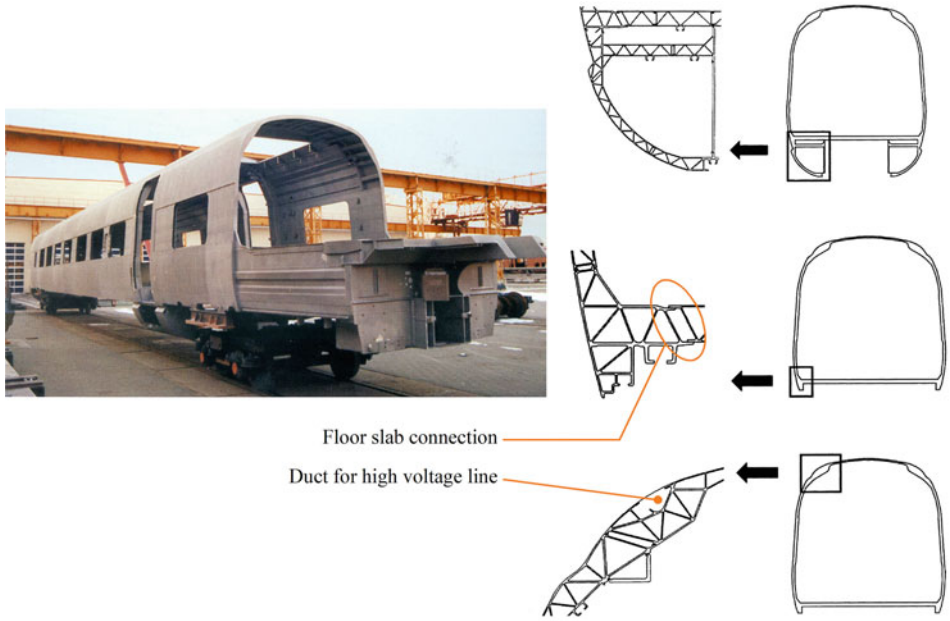

Fig. 6.21 View of the body shell of the ICE-T and sections through prominent points. (According to drawings: Bombardier)

Figure 6.21 shows a photo of the head car body shell as well as three cut-outs from the body shell – aprons below the entrances, longitudinal members and roof area. Since the ICE-T is a multiple unit, the traction equipment must be housed in the cars. Each of the ICE-T consists of head cars without drives, which accommodate the driver's cab, roof pantograph, and transformer. Additional intermediate cars are equipped with converters and two traction motors. The traction motors, which are suspended under the vehicle body, drive both wheelsets of a bogie via cardan shafts. Three cars – head car, converter car, and another intermediate car with two traction motors – form a basic module. The seven-car class 411 ICE-T consists of two basic modules supplemented by a drive-less intermediate car. The five-car class 415 ICE-T includes a basic module as well as another power converter and another end car.

To accommodate the transformers, converters, traction motors, etc., the space below the floor plate is used. As the electrical equipment is distributed among the vehicles, they are connected via a high-voltage line. This is laid in an integrated channel in the roof edge profile ("roof cove"). The head of the control car is a laminated part made of GRP and is glued to the car body. Deformation elements are added to the head piece shown in the photo in Fig. 6.21 to meet the crash standard.

Figure 6.22 shows the individual mass components for a complete second class ICE-2 intermediate carriage. The gross mass of an ICE-2 intermediate carriage is about 8300 kg. If the floor pan for accommodating various items of equipment is added (approx. 1000 kg),

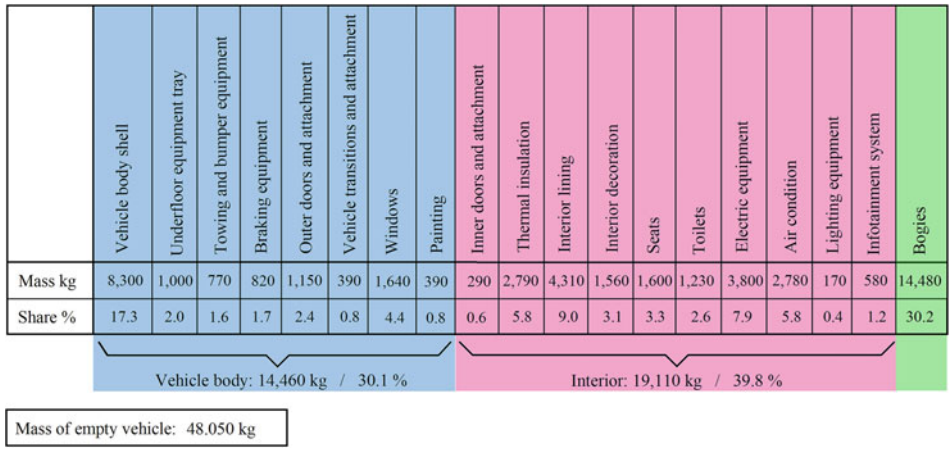

Fig. 6.22 Mass proportions of individual assemblies of a second class ICE-2 intermediate carriage (individual masses rounded to the nearest 10 kg)

the unladen mass accounts for just under 20% of the vehicle's unladen mass. The interior fittings contribute 19,110 kg to this vehicle, corresponding to almost 40%. The bogies, with a mass of around 15,000 kg, account for 30%. For a long-distance vehicle of a higher comfort level, the share of the body shell in the vehicle's unladen mass is therefore surprisingly low. A mass saving of 20% on the body shell, which could only be achieved with a great deal of design and manufacturing effort, would only result in a 4% reduction in the unladen mass. Efforts to reduce weight must therefore also be extended to exterior and interior components and bogies.

Finally, as shown in Fig. 6.9, the hybrid construction method (see Fig. 6.23) should be mentioned, which was developed from the 1990s onwards especially for light rail vehicles, e.g. light railcars and tram vehicles. Since welding of large assemblies usually requires complex jigs, measuring procedures and straightening work, hybrid construction uses joining techniques such as bolting, (blind-)riveting, setting of locking bolts and adhesive bonding instead. Figure 6.22 shows an example of the RegioSprinter,[16] a light diesel railcar for regional and local transport.

The RegioSprinter consists of two head sections, each with a drive wheelset, which are semi-mounted on a two-axle, non-driven centre section (axle arrangement A′[2′]A′). The two diesel engines are each located as underfloor engines (in Fig. 6.23a in the area of the green skirts) under the cabs. Between the boarding doors and the cabs are high-floor areas, between the doors across the centre section the vehicle is low-floor. The railcar of the

[16] For the Regiosprinter see also:
Hondius, H.: RVT from Duewag for the Dürener Kreisbahn. Der Stadtverkehr 40(1995)H. 2, pp. 10–13.

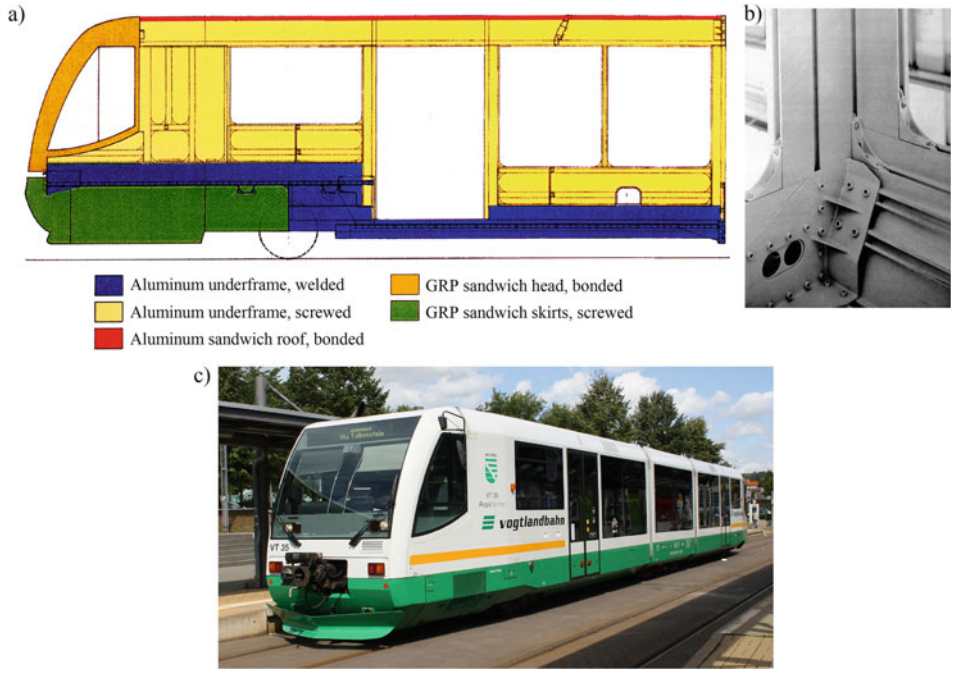

Fig. 6.23 Hybrid construction of the RegioSprinter. (**a**) Body structure, (**b**) Bolted connections between side wall and rear wall and window corners with cast nodes. (according to photos: Duewag) (**c**) Vehicle view

Vogtlandbahn shown in Fig. 6.23c also runs on a tram line in Zwickau and therefore also has flashing and brake lights in accordance with the German regulations for trams.

The car body is formed from a welded aluminum subframe onto which the side walls made of extruded aluminum profiles are screwed. Cast nodes serve as connecting pieces where profiles meet vertically (window corners; connection of side wall with rear wall). The roof as an aluminum sandwich plate is glued in place. The heads of the two end carriages made of laminated glass-fibre reinforced plastic (GRP) are also glued on. However, they do not assume any load-bearing function. The vehicle has a service mass[17] of 49,200 kg.

In the case of screwed and bonded joints, the amount of fixturing required is considerably less than for welding. Straightening work can also be largely dispensed with. In addition, only specially trained and certified skilled workers may be used for welding work. The vehicle heads made of GRP can be shaped in almost any way. This means, for example, that customer-specific designs of the vehicles of a (standard-)vehicle platform

[17] With 75% supplies and driver.

Fig. 6.24 (**a**) Low-floor centre section for a tramcar using the winding technique (Photo: André Knoerr, Geneva), (**b**) Door side and (**c**) Non-door side of a high-floor articulated tramcar with low-floor centre section using the winding technique

are possible at reasonable expense. After accidents,[18] damaged vehicle heads can be replaced relatively easily. The hybrid design therefore has a certain significance for light mainline vehicles for local and regional transport and for tram vehicles.

From 1995 onwards, over a period of several years, car body structures were manufactured from glass-fibre reinforced plastic using the winding technique. This applied in particular to low-floor centre sections retrofitted to older high-floor articulated tramcars, Fig. 6.24. The winding technique uses a rotating mandrel in the shape and internal dimensions of the structure, around which the fibre layers are wound and impregnated with resin. An inner and an outer GFRP face layer, each 5 mm thick, are wrapped around a core of 40 mm thick polymethacrylimide (PMI) rigid foam sheets. In addition, GRP ring spans are included in the structure. The low-floor center sections have two single-wheel single-axle bogies. The passenger capacity of the center section on the three-car vehicle is approximately one-third. The middle section has a share of approx. 25% in the service mass of the three-part conversion vehicle with approx. 7300 kg (total mass 29,800 kg). However,

[18] Unfortunately, collisions with road vehicles cannot be completely avoided in the case of vehicles for branch lines and in the case of tramcars and light rail vehicles.

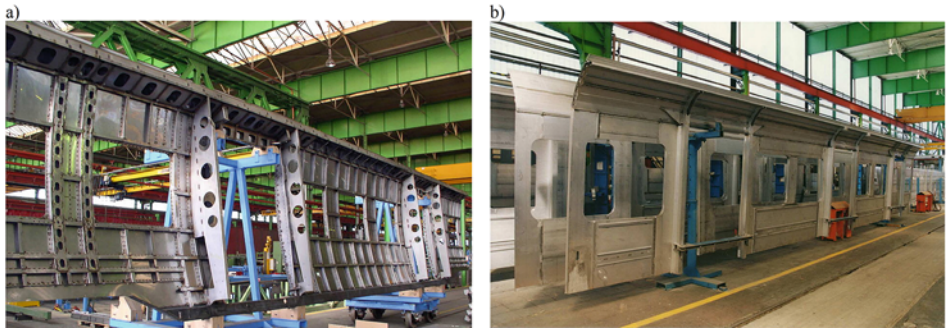

Fig. 6.25 Side walls of multiple units in steel construction (differential construction) (**a**) and in extruded aluminum construction (integral construction) (**b**). (Photos: Alstom)

the production of wound car bodies was discontinued a few years ago by the two previous manufacturers.

At the railway trade fair "Innotrans" 2018, the Chinese company CRRC presented a train of the type "New Generation Metros". The vehicles have car bodies made of carbon fiber composite. Together with other measures, this is said to have achieved a weight reduction of 13%.

In Fig. 6.25, the differential and integral construction methods are once again compared on the basis of the side walls of two multiple units. Figure 6.25a shows a cambered side wall of an electric multiple unit for Sweden. Due to the larger loading gauge there, the vehicles can be designed wider in the area of the pool of seated passengers, which improves the seating comfort or allows five instead of four seats in a row or wider central aisles. It can be seen that the window pillars and the door pillars have cut-outs to reduce weight, as does the upper longitudinal beam. Since sheet metal parts are usually cut by laser at high cutting speeds,[19] this involves only slightly longer cutting times. Smaller cut-outs can also be punched out with punching-nibbling machines with short production times. The cover plate is connected to the side wall frame from the rear by laser welding without filler material. The welding robot creates short zigzag seams. Due to the lower heat input, the necessary straightening work is considerably reduced.

In comparison, the side wall of a DB class 423 electric commuter train shown in Fig. 6.25b is much simpler and made up of fewer parts. Here, the advantages of the integral construction method in extruded aluminum profiles become apparent.

That both integral and differential construction methods are currently used side by side is shown by the last two examples. For example, the body shell of the "Railjet" vehicles of

[19] Depending on the sheet thickness and the laser power, the cutting speed for sheet steel is approximately between 1 and 20 m/min.

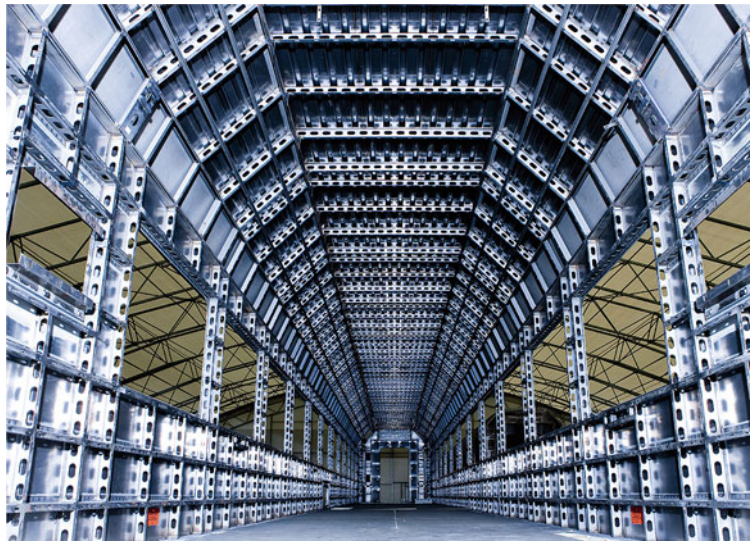

Fig. 6.26 Body of an ÖBB Railjet car made of steel. (Photo: Siemens)

the Austrian Federal Railways (ÖBB), Fig. 6.26, was built using the steel differential construction method. ÖBB relies on locomotive-hauled trains with control cars for high-speed traffic with $v_{max} = 230$ km/h. The passenger vehicles of the Railjet are steel constructions. As can be seen in Fig. 6.26, it is a differential construction of open profiles. Almost all the sections in the side walls and roof were cut out to save weight. Beaded sheet metal was used for the roof.

The base frame consists of rolled and edged profiles. A beaded sheet closes the underframe on the underside. In Fig. 6.26, the floor made of laminated wood has already been installed. Weight data for the individual vehicles are missing; only for the unit consisting of seven wagons an empty mass of 330 t is given. This means that a vehicle would have an unladen mass of approx. 47 t and would thus be within the range of an ICE-1/2 intermediate carriage with aluminum body, with comparable interior equipment but lower maximum speed. The manufacturer particularly points out the complete recyclability of the steel body.[20]

The double-deck carriages for the electric multiple unit "KISS", on the other hand, are built in aluminum integral construction, Fig. 6.27. The view into the body shell in Fig. 6.27a clearly shows the structure of the wagon body without ribs. This is particularly advantageous for double-deck wagons in terms of headroom, as the wagon height is limited by the loading gauge. As the vehicle is a multiple unit, space is needed to accommodate the electrical equipment (transformer, converter, current collector, etc.). For this reason, the

[20] ÖBB/Siemens (ed.): Railjet – Technical Brief Description. Vienna (2008); accessed on 21.01.2016 at: http://www.bahnzauber-europa.at/Railjet%20Folder.pdf/.

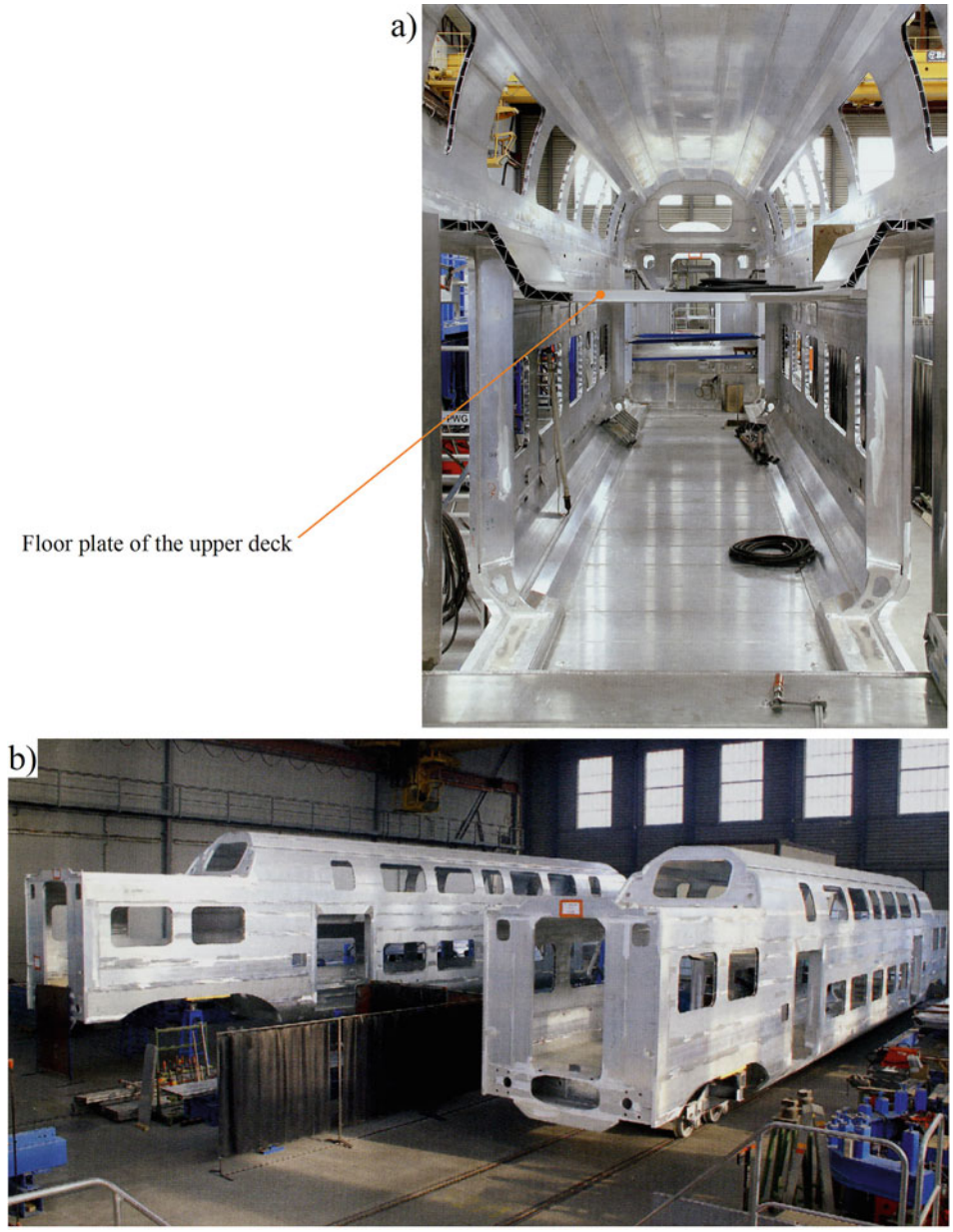

Fig. 6.27 Shells of the KISS double-deck electric multiple unit; (**a**) view into the body shell, (**b**) body-in-white. (Photos: Stadler Rail)

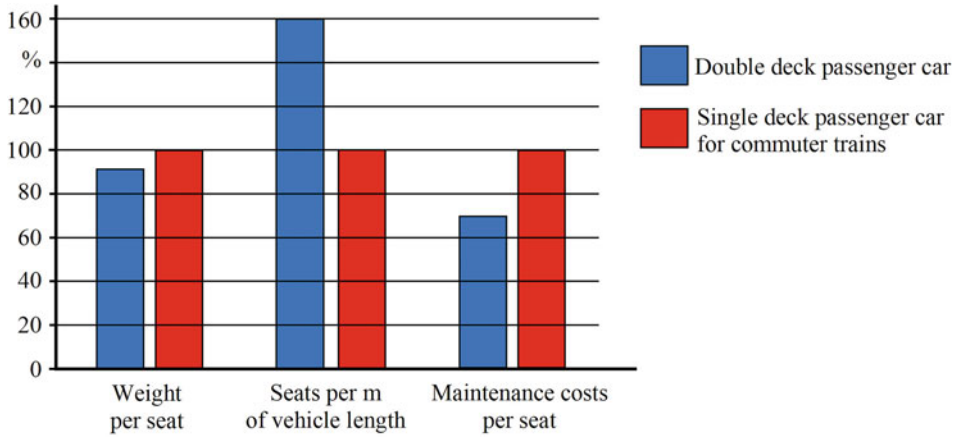

Fig. 6.28 Comparison of important characteristics of double-deck carriages with single-deck local transport carriages. (According to: Zeevenhoven, N.: Doppelstockwagen für den Einsatz im Eisenbahnverkehr. ZEV Glas. Ann. 114(1990)H. 1/2, pp. 15–23)

roof of the upper floor is not extended to the ends of the carriages. The electrical equipment is housed above the ends of the carriages.

A major advantage of the double-deck carriage (Fig. 6.28) is its larger capacity. This means that more seats can be offered than with single-deck vehicles, even with limited platform lengths. The maintenance costs per seat are lower for double-deck coaches because, for example, there are fewer running gears requiring maintenance for a given number of seats. The empty mass per seat is approx. 10% lower in double-deck coaches than in single-deck local transport coaches (e.g. 370–410 kg per seat with comparable equipment).

Figure 6.29 shows the material properties of the materials commonly used in rail vehicle construction. Load-bearing structures made of GRP and CFRP (carbon fibre-reinforced plastic) are, as shown, rare in series-produced vehicles (highlighted in grey in Fig. 6.29). The disadvantage of GRP and CFRP components is that they cannot be recycled in any meaningful way. They are usually shredded and used as filler or incinerated.

The fields highlighted in green indicate the most favourable material properties in each case. The two structural steels S235 and S335 are characterised by a high modulus of elasticity,[21] low thermal expansion and favourable procurement costs, whereby there are no cost differences for the two structural steels in some cases. Structural steels have good weldability. However, appropriate coatings are necessary for corrosion protection. The latter can be omitted with stainless steel. Stainless steels have high tensile strengths and

[21] The modulus of elasticity is decisive for the stiffness of a component, i.e. a high modulus of elasticity together with the cross-sectional area or the second-degree moment of area ensures low elastic deformations.

	Structural steel S235	Structural steel S355	Stainless steel X2CrNiN18-7	Aluminum ENAW-AlSi1Mg	GRP unidirectional	CFRP unidirectional
Density [kg/dm³]	7.85	7.85	7.9	2.7	2.6	1.8
Modulus of elasticity [kN/mm²]	210	210	200	70	40	115
Tensile strength [N/mm²]	360	470	650-850	180-250	800-1,200	1,000-1,500
Elongation at break [%]	26	22	40	8	4	1.2
Thermal expansion [10^{-6}/K]	12	12	16	24	5	0.12
Procurement costs [€/kg]	0.5-1.1*)	0.6-1.2*)	3-4*)	5.5-7**)	(4-6)	(40-60)

*) Sheet materials
**) Extruded profiles

Fig. 6.29 Comparison of material properties. (According to: Dr.-Ing. G. Köhler, lecture notes, University of Hanover)

high elongation at break. The procurement costs for semi-finished products are approx. three to five times higher than for structural steel. Steel is the material with the best recyclability.

Aluminum or aluminum alloys have only one third of the specific mass of steel. However, due to the modulus of elasticity, which is lower by a factor of 3, larger component cross-sections must be provided when designing for stiffness compared to steel, so that part of this weight advantage is lost. The procurement costs for aluminium extrusions are significantly higher than for sheet steel. For the repair of accident damage, for example, certain extruded profiles may have to be kept in stock, as subsequent reordering of vehicle-specific profiles can be associated with high costs and long delivery times.

It is therefore necessary to weigh up which construction method leads to lower manufacturing costs overall. In any case, it is worthwhile for the operator of rail vehicles to consider the life cycle costs. These also include the costs for traction energy, maintenance, servicing and disposal.

6.3 Metro, Light Rail and Tram Vehicles

The development in railway passenger carriages and railcars can also be seen in the vehicles for urban transport. With the advent of the tramway from 1881, development began with steel underframes and wooden car bodies, and continued with riveted to welded steel car bodies. Experiments with aluminum as a material and with tubular construction in aluminum and steel took place in the 1950s. While the steel differential design

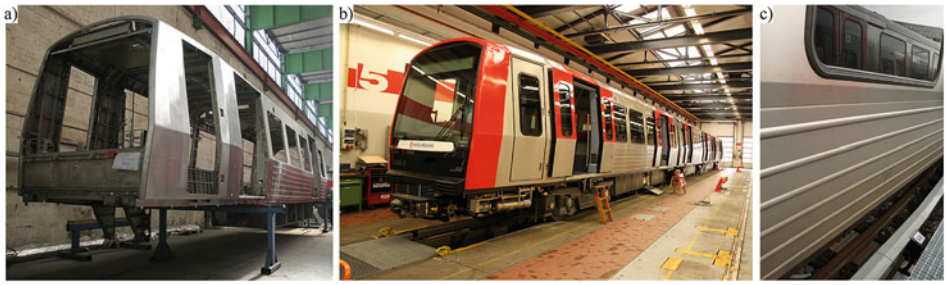

Fig. 6.30 Subway multiple unit class DT5 for Hamburg. (**a**) Body shell (photo: Alstom), (**b**) Multiple unit, (**c**) Side wall

predominated until the turn of the millennium, there were also applications of the extruded aluminum design. For the last 30 years or so, hybrid construction has been used in addition to steel construction for light rail and tram vehicles. As already shown, the plastic winding technology was only an episode of about 10 years.

Due to the strength requirements of DIN EN 12663-1, vehicles for urban mass transit can be built more lightweight than mainline vehicles. If, for example, there is no mixed traffic with other vehicles on the routes of urban railways, the urban rail vehicles are to be assigned to category P-III. Subway and light rail vehicles fall into category P-IV, tram vehicles into category P-V. In principle, the orderer or the operator determines the vehicle category in the specification [57].

The new DT 5 multiple-unit subway train for Hamburg (delivery years 2010 to probably 2019), Fig. 6.30, has a stainless steel outer skin and therefore no paint. Since Hamburg's loading gauge is relatively small, the train was given a side wall with a longitudinal fold at the level of the roll moment pole. The body is narrower at the top and bottom, as this is where crossways occur when the vehicle rolls. The pelvis, i.e. the widest point for seated passengers, is at the height of the fold. The greatest width of the car body here results in good seating comfort. The entire metro network has elevated platforms, so that the electrical equipment can be completely accommodated in boxes below the floor. Steps are not required. Power is supplied by a side conductor rail. Figure 6.30b shows the three-car multiple unit. It has a driving bogie under each of the end cars. The middle car, on which the end cars are mounted, runs on two bogies, each with one non-driven and one driven wheelset (axle arrangement Bo′(1A′ A1′)Bo′). The GRP end car heads are glued to the car body structure. The stainless steel sidewall is beaded below the longitudinal crease (Fig. 6.30a and c), smooth above. The corrugations were introduced by means of explosive forming.

There are high-floor and low-floor light rail vehicles. The city of Hannover currently only uses high-floor vehicles, of which older series are still equipped with folding steps for serving stops at street level. The extension and retraction of the folding steps requires longer stop times and makes it more difficult for people with limited mobility to get on and off. Since it is planned to convert all stops to elevated platforms, the latest type, the light rail

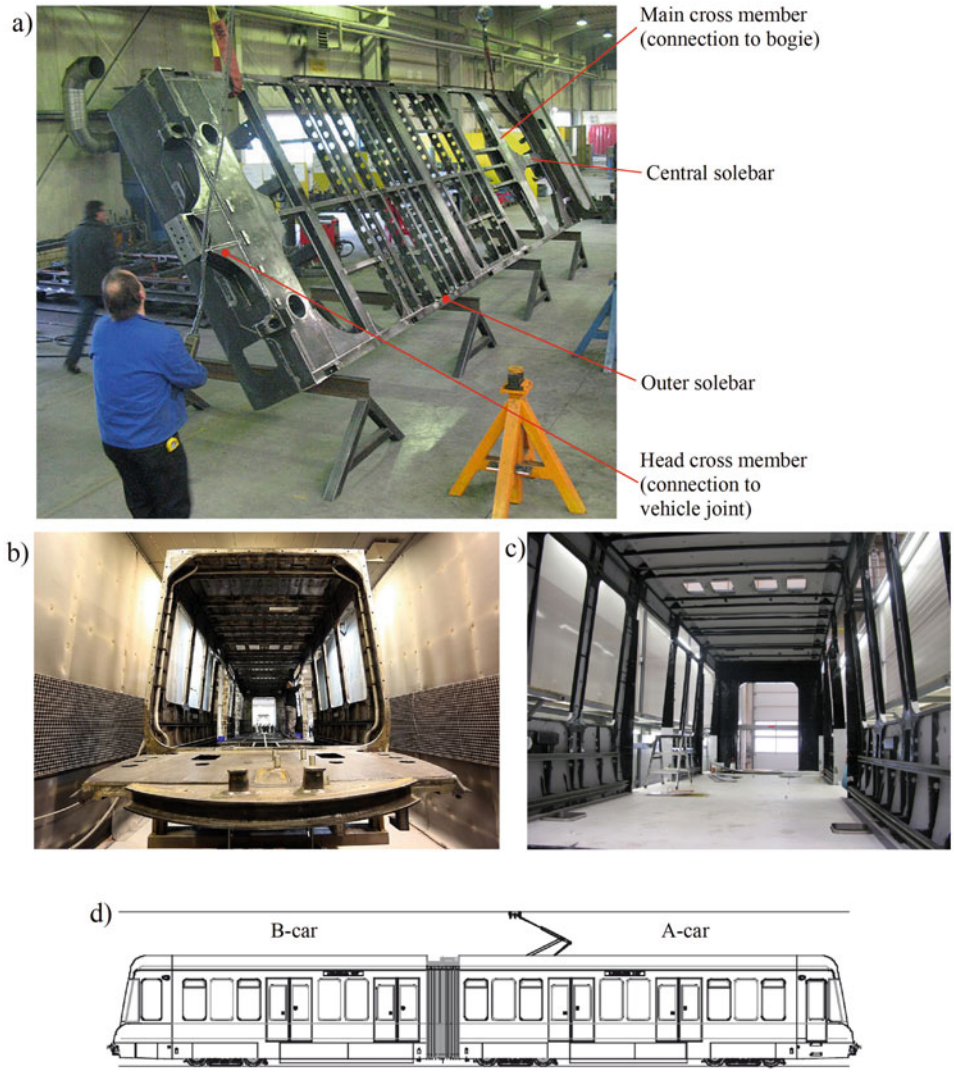

Fig. 6.31 Body of the Hanover light rail vehicle class 3000. (**a**) Underframe B-car, (**b**) Body shell A-car, (**c**) with floor and insulation (photos: Üstra), (**d**) Sketch of the vehicle. (Sketch: HeiterBlick)

vehicle class 3000, is designed as a pure high-floor vehicle (see Fig. 1.3 in Chap. 1). Shell car bodies of this type of vehicle and an outline sketch are shown in Fig. 6.31. The vehicle with the axle arrangement (Bo′2′)Bo′ consists of a front part (A-car) on a drive and a running bogie. A trailing section (B-car) with a drive bogie is mounted on the front vehicle (Fig. 6.31d). The car bodies are of steel differential construction. The underframe of the B-car with the articulated side in the foreground can be seen in Fig. 6.31a. Figure 6.31b shows the articulated end of the A-car body shell. Due to the load assumptions to be applied

for the vehicle category P-IV (longitudinal force 400 kN), the underframe and the body shell are designed to be much lighter than those of railway vehicles. The tensile and impact forces from the Scharfenberg centre buffer coupler are transmitted (Fig. 6.31a) from the rear end to the centre solebar and on to the main transverse member and from there via the outside and the then weaker designed centre solebar to the head transverse member at the vehicle joint.

Accidents with motor vehicles are not uncommon with light rail and tram vehicles operating in road space. Therefore, special attention must be paid here to the protection of passengers and the vehicle driver. On the other hand, inexpensive and quick repair options are useful. Both can be ensured by easily replaceable crash elements and crash-safe survival compartments (see Sect. 6.1.4). If possible, front and side panels should consist of several parts so that only really damaged parts need to be replaced.

Figure 6.32 shows the tramcar "Tramino" for Braunschweiger Verkehrs-GmbH. This is a four-part articulated vehicle in 100% low-floor design. On the one hand, there is therefore little construction space available for the underframe and, on the other hand, essential parts of the electrical equipment have to be accommodated on the roof. For this reason, the side walls are particularly strong and perform important load-bearing functions. The car bodies are made of steel in differential construction.

In Fig. 6.32a, the floor assembly is in the (yellow) welding jig. The prefabricated assemblies of the floor assembly are clamped in the jig and can then be tack welded and subsequently welded. The welding jigs are rotatable about the longitudinal axis so that the welders can weld[22] all the major seams in what is known as the tub position. Figure 6.32b shows parts of the side wall in the associated (green) welding jig. The top of the side wall is at the bottom, so that the welder does not have to weld the seams that are at the top in the normal position overhead, but can create them in the tub position. In Fig. 6.32c, the shell can still be seen without the outer sheeting. The side walls are braced like trusses below and above the window cutouts. The roof plate is still missing. In order to be able to carry the roof plate with the boxes for the electrical equipment, the roof edge profiles of the side wall are particularly strong. The finished vehicle is shown in Fig. 6.32d. The pleasing vehicle head is a GRP component glued onto the steel structure. The shock absorbing members below the front lights can easily be replaced including their fairings.

The four-part low-floor tramcar "Avenio" for Munich (photo see Fig. 5.53 in Chap. 5) has a welded carbody framework including the roof made of steel, Fig. 6.33a. The four modules of the vehicle are largely identical in construction. Only the GRP front and rear masks are different. The steel body of the vehicle receives a coating of cataphoretic dip-paint as corrosion protection. The body shell is clad on the outside with painted aluminum sheets by means of elastic thick-film bonding, Fig. 6.33b. This eliminates the need for body filler. Because many of the same parts are used in each module, the stocking

[22] Tub position: This allows the welder to work horizontally. The seam is in a horizontal plane, the cover layer is on top (see DIN EN ISO 6947).

Fig. 6.32 Four-part articulated tramcar "Tramino". (**a**) underframe and (**b**) side wall in welding jigs, (**c**) body shell (according to photos: Solaris), (**d**) vehicle in service

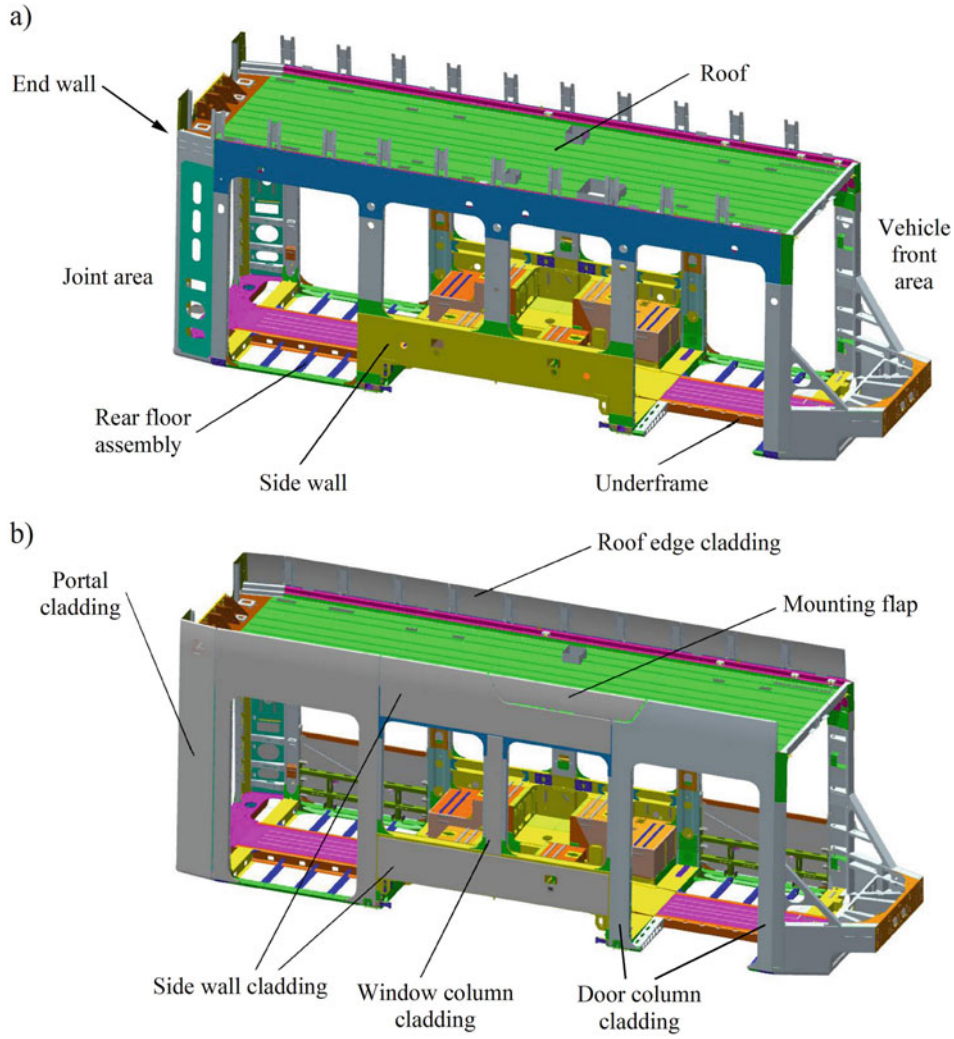

Fig. 6.33 Body of the Avenio tramcar for Munich. (**a**) Body shell, (**b**) clad body shell. (According to images: Siemens)

of spare parts for repairs is simplified. The self-supporting front mask made of GRP is glued to the body shell. It does not contribute to the strength of the body shell. Since the vehicle is low-floor over its entire length, the electrical equipment has to be accommodated on the roof. The public transport authorities in Munich have ordered the vehicle in two-, three- and four-part versions. The four-part version is already in service.

6.4 Locomotives

Locomotives are by design "traction engines" which are intended to develop high tractive and braking forces and to transmit them to the attached train via the traction and impact device. Although in train operation the whole train is braked via the continuous brake, if, for example, an electric locomotive carries out steady-state braking by means of resistor or regenerative braking, the entire braking force must be transmitted via the locomotive buffers. Based on Fig. 3.17 (Tractive force/braking force characteristics of the Class 151 electric locomotive), in double traction, for example, a tractive force of about 600 kN and a braking force of 400 kN can be transmitted in real terms between the locomotive and the wagons via the towing hook and the buffers. This requires a correspondingly strong design of the locomotive body or the locomotive frame, as these forces occur dynamically during operation. The static longitudinal forces from the load assumptions of DIN EN 12663-1 with a tractive force of 1000 kN and a compressive force of 2000 kN also apply to the design (see Fig. 6.1).

Figure 6.34 shows the structure of a diesel-electric shunting and mainline locomotive. As already shown in Chap. 3, shunting locomotives have a central driver's cab because of the frequent change of direction. All power units are housed in front and rear superstructures. This type of locomotive usually uses a bridge frame on which the superstructures are mounted as modules. The fuel tank is usually located below the central driver's cab under the frame and has a volume of approx. 2000–4000 L, depending on the

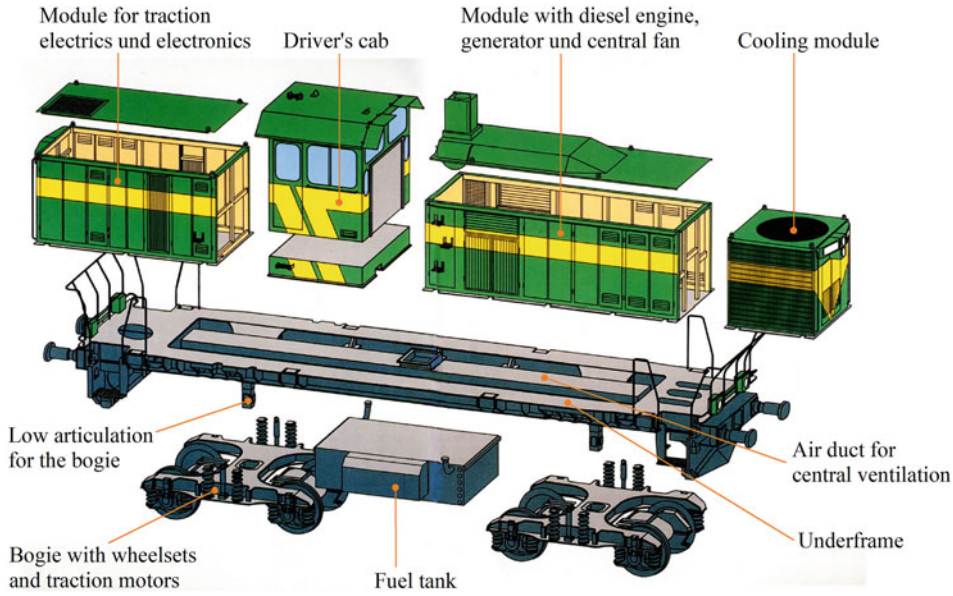

Fig. 6.34 Structure of a diesel-electric shunting and mainline locomotive. (According to drawing: Krauss-Maffei)

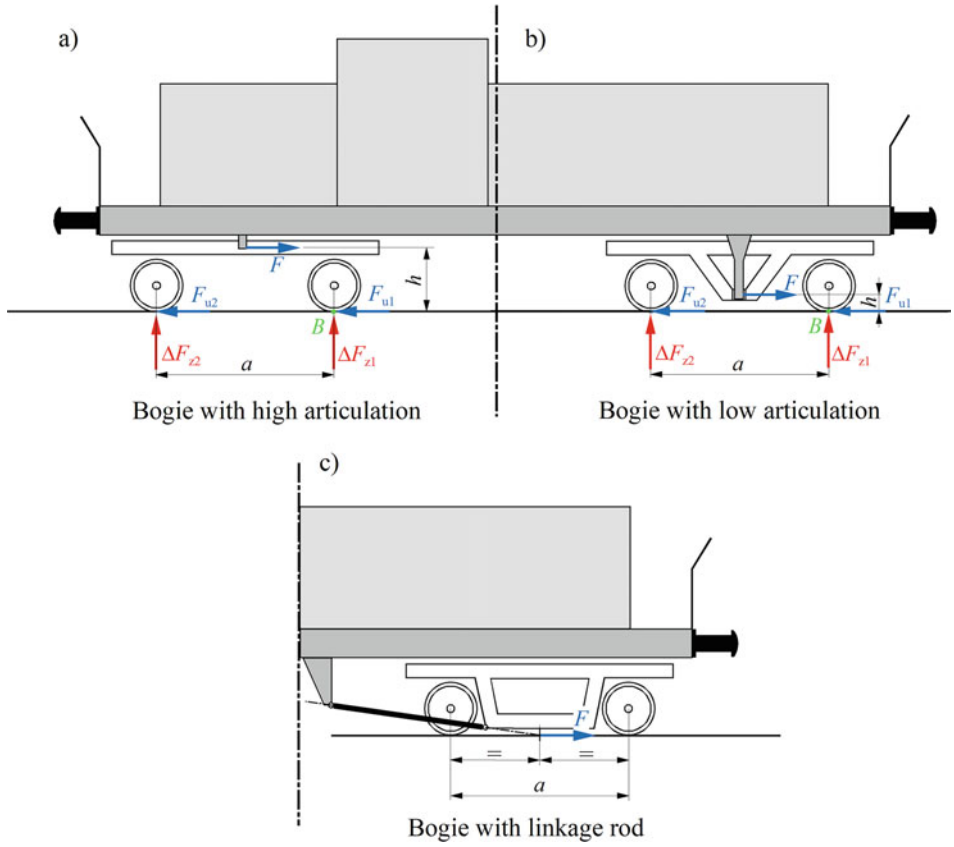

Fig. 6.35 (**a**) High linkage and (**b**) low linkage of locomotive bogies, (**c**) linkage rod

engine power and the intended use. In order to keep the axle load changes during starting and braking as low as possible, the low articulation of the bogies is preferred for locomotives. The point of power transmission between the bogie frame and the locomotive frame is as low as possible above the upper edge of the rail (see Fig. 6.35).

Let us first consider the high linkage in Fig. 6.35a: The horizontal force F between the locomotive frame and the bogie solebar is introduced at the height h above the top of the rail. This results in differences in the wheelset load at the front and rear wheelsets of the bogie, ΔF_1 and ΔF_2 respectively. We form the moment equilibrium around point B:

$$\Delta F_{z2} \cdot a + F \cdot h = 0 \rightarrow \Delta F_{z2} = -F\frac{h}{a} \qquad \text{(Wheel relief)}. \tag{6.1}$$

Also, assuming that the load on the pivots does not change due to the buffer force (which is not quite true in reality due to the buffer height and because the locomotive's center of gravity is high):

$$\Delta F_{z1} + \Delta F_{z2} = 0 \rightarrow \Delta F_{z1} = -\Delta F_{z2} \rightarrow \Delta F_{z1} = F\frac{h}{a} \qquad \text{(Wheel load)}. \qquad (6.2)$$

These would be the conditions during braking. When applying drive forces, the front wheelset in the bogie is relieved of load and the rear wheelset is loaded. The front wheelset could have a too high circumferential force with separate-axle drive and spin ("skid"). In order to keep the wheel relief as small as possible, the height h of the pivot point must be as small as possible and the wheelset distance a as large as possible. There are limits to the latter because of the curved run and the space conditions under the locomotive – hence the low linkage with small h. Another possibility to minimise the wheelset load differences is a link rod between the locomotive frame and the bogie frame as shown in Fig. 6.35c to transmit the traction and braking forces. If possible, the extension of the link rod centreline should meet the centre of the wheelset stand at the level of the top of the rail. For reasons of space, however, the use of a link rod is not always possible.

The low linkage of the locomotive in Fig. 6.34 has at the same time the function of a pivot, whereby the secondary springs of the bogie take over the transverse and outward turning movements of the bogie by means of flexicoil action. The bridge frame, which accommodates all the locomotive's assemblies and superstructures, consists of two outer solebars connected by the head and the main crossmember. The low linkages are welded to the main cross member. Between the two solebars is an air duct for routing air to the electric traction motors and the power electronics. Doors and flaps on the superstructures are used for maintenance; the superstructures can be lifted off the locomotive frame by means of a crane for larger repairs or unit replacement.

Figure 6.36 shows the underframe of a power car for the ICE-1. While the intermediate carriages are of integral aluminum construction, the vehicle bodies of the power cars are steel constructions of differential design. The side walls, which are still missing in Fig. 6.36, also perform a load-bearing function. The underframe is in the supine position, i.e. with the underside facing upwards. The bogies of the power car are connected to the locomotive body via link rods. The "towers" provided for holding the joints of the link rods are welded onto strong cross members of the underframe. This is where the propulsion and braking forces of the power car are transmitted from the bogies to the undercarriage.

Another example of the underframe and the vehicle body of an electric locomotive is shown in Fig. 6.37. This is the locomotive type "Taurus" from Siemens, which is used by various state and private railways. The underframe in the supine position, Fig. 6.37a, shows the two pivots for the low linkage of the bogies. In the centre of the head cross member can be seen the bolt-on area for the installation of the draw hook cartridge. The towing hook is longitudinally spring-mounted in the towing hook cartridge. The cartridge can be exchanged for a central buffer coupling.[23]

[23] The European railroads planned the conversion of the rolling stock to an automatic center buffer coupler for Easter 1976. However, this date was postponed indefinitely at the time because of the high costs involved. Nevertheless, the underframes of locomotives and cars are still being designed in such

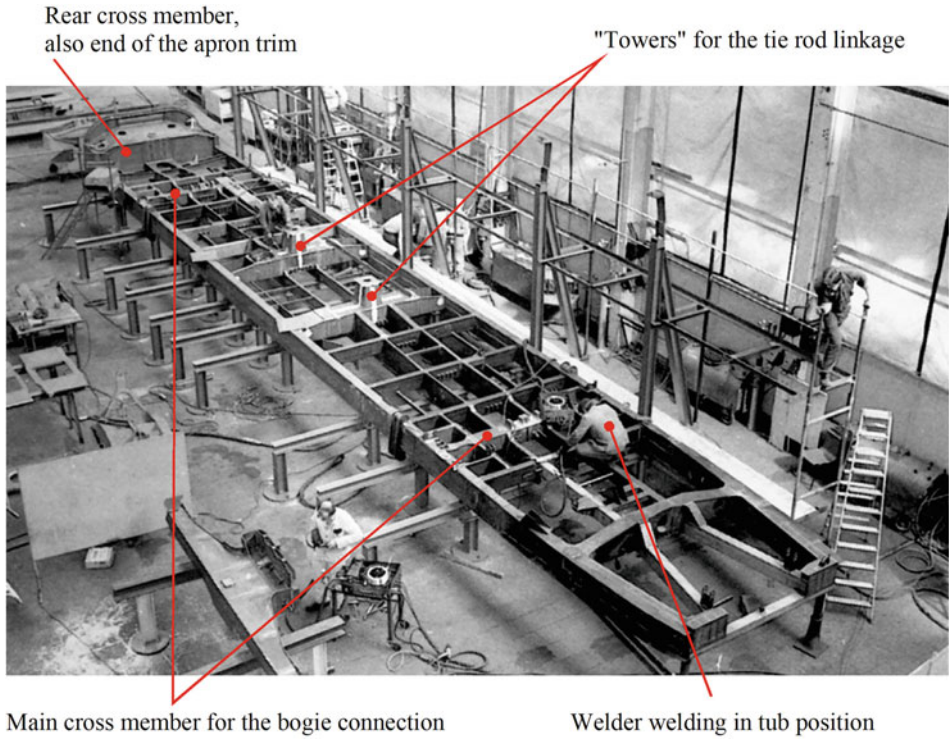

Fig. 6.36 Underframe of the power car ICE-1 (supine position). (According to photo: ARGE Triebkopf)

Figure 6.37b shows the underframe in the position of use. You can see the mountings for attaching the electrical frames in which the various electrical and electronic assemblies will be housed. Above the air ducts for the cooling air of the externally ventilated traction motors are the motor fans. The carbody shell in Fig. 6.37c consists of the underframe, side walls, partitions between the cab and engine room, and the driver's cabs (see Fig. 6.37d). The roof is a separate assembly that can later be lifted off in the workshop for repair and replacement work. The driver's cab in this example is a steel structure. The oil-cooled main transformer as a large component is located underfloor.[24] This allows a central aisle in the engine room.

A view of the inside of the vehicle body of an electric locomotive before fitting the equipment is shown in Fig. 6.38. Here, too, the underframe and the side walls as well as the bulkhead walls between the engine room and the driver's cabs form the vehicle body. The

a way that it is possible to replace the draw hook cartridge with an automatic centre buffer coupler. The then different introduction of force into the underframes is also taken into account in the design.

[24] The individual weight of the transformer is not known. Usually it is between 10 and 13 t for locomotives of this power class (6400 kW) for 16.7 Hz.

Fig. 6.37 (**a**) and (**b**) Underframe, (**c**) Vehicle body, (**d**) Locomotive driver's cab of the electric locomotive "Taurus" (according to photos: Siemens), (**e**) Locomotive in operation

Fig. 6.38 Vehicle body of a DB class 152 electric locomotive. (Photo: Krauss-Maffei)

roof is removable. The side walls are a welded construction of open edge sections and plain sheet metal. In the engine room there are plinths for the installation of the electrical frames. The cables are laid underneath. Also here there is a central aisle, which connects the two driver's cabins. The floor openings for the cooling air ducting and for the cable connections to the engines can be seen again.

6.5 Freight Wagons

The construction of freight wagons has declined sharply in Germany since the mid-1990s. The three major manufacturers Alstom, Bombardier and Siemens have ceased freight car construction. Only a few smaller manufacturers are still active in freight car construction in Germany. Freight wagons for the European market are now mainly manufactured in Eastern and South-Eastern Europe. Nevertheless, a few freight car supporting structures will be presented here.

First of all, there is a list of the types of freight wagons:

- Open wagons: high-sided wagons for general cargo and bulk goods (e.g. pit timber, scrap); low-sided wagons and stake wagons for general cargo (e.g. individual items such as machinery; long, flat and plate material),

- Covered wagons for general cargo: wagons with sliding doors (standard design); wagons with sliding walls, wagons with sliding walls and sliding roof, wagons with sliding roof or swivelling roof (for loading with fork-lift truck or crane; e.g. for palletised general cargo, paper rolls, etc.); telescopic hood wagons, wagons with sliding tarpaulins (e.g. for sheet metal coils),
- Covered cars as special cars: refrigerator cars,
- Open wagons as special wagons: low-loader wagons for heavy and bulky goods (e.g. large machines, large transformers); open double-deck wagons for car transport,
- Open wagons for bulk goods: for gravity unloading or with tipping device (e.g. for ore, coal, mineral fertilisers, grain, building materials),
- Wagons for combined transport: carrying wagons (2- and 4-axle or 6-axle articulated wagons) for container and tote transport; pocket wagons for semi-trailers; low-floor wagons for trucks and trailers,
- Vessel wagon with compressed air discharge (for powdery goods such as cement, talcum, chalk, flour as well as slightly granular goods such as semolina and quartz sand),
- Tank wagon for liquid goods (e.g. mineral oil and oil products, acids, lyes, etc.); with insulation and heating equipment (e.g. for bitumen); as compressed gas tank wagon for liquefied gases.

In the meantime, DB's freight car stock has[25] shrunk to about 80,000 units. On the other hand, the stock of private railways and wagon hire companies has grown. In addition, there are freight cars from industrial companies. Freight wagons are used throughout Europe. Many of the freight wagons running in Germany are employed by private railways and foreign railways.

Freight wagons are subjected to rough operation, particularly through shunting (assembling and breaking up train formations), but also through loading and unloading. Figure 6.39 shows an older universal underframe for two-axle freight wagons. This underframe is also prepared for the installation of the automatic centre buffer coupler and therefore has a strong central solebar. Before the decision to switch to automatic coupling, two-axle freight cars usually had a continuous drawbar as the connection between the two draw hooks, which was articulated longitudinally with springs in relation to the underframe. As a result, only outer solebars were common in the longitudinal buffer axis. However, central buffer couplings transmit both tractive and impact forces. The outer solebars are hot-rolled U-sections of mild steel, the middle longitudinal members are double-T-sections. Cross members made of lightweight double-T-sections connect the solebars.

[25] 40 years ago, the German Federal Railroad still had about 270,000 of its own freight cars. The stock has declined, among other things, because four-axle cars with higher capacity are now increasingly being used compared to two-axle cars.

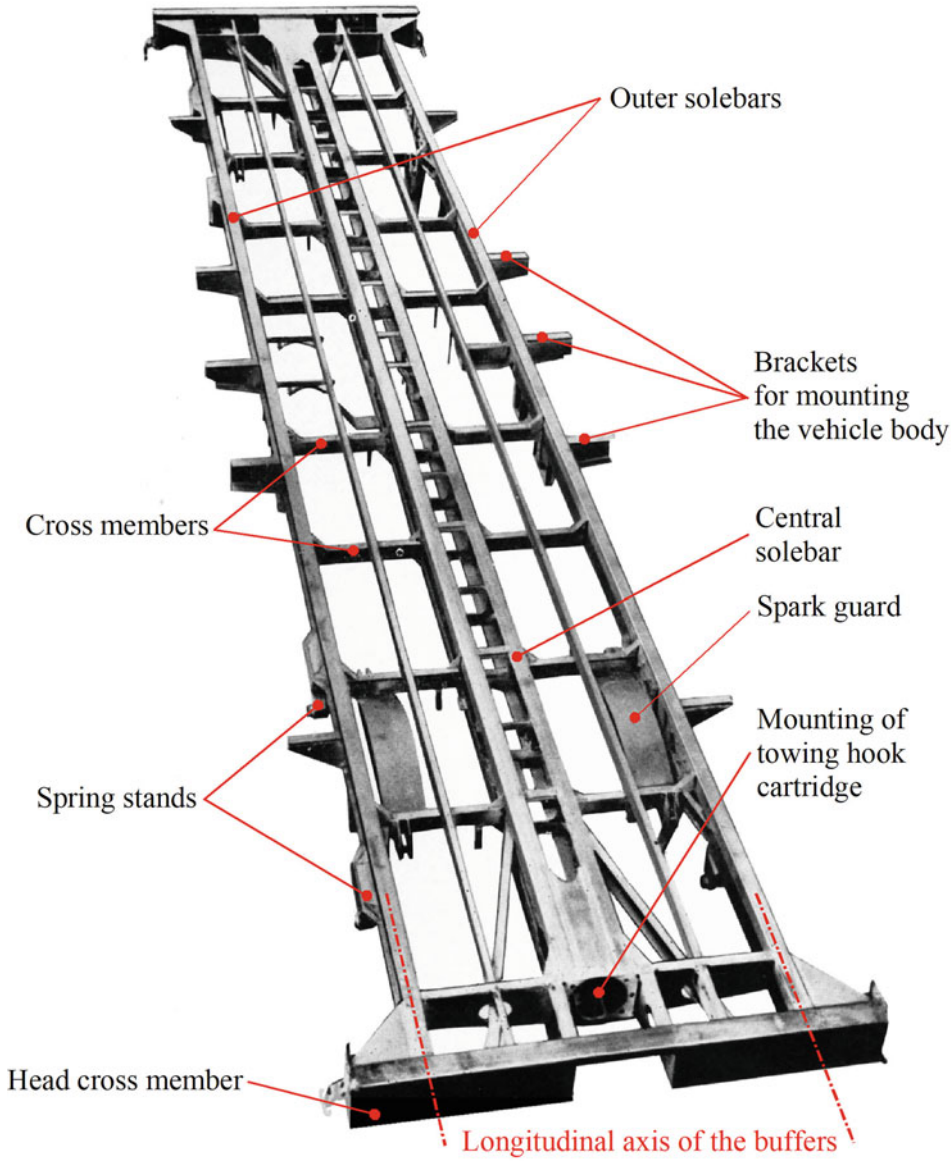

Fig. 6.39 Universal underframe for two-axle freight cars. (According to photo: Waggonfabrik Uerdingen)

The spring supports are welded on under the outer solebars for connecting the wheelsets. Spark protection plates protect the floor of the wagon, which in many freight wagon designs consists of wooden planks or laminated wood panels, from flying sparks

when braking with cast iron brake blocks. Universal underframes of this type were used, for example, for covered and open cars with high or low sides.

Figure 6.40 shows a four-axle sliding wall wagon. The sides of this vehicle each consist of two sliding walls. They allow an opening for loading and unloading over half the length of the vehicle. Using a forklift, loading and unloading is possible from a side ramp as well as from track level. As the fixed roof is kept very narrow and the sliding walls form part of the wagon roof at the top, a crane can also be used for loading and unloading. Vehicles of this type are used for transporting large-volume and heavy goods on pallets or in special load carriers, e.g. in the automotive industry for car engines and gearboxes and for pressed sheet metal parts, in the household appliance industry and in the paper industry. The internal width is 2780 mm and the loading length 21,980 mm. This means that 54 Euro pallets can be accommodated on one level.[26] With a wheelset load of 20 t, the payload is approx. 51 t with a tare weight of approx. 29 t.

The underframe of the wagon consists of two outer solebars, which are designed as fish-bellied girders (Fig. 6.40a and c) and thus correspond in their cross-section approximately to the bending moment curve of a beam under line load (see Fig. 6.2a in Sect. 6.1.1). In the middle section, however, the solebar has a straight lower edge to ensure the necessary belly clearance when driving over crests (humps). Figure 6.40b shows a section through the body of the wagon. The two solebars consist of plates welded in a double-T-shape from the lower flange, web and upper flange. The two solebars are connected by cross members of hot-rolled double-T-sections. Lightweight double-T-sections lie longitudinally on top of these, which support the wagon floor made of pine planks. The floors of covered and open freight cars are often made of wood, as it is common practice to nail wedges and squared lumber to the floor to secure the load, for example. In this type of wagon, the load can be secured by suspended partitions which can be moved longitudinally ("transport protection device" in Fig. 6.40b). There are also lashing eyes for tensioning belts or chains in the top chord of the solebar.

In the area of the buffer beam and the bogie connection (to be seen in Fig. 6.40c) the underframe is reinforced by cover plates as well as head and main cross members, as here the height of the solebars and thus their second order moment of area is reduced. Tensile and impact forces must be transferred to the outer solebars in this area. In addition, sufficient diagonal stiffness of the wagon should be achieved (corresponding to the buffer diagonal joint shown in Fig. 6.1e). Figure 6.40c shows the wagon body from below, clamped in a rotating welding jig to allow welding in the tub position.

The car body consists of the underframe, the two end walls, a central portal and the narrow roof, Fig. 6.40b and c. The roof is welded from steel sheet edge profiles and forms

[26] For shippers, the number of Euro pallets to be accommodated (base area 1200 × 800 mm) is one of the factors that counts for means of transport. Trucks according to StVZO have an internal width of approx. 2430–2460 mm and can accommodate a maximum of 38 Euro pallets on one level with a trailer or as an articulated vehicle. The payload for flatbed vehicles incl. Trailer is approx. 25 t at 40 t gross vehicle weight.

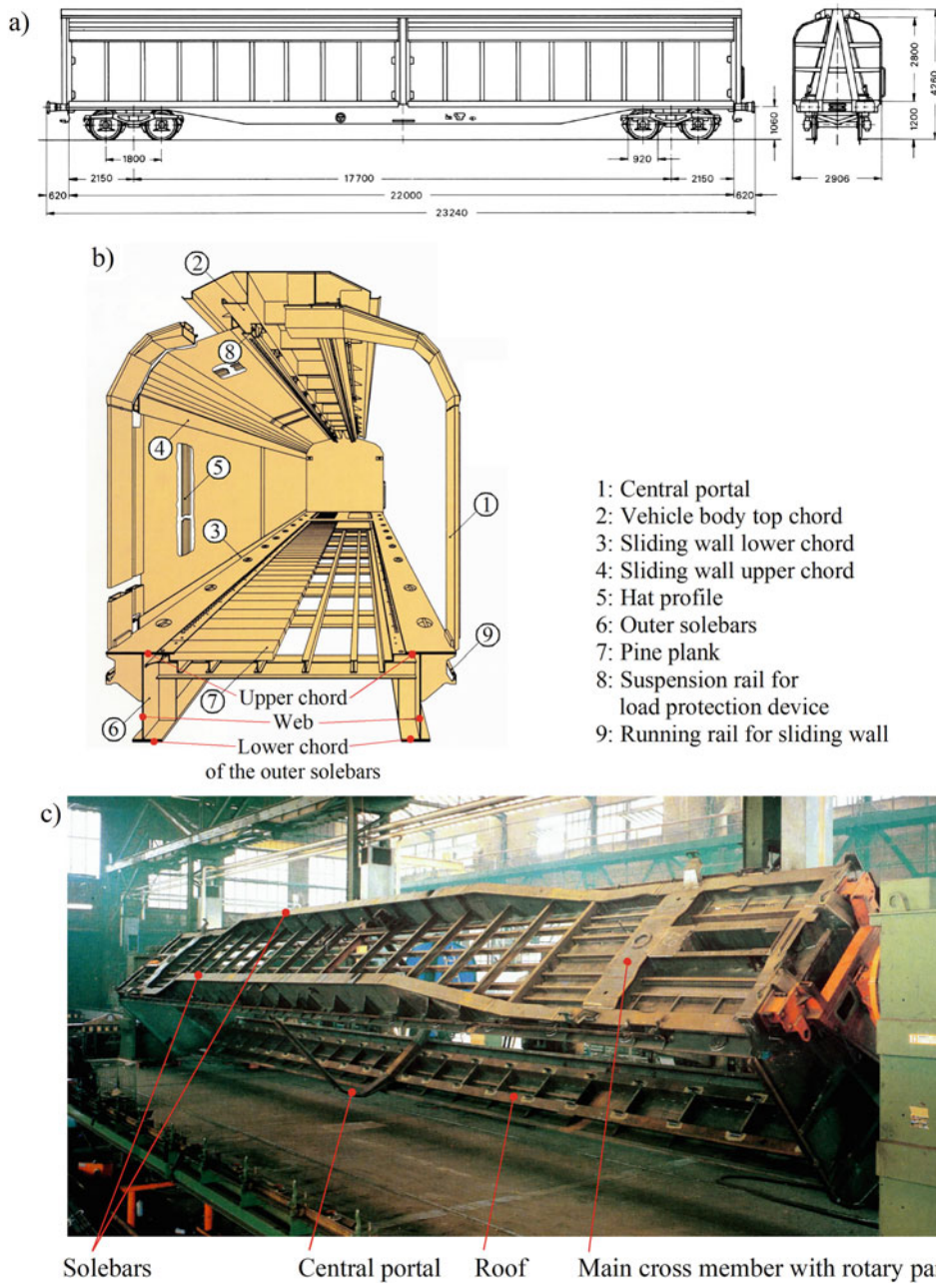

Fig. 6.40 Four-axle sliding wall car. (**a**) Dimensioned sketch, (**b**) Body construction, (**c**) Body in welding jig. (According to drawings and photo: Duewag)

the upper chord of the wagon body. The sliding walls run on rollers at the bottom of the solebar and at the top of the roof. The sliding walls themselves consist of a frame made of hollow aluminum sections. Vertical hat profiles are welded in between the sliding wall upper chord and the lower chord. The internal aluminum sliding wall cover plate is connected to the frame and hat profiles by means of spot welds.

The sliding walls are opened manually: First, the sliding wall to be opened is lifted by means of a linkage, whereby it moves away from the wagon body to such an extent that it can be pushed over the second, closed sliding wall. The closed sliding walls are sealed to the wagon body via labyrinth seals so that the load is protected from the weather.

Tank wagons are used to transport liquid cargo. In Germany, these are almost exclusively owned by industrial companies and wagon hire companies. Many of the liquid cargoes are hazardous materials. Different cargoes require adapted tank designs in each case: for mineral oil products, the tanks are usually made of structural steel; dilute acids and alkalis are transported in stainless steel tanks. For chemicals such as chlorine bleach and hydrochloric acid, there are tanks with internal rubber linings. For transporting bromine, the tanks are lined with lead. The transport of bitumen requires heat-insulated and heatable tanks to keep the contents flowable. For heating before unloading, the wagons are usually connected to stationary steam heating systems. Pressurized gas tank wagons transport pressurized, liquefied gases such as propane, butane, etc. and their mixtures, as well as liquid ammonia, for example.

Figure 6.41 shows a tank wagon for, among other things, petroleum products. The tank is made of S355J2 + N (soothed cast). The tank shell has a wall thickness of 7.0 mm, the bottoms 8.0 mm. The underframe consists of two central solebars made of double-T-profile. In the area from the buffer beam to the coupling it is extended by outer solebars, head cross members and main cross members. The brake equipment and the emptying device are attached to the central solebar. The tank has a central bend of 1° for better residual emptying. The underframe is constructed from modules so that it can be easily adapted to different tank lengths. The wagon has a dead weight of 24.6 t, so that a payload of 65.4 t is achieved with a 22.5 t wheelset load. A tank wagon with a continuous underframe has a higher tare mass.

The saddle consists of the saddle bar, which is attached to the tank, and the saddle plates. These provide the connection between the tank and the undercarriage and must, among other things, transfer the impact forces from the tank mass to the undercarriage. The saddle bar and saddle plate can be connected by welds, rivets or bolts.

A welded connection between the saddle bar and the saddle plate is shown in Fig. 6.42. There, in Fig. 6.42b, the saddle rail is outlined in blue and the saddle plate in red. In order to avoid stress peaks at the tank, the saddle plate tapers gently at the front and rear of the saddle rail. The wagon shown in Fig. 6.42 is a pressurised gas tank wagon (recognisable by the orange belly band of the tank) for liquefied ammonia. In order to reduce the heat input into the tank when exposed to sunlight, the wagon has a sunshield. This wagon also does not have a complete underframe, but rather only central solebars.

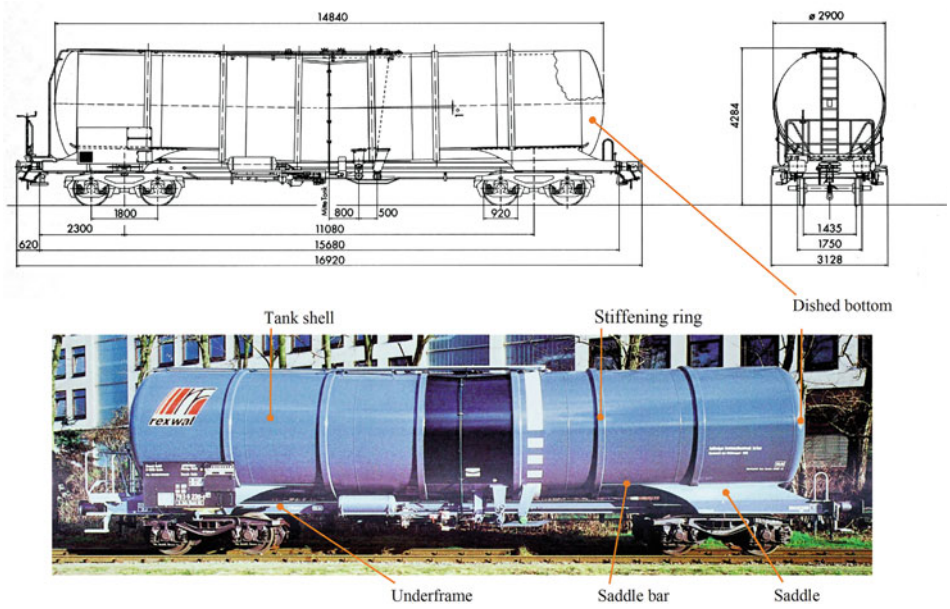

Fig. 6.41 Tank wagon 95 m^3. (According to photo and drawings: Alstom)

A tank as a tubular structure has a high bending and torsional stiffness, so that it is possible to build tank cars without an underframe. This means that low dead weights can be achieved. The transfer of impact forces from the buffer beam to the tank leads to high stresses in the connection, which can cause cracks in the tanks. For this reason, this design is no longer in common use [54]. Another disadvantage is that replacement of tanks is only possible at considerable expense. However, when the transport market changes, tank wagons are adapted to new requirements by replacing the tank.

6.6 Bogies and Running Gear

Bogies and running gears are decisive for the safety of rail transport. They are subject to high dynamic stresses. Failure during operation must be avoided at all costs. This is achieved by careful design and manufacture and by regular inspection. The requirements for the design of bogies and running gears, insofar as they are used on international lines in

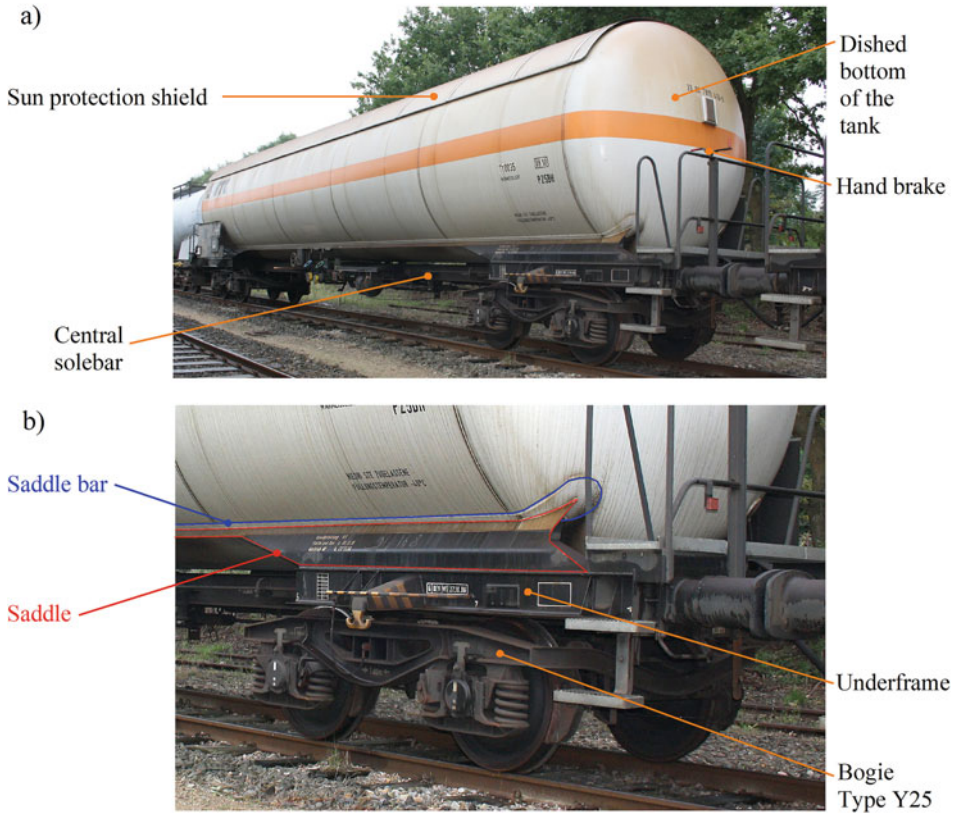

Fig. 6.42 (**a**) Pressurised gas tank wagon for ammonia, (**b**) Detail of the saddle system

Europe, are set out in DIN EN 15827,[27] among others. Numerous other regulations must be taken into account.[28]

> The supply of a bogie/chassis shall be based on a comprehensive specification. This specification must describe the functional requirements and the interfaces to the associated assemblies [. . .]. [DIN EN 15827]

The customer prepares the specification, e.g. in the form of a specification sheet, sometimes also in cooperation with the supplier. According to DIN EN 15827, the specification should include the following:

[27] DIN e. V. (Ed.): Railway applications – Requirements for bogies and running gears. DIN EN 15827, Beuth Verlag, Berlin (2011).

[28] A good overview of this can be found in [57], p. 245. The reader is strongly recommended to inform himself about the currently valid regulations if necessary.

- Connections between the bogie/running gear and the vehicle body,
- Mass of the wagon body, payload and load effects,
- Operating speed,
- Interfaces and performance of the drive and braking system,
- Track line properties,
- Static wheelset load, limits for dynamic wheel loads,
- Operating environment including environmental conditions.

The load assumptions distinguish between exceptional loads (static) and fatigue loads (dynamic, in the form of load spectra). Extraordinary loads are treated as maximum forces or accelerations. They only occur in exceptional situations or accidents:

- Extraordinary response to track excitation,
- Derailment at low speed (out of the rail into the track bed),
- Sudden application of large loads (goods wagons),
- Lateral loads during tilt condition (vertical loads and roll moments),
- Track displacement force according to Prud'Homme[29] multiplied by number of wheelsets,
- Longitudinal acceleration due to hard shunting impacts,
- Thrust forces due to turning moments at the wheelsets (as a result of skewer position in curves),
- Loads due to lifting at the bogie as well as at the wagon body.

The exceptional load conditions place demands on the static strength of the bogie/running gear. The bogie must remain fully functional under these loads. It shall be demonstrated by calculations and/or tests that no significant permanent deformation, no instability (e.g. buckling) and no breakage of the structure or of any individual part occurs.

Fatigue loads are defined by load collectives and include (see also [57]):

- Vertical loads due to track excitation, possibly supplemented by loads due to loading/unloading cycles (e.g. commuter traffic, freight vehicles),
- Lateral loads due to track excitation and curve forces,
- Loads from drive and braking,
- Loads from turning moments on the wheelsets,
- Loads due to track twists,
- Loads due to system components (engine, springs, dampers, brakes, etc.).

[29] According to Prud'Homme, lateral forces on the wheel flange can cause lateral track displacement if, over 2 m of travel, the lateral force is more than 76% of the wheel load. Derailment is not to be expected until the lateral force equals the wheel load (see: Fendrich, F. (ed.): Handbuch Eisenbahninfrastruktur. Springer Verlag, Berlin/Heidelberg (2006), p. 56).

The fatigue strength shall be verified e.g. according to the fatigue strength method. The underlying material behaviour under fatigue loading shall be based on current European or national standards.

For the design of passenger vehicles according to BOStrab, VDV publication 152 [66] applies. It was revised in 2016, as in some types of low-floor trams, in contrast to classic bogies, the turning angle of the bogie is limited (see Sects. 5.6.2 and 6.3). Even with small turning angles of the bogie, the associated vehicle part, which is connected to other vehicle parts via joints, must be taken along. This results in greater loads on certain types of low-floor running gear compared with bogies. These increased loads must be estimated by multi-body simulations or determined by line measurements [57].

The stresses in the load-bearing structures of bogies/chassis (as well as entire car bodies) are[30] calculated today with the aid of the finite element method (FEM). The FEM is used to investigate problems from strength theory (stresses and deformations with linear and non-linear material laws), from fluid mechanics (flow around and through) and from thermodynamics. Problems of electric and magnetic fields can also be investigated with the help of the FEM. The use of the FEM in the strength calculation of drive structures in the linear range, i.e. within the validity of HOOKE's law, will be briefly explained using an example.

The frame and cradle of a tram bogie are considered by means of FEM analysis. The outer frame is a welded box construction. The bogie for standard gauge has a wheelset spacing of 1800 mm. The wheelsets are mounted in the frame in the primary stage via rubber thrust springs (metal-rubber springs, MEGI springs). Each wheelset is driven by a motor-gear unit. The bogie is equipped with magnetic rail brakes. The cradle is connected to the bogie frame by vertical coil springs. Movements of the cradle vertically and in the horizontal-transverse direction are damped by hydraulic shock absorbers; horizontal-transverse movements are limited by rubber buffers. The body of the tramcar is supported on the cradle by a slewing ring (axial bearing) (see also Fig. 6.43).

The bogie frame and cradle support were constructed as an FEM model using shell elements. The frame consists of approx. 14,250 elements, the cradle of approx. 5200. The following loads were investigated against fatigue failure of the frame:

(1) Vertical load as regular load ("two-thirds load", i.e. two-thirds of all seats and standing places are occupied),
(2) Torsional force from 4% cant ramp inclination (4 mm height difference per 1 m wheel distance),

[30] Today, FEM program systems are often part of a PDM system (Product Data Management System), i.e. CAD models can be directly converted into FEM models and analyzed. Some well-known FEM programs are:
ANSYS: http://www.ansys.com (also available as student version).
LS-DYNA: http://www.dynamore.de/.
NASTRAN: http://www.mscsoftware.com/.

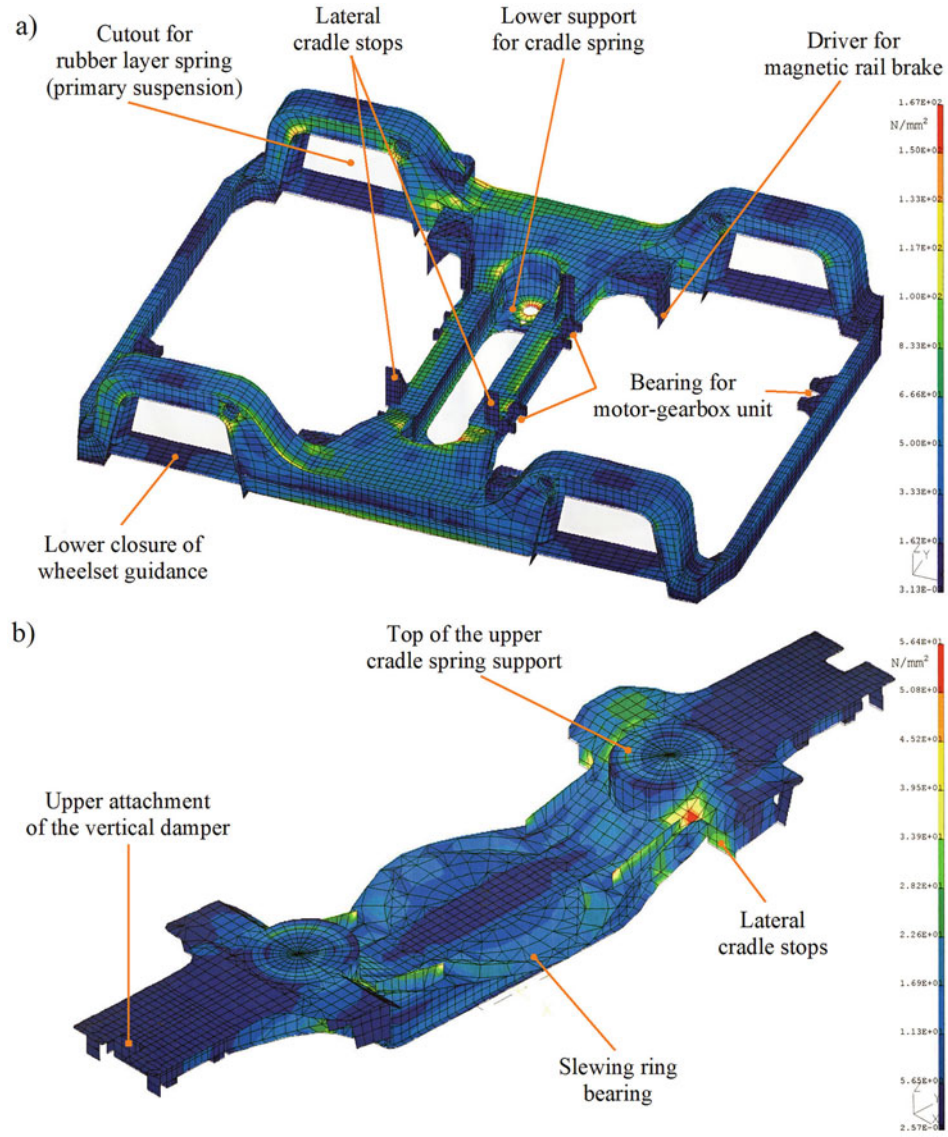

Fig. 6.43 Results of the FEM calculation for a tram bogie. (**a**) Frame and (**b**) Cradle beam

(3) Transverse impact as a regular load,
(4) Transverse impact of the motor-gearbox units,
(5) Vertical load of the motor-gearbox units,
(6) Braking as a regular load (braking in regular service).

The loads are recorded as mean value and lower and upper span (e.g. in the form $F = F_0 \pm F_a$ with F_0 = mean force and F_a = deflection force). The strength values result here from a fatigue strength diagram of the material.

The yield strength of the material was investigated for the frame:

(7) Vertical load as maximum load,
(8) Transverse impact as an exceptional load,
(9) Twisting force from 6.7% slope of cant ramp,
(10) Vertical load of motor-gear units as exceptional load,
(11) Transverse impact of the engine-gearbox units as an exceptional load,
(12) Hazard braking,
(13) Longitudinal impact when driving onto vehicle,
(14) Longitudinal impact of the engine-gearbox units when driving up.

For the cradle beam, the following load cases were investigated against fatigue failure:

(1) Vertical load as two-thirds load,
(2) Transverse impact as a regular load,
(3) Braking as a regular load.

Against yield strength were investigated:

(4) Vertical load as maximum load,
(5) Transverse impact as an exceptional load,
(6) Hazard braking,
(7) Longitudinal impact when driving onto vehicle,
1. Lifting.

Figure 6.43 shows the results of the FEM calculation for the superposition of the load cases against fatigue failure. For the frame these are the load cases 1–6, for the cradle 1–3. The maximum stresses are shown as equivalent stresses. To evaluate the fatigue strength, the mean and minimum stresses are also required. Areas of high stress can be identified from the colours of the output graph. The scales are shown on the right in Fig. 6.43a and b. The numerical values are automatically scaled by the FEM program to the maximum stresses that occurred. For the bogie frame, the maximum stresses are in the area of the lower cradle spring support with 167 N/mm^2. For the cradle support, the maximum stress is about 56 N/mm^2 in the transition between the upper cradle spring support and the lateral cradle stops.

As a further result of the FEM calculation, Fig. 6.44 shows the deformations of the cradle beam in the load case “lifting”. In this case, the empty vehicle is lifted at the running gear, e.g. after derailments, by means of hydraulic cylinders. The FEM program displays the deformations enlarged and marks the displacement of the individual elements by colors. The scale on the right in Fig. 6.44 indicates the size of the deformations: Compared to the

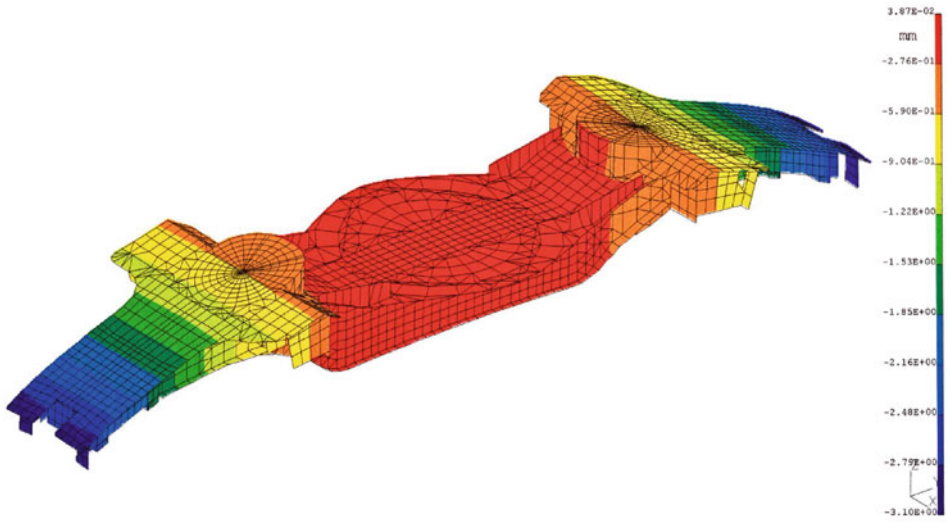

Fig. 6.44 Deformations on the cradle beam for the "Lifting" load case

centre of the cradle beam, the sides are bent downwards by about 3.1 mm. As further investigations have shown, this is a purely elastic, i.e. reversible, deformation.

The conversion of a geometry model from CAD into an FEM model requires experience, since, for example, the selected size and type of elements has an influence on the calculated stresses. If the elements are selected too large in highly loaded areas, this can falsify the calculated stresses. Likewise, experience is necessary when assessing the stresses and deformations calculated using FEM. It should be noted that weld seams in complex structures often cannot be mapped realistically or not at all. Also residual stresses in the area of weld seams cannot be captured. Nevertheless, the FEM is a tool that has contributed significantly to lightweight construction and safer design in the dimensioning of rail vehicles and their assemblies for 40 years.

Engineering in Rail Vehicle Construction

7

> The rail industry and railway operators have the common goal of putting rail vehicles into operation in high quality and under the agreed conditions. In this context, their quality-driven **development** plays a key role because increasing demands on the performance of **products** as well as ever more demanding laws and approval rules (for example in the environmental field or in the context of European harmonisation) require adjustments in the product development of rail vehicles [63, p. 4; emphasis in the original].

Over the last 25 years, the engineering processes in rail vehicle construction have changed significantly. On the one hand, the strong involvement of customers in the development and production process is decreasing. Before the privatisation of the German state railways (DB and DR), competences and capacities for development and development support were held in central offices (called "Zentralämter" at the German Federal Railway). As authorities, the state railways also had the authority to approve and commission new vehicles. With the privatisation of the Deutsche Bundesbahn and the Deutsche Reichsbahn to form Deutsche Bahn AG, the corresponding personnel capacities were reduced and the Federal Railway Authority (EBA, Eisenbahn-Bundesamt) was installed as the approval and supervisory authority.

Whereas until the 1990s the national railway companies made very detailed specifications for the vehicle to be supplied, today the rail vehicle industry is also responsible for the technical specification of the vehicle and its components.[1] Since then, the task of the rail vehicle manufacturers has been the development and production of tested and operationally ready vehicles, including the integration of all components procured from suppliers. The development, testing and approval effort for the

[1] Abele, R., Völkening, W.: On the new distribution of roles in the railway industry. Eisenbahningenieur 51(2000)H. 2, S. 24/25.

© The Author(s), under exclusive license to Springer Fachmedien Wiesbaden GmbH, part of Springer Nature 2022

J. Ihme, *Rail Vehicle Technology*,
https://doi.org/10.1007/978-3-658-36969-9_7

manufacturers has thus increased. As a result, rail vehicle manufacturers are now developing modular vehicle platforms, at least in the railway sector and to some extent also in the tram sector, which cover the needs and conditions of several customers as well as various country specifics.

On the other hand, the change in development processes affects the computer-aided methods used, such as computer-aided design (CAD), computer-aided engineering (CAE), computer-aided planning (CAP), computer-aided manufacturing (CAM), computer-aided testing (CAT) and computer-aided quality management (CAQ), which are based on the digital product model (Digital Mock-up, DMU). This is discussed in Sect. 7.2. These digital methods were introduced and further developed in the aircraft and automotive industries from about 1975 onwards . They have also been widely used in rail vehicle construction for about 35 years.

A third aspect is the increased involvement of suppliers – a trend that also originated in the automotive industry. Suppliers are transforming themselves from parts to module manufacturers, i.e. they supply production-ready, tested and ready-to-install modules for integration into the vehicles. This is associated with a shortening of the development and design process and a reduction in the vertical range of manufacture.[2] Both ultimately lead to shorter delivery times, as numerous sub-processes in product creation can be carried out in parallel. The fourth trend to be mentioned is the sharp drop in prices for rail vehicles, which has led to increasing cost pressure in the companies.

Since around 1990, the growing demands on manufacturers and suppliers have led to a process of concentration in the European rail vehicle industry. The share of electrical equipment in rail vehicles for passenger transport and locomotives is now 50% or more of the manufacturing costs. In the past, rail vehicle manufacturing therefore required cooperation between the manufacturer of the mechanical part of the vehicle (e.g. vehicle body and running gear) and the supplier of the electrical equipment. Many manufacturers[3] that were independent or belonged to steel and engineering groups until the early 1990s have been taken over by three large (electrical-)groups – Alstom, Bombardier and Siemens – or have disappeared from the market altogether. Alstom's acquisition of Bombardier's rail vehicle division was completed in 2020. These three or now two "big players" in Europe have been joined by serious competitors again in the form of the Swiss company Stadler Rail and the Spanish company CAF[4] (Construcciones y Auxiliar de Ferrocarriles S. A.). In addition, the

[2]The vertical range of manufacture refers to the share of the company's own added value in the product.

[3]Examples of takeovers in Germany: Henschel and Waggon-Union (both Thyssen group) and large parts of the DWA group (former GDR rail vehicle industry) went to Bombardier. DUEWAG (independent of the group), MaK (Krupp group) and Krauss-Maffei (Buderus group) joined Siemens; Linke-Hofmann-Busch (Salzgitter group) was taken over by Alstom. Krupp, MAN and Messerschmidt-Bölkow-Blohm gave up their rail vehicle activities.

[4]CAF acquired the bus division and Stadler Rail the tram division of Polish bus and tram manufacturer Solaris in 2018.

world's largest rail vehicle manufacturer, CRRC, has emerged in China (see Chap. 1, Fig. 1.32). Although it has not yet entered the European market to any great extent, it is increasingly occupying the markets in Asia, Africa and America.[5]

Before describing the product creation process in Sect. 7.1, the following figures illustrate[6] the complexity of a rail vehicle: A three-part multiple unit consists of 18 main assemblies, which are divided into about 100 subassemblies and represented in about 16,000 drawing items. Over a million individual parts have to be handled in production and assembly, with around 40 different materials being used. Not to forget the necessary software in the on-board computers and control units. It consists of several hundred thousand program lines.

7.1 Product Creation Process in Rail Vehicle Construction

As already described, the national railways played a major role in the development process of new rail vehicles. Figure 7.1 schematically shows the corresponding process. On the basis of a specification, one or more manufacturers were invited to submit a development offer. After receipt, examination and comparison, the railway company usually awarded the development contract to one manufacturer. In some cases, consortiums of several manufacturers were commissioned (e.g. for the ICE-1).

The development order included the development and design and usually also the construction of a prototype or a small prototype series. The entire process was supervised by the orderer. For this purpose, regular coordination meetings were held between the customer and the contractor. In addition, employees of the railway company worked for the manufacturers, called acceptors. At the Deutsche Bundesbahn, the "Quality Inspection Service" was responsible for this. It monitored the production process and also the suppliers of the vehicle manufacturer, right down to the semi-finished product and paint suppliers. The so-called acceptance test took place on the finished vehicle at the manufacturer's premises by employees of the railway company, during which conformity with the specification and the quality of workmanship were checked. Product documentation (essentially drawings, parts lists and circuit diagrams) produced by the manufacturer became the property of the railway company.

The vehicle or the prototype series were then tested in railway operation over a longer period of time up to several years. Improvements and change requests were documented and partly already implemented. After successful trial operation, a decision was made on series procurement and a new invitation to tender was issued. Depending on the offer situation, other manufacturers could also be involved in series production in addition to the

[5] https://www.produktion.de/specials/chinas-industrieriesen/das-ist-crrc-mit-400-km-h-auf-den-weltmarkt-123.html, last accessed on 07/09/2018.

[6] According to Bombardier documents.

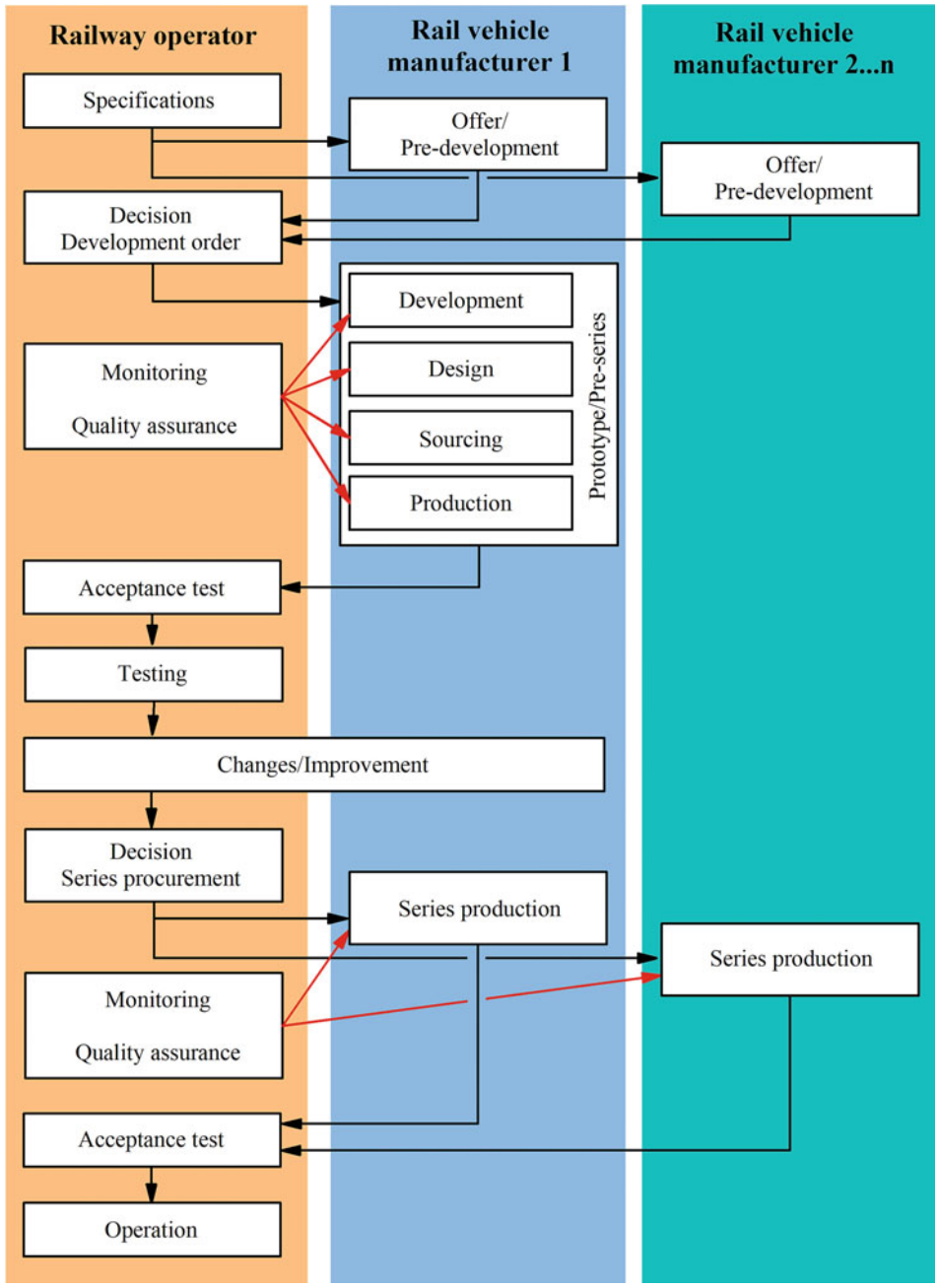

Fig. 7.1 Product creation in rail vehicle construction: the past

actual vehicle developer. This was also done because of the production capacities and the desired delivery time. It also happened that the developer was not involved in the series production. Since the technical documentation of the vehicle was available at the client, he was free to award the contract.

As already described, series production and the suppliers used for this purpose were also monitored by the client. Each individual vehicle was handed over to railway operations after the acceptance procedure. The warranty period for the manufacturer began with the operational use.

This approach has now been largely abandoned by the state-owned railway companies. In the case of vehicle developments for railway systems with special characteristics and requirements (e.g. urban underground railways, in some cases also trams), the product development process is still similar to that shown in Fig. 7.1 (e.g. underground train class DT 5 of Hamburger Hochbahn AG, Fig. 6.30, or tramcar class 3000 of ÜSTRA Hanover, Fig. 6.31). In this case, after a call for tenders, a manufacturer is selected as the developer and supplier in accordance with the offer situation. Due to the smaller order series, prototypes are often not used, but instead, for example, after the delivery of a pre-series, a delivery break is taken during which testing takes place at the customer's premises. The delivery is then continued after any design changes have been made. The series delivery is usually not divided among several manufacturers. In Germany in this case, the approval of the vehicle type is the task of a technical supervisory authority, an authority of the respective federal state.

Since the privatisation of the state railways, the product development process and the approval procedure have changed. Figure 7.2 illustrates this. The rail vehicle manufacturer takes over the development of a vehicle platform up to a prototype after market analysis and preparation of a specification. The vehicle platform (see Fig. 7.3) covers the requirements of as many potential customers as possible. Modifications according to the wishes of the customers are possible, e.g. different traction current systems, adaptation of the entrances to different platform heights, door arrangement, division of the interior spaces, etc.

The approval of a railway vehicle will only be touched upon briefly here, as the procedure will be changed in future by the installation of the "European Railway Agency"[7] (ERA) within the European Union. For the currently valid procedure, reference is made here to the "Railway Vehicles Manual" [6] and to the "Memorandum of Understanding" [15]. The approval of a rail vehicle is understood to mean the granting of a type approval, or a series approval or an authorisation for placing in service by a legally defined national institution. In the Federal Republic of Germany, this institution is the Federal Railway Authority (EBA). In the approval procedure, the manufacturer has to submit a large number of documents and proofs which have to be checked by assessment bodies.

[7] Brunn, C.; Sonnenburg, U.: Railway authority ERA – a bureaucracy monster? Privatbahn-Magazin 12(2018)H. 4, S. 12/13.

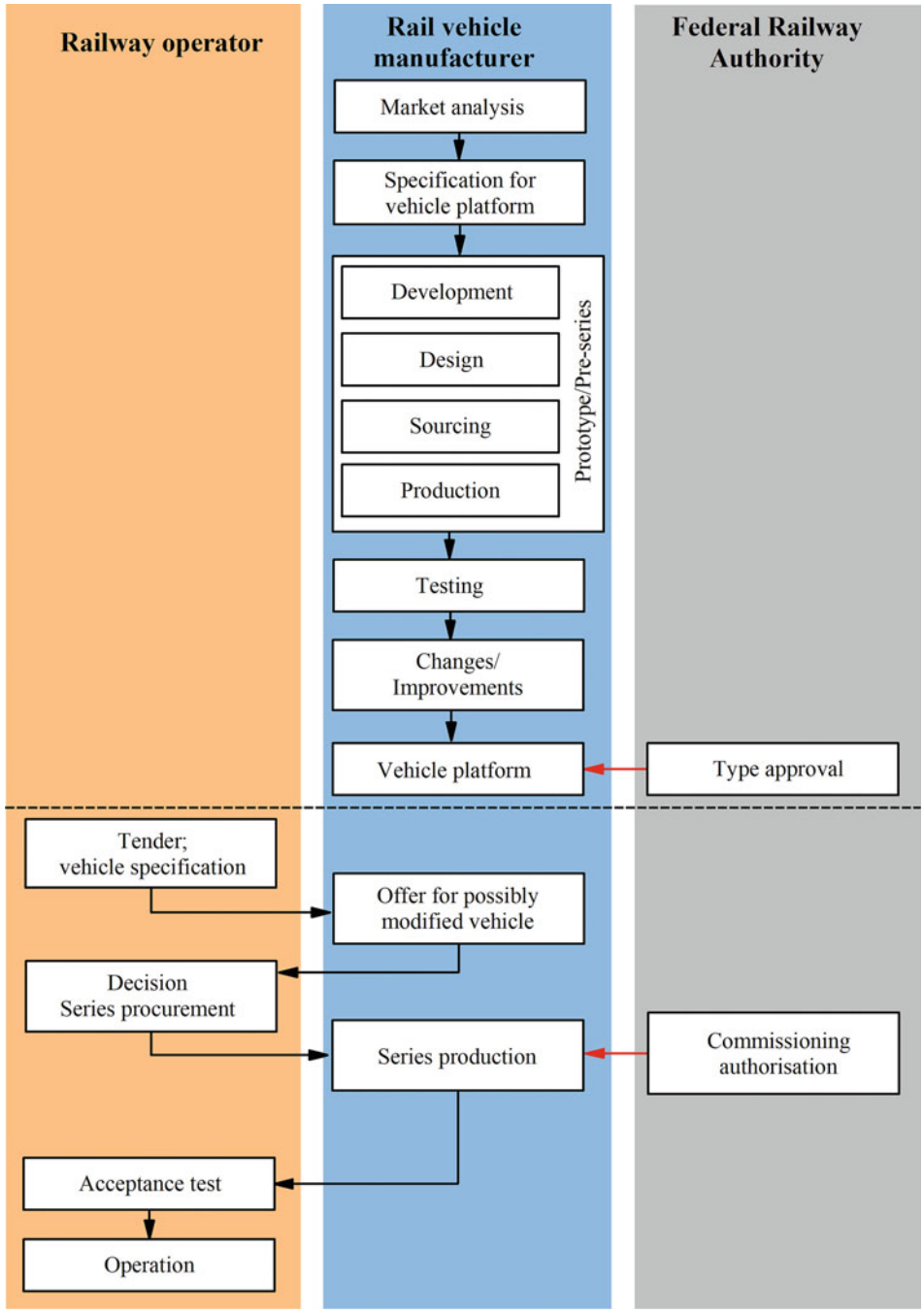

Fig. 7.2 Product creation process in rail vehicle construction: present day

Fig. 7.3 Example of vehicle platform: Bombardier TwindexxVario

A "Notified Body" (NoBo) checks whether a railway vehicle complies with the European TSI ("Technical Specifications for Interoperability", EU railway regulations)[8] and the applicable European Standards (EN). "Notified Bodies" are government-appointed and supervised private inspection bodies that act on behalf of the government and assess the conformity of products with European requirements. They issue the EC certificate of verification. This allows a vehicle to be used within the European Union once it has been approved for commissioning.

A "Designated Body" (DeBo) checks compliance with national requirements (NNTR, Notified National Technical Rules and Regulations) and issues the "NNTR Certificate of Conformity". Safety assessment bodies (Associated Body, "AssBo") are responsible for the evaluation and assessment of risks and prepare a safety assessment report. On the basis of the EC certificate of verification, the NNTR certificate of conformity and the safety assessment report, the authorisation for placing in service can then be issued by the EBA after a detailed examination of the documents.

[8] https://www.eba.bund.de/DE/RechtRegelwerk/TSI/tsi_node.html; last accessed on 12th Oct. 2018.

Since the testing of rail vehicle prototypes is now the responsibility of the manufacturer, various facilities have been set up for this purpose, e.g. the railway test ring in Velim in the Czech Republic or the Siemens test site in Wegberg-Wildenrath in Germany. There, (endurance-)tests can be carried out on ring-shaped track systems, among other things. The test sites have tracks of several gauges and traction current systems. As a rule, customers require that newly developed vehicles have successfully covered several thousand kilometres. For simple driving tests, several rail vehicle manufacturers have test tracks on their factory premises. Functional tests in cold and heat can take place, for example, in the climatic wind tunnel in Vienna (Rail Tec Arsenal) in Austria. There, air conditioning systems and vehicle heaters are tested under extreme climatic conditions.

Figure 7.3 shows an example of a vehicle platform based on the "TwindexxVario" from Bombardier[9]: The upper part of the figure shows a four-part unit, the lower part a three-part unit. Both variants have two power cars. The platform concept also provides for sets with a power car and a driving trailer as well as one to several intermediate cars. The boarding height of the power car is 600 mm in the upper part of the figure and 1150 mm in the lower part. In the upper example in Fig. 7.3, first class is located in the power car, in the lower example in the middle car (indicated by the yellow bar below the windows in the upper deck).

As already mentioned, the vertical range of manufacture in rail vehicle construction has decreased. This means that the share of suppliers in the product manufacturing process is increasing, with fewer simple parts being purchased today and more ready-to-install modules. The task for rail vehicle manufacturers is therefore to integrate these modules and ensure the quality of the end product [63].

Modules purchased from suppliers include:

- Diesel engines and gearboxes ("power packs"), cardan shafts
- Electrical drive systems (electric motors, transformers, rectifiers, inverters, etc.)
- Wheelsets with wheelset bearings and housings, also with wheelset gears and brake discs
- Springs, dampers (partly also complete running gears), air suspension systems
- Couplings (buffers, draw hooks or central buffer couplings)
- Noses or front masks (as plastic moulded parts, also completely equipped)
- Driver's cab equipment; control cabinets
- Transition devices (bellows, transition bridges)
- Doors, windows or glass panes
- Interior fittings (wall and ceiling linings, glass separating discs, retaining bars, etc.)
- Seats (passenger and driver seats)

[9]Further examples of vehicle platforms are: TRAXX locomotives from Bombardier; Coradia LINT and Coradia Continental multiple units from Alstom, KISS and FLIRT multiple units from Stadler, Vectron locomotives and Velaro high-speed trains from Siemens.

- Sanitary facilities (toilets, service and waste water tanks, washbasins, etc.)
- Air conditioning and heating systems
- Lighting systems for indoors and outdoors
- Passenger information systems (matrix displays, screens, loudspeakers, etc.)
- Brake systems (brake cylinders, air reservoirs, valves, compressors, lines, hoses, brake control, etc.)
- Current collectors
- Batteries (starting batteries, traction batteries, batteries for energy supply during vehicle standstill)

In addition, there are semi-finished products such as steel-, light metal-, rubber- and plastic profiles, sheet metal, pipes, welding filler materials, laminated panels, floor coverings and cables, as well as paints, adhesives, sealants, etc., and finally the usual fasteners such as screws, nuts, rivets, bolts, nails, split pins.

The integration of a module to be supplied is to be explained using the example of a door system. The external doors of a rail vehicle are installed in the body of the carriage during final assembly and are firmly connected to it. The mechanical closing and opening function and the tightness must be ensured by adjusting the door system during assembly. Since the door drive must be supplied with energy, a connection to the vehicle's electrical or compressed air on-board network is required.

In addition, the door system must be integrated into the overall control of the vehicle, as vehicle functions and door functions are interdependent. For example, the train can only depart when all doors are closed. On the other hand, the door must not close as long as there is still an object between the finger protection strips of the door leaves (Fig. 7.4). The closing procedure must be announced visually and acoustically outside and in the boarding area. Before a stop, only the doors on the platform side are released by the driver for the opening procedure. A released door shall then be opened by the passenger when the train is at a standstill by pressing the door pushbutton, whereby the associated step may first be extended to bridge the gap to the platform edge. Before the train departs, the doors are locked by the driver when closed and can then no longer be opened by passengers. In an emergency, it shall be possible to open the door after it has been released, even if the vehicle has no power.

The door of the ICE-3 shown in Fig. 7.5 is adapted to the outer contour of the carriage body. In addition to the interfaces to the vehicle described above, the train running sign is integrated into the door pane as a digital display and is therefore integrated into the train's passenger information system. As the vehicle operates on high-speed lines, the door seal must ensure the pressure tightness of the carriage body.[10]

[10] Train encounters as well as tunnel entrances and exits lead to large pressure surges on high-speed lines. Since these would be very unpleasant for the passengers ("pressure on the ears"), the car bodies must be designed to be pressure-tight. This also requires air-conditioning systems with controllable air intake flaps and vacuum toilets with closed waste-holding tanks.

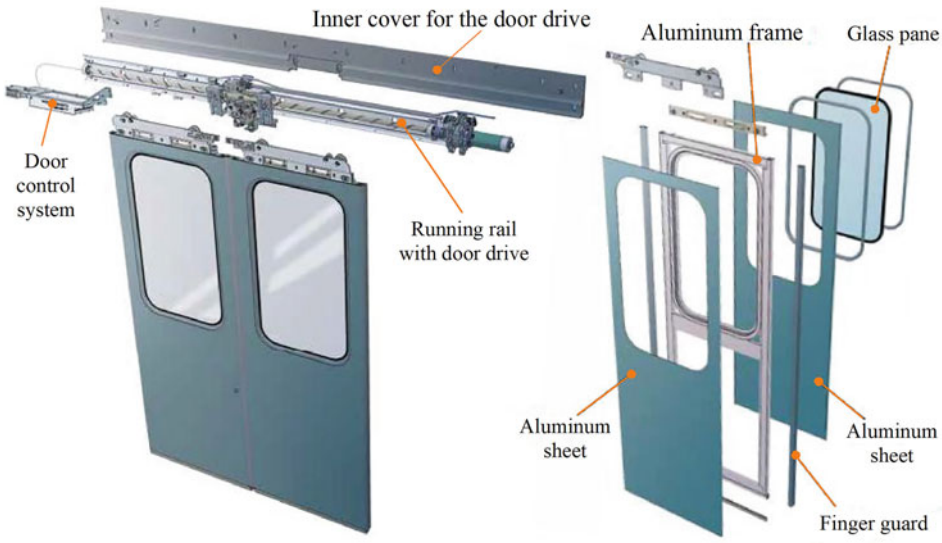

Fig. 7.4 Door system. (According to drawing: Gebr. Bode GmbH & Co KG)

Fig. 7.5 Door of the ICE-3 (Velaro-D, DB class 407)

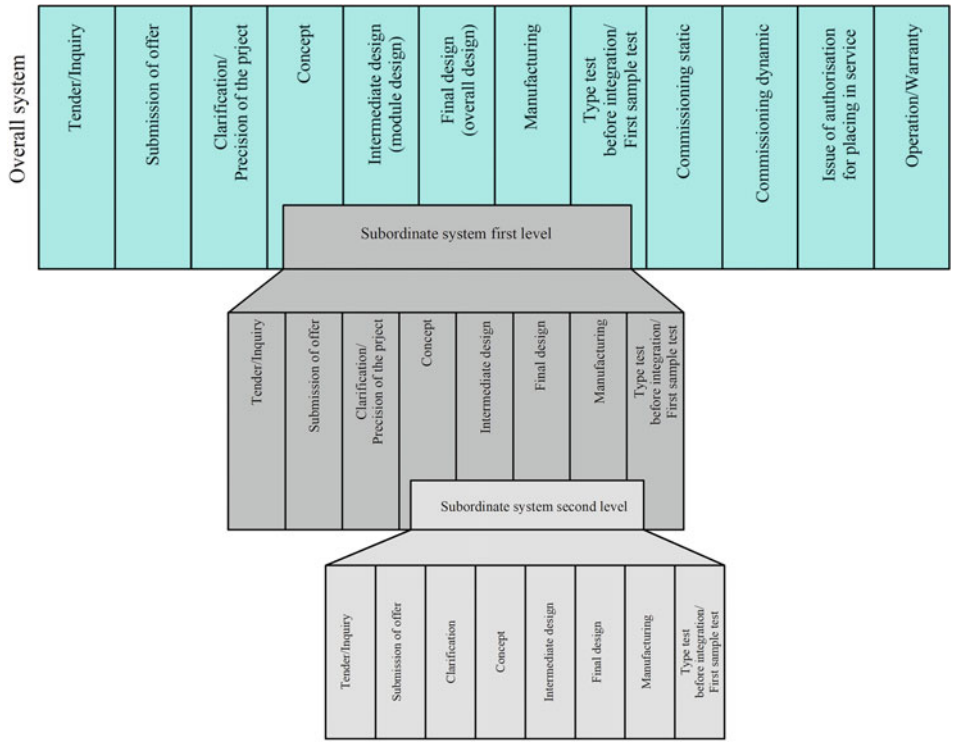

Fig. 7.6 Integration of supplier modules/systems within the product creation process. (According to [63])

The procedure for the procurement and integration of subordinate systems in the vehicle is shown in Fig. 7.6. The vehicle manufacturer draws up a specification for such a system, which is usually part of the enquiry with several suppliers. In the example of the door system the body section and the vehicle contour (see Fig. 7.5) are also sent to the suppliers as a CAD data set. The manufacturers of door systems will submit offers on this basis, but these will not yet have been designed down to the last detail. The effort required for this is not made until after the order has been placed. As a rule, the offers are explained in advance in discussions with the vehicle manufacturer and refined to the final concept.

At this point, some suppliers may withdraw their offer because they cannot meet the requirements, e.g. technically, in terms of deadlines or economically. After all clarifications have been completed, one supplier is finally awarded the contract and can bring his concept up to the "final design" (Fig. 7.6) ready for production. After approval by the vehicle manufacturer, production of the door system can then begin. In addition to semi-finished products, the door supplier will also purchase the drive and the glass panel from his suppliers and integrate them into his module. The door system is the first level, the door drive would be the second level in Fig. 7.6.

After completion of the first door system, an initial sample inspection is carried out at the supplier's premises to check that the design and function conform to the quotation. After approval, series production and delivery can begin in accordance with the vehicle manufacturer's delivery schedule. Once the first vehicle is completely assembled, static commissioning takes place on a test bench in the vehicle manufacturer's workshops. All functions that are possible without moving the vehicle are checked. Whether a door cannot be opened by passengers when the vehicle is moving, can, for example, only be checked in the dynamic commissioning during test runs on a test track.

Once all tests on the finished vehicle have been successfully completed, the approval for commissioning can finally be issued by the licensing authority. The vehicle is handed over to the operator and the warranty begins for the vehicle manufacturer and supplier.

7.2 Computer-Aided Product Creation

As already mentioned, the rail vehicle industry uses computer-based methods in product creation. They are often summarised under the term "CAx". Figure 7.7 illustrates the use of CAx methods in the product creation process.

CAD – Computer-Aided Design, has become an indispensable tool in design and development. In addition to "mechanical" design (M-CAD), i.e. the creation of the product geometry, the creation of circuit and wiring diagrams, control cabinet planning and cable routing (E-CAD) also play a role. The result of M-CAD is a three-dimensional product model, the so-called "digital mock-up" (see Fig. 7.8). It is the basis for further computer-based methods in the product creation process.

The starting point for the digital product model (Digital Mock-up, DMU) are 3D CAD models as CSG or BRep models. CSG stands for "Constructive Solid Geometry" and is a solid model. Components are assembled and represented from basic bodies such as cuboids, wedges, pyramids, prisms, cylinders, cones, spheres and toruses. The bodies have a volume and by assigning material data the system can determine e.g. masses, centers of gravity and moments of inertia. BRep is the abbreviation for "Boundary Representation" and means a surface-limited model. Here, so-called free-form surfaces can be generated, such as those used to represent the outer skin of motor cars. Initially, the BRep model has no wall thickness. However, bodies bounded by free-form surfaces can also be created. CAD systems with hybrid modelers offer both options. Figure 7.9 shows a CAD workstation in the rail vehicle industry. A complex CAD model is shown in Fig. 7.10.

On the one hand, the DMU serves as the basis of computer-aided engineering (CAE, see also Fig. 7.7). On the other hand, the DMU is also the basis of the "digital factory" via CAP and CAM, which in turn[11] contains essential components of "Industry 4.0". For "Rapid

[11] "Industry 4.0" refers to the comprehensive digitalization of industrial production with the goal of extensive self-organization. People, products, production facilities and logistics systems are

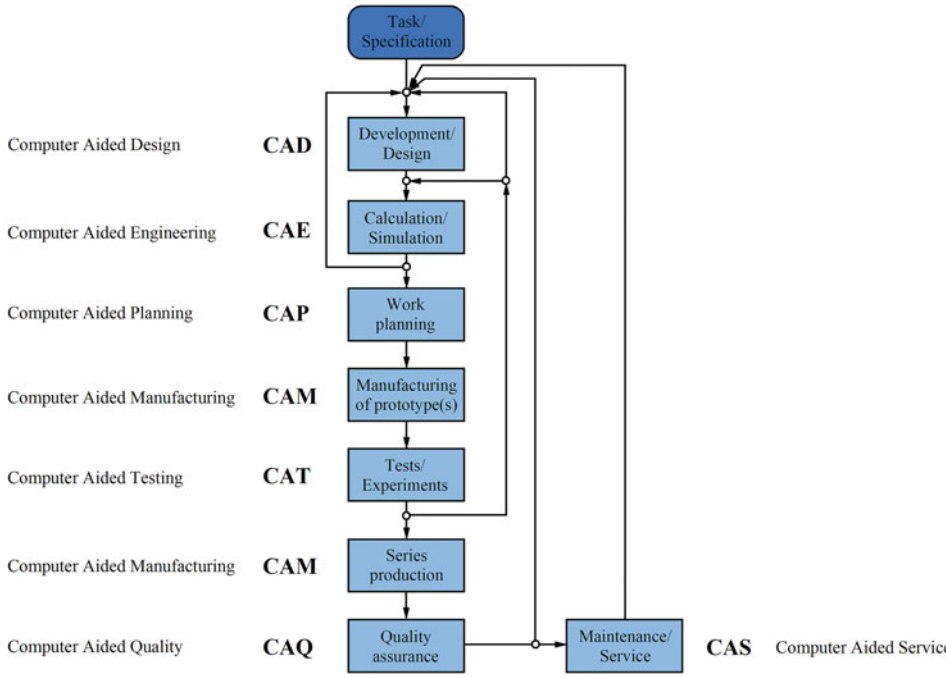

Fig. 7.7 CAx systems in product creation

Prototyping",[12] the CAD data of the product are processed and visual and functional models of the future product are created within a few hours. "Rapid tooling" enables the rapid production of prototype and pre-series tools. The aim here is also to shorten the development (partial-)processes. Especially for small series products, the production of spare parts in plastic or metal with the help of additive manufacturing processes will be a cost-saving option in the future. The spare parts would no longer have to be kept in stock in forecast quantities, but could be produced on demand with short delivery times.

As shown in Sect. 7.1, every rail vehicle has a high proportion of supplier modules and parts. If the supplier can provide 3D CAD data, the design process at the rail vehicle manufacturer is simplified. The corresponding CAD model of the module can then be directly integrated into the overall CAD model. An example of a 3D model of a module is shown in Fig. 7.11 on the basis of a "power pack", a drive module purchased from a

networked, cooperate and communicate with each other. In addition, the entire product life cycle from the product idea to recycling is to be included; see e.g.: https://www.iosb.fraunhofer.de/servlet/is/21752/Umsetzungsempfehlungen_Industrie_4.0_final_2012–10–02.pdf?command=downloadContent&filename=Umsetzungsempfehlungen_Industrie_4.0_final_2012–10–02.pdf, last accessed on 13.10.2018.

[12] Rapid prototyping and rapid tooling are additive manufacturing processes. A layer-by-layer material build-up in plastic or metal takes place on special systems.

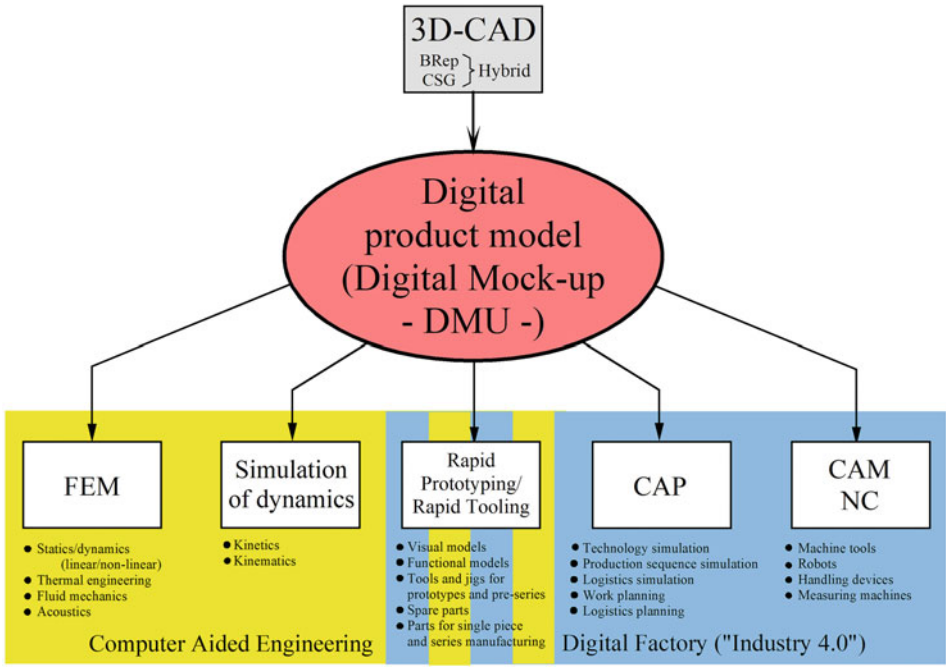

Fig. 7.8 Digital product model as starting point for computer-based engineering methods

supplier consisting of a diesel engine, hydraulic transmission, numerous auxiliary units and support frame. The drive module is arranged underfloor in the vehicle. CAD data can also be transferred between different CAD systems via CAD interfaces. An internationally standardized interface is STEP (Standard for the Exchange of Product Model Data).

The next CAx component after the creation of the product geometry data in CAD is CAE – Computer-Aided Engineering (Fig. 7.7). It comprises methods for calculating and simulating products in the creation phase. An example of this is the finite element method, see Figs. 6.43 and 6.44 in Chap. 6. The finite element method can be used to calculate static and dynamic properties (mechanical stresses and deformations under static and dynamic loads, crash, natural frequencies and natural modes). If inadequacies of the product are found, e.g. excessive mechanical stresses or inadmissible deformations, changes must be made in the product model (red feedback loop in Fig. 7.7).

Another example of the application of CAE is shown in Fig. 7.12. Here, CFD (Computational Fluid Dynamics; CFD is also based on the finite element method) was used to investigate the heat load and flow through an internally ventilated brake disc. CFD is used to simulate heat transfer problems as well as circulation and flow. It can also be used to investigate acoustics.

During braking, kinetic energy is converted into thermal energy. During deceleration or stop braking, the brake disc must store the energy generated for a short period and release it

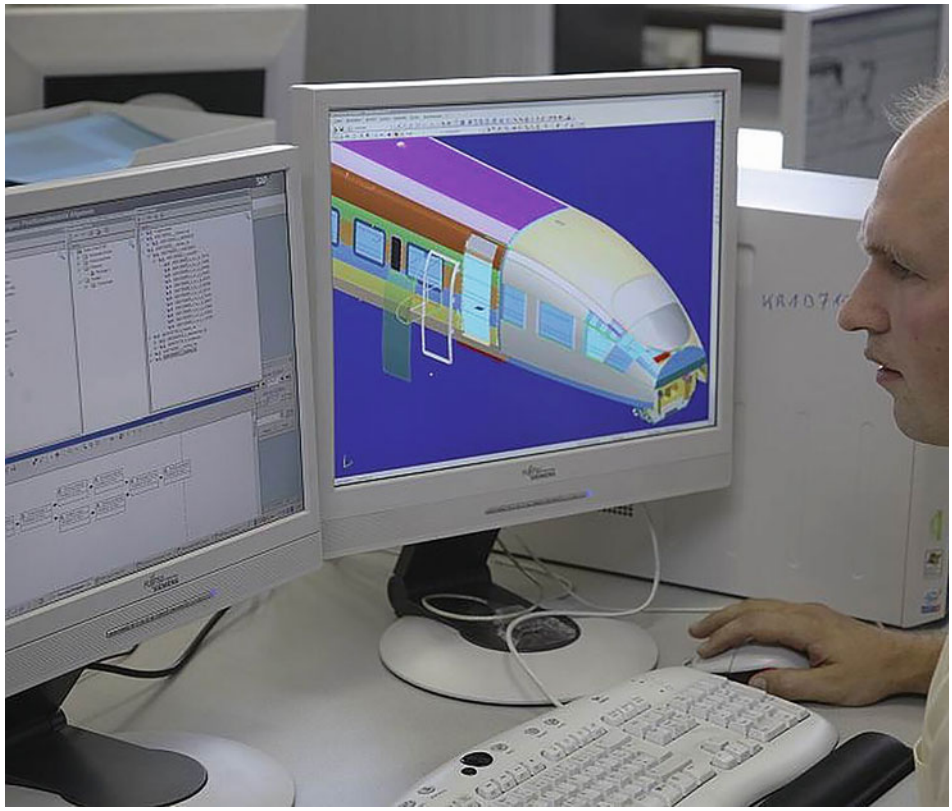

Fig. 7.9 CAD workstation. (Photo: Siemens Mobility)

to the environment via the surface. In the case of inertia braking on a downhill gradient, the thermal energy accumulating over longer periods is dissipated to the environment via the flow through the inner blading (see Fig. 4.17; Fig. 7.12 shows a section through the brake disc). In both cases the brake disc heats up. Large temperature differences in the disc can lead to cracks, very high temperatures to severe wear of the brake pads and the disc. With the help of CFD, a prediction of the brake disc can be made and many time-consuming tests can be saved.

Figure 7.13 shows the investigation of the ergonomics of a driver's cab using a human model. The accessibility of controls for different sized drivers, the field of view on the track and on display systems can be checked in the DMU.

Kinetics and kinematics (driving behaviour and vibration behaviour, freedom of movement of e.g. running gear, cardan shafts, doors, steps, current collectors) can also be investigated in simulations. In this way, development results can be secured and tests with their costs and time expenditure can be saved.

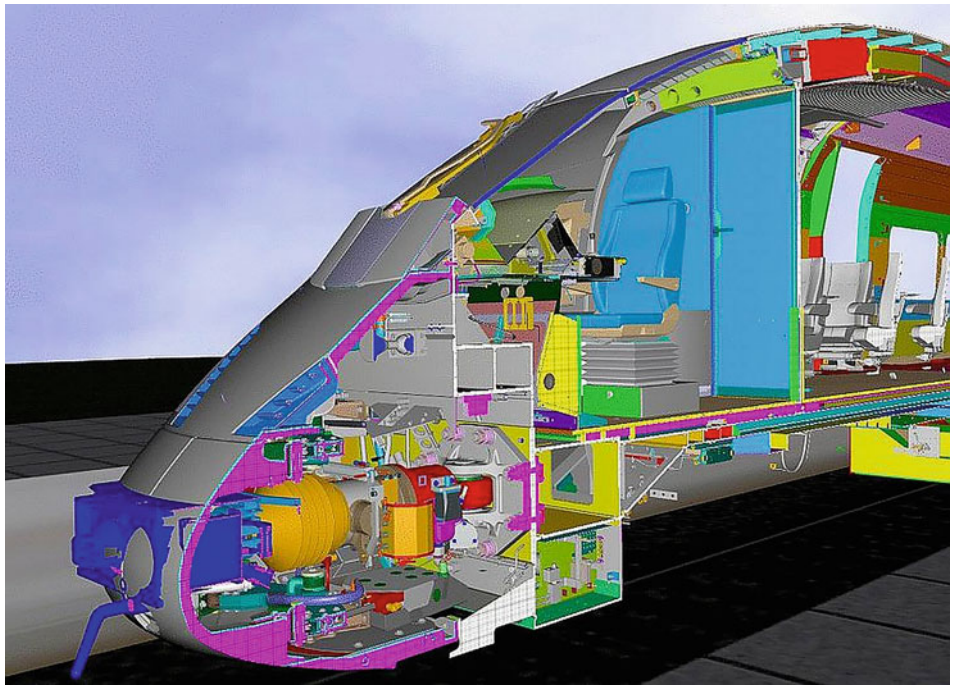

Fig. 7.10 CAD model of a high-speed train in sectional view. (Image: Siemens Mobility)

The next computer-aided method in the product manufacturing process (Fig. 7.7) is CAP (Computer-Aided Planning) systems, which are used to prepare manufacturing and assembly tasks. Work and assembly plans are created. They contain the sequence, workstation/machine, aids (tools, fixtures) as well as the time and labour requirements of the work steps to be carried out in order to obtain, for example, a finished component from a semi-finished product or an assembly from individual parts. Work schedules and assembly plans are used to instruct workers and are the basis for determining costs, capacity and deadlines. The tasks within the CAP also include the creation of NC programs (see below) for computer-controlled machine tools, for welding systems and industrial robots. In addition, there is the design of tools for forming and injection moulding machines, of fixtures for welding assemblies as well as of handling devices and aids for assembly. The planning of factories and workshop areas by means of computers is also attributed to CAP. Figures 7.14, 7.15 and 7.16 show examples from the field of computer-aided work planning.

The geometry data of the roof, roof bows and purlins are used to design the welding fixture and tensioners in Fig. 7.14. The design of such fixtures is done with the help of a CAD system, but is usually attributed to CAP. Welding fixtures are used for tacking and welding out. They are the prerequisite for dimensionally accurate welded assemblies. The

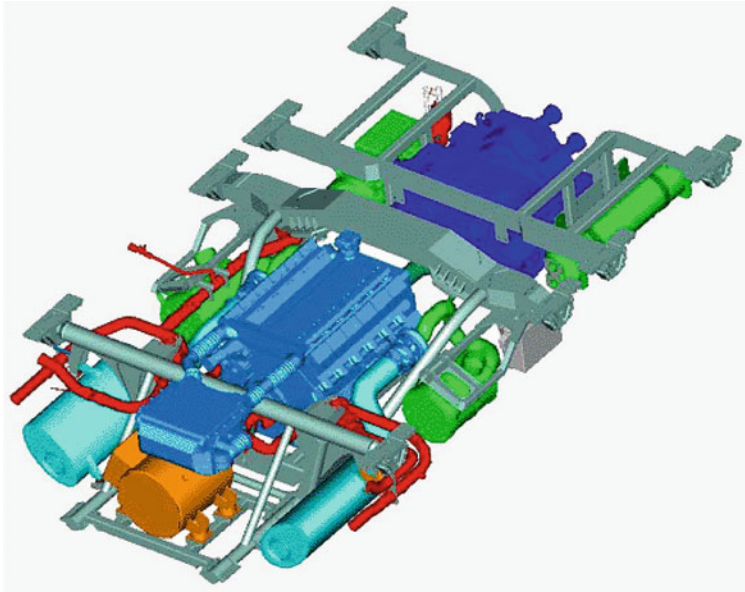

Fig. 7.11 3D CAD model of a ready-to-install drive module for a diesel railcar. (Image: Voith Turbo)

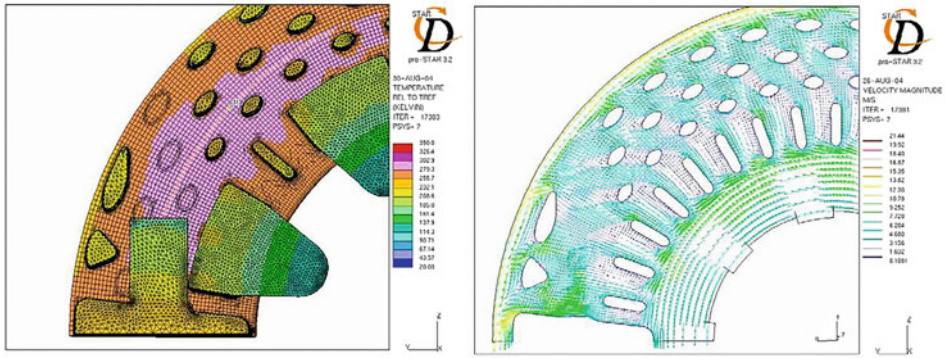

Fig. 7.12 Investigation of the temperature load of a rail vehicle brake disc (**a**) and the flow velocities inside (**b**) at a continuous braking power of 22 kW and 520 min^{-1}. (Image: Faiveley Transport)

components to be joined are inserted into the jig and fixed in the correct position with the aid of clamps.

Figure 7.15 shows a handling device for picking up and fitting bellows. The latter connect the passenger compartments of two car bodies. They are too heavy for manual handling. With the aid of the device, the bellows are removed from the delivery packaging

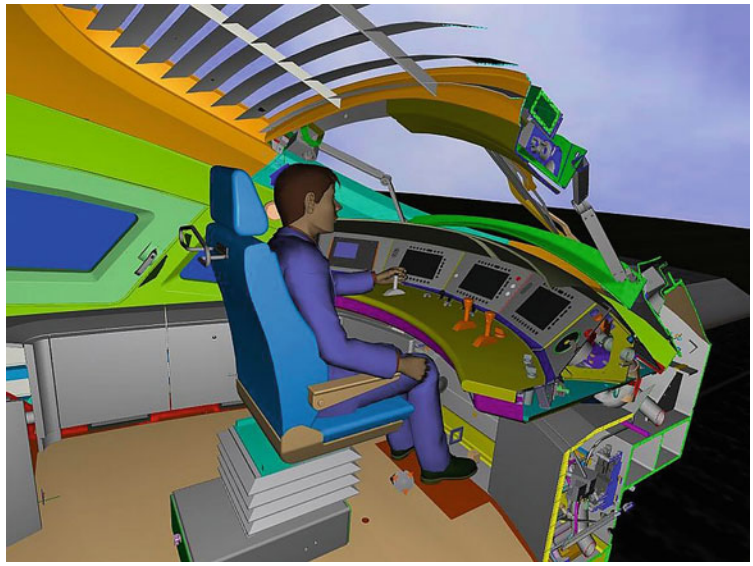

Fig. 7.13 Simulation of a driver's cab with a human model. (Image: Siemens Mobility)

Fig. 7.14 Fixture with magnetic clamps for welding passenger carriages roofs. (Photo: Minda Industrieanlagen GmbH)

and brought into the position required for assembly on the vehicle body. The task of work planning is to identify the need for handling systems, to plan and design them. In some cases, design and manufacture are also left to subcontractors.

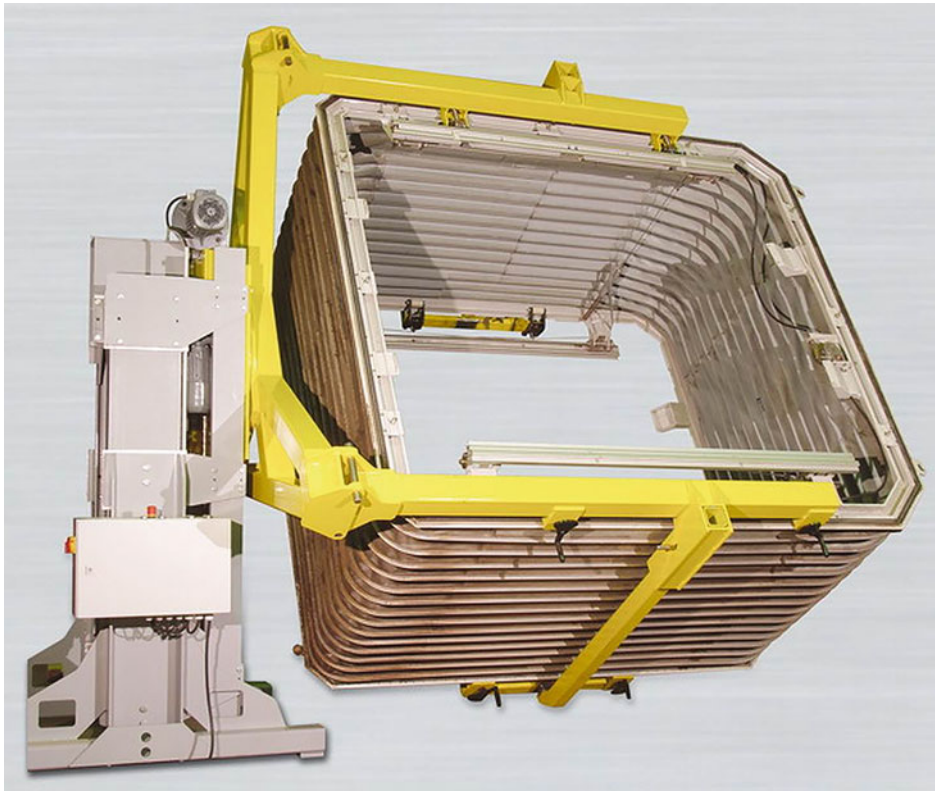

Fig. 7.15 Device for handling and mounting bellows. (Photo: Klädtke Metallverarbeitung)

Since many vehicles to be used in local transport are built with low floors, numerous parts of the drive equipment and air conditioning must be accommodated on the roof. Ladders and platforms are therefore necessary for the assembly workers in order to achieve a favourable body posture during assembly and to ensure work safety. Figure 7.16 shows the planning of such assembly stations using 3D CAD. The vehicle itself is only shown as a rough shell in order to reduce the data complexity and thus the response times of the system. The individual tools are planned to match the shapes and dimensions of the vehicle and the working environment. On the far left, a platform with railings bridges the working pit of the workshop. In front of the vehicle is a working platform for installing the front window. The mobile staircase is provided for safe access to the driver's cab from the hall floor.

The lateral yellow lifting platform is used for the installation of the side windows: The workers pick up a window, move to the lowered lifting platform and move to the installation position with the window on the lifting platform. For work on the roof equipment, the platforms shown on the right in Fig. 7.16 are provided at roof level.

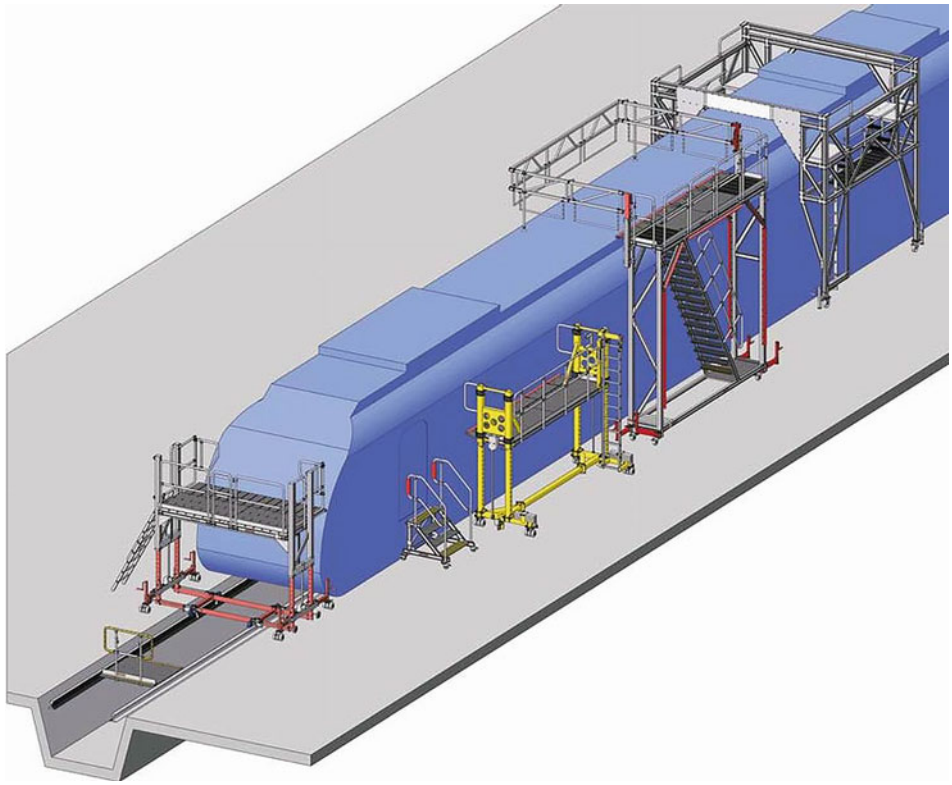

Fig. 7.16 Planning of an assembly workstation. (Image: Zarges GmbH)

CAP systems[13] can also be used to plan the facilities of new factories, factory halls, work areas and workstations. Complex assembly plants such as individual assembly workstations can be simulated and optimized on the digital model. A product can be simulated for assemblability and maintainability (e.g. accessibility of individual parts and assemblies). With a logistics simulation, capacities and throughputs of entire production areas can be determined and improved. The number of necessary conveyors, the size of buffers and storage areas as well as the cycle times of conveyors and production equipment can be simulated and optimized. Human models are also available in these systems, so that human motion sequences can be interactively checked and evaluated. In work planning on the simulation model, the ergonomics of manual assembly stations are improved, for example, or specified times for movement and work sequences are determined.

[13]For example: DELMIA from Dassault Systemès and TECNOMATIX from Siemens-PLM-Software.

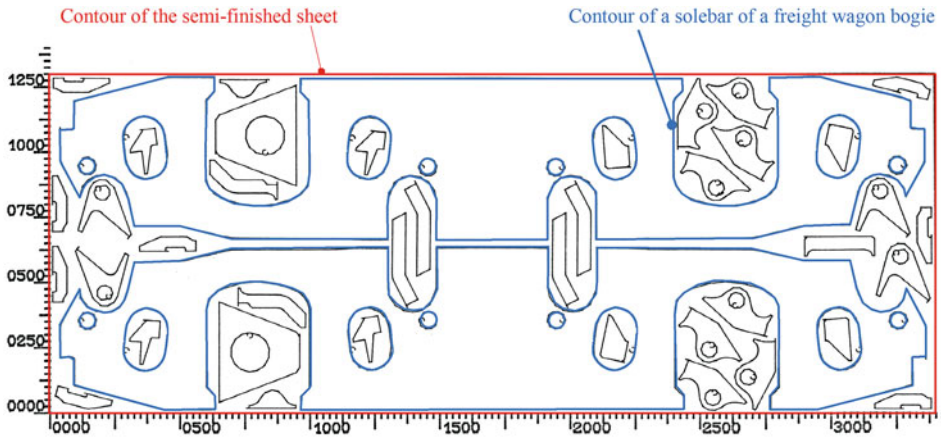

Fig. 7.17 Nesting plan for the solebars of a freight car bogie. (Image: Linke-Hofmann-Busch)

With the help of technology simulations, e.g. for sheet metal forming, component areas at risk of cracking and buckling can be identified in the simulation. For the design of injection molds, the injection, cooling and shrinking processes can be simulated. Goals in the field of CAP are the shortening of planning processes, but especially their safeguarding: The optimization of a realized plant or factory in operation is time-consuming and expensive, but usually only possible in partial areas. With the help of simulation techniques, bad investments can be avoided in factory and plant planning.

After work planning, computer-aided manufacturing and assembly can begin. CAM – Computer-Aided Manufacturing – describes the use of numerically controlled machine tools and industrial robots for manufacturing and assembly using the product geometry. Mostly CNC machines (CNC: Computer Numerical Control) are used today, which are connected to the CAM computer via a data line. The necessary control programs (NC programs) for the machine or the robot are generated from the geometry data of the product. Additional technology data is required, e.g. for milling the tool geometry, the spindle speed and the feed rate. In the CAM system, the NC programs are linked to order data as production-related product data. The latter specify, for example, the machine or system that has to process a certain number of pieces of a component or assembly at a defined date. CAM methods can be used in both prototype and series production. Figures 7.17, 7.18, 7.19, 7.20 and 7.21 show examples of computer-aided manufacturing.

Bogies are often welded together from sheet steel parts. These parts are cut from sheet metal panels using a CNC flame cutting machine. For the freight car bogie shown in Fig. 5.35, the two web plates for the solebars are burnt out of an 8 mm thick sheet. Figure 7.17 shows the so-called nesting plan. The two solebars are placed on a sheet of size 3320 × 1300 (red contour). The contour of the two solebars is highlighted in blue.

Fig. 7.18 Machining of a base plate for ICE intermediate carriages on a CNC portal milling machine. (Photo: Linke-Hofmann-Busch)

Fig. 7.19 Machining of a bogie frame on a CNC moving column milling machine. (Photo: J&S Engineering and Maintenance)

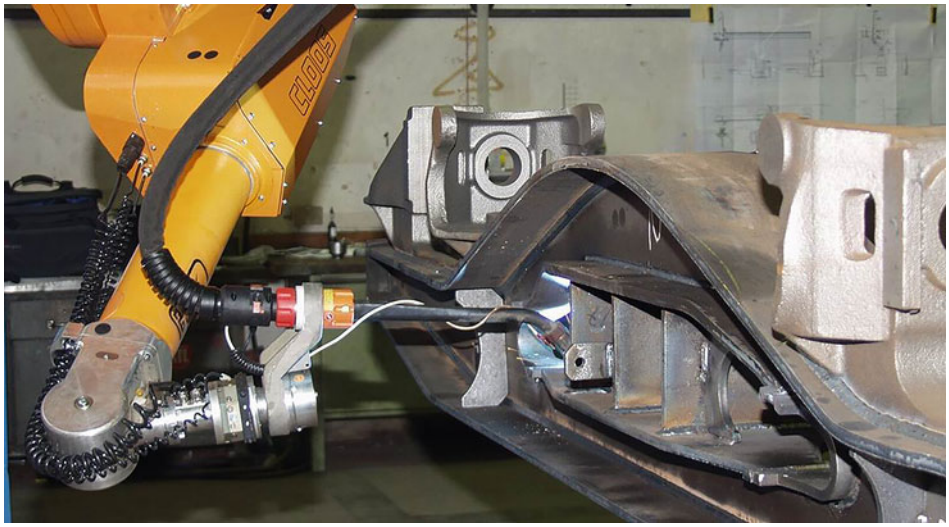

Fig. 7.20 Welding robot during seam welding of a solebar for a freight car bogie Y25. (Photo: Karl Cloos Schweißtechnik GmbH)

To reduce waste, additional (small) parts are automatically placed in the gaps on the sheet metal panel with the help of nesting software. The system recognizes when more parts can be accommodated by rotating the small part contours. The resulting nesting plan is loaded as an NC program into the control system of the flame-cutting machine, and the torch moves along the contours of the individual parts. The small three-quarter circles in Fig. 7.17 indicate the location where the torch is ignited for each part.

Figure 7.18 shows the milling of a base plate welded from extruded profiles for an ICE intermediate carriage. The base plate is clamped on the machine table with the underside facing upwards. The integrated C-profiles shown in Fig. 6.19 are milled off in sections so that square nuts can later be inserted for fastening underfloor equipment. In addition, openings for cables and air ducts are milled. The milling portal can be moved over the entire length of the base plate.

Bogie frames must also be machined after welding and after any annealing process to reduce welding residual stresses. All functional and connecting surfaces, e.g. the spring support surfaces, are milled. This is necessary, among other things, to ensure the parallelism of the wheelsets and to guarantee largely identical wheel loads. Due to the size and mass of a bogie frame, machining is carried out in one clamping operation if possible. Figure 7.19 shows a bogie frame clamped vertically on a turntable being machined on a CNC moving column milling machine.

Figures. 7.20 and 7.21 show the use of industrial robots for welding. In Fig. 7.20, the solebar of a standard steel freight wagon bogie Y25 (see Fig. 5.34) is joined to the main cross member by seam welding.

Fig. 7.21 Industrial robot with spot welding gun welding a side wall. (Photo: IGM Robotersysteme AG)

The industrial robot in Fig. 7.21 is used for spot welding. It guides the yellow welding gun with the two welding electrodes. In the case of a side wall made of aluminum, the bottom outer sheet is joined to the top side wall frame made of L and Z profiles.

Before surface treatment of rail vehicles, complete blasting of the surfaces is necessary to improve the adhesion of the primer due to the desired long service life. Figure 7.22 shows a blasting cabin in which a body shell of a commuter train is being blasted by means of a robot. The robot is connected to an overhead crane-like structure that travels on rails above the car body. In addition to the longitudinal and transverse travels possible with it, the robot can be raised and lowered vertically. The blasting gun is attached to its articulated arm. The robot's traverse paths are determined by the vehicle geometry, which the blasting gun has to cover completely on the outside and inside. For blasting the inside, the robot arm travels through the windows and end openings. Depending on the material of the car body, different blasting media are used, e.g. steel, ceramic or glass beads. During the blasting process, there are no workers inside the blasting cabin.

Another component of CAx technologies is CAT – Computer Aided Testing (Fig. 7.7). This includes, for example, the control of test facilities and processes as well as the collection, storage and evaluation of test data with the aid of computers. This comes into

Fig. 7.22 Industrial robot blasting a metro train car body in preparation for painting. (Photo: Blastman Robotics Ltd.)

question both in prototype testing and in the monitoring of series production. The latter can also be seen as a function of CAQ (see below). An example is given in Sect. 6.1.3 and in Fig. 6.3.

CAQ – Computer-Aided Quality (Management) is the computer-aided quality assurance. This ranges from the creation of test plans to the control of 3D measuring machines with the aid of CAD product data geometry to the monitoring of series production including evaluation. During the production and assembly of rail vehicles, safety-relevant production steps in particular must be monitored and documented. Likewise, protocols are created from the acceptance of a vehicle. In the case of pressure tanks for e.g. pressurised gas tank wagons (Fig. 6.42), all sheet metal blanks must be stamped with batch numbers. They are entered on a tank drawing. All weld seams are X-rayed and the X-ray images are documented in a so-called tank book. The tank book contains all documents relating to the pressure tank, including the acceptance certificates for the semi-finished products used.

The final building block of computer-aided methods is CAS – Computer-Aided Service. CAS covers two areas: Firstly, the use of the computer in the diagnosis and maintenance of products (e.g. evaluation of fault memories within the control computers in the vehicle) including the computer-aided determination of maintenance and servicing measures depending on the stress and wear of the product. For this purpose, relevant components are monitored via sensors. It is possible to report necessary maintenance measures from the

moving train to the responsible maintenance base, so that the necessary work can be planned in advance and the corresponding spare parts can be provided in time. This can increase the availability of a vehicle fleet.

CAS also includes, for example, the support of maintenance personnel through pictorial representation of maintenance procedures and display of circuit diagrams on portable computers. In the future, even more extensive support will be possible here through methods of "augmented reality" – a mixture of reality and virtual computer representation by means of special devices. On the other hand, CAS also includes computer-aided product monitoring in operation as a preliminary stage to product modification and improvement measures, e.g. by tracking complaints, repair processes as well as spare and wear part requirements.

Due to the long service life of rail vehicles of 30 to sometimes 50 years, the comprehensive documentation of the products is of great importance. Many rail vehicles are rebuilt several times in the course of their life in order to adapt them to the respective current requirements of technology and customers. Examples of this are the replacement of the interior fittings of passenger coaches, the renewal of the electrical installations in tram cars and the replacement of the tank in tank cars. Since such work is not necessarily carried out by the previous manufacturer, the product documentation should always be up to date. Product lifecycle management systems (PLM systems), in which all relevant data of the vehicles are stored over their entire life cycle, are ideal for this purpose. In addition to technical data, data such as mileage, downtimes, energy consumption, repair and maintenance costs, etc. can also be collected here.

References

1. Adler, G., Fenner, W., et al. (Hrsg.): Lexikon der Eisenbahn, 8. Aufl. Motorbuch, Stuttgart (1990)
2. Babiel, G.: Elektrische Antriebe in der Fahrzeugtechnik. ViewegVerlag, Wiesbaden (2007)
3. Baur, K.G.: Drehgestelle – Bogies. EK-Verlag, Freiburg (2006)
4. Bendel, H.: Die elektrische Lokomotive. transpress Verlag, Berlin (1994)
5. Beyer, K.-H., Degenkolbe, J., et al.: Handbuch Diesellokomotiven. transpress Verlag, Stuttgart (2005). Reprint der Ausgabe 1963
6. BMVBS (Hrsg.): Handbuch Eisenbahnfahrzeuge. Leitfaden für Herstellung und Zulassung. Bundesministerium für Verkehr, Bau und Stadtentwicklung, Berlin (2013). https://www.bmvi.de/SharedDocs/DE/Publikationen/E/handbuch-eisenbahnfahrzeuge.pdf?__blob=publicationFile. Accessed on 05.09.2018
7. BMVI (Hrsg.): Verkehr in Zahlen 2013/14. Bundesministerium für Verkehr, Bau und Stadtentwicklung/DVV Media Group, 42. Jahrgang, Hamburg (2014)
8. Bugarcic, H., Geers, L., Meyer-Plate, E.: Empfehlungen für die Festigkeitsauslegung von Personenfahrzeugen nach BOStrab. VDV-Schriften, Bd. 152. Verband Deutscher Verkehrsunternehmen (VDV), Köln (1992)
9. Büttemeier, H., Kaßner, M., Strothmann, M.: Schweißtechnisches Handbuch Schienenfahrzeugbau. Auslegung, Konstruktion, Fertigung und Qualitätssicherung. DVS Media GmbH, Düsseldorf (2010)
10. DB AG: Arbeitsmappe für die Aus- und Fortbildung von Triebfahrzeugführern auf dem Triebzug BR 402 DB AG. Dienstleistungszentrum Bildung, Berlin (1995)
11. DB Reise&Touristik AG (Hrsg.): ICE T – BR 411, 415 und 605. Hestra-Verlag, Darmstadt (2000)
12. DBCargo AG (Hrsg.): Die Güterwagen der Bahn. DBCargo AG, Berlin (2000)
13. Deinert, W.: Elektrische Lokomotiven. transpress Verlag, Stuttgart (2006). Reprint der 2. Auflage 1965
14. Deinert, W.: Eisenbahnwagen, 4. Aufl. transpress VEB Verlag für Verkehrswesen, Berlin (1981)
15. EBA (Hrsg.): Memorandum of Understanding über die Neugestaltung von Zulassungsverfahren für Eisenbahnfahrzeuge. Eisenbahn-Bundesamt, Bonn (2015). https://www.eba.bund.de/SharedDocs/Downloads/DE/Fahrzeuge/Inbetriebnahme/MoU/MoU_Neugestaltung_Zulassungsverfahren.pdf;jsessionid=29A8DC15951407BDC7BAD2E99144EA93.live21304?__blob=publicationFile&v=2. Accessed on 18.09.2018
16. Engelmann, M., Ludwig, H.: Handbuch der Dieseltriebfahrzeuge der Deutschen Bundesbahn. Vermögensverwaltung der GDL, Frankfurt/Main (1963)

© The Author(s), under exclusive license to Springer Fachmedien Wiesbaden GmbH, part of Springer Nature 2022

J. Ihme, *Rail Vehicle Technology*,
https://doi.org/10.1007/978-3-658-36969-9

17. FAG Kugelfischer (Hrsg.): FAG Rollenachslager für Schienenfahrzeuge, Publ.-Nr. 07100, FAG Kugelfischer Georg Schäfer & Co., Schweinfurt (ca. 1963)
18. Feihl, J.: Die Diesellokomotive. Aufbau – Technik – Auslegung. Transpress-Verlag, Stuttgart (1997)
19. Fiedler, J.: Bahnwesen – Planung, Bau und Betrieb von Eisenbahnen, S-, U-, Stadt- und Straßenbahnen, 4. Aufl. Werner Verlag, Düsseldorf (1999)
20. Filipovic, Z.: Elektrische Bahnen – Grundlagen, Triebfahrzeuge, Stromversorgung, 5. Aufl. Springer, Berlin/Heidelberg (2015)
21. Fischer, R., Linse, H.: Elektrotechnik für Maschinenbauer, 13. Aufl. Vieweg + Teubner, Wiesbaden (2009)
22. George, K.-D.: Fahrzeuge und maschinentechnische Anlagen. Handbuch für den Eisenbahnbetriebsleiter, Bd. 3. Aus- und Weiterbildungszentrum Verkehrsgewerbe Leipzig, Leipzig (2006)
23. Glück, H.: Aerodynamik der Schienenfahrzeuge. TÜV Rheinland, Köln (1985)
24. Gralla, D.: Eisenbahnbremstechnik. Werner, Düsseldorf (1999)
25. Hanneforth, W., Fischer, W.: Laufwerke Schienenfahrzeugtechnik. transpress VEB Verlag für Verkehrswesen, Berlin (1986)
26. Hausmann, A., Steinbügl, J.: Grundlagen des Bahnbetriebs. DB-Fachbuch, Bd. 4/10. Eisenbahn-Fachverlag, Heidelberg (2000)
27. Hegger, A., Marks-Fährmann, U., Restetzki, K.: Grundwissen Bahn. Verlag Europa-Lehrmittel, Haan-Gruiten (2014)
28. HochschulefürTechnik und Wirtschaft (Hrsg.): Tagungsband 8. Internationale Schienenfahrzeugtagung, Dresden, 2006. Eurailpress Tetzlaff-Hestra, Hamburg (2006)
29. Hochschule für Technik und Wirtschaft (Hrsg.): Tagungsband 13. Internationale Schienenfahrzeugtagung, Dresden, 2014. DVV Media/Eurailpress, Hamburg (2014)
30. Ihme, J.: Beitrag zur Laufdynamik zweiachsiger Schienenfahrzeuge im geraden Gleis. Diss, TU Braunschweig (1983)
31. Institution of Mechanical Engineers (Hrsg.): Railway Rolling Stock. IMechE Seminar Publication 1996-17, Bury St Edmunds (1996)
32. Iwnicki, S. (Hrsg.): Handbook of Railway Vehicle Dynamics. Taylor & Francis Group, Boca Raton/Florida (2006)
33. Janicki, J.: Bremstechnik und Bremsproben. Bahn Fachverlag, Berlin (2018)
34. Janicki, J., Reinhard, H., et al.: Schienenfahrzeugtechnik, 3. Aufl. Bahn Fachverlag, Berlin (2013)
35. Joachimsthaler, A.: Die elektrischen Einheitslokomotiven der Deutschen Bundesbahn, 3. Aufl. Vermögensverwaltung der GDL, Frankfurt/Main (1969)
36. Klell, M., Eichlseder, H., Trattner, A.: Wasserstoff in der Fahrzeugtechnik. Erzeugung, Speicherung und Anwendung, 4. Aufl. Springer Vieweg, Wiesbaden (2018)
37. Knorr-Bremse (Hrsg.): Grundlagen der Bremstechnik, Basics of Brake Technology, 3. Aufl. Knorr-Bremse GmbH, München (2007)
38. Knothe, K., Stichel, S.: Schienenfahrzeugdynamik. Springer, Berlin/Heidelberg (2003)
39. Koewius, A.: Aluminium-Schienenfahrzeuge Entwicklungen – Technologien – Projekte. Aluminium-Zentrale e. V., Düsseldorf. Hestra, Darmstadt (1992)
40. Krugmann, H.-L.: Lauf der Schienenfahrzeuge im Gleis – Eine Einführung. Oldenbourg Verlag, München/Wien (1982)
41. Kunicki, H.: Kraftübertragungsanlagen der Dieseltriebfahrzeuge. transpress VEB Verlag für Verkehrswesen, Berlin (1963)
42. Kuper, K., Janicki, J., Meffert, R.: Bremstechnik und Bremsproben, 2. Aufl. DB-Fachbuch 9/11. Eisenbahn-Fachverlag, Heidelberg (1992)
43. Lehmann, H.: Bahnsysteme und ihr wirtschaftlicher Betrieb. Tetzlaff, Darmstadt (1978)

44. Lübke, D. (Hrsg.): Handbuch – Das System Bahn. DVV Media Group, Hamburg (2008)
45. Mäurich, G., Matthes, H., Stößel, G.: Straßenbahnen, 2. Aufl. transpress VEB Verlag für Verkehrswesen, Berlin (1990)
46. Mitschke, M., Wallentowitz, H.: Dynamik der Kraftfahrzeuge, 5. Aufl. Springer-Verlag, Berlin/Heidelberg (2014)
47. Müller, A.: Wissenschaftliche Bewertung von alternativen, emissionsarmen Antriebskonzepten für den bayerischen SPNV. Bericht 2017-EB-008-1. Institut für Bahnfahrzeuge und Bahntechnik der Techn. Universität Dresden. Dresden (2017)
48. Müller, S.: Elektrische und dieselelektrische Triebfahrzeuge, Leistungsfähigkeit – Wirtschaftlichkeit – Arbeitsweise. Birkhäuser Verlag, Basel/Boston/Stuttgart (1979)
49. Neuber, H.D. (Hrsg.): Studie über ein Schnellverkehrssystem, Hochleistungs-Schnellbahn-Studiengesellschaft. Ottobrunn/Bundesministerium für Verkehr, Bonn (1972)
50. Pippert, H.: Antriebstechnik – Strömungsmaschinen für Fahrzeuge. Vogel-Verlag, Würzburg (1974)
51. Plett, S.: Einführung in die Technik der Bremsen. Die Lokomotivtechnik. Gewerkschaft Deutscher Lokomotivbeamten und Anwärter, Frankfurt/Main (1974). Sonderausgabe 9
52. Reinhardt, W.: Geschichte des Öffentlichen Personenverkehrs von den Anfängen bis 2014, Mobilität in Deutschland mit Eisenbahn, U-Bahn. Straßenbahn und Bus. Springer Vieweg, Wiesbaden (2014)
53. Rose, H. (Hrsg.): Lexikon der Lokomotive. Transpress Verlag, Berlin (1992)
54. Rossberg, R.R. (Hrsg.): Deutsche Eisenbahnfahrzeuge von 1838 bis heute. VDI-Verlag, Düsseldorf (1988)
55. Sachs, K.: Elektrische Triebfahrzeuge, Ein Handbuch für die Praxis sowie für Studierende in drei Bänden. Springer, Wien (1973)
56. Saumweber, E., Gerum, E., Berndt, P.J.: Grundlagen der Schienenfahrzeugbremse. Archiv für Eisenbahntechnik, Bd. 43. Hestra-Verlag, Darmstadt (1990)
57. Schindler, C. (Hrsg.): Handbuch Schienenfahrzeuge. Entwicklung – Produktion – Instandhaltung. DVV Media Group, Hamburg (2015)
58. Steimel, A.: Elektrische Triebfahrzeuge und ihre Energieversorgung, Grundlagen der Praxis, 3. Aufl. Deutscher Industrieverlag, München (2014)
59. Taschinger, O.: Stahl im Leichtbau von Eisenbahnwagen, Beratungsstelle für Stahlverwendung. Verlag Stahleisen, Düsseldorf (1967)
60. VDI (Hrsg.): Getriebe für Schienenfahrzeuge (Tagung Veitshöchheim 1999), VDI-Gesellschaft Entwicklung Konstruktion Vertrieb. VDI-Berichte, Bd. 1455. VDI Verlag, Düsseldorf (1999)
61. Voith, J.M. (Hrsg.): Hydrodynamik in der Antriebstechnik – Wandler, Wandlergetriebe, Kupplungen, Bremsen. Vereinigte Fachverlage, Mainz (1987)
62. VDB e. V. (Hrsg.): Die Bahnindustrie in Deutschland – Zahlen und Fakten zum Bahnmarkt und -verkehr. Verband der Bahnindustrie in Deutschland (VDB), Berlin (2014)
63. VDB e. V (Hrsg.): VDB-Leitfaden Quality Engineering in der Entwicklung von Schienenfahrzeugen und ihren Systemen. Verband der Bahnindustrie in Deutschland e. V., Berlin (2015). https://bahnindustrie.info/fileadmin/Leitfaeden_DE/1509a__VDB-QE-Leitfaden_DE_final.pdf. Accessed on 05.09.2018
64. VDV e. V. (Hrsg.): Der Straßenbahner. Handbuch für U-Bahner, Stadt- und Straßenbahner. Verband Deutscher Verkehrsunternehmen (VDV), Köln (2001)
65. VDV e. V. (Hrsg.): Stadtbahnsysteme – Light Rail Systems, Grundlagen – Technik – Betrieb – Finanzierung, Principles – Technology – Operation – Financing. Verband Deutscher Verkehrsunternehmen (VDV), Köln/DVV Media Group, Hamburg (2014)
66. VDV e. V. (Hrsg.): Empfehlungen für die Festigkeitsauslegung von Personenfahrzeugen nach BOStrab. VDV-Schrift 152, Verband Deutscher Verkehrsunternehmen (VDV), Köln (2016)

67. Wende, D.: Fahrdynamik des Schienenverkehrs. Teubner Verlag, Stuttgart (2003)
68. Wickens, A.H.: Fundamentals of Rail Vehicle Dynamics: Guidance and Stability. Swets & Zeitlinger, Lisse (2003)

Index

A
Acceleration resistance, 31, 39, 40, 46, 230, 235
AC motors, 63–69
Air brake
  direct-acting, 117
  indirect, 117, 118
  multi-solvent, 119
  self-acting, 118
Air resistances, 31, 33–35, 40–43, 47–50, 230
Air spring
  additional volumes, 210
  calculations, 206
  characteristics, 207, 209
  level control, 193, 206, 209, 210
  load capacity, 209, 210
  natural frequency, 209, 210
Air suspension, 193, 206–211, 278
Amplitude control, 65, 66
Assembly workstations, 290

B
Back pressure brake, 57
Ballast superstructure, 14
Bogie
  air suspension, 206
  American, 186
  basic types, 185
  cradle suspension, 188, 189
  fatigue loads, 219, 220, 266, 267
  Freight wagons, 143, 185, 186, 293
  ICE 1, 76
  Jacob's arrangement, 194, 195
  passenger carriages, 216, 226–247, 288
  Wishbones, 192
Bogie frame
  torsionally soft, 203, 205
Bogie vehicles, 143, 184, 229
Brake
  frictional, 108
  generative, 234
  hydrodynamic, 85
Brake block materials, 124
Brake block soles, 124
Brake circuit
  electrical brake, 116, 127, 129
Brake control
  electropneumatic, 121
Brake linkage, 114, 124
Brake pad moulds, 110, 117, 126, 127, 130, 285
Brake pressure regulator, 122, 123
Brake slip, 111
Brake type changes, 121
Brake weights, 140–141
Braking distance
  calculations, 134, 141
Bridge frame
  locomotives, 253
Bumps
  Freight wagon, 258–264

C
CAD models, 267, 282, 283, 286, 287
CAP systems, 290
Car bodies
  collision safety, 220, 221
  differential construction, 237, 243, 249, 250
  double-decker car, 24
  fatigue load cases, 219

© The Author(s), under exclusive license to Springer Fachmedien Wiesbaden GmbH, part of Springer Nature 2022

J. Ihme, *Rail Vehicle Technology*,
https://doi.org/10.1007/978-3-658-36969-9

Car bodies (*cont.*)
hybrid construction, 240, 241, 248
integral design, 234, 235
lever load case, 217
light rail vehicle, 116, 124, 163, 216, 221, 240, 242, 248, 249
mass fractions, 113
mixed construction, 228
sectional construction, 232
self-supporting, 229, 231
stainless steel, 234, 246, 248, 263
static tests, 220
steel construction, 232, 234, 243, 244, 248, 255
strength requirements, 215–225, 248
tensile- and compressive forces, 215
tram, 9, 17, 143, 163, 168, 184, 185, 196–202, 206, 220, 221, 225, 242, 250, 251, 267, 275, 296
tramcars, 23, 185, 197, 242, 250
tubular construction, 231, 247
vertical loads, 216, 217, 220, 266, 267, 269
winding technique, 242
Cardan drive TGV, 80
Cardan hollow shaft drive of the ICE-1, 79
Catenary, 24, 25, 59, 74, 91, 105, 108, 127, 129
Catenary voltages, 24, 60
CAx systems in product creation, 283
Clearance gauge, 21, 23
Clutches, 79, 80, 82–86, 89
Coefficient of adhesion, 51, 110, 111, 131
Commissioning, 277, 282
Computational fluid dynamics (CFD), 284, 285
Computer-aided design (CAD), 270, 272, 281–286, 289, 295
Computer-aided engineering (CAE), 272, 282, 284
Computer-aided manufacturing (CAM), 272, 282, 291
Computer-aided planning (CAP), 272, 282, 286, 291
Computer-aided quality (CAQ), 272, 295
Computer-aided service (CAS), 295, 296
Computer aided testing (CAT), 272, 294
Conicity
effective, 165, 181
Control valves, 117–120, 122, 123, 209
Converter gearbox, 87
Crash, 222, 224, 225, 239, 284
Crash elements, 222–225, 250
Current collectors, 24, 25, 27, 104, 105, 244, 279, 285
Curvature resistance, 31, 38

D
DC chopper, 63
DC motors, 61–64, 69, 70, 76, 79, 234
Δr-function, 165, 166, 177, 178, 181
$\Delta\gamma$-function, 177, 178
Demand map, 52
Development processes, 272, 273
Diesel-battery hybrid drive, 105
Diesel engine
braking torque, 82
map, 82
motor characteristic, 93
Diesel locomotive
multi-engine, 95
Differential converter gearbox, 90
Digital mock-up (DMU), 204, 206, 216, 272, 282, 285
Digital product model, 272, 282, 284
Direct current generator, 69, 91, 92
Disc brakes, 107, 110, 116, 124–126, 190, 234
Double-decker car, 24, 244, 259
Drag coefficients, 31, 40, 41, 45, 47–49
Drilling angle speed, 111, 175
Drilling slip, 173–175
Driving resistance lines, 46, 51
Driving resistances, 3, 39, 43–45, 47, 51, 73
Drum brakes, 107, 126, 127

E
Eddy current brake, 131–133
Efficiency curve
hydraulic converter, 86
Efficiency of a fuel cell system, 104
Electrical power transmission, 91–96
Electric locomotive, 10, 13, 40, 46, 58, 59, 63, 68, 73–75, 78, 91, 98, 101, 124, 223, 224, 253, 255–258
The Last Mile, 101
Extruded aluminium profiles, 235, 237, 241, 243

F
FEM analysis, 267
Final design, 281
Finite element method (FEM), 267–270, 284
Flame straightening, 230, 231
Flexicoil suspension, 191, 192
Freight traffic, 148, 180
Friction Stir Welding, 237
Fuel cells, 101–104
Fuel cell system, 103, 105
Funicular railway, 4, 7

G
Gas turbines, 96–99
Gauges, 8, 9, 16, 17, 19, 23, 39, 81, 91, 166, 167, 182, 198, 220, 243, 244, 248, 278
Geometry data, 284, 286, 291
Gradients, 4, 31, 38, 39, 45, 46, 48, 50–52, 57, 113, 134, 158, 230, 235, 285
Gravitational spring stiffness, 178
Grooved rails, 39, 161, 163, 164
Guide brake valve, 117, 121–123

H
Hand brake, 107, 114, 115
Hanover formula, 40–42, 47
Headwind surcharge, 33
Heating
  passenger trains, 98
Hollow shaft axlebox drive, 75, 78
Hybrid construction, 240, 241, 248
Hybrid drive, 99, 104, 105
Hybrid fuel cell vehicles, 105
Hybrid locomotive, 99–101
Hydrodynamic converter, 85, 86, 89
Hydrodynamic clutch, 85, 86
Hydrodynamic transmission, 86
Hydrogen, 102–105

I
Ideal delivery characteristic, 52, 57, 82, 96
Idler gear, 199
iLINT, 102–104
Impact resistance, 31, 35, 37, 48
Impulse resistor, 44
Industrial robots, 286, 291, 293–295
Integration of modules, 279

L
Landing gear
  KERF, 211
Leaf spring control arms, 189
Legal bases, 8, 9
Level control, 193, 206, 209, 210
Light rail, 6, 114, 124, 163, 216, 219, 221, 240, 242, 247–252, 275
Line resistance, 31, 38, 59
Linkage
  motor bogies, 198
Load change, 123, 140, 173, 254

M
Magnetic rail brakes, 111, 112, 129, 130, 133, 139, 190, 267
Magnification functions, 149, 154–156, 179
Material properties, 246, 247
Mechanical power transmission, 83–85
Minimum braking hundredths, 141

N
Natural frequency
  of a pendulum, 170
NC programs, 286, 291, 293
Nonlinearity
  examples, 149, 157, 158

P
Passenger traffic, 143
Pendulum length, 170
Petrol engines, 80, 82
Pointer diagram, 153, 154
Power converter control, 65
Powershift transmissions, 83–85
Power systems in Europe, 72
Product creation process, 273, 276, 281, 282
Product development process, 275
Product lifecycle management system (PLM systems), 296

R
Rack railways, 4, 6, 57
Rail profiles, 21, 163, 164, 166, 182
Rail vehicle manufacturers, 26, 271–273, 275, 278, 283
Railways, 1–5, 8–10, 13, 14, 16, 17, 19, 21, 23–26, 32, 33, 37, 38, 44, 50, 54, 56–63, 66–69, 81, 82, 91, 94, 96, 101, 105, 108, 109, 116, 117, 129–131, 134, 138, 140, 143–146, 161, 162, 186, 203, 215, 216, 221, 222, 226–248, 255, 259, 271–273, 275, 277, 278
Railway superstructure, 14
Railway systems, 2, 3, 8, 275
Railway vehicles, 5, 9–11, 39, 107–141, 143, 144, 148, 168, 184–202, 215–270, 275, 277
Rapid prototyping, 282, 283
Resistance brake, 128
Rolling resistance, 15, 31, 35–37, 45, 48, 50, 235
Rolling resistance coefficient, 36, 37, 47–49
Rubber ring spring drive, 75

Rubber roller springs, 194, 195, 211
Rubber sprung tram wheel, 18
Running resistances, 31–49, 134

S
Simulation
in frequency range, 144, 154, 155
in the time domain, 151, 157–160
Simulation programs, 151
Single-phase alternating current, 59, 61, 69, 70
Sliding walls, 46, 259, 261–263
Speed
critical, 179, 182–184
Speed gap, 82, 83
Spring-loaded brake, 116
Standard gauge, 14, 16, 18, 39, 165, 198, 267
Start-up converter, 62, 83, 86, 89
Static friction, 53, 54
Steam engine, 54–57, 63
Strength requirements
car bodies, 215–225, 248
Subsystems, 3, 4
Surface treatment, 294

T
Testing, 105, 271, 272, 275, 278, 295
Three-phase asynchronous motor, 63, 69, 70
Three-phase power transmission, 91–93
Tilting device
bodies, 24, 206
Time step integration, 159
Torque mass allowance factor, 40
Track guidance, 4, 13, 14, 143, 160, 163
Track play, 17
Track position errors, 146
Traction motors, 44, 59, 62, 63, 66, 68, 69, 71, 74, 76, 78, 91, 95, 103, 127, 129, 197, 201, 234, 239, 255, 256
Tramcar
low-floor, 197–199, 202, 242, 250
Trams, 2, 4, 9, 12, 15–17, 23–25, 39, 60, 62, 70, 76, 79, 131, 139, 143, 145, 160–163, 184, 185, 196, 197, 199, 201, 210, 216, 219–221, 225, 240–242, 247–252, 267, 268, 272, 275, 296
Traverse bearing drive, 74
Tub position
welding, 250, 261
Two-axle longitudinal drive, 76, 79

V
Vacuum brakes, 116
Vehicle boundary profile, 21
Vehicle platforms, 241, 272, 275, 277, 278
Vibration comfort, 143–145, 170, 187, 189, 210
Vibration replacement model, 152
Vibration responses, 144, 149
Vibration sensation
of man, 144

W
Wedge pack coupling, 76
Wheel hub motors, 199, 200
Wheel profile
tram, 15
Wheel set
dynamic behaviour, 164–167, 169–171, 173, 175, 177–180, 182–184
equations of motion, 151, 152, 179, 183
forces and moments, 171, 172, 177
speeds at, 171
Wheelset arrangements, 10, 13, 80
Wheelset guides, 8, 166, 168
Wheel tyre outline profiles, 160
Wheel tyres, 15–17, 111, 127, 143, 160–164, 166, 211
Wishbone, 192